

**BREAST SKIN STRAIN DURING GRAVITATIONAL
AND DYNAMIC LOADING**

Amy Zena Sanchez (nee Loveridge)

The thesis is submitted in partial fulfilment of the requirements for the award of the degree of Doctor of Philosophy of the University of Portsmouth.

April 2015

Abstract

The breast contains no muscle or bone and its primary supporting structures are reported to be the skin and Cooper's ligaments. It has been hypothesised that independent breast motion, which is already known to cause pain for many women, may also cause damage to the breast structure leading to breast ptosis (sag). Breast damage could be estimated by applying the published strain failure limits (60%) for human skin to measurements of breast skin strain. However, there have been few attempts to measure breast skin strain as gravitational deformation makes it difficult to identify the neutral breast position in which there is no external strain on the breast skin.

A gold-standard method for estimating the neutral breast position based on Archimedes' principle was developed and implemented within this thesis. Fourteen female participants, with breast sizes 30 to 34 under band and B to E cup size, had semi-permanent henna markers applied to their torso (4 markers) and left breast (an array of 17 markers including the nipple). Participants were immersed up to their neck in two fluids with mass-densities above (water) and below (soybean oil) the reported range of breast mass-densities ($919 \text{ kg}\cdot\text{m}^{-3}$ to $986 \text{ kg}\cdot\text{m}^{-3}$). The mid-point between the breast position in water and soybean oil provided the gold-standard neutral position estimate. Participants also performed nine alternative novel or previously published methods for estimating the neutral breast position. Alternative methods were assessed for accuracy and precision when estimating the gold-standard neutral nipple position. To investigate the effects of gravity and dynamic activity on the breast, participants had their breast displacement and breast skin strain assessed in the static gravity-loaded (bare-breasted) position and during an incremental-speed (bare-breasted) treadmill test (4 kph to 14 kph). Breast pain was recorded in each condition using an 11-point numerical rating scale.

The gold-standard method was implemented to obtain an accurate (measurement error $\leq 1.4 \text{ mm}$) and precise (TEM $\leq 1.2 \text{ mm}$, SD $\leq 3.7 \text{ mm}$) measurement of the neutral breast position. Evaluation of novel and previously published neutral position methods revealed that the buoyancy in water method achieved the most accurate estimation of the gold-

standard neutral nipple position (absolute differences ≤ 5.6 mm, TEM ≤ 1.2 mm, SD ≤ 2.6 mm). Comparison of the gravity-loaded and neutral breast positions demonstrated that gravity caused the nipple to move posteriorly (mean change 15.6 mm), laterally (mean change 7.5 mm) and inferiorly (mean change 25.9 mm) relative to the torso, and induced potentially damaging skin strains up to 75%. During bare-breasted incremental-speed treadmill activity the nipple was displaced furthest from the neutral position in the inferior direction (mean of 45.5 mm); a result which could not be attained using conventional measurements of nipple range of motion (ROM). Strain analysis indicated potentially damaging skin strains during the incremental-speed treadmill activity (up to 114%), particularly in the upper-outer region of the breast. This finding supports the anticipated relationship between breast motion and breast damage. Breast pain was most strongly correlated to superior nipple displacement from the neutral position during treadmill activity ($p < 0.001$, $r = 0.725$), and a significant correlation was observed between breast pain and breast skin strain ($p < 0.001$, $r = 0.361$). Combination of breast displacement and skin strain data provided a comprehensive analysis of the effect of gravity- and motion-induced breast displacements on the breast skin.

Incorporation of the neutral breast position into future biomechanical research may lead to improved assessment of breast motion and breast damage, and a deeper understanding of motion-induced breast pain. Within clinical research, identification of the neutral breast position may enable the development of breast models that are better able to predict the gravitational deformation of the breast during surgery. Consideration of the neutral breast position, and subsequent breast strain, also has applications within the field of breast support design and evaluation. A breast support garment that positions the breast in the neutral position and restricts motion to within the reversible strain limits of the skin may protect the breast from skin damage and the associated breast pain.

Contents

Abstract	i
Contents	iii
Declaration	ix
List of tables	x
List of figures	xiv
Abbreviations	xxii
Acknowledgements and dedication	xxiii
Dissemination.....	xxiv
1. Introduction	1
1.1. Rationale.....	1
1.2. Aims of the thesis	3
1.3. Thesis overview	4
2. Literature review and justification of the thesis methods	6
2.1. Introduction.....	6
2.2. The neutral breast position	6
2.3. Assessing breast position and breast motion	14
2.3.1. Participant factors.....	14
2.3.2. Static breast measurements	18
2.3.3. Dynamic breast measurements	24
2.4. Breast strain.....	42
2.4.1. Measuring breast skin strain.....	42
2.4.2. Strain as a measure of damage.....	44
2.4.3. Recovery time of the breast.....	48
2.4.4. Implications of restricting breast motion based on measures of skin strain	49
2.5. Breast pain.....	50
2.5.1. Assessment of breast pain	50
2.5.2. Relationships between breast motion and breast pain.....	52
2.5.3. Strain as a cause of pain.....	53
2.6. Evaluating the accuracy and precision of experimental methods	54
2.6.1. Accuracy assessment	55

2.6.2.	Accuracy criteria.....	63
2.6.3.	Precision assessment	64
2.6.4.	Precision criteria	68
2.7.	Summary.....	69
3.	Methodological development	71
3.1.	Overview.....	71
3.2.	Methodological study 1: A systematic review of the density of the breast to inform the fluid selected for the new gold-standard buoyancy neutral position method	72
3.2.1.	Introduction	72
3.2.2.	Aims.....	73
3.2.3.	Method.....	73
3.2.4.	Results	75
3.2.5.	Discussion.....	81
3.2.6.	Conclusion	83
3.3.	Methodological study 2: Does breathing state or measurement duration affect relative breast position?	84
3.3.1.	Introduction	84
3.3.2.	Aims.....	86
3.3.3.	Method.....	86
3.3.4.	Results	88
3.3.5.	Discussion.....	91
3.3.6.	Conclusion	93
3.4.	Methodological study 3: Using POSE estimation within breast biomechanics	94
3.4.1.	Introduction	94
3.4.2.	Aims.....	96
3.4.3.	Method.....	96
3.4.4.	Results	99
3.4.5.	Discussion.....	103
3.4.6.	Conclusion	106
3.5.	Methodological study 4: Development of the gold-standard buoyancy method for measuring the neutral breast position	107

3.5.1.	Investigation 1: Assessing camera functionality and safety concerns when using soybean oil for immersion.....	107
3.5.2.	Investigation 2: Practicality testing of the buoyancy method using water ..	116
3.5.3.	Investigation 3: Selecting a tank for the buoyancy study	121
3.5.4.	Investigation 4: Developing a calibration object for the buoyancy study ...	124
3.6.	Summary of methodological developments	129
4.	Measuring the neutral nipple position using the gold-standard buoyancy method.....	131
4.1.	Introduction.....	131
4.2.	Aims	131
4.3.	Method	132
4.3.1.	Experimental procedure	132
4.3.2.	Measurement analysis	139
4.3.3.	Accuracy analysis	140
4.3.4.	Precision analysis	142
4.4.	Results	143
4.4.1.	Neutral position measurement.....	143
4.4.2.	Quantifying the effect of gravity on the static nipple position.....	149
4.4.3.	Accuracy assessment	152
4.4.4.	Precision assessment	154
4.5.	Discussion	157
4.6.	Conclusion	162
4.6.1.	Investigating the influence of torso angle on the effect of gravity on the breast	163
5.	Developing alternative methods for identifying the neutral breast position	172
5.1.	Introduction.....	172
5.2.	Aims	175
5.3.	Stage 1: Review of methods for predicting the neutral breast position.....	175
5.3.1.	Method.....	175
5.3.2.	Results	177
5.3.3.	Discussion.....	182
5.3.4.	Conclusion	183

5.4.	Stages 2 and 3: Laboratory testing.....	184
5.4.1.	Method.....	184
5.4.1a.	Buoyancy in water	188
5.4.1b.	Breast drop	193
5.4.1c.	Static extremes	204
5.4.1d.	Drop landing	217
5.4.1e.	Zero acceleration during treadmill activity	229
5.4.1f.	Zero acceleration during jumping activity.....	234
5.4.1g.	Gravity loaded static position.....	237
5.5.	Comparison of the alternative neutral position methods against the gold- standard buoyancy method	241
5.5.1.	Neutral nipple position estimates.....	242
5.5.2.	Accuracy of the neutral nipple position estimates	243
5.5.3.	Precision of the neutral nipple position estimates	244
5.6.	Discussion	245
5.7.	Conclusion	247
6.	Incorporating the neutral nipple position into measurements of breast motion	248
6.1.	Introduction.....	248
6.2.	Aims	250
6.3.	Method.....	250
6.4.	Results	251
6.5.	Discussion	260
6.6.	Conclusion	264
7.	Static and dynamic breast strain	265
7.1.	Introduction.....	265
7.2.	Aims	268
7.3.	Method	268
7.3.1.	Experimental procedure	268
7.3.2.	Data analysis	269
7.3.2a.	Static breast skin strain	270
7.3.2b.	Peak regional breast skin strain during treadmill activity.....	276
7.3.2c.	Peak segmental breast skin strain during treadmill activity	284

7.3.2d. Instantaneous segmental breast skin strain over one gait cycle at 14 kph –
 A case study.....292

7.3.2e. Peak breast skin strain and breast pain300

7.3.2f. Error analysis of breast strain data307

7.4. Discussion311

7.5. Conclusions.....312

8. Combining breast displacement and skin strain data314

8.1. Introduction.....314

8.2. Aim.....314

8.3. Method314

8.4. Results and discussion315

8.4.1. Static data315

8.4.2. Dynamic data320

8.5. Conclusion330

9. Thesis review331

9.1. General discussion.....331

9.2. Delimitations and limitations336

9.3. Conclusions.....339

References.....340

Appendices.....369

Appendix A - Breathing state results.....370

Appendix B - Breathing duration results371

Appendix C - Participant information booklet372

Appendix D - Correlations between participant characteristics and nipple position374

Appendix E - Frontal and sagittal views of the neutral and gravity-loaded breast.....377

Appendix F - Breast drop neutral position estimates391

Appendix G - Static extreme neutral position estimates392

Appendix H - Drop landing neutral position estimates393

Appendix I - Zero acceleration neutral position estimates (treadmill running).....394

Appendix J - Zero acceleration neutral position estimates (trampoline jumping).....395

Appendix K - Numerical rating breast pain scales.....396

Appendix L - Breast skin strain results (static, 5 kph, 8 kph and 14 kph).....397

Appendix M - Static strain error estimates411

Appendix N - Favourable ethical opinion letter415

Appendix O - UPR16 Form declaring the ethical conduct of the research416

Declaration

Whilst registered as a candidate for the above degree, I have not been registered for any other research award. The results and conclusions embodied in this thesis are the work of the named candidate and have not been submitted for any other academic award.

Word count: 79,412

List of tables

Table 3.1: Mass-densities of the breast calculated from published quantitative breast data up to and including the year 2013.	77
Table 3.2: Mean left nipple position relative to the torso during 2 s measurements in normal breathing, held exhalation and held inhalation conditions.	89
Table 3.3: Absolute differences in nipple position during held exhalation and inhalation compared to each participant’s mean nipple position during 2 s of normal breathing (mm).	89
Table 3.4: Standard deviation of nipple position measurements for three repeat trials in each breathing state (mm).....	89
Table 3.5: Mean left nipple position relative to the torso during 2.00 s, 1.00 s, 0.50 s, 0.25 s, and 10.00 s of normal breathing.	90
Table 3.6: Absolute differences in nipple position compared to each participant’s mean nipple position during 10.00 s of normal breathing (mm).....	90
Table 3.7: Standard deviation of nipple position measurements for three repeat trials for each breathing duration (mm).	91
Table 3.8: Mean segment residual during running at 10 kph for three different constructions of the torso segment.	99
Table 3.9: Mean range of motion of the suprasternal notch marker about the segment origin during running at 10 kph for three different constructions of the torso segment (n = 1).....	101
Table 3.10: Mean range of motion of the left nipple marker relative to the segment origin during running at 10 kph for three different constructions of the torso segment (n = 1).....	101
Table 3.11: Properties of soybean oil.	113
Table 3.12: Practicality results for the buoyancy in water method.....	118
Table 3.13: Mean left nipple position in the LCS of the torso while immersed in water during the buoyancy practicality investigation (n = 7).	119
Table 4.1: Participant information for the 14 women who took part in the gold-standard buoyancy study.	134

Table 4.2: Mean gravity-loaded left nipple position while standing stationary in the laboratory (n = 14).....	144
Table 4.3: Mean left nipple position in water and soybean oil, and the calculated mean neutral nipple position estimated using buoyancy.....	145
Table 4.4: Change in left nipple position from the gold-standard neutral position estimated using buoyancy to the gravity-loaded laboratory position (n = 14).	149
Table 4.5: Correlations between participants' physical characteristics and their neutral and gravity-loaded nipple positions (n = 14).	151
Table 4.6: Absolute difference in measured marker locations using the gold-standard buoyancy method compared to their known locations.....	153
Table 4.7: Gravity loaded left nipple position measured during two separate testing sessions (sessions 2 and 3) within a two week period (n = 14).	155
Table 4.8: Change and standard deviation in gravity loaded left nipple positions measured during two separate testing sessions (sessions 2 and 3) within a two week period (n = 14).....	156
Table 4.9: Standard deviation of neutral nipple position measurements using the gold-standard buoyancy method (n = 14).....	157
Table 4.10: Mean and absolute difference in participant torso local co-ordinate system angle in the laboratory, the neutral position, water, and soybean oil.	167
Table 4.11: Paired sample t-test results for comparing torso local co-ordinate system angle across conditions in the buoyancy study.	168
Table 4.12: Correlation between torso local co-ordinate system angle and directional changes in nipple position when moving from the laboratory to the neutral position.....	168
Table 5.1: Previously implemented methods for identifying the neutral position of the breast.....	177
Table 5.2: Novel methods for identifying the neutral position based on counteracting the effects of gravity on the breast.	179
Table 5.3: Absolute difference (to the gold-standard value) and standard deviation in neutral nipple position measured using the buoyancy in water method.	189

Table 5.4: Paired samples t-test results and typical error of measurement (TEM) values for the buoyancy in water method.....	190
Table 5.5: Practicality results for the breast drop method.....	196
Table 5.6: Mean neutral nipple position measured using the breast drop and gold-standard methods.	198
Table 5.7: Absolute difference (to the gold-standard value) and standard deviation in neutral nipple position measured using the breast drop method.	199
Table 5.8: Paired samples t-test results (compared to gold-standard values) and typical error of measurement (TEM) values for the breast drop method.	200
Table 5.9: Practicality results for the static extreme method.	208
Table 5.10: Mean static extreme positions of the left nipple during accuracy and precision assessment of neutral position methods.	210
Table 5.11: Mean neutral nipple position measured using the static extremes and gold-standard methods.	213
Table 5.12: Absolute difference (to the gold-standard value) and standard deviation in neutral nipple position measured using the static extremes method.	214
Table 5.13: Paired samples t-test results (compared to gold-standard values) and typical error of measurement (TEM) values for the static extremes method.	214
Table 5.14: Practicality results for the drop landing method.....	221
Table 5.15: Mean neutral nipple position measured using the drop landing and gold-standard methods.	225
Table 5.16: Absolute difference (to the gold-standard value) and standard deviation in neutral nipple position measured using the drop landing method.....	226
Table 5.17: Paired samples t-test results (compared to gold-standard values) and typical error of measurement (TEM) values for the drop landing method.....	226
Table 5.18: Practicality results for the zero-acceleration during running method.	232
Table 5.19: Practicality results for the zero-acceleration during jumping method.....	235
Table 5.20: Absolute difference (to the gold-standard value) and standard deviation in neutral nipple position measured using the gravity-loaded static nipple position method.....	238

Table 5.21: Paired samples t-test results (compared to gold-standard values) and typical error of measurement (TEM) values for the gravity-loaded static nipple position method.....	239
Table 6.1: Correlations between breast pain, nipple ROM and maximum nipple displacement from the neutral nipple position during an incremental-speed treadmill test.....	260
Table 7.1: First order static breast strain calculated using the resultant distance between the suprasternal notch and nipple marker compared to peak static strain obtained using a breast array.	272
Table 7.2: Breast pain scores in the static standing condition and at each speed of the incremental-speed treadmill test.....	301
Table 7.3: Mean peak breast skin strain (occurring in any breast segment over three gait cycles) at each speed of the incremental-speed treadmill test.....	302
Table 7.4: Mean maximum change in breast skin strain compared to the static condition (in any breast segment) over three gait cycles at each speed of the incremental-speed treadmill test.....	304
Table 7.5: Correlations between breast pain, peak breast skin strain and peak change in breast skin strain during an incremental-speed treadmill test.....	304

List of figures

Figure 2.1: Breast anatomy (Haake & Scurr, 2010).....	7
Figure 2.2: Misalignment of gravity and the ground reaction force acting on the breast. ...	8
Figure 2.3: Magnetic resonance images of breasts with low and high radiological density demonstrating varying proportions of fat within the breast (Lee <i>et al.</i> , 1997).	11
Figure 2.4: International Society of Biomechanics recommended marker placement for the torso (triangles and pentagon) (Wu <i>et al.</i> , 2005), and recommended breast motion torso markers (squares and pentagon) (Zhou <i>et al.</i> , 2011), compared to torso markers used in previous breast motion studies (circles and pentagon) (Haake & Scurr, 2010; Scurr, Galbraith, Hedger, <i>et al.</i> , 2007; Whittingham <i>et al.</i> , 2012; Zhou <i>et al.</i> , 2011; Zhou, Yu, & Ng, 2012b).....	31
Figure 2.5: Breast marker placement on the nipple (pentagon) (Zhou <i>et al.</i> , 2011), and additional breast markers that have been used for assessing breast motion (white circles) (Chen <i>et al.</i> , 2012; Zhou <i>et al.</i> , 2009); breast position (black circles and squares) (Brown <i>et al.</i> , 1999; Rong, 2006; Veitch <i>et al.</i> , 2012; Wheat <i>et al.</i> , 2014); and garment design (triangles and squares) (Ying <i>et al.</i> , 2011). Dotted lines illustrate the four quadrants of the breast and the superior breast boundary.	32
Figure 2.6: The rectangular breast array used in Rajagopal's (2007) neutral breast position study (a) and the conical breast array used by Sutrada (2012) to investigate the properties of breast skin (b).	33
Figure 2.7: Construction of a torso reference frame, using the same torso marker set, defined using a medial-lateral (a) or superior-inferior (b) primary axis (Mills, Loveridge, <i>et al.</i> , 2014a).....	37
Figure 2.8: Global co-ordinate system of the laboratory (GCS) compared to the local co-ordinate system (LCS) of the torso segment used for calculation of relative breast motion (underline shows the positive direction for each LCS axis).....	39
Figure 2.9: Displacement (a), amplitude (b) and peak to peak value (ROM) (c) of example displacement data.....	40

Figure 2.10: MRI scans of the breasts while lying prone in the gravity loaded position (a) and while immersed in water (b) (Rajagopal <i>et al.</i> , 2008).....	43
Figure 2.11: Stress-strain curve for human torso skin illustrating the orientation of the collagen network within the skin during each strain phase (Daly, 1982).....	45
Figure 2.12: Strain ellipses on the (male) human chest (a) (Gibson <i>et al.</i> , 1969), and the stress-strain relationship for human abdomen skin measured parallel (A) and perpendicular (B) to the superior-inferior axis (a) (Daly, 1982).	47
Figure 2.13: Anscombe’s quartet demonstrating four different data sets with the same regression equation caused by: (a) random deviation about the regression line; (b) a linear regression line fit to quadratic data; (c) an anomalous data point influencing the gradient of the regression line; (d) an anomalous data point creating a non-infinite gradient (adapted from Anscombe, 1973).	57
Figure 2.14: Bland-Altman plot comparing two methods for measuring peak expiratory flow rate (Bland & Altman, 1986).	59
Figure 3.1: Mean calculated mass-densities of the breast from published data, up to and including the year 2013, compared to the overall mean breast mass-density and the mass-densities of water and soybean oil.....	80
Figure 3.2: Breast and torso marker set used for the methodological study on breathing.	86
Figure 3.3: Markers and landmarks used to construct three different POSE estimated torso segments to evaluate segment and origin stability and relative nipple range of motion during treadmill running at 10 kph.	98
Figure 3.4: Displacement of the suprasternal notch marker relative to the segment origin, for three different torso segment constructions, in the anterior-posterior (a), medial-lateral (b) and superior-inferior (c) directions during running at 10 kph (n = 1).	100
Figure 3.5: Displacement of the left nipple marker relative to the segment origin, for three different torso segment constructions, in the anterior-posterior (a), medial-lateral (b) and superior-inferior (c) directions during running at 10 kph (n = 1).	102
Figure 3.6: Measuring cylinders used to assess the maximum depth of field for the underwater cameras when immersed in soybean oil.....	109

Figure 3.7: Apparatus used to assess the resolution of the underwater cameras when immersed in soybean oil.	110
Figure 3.8: A 10 mm marker array filmed through 480 mm of water (a) and soybean oil (b) to assess the depth of field of the underwater cameras used in the buoyancy study.	111
Figure 3.9: Images of 10 mm and 20 mm marker arrays filmed through air (a), water (b) and soybean oil (c) taken with the underwater cameras used for the buoyancy study.	112
Figure 3.10: Immersion tank used in Investigation 2, to assess the practicality of the buoyancy method in the biomechanics laboratory using water.	117
Figure 3.11: Sputnik calibration frame used in the buoyancy practicality investigation using water.	117
Figure 3.12: Body measurements taken to assess minimum tank dimensions for the buoyancy study.	122
Figure 3.13: Tank selected for use in the buoyancy study based on the minimum dimensions required for participants to comfortably remain upright during testing.	123
Figure 3.14: Variable object used to identify the maximum calibration volume inside the D-shaped buoyancy tank.	125
Figure 3.15: Dimensions of the steel block used to construct the calibration object for the buoyancy study.	126
Figure 3.16: Maximum visible volume using three underwater cameras inside the D-shaped buoyancy tank.	127
Figure 3.17: Custom-made calibration object developed for the buoyancy study.	128
Figure 4.1: Henna marker array used in the gold-standard neutral position study.	135
Figure 4.2: Non-slip tape used on the outside (a) and inside (b) of the D-shaped tank during the buoyancy study using soybean oil.	138
Figure 4.3: Directional components of left nipple position when calculated relative to the torso segment (arrows show the positive direction along each axis).	140
Figure 4.4: Calibration markers used to evaluate measurement error for the gold-standard neutral position buoyancy method.	142

Figure 4.5: Anterior-posterior displacement of the left nipple from the neutral nipple position in the laboratory, in water and in oil. Error bars represent the standard deviation in nipple position between trials in the same condition (n = 14).....	146
Figure 4.6: Medial-lateral displacement of the left nipple from the neutral nipple position in the laboratory, in water and in oil. Error bars represent the standard deviation in nipple position between trials in the same condition (n = 14). ..	147
Figure 4.7: Superior-inferior displacement of the left nipple from the neutral nipple position in the laboratory, in water and in oil. Error bars represent the standard deviation in nipple position between trials in the same condition (n = 14).....	148
Figure 4.8: Mean (a) and individual (b) change in nipple position from the gold-standard neutral position to the gravity-loaded position (n = 14).....	150
Figure 4.9: Proposed change in breast shape during the gold-standard buoyancy study when moving from the laboratory (a) to the soybean oil (b) and water (c) immersions.....	160
Figure 4.10: The effect of torso angle (θ) on the directional components of the gravitational force at the nipple when presented in the local co-ordinate system of the torso.	164
Figure 4.11: Diagram illustrating the effect of torso local co-ordinate system rotation on measurements of anterior-posterior (A-P) and superior-inferior (S-I) nipple position.....	165
Figure 5.1: Evaluation process for determining the suitability of alternative methods used for predicting the neutral nipple position.....	174
Figure 5.2: Superior-inferior breast displacement (a) and breast acceleration (b) during a breast drop as presented by Haake & Scurr (2011).....	193
Figure 5.3: Practicality study breast drop method using the hand (a) and a Theraband (b) to support the breast.	194
Figure 5.4: Superior-inferior left nipple acceleration (above) and displacement (below) during a breast drop for a participant with breast size 32C.	195
Figure 5.5: Example static extremes and estimated neutral nipple position data viewed in the frontal plane.....	204

Figure 5.6: Diagrammatic representation of the static extremes of the left nipple in the anterior-posterior (a), medial-lateral (b), and superior-inferior (c) directions.	205
Figure 5.7: Positions used to achieve the anterior (a) and posterior (b) static extremes of the breast.	206
Figure 5.8: Positions used to achieve the medial (a) and lateral (b) static extremes of the breast.....	206
Figure 5.9: Positions used to achieve the superior (a) and inferior (b) static extremes of the breast.	207
Figure 5.10: Alterations to the medial-lateral (a) and anterior (b) positions for the static extreme method.	209
Figure 5.11: Example relative superior-inferior left nipple displacement during a drop landing.....	218
Figure 5.12: Platform used in the drop landing neutral position method.....	220
Figure 5.13: Example superior-inferior left nipple displacement for a 32C participant during a drop landing performed from four different drop heights.....	223
Figure 5.14: Example right and left heel vertical displacement data during treadmill running at 14 kph.	231
Figure 5.15: Summary of the included and excluded alternative neutral position methods evaluated in this programme of work.....	241
Figure 5.16: Anterior-posterior (a), medial-lateral (b) and superior-inferior (c) components of the gold-standard and estimated neutral nipple positions obtained using each of the alternative neutral position methods (n = 14).....	242
Figure 5.17: Anterior-posterior (a), medial-lateral (b) and superior-inferior (c) absolute difference in nipple position compared to the gold-standard position (n = 14).	243
Figure 5.18: Anterior-posterior (a), medial-lateral (b) and superior-inferior (c) standard deviation in nipple position compared to the gold-standard position (n = 14).	244
Figure 6.1: Example nipple motion data demonstrating equal nipple range of motion and differing maximum nipple displacements when measured from the neutral nipple position.....	248

Figure 6.2: Anterior-posterior (a), medial-lateral (b), and superior-inferior (c) nipple displacement for one participant (Participant 6, 32C) during three gait cycles of treadmill running at 14 kph.	253
Figure 6.3: Nipple displacement in the frontal (a) and sagittal (b) plane for one participant (Participant 6, 32C) during three gait cycles of treadmill running at 14 kph..	254
Figure 6.4: Breast pain scores at each speed of an incremental-speed treadmill test.	255
Figure 6.5: Mean left nipple range of motion at each speed of an incremental-speed treadmill test (n = 14).....	256
Figure 6.6: Mean ROM and peak displacements of the nipple from the neutral position during running at 14 kph (n = 14).....	256
Figure 6.7: Mean maximum nipple displacement from the neutral nipple position in the frontal plane during an incremental-speed treadmill test (n = 14).	258
Figure 6.8: Mean maximum nipple displacement from the neutral nipple position in the sagittal plane during an incremental-speed treadmill test (n = 14).	259
Figure 7.1: Breast marker location on the breast with reference to the Langer lines of the breast (a) (Jatoi <i>et al.</i> , 2006); and the rectangular marker pairings used for the calculation of breast strain (b).	267
Figure 7.2: Mean percentage static skin strain across the breast for 14 participants with breast sizes 32 to 34 under band and B to E cup size. The two white markers represent the locations of the suprasternal notch and the left nipple.	271
Figure 7.3: Example data demonstrating the potential for over-estimations of skin strain ($\Delta L/L_0$) arising from using the straight line approximation between breast markers.....	274
Figure 7.4: Breast regions defined for strain analysis: mid-lines (pink); upper inner (purple); upper outer (blue); lower inner (green); and lower outer (orange).	277
Figure 7.5: Mean peak skin strain values along the upper mid-line of the breast during static standing and incremental-speed treadmill activity.....	279
Figure 7.6: Mean peak skin strain values along the lower mid-line of the breast during static standing and incremental-speed treadmill activity.....	279
Figure 7.7: Mean peak skin strain values along the inner mid-line of the breast during static standing and incremental-speed treadmill activity.....	280

Figure 7.8: Mean peak skin strain values along the outer mid-line of the breast during static standing and incremental-speed treadmill activity.....	280
Figure 7.9: Mean peak skin strain values in the upper inner region of the breast during static standing and incremental-speed treadmill activity.....	281
Figure 7.10: Mean peak skin strain values in the upper outer region of the breast during static standing and incremental-speed treadmill activity.....	281
Figure 7.11: Mean peak skin strain values in the lower inner region of the breast during static standing and incremental-speed treadmill activity.....	282
Figure 7.12: Mean peak skin strain values in the lower outer region of the breast during static standing and incremental-speed treadmill activity.....	282
Figure 7.13: Breast skin segments defined within each breast region for strain analysis.	285
Figure 7.14: Peak skin strain in each breast segment while standing stationary in the laboratory.....	287
Figure 7.15: Peak skin strain in each breast segment while walking at 5 kph on the treadmill.	288
Figure 7.16: Peak skin strain in each breast segment while running at 8 kph on the treadmill.	289
Figure 7.17: Peak skin strain in each breast segment while running at 14 kph on the treadmill.	290
Figure 7.18: Longitudinal (a) and latitudinal (b) breast lines defined for case study strain analysis.	293
Figure 7.19: Longitudinal skin strain across the breast of Participant 11 (32DD) for one gait cycle during treadmill running at 14 kph.	295
Figure 7.20: Latitudinal skin strain across the breast of Participant 11 (32DD) for one gait cycle during treadmill running at 14 kph.	296
Figure 7.21: Diagrammatic representation of the points during the gait cycle (at 14 kph) for one participant (size 32DD) at which each breast skin segment experienced peak strain (red).	299
Figure 7.22: Mean static strain in each skin segment within each breast region. Error bars represent the mean typical error in each strain value (n = 14).	310
Figure 8.1: Neutral and gravity-loaded nipple position (and representative breast outline) in the frontal (a) and sagittal (b) plane (Participant 11, 32DD).	315

Figure 8.2: Static gravity-induced displacement of the nipple from the neutral nipple position in the frontal (a) and sagittal (b) plane (Participant 11, 32DD).316

Figure 8.3: Static gravity-induced displacement of the breast mid-lines from the neutral breast position in the frontal (a) and sagittal (b) plane (Participant 11, 32DD).317

Figure 8.4: Static gravity-induced skin strain on the breast mid-lines in the frontal (a) and sagittal (b) plane (Participant 11, 32DD).319

Figure 8.5: Static breast skin strain against medial-lateral (a) and superior-inferior (b) skin segment displacement from the torso segment origin (Participant 11, 32DD).320

Figure 8.6: Anterior-posterior (a), medial-lateral (b), and superior-inferior (c) nipple displacement relative to the neutral nipple position during one gait cycle of treadmill running at 14 kph (Participant 11, 32DD).321

Figure 8.7: Longitudinal skin strain on the breast mid-line during one gait cycle of treadmill running at 14 kph (Participant 11, 32DD).322

Figure 8.8: Latitudinal skin strain on the breast mid-line during one gait cycle of treadmill running at 14 kph (Participant 11, 32DD).323

Figure 8.9: Longitudinal (a) and latitudinal (b) breast skin strain at the mid-point of each skin segment during one gait cycle of treadmill running at 14 kph (Participant 11, 32DD). The locations of the breast mid-line markers are illustrated in grey.326

Figure 8.10: Marker locations used to define the longitudinal and latitudinal breast mid-lines with reference to the underlying breast anatomy.327

Figure 8.11: Resultant nipple displacement relative to the torso during one gait cycle of treadmill running at 14 kph (Participant 11, 32DD).328

Figure 8.12: Nipple displacement in the frontal plane during one gait cycle of treadmill running at 14 kph (Participant 11, 32DD).328

Figure 8.13: Breast skin strain at the instant of peak resultant nipple displacement from the torso during one gait cycle of treadmill running at 14 kph (Participant 11, 32DD).329

Abbreviations

2D	Two dimensional
3D	Three dimensional
AP	Anterior-posterior
CV	Coefficient of variation
DLT	Direct linear transform
DXA	Dual x-ray absorptiometry
FE	Finite element
GCS	Global co-ordinate system
GCV	Generalised cross validation spline
ISB	International Society of Biomechanics
LCS	Local co-ordinate system
LHS	Left heel strike
LOA	Limits of agreement
LSCS	Least-squares cubic spline
ML	Medial-lateral
MRI	Magnetic resonance image
POSE	Position and orientation segment estimation
PSA	Power spectrum analysis
QTM	Qualisys Track Manager software
RA	Residual analysis
RFS	Regularised Fourier series
RHS	Right heel strike
RM	Regression model
ROM	Range of motion
SD	Standard deviation
SEM	Standard error of measurements
SI	Superior-inferior
STN	Suprasternal notch
TEM	Typical error of measurement
UV	Ultra violet
XP	Xiphoid process

Acknowledgements and dedication

I would like to thank the following people who provided valuable support throughout this programme of work.

Firstly, I would like to thank my supervisors Professor Joanna Scurr and Dr Chris Mills for their continued academic support and guidance. I am also grateful for the additional expertise provided by Dr Afshin Anssari-Benham during the later stages of this project.

Secondly, I would like to thank the members of staff in the Department of Sport and Exercise Science and in the School of Engineering who helped me to develop and implement the experimental methods described within this thesis. In particular, I would like to thank Geoff Long and Danny White for their technical expertise and assistance during the development of the more unconventional testing protocols. Additionally, I would like to thank all of my participants for their invaluable involvement within this work.

I would also like to thank my family, friends, and colleagues, particularly those in the research office, who have made the last three years thoroughly enjoyable.

Finally, I would especially like to thank my husband Álvaro for his enduring love, support, and understanding. I dedicate this thesis to you.

Dissemination

Published articles

Mills, C., **Loveridge, A.**, Milligan, A., Risius, D., & Scurr, J. (2014a). Can axes conventions of the trunk reference frame influence breast displacement calculation during running? *Journal of Biomechanics*, 47(2), 575–578.

Mills, C., **Loveridge, A.**, Milligan, A., Risius, D., & Scurr, J. (2014b). Is torso soft tissue motion really an artefact within breast biomechanics research? *Journal of Biomechanics*, 47(11), 2606–2610.

Scurr, J., **Loveridge, A.**, Brown, N., & Mills, C. (2015). Acute changes in clinical breast measurements following bra removal: Implications for surgical practice. *Journal of Plastic, Reconstructive & Aesthetic Surgery Open*, 3, 22–25.

Conference Presentations

Loveridge, A. (2014). Incorporating the neutral breast position into measurements of breast strain. University of Portsmouth DSES Postgraduate Seminar Series, 12th November 2014.

Loveridge, A. (2012). An experimental method to predict the neutral position of the breast. University of Portsmouth Science Faculty Postgraduate Poster Day, 27th June 2012.

Awards

Awarded the Best Poster Prize at the University of Portsmouth Science Faculty Postgraduate Poster Day, 27th June 2012.

1. Introduction

1.1. Rationale

The female breast is a highly malleable structure that is easily deformed by external forces (Rajagopal *et al.*, 2008). During physical activity the breast has been reported to move up to 210 mm relative to the torso (Scurr, 2007). For many women this independent motion causes pain (Gehlsen & Albohm, 1980) and embarrassment (Bowles, Steele, & Munro, 2008) and may ultimately lead to damage of the breast structure causing breast sag (ptosis) (Page & Steele, 1999). These breast-related factors have been shown to negatively affect women's overall health and well-being by altering exercise behaviour and constituting a barrier to physical activity participation (Brown, White, Brasher, & Scurr, 2014; Burnett, White, & Scurr, 2014). Existing research has demonstrated that application of external breast support can reduce independent breast motion and the associated breast pain (Zhou, Yu, & Ng, 2011). However, the link between breast motion and breast damage has not yet been investigated and the exact cause of motion-induced breast pain remains unclear (Zhou *et al.*, 2011).

Strain (extension per unit length) has been used to evaluate the magnitude and reversibility of a biological tissue's response to external loading (Gao & Desai, 2010; Hull, Berns, Varma, & Patterson, 1996; Lim *et al.*, 2008; Miller, 2001; Toms, Lemons, Bartolucci, & Eberhardt, 2002). One of the breast's primary support systems is the skin (Hindle, 1991). Failure limits have already been established for human skin based on measures of strain, with permanent skin deformation occurring at 60% strain (Silver, Freeman, & DeVore, 2001). Measurements of strain on the breast skin could therefore be used to assess the risk of breast damage caused by independent breast motion during exercise. However, application of the 60% skin strain limit to the breast skin is difficult due to the pre-existing breast deformation (and strain) caused by gravity (Gao & Desai, 2010). It is essential that both static and dynamic skin strains are combined when assessing whether the failure limits of the breast skin have been exceeded.

Static skin strain can only be assessed by comparing the gravity-loaded breast position to the neutral breast position in which there is no external strain on the breast skin. The neutral breast position provides the zero-point from which static or dynamic extensions of the breast skin can be used to calculate total breast skin strain and to assess the risk of skin damage. Furthermore, strain on biological tissues has been associated with the sensation of pain in other areas of the body (Hirsch, Ingelmark, & Miller, 1960; Markolf, Schmalzried, & Ferkel, 1989; Micheli & Wood, 1995; Moore & Kennedy, 2000; Quinn, Lee, Ahaghotu, & Winkelstein, 2007), suggesting that breast skin strain may also be a key contributing factor to motion-induced breast pain.

Despite the potential benefits of incorporating the neutral breast position into breast biomechanical research, there have been few attempts to identify this position. Existing methods, such as the breast drop technique (Haake, Milligan, & Scurr, 2012; Haake & Scurr, 2011) or immersion of the breast in water (Rajagopal, 2007; Zain-Ul-Abdein, Morestin, Bouten, & Cornolo, 2013), have not yet been validated and there are doubts regarding their appropriateness for attaining the neutral position of the breast. It is therefore important to develop a more accurate gold-standard method for measuring the neutral breast position to enable quantification of the gravitational effects on breast position, breast strain, or breast pain. Implementation of the gold-standard method for attaining the neutral breast position also provides the opportunity to evaluate the accuracy and precision of existing methods.

Aside from the assessment of breast skin damage and breast pain, identification of the neutral breast position may have additional applications within biomechanical or clinical research, and product design. Firstly, quantification of breast displacement from the neutral breast position would allow displacements to be presented in all six anatomical directions (anterior, posterior, medial, lateral, superior and inferior). This directional distinction for measurements of breast motion has previously been unachievable due to the lack of an appropriate reference position, limiting existing research to presenting breast range of motion (ROM) along each axis (Zhou *et al.*, 2011). Implementation of the neutral breast position as the origin for measurements of breast motion would also enable a distinction to be made between breast motion that increases (away from the

neutral position) or decreases (towards the neutral position) strain on the breast skin. The concept of beneficial breast motion contradicts the currently accepted idea that minimising breast motion should correspond to less breast pain and better breast support (Mason, Page, & Fallon, 1999; Zhou, 2011), but may help explain the contradictory findings from studies investigating relationships between breast motion and breast pain (Zhou *et al.*, 2011). Within clinical research, finite element (FE) breast models are used to aid the tracking of breast structures from diagnostic images to the operating table (Azar, Metaxas, & Schnall, 2002). Mapping breast structures onto the non-loaded (neutral) breast position within these FE models has been shown to improve the tracking accuracy of the breast during deformation (Rajagopal *et al.*, 2008). From a garment design perspective, the neutral position represents the optimum position of the breast inside a bra in terms of minimising the risk of breast skin damage. A bra that positions the breast in the optimum position (neutral position) and limits breast motion to within the reversible deformation limits of the breast skin may eliminate any overloading of the breast structure, reducing the risk of ptosis and motion-induced breast pain.

1.2. Aims of the thesis

1. To establish a new gold-standard method for identifying the neutral breast position, in which there is no external strain on the breast skin.
2. To develop and evaluate the accuracy and precision of novel and existing neutral breast position methods against the gold-standard neutral position method.
3. To compare measurements of breast motion and breast pain using nipple displacement from the neutral nipple position and nipple range of motion during treadmill activity.
4. To calculate static and dynamic (during treadmill activity) skin strain from the neutral position on different regions of the breast and its relationship to breast pain.

1.3. Thesis overview

This thesis is divided into nine progressive sections each contributing to the stated aims of the research project. Initially, it is important to review the present extent of knowledge and to identify research areas which may require further investigation. Chapter 2 therefore reviews the existing research findings and methodologies within breast biomechanics, with particular focus on taking measurements of breast position; assessment of breast motion; evaluation of breast pain; and quantification of strain on the breast and other biological structures. This section also summarises the published information on breast anatomy and the physical properties of the breast structure. Anatomical information was needed to inform the development of novel neutral position methods, and subsequently to understand the extent to which breast motion may damage the breast skin and cause breast pain.

Following the review of existing literature, several methodological considerations were identified (such as marker placement, breathing state, and analysis techniques) that may impact the methods used to measure breast position. Chapter 3 therefore investigates these considerations further in a series of methodological development studies. The results presented in Chapter 3 inform the procedures used throughout the remainder of the thesis.

Having established methodologies for measuring breast position, the next stage of this thesis (chapter 4) focuses on the identification of the neutral breast position, in which there is no external strain on the breast skin. From the review of literature in Chapter 2 and the methodological developments in Chapter 3, a new gold-standard of neutral breast position measurement was proposed using buoyancy in both water and soybean oil. Chapter 4 details the new gold-standard method and presents results demonstrating the effect of gravity on static nipple position.

High financial costs and logistics associated with the new buoyancy method described in Chapter 4 meant that this method may not be feasible for use in regular laboratory testing. Chapter 5 explores several alternative methods for achieving the neutral breast

position. The alternative methods were evaluated on their theoretical underpinning, practicality within a laboratory, and accuracy and precision for predicting the neutral nipple position obtained using the gold-standard buoyancy method.

One application of the neutral breast position identified in Chapter 4 is the evaluation of breast motion relative to the optimum (neutral) breast position. Consequently, Chapter 6 evaluates breast motion during treadmill activity using measurements of maximum nipple displacement from the neutral nipple position, and compares the results to measurements of breast ROM attained using previously published methods. Based on literature identified in Chapter 2, it was anticipated that measures of maximum nipple displacement from the neutral nipple position would provide a better predictor of breast pain than nipple ROM. Therefore, Chapter 6 also investigates the relationships between breast pain and breast motion, calculated using both nipple ROM and maximum nipple displacement from the neutral position.

Another important application of the neutral breast position identified in Chapter 4 is the quantification of static and dynamic breast skin strain, due to the consequent risk of breast damage (ptosis). Chapter 7 provides an assessment of the neutral breast position using the new buoyancy method (Chapter 4) with a marker array placed over the breast. The subsequent deformations of the marker array in the static gravity-loaded position, and during dynamic treadmill activity, were used to calculate static and dynamic breast strain across the surface of the breast. Resulting magnitudes of breast skin strain were compared to reported failure limits for human skin to provide an assessment of the risk of breast skin damage associated with static and dynamic activities.

One participant's static and dynamic data are combined in Chapter 8 to demonstrate the gravity- and motion-induced effects on breast position. Data presented in this chapter also demonstrate that breast skin strains calculated using the marker array reflect and enhance the breast deformation data obtained using a single marker on the nipple in both the static and dynamic conditions. Finally, Chapter 9 provides a discussion and conclusion of the findings within the thesis. The applications of the results are discussed and recommendations are made for future research.

2. Literature review and justification of the thesis methods

2.1. Introduction

This thesis focuses on the identification of the neutral breast position and its application to measurements of breast motion and breast skin strain. This chapter provides justification for the methods implemented within this thesis by reviewing existing research findings and methodologies within breast biomechanics and other research areas associated with the thesis aims. Specifically, this chapter focuses on the following five topics: (2.2) The neutral breast position; (2.3) Assessing breast position and breast motion; (2.4) Breast strain; (2.5) Breast pain; (2.6) Evaluating the accuracy and precision of experimental methods.

2.2. The neutral breast position

The breast is positioned over the pectoralis major muscle and usually extends from the level of the second rib to the level of the sixth rib anteriorly (Gefen & Dilmoney, 2007). The breast is predominantly composed of fat and glandular tissue (Hassiotou & Geddes, 2012). The size and shape of the breast varies between women and also over time within the same woman due to the menstrual cycle, pregnancy, and during menopause (Azar *et al.*, 2002). The anatomical support for the breast is predominantly provided by the skin and the Cooper's ligaments (Mason *et al.*, 1999) (Figure 2.1). The skin has been reported to provide the primary support to the breast (Hindle, 1991), while limited internal breast support is provided by thin sheets of fibrous tissue called Cooper's ligaments (Lemaine & Simmons, 2013; Page & Steele, 1999). The work within this thesis will focus on attaining the neutral position of the breast skin, as the orientation and physical properties of the Cooper's ligaments are poorly understood making it difficult to counteract the effect of gravity on these structures (Gefen & Dilmoney, 2007).

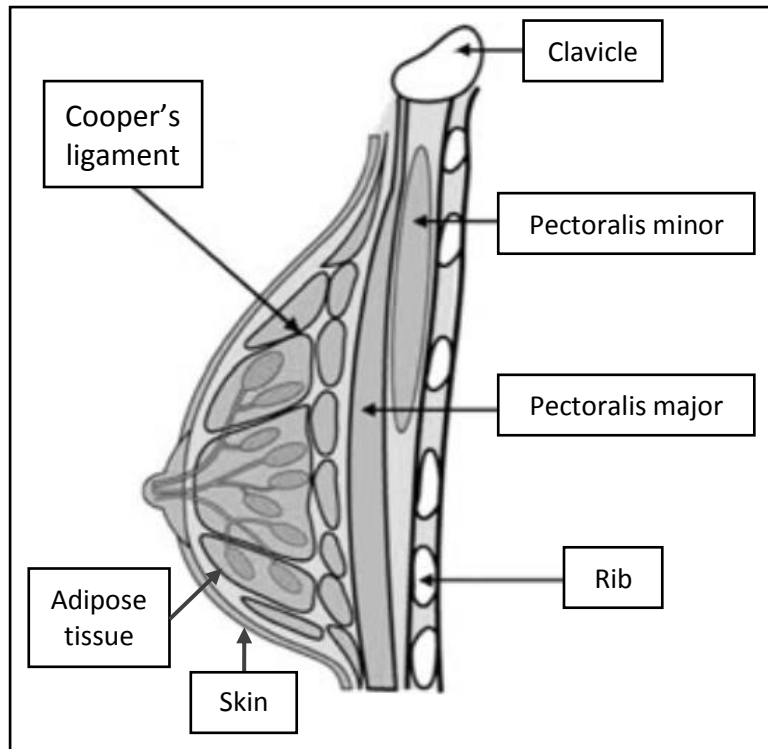


Figure 2.1: Breast anatomy (Haake & Scurr, 2010).

The neutral breast position was defined, for the purpose of this research, as the position of the breast in which there is no external strain on the breast skin. This position is referred to as the neutral breast (or nipple) position throughout this document although other authors have used the term 'stress-free', 'non-loaded', 'un-deflected' or 'zero-gravity' position of the breast (Haake & Scurr, 2011; Rajagopal *et al.*, 2008; Zain-UI-Abdein *et al.*, 2013).

The static breast position may not necessarily correspond to the neutral breast position due to the effect of gravity acting at the centre of breast mass and the reaction force acting through the contact points between the breast and the torso (Figure 2.2). These misaligned forces cause a pre-existing strain on the breast skin which may influence subsequent measures of breast motion or strain if the neutral position is not accounted for.



Figure 2.2: Misalignment of gravity and the ground reaction force acting on the breast.

The neutral breast position is a relatively new concept within breast research and as such there is a paucity of literature on this topic. There have been only four previous attempts to identify the neutral breast position. Two breast motion studies implemented a breast drop method (Haake *et al.*, 2012; Haake & Scurr, 2011), and two clinical studies used the effect of buoyancy in water (Rajagopal *et al.*, 2008; Zain-Ul-Abdein *et al.*, 2013).

The breast drop method aimed to identify the neutral position of the nipple by considering the effect of gravitational acceleration during free-fall on the supporting structures of the breast. It was assumed that if the breast was supported superiorly to its natural position then, upon release, the nipple would accelerate inferiorly with gravitational acceleration until the point just before the skin and supporting structures acted to slow it down. By recording the nipple displacement during free-fall using an optoelectronic camera system it was possible to derive nipple acceleration and to identify the position of the nipple at the latest time point where nipple acceleration was still equal to gravitational acceleration. This position was identified as the neutral nipple position (Haake & Scurr, 2011). The breast drop method was implemented in two separate studies, both with the intention of calculating breast strain during dynamic activity. However, there was no published validation procedure supporting the use of the breast drop technique for attaining the neutral nipple position. Consequently there are several

considerations regarding the theoretical underpinning, the practical implementation, and the analysis techniques associated with the breast drop method. Firstly, only the superior-inferior displacement of the nipple was considered during the breast drop. Evidence demonstrates that gravity causes the nipple to move inferiorly and laterally on the torso over time (Brown, Ringrose, Hyland, Cole, & Brotherston, 1999), suggesting that the nipple may also accelerate in multiple directions during free-fall. Isolation of inferior nipple acceleration may therefore lead to errors when predicting the neutral nipple position. Secondly, Haake *et al.* selected to use the standard gravitational acceleration value ($g = -9.81 \text{ m.s}^{-2}$) as the acceleration criteria for identification the neutral nipple position. However, nipple acceleration was calculated in the local co-ordinate system of the torso and not in the global co-ordinate system of the laboratory (Scurr, White, & Hedger, 2009). Failure to resolve the gravitational force into the torso co-ordinate system may have compromised the accuracy of the inferior breast acceleration criteria as the orientation of the torso during the breast drop was not accounted for. One final consideration of the breast drop method was the use of a single marker at the nipple to represent the breast. Only the displacement and acceleration of the nipple was recorded at each point in time, limiting this method to the identification of the neutral nipple position and not the neutral position or shape of the breast as a whole.

Considering the practical application of the breast drop method, there are many variable factors which may have produced inaccuracies in the resulting neutral nipple position estimate (such as participant breast drop technique, initial breast height, underlying muscle activity, force-extension properties of the breast, and the internal and external forces during free-fall). Haake *et al.* provide limited discussion regarding standardisation of breast drop technique which may have reduced the variability associated with this method. Finally, the use of differentiation to calculate acceleration from displacement data has been shown to produce large errors when compared to accelerometer values (Robertson, Caldwell, Hamill, Kamen, & Whittle, 2004). As the breast drop method relies on acceleration data to determine the neutral nipple position, errors in derived acceleration values may produce inaccurate estimates of the neutral nipple position.

The buoyancy method for measuring the neutral breast position is based on Archimedes' principle, asserting that an object immersed in a fluid of equal density would remain suspended in its equilibrium position (Heath, 1897). Application of this principle to the breast suggests that the static three-dimensional neutral position could be achieved by immersing the breast in a fluid of equal density to the breast tissue. The first study implementing the buoyancy method used water to support the breast while magnetic resonance images (MRI) recorded the breast position. This approach has several advantages over the breast drop method. Primarily, buoyancy is an established scientific concept and its effects have been implemented for a wide range of applications (Robens, Gast, & Straube, 1989; Turner, 1979), including the simulation of zero-gravity environments (Akin & Howard, 1992; Kowalski, 1989; Newman, 1993), giving credence to the use of this method for supporting the breast in its neutral position. Secondly, the support provided by the water over the breast surface allows the breast to be held statically in its three dimensional neutral position, which may provide measurement precision advantages compared to the dynamic breast drop method. Finally, the MRI scanner used in Rajagopal's buoyancy method enabled detailed images of the neutral breast position to be recorded.

Despite the strengths of the buoyancy neutral position method, there are theoretical and practical considerations associated with the manner in which this method was implemented in previous studies. Archimedes' principle for equilibrium between an object and the surrounding fluid requires that the fluid and object densities are equal. Both Rajagopal and Zain-UI-Abdein used water to approximate the density of the breast (Rajagopal *et al.*, 2008; Zain-UI-Abdein *et al.*, 2013). The mass-density of the breast is currently unreported, although the breast's fat content is likely to reduce its density below that of water (Figure 2.3) (Gierach *et al.*, 2011). Immersion of the breast in water may therefore have resulted in compressive breast forces, potentially causing the breast to change position or shape from its neutral position. A more accurate neutral breast position may be attainable by substituting water for an alternative fluid with a density closer to the density of the breast.

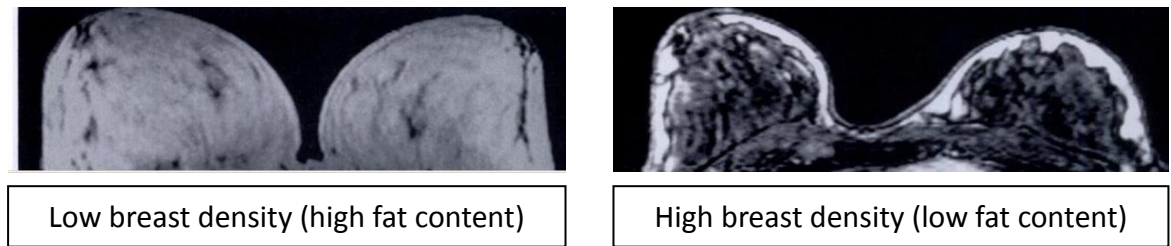


Figure 2.3: Magnetic resonance images of breasts with low and high radiological density demonstrating varying proportions of fat within the breast (Lee *et al.*, 1997).

A second consideration regarding Rajagopal's buoyancy method was the breast-only immersion performed during the measurement of neutral breast position. Isolation of the breasts was achieved while participants lay in the prone position with their breasts suspended in a water bath (Rajagopal *et al.*, 2008). The boundary of the breast tissue on the torso is difficult to define (Nie *et al.*, 2008), and attempts to isolate the breast from the torso may have resulted in incomplete immersion of the breast in water leading to errors in the measured neutral position. Subsequent implementation of the buoyancy method by Zain-UI-Abdein included a full-body immersion in water, eliminating any errors associated with incomplete breast immersion (Zain-UI-Abdein *et al.*, 2013).

The buoyancy method has potential to provide an accurate neutral breast position estimate providing that the density of the breast can be matched to the density of the surrounding fluid, and that the entire breast is immersed. In this case the gravitational force acting on the breast (in all directions) would be cancelled by the buoyancy force from the fluid. However, a small unavoidable error will always be present. In 2010, Gao and Desai identified that the disparity between gravity, acting at the breast centre of mass (COM), and the buoyancy force, acting on the breast surface, would cause the breast skin to be in equilibrium while the internal structures of the breast were still subject to gravitational deformation (Gao & Desai, 2010). Although this is a valid concern, identification of the neutral position of the breast skin alone was considered sufficient to inform many aspects of breast research.

In addition to the two previously published neutral breast position methods (Haake *et al.*, 2012; Haake & Scurr, 2011; Rajagopal, 2007; Zain-UI-Abdein *et al.*, 2013), the conceptual novelty of the neutral position provides the opportunity to develop alternative methods for attaining this position that have not yet been considered within the literature. Novel methods can be developed from the application of scientific principles to counteract the effect of gravity on the breast. Additional methods could be developed from existing testing protocols, such as treadmill running (Scurr, Galbraith, Hedger, & White, 2007), in which the neutral breast position could conceivably be attained. The work within this thesis provided the opportunity to inform the selection of suitable neutral position methods in future research by evaluating both existing and novel methods on their practicality, accuracy, and precision for measuring the neutral breast position.

The neutral breast position has several applications within biomechanical and clinical breast research, and within breast support design and evaluation. Incorporation of the neutral breast position into strain calculations, illustrated by Haake *et al.* (2013), enables the assessment of both static gravitational breast strain and dynamic motion-induced breast strain during exercise. Combination of static and dynamic breast strain measurements permits application of the strain failure limits for human tissues (such as skin) to the breast (Chandrashekar, Mansouri, Slauterbeck, & Hashemi, 2006; Noyes & Grood, 1976), enabling the risk of strain-induced breast damage to be assessed. Biomechanical assessment of breast motion could also be improved by defining the neutral breast (or nipple) position as a zero-point for measuring breast displacement. Breast displacements from the neutral position could be quantified in six anatomical directions with magnitudes that relate to the strain experienced by the breast skin (zero displacement from the neutral position represents zero skin strain). Measurements of breast motion that relate to breast strain may also correlate more strongly to breast pain than existing breast ROM measurements, as previous studies in other areas of the body have demonstrated links between strain and pain (Hirsch *et al.*, 1960; Quinn *et al.*, 2007).

Within clinical research, FE models can be used to aid the tracking of a particular breast structure from a diagnostic image to the operating table, which may otherwise be problematic due to changes in body orientation or the degree of breast compression

(Samani, Bishop, Yaffe, & Plewes, 2001). Incorporation of the neutral breast position as the reference position for FE breast models has been shown to improve the predictive results compared to models based on the gravity-loaded breast position (Rajagopal *et al.*, 2008).

Biomechanical or clinical developments resulting from consideration of the neutral breast position may inform the future design and evaluation of breast support garments. Current measures of a bra's effectiveness are based on limiting breast ROM, or 'bounce reduction' (Griffin, 2004), irrespective of the direction in which this motion occurs. This ROM method does not allow for the possibility that certain breast motion, which opposes the effect of gravity on the breast, may actually be beneficial due to the reduction in strain on the breast skin. In this context, the neutral position provides an optimum position for the breast inside a support garment in terms of minimising skin strain. A breast support garment that positions the breast in the neutral position and restricts breast motion to within the reversible strain limits of the breast skin may prevent damaging strains on the breast skin, reducing the risk of ptosis and motion-induced breast pain.

Accurate measurements of the neutral breast position could be beneficially incorporated into many areas of breast research, including the assessment of breast motion and breast strain, modelling of the breast, and the understanding of breast pain. Before developing methods to obtain the neutral breast position, it was important to consider any factors that may affect measurements of breast position, breast motion, breast strain, or breast pain.

2.3. Assessing breast position and breast motion

2.3.1. Participant factors

Numerous participant-related factors, such as hormone use; smoking history; alcohol intake; hydration level; cancer history; and education (Gapstur *et al.*, 2003; Graham, Bronskill, Byng, Yaffe, & Boyd, 1996; van Duijnhoven *et al.*, 2005), may influence kinematic breast measurements due to their reported effects on breast composition. Within this programme of work it was particularly important to consider key factors that have previously been shown to influence measurements of either breast motion or skin elasticity. Key factors were identified as: breast size (White, Scurr, & Hedger, 2010); breast symmetry (selection of the right or left breast for measurement) (Mills, Risius, & Scurr, 2014); phase of the menstrual cycle (Wojcinski *et al.*, 2012); age range (Fujimura, Haketa, Hotta, & Kitahara, 2007); and sun (ultraviolet light) exposure (Fisher *et al.*, 1997). Each of these key factors was investigated further to inform the selection of appropriate participants within this thesis.

Breast size

Most existing breast research has focused on women with breast sizes within the core bra sizing range (A to D cup), despite frequent reports that larger-breasted women experience more breast movement, need greater breast support, and experience higher levels of breast pain (Boschma, 1994; Bowles, 2012; Krenzer, Starr, & Branson, 2005; Mason *et al.*, 1999; Scurr, White, & Hedger, 2010; Zhou *et al.*, 2011). One study focusing on large breasted women (D to G cup) reported that the bare-breasted activity typically included in breast motion studies was unfeasible with this breast size due to high levels of breast pain and altered bare-breasted running mechanics (McGhee, Steele, Zealey, & Takacs, 2013). As the methods conducted within this thesis were entirely bare-breasted, it was important to select women who were comfortable performing dynamic movements without external breast support, which may have skewed the participant sample towards the smaller breast sizes.

A second size related factor to consider for this study was the effect of breast size on the neutral breast position. Based on previous literature, it is widely accepted that women with larger breasts have a larger breast mass (approximately 115 g per increase in cup size for 32 and 34 inch under bands) (Turner & Dujon, 2005). This increase in breast mass equates to an approximate increase in gravitational force on the breast of 1.13 N per cup size. It may therefore be expected that a greater change in breast position would occur for larger-breasted participants when counteracting the effects of gravity, due to the greater reduction in resultant force on the breast. Women with a larger breast mass may also have had a larger gravitational force exerted on their breasts for a prolonged period of time. Prolonged loading of biological tissues can cause a permanent extension of the tissue, implying that larger-breasted women may have already overloaded their breast skin, preventing the breast from returning to the correct neutral position during testing (Miller, 2001; Rajagopal *et al.*, 2008). The unknown relationship between breast size and gravitational remodeling of the breast skin made this factor difficult to account for during participant recruitment. Instead, participants with a range of breast sizes were recruited to investigate the accuracy and precision of neutral breast position estimates across a wide participant sample.

Right or left breast – does side matter?

Selecting only one side of the body for biomechanical measurement can have several advantages in terms of laboratory set up (all cameras or sensors can be placed on one side) and in terms of reducing testing and analysis time. This is a widely adopted practise in many areas including breast biomechanics, where several studies have reported no differences between measurements of the right and left breasts (Brown *et al.*, 1999; Chen *et al.*, 2012; McGhee *et al.*, 2007).

The breast is a variable tissue and is known to fluctuate regularly in volume (Hussain, Roberts, Whitehouse, García-Fiñana, & Percy, 1999), density (Chan *et al.*, 2011) and sensitivity (Robinson & Short, 1977) in response to changing hormone levels during the menstrual cycle. There is also evidence to suggest that most women have some degree

of breast asymmetry which itself fluctuates over the menstrual cycle (Fotouh, 2006; Manning, Scutt, Whitehouse, Leinster, & Walton, 1996). This oscillatory behaviour of the breast suggests that there is likely to be some degree of asymmetry between the breasts of any one individual at a particular time. It is possible that studies reporting no size differences between the right and left breast may have had equal numbers of women with counter-laterally larger breasts, meaning that any discrepancies were lost when presenting group mean values. This hypothesis is supported by research demonstrating that either the right or left breast can be larger for individual women at a particular time point (Hussain *et al.*, 1999). Although either breast can be larger for an individual, several studies have reported a general bias towards the left breast being larger on average (Losken, Fishman, Denson, Moyer, & Carlson, 2005; Manning, Scutt, Whitehouse, & Leinster, 1997; Page & Steele, 1999; Parmar, West, Pathak, Nelson, & Martin, 2011; Scutt, Lancaster, & Manning, 2006; Senie *et al.*, 1980; Shepherd *et al.*, 2008).

The bias towards a larger left breast should be considered when selecting a single breast to assess breast motion or breast pain. The larger breast may be expected to undergo more motion during exercise and exert larger forces on the torso. Therefore dynamic measurements of the left breast may produce stronger correlations to motion-induced breast pain than if the right breast had been selected for measurement (Mills, Risius, *et al.*, 2014). It has also been reported that skin on the left side of the body is significantly more elastic and able to return to its original shape following deformation (Smalls, Wickett, & Visscher, 2006). The left breast is therefore more likely to return quickly to its neutral position upon the counteraction of gravity.

Phase of the menstrual cycle

The menstrual cycle can be divided into the follicular (days 0 to 15) and luteal (days 16 to 28) stages, where day 0 represents the onset of menstruation (Ramakrishnan, Khan, & Badve, 2002). Several properties of the breast have been reported to fluctuate over the menstrual cycle. Mammographic density (Baines, 1998), breast volume (Hussain *et al.*, 1999), and breast tenderness (Brahmbhatt, Sattigeri, Shah, Kumar, & Parikh, 2013) have

been shown to increase, whereas breast elasticity has been reported to decrease (Wojcinski *et al.*, 2012) from the follicular to the luteal phases of the menstrual cycle.

Several authors have considered the influence of the menstrual cycle when taking breast measurements, although recommendations for obtaining stable measurements are dependent on the variable of interest. Breast motion and anthropometric studies have reported that the follicular phase is most stable for attaining breast measurements (Avşar, Aygit, Benlier, Top, & Taşkinalp, 2010; Milligan, Mills, & Scurr, 2014), whereas the luteal phase has been recommended for clinical assessment of breast composition (Graham *et al.*, 1996). Due to the number of different experimental methods implemented within this thesis, it was not possible to ensure that all participants were in a particular phase of their menstrual cycle during all data collection sessions. However, the time interval between testing sessions was kept to a minimum to reduce the influence of biological fluctuation on breast measurements.

Age range

Due to the remodelling of the breast that occurs during pregnancy (Hassiotou & Geddes, 2012), several breast related studies have focused on nulliparous women with no history of breast surgery (Ramiao, Martins, & Fernandes, 2013; Scurr, White, *et al.*, 2009; Scurr *et al.*, 2010; Scurr, White, & Hedger, 2011). This stipulation combined with the effect of convenience sampling within universities has resulted in a fairly narrow age range being represented in breast motion research, typically women aged 18 to 30 years (Zhou, 2011). Initial studies into the effect of aging on breast motion and bra requirements have found differences in both movement patterns and bra preferences between older and younger women, suggesting more work is required in this research area (Risius, Thelwell, Wagstaff, & Scurr, 2012, 2014).

The nature of this particular study requires the breast tissue to be as elastic as possible to ensure that the breast returns to its neutral position upon the removal of resultant forces. Age is a predominant factor affecting the skin's behaviour to external forces (Smalls *et al.*, 2006). It has been reported that skin over the age of 30 years (Fujimura *et*

al., 2007) is less elastic and will take longer to return to its original shape following deformation. These findings meant that an age limit of 30 years was imposed for recruitment of participants for this study.

Sun exposure

Exposure to ultraviolet (UV) radiation is not conventionally considered within breast motion research. However, skin that has been exposed to as little as 5 to 15 minutes of ultraviolet radiation (Fisher *et al.*, 1997) is reported to be less elastic and takes longer to return to its original shape following deformation than skin without UV exposure. Acute changes to the skin following UV exposure can last up to 70 days (Archambeau, Pezner, & Wasserman, 1995). In line with previous studies on human skin, participants were excluded from the neutral position study if they had exposed their breasts to UV radiation within the three months preceding testing (Gambichler, Matip, Moussa, Altmeyer, & Hoffmann, 2006), as this may prevent the breast from returning to its neutral position upon the counteraction of gravity.

Participant factors summary

Based on results from previous literature, women with a range of breast sizes, who were younger than 30 years, and who had not exposed their breasts to UV radiation within the last three months were eligible to participate within this study. All breast measurements were conducted on the left breast. Several methods can be used to obtain static or dynamic breast measurements. It was important to evaluate of these methods to ensure that appropriate breast measurements could be attained throughout this programme of work.

2.3.2. Static breast measurements

Methods for measuring (or modelling) different properties of the breast are briefly reviewed in this section before focusing specifically on static measurements of breast position.

Measuring the breast

Perhaps the most commonly conducted breast measurement is assessment of breast (or bra) size. Traditionally, breast size has been determined using torso and bust measurements taken with a tape measure (Pechter, 2008). The tape measure method is sufficiently simple to be self-administered and is popular in both commercial and scientific sectors (Greenbaum, Heslop, Morris, & Dunn, 2003; McGhee & Steele, 2010b; Wright, 2002). Categorisation of women by breast size using this technique is common practice within breast research, permitting investigation of the links between breast size and breast kinematics; breast pain; musculoskeletal injury (Greenbaum *et al.*, 2003); thoracic pain (Wood, Cameron, & Fitzgerald, 2008); posture (Coltman, McGhee, Riddiford-Harland, & Steele, 2013); anthropometric characteristics (Brown *et al.*, 2012); and diabetes risk (Janiszewski, Saunders, & Ross, 2010). However, studies have shown that single measurements of the torso and bust are insufficient to reflect the variation in breast size and shape among women (Pechter, 2008; Rong, 2006; Zheng, Yu, & Fan, 2007). Research into breast sizing and bra design has demonstrated that a single bra size, determined using the tape measure method, can incorporate a wide range of breast volumes (McGhee & Steele, 2011) and that more complex measurement techniques, such as anthropometric measurements (Zheng *et al.*, 2007) or 3D body scans (Rong, 2006) allow for a more detailed classification of breast sizes and subsequently better bra design (Lee, Hong, Kim, & Ae, 2004). McGhee and Steele (2010) and White and Scurr (2012) both advocate the use of professional bra fitting guidelines, based on five key aspects of bra fit, when assessing breast size (McGhee & Steele, 2010b; White & Scurr, 2012). This approach was implemented within this thesis to enable classification of participants based on breast size.

Breast density has been widely investigated within the literature due to the reported association with breast cancer risk (Maskarinec, Pagano, Lurie, Wilkens, & Kolonel, 2005). Mammography has typically been used to assess breast density using either a visual classification of density or quantitative calculation of the proportion of radiologically dense tissue (glandular tissue) within the breast (Boyd, Lockwood, Byng, Trichler, &

Yaffe, 1998; Ciatto, Visioli, Paci, & Zappa, 2004; Gram *et al.*, 2005; Harvey & Bovbjerg, 2004; Heng *et al.*, 2004; Maskarinec *et al.*, 2005; Ursin, Parisky, Pike, & Spicer, 2001; Vachon *et al.*, 2007). The patient discomfort associated with mammography (Sapir, Patlas, Strano, Hadas-halpern, & Cherny, 2003), combined with doubts over the ability of mammography to accurately assess breast density (Kopans, 2008), have led to the development of alternative tools for assessing breast density, such as MRI (Nie *et al.*, 2008), dual x-ray absorptiometry (DXA) (Shepherd, Kerlikowske, Smith-Bindman, Genant, & Cummings, 2002), and ultrasound or near infrared tomography (Dehghani *et al.*, 2004; Duric *et al.*, 2013). Each of these methods provides detailed information about the proportions of fat and glandular tissue within the breast, but measures of density reported using these methods do not provide mass-density estimates of the breast. The mass and mass-density of the breast are difficult to assess *in vivo*, leading to the widespread approximation of these variables within the literature, with estimated breast mass-density values ranging from 780 kg.m⁻³ (McGhee *et al.*, 2013) to 2250 kg.m⁻³ (Li, Zhang, & Yeung, 2003). The gold-standard method for assessing the neutral breast position (based on the buoyancy method) relies on matching the fluid density to the density of the breast. Further work is therefore required to establish an appropriate mass-density value for breast tissue.

Breast volume has been increasingly assessed within the literature due to the growing popularity of aesthetic and reconstructive breast surgeries, for which breast size (reduction or enhancement), shape and symmetry are typically the main surgical objectives (Farinella, Impoco, Gallo, Spoto, & Catanuto, 2006; Kececi & Sir, 2014; Kim *et al.*, 2007, 2008). Measurements of breast volume (size) are used in both pre-operative and post-operative evaluations to assess the initial need and subsequent outcomes of surgery (Brown *et al.*, 1999; Kececi & Sir, 2014; Kim *et al.*, 2007). Attempts to measure breast volume for clinical applications have included the use of thermoplastic casts (Edsander-Nord, Wickman, & Jurell, 1996); water displacement (Henseler *et al.*, 2011); ultrasound (Malini, O'Brian Smith, & Goldzieher, 1985); MRI (Hussain *et al.*, 1999); mammogram (Katariya, Forrest, & Gravelle, 1974); and 3D body scans (Veitch, Burford, Dench, Dean, & Griffin, 2012). Despite the variety of approaches, accurate measurements of breast volume are difficult to achieve due to the irregular shape of the

breast and the undefined boundary of the breast on the torso (Nie *et al.*, 2008). These factors can result in incorrect estimation of the breast volume due to partial exclusion of the breast tissue, or inclusion of additional non-breast tissue, during measurement (Henseler *et al.*, 2011; Kopans, 2008). The current limitations of breast volume measurements were important to consider when developing the gold-standard neutral breast position method as inaccurate breast volume estimates within the literature may affect calculations of breast mass-density.

Anthropometric breast measurements typically involve assessment of the distances between specific landmarks, such as the suprasternal notch to nipple distance (Avşar *et al.*, 2010). Anthropometric measurements can be taken by hand using a tape measure or callipers (Wheat, Choppin, & Goyal, 2014), or can be obtained using 2D or 3D images (Henseler *et al.*, 2013; Losken, Seify, Denson, Paredes, & Carlson, 2005; Mallucci & Branford, 2012), body scans (Farinella *et al.*, 2006), or even games consoles (Wheat *et al.*, 2014). Anthropometric breast measurements have been used to describe breast shape, aesthetics, disease risk, phenotype quality and reproductive success (Avşar *et al.*, 2010; Manning *et al.*, 1997; Moller, Soler, & Thornhill, 1995). The popularity of anthropometric breast measurements, particularly within a clinical setting, was important to consider when developing the breast measurement methods within this thesis. Implementation of a breast marker set that incorporates marker locations common within anthropometry and biomechanics research may increase the applicability of the neutral breast position within biomechanical and clinical research.

Modelling the breast

Mathematical models of the breast provide an alternative method for predicting static breast measurements and are a popular alternative to physical measurements within surgical research. The highly deformable nature of the breast has been documented to cause problems when tracking breast structures from diagnostic images to the operating table (Azar *et al.*, 2002; Dufaye, Cherouat, & Bachmann, 2013; Samani *et al.*, 2001). Several attempts have been made to model the deformation of the breast caused by external forces to improve the accuracy of mapping between surgical images and physical

locations within the breast. Advances in technology have permitted the development of complex three-dimensional FE models in which the breast volume is segmented into very small sections, each with its own mechanical properties and boundary conditions (Azar *et al.*, 2002). The accuracy of these models has been questioned due to the largely unknown physical properties of the breast (Azar *et al.*, 2002; Dufaye *et al.*, 2013; Samani *et al.*, 2001; Tanner *et al.*, 2006). Studies evaluating FE model accuracy have compared modelled locations of markers to the locations obtained with medical images under varying degrees of compression. Results demonstrate errors in position prediction ranging from 3.4 mm to 12.4 mm (Tanner *et al.*, 2006), with locations on the breast skin proving particularly difficult to predict (Azar *et al.*, 2002). The development of computer models with more detailed constraints on the component structures of the breast may ultimately improve prediction of breast deformation due to static or dynamic forces. However, due to the current limitations of breast models, a physical measurement of the breast in its neutral position remains the gold-standard method, against which the accuracy of FE models can be assessed (Rajagopal *et al.*, 2008).

Aside from complex FE analysis, the breast can also be modelled by considering the mechanical behaviour of its component structures, or by using optimisation based on experimental data. In 2007 Gefen and Dilmoney approximated the force on each of the breast's component structures (ligaments, glandular tissue, adipose tissue, and skin) during different body orientations and dynamic activities (Gefen & Dilmoney, 2007). Results indicated that the soft tissue structure within the breast that experienced the highest loading forces, during both during static and dynamic activity, were the Cooper's ligaments. However, it was acknowledged that these findings provided only a first approximation to the forces exerted on the breast due to the lack of experimental data on the physical properties of each component tissue. In 2010, an optimised breast model was created by Haake and Scurr based on comparison to experimental data. Subsequently the model was used to predict the motion of the breast under different conditions (altered stiffness and mass) (Haake & Scurr, 2010). This study demonstrated that models can be used to recreate an observed breast movement pattern, although the predicted outcomes for different scenarios were not assessed for accuracy.

Existing research on breast models has focused on developing models to recreate experimentally obtained data. The available data on the biological components of the breast structure are not yet sufficient to produce predictive models without the need for physical testing. Therefore, this thesis focused on the development of an accurate physical method for quantifying breast position.

Measuring breast position statically

Callipers and tape measure measurements can be used to take positional measurements of the breast (specifically the relative location of one point to another). Manual measurement of nipple position relative to the suprasternal notch is commonly implemented in clinical situations (Hansson, Manjer, & Ringberg, 2014). This simple manual measurement is usually quick to perform, easy to interpret, and can be conducted in a wide range of environments. The long-established nature of manual measurement methods also provides a wealth of existing data which may be particularly beneficial in clinical research aiming to distinguish between 'normal' and 'abnormal' measurement values (Brown *et al.*, 1999). Despite their advantages, many authors have identified high variability in manual measurements, with even highly trained individuals reporting different measurement values (Hansson *et al.*, 2014; Nagy *et al.*, 2008; Ulijaszek & Kerr, 1999; WHO Multicentre Growth Reference Study Group, 2006). The susceptibility to error may explain the increasing popularity of computerised systems outside of clinical research where individuals may not have the experience necessary to take valid manual measurements. Additional factors to consider with manual measurements is that the procedure quickly becomes complex if more than one breast measurement is required, and that manual measurements cannot be applied to dynamic assessments of breast position (Kim *et al.*, 2008).

Computerised measurement tools, such as 3D body scanners, MRI, digital analysis of 2D or 3D images provide the opportunity to take multiple breast measurements from the same breast image (Inui, Murase, & Tsutsumi, 2012; Mallucci & Branford, 2012; Rajagopal *et al.*, 2008; Rong, 2006). Although these tools are useful for clinical breast assessment and garment design, they are subject to the same limitation as manual measurements in

that they are predominantly intended for measurements of static breast position (Losken, Seify, *et al.*, 2005; Rong, 2006). This thesis aimed to evaluate new and existing neutral position methods, of which at least one is dynamic in nature. Therefore, measurement tools restricted to static assessment of breast position were deemed inappropriate for the aims outlined within this thesis and consideration was given to dynamic measurement methods.

2.3.3. Dynamic breast measurements

Measuring breast position dynamically

There are a range of tools available for taking dynamic measurements of human motion. Systems such as real-time 3D scanning and fluoroscopy provide highly detailed images at a specified frame rate. Real-time 3D scanning involves the repeated 3D imaging of the body to construct a dynamic assessment of body movement (D'Apuzzo, 2012; Rusinkiewicz, Hall-Holt, & Levoy, 2002). Although these devices are touted as 'real-time', currently available systems typically take between 4 and 17 seconds to complete a single 3D scan (D'Apuzzo, 2012), meaning that the measurement frequency is typically less than 0.25 Hz. Considering that Hake's breast drop study demonstrated that the breast underwent at least two oscillations within 0.6 s (Haake & Scurr, 2011), the measurement tool selected for this thesis therefore requires a higher sampling frequency than can currently be achieved with 3D scanners. Fluoroscopy measurements use X-rays to attain repeated images of the skeleton and can have sampling frequencies up to 30 Hz (Tsai, Lu, Kuo, & Lin, 2011). This technique can be useful within biomechanics where skin-mounted markers may not represent the desired motion of the underlying skeleton (Stagni, Fantozzi, Cappello, & Leardini, 2005). However, breast research is primarily concerned with the soft tissue of the breast which does not easily absorb X-rays and therefore is difficult to measure using fluoroscopy (U.S. Department of Health and Human Services, 2014).

This programme of work aimed to firstly assess the neutral position of the breast, and subsequently to incorporate this position into dynamic measurements of breast motion and breast skin strain during treadmill activity. It was therefore desirable that the same measurement tool could be used to assess both static and dynamic breast motion. The assessment of dynamic breast motion during treadmill activity requires a higher sampling frequency and a larger field of view compared to the measurement of static breast position. Video analysis and optoelectronic tracking are two prominent measurement tools that incorporate these features and that have been implemented in a wide variety of breast motion studies (Zhou *et al.*, 2011).

Video analysis typically involves the use of one or more cameras, sampling between 25 and 100 Hz, to film the breast during exercise (Mason *et al.*, 1999; McGhee *et al.*, 2007). Landmarks on the breast and body are identified prior to filming using markers which are later digitised to allow quantification of breast movement relative to the torso (Mason *et al.*, 1999). Video cameras require minimal set up prior to data collection and the video images provide a detailed qualitative record of whole breast deformation during testing. The commercial availability of video cameras also makes them a versatile measurement tool. Specifically, an internal power supply and durable outer casing are two features that allow video cameras to be used in a range of different environments including outside or underwater. Underwater video cameras have been implemented in previous breast research studies (McGhee *et al.*, 2007; Mills, Lomax, Ayres, & Scurr, 2014), and may provide an alternative measurement tool to the MRI used for assessing the neutral breast position in Rajagopal's buoyancy method (Rajagopal, 2007). Video analysis also provides flexibility with marker selection as, unlike optoelectronic systems, it does not rely on a specific marker type. Marker visibility is an important consideration within breast motion studies, particularly when assessing breast motion inside a bra as markers that are not visible through the material prevent distinction between breast and bra motion (Boschma, 1994; Mason *et al.*, 1999). Limitations of video analysis include a compromise between the field of view and sampling frequency; difficulties with low light levels; large file sizes; and time-consuming data analysis (Robertson *et al.*, 2004). Consideration should also be given to the use of video data collection within the field of breast research

as participants may not wish to be filmed bare-breasted and there may be increased ethical concerns regarding access and protection of any video images.

In contrast, automatic optoelectronic camera systems produce anonymous data as only the trajectories of specialised reflective markers are recorded (Robertson *et al.*, 2004). A second major advantage of optoelectronic camera systems is the automatic real-time (4.2 ms delay) reconstruction of 3D marker co-ordinates (Qualisys Motion Capture Systems, 2014). Up to 500 markers can be tracked simultaneously within a measurement volume that is restricted only by the number of cameras included within the system (Richards, 1999). These features allow dynamic movements to be assessed over a long period of time with minimal increases in analysis time, a substantial advantage over video data which must be digitised on a frame by frame basis to obtain quantitative data (Payton, 2008). The spatial and temporal flexibility of optoelectronic systems enabled development of a range of novel neutral position methods within this thesis with minimal data collection restrictions.

Optoelectronic camera systems have been frequently implemented for breast motion research, with systems typically consisting of between five and eight synchronised optoelectronic cameras (Scurr, Galbraith, Hedger, *et al.*, 2007; Scurr, White, & Hedger, 2011) sampling at frequencies between 100 and 250 Hz (Bennett, 2009; White, Scurr, & Smith, 2009). The majority of existing breast motion research, including the breast drop neutral position method, has used a single marker on the nipple when assessing breast motion. The assessment of breast skin strain within this thesis requires multiple markers to be applied to the breast to enable a better approximation of the breast's curved surface. Additional breast markers may necessitate the use of additional cameras to ensure that all markers are tracked correctly during dynamic activity (Van Bogart, 2000). Occlusion of markers during optoelectronic data collection results in a permanent loss of data and constitutes a primary limitation of these systems. It is therefore important to select marker locations which will not be obstructed during dynamic activity (Scurr, White, *et al.*, 2009). The risk of data loss resulting from marker obstruction may have contributed to the minimal marker sets employed in existing breast movement research, usually consisting of three or four body markers and one breast marker (Zhou, 2011).

Limitations associated with marker based motion capture systems have led to the development of several alternative non-visual motion tracking technologies. Inertial measurement units are a popular alternative system for the 3D tracking of human motion (Lee *et al.*, 2012). These units combine data from a tri-axial accelerometer, a tri-axial gyroscope and possibly a tri-axial magnetometer to provide translational and rotational tracking of the human body (Chen, Zhou, Zhang, & Ferreiro, 2013; Roetenberg, Luinge, & Slycke, 2013). Inertial measurement units are popular in the film and video game industry due to their unrestricted measurement volume, although currently available systems can be prone to measurement inaccuracies in the presence of metal objects and also require a power source (Chen *et al.*, 2013). Potential problems associated with collecting data around metal objects (such as a treadmill), and the requirement for either obstructive wires or heavy batteries (in each sensor) when using inertial measurement units meant that these were not considered suitable for collecting breast motion data within this thesis. A smaller and lighter alternative technology which has recently been developed uses infrared LEDs and photodiodes to track human motion (Lee *et al.*, 2012). However, the current tracking errors (3.3 cm and 3.6°) associated with the LED system also make it unsuitable for use within this thesis (Lee *et al.*, 2012). Highly precise electromagnetic tracking systems do currently exist (with tracking errors of 0.8 mm and 0.5°), and have been promoted for their possible application within micro-scale surgical procedures) (Nasseri *et al.*, 2012). Unfortunately due to their development within a surgical environment, these systems are currently restricted to measurement volumes that are too small for use in breast motion analysis (maximum recommended sensor-transmitter distance is 51 cm) (Nasseri *et al.*, 2012). Although human motion tracking is a rapidly developing research area, which in the future may provide a superior alternative to video or optoelectronic systems, the currently available technologies were not considered appropriate for the measurements required within this thesis.

The requirement for dynamic breast measurement for both neutral position measurement and the subsequent displacement and strain analysis, excludes the use of MRI, body scanners or manual measurements for use within this thesis. Video or optoelectronic measurements could both be used to achieve the aims of this research,

with optoelectronic capture providing longer-duration dynamic measurements and video capture providing a measurement option for methods requiring immersion in fluid. Both of these measurement methods employ markers to identify specific locations on the body. It is therefore important to establish the most appropriate marker set for assessing breast position.

Marker sets

The use of markers has been demonstrated to improve the accuracy and precision of anatomical measurements compared to the same measurement taken from a non-marked participant (Weinberg, Scott, Neiswanger, Brandon, & Marazita, 2004). The application of markers is particularly important for breast measurements because the variable structure of the breast and lack of innate anatomical landmarks (aside from the nipple) make it difficult to consistently identify the same location over repeated measurements (Farinella *et al.*, 2006).

Types of markers

A wide variety of techniques are used to mark locations on the human body, examples of markers include fluorescent, skin-mounted, bone-mounted, semi-permanent henna and permanent tattoo markers (Cappozzo, Della Croce, Leardini, & Chiari, 2005; Chuang & Gilchrest, 2012; Griffiths & Murphy, 2012; Leardini, Chiari, Della Croce, & Cappozzo, 2005; Vassileva & Hristakieva, 2007; Zhu & Zhou, 2004). Markers can be used for identifying particular joints, segments or landmarks; taking anatomical measurements; or for tracking human motion (Robertson *et al.*, 2004).

Optoelectronic and video measurement tools require the use of easily visible surface-mounted markers. Surface-mounted markers can broadly be classified as active or passive markers (Van Bogart, 2000). Active markers emit a signal (such as electromagnetic radiation) to a recording device, and passive markers are inert devices that provide contrast to the surrounding environment allowing them to be recognised during the measurement process. In a controlled laboratory environment, passive

markers are generally preferred because their light weight and independence from external power sources mean that they cause minimal interference to the participant during dynamic activities (Van Bogart, 2000). Optoelectronic camera systems require the use of specially designed retro-reflective markers (Qualisys Motion Capture Systems, 2008), whereas video cameras can be used with a variety of marker types such as adhesive tape, eyeliner or LEDs (Mason *et al.*, 1999; Mills, Lomax, *et al.*, 2014).

Typically within biomechanics, marker locations are selected based on easily recognisable landmarks to minimise inconsistencies in marker placement between sessions, although such landmarks are lacking on the breast surface (Farinella *et al.*, 2006). Within the clinical literature permanent medical tattoos are often used on the breast, enabling patients to undergo long periods of treatment without the need for re-application of skin markers (Rafi, Tunio, Hashmi, & Ahmed, 2009; Rathod, Munshi, & Agarwal, 2012). However, the painful application procedure, permanent visibility, and potential for conflict with social-religious beliefs associated with medical tattooing can cause patient discomfort (Rathod *et al.*, 2012). Surgical pens provide a cheaper, quicker and painless alternative to tattoos (Rafi *et al.*, 2009), but have limited durability (2 to 5 days) resulting in the frequent need for re-application and possible restraint from washing during treatment (Griffiths & Murphy, 2012; Rafi *et al.*, 2009; Rathod *et al.*, 2012; Tatla & Lafferty, 2002). An unconventional, cost-effective, and durable alternative to tattoos and surgical pens is the use of henna as a semi-permanent skin marker (Griffiths & Murphy, 2012; Rathod *et al.*, 2012; Wurstbauer, Sedlmayer, & Kogelnik, 2001). Henna markers can remain visible for up to 48 days without the requirement for patients to alter their normal daily activities (Wurstbauer *et al.*, 2001), although the time taken for the henna application process may be a deterrent for the use of henna within research or clinical environments (Rafi *et al.*, 2009).

Passive retro-reflective markers were selected for use within this thesis, with their locations marked semi-permanently on participants using henna. Within this thesis, breast position and breast motion were assessed relative to the torso (or reference segment), necessitating the placement of markers on both the body and the breast.

Breast and torso marker locations were evaluated to ensure relative breast position could be calculated consistently in static and dynamic conditions.

Marker locations - reference markers

Recommendations for reference marker locations suggest that at least three non-collinear markers should be placed on a rigid segment of the body in locations that are easily identifiable across individuals (Leardini *et al.*, 2005; Williams, Schmidt, Disselhorst-Klug, & Rau, 2006; Zhou *et al.*, 2011). As the breast overlies the ribcage, reference markers should be restricted to this segment and not placed on adjacent segments such as the pelvis, collar bone or shoulder that may move independently (Zhou, 2011). In a review of methodologies within breast motion studies, Zhou suggested that the marker set proposed by Scurr *et al.* in 2010 (the suprasternal notch and the left and right anterior-inferior aspects of the 10th ribs) represented a stable reference frame for assessing relative breast motion (Scurr *et al.*, 2010; Zhou *et al.*, 2011). However, subsequent research has demonstrated that markers placed on the ribs can decrease the stability of the reference segment due to high levels of marker movement caused by both breathing and relative soft tissue movement in this location (Mills, Loveridge, Milligan, Risius, & Scurr, 2014a; Whittingham, Roberts, Weir, Caine, & Forrester, 2012).

Defining an optimum reference segment for use within breast research is an ongoing challenge and a variety of existing reference systems are currently in use (Figure 2.4) (Whittingham *et al.*, 2012; Zhou *et al.*, 2011; Zhou, 2011). Interestingly, the most stable marker set, recommended by the International Society of Biomechanics (ISB), for representing torso movement (Wu *et al.*, 2005) has rarely been utilised within breast movement studies due to problems with marker obstruction caused by breast support garments (Figure 2.4) (Mills, Loveridge, *et al.*, 2014a). Existing literature presents inconclusive findings regarding the most appropriate reference marker locations for use in breast research. It was therefore important to conduct further work within this thesis to establish a suitable reference marker set before attempting to measure the neutral breast position.

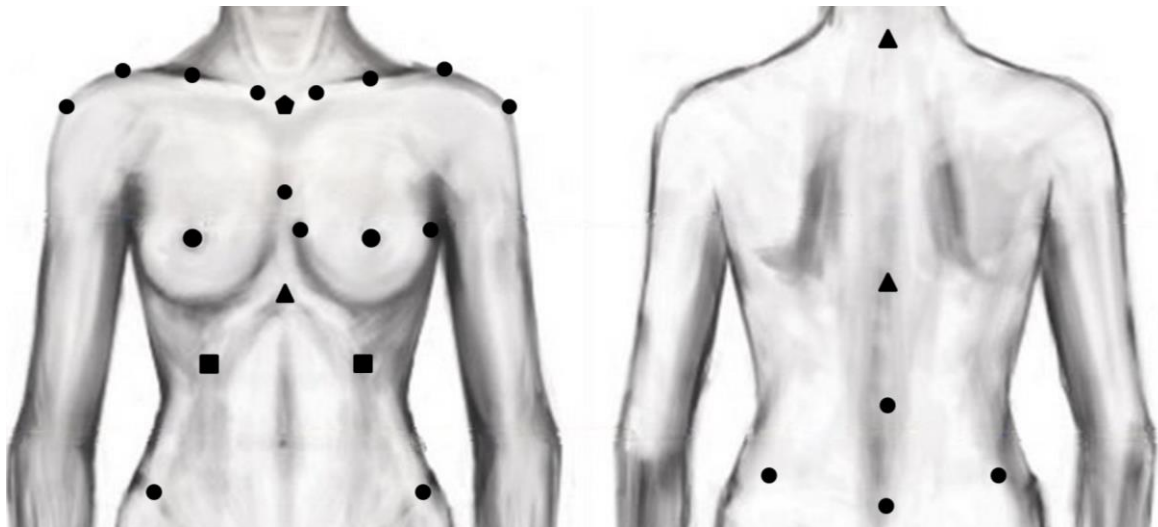


Figure 2.4: International Society of Biomechanics recommended marker placement for the torso (triangles and pentagon) (Wu *et al.*, 2005), and recommended breast motion torso markers (squares and pentagon) (Zhou *et al.*, 2011), compared to torso markers used in previous breast motion studies (circles and pentagon) (Haake & Scurr, 2010; Scurr, Galbraith, Hedger, *et al.*, 2007; Whittingham *et al.*, 2012; Zhou *et al.*, 2011; Zhou, Yu, & Ng, 2012b).

Marker locations - breast markers

As the breast contains only one easily identifiable landmark, it is not surprising that the nipple has been the prominent choice of marker location in previous breast motion research (Zhou *et al.*, 2011). Many studies have selected only the nipple marker to represent gross breast motion as this marker has been reported to experience maximum displacements during exercise when compared to markers on other breast locations (Chen, Wang, & Jiang, 2012; Zhou, Yu, Ng, & Hale, 2009). Additional markers have been included in some studies to enable more detailed analysis of breast deformation during exercise (Chen *et al.*, 2013; Zhou *et al.*, 2009); to reflect markers used in bra design (Ying, Wang, Liu, & Zhang, 2011); or for consistency with anthropometric or clinical measurements (Brown *et al.*, 1999; Rong, 2006; Veitch *et al.*, 2012; Wheat *et al.*, 2014) (Figure 2.5).

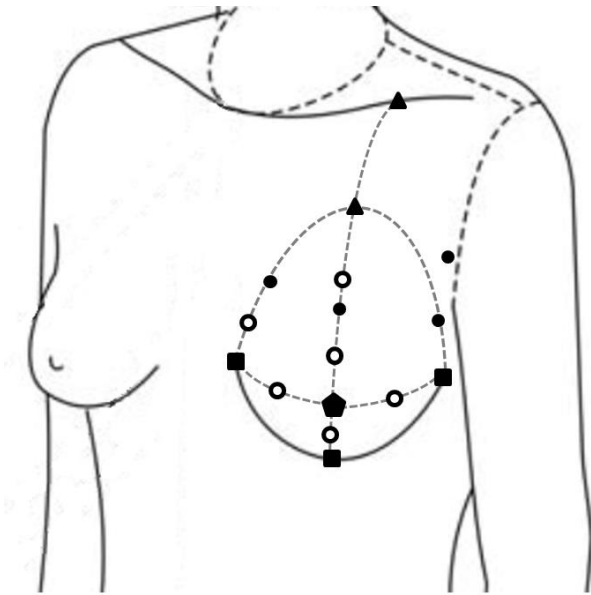


Figure 2.5: Breast marker placement on the nipple (pentagon) (Zhou *et al.*, 2011), and additional breast markers that have been used for assessing breast motion (white circles) (Chen *et al.*, 2012; Zhou *et al.*, 2009); breast position (black circles and squares) (Brown *et al.*, 1999; Rong, 2006; Veitch *et al.*, 2012; Wheat *et al.*, 2014); and garment design (triangles and squares) (Ying *et al.*, 2011). Dotted lines illustrate the four quadrants of the breast and the superior breast boundary.

The application of additional markers to the breast provides more detailed information about static breast shape and dynamic breast motion compared to data obtained using a single nipple marker. Multiple breast markers are particularly important for the assessment of strain on the breast skin. More markers, with smaller inter-marker spacing, enable a better approximation of the breast's curved surface and therefore more accurate calculations of skin strain. Currently, a wide discrepancy exists in the number of breast markers employed in biomechanical breast research (up to 6 markers) compared to the high numbers of 'virtual markers' (nodes) incorporated into clinical breast models (up to 5184 markers) (Rajagopal, 2007; Zhou, 2011). Although current data collection and analysis methods for assessing dynamic breast motion do not permit the same level of detail provided by virtual models, there is scope to develop a more extensive marker array for the assessment of breast strain within this thesis than those used in previous breast motion publications.

Marker locations – breast marker arrays

The breast can be divided into four regions centred on the nipple: the upper-inner quadrant; the upper-outer quadrant; the lower-inner quadrant; and the lower-outer quadrant (Figure 2.5) (Lemaine & Simmons, 2013). This division of the breast into regions has been implemented in both clinical and bra design research (Ramiao *et al.*, 2013; Zhou *et al.*, 2012b). A similar division of the breast for biomechanical breast research may aid the application of breast motion results to clinical or garment design developments.

To obtain measurements of breast motion and breast skin strain for each region of the breast during dynamic activity, at least one marker must be used within each region to create a marker array. Due to the hemispherical shape of the breast, once the breast regions have been defined, it is possible to apply either a rectangular (Figure 2.6 a) or conical (Figure 2.6 b) marker array to the breast. Use of a rectangular breast array was demonstrated by Rajagopal in a neutral breast position study using buoyancy in water (Rajagopal, 2007). Sutradhar and Miller illustrated the application of a conical breast array when investigating the properties of breast skin in different regions of the breast (Sutradhar & Miller, 2012).

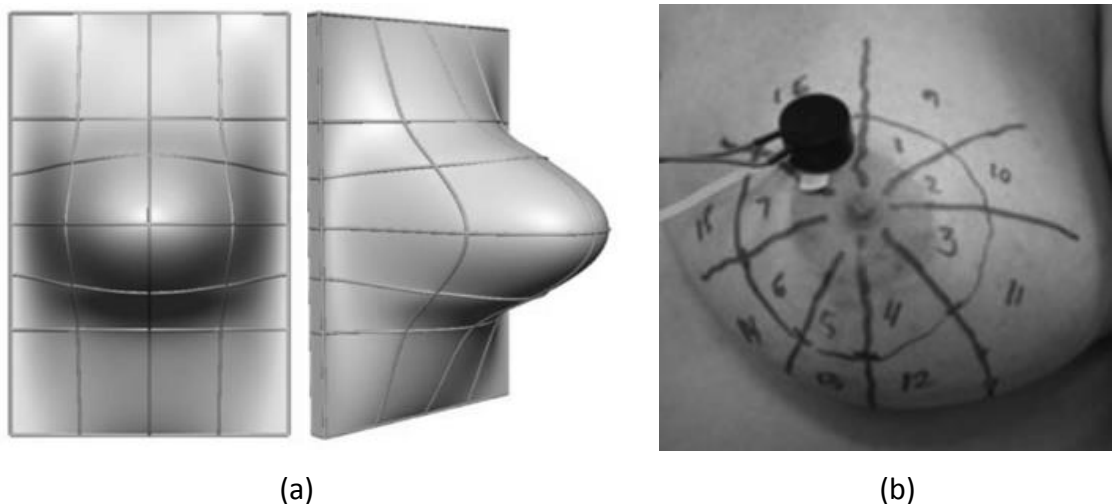


Figure 2.6: The rectangular breast array used in Rajagopal's (2007) neutral breast position study (a) and the conical breast array used by Sutrada (2012) to investigate the properties of breast skin (b).

Due to the limited investigation into the behaviour of different breast regions, there has been no evaluation regarding the most appropriate selection of marker array for the breast, although rectangular arrays are the conventional selection for biomechanical studies investigating soft tissue deformation in other areas of the body (Camomilla, Donati, Stagni, & Cappozzo, 2009; Gao & Zheng, 2008; Leardini *et al.*, 2005; Mills, Scurr, & Wood, 2011; Tsai *et al.*, 2011). Based on the preference towards rectangular arrays within other soft tissue research, a rectangular array was selected for the evaluation of breast strain within this thesis.

Once participant criteria and data collection methods had been determined, it was important to establish appropriate data analysis methods to obtain dynamic breast measurements. Data analysis factors included data filtering and the subsequent calculation method used to quantify the motion of the breast and torso.

Data filtering

During dynamic measurement of human motion using video or optoelectronic camera systems, small errors in marker tracking or digitising can cause high-frequency noise in the resulting positional data. Within biomechanics it is customary to filter the positional co-ordinates of markers to reduce noise before further analysis is conducted. Filtering is particularly important if deriving velocity or acceleration data, as small errors in displacement are magnified during differentiation (Robertson *et al.*, 2004).

There are a number of accepted processes utilised within biomechanics to remove noise, although low-pass Butterworth filters have been the most common technique within breast motion research. Reported cut-off frequencies have ranged from 4 Hz (Mason *et al.*, 1999) to 13 Hz (Mills, Loveridge, *et al.*, 2014a) for breast displacement data collected during treadmill running. When selecting an appropriate cut-off frequency the power spectrum of the signal (Mills, Loveridge, *et al.*, 2014a), the sampling frequency (Yu, Gabriel, Noble, & An, 1999) and the intended data processing methods (Giakas & Baltzopoulos, 1997b) should all be considered. The data analysed within this thesis consists predominantly of displacement data although some of the alternative neutral

position methods also require the derivation of velocity and acceleration. In 1997 Giakas identified that velocity and acceleration data may require different cut-off frequencies to the frequency used for displacement analysis (Giakas & Baltzopoulos, 1997b). To investigate this further Giakas implemented four different filtering techniques when deriving velocity and acceleration data from displacement. Results demonstrated that double filtering of data (*i.e.* filtering displacement and derived data separately) produced large errors in velocity and acceleration and were therefore considered unsuitable methods for processing kinematic data. The most accurate derived data was achieved by filtering displacement data using the optimum velocity/acceleration cut-off frequency (Giakas & Baltzopoulos, 1997b).

Although the Butterworth filter has been popular within breast research studies, there are several alternatives that are commonly implemented in other areas of biomechanical research (Robertson *et al.*, 2004). The accuracies of six different filtering methods applied to video analysis of a gait cycle were assessed in a second study by Giakas and Baltzopoulos (1997a). These methods were: power spectrum analysis (using a Butterworth filter) (PSA); generalised cross validation spline (GCV); least-squares cubic spline (LSCS); regularised Fourier series (RFS); regression model (RM); and residual analysis (RA). Results showed that the RFS, RM and RA filtering methods performed poorly in most derivatives (displacement, velocity and acceleration). Overall the PSA and GCV methods produced the most accurate filtered data, with PSA performing well with displacement and velocity data, and GCV performing well with displacement and acceleration data. These findings justify the use of a Butterworth filter for breast displacement data obtained using treadmill activity. However, considering that some methods presented within this thesis incorporate both displacement and acceleration data and that the GCV filtering method performed well with both these data types, a GCV filter was selected for use within this thesis. Filtered displacement data was then used to quantify breast motion relative to the torso.

Calculation of relative breast motion

Incorporation of the neutral breast (or nipple) position into dynamic measures of breast motion and breast skin strain requires a consistent reference frame to be identified in both the static and dynamic conditions. This is typically achieved using a torso reference segment, which allows the displacement and rotation of the torso to be accounted for when calculating relative breast motion (Scurr, White, *et al.*, 2009; Zhou *et al.*, 2011).

Constructing the torso reference segment

Previous studies that have used a torso reference segment when calculating breast motion have often provided limited details regarding the methods used when constructing their local co-ordinate system (LCS). A recent study by Mills *et al.* found that the order in which reference axis are created during data analyses caused a significant difference in the measured magnitude of relative breast ROM (Mills, Loveridge, *et al.*, 2014a). Mills compared two torso reference segments created using the same data set (the same dynamic trial was duplicated for analysis). The first segment was constructed with a medial-lateral primary axis (Figure 2.7 a) (Scurr *et al.*, 2010), and the second used a superior-inferior primary axis (Figure 2.7 b) (Zhou, Yu, & Ng, 2012a). A significant decrease in superior-inferior relative breast ROM was found during running in a sports bra when using a reference segment with a superior-inferior primary axis. Mills' results illustrate that the construction of the reference segment can affect the measured magnitude of relative breast motion. The ISB specify that a superior-inferior primary axis should be used for reference segments (Wu *et al.*, 2005) as this is anticipated to remain the most stable during dynamic activity (Kontaxis, Cutti, Johnson, & Veeger, 2009). The analysis within this thesis therefore used torso segments constructed with a superior-inferior primary axis.

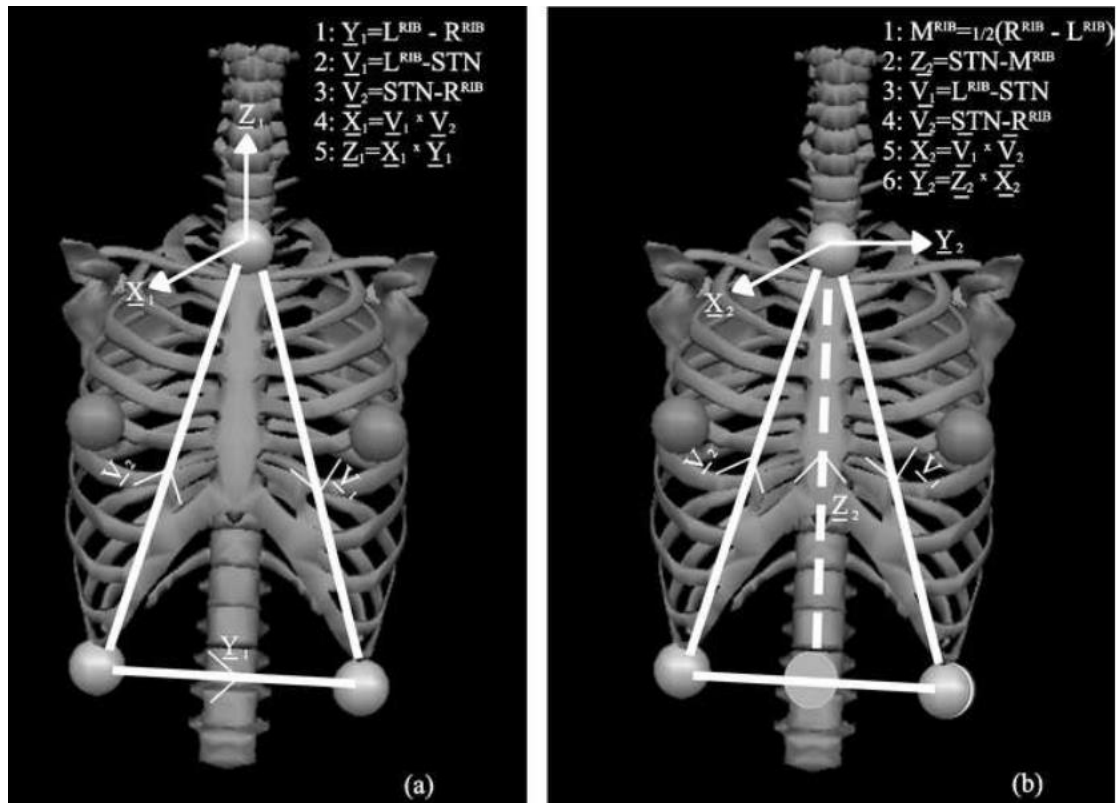


Figure 2.7: Construction of a torso reference frame, using the same torso marker set, defined using a medial-lateral (a) or superior-inferior (b) primary axis (Mills, Loveridge, *et al.*, 2014a).

Further investigation into reference segment stability within breast motion research has demonstrated that torso segments created with the inclusion of rib markers produce smaller measurements of relative breast ROM compared to segments without markers on the ribs (Whittingham *et al.*, 2012). Large amounts of soft tissue motion over the ribs has been suggested to cause inter-marker movement on the torso resulting in segment instability and reduced relative breast motion (Whittingham *et al.*, 2012). As discussed previously, there are limited alternative marker placements on the torso due to obstructions caused by breast support garments, or possibly the breasts themselves in the case of dynamic testing. Position and orientation segment estimation (POSE) calculations can improve the stability of the torso segment created using rib markers within breast research (Mills, Loveridge, Milligan, Risius, & Scurr, 2014b). During POSE calculations the dynamic torso segment is defined using the least squares method to the corresponding static marker locations. The segment length is fixed and any inter-marker movement is classified as error. Although this method eliminates torso segment

deformation, a second problem is introduced. Using the marker set illustrated in Figure 2.7, the POSE estimated torso segment is weighted towards the rib markers. Any soft tissue at the ribs therefore causes a translation of the entire torso segment (including the origin of the LCS) in the direction of soft tissue motion. This problem was identified by Mills although a solution was not discussed (Mills, Loveridge, *et al.*, 2014b). For this thesis in particular it is important to have a stable reference frame and LCS origin when measuring breast motion. Any changes in the LCS of the torso may result in errors when incorporating the static neutral breast position into dynamic measurements of breast motion. Adaptations to published segment construction procedures were therefore investigated in this thesis to evaluate how the effect of soft tissue movement on the LCS origin could be minimised.

Calculating relative breast motion

Once a torso reference frame has been constructed, the co-ordinates of the breast marker(s) can be transformed from the global co-ordinate system (GCS) into the local co-ordinate system (LCS) of the torso (Figure 2.8) (Scurr, White, *et al.*, 2009). The exact calculations involved in the transformation are dictated by the construction of the LCS when creating the torso segment. The position of each marker on the breast can be defined by its displacement along the anterior-posterior, medial-lateral and superior-inferior axes of the torso, as opposed to the x, y and z co-ordinates of the marker in the GCS. Calculation of breast motion in the LCS enables relative breast motion to be assessed, without the influence of torso position or orientation within the laboratory.

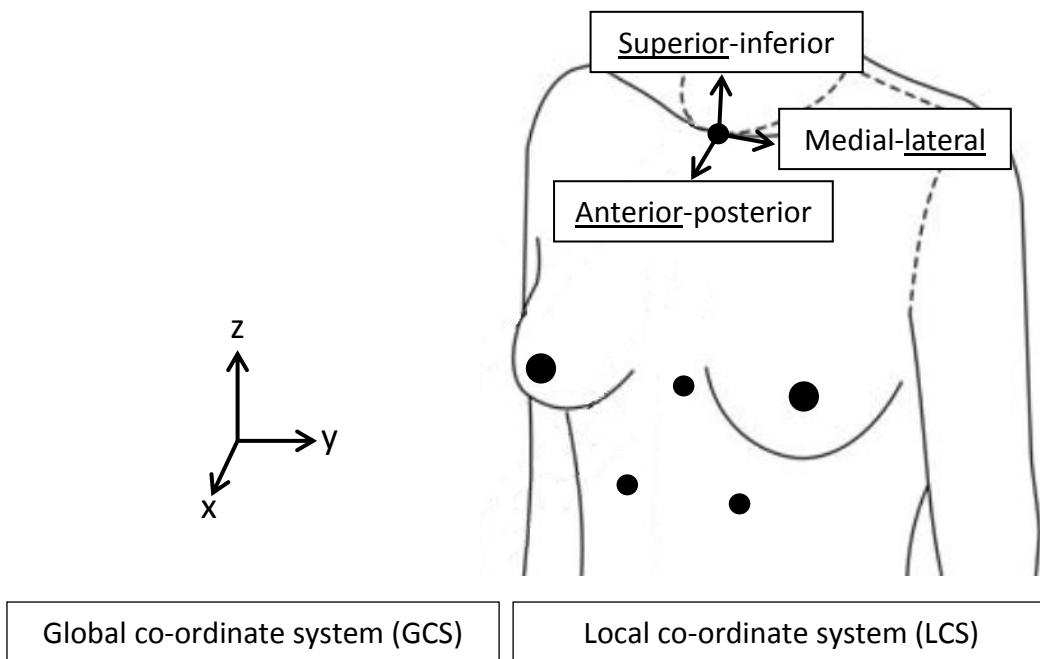


Figure 2.8: Global co-ordinate system of the laboratory (GCS) compared to the local co-ordinate system (LCS) of the torso segment used for calculation of relative breast motion (underline shows the positive direction for each LCS axis).

Reporting relative breast motion

The extent of breast motion that occurs during dynamic activity is a commonly reported variable within breast motion research (Zhou *et al.*, 2011). As the breast is constrained by its attachment points to the torso, dynamic breast motion typically displays a wave-like movement pattern when plotted over time, with the complexity of the corresponding wave equation depending upon on the activity being performed (illustrated by data presented in Campbell's (2007) study on breast motion). There are several scientific terms used to describe properties of waves, and the following are relevant to breast biomechanics (Figure 2.9):

Displacement: A distance from a specified origin in a specified direction. It is the vector equivalent of the scalar distance (adapted from Issaacs, 2009).

Amplitude: the maximum difference of the disturbed quantity from its mean value (Issaacs, 2009).

Peak to peak value: Generally, [for a sinusoidal signal] the peak-to-peak value is twice the amplitude (Issaacs, 2009). (This is often referred to as ROM within biomechanics).

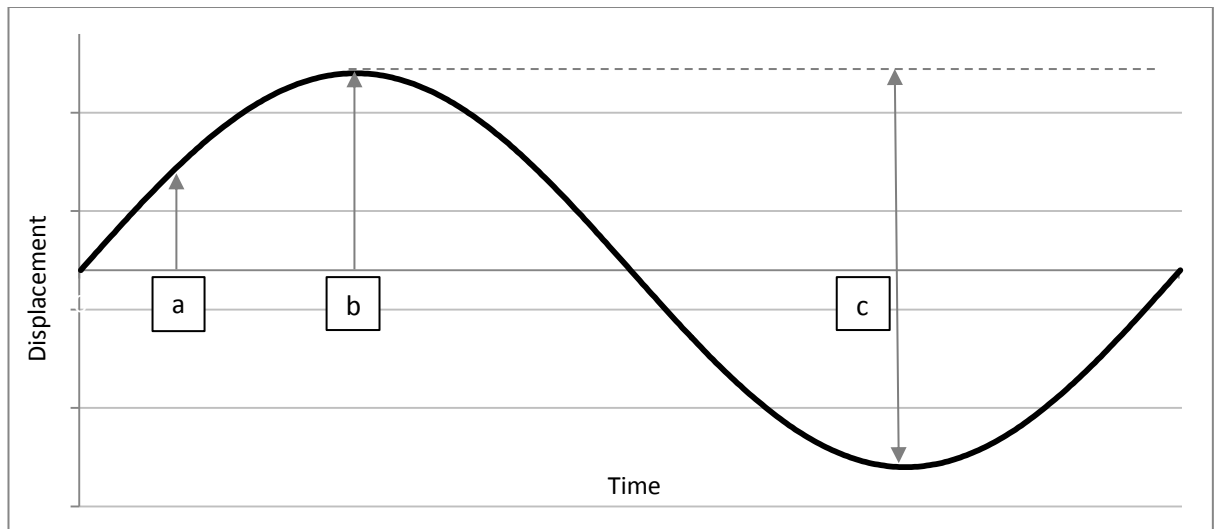


Figure 2.9: Displacement (a), amplitude (b) and peak to peak value (ROM) (c) of example displacement data.

When reviewing published studies within breast biomechanics it became clear that there was some degree of confusion over the terms used to describe breast motion. A large portion of the literature report displacement when referring to the peak to peak (or ROM) value (Boschma, 1994; Bridgman, Scurr, White, Hedger, & Galbraith, 2010; Campbell, Munro, Wallace, & Steele, 2007; McGhee *et al.*, 2013; Scurr *et al.*, 2010; Scurr, White, & Hedger, 2011). One study described their measurements using both displacement and amplitude but did not make it clear which one they had actually calculated, leaving the possibility that they too were referring to ROM (Mason *et al.*, 1999). Only one study, conducted by Zhou *et al.* in 2012, was found to present displacement data (based on the scientific definition of displacement), making the distinction between maximum displacement (how far the breast moved from its original position) and what Zhou referred to as 'range-of-displacement' (peak to peak measurement of displacement) (Zhou *et al.*, 2012b). This confused terminology may lead to difficulties comparing data between studies; and may also cause problems in future if a distinction between breast position (displacement from a defined origin), and motion (ROM) is needed.

One application of the neutral nipple position is its incorporation as the motion origin into measurements of nipple motion during exercise. In this situation, the difference between ROM and displacement is important. Displacement represents the extent of motion away from the neutral position, enabling the distinction between movements that increase the load on the breasts (away from the neutral position) and those that decrease it (towards the neutral position). In contrast, ROM represents the total amount of motion that occurs along a particular axis, with no consideration for the optimum nipple position. From a physics perspective it may be expected that motion-induced breast pain is caused by excessive extension of the breast tissue. Therefore, breast pain should be more strongly correlated to measures of displacement (representing skin extension from the neutral position), than to the magnitude of breast motion (ROM) measured from an undefined or arbitrary position. One aim of this thesis was therefore to investigate whether nipple displacement provided a stronger correlation to breast pain than the existing measures of nipple ROM.

Due to the important distinction between displacement and ROM, and for consistency with other scientific disciplines, the scientific terms for motion analysis were used throughout the document to minimise confusion when interpreting results. The measurements made within this thesis are typically measurements of breast and torso markers taken with video or optoelectronic camera systems. The term 'position' therefore refers to the 3D co-ordinates of a marker; 'displacement' refers to the distance a marker has moved in a specified direction from a specified origin; 'maximum displacement' (amplitude) refers to the maximum distance travelled by a marker in a specified direction from a specified origin; and 'ROM' (peak to peak) refers to the maximum distance travelled by a marker along a specified direction.

Identification of the neutral breast position within this thesis not only has applications to the assessment of breast motion but also enables the assessment of static and dynamic breast skin strain, which has not previously been attempted within the literature. Consequently, there are several factors that should be considered before developing a novel method to quantify strain on the breast skin.

2.4. Breast strain

2.4.1. Measuring breast skin strain

Strain (extension per unit length) is a mechanical variable that is commonly used to evaluate the magnitude and reversibility of a biological tissue's response to external loading (Gao & Desai, 2010; Hull *et al.*, 1996; Lim *et al.*, 2008; Miller, 2001; Toms *et al.*, 2002). In other areas of the body, strain can be assessed using displacement transducers (such as extensometers, liquid metal strain gauges or Hall effect strain gauges) or optical systems (such as photography, visual displacement analysis, or automatic tracking) (Smutz, Drexler, Berglund, Growney, & An, 1996). The breast is classified as a very soft tissue, meaning it is easily distorted by external forces (Gao & Desai, 2010). Optical systems therefore offer an advantage for assessing breast strain as there is minimal contact required for strain measurements to be taken (aside from the application of light-weight markers) (Gao & Desai, 2010).

Measurements of strain are typically used to identify the failure limits of biological tissues (*i.e.* the amount of extension that can occur before the tissue breaks) enabling the risk of damage to be assessed during application of external loads (Chandrashekar *et al.*, 2006; Noyes & Grood, 1976; Provenzano, Heisey, Hayashi, Lakes, & Vanderby Jr., 2002; Quinn *et al.*, 2007). Application of the published failure limits for human skin to measurements of breast skin strain may enable the risk of breast damage (ptosis) to be assessed.

The calculation of strain on the breast skin requires measurements of skin length to be taken in both the loaded (L) and neutral (L_0) conditions (Equation 2.1).

Equation 2.1:
$$\text{Strain} = 100 \cdot \left(\frac{(L - L_0)}{L_0} \right)$$

Constant gravitational loading means that the static breast position does not necessarily correspond to the neutral position of the breast (Figure 2.2). In one study by Scurr *et al.*

in 2009, the static effect of gravity was not considered, and the gravity-loaded breast position was used as the reference state for breast strain calculations. Results demonstrated that larger-breasted women experienced less breast strain than their smaller-breasted counterparts (Scurr, Bridgman, Hedger, & White, 2009). Scurr's counter-intuitive results may have been due to the larger-breasted women having a greater pre-existing static strain on their breast tissue that was not taken into account when attempting to quantify breast strain.

Static breast skin strain caused by gravity acting on the breast can only be quantified by counteracting the effect of gravity on the breast and identifying the neutral breast position. Subsequent extension of the breast skin in static or dynamic conditions can then be combined to calculate total strain on the breast skin. As discussed in section 2.2, Rajagopal (2007) used the buoyant force from water to support the breast in its neutral position. Although Rajagopal did not directly investigate breast strain, results demonstrated a 16.9 mm increase in breast projection in the gravity-loaded prone position compared to the breast immersed in water (Figure 2.10) (Rajagopal, 2007). Using Equation 2.1, a first order approximation of 38% static breast strain can be calculated using Rajagopal's data. This finding supports the idea that gravity causes a measurable static strain on the breast, which if neglected, may cause errors in the assessment of total breast strain and the subsequent relationships between strain, damage and pain.

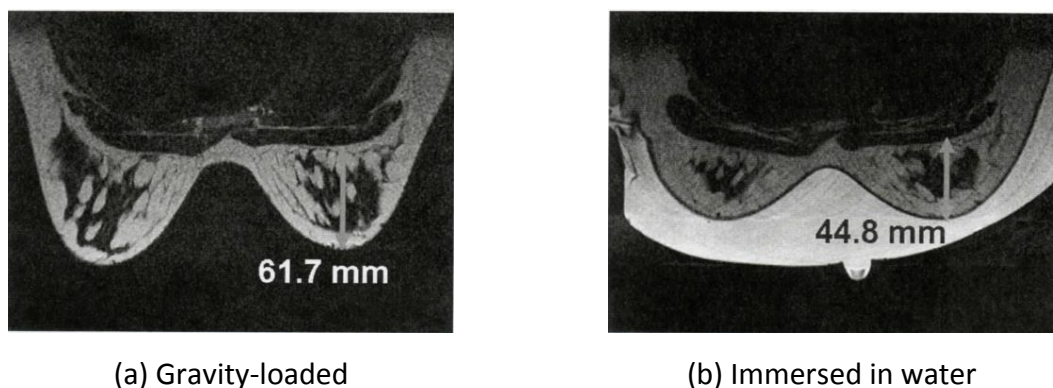


Figure 2.10: MRI scans of the breasts while lying prone in the gravity loaded position (a) and while immersed in water (b) (Rajagopal *et al.*, 2008).

Attempts to counter the effect of gravity using the breast drop method before measuring strain on the breast during treadmill activity were conducted by Haake and Scurr in 2011, and again by Haake *et al.* in 2013. The use of a single nipple marker in the breast drop method meant that the reported strain values may not represent the strain on any particular structure within the breast, but rather the percentage extension of the vector extending through the breast from the suprasternal notch to the nipple. Results indicated that static breast strain increased with increased breast size in the no-bra condition; application of external breast support reduced static strain, particularly for the larger breast sizes; and breast pain during exercise was related to peak dynamic breast strain (Haake *et al.*, 2012; Haake & Scurr, 2011). Each of these findings support the use of breast strain data within breast motion research to inform breast support design and to better understand motion-induced breast pain.

The work within this thesis aimed to improve on the existing measures of static and dynamic strain, firstly by implementing a gold-standard measurement of the neutral breast position, and secondly by using a marker array to provide a better approximation of strain on the breast skin. More accurate assessment of skin strain enables the risk of breast damage caused by static and dynamic loading to be estimated.

2.4.2. Strain as a measure of damage

One of the breast's primary supporting structures is the skin (Hindle, 1991). Human skin exhibits viscoelastic and highly anisotropic mechanical behaviour, which is largely determined by the dermis layer (Daly, 1982; Wu, Thalmann, & Thalmann, 1995). The dermis is mainly composed of collagen fibres (approximately 70% in dry weight), providing strength; and elastin fibres (2 to 4% in dry weight) providing elasticity (Igarashi, Nishino, & Nayar, 2005). In the young adult collagen fibres are loosely interwoven, wavy and randomly orientated, with the fibre density increasing with age (Silver *et al.*, 2001).

The biomechanical properties of the skin vary directionally, regionally, and between individuals (Clark, Cheng, & Leung, 1996; Finlay, 1970). However, existing research has

identified three distinct phases of normal human skin extension (Figure 2.11) (Daly, 1982; Finlay, 1970; Silver *et al.*, 2001; Wu *et al.*, 1995). At low strains the collagen fibres are loosely interwoven and there is little resistance to deformation (phase A in Figure 2.11). At increasing strains the collagen fibres align in the direction of loading and begin to resist extension (phase B in Figure 2.11), until eventually failure occurs (phase C in Figure 2.11) (Daly, 1982). The reported strain values at which each skin extension stage occurs are varied within the literature. Due to ethical considerations associated with testing skin to failure, skin strain data have commonly been obtained from porcine or cadaver skin samples (Gallagher *et al.*, 2012; Winter, 2006). Results from these studies suggest that the onset of skin resistance occurs at strains between 16% and 48% (Stark, 1977), and the onset of skin failure occurs at strains between 16% (Lim, Hong, Chen, & Weerasooriya, 2011) and 126% (Gallagher *et al.*, 2012; Ní Annaidh, Bruyère, Destrade, Gilchrist, & Otténio, 2012). The wide-ranging results presented for the different stages of skin extension may be due to differences in skin sampling techniques, sample preservation procedures, or strain measurement systems. To enable breast skin damage to be estimated within this programme of work it was necessary to define appropriate strain values to represent the onset of skin resistance and skin failure. These strain values were defined as 30% for skin resistance and 60% for skin failure based on the representative strain values for human skin reported by Silver *et al.* (2001).

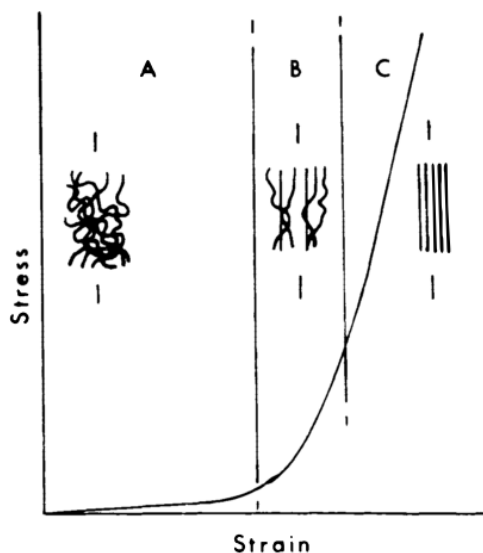


Figure 2.11: Stress-strain curve for human torso skin illustrating the orientation of the collagen network within the skin during each strain phase (Daly, 1982).

The orientation in which strain measurements are taken can influence the stress-strain behaviour of skin. Although the network of collagen fibres within the skin has been described as random within the literature (Daly, 1982; Silver *et al.*, 2001), a slight directional bias was demonstrated by Langer for many different skin sites over the human body (Langer, 1861). Gibson *et al.* (1969) illustrated the directional variation in the skin strain response measured on the (male) chest (Figure 2.12 a), and the effect of measurement orientation on the stress-strain relationship of human skin was later shown by Daly in 1982 (Figure 2.12 b). The lines indicating the direction of increased skin tension are often referred to as Langer lines (Flynn, Taberner, & Nielsen, 2011). The presence of Langer lines in the skin of the breast means that the same magnitude of external stress (force per unit area) may cause differing amounts of skin strain when measured in perpendicular directions. Additionally, the failure limits of the skin may also be different in different directions, for example Figure 2.12 b indicates that human abdomen skin can extend further in the superior-inferior direction than the medial-lateral direction before the onset of skin failure. It is therefore important to evaluate skin strain in perpendicular directions on the breast and to consider how the magnitude of skin strain measured in each direction represents the risk of skin damage on the breast (Carmichael, 2014; Daly, 1982; Gibson, Stark, & Evans, 1969; Ottenio, Tran, Ní Annaidh, Gilchrist, & Bruyère, 2014).

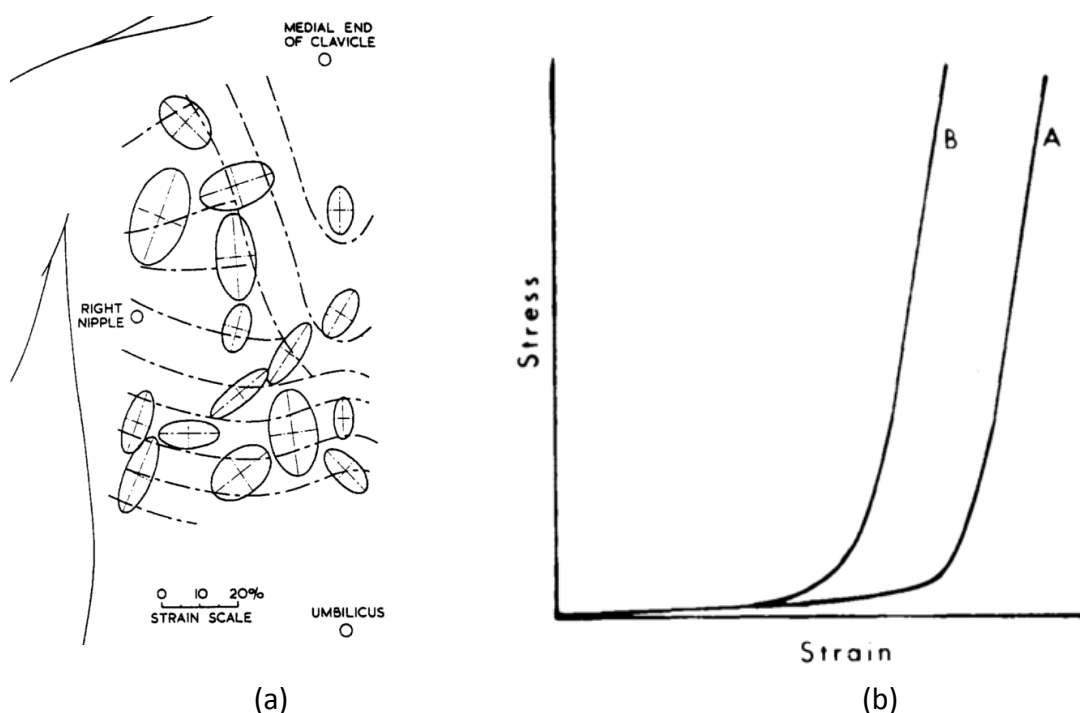


Figure 2.12: Strain ellipses on the (male) human chest (a) (Gibson *et al.*, 1969), and the stress-strain relationship for human abdomen skin measured parallel (A) and perpendicular (B) to the superior-inferior axis (a) (Daly, 1982).

The rate at which human skin is strained can also influence the skin's mechanical behaviour. Results obtained from human back skin have shown that increased strain rates (from 0.06 s^{-1} to 167 s^{-1}) caused an increase in the ultimate tensile strength of skin but did not affect the strain limit at which skin failure occurred (Otténio *et al.*, 2014). The lack of dependence between skin failure limit and strain rate has also been demonstrated in animal studies (Haut, 1989; Vogel, 1972). These results imply that the same failure limits may be applied to measurements of breast skin strain obtained in a range of static or dynamic conditions without the need to control skin strain rate during data collection.

Within this thesis, strain-induced skin damage refers to the small permanent extension that has been reported to occur when biological tissues experience strain above their failure limit (Rigby, Hirai, Spikes, & Eyring, 1959). Elsewhere in the literature, excessive stretching of the skin has been reported to cause additional damage in the form of striae distensae (stretch marks) (Henry, Piérard-Franchimont, Pans, & Piérard, 1997; Hermanns & Piérard, 2006). Despite their name, there is increasing evidence to suggest that stretch

marks are not primarily caused by stretching of the skin (Chang, Agredano, & Kimball, 2004). Instead, the formation of stretch marks are due to an underlying fault in the structure of the skin, caused either by defects in the collagen, elastin, and fibronectin genes (Al-Himdani, Ud-Din, Gilmore, & Bayat, 2014; Chang *et al.*, 2004; Lee, Rho, Jang, Suh, & Song, 1994); altered fibroblast metabolism (Di Lernia, Bonci, Cattania, & Bisighini, 2001; Lee *et al.*, 1994); topical steroid application (Gilmore, Vaughan, Madzvamuse, & Maini, 2012); or hormonal changes (specifically adrenocorticotrophic and cortisol) (Al-Himdani *et al.*, 2014). Consequently, stretch marks are not anticipated to be caused solely by excessive strain on the skin and were not considered to signify strain-induced damage within this thesis. Although the estimation of breast skin damage using measures of strain was a key outcome of the work conducted within this thesis, consideration was also given to the temporary effects associated with non-damaging skin strains below 60%.

2.4.3. Recovery time of the breast

Providing that strain does not exceed the non-reversible limit for a biological tissue, the tissue will eventually return to its pre-strained state. The time taken for this process to occur is termed the recovery time of the tissue (Provenzano, Lakes, Keenan, & Vanderby Jr., 2001). The breast is a complex structure that experiences a constant static strain due to gravity and an additional dynamic strain during exercise. The recovery time of the breast has not yet been studied and most stress-strain studies on other biological tissues have focused on dynamic loading, with only a few considering the effect of prolonged static loading on tissues. Prolonged loading on ligaments has been shown to result in periods of extension lasting up to 24 hours (Chu *et al.*, 2003). Static loading of tendons over a period of 24 hours produced an irreversible rearrangement of the tendon, even at low strain values (Rigby *et al.*, 1959). The viscoelastic behaviour of skin means that permanent skin extension can also occur as a result of extended loading periods (Findley & Davis, 2013). This effect is sometimes referred to as 'creep' and a loading period of only 15 minutes has been shown to produce a significant increase in skin length that persisted for at least one year (Hirshowitz, Kaufman, & Ullman, 1986). Permanent skin extension resulting from creep has been used beneficially within the field of reconstructive surgery when additional tissue length is required (Hirshowitz *et al.*, 1986).

However, prolonged gravitational loading on the skin and ligaments of a healthy breast may result in breast ptosis.

During the data collection aspects of this thesis, dynamic loading of the breast was kept to a minimum and static rest periods were implemented between activities to minimise the effect of prolonged breast extension from one measurement trial affecting the data obtained in the following trials. It was acknowledged that the lifetime exposure to gravity may have caused a pre-existing breast extension for participants, which may have affected measurements of the neutral breast position and the subsequent calculation of breast skin strain.

Demonstration of strain-induced skin damage within the literature could be used to inform the development of breast support garments that protect the breast from ptosis by immobilising the breast in the neutral position. This is a novel concept within garment design and it was important to consider the consequences associated with confining the breast to remain in this neutral position.

2.4.4. Implications of restricting breast motion based on measures of skin strain

Despite mounting evidence recognising the benefits of wearing external breast support (Greenbaum *et al.*, 2003; Mason *et al.*, 1999; Scurr, White, & Hedger, 2011; Wilson & Sellwood, 1976), the prolonged use of tight-fitting garments (such as sports bras) has been linked to several negative health implications. Sustained pressure on the skin (particularly of the torso) has been found to prolong the menstrual cycle (Kikufuji & Tokura, 2002), increase heart rate (Mori, Kioka, & Tokura, 2002), disrupt hormone secretion (Mori *et al.*, 2002), and cause anatomical distortion (Wang, Chen, & Lin, 2011).

Focusing on the direct implications of minimising the effects of external loading on the breast, perhaps the biggest concern is atrophy of the breast tissues. Atrophy of bones and muscles is a well-documented phenomenon that occurs if the tissue becomes disused, or if typical loading is reduced (Belavý *et al.*, 2009; Cavanagh, Licata, & Rice, 2005). It could therefore be suggested that application of external support to the breast

may inhibit the development of the breast's own natural support system (Hunter & Togan, 1985). However, the breast's internal structure is maintained by ligaments and does not contain any bone or muscle. There is limited research on ligament atrophy although it has been documented to occur following bone deformity or prolonged fixation of a joint (Klein, Heiple, Torzilli, Goldberg, & Burstein, 1989; Wright & Schuknecht, 1972). One study investigating atrophy of ligaments in the knee following prolonged periods of disuse, without immobilisation, found that there was no qualitative or quantitative evidence of ligament atrophy, or loss of ligament strength, despite a marked occurrence of bone atrophy (Klein *et al.*, 1989). Klein's findings suggest that ligaments do not weaken if loading is reduced, unless complete restriction of motion is also present.

Results presented within the literature suggest that complete fixation of breast position may cause the natural breast support system to weaken. Therefore, an ideal breast support garment could restrict breast motion sufficiently to prevent overloading of the breast structure, but without rigidly fixing the breast's position against the torso. A garment which supports the breast in the neutral position, and restricts breast motion within the reversible skin limits of the breast skin, may enable the risk of breast damage to be minimised without compromising the natural support system of the breast. Breast support garments that protect the breast from gravitational or dynamic loading may also lead to reduced levels of motion-induced pain, which is reported to affect up to 72% of exercising females (Gehlsen & Albohm, 1980).

2.5. Breast pain

2.5.1. Assessment of breast pain

Individual pain perception is a difficult variable to quantify (Kane, Bershady, Rockwood, Saleh, & Islam, 2005). Pain assessment is important for clinical assessment of a patient's recovery or the effectiveness of a particular intervention, and consequently numerous pain assessment techniques have been reported within the literature. Breast pain can be classified into the following 3 categories: (1) cyclical mastalgia, defined as breast pain associated with the menstrual cycle; (2) non-cyclical mastalgia, defined as constant or

irregular breast pain with no relationship to menstruation; and (3) costochondritis, defined as inflammation of the area of the junction of the rib and cartilage (Maltz *et al.*, 2013).

Evaluation of pain is particularly challenging when aiming to compare pain scores across individuals as experiences of pain cannot be shared among individuals, making it difficult to standardise pain perception using a numeric scale. Non-cyclical breast pain has been widely investigated within the literature. In 2003, Sapir *et al.* produced a summary of 22 different studies assessing breast pain during mammograms. Techniques for quantifying breast pain included 3-, 4-, 5- and 6-point verbal scales; 10-point numeric scales; visual analog scales; brief pain inventories; McGill pain questionnaires; and state-trait and anxiety inventories (Sapir *et al.*, 2003). Comparisons of different pain scales for reporting breast pain during mammography found that validated pain measures, such as visual analog scales or McGill pain questionnaires, resulted in more frequent reports of breast pain compared to pain assessed using non-validated pain measures (Kornguth, Keefe, & Conaway, 1996). This discrepancy suggests that the method used to measure pain can have important implications on breast pain studies.

Assessment of motion-induced breast pain was first proposed by Mason *et al.* in 1999. Mason implemented a 11-point numerical rating scale as a versatile pain measure that could be used in a variety of situations (Mason *et al.*, 1999). This 11-point scale has subsequently been widely implemented within breast motion research (Haake *et al.*, 2012; McGhee *et al.*, 2007; Scurr, Bridgman, *et al.*, 2009; Scurr *et al.*, 2010; Scurr, White, Milligan, Risius, & Hedger, 2011b), and was used to assess motion-induced breast pain within this thesis. As the aim of this thesis was to investigate the effect of incorporating the neutral breast position on the relationships between breast motion and breast pain, it was beneficial to use the same pain assessment scale as previous studies to allow direct comparison of results. However, it was acknowledged that differing individual perceptions of pain may produce inconsistent pain scores across individuals during exercise (Kane *et al.*, 2005).

2.5.2. Relationships between breast motion and breast pain

During physical activity the breast has been reported to move up to 210 mm relative to the torso (Scurr, 2007). For many women this independent motion causes pain (Gehlsen & Albohm, 1980) which can negatively affect their overall health and well-being (Brown *et al.*, 2014; Burnett *et al.*, 2014). The biomechanical investigation into breast motion is therefore motivated by a desire to alleviate excessive breast motion and its negative consequences, particularly during exercise (Hadi, 2000; Page & Steele, 1999; Scurr, White, & Hedger, 2011; Zhou *et al.*, 2011).

Over the past few decades, increasing numbers of studies have been conducted to improve the understanding of breast pain experienced by active females (Haake *et al.*, 2012; Mason *et al.*, 1999; McGhee *et al.*, 2007, 2013; Page & Steele, 1999; Scurr, Galbraith, Wood, & Steele, 2007; Zhou *et al.*, 2011). Generally these studies have involved the quantification of breast kinematic variables and the assessment of breast pain in different breast support conditions during dynamic activity. Kinematic measures of the breast have included ROM, trajectory, extension, velocity, acceleration, and force (McGhee *et al.*, 2013; Milligan *et al.*, 2014; Scurr, White, Milligan, *et al.*, 2011b; Zhou *et al.*, 2011). Results demonstrate that the application of breast support garments can reduce the magnitude of each of these variables and can reduce the breast pain associated with exercise (McGhee, Steele, & Zealey, 2010; Monari, Desloovere, Bar-On, Molenaers, & Jaspers, 2013; Scurr *et al.*, 2010; Steele, 2013).

Attempts to identify specific causes of breast pain using kinematic measures display inconclusive results. Breast ROM (White, Scurr, & Hedger, 2008), breast velocity (McGhee *et al.*, 2007; Scurr *et al.*, 2010), and breast acceleration (Haake *et al.*, 2012) have all been identified as primary factors for motion-induced breast pain. Yet, in similar studies, no relationships were observed between either breast pain and ROM (Mason *et al.*, 1999; McGhee & Steele, 2010a), velocity (McGhee & Steele, 2010a), or acceleration (Scurr *et al.*, 2010). It has been suggested that these conflicting results may be due to inconsistencies within breast motion research (Zhou *et al.*, 2011). Factors such as participant selection, kinematic data collection methods and pain assessment techniques

may all affect the relationships observed between breast motion and breast pain. Strain (or tension) on the breast has also been hypothesised to cause motion-induced breast pain (Mason *et al.*, 1999; Scurr, Bridgman, *et al.*, 2009), although this relationship has not yet been investigated due to the lack of existing breast strain data.

2.5.3. Strain as a cause of pain

Strain has been linked to the perception of pain in muscles (McArdle, Katch, & Katch, 2010); ligaments (Hirsch *et al.*, 1960; Quinn *et al.*, 2007); and tendons (Micheli & Wood, 1995). One study investigating the effect of incrementally increased strain on ligaments in the ankle found that the onset of pain (at 20° ankle rotation) preceded the subsequent failure of either the bone or the ligaments (at 41° rotation) (Markolf *et al.*, 1989). These results support the relationships between displacement (ankle rotation), pain and strain, which are hypothesised to be present in the breast. Although links between strain and pain have been established for some biological tissues, there has been little investigation into pain caused by strain on the skin.

Within the skin, mechanoreceptors are responsible for detection of mechanical stimuli such as stretching (or strain) (Kiernan & Rajakumar, 2013). Skin strain has been found to provide important information regarding perceptions of human joint position and movement. In one study by Edin (1995), application of artificial skin strain to the fingers created the illusion of movement, and restriction of skin strain inhibited participants' perceptions of up to 90° finger flexion (Edin & Johansson, 1995). Further work by Edin demonstrated similar results using static and dynamic skin strain on the knee joint (Edin, 2001). Edin's work demonstrates that information from skin mechanoreceptors can override contradicting information from other proprioceptive mechanisms such as muscle fibres, illustrating the high sensitivity of the body to strain exerted on the skin (Edin, 2004). However, the neural pathways responsible for proprioception are not necessarily the same as those responsible for the experience of pain (Kiernan & Rajakumar, 2013).

The breast is a key region of interest when considering pain caused by skin strain. The skin and nipple of the female breast are richly innervated making this area particularly

sensitive to sensations of pain (Robinson & Short, 1977; Wallace, Wallace, Lee, & Dobke, 1996). This sensitive skin supports the breast mass against the effects of gravity, controls the motion of the breast against the torso, and undergoes cyclical deformations resulting from fluctuations in breast volume and shape during the menstrual cycle (Hindle, 1991; Manning *et al.*, 1996; Milligan *et al.*, 1975). These factors may explain the prevalence of breast pain, which is reported to be experienced by over 60% of premenopausal women (Ader & Shriver, 1998), though the exact physical mechanisms of breast pain are poorly understood (Gopinath *et al.*, 2005). One study investigating the neural causes of breast pain found that women who experienced breast pain tended to have abnormal innervation of the breast skin, possibly resulting from nerve damage caused by stretching (Gopinath *et al.*, 2005). Nerve stretching has previously been attributed to increases in breast size (Chadbourne *et al.*, 2001), although it was proposed within this thesis that nerve stretching may also occur if the skin is strained excessively by gravity or exercise induced breast motion. Measurement of skin strain on the breast during dynamic activity may therefore provide a better predictor of motion-induced breast pain than the previously investigated kinematic variables of the breast (Zhou *et al.*, 2011).

Having reviewed the existing literature on the neutral breast position, and considered factors associated with the measurement of breast motion, breast strain, and breast pain data, the final aspect of this chapter focuses on the evaluation of experimental methods. This thesis has two aims related to the development of methods for measuring the neutral breast position, making it important to establish appropriate assessment criteria for determining the accuracy and precision of each method before evaluating suitability for use in future research.

2.6. Evaluating the accuracy and precision of experimental methods

When conducting scientific research it is imperative that measurements are sufficiently accurate and precise to allow appropriate conclusions to be drawn from the data collected (Atkinson & Nevill, 1998). The evaluation of accuracy and precision are typically combined when reporting the validity of a particular measurement tool or testing method

(Currell & Jeukendrup, 2008). However, accuracy and precision are two distinct concepts and are therefore discussed separately within this section.

2.6.1. Accuracy assessment

The term accuracy refers to the ability of a measurement to assess the true value of a particular variable (Hopkins, 2000a). Generally the accuracy of a measurement tool (or method) is evaluated by comparing the measured data to the corresponding 'gold-standard' data values (Azar *et al.*, 2002; Edgecomb & Norton, 2006; Gutierrez-Farewik, Bartonek, & Saraste, 2006; Lee, 2011; MacNeil & Boyd, 2007; Rajagopal., 2007; Samani *et al.*, 2001; Stagni *et al.*, 2005; Tanner *et al.*, 2006). The nature in which comparisons are made between two data sets depends on the type of data that has been collected (Batterham & George, 2000). Nominal data can be assessed for accuracy using a kappa coefficient, although this type of data is not typically examined within biomechanics (Hopkins, 2000a). More commonly, biomechanical studies are concerned with interval-ratio data, which can be assessed for accuracy either using statistical comparisons between two complete data sets, or by direct comparisons between individual data points.

Correlation

Correlation analysis has been used in a range of studies evaluating the accuracy of a measurement tool against a corresponding gold-standard method (Edgecomb & Norton, 2006; Henseler *et al.*, 2011; Heymsfield *et al.*, 1989; MacNeil & Boyd, 2007; Mayagoitia, Nene, & Veltink, 2002). Pearson's product moment correlations in particular are frequently implemented when assessing the strength of the relationship between two sets of measurements (Boyd, Lockwood, Byng, Little, *et al.*, 1998; Currell & Jeukendrup, 2008; Koff & Benavage, 1998; Segal, Gutin, Presta, Wang, & Van Itallie, 1985; Smalls *et al.*, 2006; Smith & Havenith, 2012; White *et al.*, 2008; White, Scurr, & Hedger, 2009), where a correlation coefficients of 0.5, 0.3, and 0.1 indicate strong, moderate, and weak relationships respectively (Field, 2009). However, the use of correlations to evaluate the accuracy of measurements has been criticised within the literature due to the inability of

the correlation coefficient alone to evaluate the degree to which measured values replicate the gold-standard results (Bland & Altman, 1986; Bruton, Conway, & Holgate, 2000; Sonnergaard, 2006). For example, two methods would be perfectly correlated, without producing the same data results, if one system consistently gave results that were twice as big as the other. Correlations may therefore be appropriate when investigating whether two variables are related but not for assessing the accuracy of measured data against gold-standard values (Bland & Altman, 1986; Bruton *et al.*, 2000; Currell & Jeukendrup, 2008).

Regression

Regression analysis is conventionally used to predict the value of an outcome based on a related variable (Field, 2009). Regression can also be used to assess accuracy by graphically plotting the 'gold-standard' values against the measured values for a selected variable and creating a best-fit line (Field, 2009; Hopkins, 2000a). Comparison of the best-fit line equation to the equation of the identity line ($y = x$, $R^2 = 1$) provides an assessment of measurement accuracy because the identity line represents the most accurate scenario in which all measured values are equal to the gold-standard measurements. Three measures of accuracy can be obtained from regression analysis: the change in error over a range of measurement values (gradient); the presence of systematic bias (intercept); and the degree of variation between measurements (coefficient of determination (R^2)) (Atkinson & Nevill, 1998; Field, 2009).

The ability to represent three distinct components of accuracy using regression analysis has led to this method being recommended within the literature for evaluating measurement accuracy against gold-standard data (Hopkins, 2004). However, regression analysis may not always provide an appropriate assessment of accuracy. In 1973 Francis Anscombe demonstrated that four very different data sets produced the same regression equation (Figure 2.13), potentially leading to incorrect conclusions being drawn from regression analysis if the data is not visually inspected beforehand (Anscombe, 1973). Data sets that contain a small numbers of trials are particularly susceptible to misleading regression equations as a single outlier can have a considerable effect on the derived

regression equation (Figure 2.13 c and d). It is therefore recommended that sample sizes of at least 20 are used for this type of analysis (Hopkins, 2000a), with larger sample sizes typically leading to more appropriate regression models (Field, 2009).

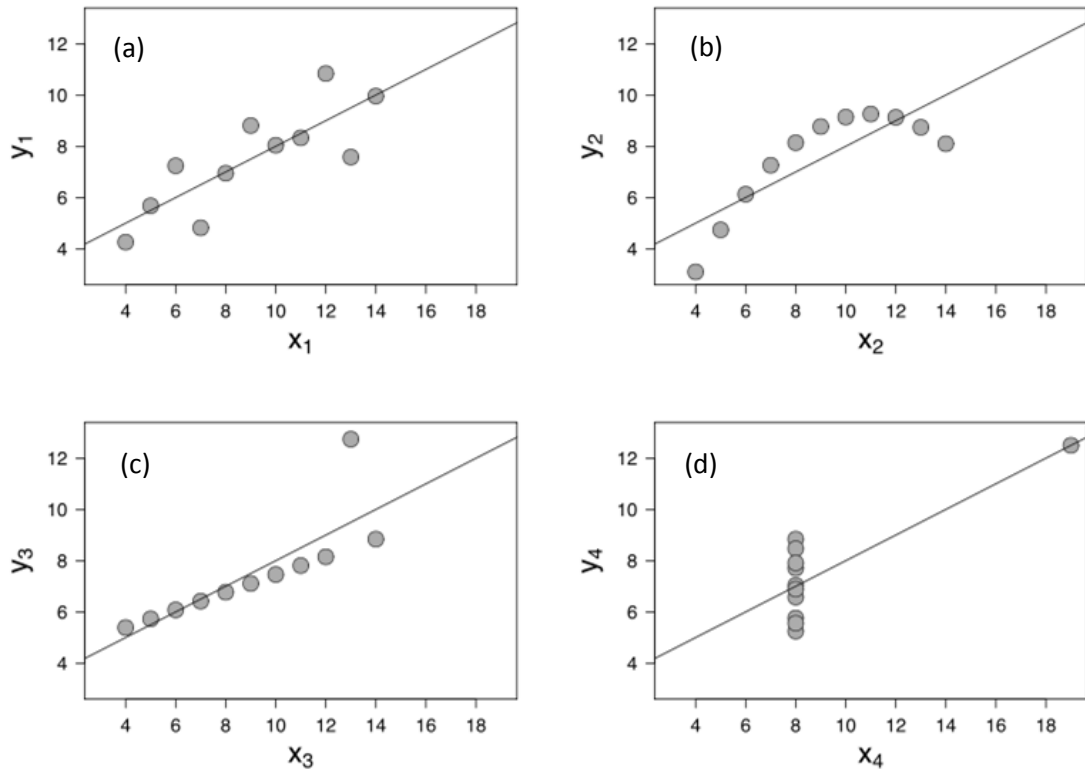


Figure 2.13: Anscombe's quartet demonstrating four different data sets with the same regression equation caused by: (a) random deviation about the regression line; (b) a linear regression line fit to quadratic data; (c) an anomalous data point influencing the gradient of the regression line; (d) an anomalous data point creating a non-infinite gradient (adapted from Anscombe, 1973).

Paired samples t-test

An alternative statistical test that is commonly used for accuracy assessment is the paired samples t-test (Coutts & Duffield, 2010; Edgecomb & Norton, 2006; Gutierrez-Farewik *et al.*, 2006; Weinberg *et al.*, 2004). Paired samples t-tests can be used to assess whether there is a statistically significant difference ($p < 0.05$) between the mean values of gold-standard measurements compared to the mean values obtained using an alternative

method (Atkinson & Nevill, 1998). In the case of accuracy assessment, a non-significant difference between the gold-standard value and the measured value may indicate that the two methods are interchangeable (Henseler *et al.*, 2011). However, the significance level (p value) represents the probability that an observed difference occurred due to chance variation alone (Knudson, 2009), and does not represent the magnitude of a reported effect (Gissane, 2012). It is therefore possible to find no significant difference between two sets of data if large absolute differences between paired values are accompanied by high levels of variation within each data set (Atkinson & Nevill, 1998). Conversely, a statistically significant difference can be observed between two measurements that does not correspond to a practically significant value (Gissane, 2013; Morrow Jr. & Jackson, 1993). In one study evaluating the accuracy of 3D photogrammetry for taking anthropometric measurements, for example, it was concluded that although measurements taken with photogrammetry demonstrated a statistically significant ($p < 0.05$) difference to calliper measurements, the magnitude of the differences were not clinically significant (differences < 2 mm) leading to the conclusion that photogrammetry could be used to accurately measure anthropometric distances (Weinberg *et al.*, 2004).

Several authors have warned against the over-reliance on statistical significance and have promoted the inclusion of alternative analyses, such as limits of agreement or absolute error, which provide information about the practical significance of any discrepancies between measurement systems (Atkinson & Nevill, 1998; Batterham & George, 2000; Batterham & Hopkins, 2006; Gissane, 2012; Hopkins, 2001; Knudson, 2009). Information about the practical significance of t-test results can be gained from reporting the effect size alongside the significance value (Currell & Jeukendrup, 2008; Knudson, 2009). Effect sizes indicate the magnitude of the measured difference between measurement methods (Knudson, 2009). The use of the correlation coefficient (r) for calculating effect size was promoted by Field in 2009, where effect sizes are defined as: small = 0.1; med = 0.3; and large = 0.5 (Field, 2009).

Limits of agreement

Limits of agreement (LOA) analysis, for the purpose of assessing the accuracy, identifies the limits in which 95% of the measurements taken using a particular measurement method would lie compared to the gold-standard reference values (Hopkins, 2000a). In 1986 Bland and Altman published a paper in the *Lancet* strongly recommending the LOA method, accompanied by a visual display of the data (Bland-Altman plot) (Figure 2.14), for comparing two methods for measuring the same variable (Bland & Altman, 1986). The Bland-Altman plot is constructed by plotting the difference between the gold-standard and measured values (y) against the mean of the gold-standard and measured values (x). The mean and standard deviations (SD) of the differences are then calculated, and the 95% LOA are identified (typically using: $LOA = \text{mean} \pm 1.96 \text{ SD}$, although strictly this only applies to large sample sizes where the factor of 1.96 approximates the cumulative probability and degrees of freedom from the t-distribution) (Hopkins, 2000b).

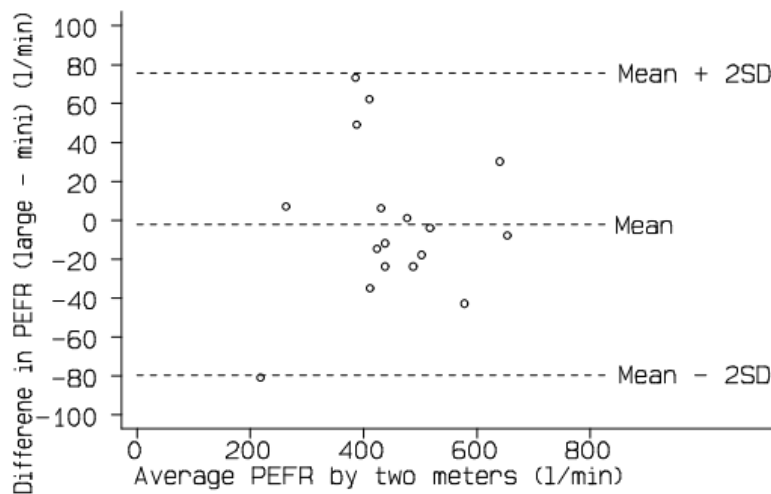


Figure 2.14: Bland-Altman plot comparing two methods for measuring peak expiratory flow rate (Bland & Altman, 1986).

Accuracy assessments using LOA are in the original units of measurement, which is beneficial compared to dimensionless quantities such as the p-value or correlation coefficient because it allows researchers to interpret results with reference to their individual research requirements (Batterham & George, 2000; Bruton *et al.*, 2000).

Despite the popularity of the Bland-Altman's plot within the literature (Bland & Altman, 1986; Currell & Jeukendrup, 2008; Hofstra *et al.*, 1997; Jobson *et al.*, 2007; Kelly & Sale, 2008; Lamb, Eston, & Corns, 1999; Reilly & Atkinson, 2009; Wheat *et al.*, 2014), there are limitations associated with using LOA to assess accuracy. In 2000 Hopkins identified several reasons not to use LOA to assess measurement accuracy: LOA cannot be used to assess the accuracy of a single measurement; 95% LOA may not be suitable for detecting true changes in individual results over time; and LOA applications are limited to the evaluation of test-retest situations (Hopkins, 2000b). Hopkins then went on to publish further work demonstrating that Bland-Altman plots incorrectly identify bias in measurements when assessed against a gold-standard calibration value (Hopkins, 2004). Instead, Hopkins promotes an absolute measure of error to assess the accuracy of one measurement system against another (Hopkins, 2000b).

Absolute difference and percentage error

The absolute error in terms of accuracy assessment represents the magnitude of the difference between a measured value ($x_{MEASURED}$) and the corresponding gold-standard value ($x_{GOLD-STANDARD}$). There are several terms used to represent this value within the literature: 'root mean square (RMS) error', 'typical error', 'mean error', 'mean difference', 'mean squares error', 'absolute difference' (Batterham & George, 2000; Henseler *et al.*, 2011; Hopkins, 2000a; Tanner, White, Guarino, Douek, & Hawkes, 2009; Weinberg *et al.*, 2004). The term 'absolute difference' is used within this document to represent this value, which is calculated using the following equation.

$$\text{Equation 2.2: } \quad \textit{Absolute difference} = ((x_{MEASURED} - x_{GOLD-STANDARD})^2)^{1/2}$$

The absolute difference method directly compares the value obtained using one measurement method to the value obtained for the same condition using the gold-standard method. When applying this type of analysis across a sample of participants or over multiple trials, the group differences can be presented as a mean difference; a range of differences across the sample or as the maximum difference observed within the sample. Each of these expressions can be useful for reporting accuracy. Firstly, the mean

absolute difference provides information about the typical error associated with a measurement tool and this can be useful when comparing several different measurement methods, or when optimising a certain measurement protocol for the same variable (Edgecomb & Norton, 2006; Tanner *et al.*, 2009). Secondly, the range of absolute difference values can be used to indicate the presence of heteroscedasticity within the data (larger absolute differences at larger gold-standard values), and to assess the accuracy of the measurement method over the sample data range. Thirdly, the maximum absolute error is important, particularly in clinical studies, when there are pre-defined limits for the acceptable accuracy and researchers must demonstrate that a new measurement method does not exceed these boundaries (Duan, Yuan, Liao, Si, & Zhao, 2011; Henseler *et al.*, 2011; Weinberg *et al.*, 2004).

Absolute differences can also be presented as a percentage of the measured data value, resulting in an assessment of relative error (Heymsfield *et al.*, 1989). Relative error can be more appropriate for heteroscedastic data (Hopkins, 2000a) as the error scales with the data values, although it is important to define the range of values for which a relative error value has been calculated to prevent incorrect comparisons between studies (Weinberg *et al.*, 2004). Presentation of absolute accuracy values, and relative accuracy where appropriate, has been commonly recommended within the literature (Batterham & George, 2000; Chiari, Della Croce, Leardini, & Cappozzo, 2005; Hopkins, 2000b; Knudson, 2009; Weinberg *et al.*, 2004). Advantages of presenting absolute differences include the easy interpretation of results for comparative purposes (it is in the original units of measurement); the lack of dependence on the size of the measurement; and the fact that it requires few assumptions about the data (Weinberg *et al.*, 2004). However, it is important to acknowledge the limitations of extrapolating these types of error values to other participant populations as the error magnitude may depend on the specific participant sample selected (Hopkins, 2000b).

Accuracy assessment – summary

The specific selection of accuracy analysis depends partly on the data collected and partly for the intended outcomes of the research. As this thesis addressed two separate

objectives regarding the identification of the neutral breast position, firstly to develop a new gold-standard method (based on buoyancy) and secondly to evaluate several alternative, more practical, methods on their ability to replicate this position, two separate accuracy analyses were required.

Assessing the accuracy of the new gold-standard method for achieving the neutral breast position posed an unusual challenge. Typically, evaluation of a new measurement method involves comparing measurements to corresponding gold-standard values (Hopkins, 2004). However, in this case the new method itself represents the gold-standard, making it illogical to assess the accuracy of the new method against previously implemented, potentially less accurate, methods. In this instance, the only available option was to assess the accuracy of the gold-standard method against known calibration values. This type of analysis has occasionally been presented in the literature when assessing the accuracy of a single measurement device before collecting data (Betzler, 2010; Hennessey *et al.*, 2014; Milligan, Mills, & Scurr, 2014). Attention is drawn to the fact that accuracy assessment using calibration values provided an assessment of 'measurement accuracy' but not the accuracy to which the breast position using the gold-standard method replicated the true neutral breast position. In this case the accuracy assessment aimed to identify the maximum measurement error associated with the gold-standard method, which can be quantified using the absolute difference between the measured and known calibration values.

The evaluation of alternative methods for measuring the neutral breast position can be achieved with a more conventional approach, using the 'gold-standard' neutral breast position data to assess each of the alternative methods. As the alternative neutral position methods were anticipated to have diverse applications, from biomechanical and clinical research to product development, it was important to provide an absolute measure of accuracy which could be used to evaluate the suitability of each method for different research areas (Batterham & George, 2000; Hopkins, 2000b). The absolute difference, and paired samples t-tests with effect sizes, can be combined to evaluate whether there are either clinically or statistically significant differences between the alternative and gold-standard methods. A non-significant difference between a particular

method and the gold-standard method, combined with low absolute differences and large effect sizes, implied that the alternative method closely replicates the gold-standard results over the selected participant sample. Correlations, regression and LOA were not considered appropriate for assessing accuracy within this thesis due to their susceptibility to error when implemented on a small sample size (< 20 participants) (Hopkins, 2000a).

2.6.2. Accuracy criteria

When implementing absolute measures of accuracy, such as the absolute difference, it is important to implement accuracy criteria defining how large the difference between the measured values and the gold-standard (or calibration) values can be before the measurement method being evaluated is deemed unsuitable. It is recommended that these criteria are defined before data collection to allow unbiased evaluation of each measurement method (Atkinson & Nevill, 1998; Bland & Altman, 1986). Again a distinction was made between the measurement accuracy assessed in the gold-standard neutral breast position method, and the overall accuracy assessed for the alternative neutral breast position methods.

The gold-standard neutral position breast method proposed in this thesis was intended to provide a more accurate measurement of the neutral breast position than the two existing methods that have been implemented in both biomechanical (Haake & Scurr, 2011) and clinical research (Rajagopal, 2007). Although there has been limited discussion regarding acceptable measurement accuracy within the biomechanical literature (Atkinson & Nevill, 1998), clinical research often requires the demonstration that measurement error does not exceed a clinically significant measurement value (Dehghani *et al.*, 2004; Henseler *et al.*, 2011; Weinberg *et al.*, 2004). In the case of anthropometric measurements 2 mm represents the maximum clinically acceptable measurement error (Aung, Ngim, & Lee, 1995; Weinberg *et al.*, 2004). It was therefore appropriate to specify that the gold-standard method should meet this 2 mm measurement accuracy requirement if it is to replace the current methods for assessing the neutral breast position (Rajagopal, 2007; Zain-UI-Abdein *et al.*, 2013).

The alternative neutral position methods were developed with the intention of providing a simple method for assessing the neutral breast position within a laboratory environment. These alternative methods were not anticipated to recreate the neutral position of the entire breast surface due to the high levels of variance reported in dynamic breast movement data (Milligan *et al.*, 2014). Instead the focus of these methods was on replicating the neutral position of the nipple which is frequently used to represent the gross position of the breast (Bridgman, Scurr, White, Hedger, & Galbraith, 2010; Chen *et al.*, 2012; Haake *et al.*, 2013; Haake & Scurr, 2010; Mason *et al.*, 1999; McGhee, Steele, & Zealey, 2010; Scurr *et al.*, 2010; Scurr, White, *et al.*, 2009; White, Mills, & Scurr, 2012; Zhou *et al.*, 2011, 2012b, 2009). Accuracy assessment of these alternative methods incorporates the degree to which the gold-standard neutral nipple position is replicated in addition to the inherent measurement error. In this case, the acceptable accuracy criteria must take into account the stability of the breast on the torso as well as the measurement error associated with each method. The previously implemented buoyancy and breast drop methods for estimating the neutral nipple position were not evaluated for accuracy and therefore cannot be used for comparison within this thesis (Haake *et al.*, 2013; Haake & Scurr, 2011; Rajagopal, 2007; Zain-Ul-Abdein *et al.*, 2013). However, previous research has reported that 5 mm is the maximum achievable accuracy for measuring relative nipple position due to the effects of breathing and fluctuating torso angle (Hansson *et al.*, 2014). A 5 mm criterion was therefore used to evaluate whether the alternative neutral position methods could accurately replicate the gold-standard neutral nipple position.

2.6.3. Precision assessment

Precision quantifies the difference between repeated measurements of the same value. Several alternative terms for precision, such as 'repeatability', 'reliability', 'reproducibility', 'consistency', 'agreement', 'concordance', and 'stability', have been used within the literature (Atkinson & Nevill, 1998; Batterham & George, 2000). The selection of different terms for precision within the same study can be helpful when distinguishing between measurements taken at different time intervals, with different apparatus, or by different individuals, however as this thesis predominantly focused on measurement tools

(methods for assessing the neutral breast position) applied by the same individual over a short time period then the term precision is used throughout the document.

In a review of statistical methods for assessing measurement error in sports medicine Atkinson and Nevill stated that precision was key when evaluating measurement tools, since an imprecise tool would never give accurate results over repeated measurements (Atkinson & Nevill, 1998). There are two types of precision analysis described within the literature, one evaluates relative precision (*i.e.* how precisely do individuals maintain their rank within a group) and the other assesses absolute precision (*i.e.* how precisely can the same variable be measured over repeated trials). Relative precision is often used to evaluate the ability of a test to distinguish between individuals based on their score and is represented using correlation coefficients or regression analysis (Atkinson & Nevill, 1998). Absolute precision can be used to compare the precision of different measurement methods and is applicable to the type of data presented within this thesis. Calculations of absolute precision include the coefficient of variation (CV), standard error of measurements (SEM), limits of agreement (LOA), standard deviation (SD), and typical error of measurement (TEM) (Atkinson & Nevill, 1998; Betzler, 2010).

Coefficient of variation (CV)

The CV method of assessing precision can express the standard deviation of the measure as a percentage of the mean value, making it easier to compare the amount of variation between different protocols. Although this type of precision analysis is popular within the literature there are several limitations with this method. Most importantly for the data explored within this thesis, CVs are not appropriate for values not bounded by zero as it is assumed that the error approaches zero near zero measurement values (Atkinson & Nevill, 1998). As the position of the breast is not bounded by zero, CV analysis was not appropriate for evaluating the precision of the methods used to measure the neutral breast position.

Standard error of measurement (SEM)

Due to limited participant sample sizes there are several different approximations for SEM within the literature (Weir, 2005) leading to some degree of confusion when reporting this variable (Atkinson & Nevill, 1998). Both SEM and LOA (as described in the previous section) have been promoted for precision assessment (Atkinson & Nevill, 1998; Hopkins, 2000a), although both methods are susceptible to errors due to their underpinning assumption of homoscedasticity (Batterham & George, 2000). When taking biological measures heteroscedasticity is often present within the data (Atkinson & Nevill, 1998), violating the assumptions required for SEM and LOA precision analysis. A second important factor to consider with implementing SEM or LOA is the requirement for a large sample size (minimum sample sizes between 20 and 50 participants recommended) (Atkinson & Nevill, 1998; Hopkins, 2000a; Morrow Jr. & Jackson, 1993), which were not achieved for the methods evaluated in this thesis.

The number of repeat trials conducted within this research constitutes a limitation in terms of assessing the precision of each neutral position method. Higher numbers of repeat trials within each method were unachievable due to the number of different methods incorporated into the neutral position study. The high variability of the breast tissue over time (Hussain *et al.*, 1999; Milligan, Drife, & Short, 1975; Wojcinski *et al.*, 2012) meant that a compromise had to be made between the number of participants, the number of different neutral position methods, and the number of trials completed within each session. Considering that the evaluation of the alternative neutral position methods was intended to assess which methods were likely to produce accurate neutral nipple position estimates across a range of participants, and not to validate each testing procedure, it was decided to include only three trials of each feasible method. Measures of precision that can be applied to small numbers of trials include standard deviation (SD) and typical error of measurement (TEM) (Hopkins, 2000a).

Standard deviation (SD)

The SD of repeated measurements of the same variable provides a basic assessment of the variation between measurements in the original measurement units. Standard deviations are commonly reported within biomechanics (Azar *et al.*, 2002; Beck, Foerster, Buchröder, Schmidt, & Döring, 2014; Campbell, Munro, Wallace, & Steele, 2007; Chen *et al.*, 2012; Nie *et al.*, 2008; Stagni *et al.*, 2005; Zhou *et al.*, 2009, 2011), and can be used to compare the precision of different measurement tools (Leardini *et al.*, 2005). Standard deviations are typically used to represent precision when evaluating a small number of repeat trials, or when comparing measured values to calibration data (Betzler, 2010; Duan *et al.*, 2011; Edsander-Nord *et al.*, 1996; Malini *et al.*, 1985; Milligan *et al.*, 2014).

Typical error of measurement (TEM)

The TEM quantifies the SD of measurements once any changes in the mean have been accounted for and represents the expected variation resulting from multiple repeat trials (Hopkins, 2000a). Calculated TEMs are widely implemented within anthropometric studies to evaluate the precision of repeated measurements on the same individual (Nagy *et al.*, 2008). The standard calculation for TEM is based on two measurements of the same variable (Equation 2.3) (Weinberg *et al.*, 2004), although a slightly more complex version is available on Hopkins' website for calculating TEM using three repeat measurements (Hopkins, 2000a).

Equation 2.3:
$$\text{TEM} = \left(\frac{\sum(\text{Difference between measurements})^2}{2(\text{No. of individuals measured})} \right)^{1/2}$$

The TEM provides an assessment of precision for a sample group as a whole, allowing simple comparison between methods. The lack of dependence on sample size, and simple interpretation of results, has led to TEM being promoted for use in precision studies (Hopkins, 2000b; Weinberg *et al.*, 2004).

Precision assessment – summary

Due to the number of different methods implemented within this thesis, each with three repeat trials, precision evaluation was limited to the SD and TEM methods. Precision was assessed for each individual within the sample group using SD, whereas and the precision of each method across the whole sample group was assessed using the TEM calculation for three repeat trials.

2.6.4. Precision criteria

Definitions of adequate precision have rarely been discussed within the literature (Atkinson & Nevill, 1998), with authors suggesting that the precision criteria should be defined according to the intended outcomes of the study (Batterham & George, 2000). Standard deviation is typically used to assess the precision of measurement tools across repeated trials using a fixed measurement value (such as a calibration object). Highly precise limits are imposed in these cases (up to 0.5 mm) as repeated measurements are expected to produce exactly the same value (Betzler, 2010). However, breast position is unlikely to remain fixed between consecutive measurements, meaning higher standard deviations are anticipated between trials. It was therefore suggested that acceptable criteria for SD of measurements within this study could be defined using the typical SDs present in the existing methods for measuring static nipple position using optoelectronic cameras (Scurr, White, Milligan, *et al.*, 2011b). This precision criterion was calculated in section 4.4.4 by assessing the maximum resultant SD in relative nipple position for 14 participants over six static trials using the optoelectronic camera system.

Acceptable precision criteria have been defined for TEMs within the anthropometric literature, where the magnitude of acceptable TEM depends on what body part is being assessed. 'Expert' anthropometric TEM criteria for measurements of length vary from 1.6 mm (WHO Multicentre Growth Reference Study Group, 2006) to 31 mm (Ulijaszek & Kerr, 1999). Research focused on breast measurements have reported acceptable TEM values up to 3.5 mm (Brown, Ringrose, Hyland, Cole, & Brotherston, 1999). Consequently this TEM criterion was implemented to evaluate precision within this thesis.

2.7. Summary

In this chapter a review of existing knowledge and research methods within breast biomechanics were outlined, with a focus on taking breast measurements, assessing breast strain, considerations for assessing pain, and evaluating experimental methods. It was proposed that to understand the relationships between breast motion; the risk of breast damage; and motion-induced breast pain, it is necessary to incorporate the neutral breast position into assessments of these three variables. The neutral breast position represents the position in which there is no external strain on the breast skin. This position therefore provides a meaningful zero-point for quantifying breast motion, enabling the distinction between motions that increase or decrease the strain on the breast during dynamic activity. The neutral position also provides the reference position for assessing static strain on the breast caused by gravity. The inclusion of static strain is required to estimate the risk of breast skin damage using the published skin strain failure limits.

Further applications of the neutral breast position were also identified within clinical research and in relation to the development and assessment of breast support garments. Experimentally obtained data on the neutral breast position may enable the development of improved FE breast models for predicting the deformation of the breast in a clinical setting. In terms of breast support garment design and assessment, the neutral position represents the optimum breast position in terms of minimising skin strain. Developing and evaluating breast support garments on their ability to control motion about the neutral position may therefore provide an improved evaluation of breast support in terms of minimising the risk of breast damage and motion-induced breast pain compared to existing measures of breast ROM.

A scarcity of literature on the neutral breast position was identified. Two published methods (breast drop and buoyancy) exist for identifying the neutral breast position but neither method has been validated within the literature for this purpose. This thesis aimed to establish a gold-standard method for measuring the neutral breast position.

Chapter 2: Literature review and justification of the thesis methods

The existing breast drop and buoyancy methods could then be evaluated, alongside novel methods, against the gold-standard method for their accuracy and precision when estimating the neutral breast position. The following chapter focuses on the refinement of the data collection and analysis methods selected for use within the thesis based on the literature review.

3. Methodological development

3.1. Overview

The first aim of this thesis was to develop a new gold-standard method for measuring the neutral breast position. Within the literature review the buoyancy method was identified as having a strong theoretical underpinning. However, the use of water to support the breast in previous buoyancy studies may have led to inaccurate neutral position estimates as the breast's fat content may lower its mass-density below that of water. A more accurate gold-standard estimate of the neutral breast position may be achievable by substituting the water in the buoyancy method for an alternative fluid with a mass-density equal to breast tissue. The first methodological consideration was therefore the selection of an appropriate fluid for use in the buoyancy method based on published breast (radiological) density data (investigated in section 3.2). Once an appropriate fluid had been selected for the new gold-standard neutral position method, it was then important to consider the factors identified within the literature review that may influence the measurement of breast position. The effects of participant breathing state, and different torso segment constructions, on measurements of relative nipple position were investigated in sections 3.3 and 3.4. Section 3.5 focused on the practical implementation of the buoyancy method within a biomechanics laboratory. The results from these methodological studies informed the experimental procedures and data analysis methods used throughout the remainder of the thesis.

3.2. Methodological study 1: A systematic review of the density of the breast to inform the fluid selected for the new gold-standard buoyancy neutral position method

3.2.1. Introduction

The buoyancy method is based on Archimedes' principle which states that the buoyancy force experienced by an object immersed in a fluid is proportional to the volume it displaces, and the proportionality constant is the density of the displaced fluid multiplied by gravitational acceleration (Equation 3.1) (Huerta, Sosa, Vargas, & Ruiz-Suárez, 2005).

Equation 3.1:
$$F_{\text{Buoyancy}} = (g \rho_{\text{Fluid}}) V_{\text{Displaced}} = m.g = \text{weight}$$

where g is gravitational acceleration, ρ_{Fluid} is the density of the displaced fluid and $V_{\text{Displaced}}$ is the volume of the displaced fluid.

Applying this principle to the breast, if the breast is immersed in a fluid of equal mass-density to the breast tissue then the buoyancy force will be equal to the breast weight, and the breast will remain suspended in its equilibrium position. This type of immersion would almost completely counteract the effect of gravity on the breast, with only a small theoretical inaccuracy occurring because gravity acts through the centre of mass of the breast whereas buoyancy acts at the breast surface (Gao & Desai, 2010).

The buoyancy method has been used in two previous studies, in which breast mass-density was approximated using water (Rajagopal *et al.*, 2008; Zain-Ul-Abdein *et al.*, 2013). The breast is primarily composed of fat and glandular tissue, with the proportion of fat ranging from 19% to 90% of the total breast volume (Figure 2.3) (Gefen & Dilmoney, 2007; Hassiotou & Geddes, 2012; Lee *et al.*, 1997; Vandeweyer & Hertens, 2002). Human body fat typically has a mass-density of 900 kg.m^{-3} (Durnin & Womersley, 1974), whereas glandular tissue is reported to have a mass-density of 1050 kg.m^{-3} (Katch *et al.*, 1980). The presence of fat within the breast means that the overall breast mass-density is likely to be lower than that of water (994 kg.m^{-3} at 35°C) (Kell, 1975). Immersion of the breast

in water, with a comparably higher mass-density, may therefore have resulted in compressive forces acting on the breast in previous studies implementing the buoyancy method, potentially leading to errors in the resulting measurements of neutral breast position.

A scarcity of data is available on the mass-density of the breast making the selection of a suitable immersion fluid difficult. Reported values of breast density commonly refer to the radiological density of the breast, measured using mammography or MRI, which does not directly correspond to the mass-density of the breast required for the application of Archimedes' principle. This methodological study aimed to systematically review the breast density literature; convert radiological density data into mass-density data; and to select a suitable fluid for the development of the gold-standard neutral position method.

3.2.2. Aims

1. Systematically review the breast density literature.
2. Calculate the mass-density of the breast from published quantitative data on density-related variables.
3. Select a suitable fluid, with a mass-density equal to the calculated breast mass-density, for use in the gold-standard neutral position method.

3.2.3. Method

A literature search was performed using Medline (from the beginning of the database to February 2013) for studies (in English) reporting quantitative measurements of any variable associated with breast mass-density (*i.e.* mass, weight, volume, component tissue ratios, or radiological density). Studies were excluded if measurements were made qualitatively; if density measurements were categorised; if any assumptions were made regarding breast density within the study; if the measurement method was unclear; or if there were insufficient data to calculate density. The abstracts of the selected studies

were screened and any irrelevant articles were rejected. The full articles of remaining studies were retrieved and reviewed again for their relevance to this study. Reference lists within these articles were also checked for relevance. Any articles that were not available in the University-subscribed journals were obtained through inter-library loan. All relevant literature was stored in an electronic database (Mendeley desktop, version 1.11, Medeley Ltd.) and quantitative breast data values were copied to Excel.

The calculation of mass-density for the breast depended on the specific variables presented within each study. For studies reporting the ratio of fat to glandular tissue in the breast, the mass-density can be approximated using the known densities of these tissues (fat: $\rho_F = 900 \text{ kg.m}^{-3}$; glandular tissue: $\rho_G = 1050 \text{ kg.m}^{-3}$) (Durnin & Womersley, 1974; Katch *et al.*, 1980). Assuming that the breast is composed entirely of these two tissues, an estimate for breast mass-density (ρ_B) can be calculated as demonstrated by Equation 3.2, Equation 3.3, and Equation 3.4, where X is the proportion of fat (mass) in the breast; A is the proportion of fat (volume) in the breast; V_F is the volume of fat in the breast; and V_B is the volume of the breast. For longitudinal or intervention studies that presented more than one measurement on the same participant, the baseline data values were used for the calculation of mass-density.

$$\text{Equation 3.2} \quad \rho_B = \frac{1}{\left(\frac{X}{0.9}\right) + \left(\frac{1-X}{1.05}\right)} \quad (\text{Katch } et \text{ al.}, 1980)$$

$$\text{Equation 3.3:} \quad \rho_B = A \rho_F + (1 - A) \rho_G \quad (\text{Katch } et \text{ al.}, 1980)$$

$$\text{Equation 3.4:} \quad \rho_B = \rho_G - \frac{V_F}{V_B} (\rho_G - \rho_F) \quad (\text{Vandeweyer \& Hertens}, 2002)$$

Some studies included within this systematic review reported measures of breast mass (m_B) and breast volume (V_B). These variables were used to calculate breast mass-density using the standard density equation (Equation 3.5).

Equation 3.5:
$$\rho_B = \frac{m_B}{V_B} \quad (\text{Parmar } et al., 2011)$$

Once the mass-densities of the breast had been calculated from the literature identified in the systematic review, the next stage of this study focused on the selection of an appropriate fluid for use in the neutral position method. A range of sources, including websites, technical handbooks and scientific papers, were searched for fluids with densities (at body temperature) that matched the calculated breast mass-density. Secondary selection criteria were also imposed to eliminate any fluids that would be inappropriate for use in the gold-standard buoyancy method. The secondary criteria were: non-hazardous; non-reactive; not an irritant to skin/eyes; translucent (for measurements to be taken with a camera); and to a lesser extent, easily accessible and financially viable.

3.2.4. Results

Twenty three studies with quantitative measurements of breast density-related variables were identified within the systematic review of literature (Table 3.1). These studies incorporated 17,593 women with an age range of 18 to 90 years, the published quantitative breast data was used to calculate an approximate mass-density for the breast. The mean calculated mass-density from each study ranged from 919 kg.m⁻³ to 986 kg.m⁻³, with an overall mean mass-density value of 948 kg.m⁻³(Table 3.1).

The wide variation in calculated breast mass-density across the 17,593 women included within this review demonstrated that it was not possible to select a single fluid that would match the mass-density of every woman's breasts. However, considering Archimedes' principle, the breast should float in a fluid with higher relative mass-density and sink in fluid with lower relative mass-density. Therefore, it may be possible to identify the

boundaries of the neutral breast position by immersing the breast in two different fluids that have mass-densities either side of the calculated breast mass-density values.

Based on the mass-density criteria defined by the range of breast mass-densities, and considering the secondary criteria detailed previously, the two most appropriate fluids for the buoyancy experiment were identified as water (994 kg.m^{-3}) (Kell, 1975) and soybean oil (909 kg.m^{-3}) (Pryde, 1980). The mean calculated breast mass-density (948 kg.m^{-3}) lies almost exactly midway between the mass-densities of these two fluids (Figure 3.1), enabling the neutral breast position to be estimated using the midpoint between the breast position in water and the breast position in soybean oil.

Table 3.1: Mass-densities of the breast calculated from published quantitative breast data up to and including the year 2013.

Study	Method	Number of participants	Age of participants (years)	Mean breast density (kg.m ⁻³)
Mammographic densities and risk of breast cancer. (Saftlas <i>et al.</i> , 1991)	Digitised mammogram	567	35-74	946
Quantitative correlation of breast tissue parameters using magnetic resonance and X-ray mammography. (Graham <i>et al.</i> , 1996)	MRI (water content)	42	40-50	957
	Mammogram (percentage density)	42		983
Fatty and fibroglandular tissue volumes in the breasts of women 20-83 years old. (Lee <i>et al.</i> , 1997)	MRI	40	20-83	950
	Mammogram	40		986
The relationship of anthropometric measures to radiological features of the breast in premenopausal women. (Boyd, Lockwood, Byng, Little, <i>et al.</i> , 1998)	Digitised mammogram	273	29-51	959
Ethnic differences in mammographic densities. (Maskarinec, Meng, & Ursin, 2001)	Digitised mammogram	514	35-85	941

Comparison of mammographic densities and their determinants in women from Japan and Hawaii. (Maskarinec, Nagata, Shimizu, & Kashiki, 2002)	Digitised mammogram	523	40 +	944
Measurement of breast density with dual X-ray absorptiometry: feasibility. (Shepherd <i>et al.</i> , 2002)	DXA scanning and mammogram	8	No data	942
Quantification of glands and fat in breast tissue: An experimental determination. (Vandeweyer & Hertens, 2002)	Mastectomies - volume analysis	21	27-83	950
A cross-sectional investigation of breast density and insulin-like growth factor I. (Maskarinec, Williams, & Kaaks, 2003)	Digitised mammogram	263	34-46	958
Risk factors for breast cancer associated with mammographic features in Singaporean Chinese women. (Heng <i>et al.</i> , 2004)	Digitised mammogram	803	45-69	938
Insulin-like growth factor-I, IGF-binding protein-3, and mammographic breast density. (Diorio <i>et al.</i> , 2005)	Digitised mammogram	1574	54.1 (mean)	941
Percentage density, Wolfe's and Tabár's mammographic patterns: agreement and association with risk factors for breast cancer. (Gram <i>et al.</i> , 2005)	High-cancer-risk digitised mammogram	987	55-71	938
Measurements of breast density: no ratio for a ratio. (Haars, van Noord, van Gils, Grobbee, & Peeters, 2005)	Digitised Xeromammogram (postmenopausal)	418	49-65	935
Mammographic density and breast cancer risk: the multiethnic cohort study. (Maskarinec <i>et al.</i> , 2005)	Digitised mammogram	1274	No data	945

Mammographic features and subsequent risk of breast cancer: a comparison of qualitative and quantitative evaluations in the Guernsey prospective studies. (Torres-Mejía <i>et al.</i> , 2005)	Digitised mammogram	3211	40-80	945
Longitudinal trends in mammographic percent density and breast cancer risk. (Vachon <i>et al.</i> , 2007)	Digitised mammogram	1085	50+	944
Association of mammographic density with the pathology of subsequent breast cancer among postmenopausal women. (Ghosh <i>et al.</i> , 2008)	Digitised mammogram	286	40+	943
Age-specific trends in mammographic density: the Minnesota breast cancer family study. (Kelemen <i>et al.</i> , 2008)	Digitised mammogram	1689	40-90	939
Development of a quantitative method for analysis of breast density based on three-dimensional breast MRI. (Nie <i>et al.</i> , 2008)	MRI	4	No data	919
Mammographic density does not differ between unaffected BRCA1/2 mutation carriers and women at low-to-average risk of breast cancer. (Gierach <i>et al.</i> , 2011)	Digitised mammogram	262	No data	953
Mammographic breast density and subsequent risk of breast cancer in postmenopausal women according to tumour characteristics. (Yaghjian <i>et al.</i> , 2011)	Digitised mammogram	3667	No data	936
	Total/range/mean value	17,593	18-90	948

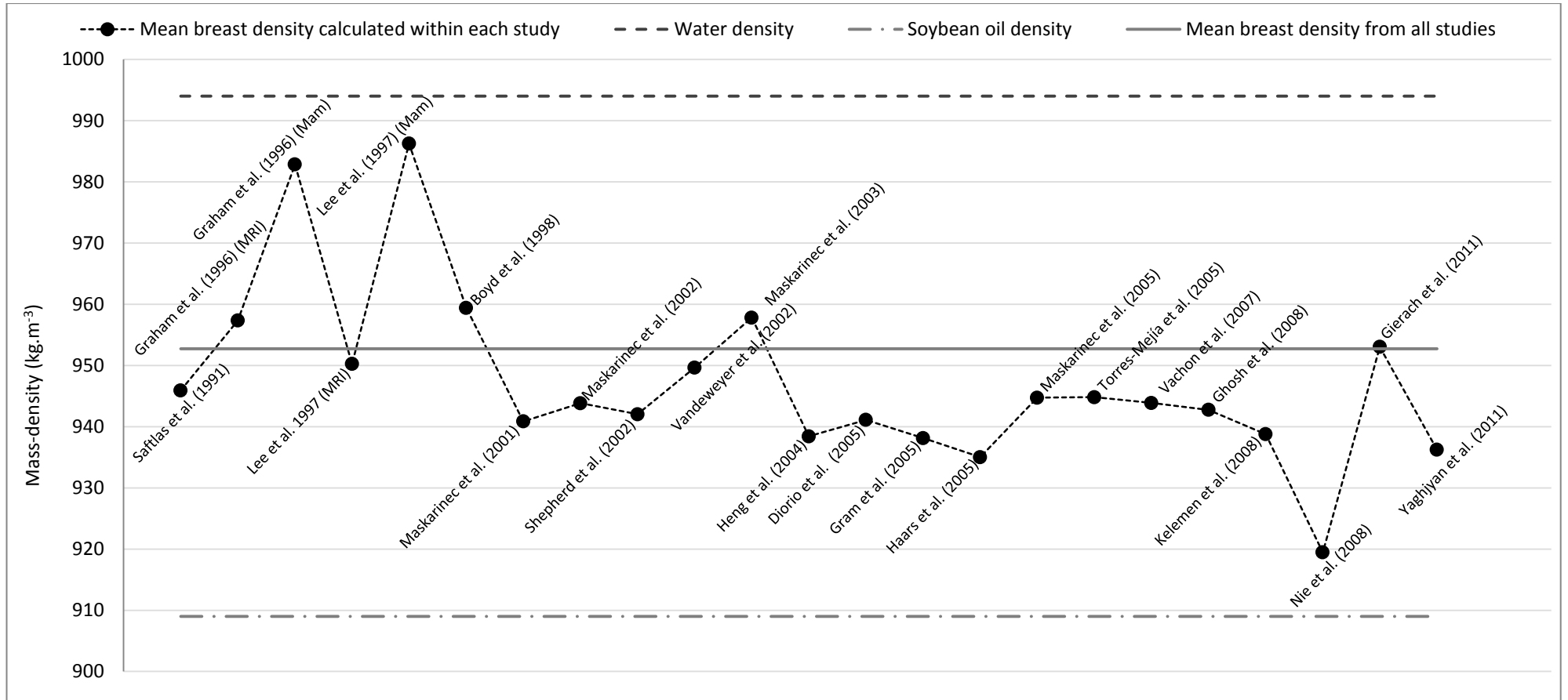


Figure 3.1: Mean calculated mass-densities of the breast from published data, up to and including the year 2013, compared to the overall mean breast mass-density and the mass-densities of water and soybean oil.

3.2.5. Discussion

Quantitative data from twenty three studies was successfully used to calculate an estimate of breast mass-density. Two key assumptions were made during the calculation process, firstly that the breast was entirely composed of fat and glandular tissue, and secondly that the quantitative results presented in each density-related study provided accurate data for the breast. Disregard for other tissues within the breast (*e.g.* breast skin) may have resulted in small inaccuracies when calculating density based on only two tissue types (fat and glandular tissue). Of greater concern was the accuracy of the published data used for calculating mass-density. In a review of radiological breast density assessment in 2008, Kopans raised several concerns about the validity of mammograms for assessing the composition of the breast (Kopans, 2008). Kopans reported that it was impossible to accurately assess three-dimensional breast composition using mammography. Reasons included the inability to use two mammographic images to accurately assess 3D tissue volumes; the non-validated assumption that mammographic measurements reflect the true volume ratios of tissues; variations in breast compression during measurement and the incomplete assessment of breast tissue due to the ill-defined breast boundary (Kopans, 2008). Considering that nineteen out of the twenty three studies included in this systematic review incorporated mammographic measurements of breast composition, errors arising from mammographic assumptions may therefore have had a large effect on the calculated breast mass-density values. However, some reassurance can be gained from the MRI data included in this review. Data obtained using MRI provide a more accurate 3D assessment of breast structure due to the high number of measurements taken at incrementally increasing depths of the breast (Nie *et al.*, 2008). Breast mass-densities calculated from MRI data may therefore provide more accurate results. Data in Table 3.1 indicate that mass-density values obtained from MRI data were not dissimilar to the overall mean mass-density value calculated across all studies, suggesting that errors associated with mammography were distributed symmetrically about the mean mass-density value.

The data in Figure 3.1 indicates a gradual trend for decreasing breast mass-density over the 20-year data sample. This was an interesting finding and could be explained by

improvements in data analysis techniques. Early attempts to quantify mammographic images involved the identification of fatty and glandular breast regions using a china marker and then taking measurements of area by hand using a planimeter (Saftlas *et al.*, 1991). In contrast, more modern techniques involve complex computerised processes. Mammographic images are enhanced using contrast adjustment, image darkening to remove unwanted tissue, and background deletion to isolate the breast. Analysis can then be automated based on a pre-defined threshold colour values for every pixel of the breast image, percent (radiological) density can then be precisely quantified by calculating the percentage of dark pixels (representing glandular tissue) within the breast image (Gierach *et al.*, 2011; Yaghjian *et al.*, 2011). Increased precision and reduced human error associated with modern mammographic analysis may indicate that the higher breast mass-densities calculated from early studies may be due to measurement error, and that breast mass-density is actually lower than the calculated mean value. On the other hand, there may be a genuine trend for decreasing breast mass-density over the 20 year sample period caused by the increase in worldwide obesity rates leading to higher percentages of fatty tissue in the breast (Popkin & Doak, 1998; Sturm, Ringel, & Andreyeva, 2004; World Health Organization, 2000).

Despite the presence of real or erroneous trends within the mass-density data, it was observed that none of the calculated mass-density values were outside of the mass-density boundaries formed by water and soybean oil (Figure 3.1). Since these data values encompass results from 17,593 women aged between 18 and 90 years, it was assumed that all of the women recruited within this thesis would also have breasts with a mass-density between water and soybean oil. Consequently, immersion of the breast in water and soybean oil would result an over-and under-compensation for the effects of gravity respectively. The neutral breast position can then be estimated using the mid-point between the two immersed breast positions.

3.2.6. Conclusion

The systematic review of breast density data revealed that breast mass-density ranged from 919 kg.m^{-3} to 986 kg.m^{-3} , with an overall mean mass-density value of 948 kg.m^{-3} . The wide range of breast mass-density values prevented the selection of a single fluid for use in the gold-standard neutral position method. Immersion of the breast in two separate fluids, with densities above (water) and below (soybean oil) the range of reported breast mass-densities permits the boundaries of the neutral position to be identified. The mid-point between the breast positions in water and soybean oil can then be used to estimate the neutral breast position with more accuracy than could be achieved using a single fluid in isolation.

The next stage of this thesis investigated factors that may affect the accuracy or precision of breast measurements to ensure the most appropriate methodologies are implemented in both static and dynamic measurements of breast position.

3.3. Methodological study 2: Does breathing state or measurement duration affect relative breast position?

3.3.1. Introduction

When establishing a gold-standard method for assessing the neutral breast position it was important to minimise any factors that may cause imprecise or inaccurate measurements of the breast. Existing research has shown that breathing can have a significant effect on measured breast size, specifically with the expansion and contraction of the ribcage causing changes of up to six inches in the under band measurement depending on respiration state (McGhee & Steele, 2006).

The calculation of relative breast position (or motion) requires the construction of a reference plane on the torso. The ribs are a recommended location for reference markers within breast biomechanics research (Zhou *et al.*, 2011), although recent research has suggested that the instability of rib markers can effect measurements of breast motion (Whittingham *et al.*, 2012). Soft tissue motion has been suggested as a primary cause of marker instability at the ribs (Mills, Loveridge, *et al.*, 2014a; Whittingham *et al.*, 2012), though rib movement caused by breathing may also be a contributing factor (Mills, Loveridge, *et al.*, 2014a). Considering that some of the methods implemented within this thesis (including the gold-standard neutral position method) were stationary in nature, it was important to assess the effect of breathing on the accuracy and precision of static breast measurements.

During inspiration the ribs move anteriorly, laterally and superiorly, with the converse motion occurring during expiration (De Groote, Wantier, Cheron, Estenne, & Paiva, 1997). Construction of a torso reference plane from markers placed on the ribs may therefore result in changes in reference plane and local co-ordinate system (LCS) orientation during the normal breathing cycle. It was postulated that changes in the orientation of the LCS may cause an apparent change in static breast position even if no breast movement has occurred. Several authors have acknowledged the potential for breathing to affect measurements of static breast position but have selected not to standardise breathing

state when taking measurements of the breast (Barbosa *et al.*, 2012; McGhee & Steele, 2010b). It has been reported that a relaxed end expiration state provides the optimum assessment of bra size (McGhee & Steele, 2006), suggesting that a specific breathing state may correspond to improved breast measurements, although the effect of breathing state on measurements of breast position has not yet been assessed within the literature.

The duration of breast measurement (*i.e.* the number of frames of data recorded using video or optoelectronic camera systems) was a second aspect to consider within this thesis. If breathing was found to have a measurable effect on nipple position then the proportion or number of breathing cycles incorporated during measurement trials may affect the resulting mean measured nipple position. Normal resting breathing frequency is 16.6 breaths per minute (0.3 breaths per second) (Mead, 1960) whereas the typical duration of static breast measurement trials has been approximately 2 seconds (Haake & Scurr, 2011). Calculation of mean static breast positions may therefore incorporate incomplete breathing cycles, and may not represent the typical breast position over a longer time period. Although increasing measurement durations has limited impact on optoelectronic data analysis, significant time implications are associated with video analysis. Within this thesis video cameras were used to obtain breast positional data in water and soybean oil at a sampling frequency of 25 Hz. Considering that each marker on the breast and torso (21 in total) had to be manually digitised every measurement frame for all participants, in both water and soybean oil conditions, increasing the measurement duration would have significant time implications for analysis of the neutral breast position. It was therefore beneficial to identify the minimum measurement duration required to achieve an acceptably accurate and precise measure of mean static nipple position.

3.3.2. Aims

1. To assess the effect of breathing state on the accuracy and precision of static measurements of nipple position.
2. To assess the effect of measurement duration on the accuracy and precision of static measurements of nipple position.

3.3.3. Method

Twelve participants with breast sizes ranging from 30 to 34 inch under band and A to GG cup size gave informed consent to take part in this study. Participants had a mean (SD) age of 26 (3) years, height of 1.67 (0.05) m and mass of 64 (10) kg. Four retro-reflective 12 mm diameter spherical markers were placed on the suprasternal notch, the anterior-inferior aspect of the 10th ribs and on the left nipple using hypoallergenic tape (Scurr *et al.*, 2010) (Figure 3.2). Eleven Qualisys Oqus optoelectronic cameras (Qualisys, Sweden) were positioned in an arc around the centre of the biomechanics laboratory and were calibrated using a Qualisys calibration frame and wand.

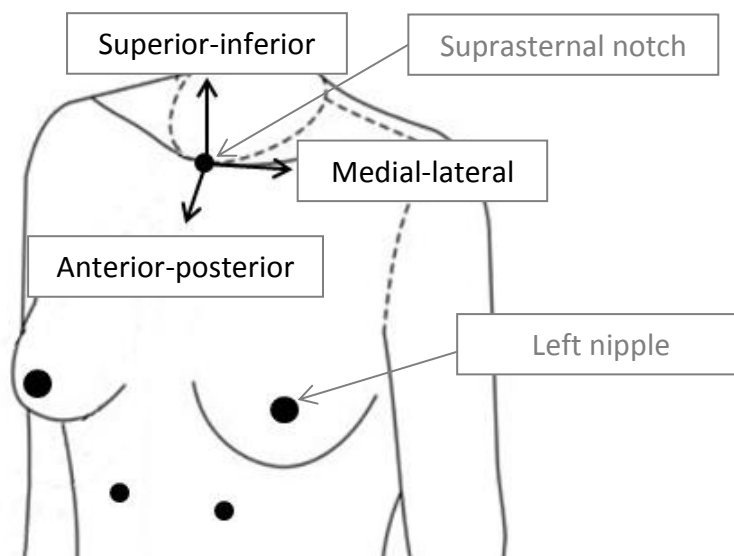


Figure 3.2: Breast and torso marker set used for the methodological study on breathing.

Participants stood in the centre of the laboratory with their arms by their sides and their shoulders relaxed. Optoelectronic recordings of the breast and torso markers were taken at 200 Hz using Qualisys Track Manager (QTM) software (Qualisys, Sweden). Participants performed at least two familiarisation trials for each breathing condition before any measurements of nipple position were taken.

The effect of breathing state on mean measured nipple position was investigated using three repeat trials of the following three conditions:

- (1) 2 s breathing normally
- (2) 2 s held breath in a comfortable expiration position (exhale)
- (3) 2 s held breath in a comfortable inhalation position (inhale)

The 2 s trials represent a typical duration of static breast measurement within breast motion research (Haake & Scurr, 2011).

The effect of measurement duration on mean measured nipple position was investigated using three repeat trials of the following four conditions:

- (4) 10.00 s breathing normally
- (5) 2.00 s breathing normally
- (6) 1.00 s trials breathing normally
- (7) 0.50 s trials breathing normally
- (8) 0.25 s trials breathing normally

The 10 s measurement trials were collected to represent the typical static breast position incorporating multiple breathing cycles. The 2 s normal breathing trials were collected to represent typical static breast measurement duration. The shorter duration trials were created by cropping the same three 2 s trials to increasingly shorter durations, ensuring that any measured changes in nipple position across conditions were due to measurement duration (*i.e.* the proportion of the breathing cycle incorporated) and not due to other factors such as changes in posture between trials or trials taken at different points in the breathing cycle.

The 3D trajectories of the breast and torso markers were identified within QTM and were exported to Visual 3D (v4.96.4, C-motion) for further analysis. A POSE estimation method was used to create the torso reference segment using the suprasternal notch as the proximal end of the segment and the right and left rib markers as the distal ends of the segment. The origin of the LCS was defined at the proximal end of the torso segment. Raw marker co-ordinate data were filtered using a generalised cross-validatory quintic spline and the torso segment was recalculated. Mean three dimensional left nipple positions were then calculated relative to the torso segment for each measurement trial.

The reference breathing state was 2 s of normal breathing (1), and the reference breathing duration was 10 s (4). Accuracy was assessed using absolute differences for individual participant data and paired samples t-tests for group data. Acceptable accuracy was defined for absolute differences below 5.0 mm. Statistically significant differences ($p < 0.05$) between conditions indicated that the typical nipple position over 10 s was not replicated in the alternative breathing state.

The precision of nipple position measurements in each condition were assessed using SD for individual participant data and TEMs for group data. Acceptable maximum TEM values were defined as 3.5 mm. The SD values were evaluated by comparison to the reference breathing condition, with smaller SDs indicating more precise within-participant measurements of nipple position.

3.3.4. Results

Breathing state results

The mean nipple positions in each condition are presented in Table 3.2 (individual data are available in Appendix A), and accuracy and precision data are presented in Table 3.3 and Table 3.4 respectively.

Table 3.2: Mean left nipple position relative to the torso during 2 s measurements in normal breathing, held exhalation and held inhalation conditions.

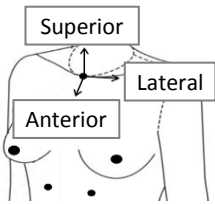
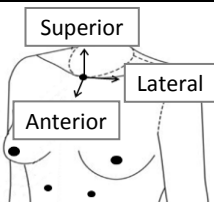
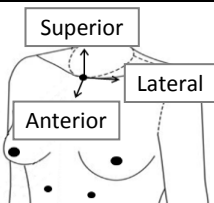
	Mean left nipple position (mm)		
	Anterior-posterior	Medial-lateral	Superior-inferior
(1) 2 s normal breathing	48.0	103.7	-176.8
(2) 2 s held exhale	49.1	101.6	-178.9
(3) 2 s held inhale	56.7	105.2	-170.4

Table 3.3: Absolute differences in nipple position during held exhalation and inhalation compared to each participant’s mean nipple position during 2 s of normal breathing (mm).

	Absolute difference in nipple position (mm)					
	Anterior-posterior		Medial-lateral		Superior-inferior	
	Mean	Peak	Mean	Peak	Mean	Peak
(1) 2 s normal breathing	-	-	-	-	-	-
(2) 2 s held exhale	2.0	7.2	2.3*	9.7	2.5*	5.2
(3) 2 s held inhale	8.7*	14.1	2.6	4.4	6.4*	14.4

* denotes a significant difference ($p < 0.05$)

Table 3.4: Standard deviation of nipple position measurements for three repeat trials in each breathing state (mm).

	Standard deviation in nipple position (mm)					
	Anterior-posterior		Medial-lateral		Superior-inferior	
	Mean	Peak	Mean	Peak	Mean	Peak
(1) 2 s normal breathing	0.7	1.6	0.3	0.5	0.5	1.2
(2) 2 s held exhale	0.7	1.4	0.8	3.0	0.9	1.9
(3) 2 s held inhale	1.0	3.7	0.9	3.7	0.9	2.0

Calculated TEM values for all breathing states were within the acceptable precision criteria (3.5 mm). The largest TEM value was 1.6 mm in the anterior-posterior component of nipple position during the 2 s held inhalation condition (Appendix A).

Breathing duration results

The mean nipple positions in each condition were presented in Table 3.5 (individual data are available in Appendix B), and accuracy and precision data are presented in Table 3.6 and Table 3.7 respectively.

Table 3.5: Mean left nipple position relative to the torso during 2.00 s, 1.00 s, 0.50 s, 0.25 s, and 10.00 s of normal breathing.

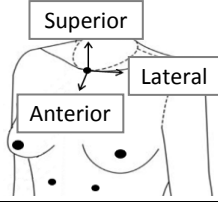
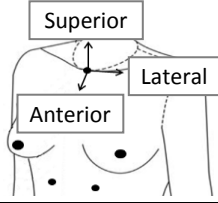
	Mean left nipple position (mm)		
	Anterior-posterior	Medial-lateral	Superior-inferior
(4) 10.00 s normal breathing	47.8	104.2	-174.5
(5) 2.00 s normal breathing	48.0	103.7	-176.8
(6) 1.00 s normal breathing	48.1	103.6	-176.7
(7) 0.50 s normal breathing	48.2	103.6	-176.6
(8) 0.25 s normal breathing	48.2	103.6	-176.6

Table 3.6: Absolute differences in nipple position compared to each participant’s mean nipple position during 10.00 s of normal breathing (mm).

	Absolute difference in nipple position (mm)					
	Anterior-posterior		Medial-lateral		Superior-inferior	
	Mean	Peak	Mean	Peak	Mean	Peak
(4) 10.00 s normal breathing	-	-	-	-	-	-
(5) 2.00 s normal breathing	1.1	2.9	1.2	4.6	2.3*	5.2
(6) 1.00 s normal breathing	1.0	2.7	1.2	4.7	2.3*	5.2
(7) 0.50 s normal breathing	1.0	2.8	1.2	4.7	2.3*	5.2
(8) 0.25 s normal breathing	1.0	2.8	1.2	4.6	2.2*	5.2

* denotes a significant difference (p < 0.05)

Table 3.7: Standard deviation of nipple position measurements for three repeat trials for each breathing duration (mm).

	Standard deviation in nipple position (mm)					
	Anterior-posterior		Medial-lateral		Superior-inferior	
	Mean	Peak	Mean	Peak	Mean	Peak
(4) 10.00 s normal breathing	0.6	1.6	0.4	1.0	1.0	3.0
(5) 2.00 s normal breathing	0.7	1.6	0.3	0.5	0.3	0.5
(6) 1.00 s normal breathing	0.7	1.6	0.4	0.9	0.4	1.9
(7) 0.50 s normal breathing	0.7	1.6	0.4	1.1	0.6	1.3
(8) 0.25 s normal breathing	0.7	1.4	0.5	1.2	0.5	1.2

TEM values for all breathing states were within the acceptable precision criteria (3.5 mm). The largest TEM value was 1.2 mm in the superior-inferior component of nipple position during the 10.00 s condition (Appendix B).

3.3.5. Discussion

Standardisation of breathing during breast measurements has had limited discussion within the literature. For the majority of breast motion studies it may not be feasible to standardise breathing state due to the dynamic or prolonged nature of the testing. However, breathing state could be standardised for short-duration static measurements of breast position such as those required for the new gold-standard neutral position method.

Results of this study demonstrated that both exhalation and inhalation conditions had a measurable effect on relative nipple position. During held exhalation nipple position was up to 9.7 mm different to the normal breathing position in the medial-lateral direction (Table 3.3). Inhalation had a greater effect on nipple measurements, with up to 14.4 mm and 14.1 mm differences in the superior-inferior and anterior-posterior directions respectively when compared to the measurement taken during normal breathing (Table 3.3). Statistically significant differences were observed in two out of three components of

nipple position for both exhalation and inhalation conditions compared to the normal breathing condition. Although TEM values were all within acceptable limits, analysis of within-participant SD demonstrated that the mean measurement of nipple position was most precise, in all three directions, for the normal breathing state (Table 3.4). These findings suggested that attempts to control breathing state during measurements of nipple position using optoelectronic camera systems results in significantly different and less precise measurements than those taken in the uncontrolled normal breathing state.

Investigation into the effects of measurement duration on static nipple position demonstrated similar results for all durations of 2.00 s or below, with maximum differences between conditions of 0.2 mm (Table 3.6). However, larger differences were observed when comparing each duration condition to the 10.00 s measurement intended to replicate the typical breast position. The superior-inferior direction in particular produced a maximum difference of 5.2 mm in the short duration measurements compared to the 10.00 s recording, and therefore exceeds the maximum acceptable accuracy criteria outlined in this thesis (5.0 mm) (Table 3.6). Although this may suggest that short measurement durations do not produce a representative measurement of the mean nipple position, results of this study also demonstrated that the 10.00 s measurements had the highest SD values of all conditions in the superior-inferior direction (Table 3.7). The mean SD in this direction was 1.0 mm with a maximum value of 3.0 mm. This relatively high within-participant variation in the reference condition may partially account for the discrepancies observed in comparison to shorter duration measurements of nipple position. It was proposed that this variation may have been due to participants' inability to remain completely stationary for the entire 10.00 s measurement, possibly resulting in small posture fluctuations that may have affected measurements of nipple position. As the gold-standard assessment of the neutral nipple position required highly precise nipple measurement, shorter duration breast measurements may minimise within-participant variation between trials.

The results of this study also demonstrate that measurement durations of 0.25 s can accurately and precisely replicate the same measurement value as recordings taken with the standard 2.00 s duration. Considering that these measurement durations correspond

to approximately 6 and 50 frames of 25 Hz video data respectively, the option to select shorter measurement durations without compromising data quality was particularly beneficial for analysis of the buoyancy neutral position data where each frame had to be digitised manually.

3.3.6. Conclusion

Controlling breathing state during measurements of relative nipple position using an optoelectronic camera system resulted in significantly different, and less precise, measurements to those obtained in the uncontrolled normal breathing state. The normal uncontrolled breathing condition was therefore selected for measurements of breast position within this thesis.

Measurement durations between 0.25 s and 2.00 s produced similar results in terms of accuracy and precision, with absolute differences and SD values all within 0.5 mm when compared between these conditions. Statistically significant differences, and higher SD values, were present in the superior-inferior component of nipple position when measuring for 10.00 s, suggesting that longer measurement durations cannot be used to accurately and precisely measure static breast position. Static breast measurement durations were therefore kept between 0.25 s and 2.00 s within this thesis, with the shortest duration used for data requiring manual digitisation.

3.4. Methodological study 3: Using POSE estimation within breast biomechanics

3.4.1. Introduction

The appropriate selection of breast and torso marker locations and the subsequent definition of the torso reference segment are ongoing challenges within breast motion research. The torso marker set developed by Scurr *et al.* (2010) represents the recommended torso marker set for use in breast motion studies (Zhou *et al.*, 2011). Scurr's torso marker set consists of markers placed on the suprasternal notch and right and left ribs. However, marker placement on the ribs has been shown to reduce the stability of the torso reference segment and to alter measurements of relative breast motion using POSE (Mills, Loveridge, *et al.*, 2014b; Whittingham *et al.*, 2012). Segment stability refers to the degree of inter-marker movement that occurs between the markers used to define the torso reference segment. Generally, within biomechanics skin-mounted markers are used to approximate the underlying skeleton during physical activity. This approach enables the application of rigid body mechanics to sporting movements providing that any inter-marker motion is assumed to be error caused by soft tissue motion over the skeleton (Cappozzo *et al.*, 2005; Stagni *et al.*, 2005).

The breast's location on the torso means that the reference segment consists of a non-rigid thorax overlaid with deformable soft tissue (Mills, Loveridge, *et al.*, 2014b). Combined with the additional problem of obstruction caused by breast support garments, it becomes difficult to select stable marker locations that will not experience relative motion during dynamic activity. However, creating a stable torso segment was critical to the assessment and comparison of neutral breast position methods incorporating differing levels of physical activity (and therefore soft tissue motion).

Segment instability caused by inter-marker movement can be reduced using POSE estimation, in which a least squares method is used to fit the marker positions onto their static locations and the error is quantified by the segment residual value (Cappozzo *et al.*, 2005; Lu & O'Connor, 1999). Application of POSE estimation to the torso results in a fixed length segment which moves with six degrees of freedom based on the motion of the

reference markers (Lu & O'Connor, 1999). Consequently, excessive motion at any of the reference markers causes the whole torso segment, including the origin, to be displaced in the direction of motion. To allow accurate comparisons between breast measurements within this thesis it was important that the measurement origin remained at the same location (suprasternal notch) irrespective of the static or dynamic nature of the measurement condition.

The potential for segment origin movement when using POSE estimation has only recently been recognised within the breast biomechanics literature (Mills, Loveridge, *et al.*, 2014b), and there has not yet been an attempt to investigate the magnitude of the problem or to propose a solution. This methodological study therefore aimed to examine whether the addition of torso tracking markers, or fixing the relative location of the reportedly unstable rib markers (Whittingham *et al.*, 2012), could improve the stability of the torso segment during dynamic activity. The effect of torso stability on measurements of breast motion was also assessed by calculating nipple ROM relative to each torso segment during five running gait cycles at 10 kph. This method of assessing breast motion was selected due to its popularity within the literature, allowing comparisons to be made to published data (Chen *et al.*, 2012; Haake & Scurr, 2010; Mills, Loveridge, *et al.*, 2014a; Risius, Milligan, Mills, & Scurr, 2014; Scurr, White, *et al.*, 2009; Scurr, White, Milligan, *et al.*, 2011b).

3.4.2. Aims

1. To quantify the segment residual and origin shift that occurs in the torso segment when using POSE estimation during treadmill running at 10 kph when the following torso marker sets are implemented:
 - (a) The recommended breast motion torso marker set developed by Scurr *et al.* (2010).
 - (b) The recommended breast motion torso marker set, with the addition of a tracking marker on the xiphoid process.
 - (c) The recommended breast motion torso marker set, with the addition of a tracking marker on the xiphoid process, and substitution of the rib markers for landmarks based on their static location relative to the suprasternal notch marker.
2. To assess the effect of torso segment stability on measurements of nipple ROM during treadmill running.
3. To select an appropriate torso segment construction for comparing nipple positions between static and dynamic measurement trials.

3.4.3. Method

Following favourable ethical opinion, one female participant gave informed consent to take part in this study. The participant had a breast size of 34B; age of 21 years, height of 1.76 m; and a mass of 72 kg. Five retro-reflective 12 mm diameter spherical markers were placed on the suprasternal notch (STN), the anterior-inferior aspect of the 10th ribs, the xiphoid process (XP) and on the left nipple using hypoallergenic tape (Scurr *et al.*, 2010; Wu *et al.*, 2005). An additional 19 mm diameter retro-reflective spherical marker was attached to the participant's left heel to aid with the identification of gait cycles.

Eleven Qualisys Oqus optoelectronic cameras were positioned in an arc around the treadmill (Powerjog, H/P/Cosmos Mercury, Germany) and were calibrated using a Qualisys calibration frame and wand.

Prior to collecting dynamic data, the participant stood stationary on the treadmill with her arms relaxed by her sides. A 2 s recording of the retro-reflective markers was taken at 200 Hz with the optoelectronic camera system. The participant then performed a self-selected warm up on the treadmill before the speed was increased to 10 kph. Once the participant was in a comfortable running stride at 10 kph, the retro-reflective markers were recorded at 200 Hz for five gait cycles using the optoelectronic cameras.

The 3D trajectories of the retro-reflective markers were identified within the Qualisys Track Manager (QTM) software and were exported to Visual 3D for further analysis. The 2 s static trial was used to create three different POSE estimated torso segments. The proximal end of each segment defined the segment origin.

Segment 1: This segment was created using the recommended breast motion marker set.

The proximal end of the segment was defined using the STN marker and the right and left rib markers defined the lateral and medial aspects of the distal end of the segment. The model was tracked in the dynamic trial using the STN and the two rib markers (Figure 3.3a).

Segment 2: This segment was created using the recommended breast motion marker set

with an additional marker on the XP. The proximal end of the segment was defined using the STN marker and the right and left rib markers defined the lateral and medial aspects of the distal end of the segment. The model was tracked in the dynamic trial using the STN, XP, and the two rib markers (Figure 3.3b).

Segment 3: This segment was created using the recommended breast motion marker set

with an additional marker on the XP. The two rib markers were substituted for rib landmarks which were created along the STN to right/left rib vector at

a fixed distance determined by the static STN to right/left rib distance. The proximal end of the segment was defined using the STN marker and the right and left fixed rib landmarks defined the lateral and medial aspects of the distal end of the segment. The model was tracked in the dynamic trial using the STN, XP, and the two fixed rib landmarks (Figure 3.3c).

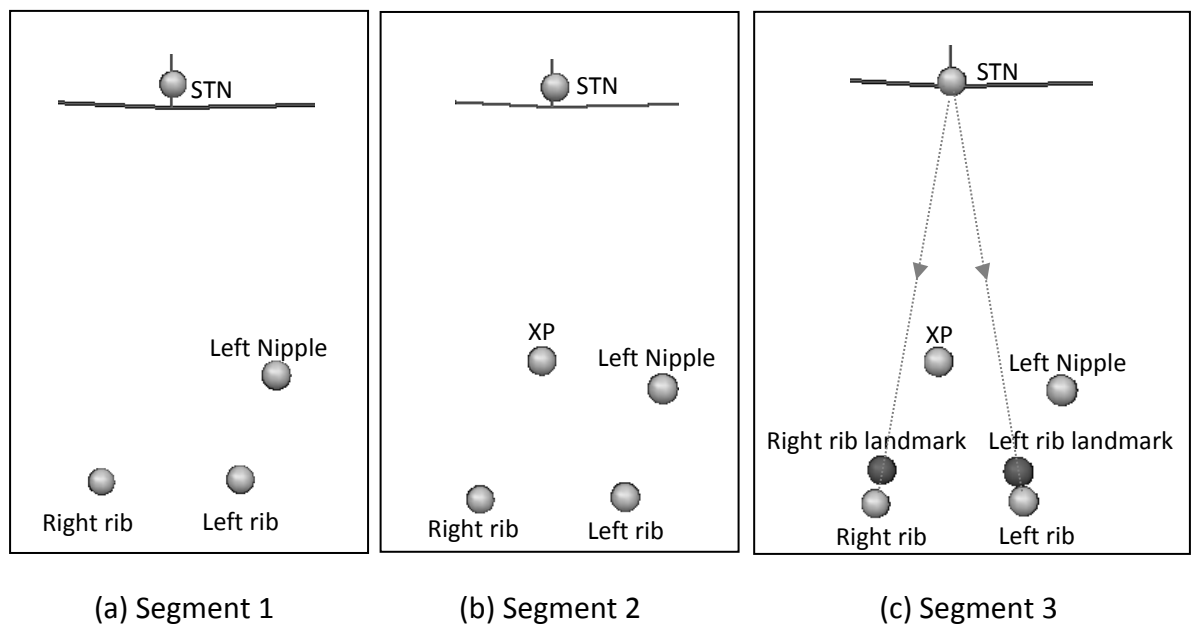


Figure 3.3: Markers and landmarks used to construct three different POSE estimated torso segments to evaluate segment and origin stability and relative nipple range of motion during treadmill running at 10 kph.

The dynamic trial was then triplicated and one copy was assigned to each torso segment (segments 1, 2 and 3). For each dynamic trial, raw marker co-ordinate data were filtered using a generalised cross-validatory quintic spline and each torso segment was recalculated. Gait cycles were identified using the anterior-posterior velocity of the heel marker (derived from the filtered heel marker displacement) (Zeni Jr, Richards, & Higginson, 2008) and event markers were used to identify the start of each gait cycle. The mean segment residual was calculated over the five gait cycles for each torso segment to evaluate stability. The extent to which POSE estimation caused a shift in the torso segment origin was assessed by calculating the displacement and ROM of the STN marker (intended origin) relative to each torso segment (actual origin). The displacement of the left nipple marker relative to each torso segment was also calculated to investigate the

effect of torso segment construction on measurements of nipple motion. The difference between the maximum and minimum values of relative left nipple and STN marker displacements in each direction were used to calculate ROM values for the origin shift and nipple motion variables.

3.4.4. Results

Table 3.8: Mean segment residual during running at 10 kph for three different constructions of the torso segment.

	Segment residual (mm)
Segment 1	6.8
Segment 2	7.7
Segment 3	5.6

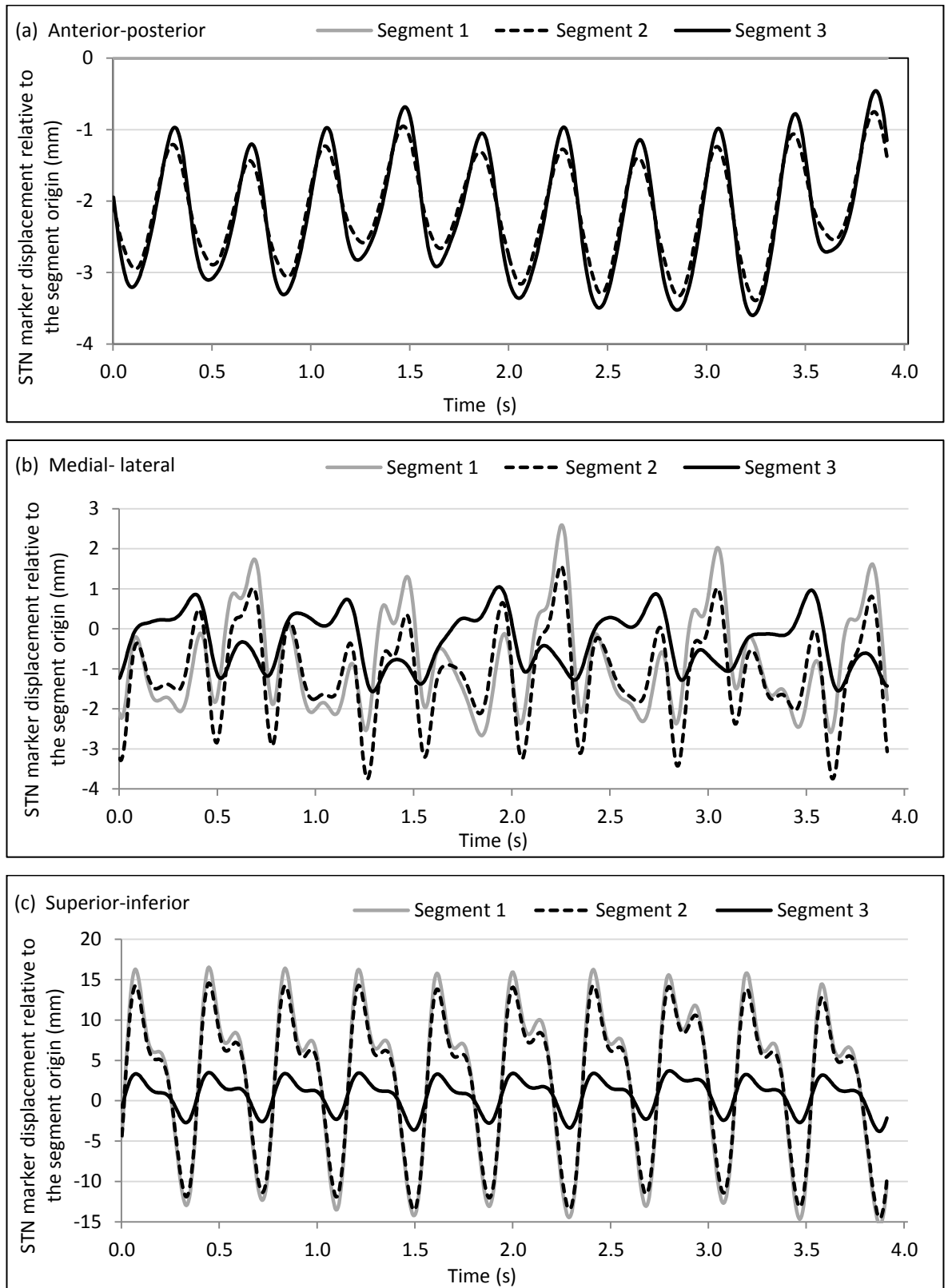


Figure 3.4: Displacement of the suprasternal notch marker relative to the segment origin, for three different torso segment constructions, in the anterior-posterior (a), medial-lateral (b) and superior-inferior (c) directions during running at 10 kph ($n = 1$).

Table 3.9: Mean range of motion of the suprasternal notch marker about the segment origin during running at 10 kph for three different constructions of the torso segment (n = 1).

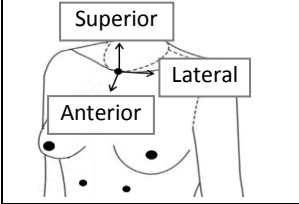
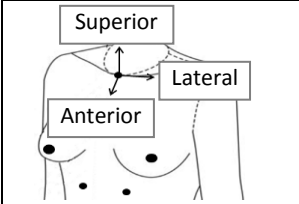
	ROM of the STN marker (mm)		
	Anterior-posterior	Medial-lateral	Superior-inferior
Segment 1	0.0	4.5	30.4
Segment 2	2.2	4.6	27.3
Segment 3	2.6	2.3	6.7

Table 3.10: Mean range of motion of the left nipple marker relative to the segment origin during running at 10 kph for three different constructions of the torso segment (n = 1).

	ROM of the left nipple marker (mm)		
	Anterior-posterior	Medial-lateral	Superior-inferior
Segment 1	0.0	4.5	30.4
Segment 2	2.2	4.6	27.3
Segment 3	2.6	2.3	6.7

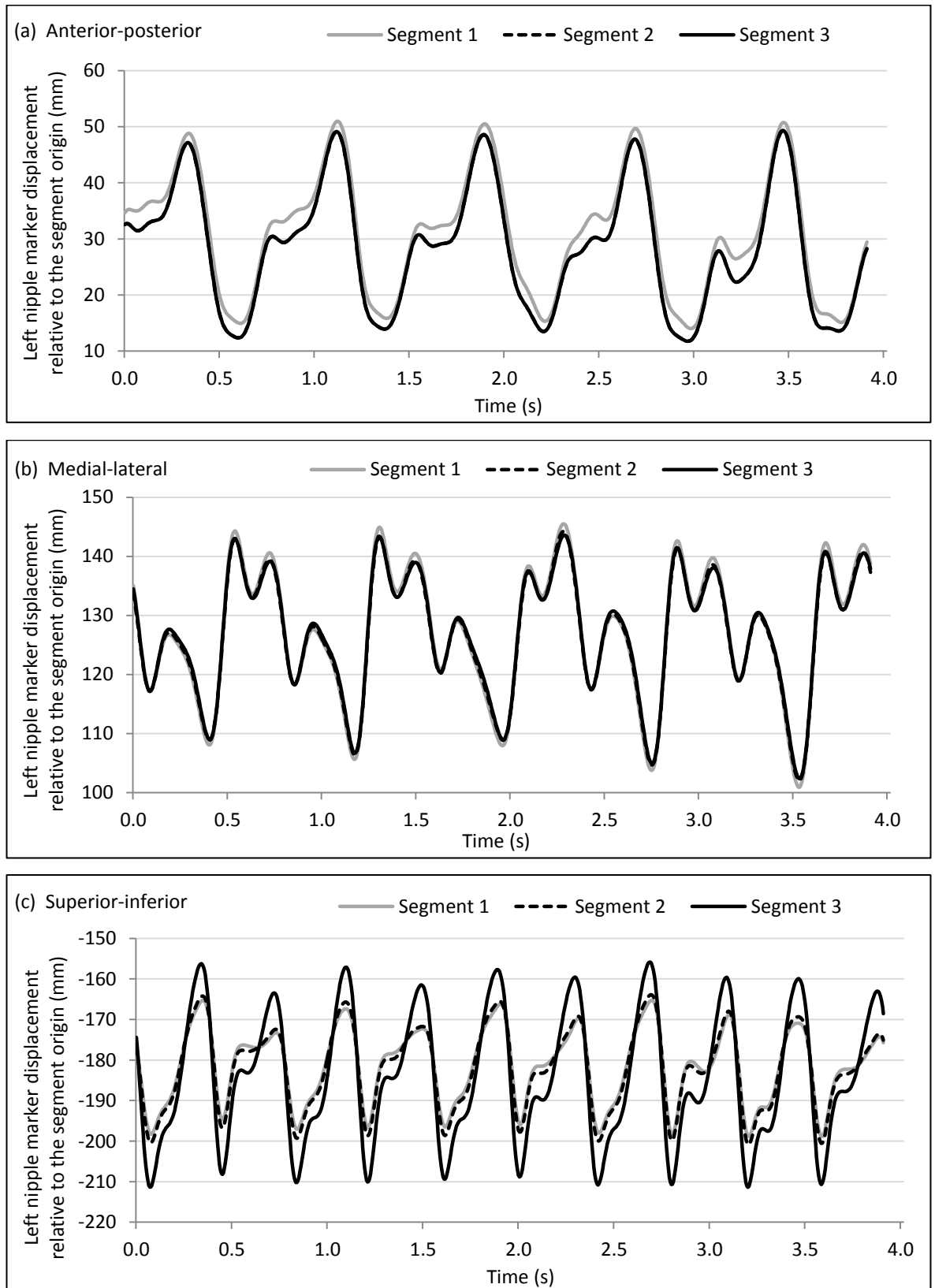


Figure 3.5: Displacement of the left nipple marker relative to the segment origin, for three different torso segment constructions, in the anterior-posterior (a), medial-lateral (b) and superior-inferior (c) directions during running at 10 kph (n = 1).

3.4.5. Discussion

Based on previous literature it was assumed that markers on the ribs would provide the largest contribution to torso segment instability within this study (Mills, Loveridge, *et al.*, 2014b; Whittingham *et al.*, 2012). It was therefore anticipated that the addition of a tracking marker on the XP, and the subsequent fixing of the ribs using landmarks, would provide more stable torso segments, with lower segment residuals, from which to calculate relative nipple position.

The data in Table 3.8 indicate that although the torso segment was more stable with fixed ribs, the addition of a tracking marker actually decreased the segment stability compared to the same segment without a tracking marker. This result may be explained by considering the number of markers used for torso segment construction in each condition. The recommended breast motion torso segment (segment 1) is defined using only three torso markers, the minimum number of markers required to construct a reference plane (2D). In this case, the least squares calculation during POSE estimation incorporates a 2D correction of inter-marker movements. The reference markers can never move outside of the reference plane as the locations of all three markers determine the reference plane orientation. The incorporation of an additional tracking marker on the XP (segment 2), outside of the plane defined by the STN and ribs (segment 1), produces a three dimensional torso segment. Any inter-marker movement therefore has to be corrected for in three dimensions during POSE estimation. Considering that the segment residual is a resultant value, for which one component will always be zero for a reference plane (segment 1), it may be expected that segments created from four or more markers would produce higher residual values even if the individual locations of markers are more stable. This factor is illustrated in Table 3.9 where it was demonstrated that the STN marker could not move anteriorly out of the reference plane.

Despite the use of four markers in the construction of segment 3, this segment demonstrated the lowest segment residual and was therefore anticipated to provide the most stable reference frame for breast measurements within this thesis. It was also highlighted that the use of four markers creates redundancy in the torso segment as the

segment can still be constructed if one marker is obstructed. This redundancy reduced the risk of data loss due to marker obstruction, which may otherwise have resulted in data loss during the more dynamic measurements assessed within this thesis.

The second factor investigated in this study was the effect of segment instability on the segment origin. Typically, breast measurements are presented relative to the STN (Zhou *et al.*, 2011). However, it had recently been suggested that POSE estimation during analysis of dynamic breast motion may cause the measurement origin to shift away from the STN marker (Mills, Loveridge, *et al.*, 2014b), potentially invalidating the use of the STN as an anatomical reference point. This study represented the first attempt to investigate the effect of segment instability on the origin position of the reference segment. Results demonstrated that the STN marker was displaced from the segment origin during treadmill running (Figure 3.4), and that the measurement origin does not remain at the STN during dynamic breast measurements. When the recommended breast motion marker set was used to construct the torso segment (segment 1), the magnitude of this origin shift was largest in the superior-inferior direction, with a ROM value of 30.4 mm (Table 3.9). Application of a tracking marker on the XP had a beneficial effect, reducing the origin shift to 27.3 mm in the superior-inferior direction. However, a greater improvement was observed when the rib markers were replaced with fixed rib landmarks (segment 3), in which case the origin shift decreased to 6.7 mm in the superior-inferior direction (Table 3.9).

Constraining the STN to rib distance based on the static rib locations in segment 3 enabled the segment origin to better approximate the STN in both the superior-inferior and medial-lateral directions (Table 3.9). Although a slight increase in the anterior-posterior origin shift was observed for segment 3 compared to segments 1 and 2. This may have occurred because although the rib landmarks were fixed relative to the STN marker in distance, their relative orientations were still defined using the unstable rib markers. The angular effects of soft tissue motion at the ribs may have been exaggerated by the rib landmarks for instances where the ribs had moved towards the STN marker. For example, if the resultant STN to rib marker distance (hypotenuse) is fixed and the ribs move closer to the STN superiorly, then Pythagorean Theorem dictates that the anterior

distance to the ribs must increase, potentially causing increased origin shift in the anterior-posterior direction. The fixed rib segment (segment 3) provided the most stable torso origin when considering all three directions of motion, with a notable improvement occurring in the superior-inferior direction during running.

The final aspect of this study considered the effect of torso segment construction on measurements of nipple displacement and ROM. Figure 3.5 demonstrates that nipple displacement was affected by the different torso segment constructions. A comparison between Figure 3.4 and Figure 3.5 demonstrates that larger STN displacements correspond to smaller nipple displacements when compared between the three segment constructions. This effect can also be observed in the ROM data presented in Table 3.10. When STN ROM decreased from 30.4 mm to 6.7 mm in the superior-inferior direction from segment 1 to segment 3, the corresponding nipple ROM increased from 31.2 mm to 53.3 mm. The magnitude of this change (22.1 mm in nipple ROM) may have important implications on measurement accuracy within this thesis and subsequently on the recommendations made for future research and bra design based on measurements of the neutral breast position. It was also interesting to note that the decrease in ROM of the STN marker between segments 1 and 3 (23.7 mm) was almost equal to the increase in nipple ROM (22.1 mm). This finding suggested that increased movement of the rib markers (causing the segment origin to be displaced from the STN marker) accounted for almost the entire decrease in measured nipple ROM. Results of this study suggest that the soft tissue over the rib markers moved in phase with the soft tissue of the breast, causing the torso segment origin to follow a similar displacement pattern to the nipple marker, only with reduced amplitude; resulting in smaller measurements of relative nipple position. The selection of torso reference frame may account for the large differences in nipple ROM reported in the literature (Zhou *et al.*, 2011).

It was proposed that without fixing the locations of the rib markers during construction of the torso reference segment it is not possible to accurately present positional breast data relative to the STN. Fixing the rib markers improved the stability of the segment origin relative to the STN marker, and provided an appropriate solution for comparisons of

breast data between different experimental conditions, or between individuals, with differing levels of soft tissue motion.

3.4.6. Conclusion

The previously published breast motion torso marker set was found to produce a torso segment (segment 1) with a residual of 6.8 mm during treadmill running at 10 kph. Using this segment, the torso origin position shifted away from the STN marker by up to 30.4 mm. The stability of the torso segment and segment origin was improved by adding a marker on the XP and fixing the location of the rib markers using landmarks (segment 3). For the same dynamic trial segment 3 had a residual of 5.6 mm and a maximum origin shift of 6.7 mm. The fixed rib approach was therefore selected for implementation within the thesis. One consideration with this new torso segment was the highly individual nature of each torso model. Due to differences in suprasternal notch to rib distance between individuals, each participant would require a separate construction of their torso segment during data analysis.

3.5. Methodological study 4: Development of the gold-standard buoyancy method for measuring the neutral breast position

Due to the novelty of the buoyancy method within a biomechanics setting, it was important to ensure that each aspect of the testing could be performed successfully using the available facilities. Several investigations were therefore performed to evaluate each aspect of the method prior to conducting the full-scale buoyancy method. These investigations assessed camera functionality and participant safety when using soybean oil; evaluating the practicality of the buoyancy testing procedure using water; the selection of an appropriate tank for use in the buoyancy study; and the development of a calibration object for taking measurements of the breast through fluid using video cameras.

3.5.1. Investigation 1: Assessing camera functionality and safety concerns when using soybean oil for immersion

Introduction

Following the systematic review of breast density (section 3.2), this thesis aimed to develop a gold-standard method for measuring the neutral breast position using buoyancy in both water and soybean oil. It was important to identify any alterations that may be required for the successful implementation of the buoyancy method in soybean oil. Primarily, the use of soybean oil was anticipated to reduce the visibility of the breast and torso markers in the buoyancy study and also to increase the safety requirements for testing participants. These factors were investigated in this section to inform the testing procedures used for the full buoyancy study.

Aims

1. Identify whether the underwater cameras have sufficient depth of field to record marker positions on participants when filming through soybean oil.
2. Assess whether the underwater cameras have sufficient resolution to distinguish between adjacent markers when filming through soybean oil.
3. Evaluate the safety concerns associated with immersing participants in soybean oil.

Method

Camera depth of field

The underwater camera (VB5C6 Submersible Colour Camera, Videcon PLC) depth of field was evaluated by placing a marker array (10 mm marker intervals) beneath several measuring cylinders with heights ranging from 120 mm to 480 mm (Figure 3.6). Each measuring cylinder was filled with soybean oil and an underwater camera was suspended vertically above each cylinder with the lens immersed in oil. A static image of the marker array was taken using the underwater camera in each cylinder to evaluate whether the marker array remained visible when filmed through increasing depths of oil. This process was then repeated in water for comparison.

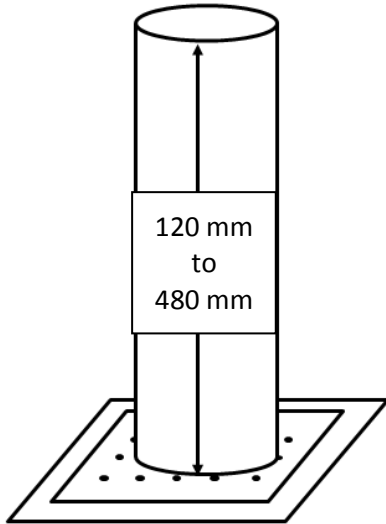


Figure 3.6: Measuring cylinders used to assess the maximum depth of field for the underwater cameras when immersed in soybean oil.

Camera resolution

Based on the rectangular breast marker array previously implemented in Rajagopal's (2007) buoyancy study (Figure 2.6 a), it was anticipated that the typical inter-marker distances would be approximately 20 mm, with no two markers separated by less than 10 mm (depending on torso and breast size). These distances provided the criteria for suitable camera resolution within this investigation.

Two marker arrays were drawn with waterproof eyeliner onto an acetate sheet, one with 10 mm marker spacing and the second with 20 mm marker spacing. The acetate was fixed to one end of a tank measuring 380 x 290 x 250 mm, and an underwater camera was attached to the opposite end using a suction pad (Figure 3.7). A static image of the markers was taken with the underwater camera with the tank filled with air, water and soybean oil. Images were then visually assessed to check that adjacent markers could be distinguished in images taken through all three fluids. Although this method was similar to the depth of field aspect of the investigation, it was anticipated that complete immersion of the camera in a larger quantity of soybean oil may have affected its functionality or resulted in insufficient light levels to identify markers.

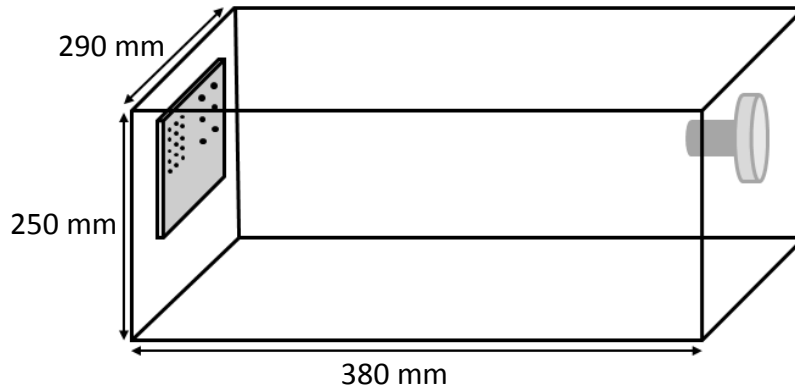


Figure 3.7: Apparatus used to assess the resolution of the underwater cameras when immersed in soybean oil.

Safety considerations

The final aspect of this investigation assessed the best safety protocols to implement when manoeuvring participants into and out of a tank filled with soybean oil. The slippery nature of the soybean oil meant that the primary concern was the safe movement of the participant into and out of the buoyancy tank when their hand and feet were covered in oil. To assess the risk of slipping during the buoyancy study one participant immersed their hands and feet in soybean oil before walking across the laboratory and climbing onto the first two rungs of a ladder (for entry into the tank). Various different methods were implemented to minimise the risk of slipping on each surface, including: non-slip shoes; non slip tape; non slip paint; non-slip rubber matting; and placing towelling on the floor. Several methods were also tested for their ability to remove the oil from the participant's skin following testing: sponges; washing up liquid; rubber squeegee; and towels.

Additional safety concerns associated with the use of soybean oil in the buoyancy study were the effect of prolonged contact with human skin and the safety procedures associated with handling and disposal of large quantities of oil. These were investigated using the known properties of soybean oil recorded on a material safety data sheet (Cargill, 2009).

Results

Camera depth of field

When filming through a depth of 480 mm, the 10 mm marker array could be seen in both the water and soybean oil conditions (Figure 3.8). This distance therefore represents the maximum acceptable camera to participant distance for the full buoyancy study. Comparison between the water (Figure 3.8 a) and soybean oil (Figure 3.8 b) images demonstrated that visibility was slightly reduced in the oil, although the markers were still sufficiently clear at this depth to be identified for data analysis.



Figure 3.8: A 10 mm marker array filmed through 480 mm of water (a) and soybean oil (b) to assess the depth of field of the underwater cameras used in the buoyancy study.

Camera resolution

Static images of both the 10 mm and 20 mm marker arrays were clear when filmed through all three fluids (air, water and oil) (Figure 3.9). It was anticipated that no markers on the breast or torso would be placed closer than 10 mm apart. Therefore, results of this investigation demonstrate that sufficient resolution for measuring breast position could be achieved using underwater cameras in soybean oil.

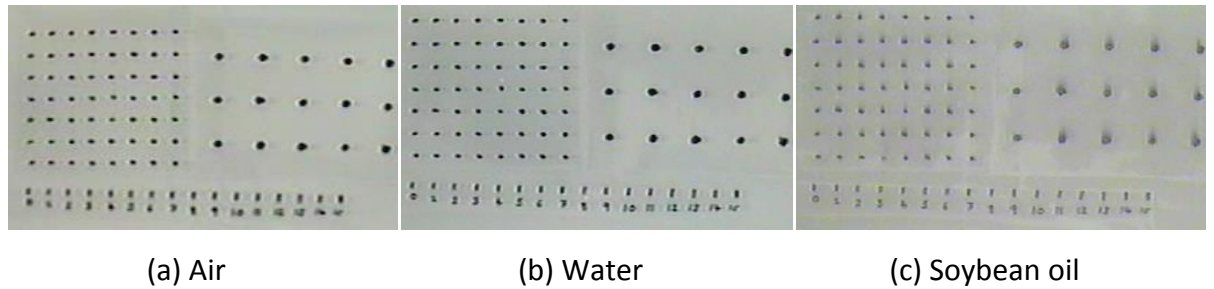


Figure 3.9: Images of 10 mm and 20 mm marker arrays filmed through air (a), water (b) and soybean oil (c) taken with the underwater cameras used for the buoyancy study.

Safety considerations

The participant used in this investigation was able to complete all required tasks following hand and foot immersion in soybean oil. Comparison of the various anti-slip surfaces demonstrated that non-slip tape provided the most friction on wet and highly slippery areas such as the rungs of the ladder and the inside of the tank. The squeegee was most effective at removing most of the oil from the participant's skin although a thorough wash with washing up liquid was still required afterwards.

Using data presented in the materials safety data sheet for RBD soybean oil (Cargill, 2009) a list of properties that may have affected the procedures used in the buoyancy study were recorded in Table 3.11.

Table 3.11: Properties of soybean oil.

Inhalation	High concentrations may be irritating to the respiratory system.
Eye contact	May cause temporary eye irritation.
Skin contact	Prolonged contact may cause skin dryness.
Ingestion	No harmful effects (seek medical attention if more than 0.5 litres are ingested).
Spillage procedure	Absorb spill with vermiculite or other inert material, then place in a container for chemical waste.
Boiling point	> 260°C
Flash point	> 260°C
Incompatible materials	Strong oxidizing agents.
Stability	Stable.
Toxicity	No adverse health effects noted.
Carcinogens	None.
Disposal methods	Do not discharge into drains, water courses or onto the ground.

Discussion

This investigation assessed the feasibility of adapting the buoyancy method to incorporate immersion in soybean oil. Due to the novelty of this approach it was unclear whether the required measurements of breast and torso markers could be achieved using the available underwater cameras. The first aspect of this investigation demonstrated that markers separated by 10 mm were visible through both water and oil up to a depth of 480 mm (Figure 3.8). This distance represented the maximum participant to camera distance permitted during the buoyancy study.

Investigation into the effect of a larger volume of soybean oil (approximately 27 litres) on marker visibility and camera resolution demonstrated that both 10 mm and 20 mm marker arrays were clearly visible in air, water and soybean oil (Figure 3.9). Comparison of the images obtained during the resolution investigation (Figure 3.9 a, b and c) show that the colour of the soybean oil (dark yellow) did not negatively affect the quality of the marker image.

The risk of slipping in the soybean oil was reduced by applying non-slip tape to the base of the tank and to the rungs and handrails of the ladder. The same tape was applied to all exposed surfaces in the full buoyancy study. Following hand and foot immersion in oil the most effective method for removing the oil was using a rubber squeegee followed by a thorough washing in washing up liquid. In the full buoyancy study the immersion tank was placed as close as possible to the shower facilities. A bucket and squeegee were provided adjacent to the tank for participants to remove most of the oil from their skin before showering with washing up liquid.

Investigation into the properties of soybean oil demonstrated that there was no toxicity risk associated with human contact although inhalation, ingestion and prolonged contact may have caused irritation. To reduce these risks in the full buoyancy study participant immersion time in the soybean oil was kept to a minimum, participants were only immersed up to the top of their torso and face masks were provided to prevent accidental ingestion. The flash point and boiling point of the oil (Table 3.11) were much higher than the thermoneutral temperature of human immersion (35°C) (Nakanishi, Kimura, & Yokoo, 1999), resulting in a minimal fire risk during the buoyancy testing. Organic oil absorbent granules (ISOL8, Environmental Absorbents, UK) were purchased for the clean-up of spillages during the buoyancy study and, on completion of the testing, the soybean oil was collected and disposed of in accordance with Government regulations by an external company (Envirogroup, UK). One important property of soybean oil was its incompatibility with oxidising agents, such as chlorine. Chlorine is commonly added to water to prevent the spread of diseases (Robinton & Mood, 1966), however its incompatibility with soybean oil meant that the oil could not be chlorinated for use in the buoyancy study. Instead, to reduce the risk of cross-contamination between participants, each participant washed thoroughly with anti-microbial gel (Clinitex, Rosebank Healthcare products, UK) before entering the immersion tank filled with soybean oil.

Conclusion

Results demonstrated that the underwater cameras had sufficient depth of field and resolution to be used for recording the breast marker array in both water and soybean oil. The risk of participants slipping during the buoyancy study was reduced using non-slip tape on exposed surfaces and the soybean oil could be successfully removed from the skin using a squeegee and washing up liquid. The duration of immersion in soybean oil was minimised to reduce the risk of skin, eye or respiratory system irritation associated with prolonged contact. As the soybean oil could not be chlorinated, participants were required to shower with anti-microbial gel prior to entering the buoyancy tank to minimise the risk of cross-contamination between participants. Spillages were absorbed using oil absorbent granules and the soybean oil was disposed of correctly by an external company.

This investigation demonstrated that, in principle, the buoyancy neutral position study could be conducted in both water and soybean oil. However, the full testing procedure had not yet been conducted in a biomechanical environment. The next stage of this methodological study therefore investigated the feasibility of the buoyancy testing using water.

3.5.2. Investigation 2: Practicality testing of the buoyancy method using water

Introduction

As the buoyancy method had only previously been implemented within a clinical setting, this investigation aimed to evaluate whether this method could be implemented within the biomechanics laboratory, and whether nipple position could be recorded using video cameras during immersion. Due to the cost and logistical problems associated with large quantities of soybean oil, this investigation used water to aid development of the buoyancy testing procedure before implementing the finalised method in both water and soybean oil within the full buoyancy study (Chapter 4).

Aims

1. To implement the buoyancy method using water within the biomechanics laboratory.
2. To attain a three dimensional measurement of the nipple position using video cameras when immersed in water.

Method

Seven female participants with breast sizes ranging from 30 to 34 inch under band and A to HH cup size gave informed consent to take part in this investigation. A large immersion tank measuring 2.16 x 1.38 x 1.57 meters was filled with chlorinated water at 35°C and three 25 Hz underwater cameras were fixed to three walls of the tank using suction pads (Figure 3.10). The cameras were calibrated using a sputnik calibration frame (Figure 3.11). The centre of the calibrated volume was marked on the edges of the water tank to allow correct positioning of participants during testing.

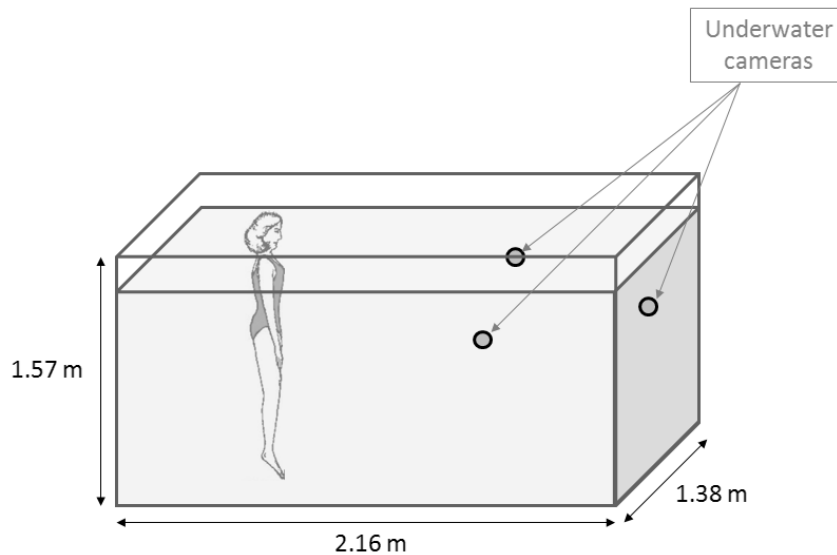


Figure 3.10: Immersion tank used in Investigation 2, to assess the practicality of the buoyancy method in the biomechanics laboratory using water.

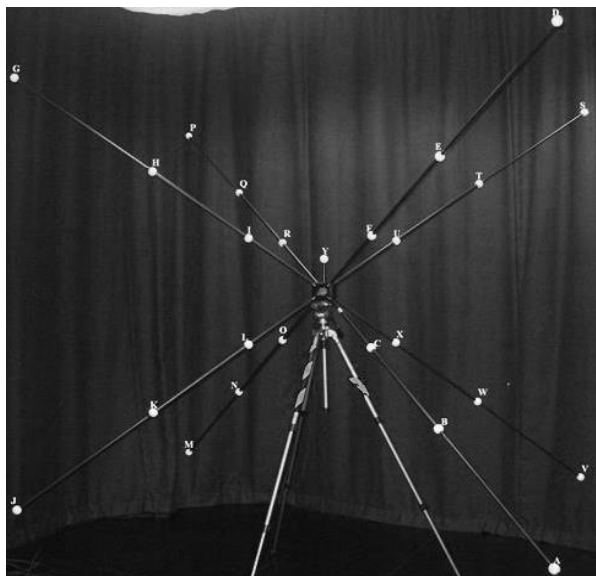


Figure 3.11: Sputnik calibration frame used in the buoyancy practicality investigation using water.

Each participant had the marker set described in section 3.3 applied by hand using waterproof eyeliner (Figure 3.2). Participants then stood bare-breasted, with their arms by their sides, in the centre of the calibrated volume with the water level just covering the marker on their suprasternal notch. Once any water movement had subsided, a short video recording (four frames) was taken from all three video cameras simultaneously

using an external trigger. This recording duration was the maximum length achievable with the external trigger used in this practicality investigation. The recording process was performed three times with the participant moving freely between trials.

The nipple and body markers in each video recording were digitised manually using SIMI software (version 8.5.5, Tracksys Ltd). The 3D co-ordinates of each marker were reconstructed using a 16 order direct linear transform (16-DLT) within SIMI and were exported to Visual 3D (v4.82.0, C-Motion) for further analysis. The DLT calibration method has been the most popular method for reconstructing underwater data in existing literature (Kwon & Casebolt, 2006). POSE estimation was used in Visual 3D to create a torso segment in which the proximal and distal ends of the segment were defined using the suprasternal notch and rib markers respectively. The mean position of the left nipple marker across the three trials was calculated in the LCS of the torso and was used to represent each participant's mean nipple position in water.

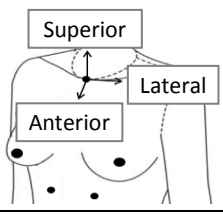
The buoyancy method was deemed practical if participants were able to complete the required tasks during data collection, and if the data collected could be used to measure nipple position in the LCS of the torso. These two criteria had to be achieved before the gold-standard buoyancy method could be conducted. Any problems with the implementation of the buoyancy method were also identified and overcome within this investigation.

Results

Table 3.12: Practicality results for the buoyancy in water method.

Practicality measure	Outcome
Method implemented successfully?	Yes
Could the nipple position be measured?	Yes

Table 3.13: Mean left nipple position in the LCS of the torso while immersed in water during the buoyancy practicality investigation (n = 7).

	Breast size	Left nipple position (mm)		
		Anterior-posterior	Medial-lateral	Superior-inferior
Participant A	32A	47.1	97.3	-139.3
Participant B	32C	57.5	97.4	-149.8
Participant C	32C	48.6	107.5	-120.5
Participant D	34C	57.6	96.4	-142.7
Participant E	34D	70.0	90.0	-120.7
Participant F	34DD	76.0	123.2	-126.1
Participant G	30 HH	99.7	113.1	-169.1
Mean		65.2	103.6	-138.3

Discussion

The buoyancy method was piloted successfully with all seven participants in water. All participants were willing and able to perform the required task. Most notably this method did not cause discomfort to the large-breasted participants, which had been a limitation for previous studies implementing bare-breasted activities (McGhee *et al.*, 2007). However, it was observed that some participants found it difficult to maintain a static standing position in the water. The buoyancy method was therefore adapted for the gold-standard buoyancy study; measurements of nipple position were taken while participants sat in a stationary upright position.

The nipple and body markers were easily visible through the water and did not wash off or smudge during testing. Manual digitisation of the calibration frame and participant measurement trials from the three video cameras enabled the reconstruction of 3D co-ordinate data for each marker within SIMI. The 3D co-ordinate data was then successfully exported to Visual 3D where relative nipple position was calculated in the LCS of the torso. The compatibility between video data collected using SIMI and the data analysis

software (Visual 3D) typically used for optoelectronic data, was an important consideration within this thesis. There were several occasions within this thesis where comparisons were made between breast measurements taken with optoelectronic and video camera systems. It was therefore important to ensure that raw data collected using both of these systems could be analysed in precisely the same manner, to avoid incorrect conclusions arising from inconsistencies in data analysis processes such as those discussed in section 2.3.

Although mean nipple position could be measured in this investigation (Table 3.13), the short measurement duration (4 frames, 0.16 s) achievable using the external trigger was not acceptable for use in the gold-standard buoyancy study. Recording durations of at least 10 frames (0.4 s) are required to implement a generalised cross-validators data filter, which had been identified as the most appropriate filtering technique for the data within this thesis (section 2.3.3). Measurement durations of at least 0.25 s had also been shown to accurately represent the mean nipple position measured over a standard 2 s static measurement trial (section 3.3). To enable longer duration measurement trials in the gold-standard buoyancy study the external recording trigger was not used to start the video recordings. Instead, each of the three cameras set to record continuously for 3 s and a light emitting diode (LED) was switched on used to identify a synchronised start point in each measurement trial from which 10 frames of data could be analysed.

A large immersion tank (4680 litres) was used successfully in this preliminary buoyancy testing using water. However, use of the same tank for buoyancy testing in soybean oil would have incurred significant financial costs, as the price of soybean oil was approximately £1 per litre at the time of testing. It was therefore beneficial to further investigate the minimum volume of fluid required to replicate the full buoyancy method in both water and soybean oil.

Conclusion

Participants were able to complete the buoyancy testing procedures in the biomechanics laboratory, and 3D measurements of nipple position could be taken underwater using

three synchronised video cameras. Three adaptations to the buoyancy method were implemented following the practicality testing. Firstly, a sitting position was adopted during measurement trials to improve the precision of the neutral nipple measurements. Secondly, the external recording trigger was substituted for longer video recordings synchronised with an LED signal, enabling the consistent application of generalised cross-validatory spline filters (requiring 10 frames of data) to all neutral position data collected within this thesis. Finally, further work was required to investigate whether a smaller tank could be used during the full buoyancy testing to reduce the financial costs associated with implementation of this method using soybean oil.

3.5.3. Investigation 3: Selecting a tank for the buoyancy study

Introduction

One of the main concerns with the buoyancy method was the potential cost associated with performing this experiment in soybean oil. Therefore, time was spent analysing the minimum tank dimensions (and therefore volume) required to ensure that participants could sit comfortably in an upright position while their breast and body were immersed in fluid.

Aim

1. Select a suitable tank for use in the buoyancy study based on the minimum tank dimensions required for participants to comfortably remain upright during immersion.

Method

Five participants gave informed consent to take part in this investigation. Participants sat cross-legged on the floor and the following measurements were taken using a tape measure: suprasternal notch to floor height (Figure 3.12 a); the maximum width of the

body (Figure 3.12 b); and the maximum depth of the body (Figure 3.12 c). The largest values of each measurement were used to define the minimum required tank dimensions.

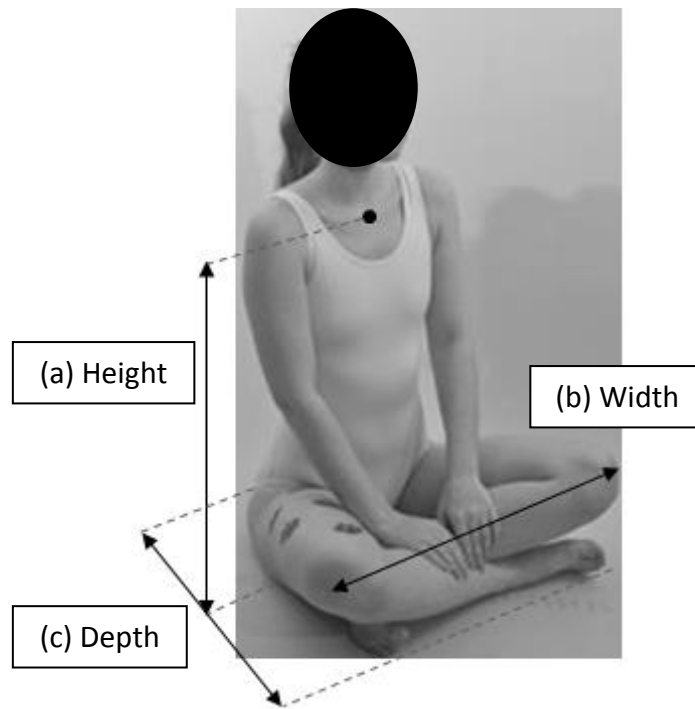


Figure 3.12: Body measurements taken to assess minimum tank dimensions for the buoyancy study.

Results

The largest sitting dimensions of the women measured were 600 mm x 700 mm x 720 mm. However, some participants found it uncomfortable to sit cross legged on the floor and struggled to keep their back straight and torso upright in this position. It was therefore decided to introduce a small stool into the tank for participants to sit on. The smallest adjustable stool available had a minimum height of 270 mm (maximum height 540 mm), therefore increasing the height requirement of the tank to 870 mm, with the width and depth measurements unaffected. A suitable 600 litre D-shaped tank was identified and purchased for use in the gold-standard neutral position study (Figure 3.13).

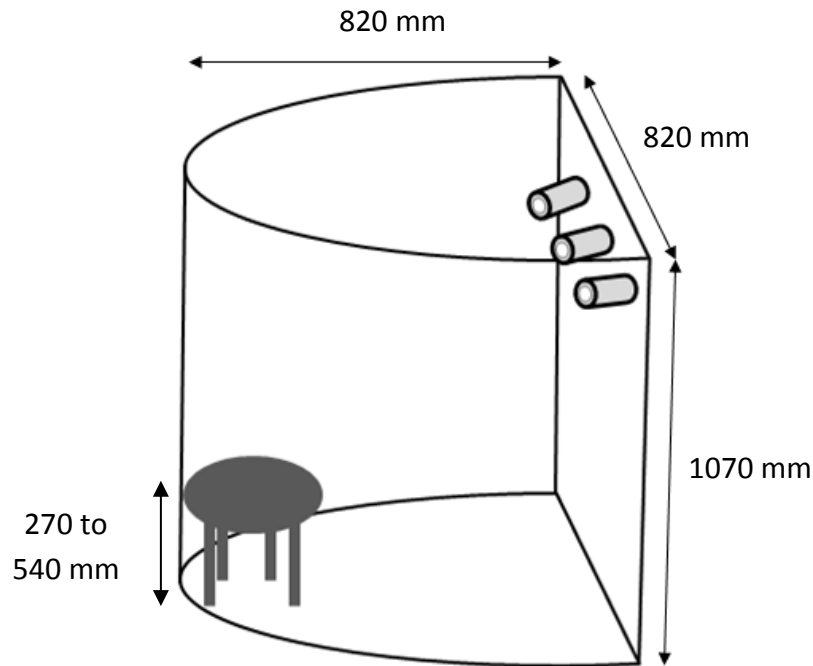


Figure 3.13: Tank selected for use in the buoyancy study based on the minimum dimensions required for participants to comfortably remain upright during testing.

Discussion

A 600 litre D-shaped tank was purchased for the buoyancy neutral position study. The shape of the tank meant that participants could sit with their back to the narrow curved wall while still having sufficient space in front and to the side for them to sit comfortably in the required upright position. A square tank of the same dimensions would have required a larger volume of soybean oil to attain the same depth of fluid for the buoyancy study and was not considered necessary for participants to achieve the correct posture.

The minimum depth requirement of the tank was 870 mm based on measurements of participants within this investigation. However, a deeper tank was selected so that the tank did not have to be completely filled during testing. The additional height of the tank above the required fluid level was anticipated to reduce the risk of spillage during testing.

Conclusion

A 600 litre D-shaped tank was purchased for use in the buoyancy study. The dimensions of the tank (820 x 820 x 1070 mm) were sufficient to enable participants to maintain an upright position while sitting. The selection of a smaller tank than had been used in the practicality investigation (section 3.5.1) meant that the sputnik calibration frame (Figure 3.11) was too big to be used in the buoyancy study. The next stage of this methodological study therefore focused on developing a new calibration object for use in the buoyancy study.

3.5.4. Investigation 4: Developing a calibration object for the buoyancy study

Introduction

To obtain quantitative measurement data from video recordings it was first necessary to calibrate the required measurement volume using an object with known dimensions (Zhang, 2001). The sputnik calibration frame used in investigation 1 was too big to be used in the tank selected for the full buoyancy study (section 3.5.3). Therefore a new smaller calibration object had to be constructed. To develop an appropriate calibration object it was necessary to identify the maximum camera field of view achievable within the D-shaped tank. The camera field of view dictated the maximum dimensions of the calibration object, and subsequently the maximum volume available for taking breast measurements. Considering that the buoyancy method involved measuring the breast through fluid (water and soybean oil) it was necessary to ensure sufficient calibration points were visible within the measurement volume to allow for fluid distortion to be accounted for during data analysis. Video data were analysed using the SIMI software which specified that at least 16 calibration points needed to be visible to all cameras for a 16-DLT calibration method to be applied, allowing fluid distortion to be accounted for.

Aims

1. Identify the maximum field of view of the three underwater cameras in the D-shaped tank used for the buoyancy study.
2. Construct a calibration object with at least 16 calibration points visible to all cameras inside the tank used for the buoyancy study.

Method

The three underwater cameras were attached using suction pads to the flat wall of the D-shaped tank selected for use in the buoyancy study (Figure 3.13), and the tank was filled with water. A variable object was constructed using 10 plastic 300 mm rulers (Figure 3.14), immersed in the water, and observed using the three underwater cameras. The dimensions of the variable object were gradually increased until the largest volume that could be seen by all three cameras was achieved. At this point, the dimensions of each side were recorded and used to define the maximum visible calibration volume attainable within the tank.

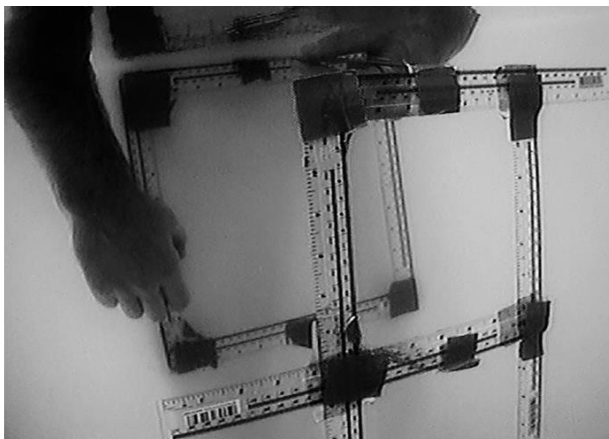


Figure 3.14: Variable object used to identify the maximum calibration volume inside the D-shaped buoyancy tank.

Once the maximum visible volume inside the tank had been established a new calibration object could be constructed. A steel block measuring 60 mm x 55 mm x 35 mm provided

the core of the new calibration object. Seven 5 mm diameter holes were drilled through the block as illustrated in Figure 3.15.

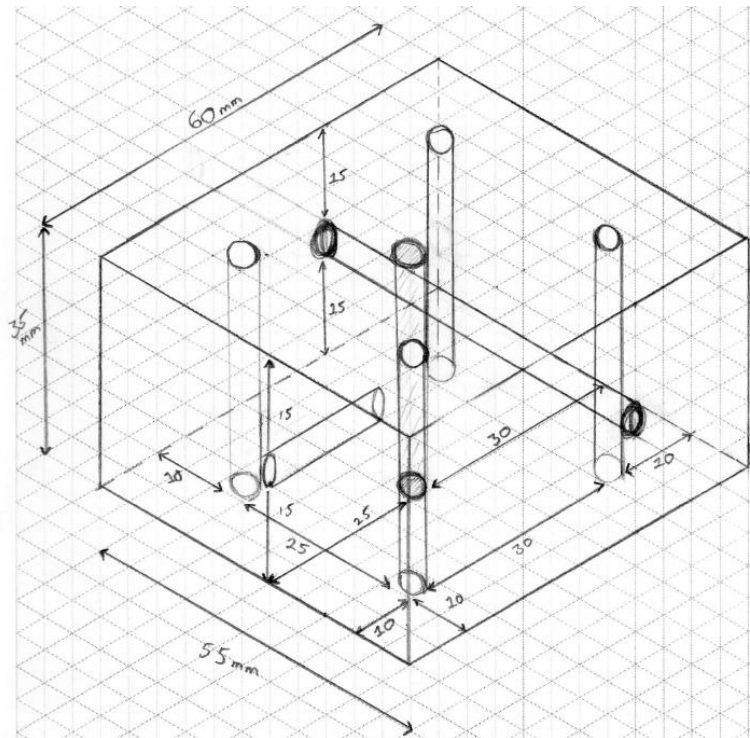


Figure 3.15: Dimensions of the steel block used to construct the calibration object for the buoyancy study.

Four steel rods (5 mm diameter) were threaded vertically through the corners of the steel block, and bent in such a way that they extended to each corner of the calibration volume identified previously. Three additional rods were inserted to the steel block, one vertically extending towards the top and bottom of the calibration volume; the second horizontally extending towards the right and left sides of the calibration volume; and the third horizontally extending towards the front of the calibration volume. The rods were secured in place using a water and oil resistant epoxy putty (Quick Steel reinforced epoxy putty, CarGo, UK). Thirty six rubberised beads (20 mm diameter) were then drilled using a 5 mm drill bit and were threaded onto the steel rods so that they were distributed throughout the measurement volume. The beads were glued in place and an additional 350 mm x 300 mm frame was constructed from the steel rods and attached to the back of the calibration frame using epoxy putty, improving the rigidity of the calibration frame. Once complete the 3D positional co-ordinates of each bead were measured by the

University engineering department using a co-ordinate measuring machine (CMM) (BN706, Mitutoyo UK) with an accuracy of 0.005 mm.

Results

The maximum visible volume using the three underwater cameras inside the D-shaped tank was a trapezoidal prism with a 350 mm square back face; a 250 mm square front face; and a depth of 300 mm (Figure 3.16). This volume defined the maximum dimensions of the calibration object used for the buoyancy study.

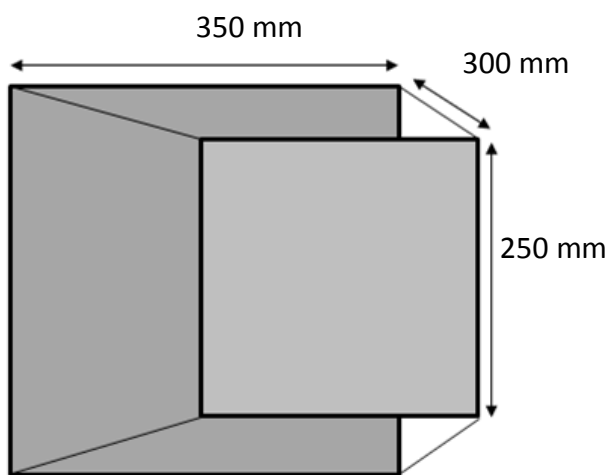


Figure 3.16: Maximum visible volume using three underwater cameras inside the D-shaped buoyancy tank.

A custom-made calibration frame was developed with maximum dimensions equal to the maximum visible volume in the buoyancy tank (Figure 3.17). A total of 36 calibration points were distributed throughout the visible volume to ensure that at least 16 markers would be visible to all cameras during data analysis.

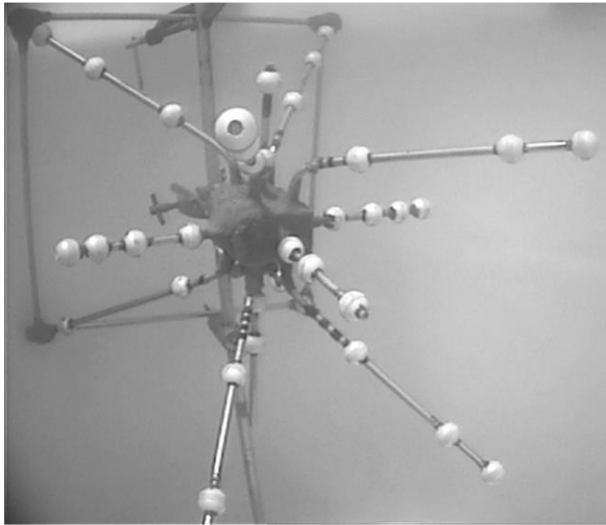


Figure 3.17: Custom-made calibration object developed for the buoyancy study.

Discussion

The maximum visible volume inside the D-shaped buoyancy tank defined the maximum dimensions of the calibration object used for the buoyancy study, and also the maximum torso and breast dimensions for any participants used in the full-scale testing. Any calibration points or participant markers that lay outside of this volume may have been lost during data collection.

A calibration object was successfully constructed that met the requirements for the buoyancy study. The maximum dimensions of the object were defined using the visible volume identified previously and a total of 36 markers were used to ensure that a 16-DLT calibration method could be applied within SIMI. The steel core and steel rods used in the calibration frame were selected to be as small as possible without compromising the strength or rigidity of the object. It was crucial that the calibration object remained rigid throughout repeated immersions (in water and soybean oil) and through repeated cycling of temperatures between room temperature (approximately 21°C) and the temperature of the fluid (up to 37.1°C). Any deviations in relative marker positions on the calibration object may have caused inaccurate calibrations and consequently inaccurate breast measurements in the buoyancy study. On the other hand, the use of excessively thick

steel during construction of the calibration object may have obscured several markers from the view of each camera.

Conclusion

A custom made calibration frame was constructed for use in the buoyancy study (Figure 3.17). The dimensions of the object, and the distribution of markers throughout the measurement volume, were designed to permit a 16-DLT calibration method within the SIMI software.

3.6. Summary of methodological developments

This chapter aimed to establish the most appropriate experimental methods for measuring the neutral breast position, with a particular focus on developing the buoyancy method already established within the literature. Systematic review of the mass-density of the breast revealed that the calculated breast mass-densities of 17,593 women aged 18 to 90 years, varied from 919 kg.m^{-3} to 986 kg.m^{-3} (Table 3.1). A gold-standard estimate of the neutral breast position was proposed using the mid-point between the breast positions in two fluids with mass-densities above (water) and below (soybean oil) the reported range of breast mass-densities (section 3.2). Investigation into the influence of breathing state and duration on measurements of nipple position demonstrated that the most accurate and precise measurement of static relative nipple position could be obtained in the uncontrolled breathing state using measurement durations between 0.25 s and 2.00 s (section 3.3). A novel method for constructing the torso segment was developed to reduce the influence of soft tissue motion on the origin position of the torso, enabling a better comparison of nipple position calculated in static and dynamic testing conditions (section 3.4). The novel torso segment was constructed using the recommended breast motion marker set, with an additional tracking marker on the xiphoid process and the rib markers replaced with fixed rib landmarks. Feasibility assessment of the proposed gold-standard buoyancy method demonstrated that the method could be performed in water, and that minimal adaptations were required to implement the buoyancy method using soybean oil (section 3.5).

The methodological developments established within this chapter were subsequently implemented in a study investigating the gold-standard measurement of the neutral nipple position using immersion in both water and soybean oil.

4. Measuring the neutral nipple position using the gold-standard buoyancy method

4.1. Introduction

This chapter focused on the implementation of the new gold-standard buoyancy method (using water and soybean oil) to measure the neutral (unloaded) position of the nipple. The nipple has been commonly used to represent the breast in breast motion research and also provides an important anatomical landmark for clinical measurements (Chen *et al.*, 2012; Hansson *et al.*, 2014; Zhou *et al.*, 2011). Identification of the neutral nipple position therefore enables the direct inclusion of the neutral position into biomechanical measures of nipple motion and clinical measures such as suprasternal notch to nipple distance. The static gravity-loaded nipple position was also included within this chapter to enable the effect of gravity on breast position to be quantified. A more detailed assessment of the neutral breast position is presented in Chapter 7 for the assessment of breast strain. The accuracy and precision of the new gold-standard method was evaluated using absolute difference, paired samples t-tests, standard deviations and TEMs, with the acceptability criteria for each variable outlined in sections 2.6.2 and 2.6.4.

4.2. Aims

1. Determine the three dimensional position of the nipple when fully supported in water and in soybean oil, and calculate the neutral position as the mid-point between these two positions.
2. Evaluate the effect of gravity on the breast by comparing the neutral (unloaded) nipple position to the gravity-loaded nipple position in the laboratory.
3. Assess the accuracy and precision of the gold-standard buoyancy method for measuring the neutral nipple position.

4.3. Method

4.3.1. Experimental procedure

Following institutional ethical approval, 14 females, with breast sizes ranging from 30 to 34 inch under band and B to E cup size, gave written informed consent to take part in this study. All participants were aged between 20 and 27 years, were nulliparous, had not undergone surgical procedures on their breasts, had not exposed their breasts to UV radiation within the last three months, and were recreationally active.

Participants in this study attended an initial screening session followed by three separate experimental testing sessions. The first experimental session involved the application of the breast and torso marker set using henna, while the second and third sessions incorporated the buoyancy testing in water and soybean oil respectively. The time taken to complete all three testing sessions was kept within 22 days to minimise the requirement for re-application of the henna markers which had a reported durability of up to 42 days on the breast skin (Wurstbauer *et al.*, 2001). The time interval between the second and third testing sessions was kept within a 14 day period to minimise any changes in breast size or shape that may have occurred between testing sessions (Hussain *et al.*, 1999).

Session 0: Initial screening

Prior to participating in this study each participant attended an initial screening session in the biomechanics laboratory. Participants completed a health history questionnaire and had a skin test involving henna application to their torso. Women with medical contraindications or who had a reaction to the henna application were excluded from further participation in this study. Participants who met the inclusion criteria had their height and mass measured, and their bra size assessed by a trained bra fitter using best-fit criteria (McGhee & Steele, 2010b). The bra used to fit each participant was the Marks and Spencer seam-free plain under-wired non-padded T-Shirt bra, made from 92% cotton and 8% elastane. A breast health questionnaire was used to record any factors that may

have influenced the elasticity of the participants' breast skin, and therefore their measured neutral breast positions. Participants were ordered in ascending cup size within each cross grading group and were each allocated a participant number to allow comparison of individual data across conditions without compromising participant anonymity. Participant measurements and information obtained through the breast health questionnaire that may have influenced the measured neutral breast position was recorded in Table 4.1. During this session participants were provided with an information leaflet detailing the procedures and requirements for each subsequent testing session (Appendix C).

Table 4.1: Participant information for the 14 women who took part in the gold-standard buoyancy study.

Participant Number	Cross grading group	Breast size	Age (years)	Height (m)	Mass (kg)	BMI (kg.m ⁻²)	Participation in bare-breasted exercise (no. of times)	Sports bra use	Previously sunburnt on chest?	Days between testing sessions 2 and 3 (days)
Participant 1	34A	32B	23	1.67	59	21.2	1-5	Very often	Yes	6
Participant 2		32B	25	1.74	61	20.1	1-5	Always	No	2
Participant 3		32B	27	1.71	68	23.3	1-5	Very often	Yes	6
Participant 4	34B	34B	21	1.76	72	23.2	1-5	Very often	Yes	2
Participant 5		32C	22	1.59	60	23.7	1-5	Never	No	2
Participant 6		32C	25	1.65	54	19.9	6-10	Sometimes	No	8
Participant 7	34C	32D	20	1.55	54	22.5	1-5	Rarely	Yes	3
Participant 8		32D	22	1.65	65	23.9	1-5	Always	No	14
Participant 9		32D	22	1.73	63	21.0	6-10	Always	No	8
Participant 10	34D	34D	26	1.79	74	23.2	10-30	Always	No	7
Participant 11		32DD	21	1.61	59	22.9	1-5	Sometimes	No	3
Participant 12		30E	24	1.64	63	23.6	1-5	Always	Unknown	3
Participant 13	34DD	34DD	23	1.69	82	28.7	1-5	Always	No	2
Participant 14		34DD	26	1.62	65	24.8	30+	Always	Yes	2
Mean/mode			23	1.67	64	23.0	1-5	Always	No	5
Standard deviation			2	0.07	8	2.2				4

Session 1: Marker application

During the first session a semi-permanent marker set was applied to the breast and torso using henna (Figure 4.1). The locations of the breast markers were based on Rajagopal's rectangular breast array illustrated in Figure 2.6 (section 2.3.3). The henna markers were covered with surgical dressing (Tegaderm film, 3M, USA) for up to two days to ensure maximum absorption and persistence (Wurstbauer *et al.*, 2001). Participants were asked to refrain from prolonged contact with water following marker application and were sent a daily email reminder to check that all markers were still visible until all three testing sessions had been completed. Each participant was also provided with a sterile surgical marker pen (Cory Bros, UK) to apply over any henna marks that had faded.

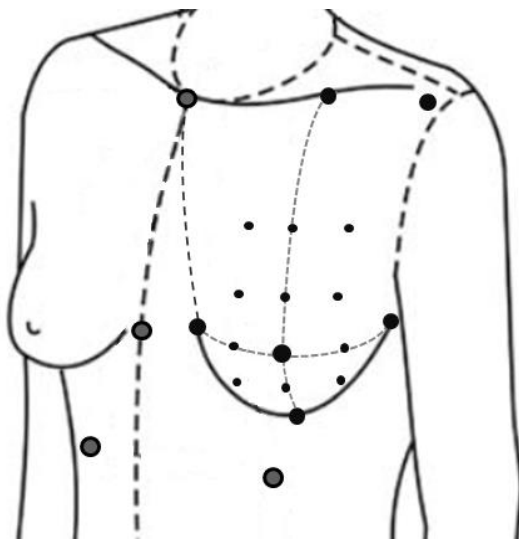


Figure 4.1: Henna marker array used in the gold-standard neutral position study.

The torso marker set was based on the recommended breast motion marker set (Scurr *et al.*, 2010) with an additional tracking marker on the xiphoid process as recommended by ISB (Wu *et al.*, 2005) and evaluated in section 3.4. A marker array was used over the breast to allow the subsequent evaluation of strain on the breast skin. However, only the nipple marker will be used in this chapter to provide a single value for the neutral breast position that could be incorporated into measurements of breast motion obtained using the nipple marker.

Session 2: Static testing in the laboratory and buoyancy testing in water

The second testing session included measurements of the static gravity-loaded nipple position followed by implementation of the buoyancy method using water. The gravity-loaded measurements were performed in the biomechanics laboratory. Eleven optoelectronic cameras (Oqus, Qualisys, Sweden) were set up in an arc around the centre of the laboratory and were calibrated using the standard Qualisys calibration axis and wand. Retro-reflective markers were applied over the participants' henna markers using hypoallergenic tape: 12 mm diameter spherical markers were used for the torso markers; 12 mm diameter flat circular markers were used for the nipple; and 6 mm diameter flat circular markers were used for the 16 other breast markers. Participants stood stationary in the centre of the biomechanics laboratory with their back straight and their arms relaxed by their sides. The 3D position of each marker was recorded at 200 Hz for three 1 s trials. The mean nipple position from these trials represented the gravity-loaded nipple position for each participant at the time of buoyancy testing in water.

Participants then completed the buoyancy testing in water in the customised 600 litre D-shaped tank (Figure 3.13). The tank was filled with chlorinated water and heated to 35°C using an immersion heater. This temperature represented the thermoneutral temperature for stationary water immersion (Nakanishi *et al.*, 1999). The water temperature in the tank was measured continuously (to the nearest 0.1°C) using a digital LCD underwater thermometer (Digiflex, UK), and a temperature between 32.4°C ($\rho_{\text{water}}^{32^\circ} = 995 \text{ kg.m}^{-3}$ (Kell, 1975)) and 37.1°C ($\rho_{\text{water}}^{37^\circ} = 993 \text{ kg.m}^{-3}$ (Kell, 1975)) was maintained throughout testing. The three underwater cameras were attached to the flat wall inside of the tank using suction pads. An adjustable shower stool was used in this study to allow participants to maintain a stationary upright torso position during measurements of the neutral nipple position (section 3.5.1). The adjustable shower stool was placed against the curved wall of the tank and was adjusted so that each participant's breast and torso markers were below the water level. The cameras were calibrated prior to each participant's testing session using the custom made star-shaped calibration frame (described in section 3.5.3) (Figure 3.17). Following calibration, water was carefully

removed from the tank to compensate for the water displacement that occurred as each participant entered the tank (0.001 m^3 per kg of participant mass).

The four spherical retro-reflective markers on each participant's torso were removed and black waterproof eyeliner was used to darken the henna torso markers. Eyeliner was also applied to the centre of each flat retro-reflective marker on the breast, ensuring that each marker was clearly visible in the camera image. Two stepladders were used to aid access to the tank, one on the outside and the other on the inside of the tank (the latter was removed before taking measurements). When inside the tank, participants sat as still as possible with their suprasternal notch marker just below the water level, their arms by their sides, their back straight and their shoulders relaxed. The buoyancy measurements commenced once any water movement had subsided. Each video camera was set to record for 3 s at 25 Hz. Once all cameras were recording a waterproof LED was illuminated to identify a synchronised start-point in each camera view for data analysis. Video data was analysed for 0.4 s following LED illumination (section 3.3). This process was repeated three times for each participant.

Session 3: Static testing in the laboratory and buoyancy testing in soybean oil

Participants attended the third testing session within two weeks of completing the water testing. During this session measurement of the gravity-loaded nipple position was repeated and the buoyancy testing was performed using soybean oil. The gravity-loaded measurements were performed in the biomechanics laboratory following the same procedure described for session 2. The mean nipple position from the three static trials taken during this session represented the gravity-loaded nipple position for each participant at the time of buoyancy testing in soybean oil.

Prior to conducting the buoyancy testing in soybean oil, the D-shaped tank was thoroughly dried and non-slip tape (black/yellow anti-slip self-adhesive tape, Faithfull tools, UK) was applied to the base and top of the tank, the shower stool, the steps and handrails of the ladders, and any other areas where there was a risk of participants slipping (Figure 4.2 a). Non-slip tape was also applied around the suction pads attached

to the video cameras to prevent them from slipping on the tank wall during testing (Figure 4.2 b). For 24 hours prior to conducting the buoyancy testing, the soybean oil was placed in a heat chamber at 37°C to raise the oil temperature just above the thermoneutral temperature of 35°C (Nakanishi *et al.*, 1999).



(a)

(b)

Figure 4.2: Non-slip tape used on the outside (a) and inside (b) of the D-shaped tank during the buoyancy study using soybean oil.

All 14 participants completed the buoyancy in soybean oil testing on the same day. On the morning of the study the D-shaped tank was filled with the warm soybean oil (Figure 4.2 b). The temperature of the oil was measured continuously using the digital thermometer and the immersion heater was used to warm the oil between participants. A temperature between 30.9°C ($\rho_{\text{oil}}^{30^\circ} = 913 \text{ kg.m}^{-3}$ (Esteban, Riba, Baquero, Rius, & Puig, 2012)) and 32.9°C ($\rho_{\text{oil}}^{37.8^\circ} = 909 \text{ kg.m}^{-3}$ (Pryde, 1980)) was maintained for the duration of the oil testing. The oil was not chlorinated during testing. To minimise the risk of contamination, participants were required to shower with anti-microbial gel (Clinitex, Rosebank Healthcare products, UK) before entering the tank. Once inside the tank, the measurement procedure described for session 2 was repeated in the soybean oil.

4.3.2. Measurement analysis

The 3D trajectories of the torso and breast markers collected in the biomechanics laboratory with the optoelectronic camera system were identified in QTM and exported to Visual 3D. The data collected in the buoyancy testing was initially analysed using SIMI. The calibration recordings for each participant were manually digitised in SIMI and a 16 order DLT was used to correct for any distortion caused by the fluid. The participant files (torso and nipple markers) were also digitised manually in SIMI for the 10 video frames (0.4 s) following the LED illumination, enabling a cross-validatory spline filter to be used. Each participant file was assigned to the corresponding calibration file (taken with the same camera for the same participant), allowing the 3D trajectories of each marker to be reconstructed and exported to Visual 3D.

Within Visual 3D, torso segments were defined using the STN, XP, and two fixed rib landmarks as described for segment 3 in section 3.4. Four separate torso models were constructed for each participant in each measurement condition (laboratory (session 2), laboratory (session 3), water, and oil). Multiple models were required because the distance from the STN to rib markers was different in each testing condition, requiring the construction of unique rib landmarks, and therefore torso model definitions, for each set of measurements. Each participant's measurement trials were then assigned to their corresponding torso model within Visual 3D. The 3D co-ordinate data from each trial was filtered using a generalised cross-validatory quintic spline and the mean position of the left nipple marker was calculated in the water, oil and laboratory conditions relative to the torso (Figure 4.3).

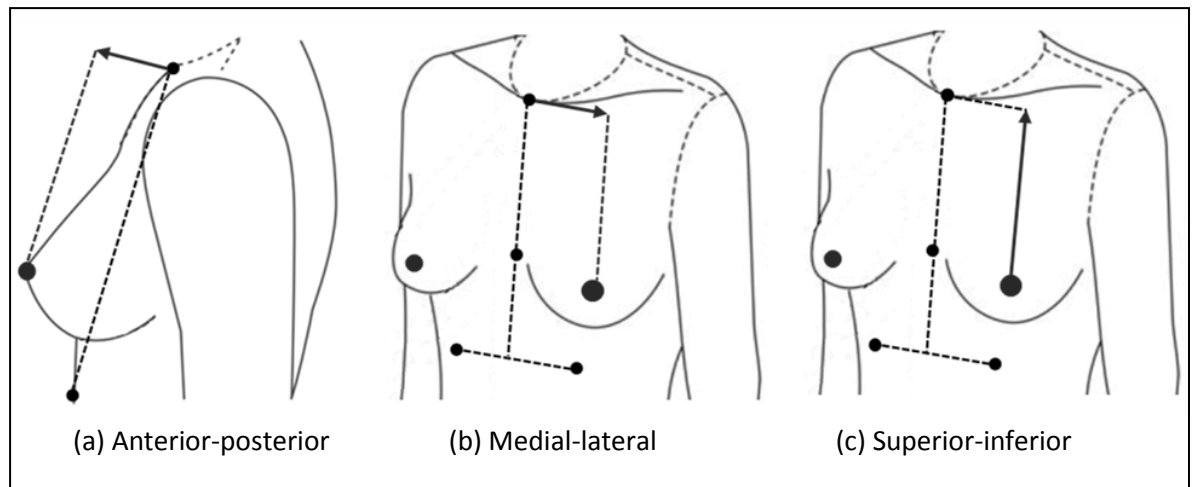


Figure 4.3: Directional components of left nipple position when calculated relative to the torso segment (arrows show the positive direction along each axis).

Three trials were used to calculate mean nipple position in the water and oil conditions, whereas six trials were used in the laboratory condition (three from each testing session) to represent the mean nipple position over the duration of the study. The mid-point between the mean nipple position in oil and water was calculated in Excel, and was used to provide the gold-standard estimate of the neutral breast position for each participant. Comparisons between the neutral nipple position and the mean gravity-loaded nipple position in the laboratory were used to evaluate the gravitational effect on nipple position. Pearson's correlations were performed using SPSS (IBM SPSS statistics version 20) to investigate the relationships between participants' physical characteristics (Table 4.1) and their neutral and gravity-loaded nipple positions. Correlation coefficients of ± 0.1 , ± 0.3 , and ± 0.5 indicated small, moderate and large effect sizes (Field, 2009).

4.3.3. Accuracy analysis

As discussed in section 2.6.1, the buoyancy method presented in this chapter represents the gold-standard method for measuring the neutral nipple position. As such, the accuracy of this method cannot be assessed by comparing the results to an alternative, more accurate, technique. However, it was possible to calculate the measurement error

Chapter 4: Measuring the neutral nipple position using buoyancy

associated with this method by calculating the absolute difference between measurements of the calibration object and its known dimensions. Maximum measurement error must not have exceeded 2 mm if the new gold-standard method was to be recommended for use in place of the previously published methods (section 2.6.2).

To evaluate the measurement error associated with the gold-standard buoyancy method three calibration trials, consisting of three camera views of the same calibration frame, were selected from the water condition and three from the oil condition. These files were selected based on the digitising error reported within the SIMI software. The three least accurately digitised calibration trials were selected in each condition to enable the maximum measurement error to be calculated.

Each of the selected calibration files were duplicated to provide a calibration and measurement version of the same file. Six calibration points were used to represent the known locations of six breast and torso markers (STN, right and left ribs, XP, right and left nipples) (Figure 4.4). These six points were deleted from each calibration file and each camera was re-calibrated using the remaining calibration points. The measurement files were then imported to SIMI and allocated to the corresponding calibration file. The six markers were manually digitised for 10 frames in each trial and the 3D co-ordinates of each marker were reconstructed in SIMI and exported for analysis in Visual 3D.

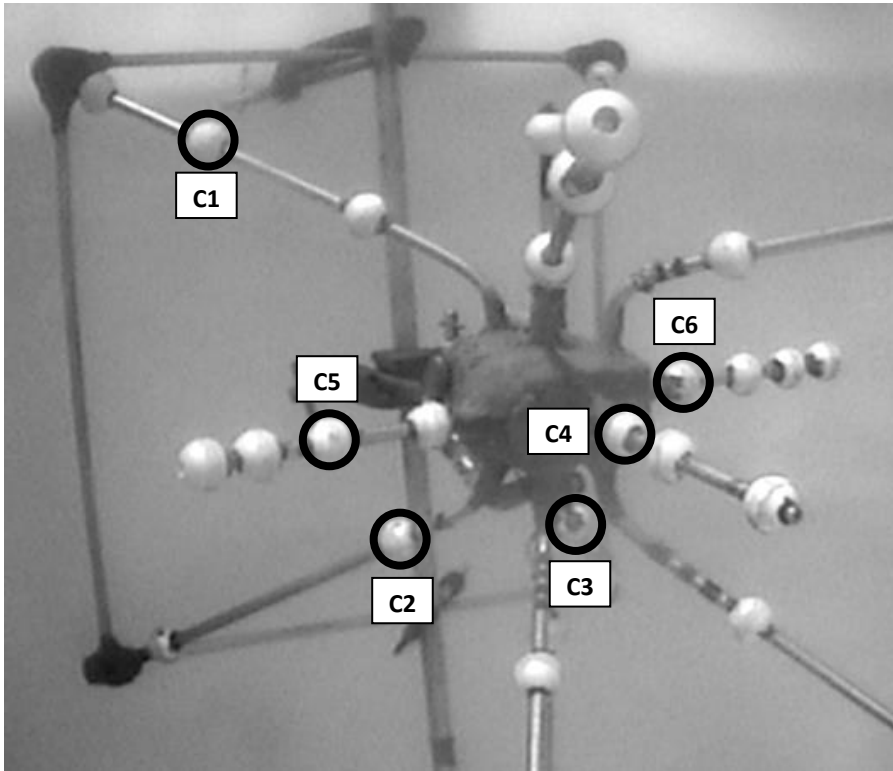


Figure 4.4: Calibration markers used to evaluate measurement error for the gold-standard neutral position buoyancy method

Within Visual 3D, the measurement trials were analysed using the same process applied to the participant trials collected in this study. The 3D co-ordinate data from each trial was filtered using a generalised cross-validators quintic spline and the mean position of each marker was calculated in the water and oil conditions. The mid-point between marker positions in water and oil were used to estimate the neutral position of each marker. The absolute difference between the measured neutral position and the known location of each marker was used to assess the measurement error for the buoyancy method. Resultant values were included as these are typically used when reporting the accuracy of a measurement tool (Betzler, 2010).

4.3.4. Precision analysis

The gold-standard buoyancy method was assessed for precision using individual participant SDs and TEM for the participant group (section 2.6.3). Individual SD was calculated for each component of the neutral nipple position before calculating the mean

within-participant SD across all participants. Acceptable SD criteria were established by calculating the mean within-participant SD of the six repeat measurements of static nipple position in the laboratory. The maximum resultant value was used to represent the typical maximum SD present within static breast measurements taken over a two week period, and defined the acceptable within-participant precision criterion for use throughout this thesis. The TEM was calculated using the spreadsheet provided by Hopkins, permitting multiple trials to be compared against each other (Hopkins, 2000a). Acceptable precision was defined for TEMs below 3.5 mm (section 2.6.4).

4.4. Results

4.4.1. Neutral position measurement

The individual-specific gravity-loaded and neutral nipple positions (calculated from the mid-point between each participant's nipple position in water and oil) are shown in Table 4.2 and Table 4.3 respectively. The displacements of the nipple from the calculated neutral nipple position in each condition for each participant are plotted in Figure 4.5, Figure 4.6, and Figure 4.7.

Table 4.2: Mean gravity-loaded left nipple position while standing stationary in the laboratory (n = 14).

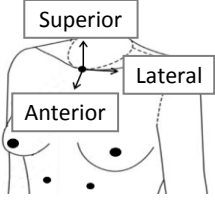
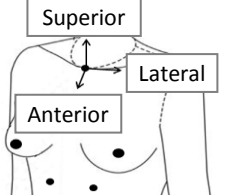
	Cross grading group	Breast size	Gravity-loaded nipple position (mm)		
			Anterior-posterior	Medial-lateral	Superior-inferior
Participant 1	34A	32B	35.2	88.7	-155.2
Participant 2		32B	28.7	80.6	-178.4
Participant 3		32B	43.9	97.4	-152.5
Participant 4	34B	34B	13.3	130.1	-185.9
Participant 5		32C	42.6	100.9	-161.8
Participant 6		32C	42.2	96.8	-163.7
Participant 7	34C	32D	32.6	95.0	-147.9
Participant 8		32D	25.5	129.9	-153.2
Participant 9		32D	30.3	106.7	-169.4
Participant 10	34D	34D	40.8	112.9	-167.2
Participant 11		32DD	46.9	103.5	-151.6
Participant 12		30E	61.9	102.5	-179.4
Participant 13	34DD	34DD	66.1	104.5	-212.0
Participant 14		34DD	50.9	111.5	-174.5
Mean			40.0	104.4	-168.1
Standard deviation			14.1	13.8	17.3

Table 4.3: Mean left nipple position in water and soybean oil, and the calculated mean neutral nipple position estimated using buoyancy.



	Cross grading group	Breast size	Nipple position in water (mm)			Nipple position in oil (mm)			Neutral nipple position (mm)		
			Anterior-posterior	Medial-lateral	Superior-inferior	Anterior-posterior	Medial-lateral	Superior-inferior	Anterior-posterior	Medial-lateral	Superior-inferior
Participant 1	34A	32B	47.3	86.9	-134.1	46.0	84.5	-135.0	46.6	85.7	-134.5
Participant 2		32B	41.5	73.2	-164.0	46.8	74.0	-166.0	44.2	73.6	-165.0
Participant 3		32B	46.0	90.3	-128.2	50.2	93.9	-132.6	48.1	92.1	-130.4
Participant 4	34B	34B	27.7	126.7	-152.1	21.2	128.7	-154.6	24.5	127.7	-153.4
Participant 5		32C	54.0	100.7	-131.4	50.8	107.1	-138.5	52.4	103.9	-135.0
Participant 6		32C	54.3	94.0	-147.5	56.6	89.1	-142.4	55.4	91.6	-145.0
Participant 7	34C	32D	48.4	88.1	-126.0	46.7	87.5	-126.9	47.6	87.8	-126.4
Participant 8		32D	45.8	121.1	-122.5	56.4	111.9	-129.1	51.1	116.5	-125.8
Participant 9		32D	42.1	104.0	-139.0	46.7	100.4	-150.2	44.4	102.2	-144.6
Participant 10	34D	34D	54.5	95.2	-149.3	52.1	99.2	-157.2	53.3	97.2	-153.2
Participant 11		32DD	65.0	92.0	-127.6	62.7	92.1	-130.3	63.8	92.0	-129.0
Participant 12		30E	89.4	83.7	-143.9	81.5	92.7	-146.5	85.4	88.2	-145.2
Participant 13	34DD	34DD	83.7	90.8	-172.8	83.0	91.1	-179.4	83.4	90.9	-176.1
Participant 14		34DD	73.6	107.3	-123.5	74.8	107.3	-134.2	74.2	107.3	-128.8
Mean			55.2	96.7	-140.1	55.4	97.1	-144.5	55.3	96.9	-142.3
Standard deviation			17.1	14.4	15.5	16.2	13.5	15.5	16.5	13.7	15.3

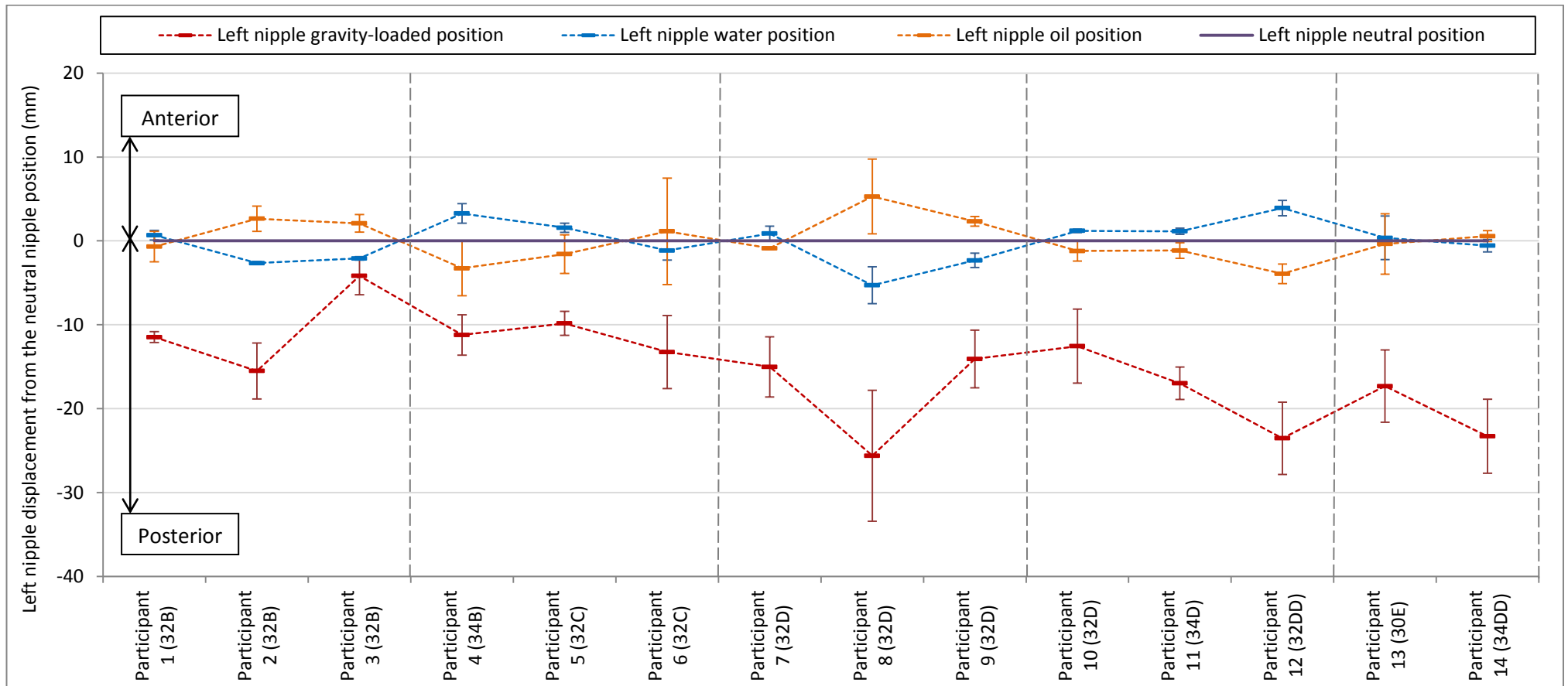


Figure 4.5: Anterior-posterior displacement of the left nipple from the neutral nipple position in the laboratory, in water and in oil. Error bars represent the standard deviation in nipple position between trials in the same condition (n = 14).

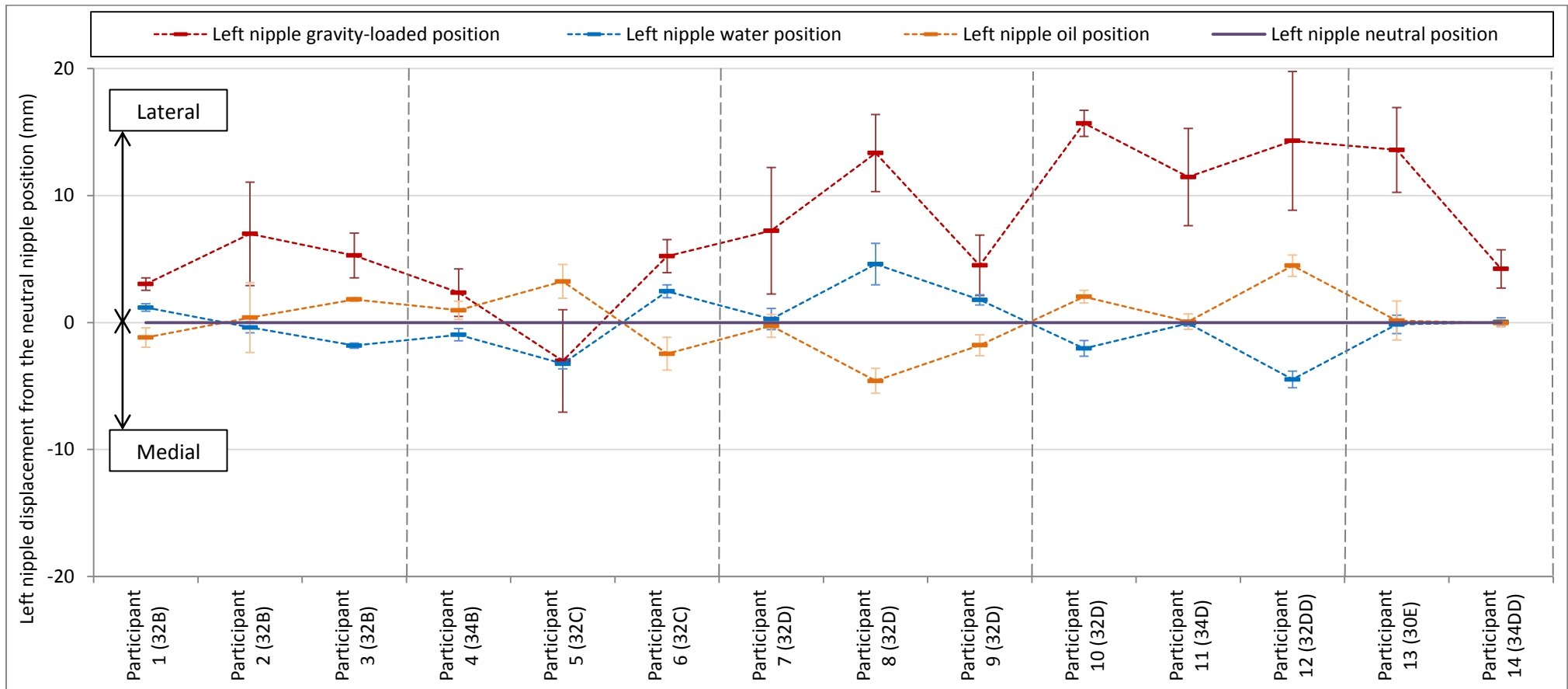


Figure 4.6: Medial-lateral displacement of the left nipple from the neutral nipple position in the laboratory, in water and in oil. Error bars represent the standard deviation in nipple position between trials in the same condition (n = 14).

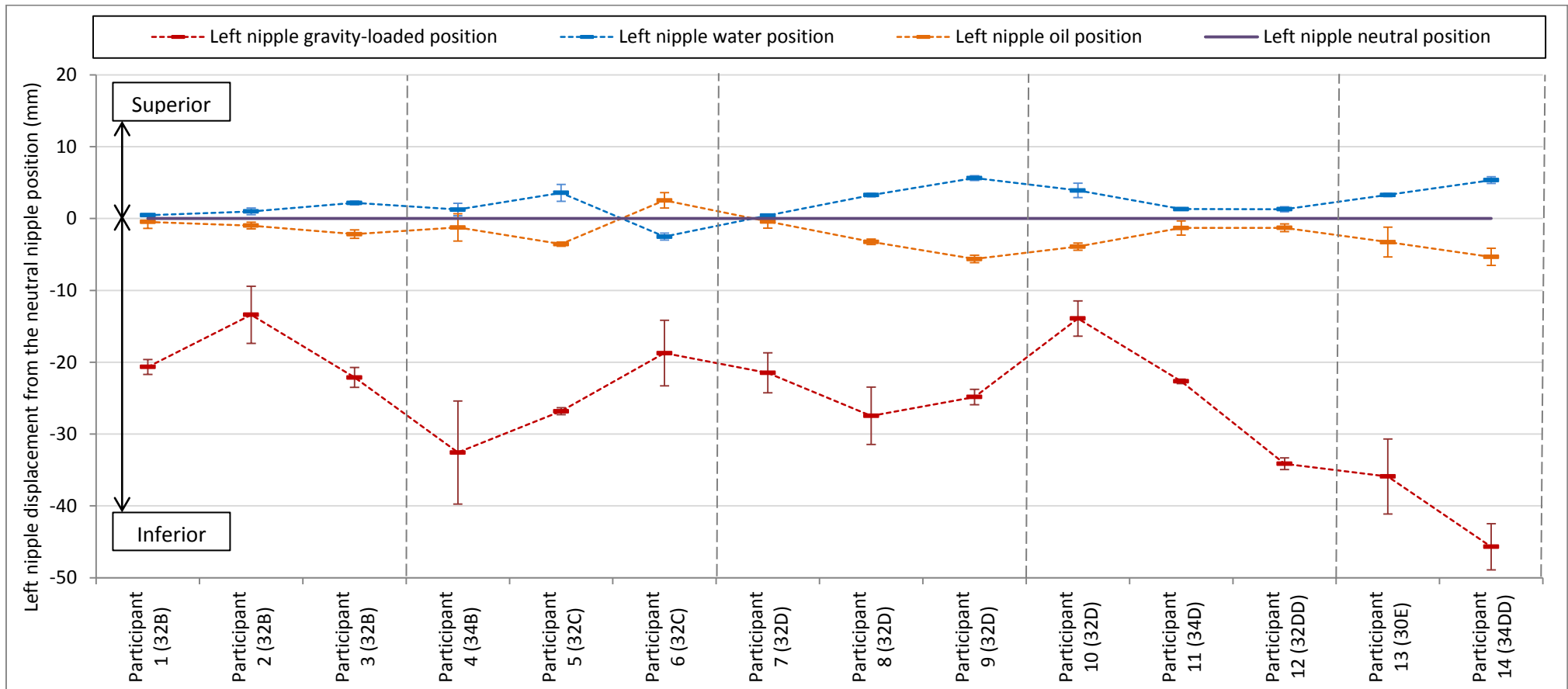
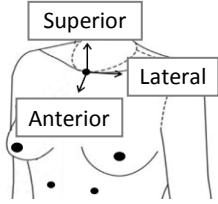


Figure 4.7: Superior-inferior displacement of the left nipple from the neutral nipple position in the laboratory, in water and in oil. Error bars represent the standard deviation in nipple position between trials in the same condition (n = 14).

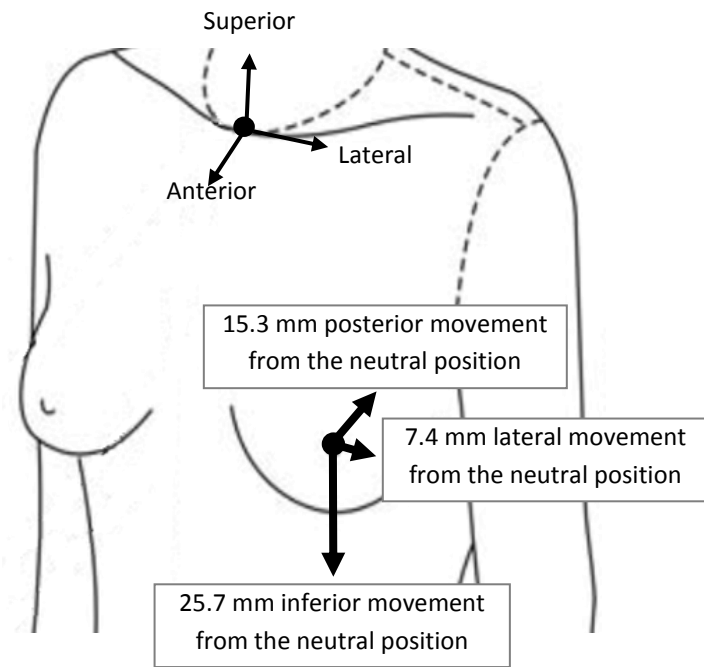
4.4.2. Quantifying the effect of gravity on the static nipple position

The effect of gravity on the static position of the nipple was assessed by comparing each participant's gold-standard neutral nipple position, measured using buoyancy in water and oil, to their gravity-loaded nipple position measured in the laboratory (Table 4.4).

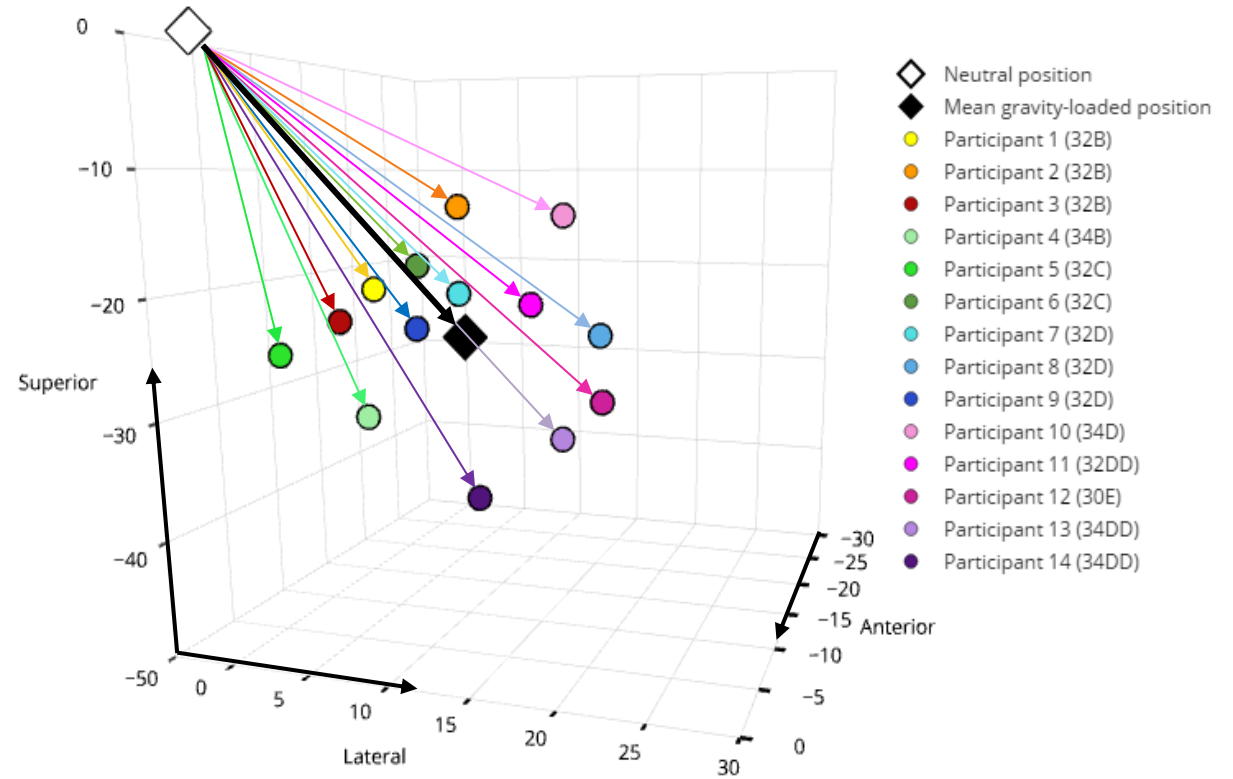
Table 4.4: Change in left nipple position from the gold-standard neutral position estimated using buoyancy to the gravity-loaded laboratory position (n = 14).

	Cross grading group	Breast size	Change in nipple position (mm)		
			Anterior-posterior	Medial-lateral	Superior-inferior
Participant 1	34A	32B	-11.5	3.0	-20.7
Participant 2		32B	-15.5	7.0	-13.4
Participant 3		32B	-4.2	5.3	-22.1
Participant 4	34B	34B	-11.2	2.4	-32.6
Participant 5		32C	-9.8	-3.0	-26.8
Participant 6		32C	-13.2	5.2	-18.7
Participant 7	34C	32D	-15.0	7.2	-21.5
Participant 8		32D	-25.6	13.4	-27.5
Participant 9		32D	-14.1	4.5	-24.8
Participant 10	34D	34D	-12.5	15.7	-13.9
Participant 11		32DD	-17.0	11.5	-22.7
Participant 12		30E	-23.5	14.3	-34.1
Participant 13	34DD	34DD	-17.3	13.6	-35.9
Participant 14		34DD	-23.3	4.2	-45.7
Mean			-15.3	7.4	-25.7
Standard deviation			5.8	5.5	8.9

For all participants the static gravity-loaded nipple position posterior and inferior to their neutral nipple position. All but one participant (Participant 5) had a gravity-loaded nipple position lateral to their neutral nipple position. The mean change in nipple position for all participants was illustrated in Figure 4.8 a, and individual participant data were shown in Figure 4.8 b.



(a)



(b)

Figure 4.8: Mean (a) and individual (b) change in nipple position from the gold-standard neutral position to the gravity-loaded position (n = 14).

Table 4.5: Correlations between participants' physical characteristics and their neutral and gravity-loaded nipple positions (n = 14).

	Condition	Pearson's correlation coefficient (r)		
		Anterior-posterior	Medial-lateral	Superior-inferior
Breast size (cross grade)	Neutral	0.724*†	0.166	-0.102
	Gravity-loaded	0.583*†	0.391	-0.391
Age (years)	Neutral	0.249	-0.282	-0.166
	Gravity-loaded	0.346	-0.235	-0.113
Height (m)	Neutral	-0.359	0.119	-0.611*†
	Gravity-loaded	-0.293	0.190	-0.400
Mass (kg)	Neutral	0.197	0.304	-0.596*†
	Gravity-loaded	0.232	0.458	-0.703*†
BMI (kg.m ⁻²)	Neutral	0.572*†	0.267	-0.217
	Gravity-loaded	0.554*†	0.402	-0.536*†

* denotes a significant correlation ($p < 0.05$), † denotes a large effect size ($r > 0.5$)

Correlation data were presented graphically in Appendix D.

Based on previous results reporting relationships between anthropometric measurements and breast mass (Brown *et al.*, 2012; Brown *et al.*, 1999), it was anticipated that measurements of nipple position may be correlated to participant age; mass; breast size; and BMI. Although the data in Figure 4.5 to Figure 4.8 suggest a slight trend for larger-breasted participants to have more anterior, lateral, and inferior gravity-loaded nipple positions, significant correlations were not present in all directions. Correlation results demonstrate that the majority of the participants' physical characteristics considered within this study did not correlate to measurements of the neutral or gravity-loaded nipple position (Table 4.5). Additional factors such as breast shape or composition may have affected the participants' neutral and gravity-loaded nipple positions. This result highlights the importance of conducting individual-specific measurements of nipple position within breast research.

In the neutral position, a strong negative correlation was observed between superior-inferior nipple position and both participant height and mass, which could be explained

by considering that the breast is typically proportional to the torso (Macéa & Fregnani, 2006). Taller (and heavier) participants with longer torsos may therefore have more inferior nipple positions relative to the suprasternal notch compared to participants with shorter torsos. It was interesting to observe that in the superior-inferior direction the relationship between nipple position and height weakens in the gravity-loaded condition whereas the relationship between mass and nipple position strengthens (Table 4.5). This result may suggest that differences in breast mass are more important than differences in torso dimensions when considering the gravity-loaded nipple position.

The strong positive correlation observed between anterior-posterior nipple position and breast size may be a consequence of the method used to classify breast sizes. Breast size classifications are based on measurements of torso and breast circumference, with these measurements providing the basis for under band and cup size respectively (Chen, LaBat, & Bye, 2011) . As the participants within this study all had similar torso measurements (under band: 30 to 34 inches), their breast size classifications were effectively based on the anterior projection of their breasts from their torso. It was therefore not surprising to observe that the anterior-posterior position of the nipple was most strongly correlated to breast size.

4.4.3. Accuracy assessment

The absolute differences between the measured and known marker positions were presented in Table 4.6. All absolute differences were below 1.2 mm and were within the acceptable measurement error limit (2 mm).

Table 4.6: Absolute difference in measured marker locations using the gold-standard buoyancy method compared to their known locations.

Marker	Calibration marker co-ordinates (mm)				Measured co-ordinates using the buoyancy method in water and oil (mm)				Absolute difference (mm)			
	X (medial-lateral)	Y (anterior-posterior)	Z (superior-inferior)	Resultant	X (medial-lateral)	Y (anterior-posterior)	Z (superior-inferior)	Resultant	X (medial-lateral)	Y (anterior-posterior)	Z (superior-inferior)	Resultant
C1	24.8	-44.5	240.8	246.1	24.7	-44.5	240.1	245.4	0.1	0.0	0.7	0.7
C2	84.4	-102.9	72.1	151.4	83.9	-101.5	72.3	150.2	0.5	1.4	0.2	1.1
C3	182.3	-94.6	58.0	213.4	182.3	-94.2	58.8	213.4	0.0	0.4	0.8	0.1
C4	127.1	-206.1	138.8	279.1	126.6	-206.9	139.3	279.7	0.5	0.8	0.5	0.6
C5	27.1	-162.0	139.3	215.4	27.4	-161.1	139.1	214.6	0.3	0.9	0.1	0.7
C6	225.0	-162.2	139.3	310.4	224.7	-161.0	139.5	309.6	0.3	1.2	0.2	0.7
Mean	111.8	-128.7	131.4	236.0	111.6	-128.2	131.5	235.5	0.3	0.8	0.4	0.7

4.4.4. Precision assessment

Defining acceptable precision criteria using standard deviations

Each participant's mean static gravity-loaded nipple position in testing sessions 2 and 3 are shown in Table 4.7. The change in nipple position between sessions and the within-participant SD of these measurements was calculated in Table 4.8. The maximum resultant SD present within the static breast measurements taken over a two week period was 5.0 mm (Table 4.8). This value was therefore used to define acceptable precision for SD throughout this thesis.

Table 4.7: Gravity loaded left nipple position measured during two separate testing sessions (sessions 2 and 3) within a two week period (n = 14).

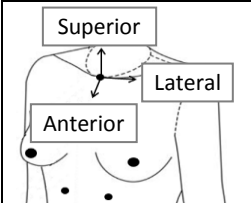
Participant Number	Cross grading group	Breast size	Time between sessions (days)	Gravity-loaded nipple position during session 2 (mm)				Gravity-loaded nipple position during session 3 (mm)			
				Anterior-posterior	Medial-lateral	Superior-inferior	Resultant	Anterior-posterior	Medial-lateral	Superior-inferior	Resultant
Participant 1	34A	32B	6	35.6	88.4	-154.3	181.3	34.8	89.0	-156.1	183.0
Participant 2		32B	2	31.5	78.9	-180.8	199.8	25.9	82.3	-176.0	196.1
Participant 3		32B	6	42.5	98.8	-152.4	186.5	45.4	96.0	-152.6	185.9
Participant 4	34B	34B	2	15.0	128.5	-192.4	231.9	11.5	131.6	-179.4	222.8
Participant 5		32C	2	41.9	104.5	-161.4	196.8	43.2	97.2	-162.2	194.0
Participant 6		32C	8	46.1	95.8	-167.8	198.7	38.2	97.8	-159.6	191.0
Participant 7	34C	32D	3	29.3	99.5	-145.6	178.7	35.8	90.6	-150.3	179.1
Participant 8		32D	14	18.4	132.3	-149.8	200.7	32.5	127.4	-156.7	204.6
Participant 9		32D	8	33.4	104.6	-168.6	201.2	27.2	108.8	-170.3	203.9
Participant 10	34D	34D	7	44.1	113.3	-168.6	207.9	37.4	112.5	-165.7	203.8
Participant 11		32DD	3	45.4	107.0	-151.4	190.8	48.3	100.0	-151.9	188.2
Participant 12		30E	3	65.8	97.6	-179.8	214.9	58.0	107.4	-178.9	216.6
Participant 13	34DD	34DD	2	67.7	107.2	-207.4	243.1	64.4	101.9	-216.6	247.9
Participant 14		34DD	2	50.1	112.4	-171.8	211.3	51.8	110.6	-177.3	215.3
Mean			5	40.5	104.9	-168.0	203.1	39.6	103.8	-168.1	202.3
Standard deviation			4	15.1	14.1	17.7	18.0	13.7	13.9	17.4	18.6

Table 4.8: Change and standard deviation in gravity loaded left nipple positions measured during two separate testing sessions (sessions 2 and 3) within a two week period (n = 14).

Participant Number	Cross grading group	Breast size	Time between sessions (days)	Change in nipple position between sessions 2 and 3 (mm)				Standard deviation in nipple position during sessions 2 and 3 (mm)			
				Anterior-posterior	Medial-lateral	Superior-inferior	Resultant	Anterior-posterior	Medial-lateral	Superior-inferior	Resultant
Participant 1	34A	32B	6	-0.8	0.7	-1.8	1.7	0.7	0.5	1.0	1.1
Participant 2		32B	2	-5.6	3.3	4.7	-3.6	3.3	4.1	4.0	2.4
Participant 3		32B	6	2.9	-2.8	-0.2	-0.6	2.2	1.8	1.4	1.1
Participant 4	34B	34B	2	-3.5	3.0	13.0	-9.1	2.4	1.9	7.2	5.0
Participant 5		32C	2	1.3	-7.3	-0.8	-2.8	1.4	4.0	0.5	1.6
Participant 6		32C	8	-7.9	2.0	8.2	-7.6	4.3	1.3	4.6	4.2
Participant 7	34C	32D	3	6.5	-9.0	-4.7	0.3	3.6	5.0	2.8	0.8
Participant 8		32D	14	14.1	-4.9	-6.9	3.9	7.8	3.0	4.0	2.2
Participant 9		32D	8	-6.2	4.2	-1.7	2.7	3.4	2.4	1.1	1.5
Participant 10	34D	34D	7	-6.7	-0.8	2.9	-4.1	4.4	1.0	2.5	2.8
Participant 11		32DD	3	2.9	-6.9	-0.5	-2.7	1.9	3.8	0.3	1.5
Participant 12		30E	3	-7.8	9.8	1.0	1.6	4.3	5.5	0.8	1.1
Participant 13	34DD	34DD	2	-3.3	-5.3	-9.1	4.7	2.4	3.3	5.2	2.8
Participant 14		34DD	2	1.7	-1.8	-5.5	4.0	1.6	1.5	3.2	2.2
Mean			5	-0.9	-1.1	-0.1	-0.8	3.1	2.8	2.8	2.2
Maximum			14	14.1	9.8	13.0	-9.1	7.8	5.5	7.2	5.0

Precision assessment of the gold-standard buoyancy method

Table 4.9: Standard deviation of neutral nipple position measurements using the gold-standard buoyancy method (n = 14).

	Cross grading group	Breast size	Standard deviation in neutral nipple position measurements (mm)		
			Anterior-posterior	Medial-lateral	Superior-inferior
Participant 1	34A	32B	1.2	0.5	0.5
Participant 2		32B	0.7	1.4	0.4
Participant 3		32B	0.5	0.2	0.3
Participant 4	34B	34B	1.5	0.6	1.3
Participant 5		32C	1.3	0.7	0.5
Participant 6		32C	3.7	0.9	0.5
Participant 7	34C	32D	0.4	0.8	0.5
Participant 8		32D	3.3	1.0	0.3
Participant 9		32D	0.3	0.6	0.1
Participant 10	34D	34D	0.7	0.3	0.8
Participant 11		32DD	0.6	0.3	0.4
Participant 12		30E	1.0	0.6	0.2
Participant 13	34DD	34DD	2.5	0.4	1.1
Participant 14		34DD	0.6	0.1	0.4
Mean			1.3	0.6	0.5
Maximum			3.7	1.4	1.3

All SDs were within the acceptable 5.0 mm criteria. Calculated TEM values for the buoyancy measurements were 1.2 mm in the anterior-posterior direction, 0.6 mm in the medial-lateral direction and 0.6 mm in the superior-inferior direction. All TEMs were within the acceptable limit of 3.5 mm for precision.

4.5. Discussion

This study was the first to estimate the neutral position of the nipple by using two fluids with densities above and below the reported densities of breast tissue. Water has a higher mass-density (at temperatures between 32.4° and 37.1° used in this study) than

the breast (determined in section 3.2) and exerts a buoyancy force that over-compensates for the effect of gravity on the breast. Conversely soybean oil has a lower mass-density (at temperatures between 30.9° and 32.9° used in this study) than the breast and exerts a buoyancy force that under compensates for the effect of gravity on the breast. Calculation of the mid-point between the nipple position in water and the nipple position in oil should therefore provide a more accurate estimate of the neutral nipple position than could be obtained using either fluid in isolation.

Results from this study demonstrate that the counteraction of gravity using buoyancy caused the nipple to move superiorly, medially and anteriorly with respect to the torso (Table 4.4). As the static nipple measurements were taken with participants in an upright position, with gravity acting predominantly inferiorly on the breast, it was anticipated that the largest change in nipple position would be in the superior direction during the buoyancy measurements. Results confirmed this assumption as the movement from the gravity-loaded to the neutral nipple position was largest in the superior direction (up to 45.7 mm) (Table 4.4).

Based on previous literature reporting that landmarks on the breast surface, including the nipple, move inferiorly and laterally with age it was proposed that gravity may also have a small component acting laterally on the breast due to the curved shape of the torso (Brown *et al.*, 1999). All participants but one experienced a medial nipple movement from the gravity-loaded to the neutral nipple position (up to 15.7 mm) (Table 4.4). However, the medial-lateral component of nipple position was the least affected during this buoyancy study suggesting that the lateral effect of gravity on the breast is minimal while in the upright position. The lateral movement of the breast reported in previous studies may have been due to the long-term effects of gravity acting on the breast in many different orientations, during different activities, and including contributions from changes in breast shape and composition that can occur over prolonged periods of time (Brown *et al.*, 1999; Razzano, D'Alessio, & D'Alessio, 2014; Soltanian, Liu, Cash, & Iglesias, 2012).

Perhaps the most interesting finding within this study was the extent of anterior nipple movement that occurred when comparing the gravity-loaded and neutral nipple positions (up to 25.6 mm) (Table 4.4). All participants experienced an anterior movement of the nipple in the buoyancy condition. This result may be explained by two contributory factors. Firstly, the marker set used to construct the torso segment caused the superior-inferior axis of the LCS to tilt backwards with respect to the global vertical axis (discussed further in section 4.6). This backwards tilt of the torso introduced a posterior component to the gravitational force on the breast, causing the nipple to move anteriorly when the effect of gravity was counteracted using buoyancy. Secondly, the redistribution of breast tissue in the buoyancy condition may have contributed to the anterior movement of the nipple when compared to the laboratory position. It was proposed that the gravity-loaded breast typically forms a tear-drop shape with a large portion of breast mass sitting at the base of the breast, in fluid the breast mass may distribute more equally within the breast, creating a more symmetrical hemispherical or conical shape, and consequently a more anterior nipple position (Figure 4.9). Changes in breast shape due to gravity were illustrated in the frontal and sagittal breast plane for each participant in Appendix E.

Comparisons between the gravity-loaded nipple position and the neutral position estimated using buoyancy support the use of Archimedes' principle to counteract the effect of gravity on the breast. However, closer inspection of the data collected using the two fluids highlighted some interesting findings. It was originally assumed that the three conditions (laboratory, oil and water) offered increasing levels of support to the breast against the effects of gravity. It followed from this, that any change in breast position between the laboratory and the oil would be replicated and exaggerated in water. However, some individuals experienced the contrary effect, with oil creating a greater change in position than water.

In the anterior-posterior direction six participants had a more anterior nipple position during oil immersion compared to their nipple position during water immersion (Figure 4.5). This finding may have been due to differing degrees of torso tilt in the two buoyancy testing sessions, causing the breast to be flattened or pulled away from the torso. The stability of torso angle within this study was investigated further in section 4.6. Another

possible explanation could have been an increase in breast size between measurements of the nipple position in water and the same measurement taken up to two weeks later in soybean oil. However, the prevalence of this inverted result across the sample group, including two women with measurements taken only two days apart suggests that changes in breast size were not solely responsible for the more anterior nipple position in oil when compared to water. Instead, it was considered that not only did the water exert a greater lift force on the breast, but it also provided a greater compressive force over the breast surface compared to the soybean oil. The additional compression exerted on the breast during immersion in water may have been sufficient to induce a change in breast shape between the oil and water immersions. It has been reported that several variations of breast shape are present within the female population (Rong, 2006). It was therefore proposed that individuals who had a more anterior nipple position in oil may have had more conical natural breast shapes. The breast may have been lifted into its natural cone shape in the soybean oil (Figure 4.9 b) but then compressed into a hemispherical shape, reducing the anterior displacement of the nipple, in the water (Figure 4.9 c).

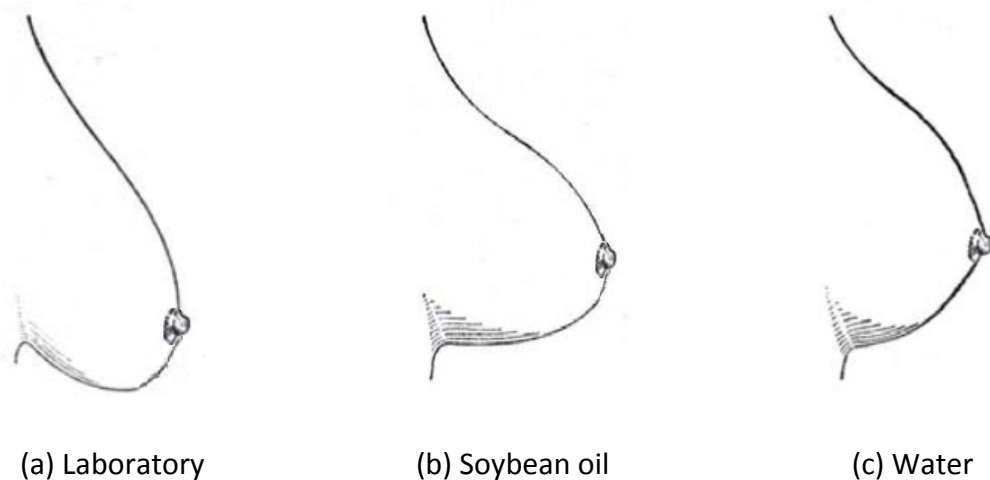


Figure 4.9: Proposed change in breast shape during the gold-standard buoyancy study when moving from the laboratory (a) to the soybean oil (b) and water (c) immersions.

In the medial-lateral direction, five participants demonstrated a more medial nipple position in soybean oil than in water. Again this was contradictory to the assumption that water would have the largest effect on nipple position when compared to the gravity-

loaded nipple position in the laboratory. However, the effect of gravity in the lateral direction was limited in this study as measurements were taken in the upright position. Consequently, the magnitudes of the differences in medial-lateral nipple position were generally smaller than the standard deviations observed in this direction (Figure 4.6). Only one participant (participant 8) had a medial movement in nipple position from water to soybean oil that was greater than the SD in her static nipple position. This participant had the greatest time interval between testing sessions (14 days), and had a large change in static nipple position between testing sessions (14.1 mm, -4.9 mm and -6.9 mm in each direction) (Table 4.8). These findings suggest that this participant experienced a change in breast size or shape between testing sessions which may have produced unexpected results when comparing the neutral nipple position to the mean gravity-loaded nipple position. It was therefore suggested that future implementation of repeated buoyancy experiments in different fluids ensure that all measurements are taken over a time period of less than 14 days. Efforts were made to minimise the time intervals between testing sessions within this study although factors such as participant and laboratory availability and limited resources meant that not all participants could complete this study within the desired time frame.

Comparisons of the superior-inferior nipple position in the laboratory, in water and in soybean oil demonstrated consistent results, with the nipple moving superiorly from the laboratory to soybean oil and from soybean oil to water (Figure 4.7). Only one participant (Participant 6) exhibited a more superior nipple position in soybean oil than in water. This result was the most perplexing of the inverted water and soybean oil data as the denser fluid (water) should have provided the greatest lift to the breast, resulting in the most superior nipple position. Again it was proposed that either a change in torso angle, or a change in breast size or shape, accounted for the more superior nipple position in soybean oil.

As this chapter implemented a novel method for estimating the neutral nipple position, it was important to establish the accuracy and precision of this method before assessing its suitability for use in future research. The mean resultant measurement error associated with this buoyancy method was 0.7 mm, with a maximum error in any directional

component of a single marker of 1.4 mm (Table 4.6). This level of accuracy compares favourably to other commercially available systems for measuring human motion (Richards, 1999), and is acceptable for use within biomechanical or clinical research (Aung *et al.*, 1995; Weinberg *et al.*, 2004). It is emphasised that the maximum reported measurement error (1.4 mm) represents a worst case scenario as it was calculated with six missing markers using the calibration recordings with the highest digitising error. All participant measurements were calculated using the full calibration recordings, enabling more accurate positional data to be obtained.

The buoyancy method was evaluated for precision using SD and TEM calculations. The TEM criteria for acceptable measurement precision was defined as 3.5 mm based on previously reported values for anthropometric measurements of the breast (Brown *et al.*, 1999). The maximum TEM for the buoyancy method was 1.2 mm in the anterior-posterior direction corresponding to an acceptable level of precision across the measured group of participants. Within-participant SD was calculated to provide a measure of precision that could distinguish between participants within the sample group. Acceptable SD values were defined using the maximum resultant SD present in repeated measures of static nipple position using the optoelectronic camera system. The maximum resultant SD in static nipple position was 5.0 mm (Table 4.8), representing the typical level of precision achievable in measurements of nipple position over a two week period. Interestingly this SD value matches the reported error associated with static breast measurements caused by fluctuations in posture (Hansson *et al.*, 2014). The SDs in nipple position measured using the buoyancy method were all within the acceptable precision limits, with the maximum within-participant SD calculated as 3.7 mm in the anterior-posterior direction (Table 4.9).

4.6. Conclusion

The mean change in left nipple position between the laboratory and the neutral position for 14 female participants was 15.3 mm anteriorly, 7.4 mm medially, and 25.7 mm superiorly (Figure 4.8). The buoyancy method demonstrated acceptable accuracy

(measurement errors ≤ 1.4 mm) and precision (TEM ≤ 1.2 mm, SD ≤ 3.7 mm) to be implemented within future research.

Overall the results from this study followed the anticipated behaviour of the breast during immersion based on Archimedes' principle. However, some participants experienced contrary results which may have been due to changes in breast size or shape, or a change in posture, between testing sessions. It was recommended that future implementation of the buoyancy method should ensure that all measurements are completed within as shorter time span as possible, not exceeding 14 days. Although attempts were made to standardise posture within this study, small torso rotations may have occurred between measurements, particularly in the transition from the laboratory (standing) to the buoyancy conditions (sitting). To investigate this further, the following section compares the torso angle between conditions to assess its potential to affect measurements of nipple position.

4.6.1. Investigating the influence of torso angle on the effect of gravity on the breast

Introduction

As gravity acts along the global vertical axis, any deviation of the torso away from this axis causes the directional distribution of gravity to be altered when considered in the LCS of the torso (Figure 4.10). This had implications for the expected behaviour of the breast during the buoyancy study. For example, an increased backwards tilt of the torso in the laboratory would increase the posterior and decrease the inferior components of gravity on the breast, potentially causing increased anterior movement and decreased superior movement of the nipple when moving from the laboratory to the buoyancy condition.

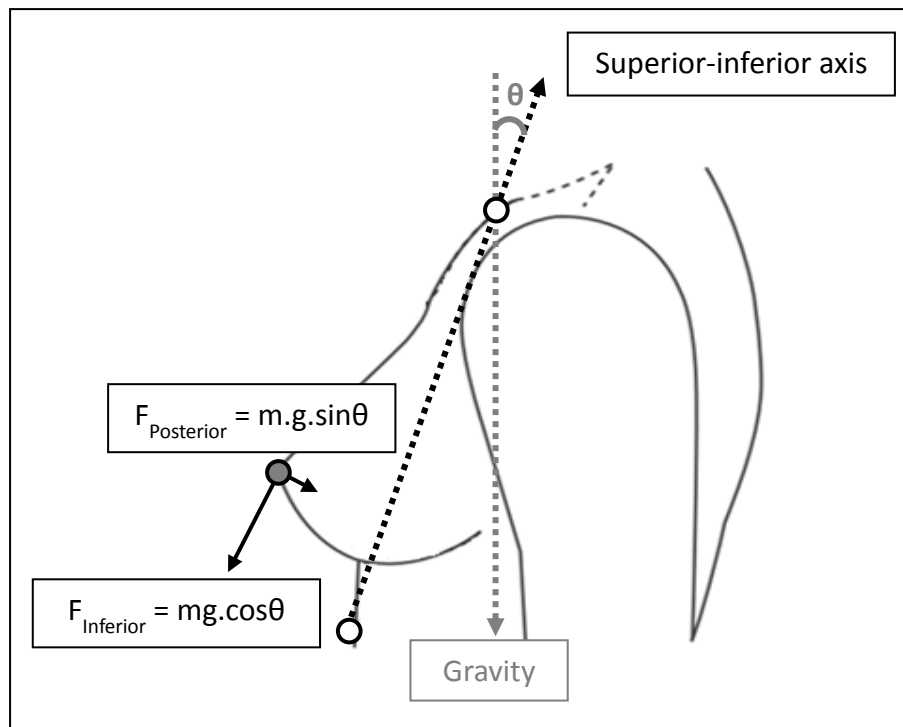


Figure 4.10: The effect of torso angle (θ) on the directional components of the gravitational force at the nipple when presented in the local co-ordinate system of the torso.

Changes in torso angle between the water and soybean oil measurements may also explain the inverted results discussed in section 4.5, as any rotation of the LCS may alter the directional components of nipple position calculated within each immersion condition. Figure 4.11 illustrates that the global positions of the STN (white) and nipple (grey) markers could be the same in two measurement conditions, but that a deviation in torso LCS angle would cause an apparent change in relative nipple position. Specifically, a backward tilt of the torso LCS (Figure 4.11 b) would make the nipple appear more inferior and posterior than if measured with the torso in the upright position (Figure 4.11 a). To investigate whether these effects were present in the gold-standard buoyancy results this section investigated the torso LCS angle of each participant in the buoyancy study in each condition (laboratory, water, soybean oil, and neutral position).

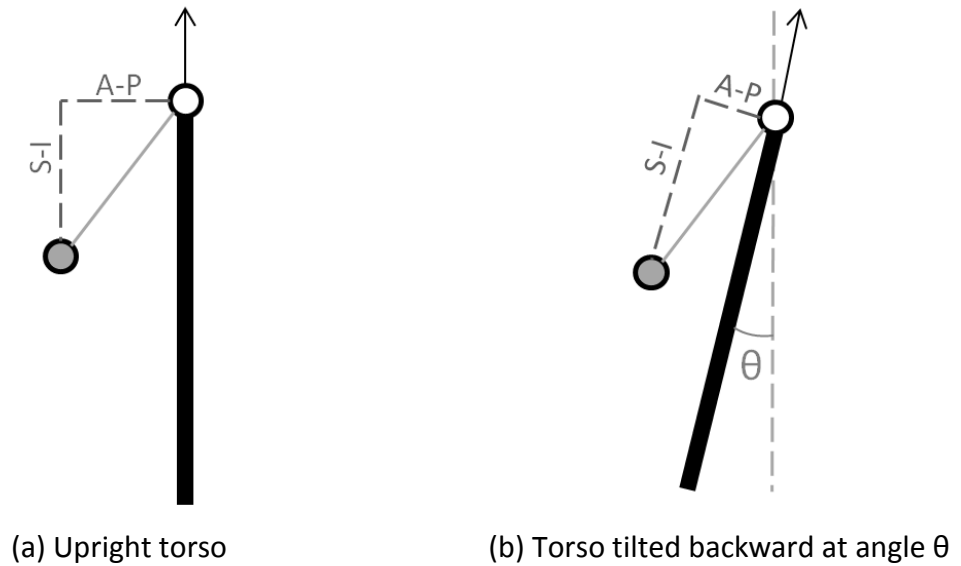


Figure 4.11: Diagram illustrating the effect of torso local co-ordinate system rotation on measurements of anterior-posterior (A-P) and superior-inferior (S-I) nipple position.

Aims

1. Investigate whether increasing the torso LCS angle in the laboratory related to increased anterior and decreased superior nipple movement from the laboratory to the neutral position.
2. Investigate whether the transition from standing in the laboratory to sitting in the neutral position study affected the torso LCS angle.
3. Investigate whether the transition from water to soybean oil in the neutral position study affected the torso LCS angle.

Method

Torso angle data was obtained from the buoyancy trials described in section 4.3. The angle of the torso LCS was defined as the degree of rotation between the superior-inferior torso axis and the vertical axis of the laboratory (defined perpendicularly to the ground in all conditions) as shown in Figure 4.10. Mean torso LCS angle was calculated using Visual 3D for each participant in the laboratory, in water, in oil, and in the neutral (mid-point between water and oil) conditions. Absolute differences and paired sample t-tests were used to compare torso angle in the laboratory and the neutral position, and torso angle in water and soybean oil. A Pearson's correlation was performed using SPSS (IBM SPSS statistics version 20) to compare each participant's torso LCS angle (in the laboratory) to their changes in anterior-posterior and superior-inferior components of nipple position between the gravity-loaded and neutral conditions. Correlation coefficients of ± 0.1 , ± 0.3 , and ± 0.5 indicated small, moderate and large effect sizes (Field, 2009).

Results

Chapter 4: Measuring the neutral nipple position using buoyancy

Table 4.10: Mean and absolute difference in participant torso local co-ordinate system angle in the laboratory, the neutral position, water, and soybean oil.

Participant Number	Cross grading group	Breast size	Torso angle (°)				Absolute difference in torso angle between conditions (°)	
			Laboratory	Neutral position	Water	Soybean oil	Laboratory and neutral position	Water and soybean oil
Participant 1	34A	32B	4	5	8	2	1	6
Participant 2		32B	7	12	14	10	5	4
Participant 3		32B	4	5	6	5	1	1
Participant 4	34B	34B	14	11	10	12	3	2
Participant 5		32C	11	11	9	13	0	4
Participant 6		32C	13	9	10	9	4	1
Participant 7	34C	32D	10	12	14	10	2	4
Participant 8		32D	12	5	3	7	7	4
Participant 9		32D	10	8	8	9	2	1
Participant 10	34D	34D	8	13	17	8	5	9
Participant 11		32DD	8	12	17	7	4	10
Participant 12		30E	15	8	8	7	7	1
Participant 13	34DD	34DD	15	11	10	12	4	2
Participant 14		34DD	12	8	5	11	4	6
Mean			10	9	10	9	4	4
Standard deviation			4	3	4	3	4	5

Chapter 4: Measuring the neutral nipple position using buoyancy

Absolute differences in individual torso LCS angle between the standing laboratory condition and the sitting neutral position ranged from 0° to 7° (Table 4.10), and were not statistically significant (Table 4.11). Additionally, there was no significant change in torso LCS angle (1° to 10°) between the water and oil conditions (Table 4.10 and Table 4.11).

Table 4.11: Paired sample t-test results for comparing torso local co-ordinate system angle across conditions in the buoyancy study.

Torso angle comparison conditions	t-value	Significance (p)	Effect size (r)
Laboratory and neutral position	0.847	0.413	0.229
Water and soybean oil	0.933	0.368	0.250

Torso LCS angles in all conditions were found to be normally distributed using the Shapiro-Wilk test. Pearson correlation results demonstrated strong significant relationships between torso LCS angle in the laboratory and the change in both the anterior-posterior and superior-inferior components of nipple (Table 4.12). The positive direction of both relationships does not support the theory that increased torso angle in the gravity-loaded laboratory condition results in larger anterior-posterior and smaller superior-inferior changes in nipple position to the neutral position.

Table 4.12: Correlation between torso local co-ordinate system angle and directional changes in nipple position when moving from the laboratory to the neutral position.

	Pearson correlation	Significance (p)
Laboratory torso angle and change in anterior-posterior nipple movement to the neutral position	0.545*	0.044
Laboratory torso angle and change in superior-inferior nipple movement to the neutral position	0.622*	0.018

* denotes a significant difference ($p < 0.05$)

Discussion

The initial aspect of this study investigated whether the transition from standing to sitting between the gravity-loaded and neutral nipple position measurements may have compromised the standardisation of participant torso position leading to apparent changes in relative nipple position. Absolute differences and paired-sample t-tests demonstrated that the largest stand-to-sit angle change in torso LCS was 7° , which was not significant and was smaller than the largest angle change within the two sitting conditions (10° change from water to oil). This result suggests that the transition from standing to sitting did not negatively affect participants' ability to remain upright during measurements of nipple position.

The torso LCS angle in water and soybean oil was also investigated following the counter-intuitive observation that some participants experienced a greater change in nipple position during the oil immersion than during the water immersion (section 4.5). Participants 2, 3, 8 and 9 had the largest inverted buoyancy results in the anterior-posterior direction, where the nipple position was more anterior in oil than in water (Figure 4.5). However, evaluation of their torso LCS angles in water and oil demonstrated that participants 2 and 3 tilted forwards in the oil by 4° and 1° respectively, while participants 8 and 9 had precisely the opposite result, tilting backwards in the oil by 4° and 1° respectively (Table 4.10). These opposing results suggest that it was not torso tilt, but possibly changes in breast shape that caused the inverted buoyancy results in the anterior-posterior direction. In the superior-inferior direction, only Participant 6 had a more superior nipple position in the oil than in the water (Figure 4.7). Analysis of this participant's torso angle in water and oil showed that they had only a 1° change in torso angle between conditions, suggesting again that changes in torso angle were not responsible for the inverted data. The suggestion that torso angle did not affect measurements of nipple position was supported by paired samples t-test results showing no significant differences between torso angle in the laboratory and in the neutral position, or between water and soybean oil (Table 4.11).

Following the observation that the change in anterior posterior nipple position between the laboratory and the neutral position was much larger than expected (section 4.4.2), this study also investigated the effect of torso LCS angle in the gravity-loaded condition on changes in nipple position. Results demonstrated that all participants had a slightly backward tilting torso LCS relative to the global vertical axis in the laboratory, with the degree of rotation ranging from 4° to 15°. Resolution of the gravitational force into the LCS of the torso therefore results in inferior forces ranging from 9.78 N to 9.47 N; and posterior forces ranging from 0.68 N to 2.54 N per unit of breast mass respectively (Figure 4.10). This finding demonstrates that the inferior component of gravity on the breast cannot be assumed to have a magnitude of $9.81 \text{ N}\cdot\text{kg}^{-1}$ as has been asserted in previous studies (Haake *et al.*, 2012; Haake & Scurr, 2011).

The multi-directional effect of gravity on the nipple when considered in the LCS of the torso highlights the potential problem associated with the assumption that gravity is an inferior force on the breast (discussed previously in section 2.2). Gravity was shown to act predominantly in the inferior and posterior directions of the breast in section 4.4.2, leading to the suggestion that participants with the largest torso LCS angles would experience a larger anterior and smaller superior movement of the nipple to the neutral position. Correlation results indicated that both anterior and superior nipple movement increased with torso LCS angle, suggesting that torso LCS angle was not the primary cause of the anterior movement of the nipple to the neutral position (Table 4.12). Breast size may have been an alternative causal factor for the observed increases in both torso LCS angle and the change in nipple position between the laboratory and the neutral position. Breast size has previously been related to BMI (Brown *et al.*, 2012) so it was feasible that participants with larger breasts also had higher BMIs and more subcutaneous fat below the rib markers. This may have caused the distal end of the torso segment to project forwards leading to a greater torso LCS angle. An upward trend was demonstrated in BMI and breast size for the participants within this study (Table 4.1), although the level of subcutaneous fat on the torso was not assessed. The range of breast sizes included within this study meant that there were insufficient participants within each breast size group to evaluate the independent effect of torso LCS angle on changes in nipple position.

Conclusion

All participants in the buoyancy study had a torso LCS that was tilted backwards relative to the global vertical axis when standing in the laboratory (between 4° and 15°). Torso tilt reduced the inferior effect of gravity on the breast to a minimum of 9.47 N.kg⁻¹, and increased the posterior effect to a maximum of 2.54 N.kg⁻¹. No significant differences were found between torso LCS angle in the laboratory (standing) and neutral (sitting) conditions or between the two immersion conditions, suggesting that participants were able to maintain similar torso orientations in all conditions. Strong positive correlations were observed between torso LCS angle and both the anterior-posterior and superior-inferior components of nipple movement, which could not be explained by the effect of torso LCS tilt on gravitational distribution on the nipple. Consequently, movement of the nipple between the laboratory and the neutral position presented in section 4.4.2 were not found to be affected by torso LCS angle.

Successful implementation of the gold-standard neutral position method in this chapter provides the data required to assess the accuracy and precision of previously published and newly developed alternative neutral position methods. The next stage of this thesis evaluates the suitability of alternative neutral position methods for use within future breast research.

5. Developing alternative methods for identifying the neutral breast position

5.1. Introduction

The potential benefits of incorporating the neutral breast position into measurements of breast motion and breast strain have already been discussed within this thesis (section 2.2). Previous attempts have been made to identify the neutral breast or nipple position using the buoyant force of water (Rajagopal, 2007; Zain-UI-Abdein *et al.*, 2013) and the breast drop method (Haake *et al.*, 2012; Haake & Scurr, 2011). Limitations associated with the two existing neutral position methods led to the development of a new gold-standard method in Chapter 4 using the buoyant force from water and soybean oil. Although the new gold-standard method was successfully implemented within this thesis, the financial and logistical issues associated with this method may limit its application within future research. Consequently, researchers may select to use a previously published, easier to implement, method to identify the neutral breast position within their work. It was therefore considered important to evaluate the accuracy and precision of the previously published neutral position methods against the gold-standard values, presented in Chapter 4, to investigate whether these alternative methods provide an appropriate approximation of the neutral position. Due to the relative novelty of the neutral position concept, there was also potential within this thesis to develop alternative novel methods that have not yet been considered for measuring the neutral position.

Figure 5.1 illustrates the overall structure of this study; the first aspect of this chapter focused on compiling a comprehensive summary of existing and novel neutral position methods. Existing methods consisted of the buoyancy in water method, the breast drop method and the static gravity-loaded method. Although the static gravity-loaded breast position was not intended to represent the neutral position of the breast, it has been previously implemented in place of the neutral position for calculations of breast extension and breast strain (Scurr, Bridgman, *et al.*, 2009; Scurr, White, Milligan, Risius, & Hedger, 2011a). Comparison of the gravity-loaded and gold-standard neutral nipple positions therefore provides an indication of the error associated with neglecting the

Chapter 5: Developing alternative methods for identifying the neutral breast position

gravitational effect on the breast when assessing breast kinematics. Novel neutral position methods were developed from fundamental scientific principles with an aim to either counteract the effect of gravity on the breast, or to identify the breast position in which there was no external strain on the breast skin. The existing and novel neutral position methods were evaluated in the first stage of this study on the strength of their underlying theory (*i.e.* does the method use established scientific principles; and how many assumptions or approximations have to be made) and their anticipated practicality within a laboratory environment.

Neutral position methods identified as having a strong or untested theoretical underpinning and that were feasible to implement within the biomechanics laboratory were then taken forward to a series of small scale practicality studies. Methods that were conducted successfully in the laboratory, and for which a neutral position estimate could be achieved, were implemented in a full scale accuracy and precision study. The full-scale study involved the same 14 participants that completed the gold-standard buoyancy testing. Each participant performed all of the alternative neutral position methods alongside the water and soybean oil buoyancy testing (within sessions 2 and 3 described in chapter 4). The neutral nipple position estimate for each method could then be compared to the gold-standard measurement for each participant. Neutral position methods that could accurately and precisely (based on the criteria developed in section 2.6) estimate the gold-standard neutral nipple position may provide a simple alternative to immersion in water and soybean oil within future research.

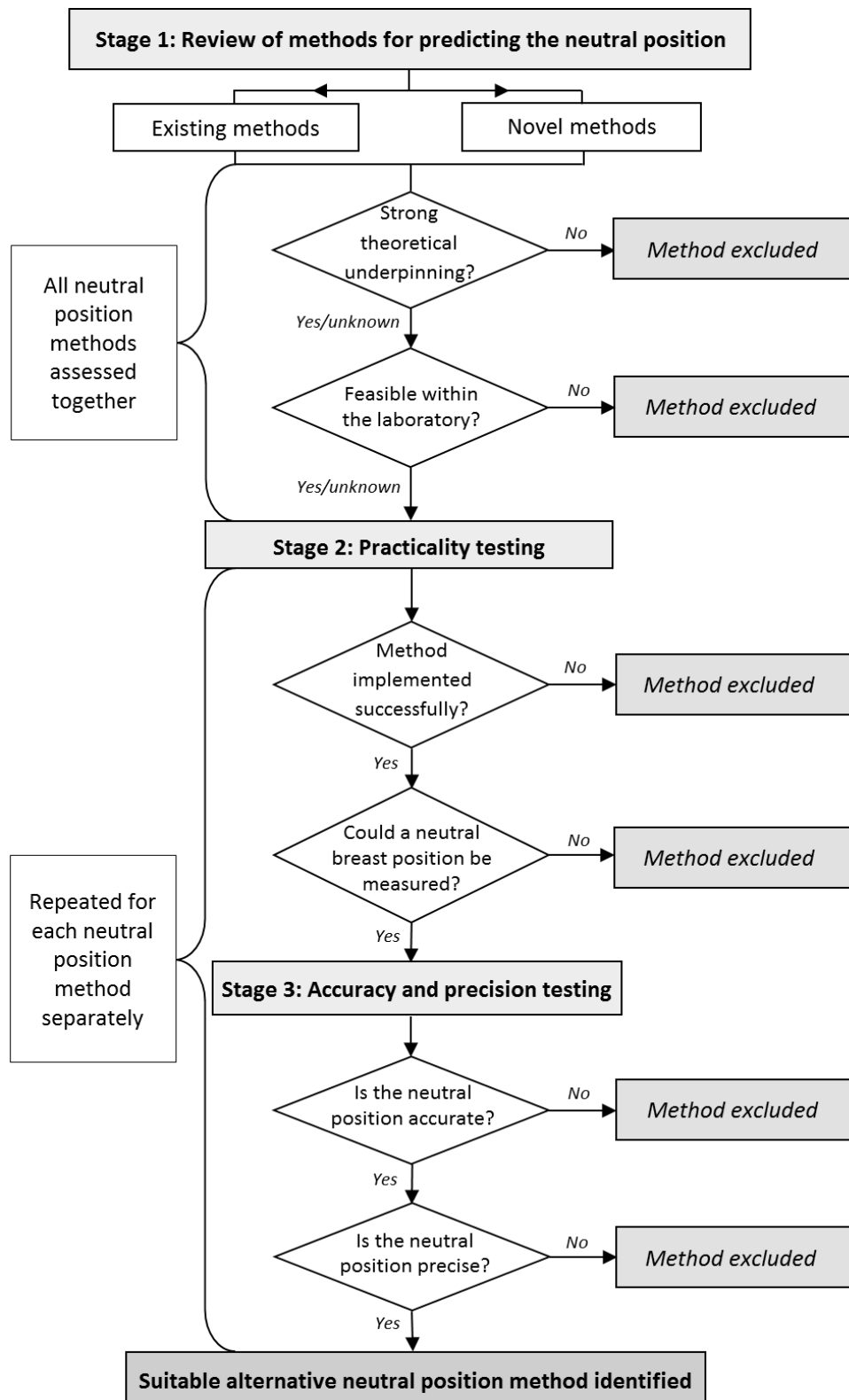


Figure 5.1: Evaluation process for determining the suitability of alternative methods used for predicting the neutral nipple position.

5.2. Aims

1. Compile a comprehensive list of existing methods for measuring the neutral nipple position
2. Develop a range of novel methods for estimating the neutral nipple position based on scientific principles.
3. Evaluate existing and novel neutral position methods on the strength of their theoretical underpinning and their suitability for implementation within a laboratory environment.
4. Identify practical neutral position methods based on their successful implementation and attainment of a neutral nipple position estimate during small scale studies.
5. Evaluate the accuracy and precision of the shortlisted neutral position methods in a full scale study by comparing the estimated to the gold-standard neutral nipple position measurements for each participant.

5.3. Stage 1: Review of methods for predicting the neutral breast position

5.3.1. Method

A systematic review of existing literature up to and including publications in the year 2013 was performed to compile a list of existing neutral position methods. Literature was initially obtained by searching electronic databases for keywords, such as 'neutral breast position', 'non-loaded breast', 'zero-gravity', 'breast strain', 'breast extension', 'stress-free breast', and 'un-deflected breast'. Secondly, the abstracts were screened and any irrelevant articles were rejected. Thirdly, the full articles were retrieved and reviewed again for their relevance to this study. Reference lists within these articles were also

Chapter 5: Developing alternative methods for identifying the neutral breast position checked for relevance. Any articles that were not available in the University-subscribed journals were obtained through inter-library loan.

To achieve the second aim of this study time was spent developing novel methods for attaining the neutral nipple position. Novel methods were based on scientific principles that enabled the nipple position to be measured either when there was no external strain on the breast skin, or when the effect of gravity had been counteracted. All neutral position methods (existing and novel) were then evaluated on their theoretical underpinning and feasibility for use in the laboratory. Methods were considered to have a strong theoretical underpinning if their underlying concepts were based on established scientific principles and if they could be applied to the breast with minimal use of assumptions or approximations. Theoretical underpinning was classified as 'untested' if there was a scarcity of evidence demonstrating that the scientific concepts used would successfully counteract the effect of gravity or to eliminate surface strain on the breast. Methods were regarded as feasible if they could be implemented in the available laboratory space, within the time and financial constraints of this project. These criteria were used to create a shortlist of methods that were taken forward to the second stage of this study involving practicality testing.

5.3.2. Results

Table 5.1: Previously implemented methods for identifying the neutral position of the breast.

Method	Neutral position definition	Evaluation	
		Theoretical underpinning	Achievable within the laboratory
Buoyancy in water	The neutral position was measured with the breast supported in three dimensions by the buoyancy force from water (Rajagopal, 2007; Zain-UI-Abdein <i>et al.</i> , 2013)	Strong: This method is based on a well-established concept (Archimedes' principle), although work within this thesis has demonstrated that water may be denser than breast tissue, potentially leading to errors in the resulting neutral position.	Yes: This method had already been implemented within this thesis.
Breast drop	The neutral position was identified as the final position of the breast while falling, when breast acceleration is still that of gravity (<i>i.e.</i> just before the supporting tissues of the breast act to slow it down) (Haake <i>et al.</i> , 2012; Haake & Scurr, 2011).	Untested: This method only considers inferior breast acceleration, which may not account for all directional components of gravity acting on the breast.	Yes: This method has previously been performed in a laboratory environment.

Chapter 5: Developing alternative methods for identifying the neutral breast position

<p>Static extremes</p>	<p>The neutral position was estimated as the mid-point between the extreme positions of the breast when deformed statically by gravity (Scurr, White, Milligan, <i>et al.</i>, 2011a).</p>	<p>Untested: There has been no evaluation of whether the static extreme positions of the breast relate to the neutral position.</p>	<p>Yes: This method has previously been performed in a laboratory environment.</p>
<p>Mathematical modelling</p>	<p>The effect of gravity was countered mathematically based on the mechanical properties of the breast. Existing models have ranged from simple conical approximations of breast shape to complex finite-element analysis based on data from MRI scans (Azar <i>et al.</i>, 2002; Z. Gao & Desai, 2010; Gefen & Dilmoney, 2007; Haake & Scurr, 2010; Ng & Sudharsan, 2001, 2004; Rajagopal, 2007; Zain-UI-Abdein <i>et al.</i>, 2013).</p>	<p>Weak: Due to the unknown mechanical properties of the breast, current breast deformation models have large inaccuracies, up to 12.4 mm, when predicting breast position (Tanner <i>et al.</i>, 2006) (section 2.3.2).</p>	<p>Yes: This method has previously been performed in clinical laboratory environments.</p>
<p>Gravity-loaded breast position</p>	<p>The natural gravity-loaded breast position was not intended to represent the neutral breast position. However, it has been used in place of the neutral position in previous research aiming to quantify breast extension and breast strain (Scurr, Bridgman, <i>et al.</i>, 2009; Scurr, White, Milligan, <i>et al.</i>, 2011a).</p>	<p>The gravity-loaded breast position would only represent the neutral position if gravity had no effect on static breast position.</p>	<p>Yes: This method had already been implemented within this thesis.</p>

Table 5.2: Novel methods for identifying the neutral position based on counteracting the effects of gravity on the breast.

Method	Neutral position definition	Evaluation	
		Theoretical underpinning	Feasible within the laboratory
Extensometer	An extensometer consists of two plates that can be incrementally moved closer or further from one another. If an extensometer is placed on the skin and the plates are gradually brought closer together then the skin between them begins to wrinkle (Clark <i>et al.</i> , 1996; Jacquet, Josse, Khatyr, & Garcin, 2008). The distance between the plates at the wrinkle point represents the neutral (un-extended) length of the skin. This method could be applied to the breast skin to assess the neutral breast position.	Strong: This method has been applied to skin on other areas of the body to identify zero-strain states.	No: This method would be exceptionally time-consuming and invasive if used across the entire surface of the breast. The highly deformable breast tissue may also cause problems when attempting to segment the breast for measurement.

Chapter 5: Developing alternative methods for identifying the neutral breast position

Terminal velocity	<p>At terminal velocity the forces of gravity and drag are balanced, providing a state in which there are no resultant forces on the falling body (Scheck, 2010). This provides the potential to measure the neutral breast position when there are no forces acting to deform the breast tissue.</p>	<p>Strong: Assuming that there is no relative motion between the breast and body at terminal velocity then the breast would be in its equilibrium position, unaffected by gravity.</p>	<p>No: Calculations demonstrate that fall heights of approximately 920 m in air, and 1.1 m in water, would be required to reach terminal velocity, which were both unachievable within the laboratory.</p>
Drop landing	<p>Considering the damped oscillations that occur during a breast drop (about the stationary breast position) (Haake & Scurr, 2011), it was proposed that during the initial stage of free-fall the breast would oscillate about its neutral position. The neutral position could therefore be identified during the flight phase of a drop landing.</p>	<p>Untested: There has not been any prior investigation into breast movement during free-fall, so it was unknown whether damped oscillation behaviour would occur.</p>	<p>Untested: Further work was required to assess the drop height required for this method before it could be classified as achievable in the laboratory (see section 5.4.1d).</p>

Chapter 5: Developing alternative methods for identifying the neutral breast position

<p>Zero-acceleration in free-fall</p>	<p>Newton's second law states that the resultant force on an object is proportional to the rate of change of momentum. This implied that if there were no resultant forces on the breast at a particular instant (<i>i.e.</i> zero acceleration), and there was no ground reaction force, then the breast may be in its neutral position. The neutral breast position could therefore be identified from instances of zero acceleration during flight (<i>e.g.</i> when running or jumping).</p>	<p>Untested: There may not be any occurrences of zero-acceleration during dynamic activity; or alternatively any zero-points identified may correspond to constant velocity and not to a consistent neutral position.</p>	<p>Yes: This method would use activities already implemented within biomechanics laboratories (<i>e.g.</i> running or jumping).</p>
<p>Force-measuring bra</p>	<p>It may be possible to create a breast support garment fitted with force-measuring devices to measure the forces exerted on the breast. The garment could then be fitted to a static participant and adjusted until the force in all three directions was in equilibrium with gravity, thus reproducing the neutral breast position.</p>	<p>Strong: This method had the potential to counteract the force of gravity in multiple directions across the breast's surface.</p>	<p>No: Due to the highly deformable breast tissue, an adjustable bra would have to exert equal and opposite force (to gravity) across the entire surface of the breast without causing it to deform within itself. This was not considered achievable within the laboratory.</p>

5.3.3. Discussion

Four different methods were identified from previous literature for determining the neutral breast position. The static gravity-loaded breast position was also incorporated into the list of existing neutral position methods as it had previously been used instead of the neutral position within breast research. In addition, five novel methods were conceived based on fundamental scientific principles. These methods were evaluated based on their theoretical underpinning and their suitability for a laboratory environment. As this was an exploratory study, it was deemed important to take as many different methods as possible through to the practical stages of testing. However, four methods were excluded during this initial stage of evaluation. Mathematical modelling of the breast was excluded due to the many unknown properties of the breast. As discussed in section 2.3.2, existing breast models are prone to large errors when predicting deformations and insufficient data are available on the physical properties of the breast to produce accurate predictive breast models. Physical measurement of the breast therefore remained the most accurate option for estimating the neutral position. The extensometer and force-measuring bra methods were excluded from this study due to the difficulty in applying these procedures to the highly malleable breast tissue. The terminal velocity method was also excluded due to the unattainable drop height required, although the drop landing method was conceptually similar and was included in the subsequent stage of this study. All other neutral position methods were taken forward to the second stage of evaluation within this chapter.

5.3.4. Conclusion

Shortlisted neutral position methods that were taken forward to the second stage of testing in the laboratory were as follows:

Existing methods

- Buoyancy in water
- Static extremes
- Breast drop
- Gravity-loaded static position

Novel methods

- Drop landing
- Zero acceleration in free-fall

Neutral position methods excluded from further testing based on the results of stage 1 were as follows:

- Mathematical modelling
- Extensometer
- Terminal velocity
- Force-measuring bra

5.4. Stages 2 and 3: Laboratory testing

5.4.1. Method

The practicality (stage 2), accuracy (stage 3), and precision (stage 3) of each neutral position method was assessed in this section. Practicality was assessed using two criteria: (1) Could the method be implemented successfully in the laboratory? ; (2) Could a neutral nipple position estimate be achieved? Neutral position methods that met these two practicality criteria were taken forward to stage 3 of this study. In stage 3 each neutral position method was implemented alongside the gold-standard buoyancy method, using the same 14 participants, to assess the accuracy and precision of the predicted neutral nipple position. The buoyancy in water method was implemented in the buoyancy tank (Figure 3.13) using the procedures described in section 4.3.2. All other neutral position methods were performed in the biomechanics laboratory where eleven Qualisys Oqus cameras were set up an arc around the centre of the laboratory. The cameras were calibrated using the standard Qualisys calibration axis and wand. Retro-reflective markers (12 mm diameter) were applied to the torso and left nipple using hypoallergenic tape. The recommended breast biomechanics marker set (Figure 3.2) was used for the practicality testing (stage 2). During stage 2 it was observed that soft tissue motion had a negative effect on the stability of the recommended torso marker set, which led to the development of an improved torso marker set (described in section 3.4) with an additional tracking marker on the xiphoid process and fixed rib landmarks (Figure 4.1). This improved torso marker set was implemented for the accuracy and precision testing (Stage 3) within this study.

Chapter 5: Developing alternative methods for identifying the neutral breast position

Participants performed a number of familiarisation trials of each method before three measurements of the estimated neutral nipple position were taken. A detailed description of each neutral position method is presented in the following sections:

5.4.1a Buoyancy in water

5.4.1b Breast drop

5.4.1c Static extremes

5.4.1d Drop landing

5.4.1e Zero acceleration during treadmill activity

5.4.1f Zero acceleration during jumping activity

5.4.1g Gravity loaded static position

Data analysis

Optoelectronic data were analysed using the QTM software to reconstruct the 3D trajectories of the nipple and torso markers before exporting the co-ordinate data to Visual 3D for further analysis. Underwater data for the buoyancy in water method was collected using underwater cameras, the 3D trajectories of the nipple and torso markers were reconstructed in SIMI and exported to Visual 3D for further analysis.

Two analysis methods were implemented within Visual 3D in stage 2 and stage 3 of this study. Practicality testing (stage 2) used a torso segment defined by the suprasternal notch marker (proximal end) and the two rib markers (distal end). A POSE estimation method was used to create the torso reference frame with the origin at the proximal end of the segment (segment 1 described in section 3.4.3). Raw co-ordinate data were filtered using a second-order Butterworth filter with a cut off frequency of 13 Hz, which was determined based on the sampling frequency using the equation provided by Yu (1999) (Yu *et al.*, 1999). Left nipple position was then calculated in three dimensions relative to the torso segment origin.

During the accuracy and precision testing (stage 3), several alterations were made to the analysis methods to improve the quality of the neutral nipple position data. Firstly, a

Chapter 5: Developing alternative methods for identifying the neutral breast position

more stable torso segment construction method was implemented in Visual 3D (segment 3 described in section 3.4.3). The addition of a torso marker on the xiphoid process and substitution of the rib markers using fixed landmarks enabled a more stable torso origin to be defined at the proximal end of the segment. A stable torso segment was particularly important within this study as nipple position measurements were compared between a range of dynamic and static conditions which were anticipated to induce differing levels of soft tissue movement. Secondly, a generalised cross-validatory (quintic) spline was used to filter the co-ordinate data of each marker during stage 3 of this study. This filtering technique has been shown to be more appropriate for studies using both displacement and acceleration data (*i.e.* the breast drop method) than the Butterworth filter used in stage 2 (Giakas & Baltzopoulos, 1997a). In both stages of the laboratory testing the mean neutral position of the left nipple, relative to the torso, was calculated from three trials of each method for each participant.

Accuracy was assessed using absolute differences in mean neutral nipple position, measured using the alternative and gold-standard neutral position methods calculated using Equation 2.2 (section 2.6.1), and paired samples T-tests conducted using SPSS (IBM SPSS statistics version 20). The correlation coefficient (r) was used for calculating effect size where effect sizes were defined as: small = 0.1; moderate = 0.3; and large = 0.5 (Field, 2009). Standard deviations were calculated in Excel and typical error of measurement was evaluated using the spreadsheet provided on Hopkins's website (Hopkins, 2000a). As this study used a progressive multi-stage approach to evaluate each neutral position method, clear criteria had to be defined at each stage of testing. The criteria for progression through each stage of this study were defined as:

Stage 2

- (1) Successful implementation in the laboratory?
- (2) Estimate of the neutral nipple position achieved?

Stage 3

Acceptable accuracy

- (1) Absolute difference (to the gold-standard neutral nipple position) ≤ 5 mm.
- (2) Paired samples t-tests (between the gold-standard and alternative neutral position methods) demonstrate no significant difference in nipple position ($p < 0.05$).

Acceptable precision

- (1) Within-participant standard deviations ≤ 5 mm (based on peak resultant value during static nipple measurements assessed in section 4.4.4)
- (2) Typical error of measurement (TEM) ≤ 3.5 mm.

5.4.1a. Buoyancy in water

Introduction

Prior to the work undertaken within this thesis, the buoyancy in water method had been used within a clinical setting to measuring the neutral breast position (Rajagopal, 2007; Zain-Ul-Abdein *et al.*, 2013). Although an improved gold-standard neutral position method was developed in Chapter 4, it was anticipated that future research may select to use the water only buoyancy study due to its previous clinical implementation and the higher financial and time-related costs associated with immersion in soybean oil. It was therefore important to evaluate the accuracy and precision of the water-only neutral position method against the gold-standard method to investigate the error in neutral position estimate associated with the potentially mismatched mass-densities of the breast and water.

Stage 2: Buoyancy in water practicality testing

The buoyancy in water method was previously described and successfully implemented in section 3.5.2, and was taken straight forward to Stage 3 for accuracy and precision assessment against the gold-standard method.

Stage 3: Buoyancy in water accuracy and precision testing

Accuracy and precision method

The accuracy and precision testing of the buoyancy in water method was described in section 4.3 (session 2).

Accuracy and precision results

The mean neutral nipple positions measured using the buoyancy in water and gold-standard methods were presented in Table 4.3. Accuracy and precision results are shown in Table 5.3 and Table 5.4 respectively.

Table 5.3: Absolute difference (to the gold-standard value) and standard deviation in neutral nipple position measured using the buoyancy in water method.

	Breast Size	Absolute difference (mm)			Standard deviation (mm)		
		Anterior-posterior	Medial-lateral	Superior-inferior	Anterior-posterior	Medial-lateral	Superior-inferior
Participant 1	32B	0.7	1.2	0.5	0.6	0.3	0.2
Participant 2	32B	2.6	0.4	1.0	0.2	0.4	0.5
Participant 3	32B	2.1	1.8	2.2	0.2	0.2	0.2
Participant 4	34B	3.3	1.0	1.2	1.2	0.5	0.9
Participant 5	32C	1.6	3.2	3.6	0.5	0.4	1.2
Participant 6	32C	1.1	2.5	2.5	1.1	0.5	0.5
Participant 7	32D	0.9	0.3	0.4	0.9	0.8	0.1
Participant 8	32D	5.3	4.6	3.3	2.2	1.6	0.2
Participant 9	32D	2.3	1.8	5.6	0.9	0.4	0.3
Participant 10	34D	1.2	2.0	3.9	0.2	0.6	1.0
Participant 11	32DD	1.1	0.1	1.3	0.4	0.2	0.2
Participant 12	30E	3.9	4.5	1.3	0.9	0.7	0.4
Participant 13	34DD	0.4	0.2	3.3	2.6	0.7	0.2
Participant 14	34DD	0.6	0.0	5.3	0.7	0.3	0.5
Mean		1.9	1.7	2.5	0.9	0.6	0.5
Maximum		5.3	4.6	5.6	2.6	1.6	1.2

Table 5.4: Paired samples t-test results and typical error of measurement (TEM) values for the buoyancy in water method.

Buoyancy in water	Anterior-posterior	Medial-lateral	Superior-inferior
t-value (t)	0.119	0.311	-3.772
Significance (p)	0.907	0.761	0.002*
Effect size (r)	0.033	0.086	0.723†
TEM (mm)	1.2	0.5	0.5

* denotes a significant difference ($p < 0.05$), † denotes a large effect size ($r > 0.5$)

Discussion

It was interesting to note that many of the absolute differences between the water only and gold-standard buoyancy methods were above the 1.4 mm maximum measurement error associated with the buoyancy method (identified in section 4.4.3). This implied that there was a measurable change in nipple position caused by the density mismatch between the breast and water, an effect that had previously been described as trivial in the literature (Zain-Ul-Abdein *et al.*, 2013). Accuracy assessment of the buoyancy in water method demonstrated that three participants (Participants 8, 9 and 14) had an absolute difference (to the gold-standard measurement value) in one component of nipple position that exceeded the acceptable accuracy criteria (Table 5.3). The data from these three participants prevented the buoyancy in water method from being recommended as an accurate method for estimating the neutral nipple position, despite its previous implementation within clinical research. However, it was acknowledged that the water method demonstrated acceptable accuracy for the majority of participants and that there may have been external factors that caused the reduced accuracy for the remaining three participants. Inspection of the participant information (Table 4.1) revealed that participants 8 and 9 had the longest time intervals between the water and soybean oil testing sessions (14 and 8 days respectively). The extended time interval may have led to a change in breast size between testing sessions that increased the absolute difference in nipple position between the buoyancy in water and gold-standard measurements. This suggestion is supported by the observation that all participants, but

Chapter 5: Developing alternative methods for identifying the neutral breast position particularly participant 8, experienced a change in their measured gravity-loaded nipple positions between the water and soybean oil testing sessions (Table 4.8).

The varying time intervals between water and soybean oil immersion constituted a limitation of this study. The time required to implement all the neutral position methods on each individual and the constraint that all participants had to complete the soybean oil testing on the same day meant that the water immersion was up to 14 days before the soybean oil immersion for some participants. However, not all participants who had absolute differences in nipple position of more than 5 mm had a long time interval between immersions. Participant 14 had only a 2 day interval between testing sessions but a maximum absolute difference in nipple position of 5.3 mm, although this participant had performed bare-breasted exercise on more than 30 occasions and had previously been sunburnt on her breasts (Table 4.1). These factors were identified in the literature review as contributors to skin damage, meaning that this participant's breast skin may have been damaged preventing the breast from returning to its correct neutral position during the gold-standard neutral position measurements.

Paired sample t-tests showed no significant difference in anterior-posterior or medial-lateral nipple position between the buoyancy in water and the gold-standard neutral position methods. A statistically significant difference, and large effect size, was observed in the superior-inferior component of nipple position between the two neutral position methods. The distinction between statistical and clinical significance has been stressed within the literature as discussed in section 2.6.1 (Hopkins, 2002). It was proposed that in this case, a statistically significant difference was observed in the superior-inferior component of nipple position due to the consistent directional movement from water to the gold-standard measurement, which was not present in the other directions. Clinically significant (> 5mm) differences were observed in the anterior-posterior and superior-inferior directions.

Acceptable precision was demonstrated for the buoyancy in water method using both SD (all values ≤ 2.6 mm) and TEM (all values ≤ 1.2 mm). A high level of precision was anticipated with this method due to its static nature.

Conclusion

Acceptable accuracy was achieved using the buoyancy in water method for 11 out of the 14 participants. For the remaining three participants the maximum absolute difference to the gold-standard measurements (5.6 mm) was close to the maximum error criteria (5 mm), suggesting that stricter inclusion criteria, and a reduced time interval between testing sessions, may enable this method to achieve acceptable accuracy in future research. Acceptable precision was achieved when estimating all three components of the neutral nipple position.

5.4.1b. Breast drop

Introduction

The breast drop method has been used in previous breast motion research to identify the neutral breast position prior to calculating breast strain (Haake *et al.*, 2012; Haake & Scurr, 2011). The breast drop method and its underpinning theory were described in section 2.2. The aim of this method was to estimate the neutral breast position using the displacement of the nipple at the latest time point during free-fall where nipple acceleration was still equal to that due to gravity (*i.e.* at the point just before the supporting structures begin to extend) (Figure 5.2). This may occur on more than one occasion due to multiple breast oscillations, giving the possibility of deriving more than one estimate of the neutral position using this method.

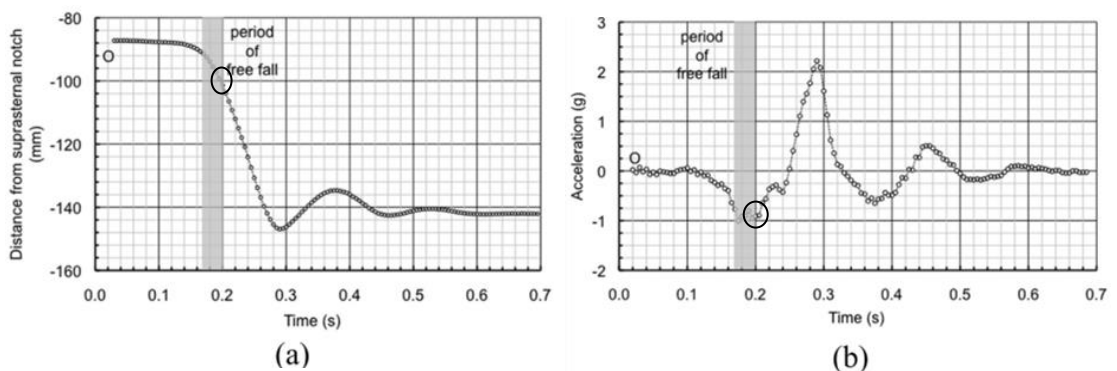


Figure 5.2: Superior-inferior breast displacement (a) and breast acceleration (b) during a breast drop as presented by Haake & Scurr (2011).

Stage 2: Breast drop practicality testing

Practicality method

Five participants gave informed consent to take part in this practicality study (breast sizes 32 to 34, C to DD). Each participant had four retro-reflective markers applied to their breast and torso as described previously (Figure 3.2).

Chapter 5: Developing alternative methods for identifying the neutral breast position

During this practicality study two versions of the breast drop were performed. The first version followed the procedure described by Haake and Scurr (2011). Participants were asked to lift their left breast and support it with their right hand (Figure 5.3 a). The left arm remained relaxed by their side in order to minimise any muscle activity that may affect the position of the left nipple. Participants then released their breast and the resulting motion of the breast was tracked at 200 Hz using the optoelectronic camera system. The second version of the breast drop method was included in an effort to establish a standardised lifting technique. Ideally this would ensure that the breast was lifted directly upwards using an equal force across its surface. This was attempted by using a Theraband stretched over the breast (Figure 5.3 b). Participants held the band at either end and lifted directly upwards (ensuring the breast was not pulled to either side). They then rolled the band upwards off the breast to initiate the breast drop. Participants performed both versions of the breast drop three times.

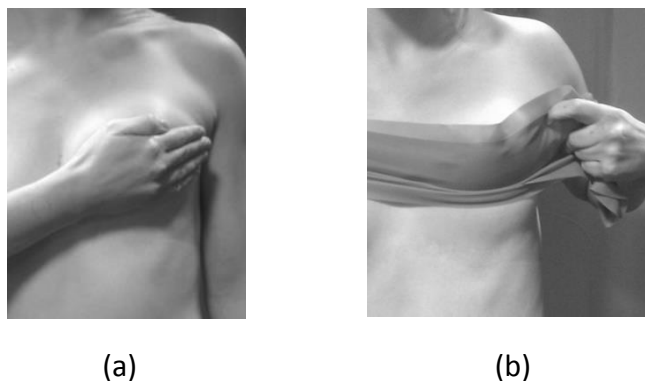


Figure 5.3: Practicality study breast drop method using the hand (a) and a Theraband (b) to support the breast.

Marker positional data was identified in QTM and exported to Visual 3D. Co-ordinate data were filtered and the relative left nipple position was calculated as previously described (section 5.4.1). The second derivative of the superior-inferior relative nipple displacement was used in Visual 3D to calculate nipple acceleration. Acceleration was then divided by 9.81 to find acceleration in multiples of gravitational acceleration (g).

Time points at which nipple acceleration was equal to gravitational acceleration (-1 g) were identified in Visual 3D. The final frame number during the initial breast drop, and

Chapter 5: Developing alternative methods for identifying the neutral breast position

any subsequent frames in which acceleration was equal to -1 g, were noted (Figure 5.4 a) and used to identify the corresponding left nipple displacement (Figure 5.4 b). This three dimensional displacement data represented the estimated neutral nipple position(s) using this method.

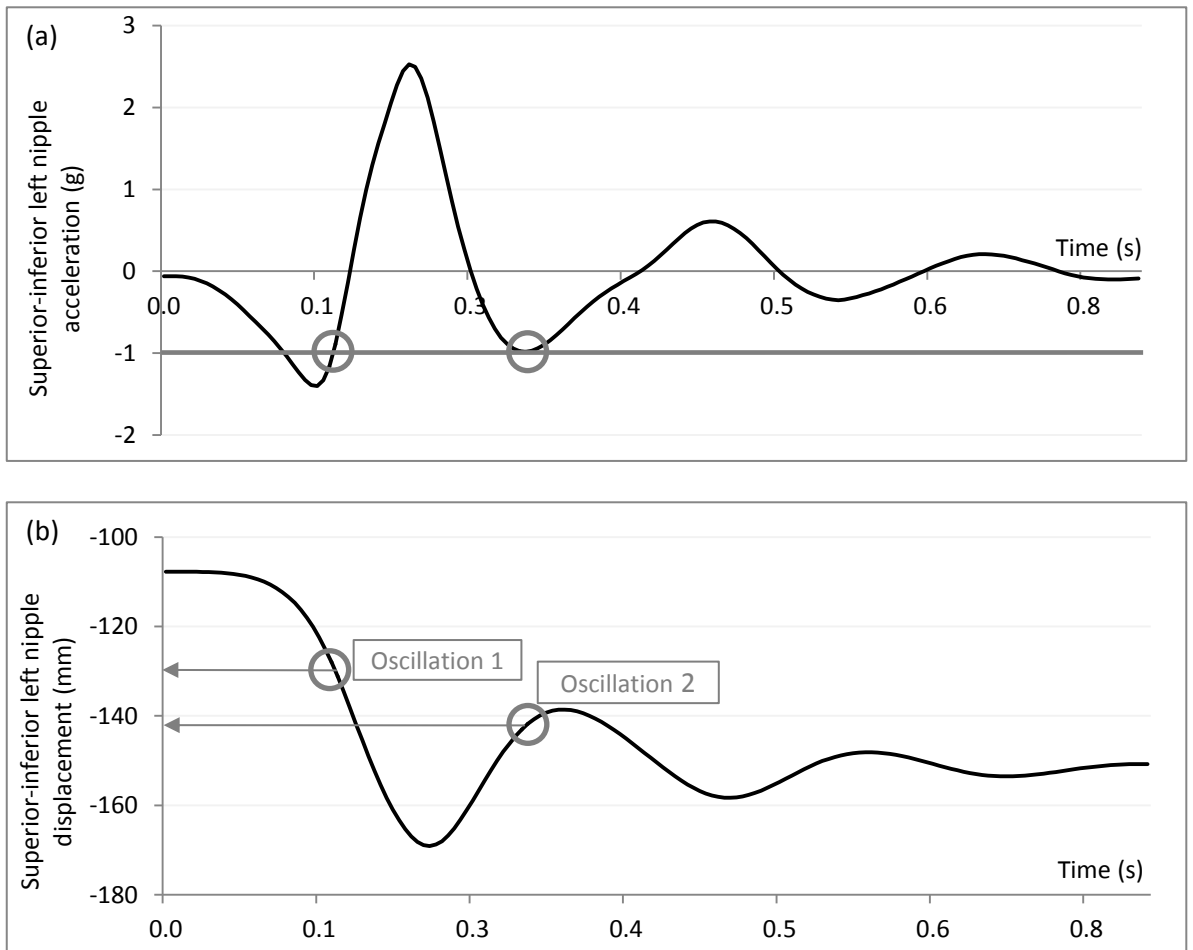


Figure 5.4: Superior-inferior left nipple acceleration (above) and displacement (below) during a breast drop for a participant with breast size 32C.

Practicality results

Table 5.5: Practicality results for the breast drop method.

Practicality measure	Outcome
Successful implementation in the laboratory?	Yes (hand only)
Estimate of the neutral nipple position achieved?	Yes

Estimated neutral position data from this practicality study were presented in Appendix F.

Practicality discussion

This method was quick to perform in the laboratory, and minimal participant movement meant that a simple camera set-up could be used. Participants were able to complete the breast drop repeatedly using the hand release method. The introduction of a Theraband aimed to improve the consistency of the breast drop method, although in practise this version was awkward during testing. On several occasions the band rolled off the breast very quickly causing the participant to turn their head and change their torso position. This was not only a practical problem but also undermined the theory underpinning the breast drop method as forces perpendicular to gravity were introduced to the breast. As mentioned previously, the breast drop method only took into account superior-inferior nipple acceleration due to the assumption that gravity acts inferiorly on the breast. Therefore, if participants rotate their torso during the trial, creating additional forces on the breast, then the breast drop theory is no longer valid. For this reason the Theraband method was excluded from stage 3 of this study.

At least one estimate of the neutral nipple position was achieved for all the participants in the practicality testing but there were also several unsuccessful trials. Data loss was largely due to obstruction of the nipple marker, although there were also instances where the nipple marker did not demonstrate the expected acceleration pattern required for estimation of the neutral position. These intermittent problems indicated variation in technique between trials and between participants. In some cases improved data was obtained following several practice breast drops, though this method remained

Chapter 5: Developing alternative methods for identifying the neutral breast position problematic for larger-breasted individuals who struggled to support their whole breast without compressing it against their torso.

Practicality conclusion

The breast drop method using hand support was taken forward for accuracy and precision assessment in stage 3. The Theraband method was excluded from stage 3 of this study due to problems with participant posture and marker obstruction.

Stage 3: Breast drop accuracy and precision testing

Accuracy and precision method

Stage 3 testing for the breast drop method took place on the same day as the gold-standard buoyancy data was collected in water, with the same 14 participants (Table 4.1) using the same marker set (Figure 4.1). Each participant performed several practice breast drop familiarisation trials to ensure minimal torso movement and the rapid release of the breast to minimise marker obstruction. Following the familiarisation period, three breast drops were recorded at 200 Hz using the optoelectronic camera system. Data was identified in QTM, filtered in Visual 3D using a generalised cross validatory (quintic) spline, and converted to relative data as described in section 5.4.1. The mean neutral position estimate was then calculated for each participant as described in the practicality study. For some participants a second neutral position estimate was obtained if the breast completed more than one oscillation in which the inferior nipple acceleration was equal to -1 g.

Accuracy and precision results

Table 5.6: Mean neutral nipple position measured using the breast drop and gold-standard methods.

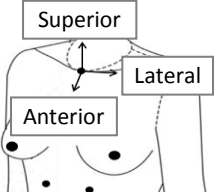
	Breast Size	Estimated neutral nipple position using breast drop (oscillation 1) (mm)			Estimated neutral nipple position using breast drop (oscillation 2) (mm)			Gold-standard neutral nipple position (mm)		
		Anterior-posterior	Medial-lateral	Superior-inferior	Anterior-posterior	Medial-lateral	Superior-inferior	Anterior-posterior	Medial-lateral	Superior-inferior
Participant 1	32B	No occurrences of equal inferior nipple and gravitational acceleration						46.6	85.7	-134.5
Participant 2	32B	No occurrences of equal inferior nipple and gravitational acceleration						44.2	73.6	-165.0
Participant 3	32B	No occurrences of equal inferior nipple and gravitational acceleration						48.1	92.1	-130.4
Participant 4	34B	No occurrences of equal inferior nipple and gravitational acceleration						24.5	127.7	-153.4
Participant 5	32C	No occurrences of equal inferior nipple and gravitational acceleration						52.4	103.9	-135.0
Participant 6	32C	No occurrences of equal inferior nipple and gravitational acceleration						55.4	91.6	-145.0
Participant 7	32D	42.6	83.6	-111.7	-	-	-	47.6	87.8	-126.4
Participant 8	32D	29.8	121.5	-95.1	-	-	-	51.1	116.5	-125.8
Participant 9	32D	30.5	103.5	-118.6	31.3	108.0	-154.2	44.4	102.2	-144.6
Participant 10	34D	60.7	99.0	-132.4	50.7	108.8	-162.1	53.3	97.2	-153.2
Participant 11	32DD	No occurrences of equal inferior nipple and gravitational acceleration						63.8	92.0	-129.0
Participant 12	30E	80.1	83.6	-128.3	60.1	117.0	-157.8	85.4	88.2	-145.2
Participant 13	34DD	No occurrences of equal inferior nipple and gravitational acceleration						83.4	90.9	-176.1
Participant 14	34DD	No occurrences of equal inferior nipple and gravitational acceleration						74.2	107.3	-128.8
Mean		48.7	98.3	-117.2	47.3	111.3	-158.0	55.3	96.9	-142.3
Standard deviation		21.6	15.8	14.8	14.7	5.0	3.9	16.5	13.7	15.3

Table 5.7: Absolute difference (to the gold-standard value) and standard deviation in neutral nipple position measured using the breast drop method.

	Breast Size	Breast drop – Oscillation 1						Breast drop – Oscillation 2					
		Absolute difference (mm)			Standard deviation (mm)			Absolute difference (mm)			Standard deviation (mm)		
		Anterior-posterior	Medial-lateral	Superior-inferior	Anterior-posterior	Medial-lateral	Superior-inferior	Anterior-posterior	Medial-lateral	Superior-inferior	Anterior-posterior	Medial-lateral	Superior-inferior
Participant 7	32D	5.0	4.2	14.7	Insufficient trials			No second oscillation					
Participant 8	32D	21.3	5.0	30.7	Insufficient trials			No second oscillation					
Participant 9	32D	13.9	1.8	26.0	0.9	2.2	6.3	13.1	5.8	9.6	3.2	1.1	1.4
Participant 10	34D	7.4	1.8	20.8	0.7	1.5	0.5	2.7	11.6	8.8	2.3	1.8	1.2
Participant 12	30E	5.3	4.6	17.0	0.3	6.6	9.5	25.4	28.8	12.5	Insufficient trials		
Mean		10.6	3.5	21.8	0.6	3.4	5.4	13.7	15.4	10.3	2.7	1.4	1.3
Maximum		21.3	5.0	30.7	0.9	6.6	9.5	25.4	28.8	12.5	3.2	1.8	1.4

Table 5.8: Paired samples t-test results (compared to gold-standard values) and typical error of measurement (TEM) values for the breast drop method.

Breast drop	Breast drop – Oscillation 1			Breast drop – Oscillation 2		
	Anterior-posterior	Medial-lateral	Superior-inferior	Anterior-posterior	Medial-lateral	Superior-inferior
t-value (t)	1.579	0.068	-7.450	2.088	-2.232	9.230
Significance (p)	0.189	0.949	0.002*	0.172	0.155	0.012*
Effect size (r)	0.620†	0.034	0.966†	0.828†	0.845†	0.988†
TEM (mm)	0.3	4.6	5.2	Insufficient trials		

* denotes a significant difference ($p < 0.05$), † denotes a large effect size ($r > 0.5$)

Discussion

Although the breast drop method was implemented successfully during practicality testing (stage 2), a neutral nipple position estimate could only be obtained for 5 out of the 14 participants tested in the full scale testing (stage 3) (Table 5.6). The neutral position could not be estimated for the other 9 participants due to the inferior acceleration of their nipple markers never reaching -1 g. The limited success in stage 3 of this study may have been due to the restricted participant sample leading to different breast kinematics being observed (younger participants who had minimal exposure to skin damaging factors such as UV radiation). However, it was more likely that the discrepancy in success rates between stage 2 and stage 3 of this study occurred because of changes in the filtering technique used on the displacement data. The displacement data in the practicality testing was filtered using a low-pass Butterworth filter whereas the accuracy and precision testing implemented a generalised cross-validatory quintic spline filter as recommended for the derivation of acceleration from displacement data (Giakas & Baltzopoulos, 1997a). The acceleration data derived from the spline filtered displacement (accuracy and precision testing) was typically much smoother than the acceleration data derived from Butterworth filtered displacement (practicality study). Using the Butterworth filter in the practicality study may have resulted in several false-positive neutral estimates where spikes in the nipple acceleration data may have produced incorrect measurements of the neutral nipple position as acceleration crossed the -1 g mark.

The nature of the data obtained using the breast drop method was inherently difficult to process due to the short duration of each breast drop trial. The nipple marker was typically obscured at the initial stage of the breast drop due to the location of the hand used to support the breast. The nipple marker then became visible during the release and oscillation phases of the breast drop during which acceleration was calculated. Applying filters (spline or Butterworth) to displacement data before deriving acceleration commonly causes endpoint errors, in which the acceleration signal behaves erratically following gaps in the displacement data (Vint & Hinrichs, 1996). Unfortunately, using this method, the point of interest in the acceleration data (immediately following release) was

almost always preceded by a large gap in the displacement data caused by the hand occluding the nipple marker. Therefore, derivation of acceleration from the nipple marker displacement during a breast drop may be unavoidably prone to errors due to the filtering process applied to the data.

Despite the small number of successful trials of the breast drop method in stage 3 of this study the accuracy and precision evaluations were still performed, although the results were interpreted with caution due to the small sample size. The only component of the neutral nipple position estimated using the breast drop that achieved acceptable accuracy (using absolute difference) was the medial-lateral component (Table 5.7). All other directional components of the neutral nipple position were outside of the acceptable accuracy criteria. The gold-standard neutral position method demonstrated that the effect of gravity on nipple position was predominantly in the inferior and posterior position (Figure 4.8). Accurate estimation of these two components of nipple position may therefore be more important than the accurate estimation of the medial-lateral component, which only differed from the gravity-loaded position by an average of 7.4 mm. Statistical testing demonstrated no significant difference between the anterior-posterior and medial-lateral neutral nipple positions measured using the breast drop and gold-standard methods (Table 5.8), although absolute differences in these directions were up to 25.4 mm and 28.8 mm respectively (Table 5.7). A large absolute difference, combined with no statistical difference (to the gold-standard neutral nipple position), indicates that the neutral nipple position estimates using the breast drop method were distributed about the gold-standard measurement.

Precision assessment demonstrated acceptable within-participant precision (using SD) in the anterior-posterior direction but not in the medial-lateral or superior-inferior directions (Table 5.7). The group precision assessed using TEM values demonstrated acceptable precision in the anterior-posterior and medial-lateral directions, but not in the superior-inferior direction. Although these results may indicate acceptable precision in at least one component of nipple position, many participants had insufficient trials to calculate SD or TEM values suggesting that the breast drop method was not precise as participants could not replicate the method successfully.

Conclusion

Although initial practicality testing demonstrated that the breast drop method was achievable within the laboratory, there were a high number of unsuccessful trials during the accuracy and precision testing. This was predominantly due to not achieving the required nipple acceleration values for predicting the neutral nipple position, which may have been caused by the application of a spline filter to the displacement data. Accuracy and precision assessment of the breast drop method was limited due to the small number of trials successfully completed. Results demonstrated that the breast drop method was not accurate or precise when estimating the superior-inferior component of the neutral nipple position. The anterior-posterior component of nipple position was estimated precisely, but was not accurate, and the medial-lateral component was accurate but not precise (when assessed using SD). In conclusion, due to the poor success rate, and limited accuracy and precision, the breast drop method was not recommended for future research aiming to identify the neutral nipple position.

5.4.1c. Static extremes

Introduction

The static extreme method was based on a study by Scurr *et al.* in 2011 (Scurr, White, Milligan, *et al.*, 2011a) in which the maximum static displacement of the breast in each direction was recorded to quantify the additional breast movement that occurred during dynamic activity.

This method was selected as a possible technique for identifying the neutral breast position as it was hypothesised that the breast would move symmetrically about its neutral position when deformed by gravity alone. The neutral nipple position could therefore be estimated using the mid-point between the two static extremes along each axis of movement (anterior-posterior, medial-lateral and superior-inferior) (Figure 5.5).

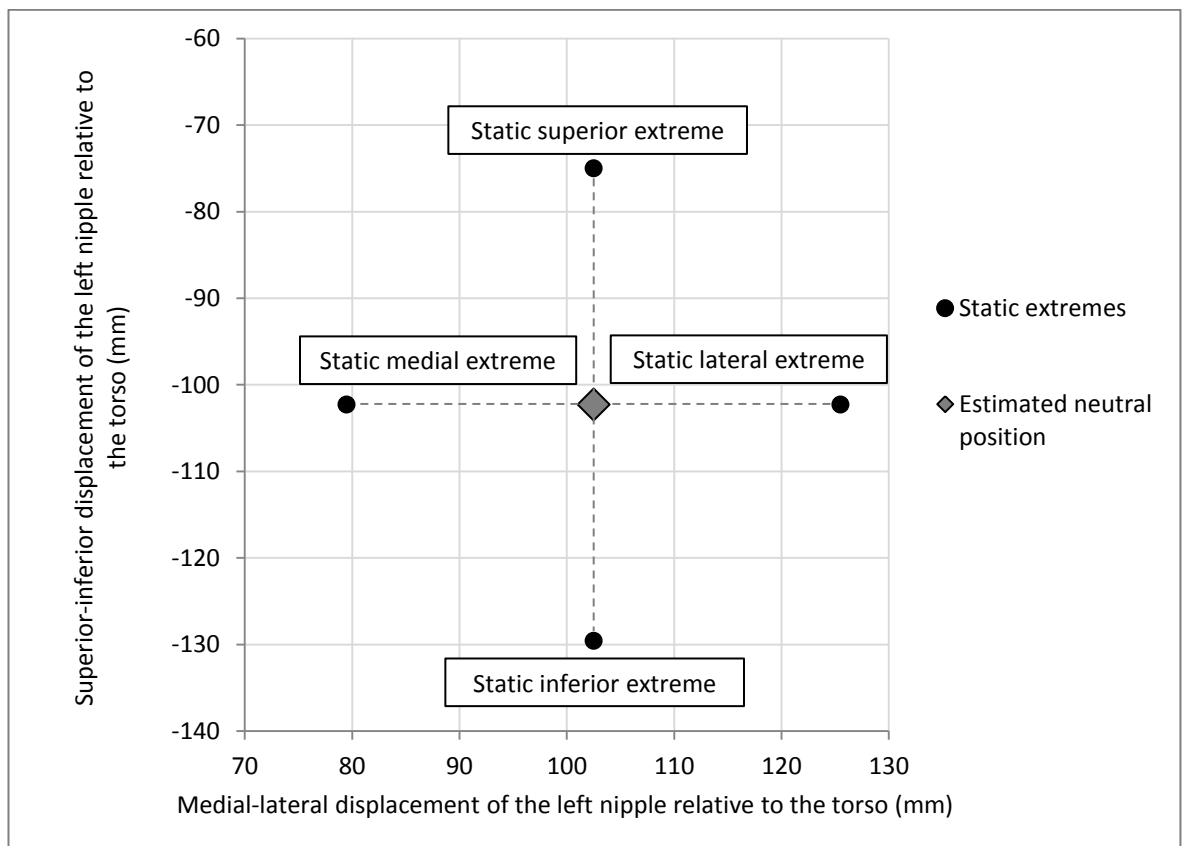


Figure 5.5: Example static extremes and estimated neutral nipple position data viewed in the frontal plane.

The static extreme method for estimating the neutral nipple position focused on aligning each of the three axes of the body to gravity, and recording the resulting position of the nipple relative to the torso. The minimum and maximum position along each axis formed the six points that defined the static extremes of the nipple from which the neutral position estimate could then be calculated.

Stage 2: Static extremes practicality testing

Practicality method

Six participants gave informed consent to take part in this practicality study (breast sizes 32 to 34, C to HH). Each participant had four retro-reflective markers applied to their nipple and torso as described previously (Figure 3.2). Participants attained six different stationary body positions in the biomechanics laboratory (bare-breasted). Each position aimed to align gravity with a different anatomical direction (Figure 5.6) while five 1 s optoelectronic recordings were taken at 200 Hz. Participants kept their back straight and arms relaxed by their sides where possible.

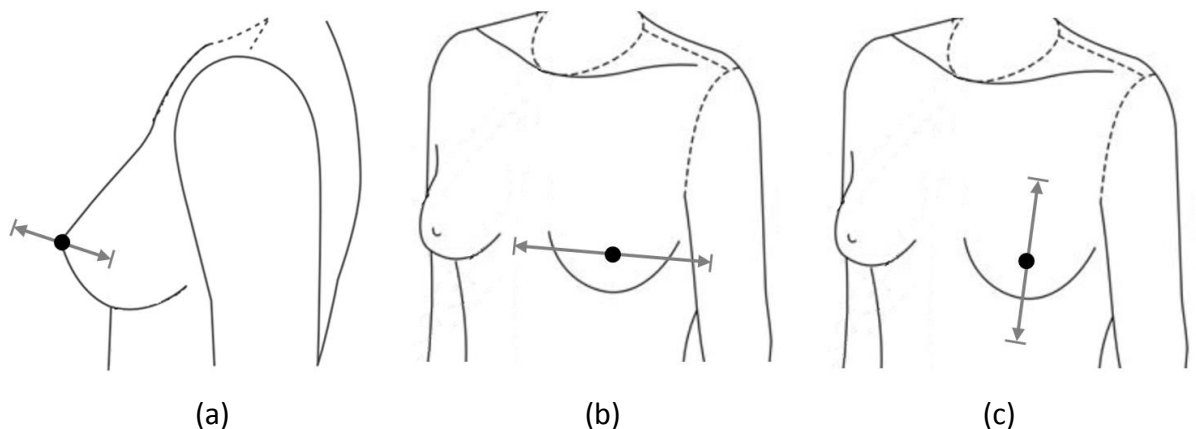


Figure 5.6: Diagrammatic representation of the static extremes of the left nipple in the anterior-posterior (a), medial-lateral (b), and superior-inferior (c) directions.

Chapter 5: Developing alternative methods for identifying the neutral breast position

The anterior extreme of the left nipple was determined with the participants on their hands and knees on top of the table (Figure 5.7 a). Participants kept their back straight and then bent their arms to the point at which their spine was parallel to the floor. The posterior extreme of the left nipple was determined with the participants lying on their back (Figure 5.7 b). Participants lay on a table with their head and spine supported and their legs flat.

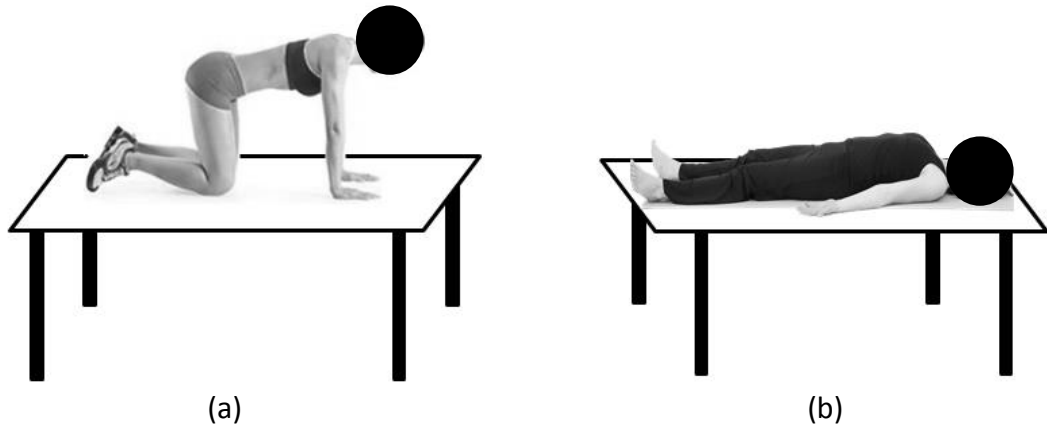


Figure 5.7: Positions used to achieve the anterior (a) and posterior (b) static extremes of the breast.

The medial and lateral extremes of the left nipple were determined with the participants lying on their right (Figure 5.8 a) and left side (Figure 5.8 b). Two padded tables were used to allow a gap for the shoulder and breast to lie below the horizontal. A strap was used to support the arm underneath the table, which allowed the arm to rest by the side without compromising the straight body position or initiating muscle activity which may have affected nipple position.

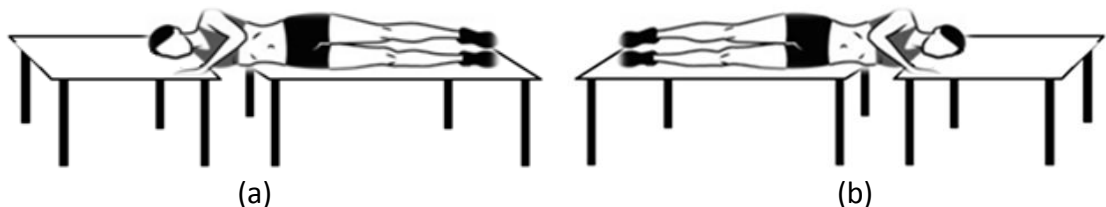


Figure 5.8: Positions used to achieve the medial (a) and lateral (b) static extremes of the breast.

The superior extreme of the left nipple was determined when the participants were inverted by 180° using an inversion table (Confidence PRO folding inversion table) (Figure 5.9 a). The speed of inversion was controlled to minimise participant discomfort. While inverted, participants hung vertically from the inversion table supported only by their ankles. They were asked to look straight ahead and to keep their arms by their sides while maintaining a straight back. The inferior extreme of the left nipple was measured while participants stood upright with their back straight and their arms relaxed by their sides (Figure 5.9 b).



(a)



(b)

Figure 5.9: Positions used to achieve the superior (a) and inferior (b) static extremes of the breast.

The mean relative left nipple position was calculated in each position (as described in section 5.4.1) to provide the six static extreme positions. The midpoint along each axis was then used to estimate the neutral nipple position.

Practicality results

Table 5.9: Practicality results for the static extreme method.

Practicality measure	Outcome
Successful implementation in the laboratory?	Yes
Estimate of the neutral nipple position achieved?	Yes

Estimated neutral position data from this practicality study were presented in Appendix G.

Practicality discussion

All participants included in this practicality study were able to complete this testing protocol and an estimate of the neutral nipple position was achieved for 5 out of the 6 participants included in stage 2. The missing data was caused by marker obstruction during the hands and knees position (Figure 5.7 a). This position was subsequently altered in stage 3 of this study to a kneeling only position with the arms held behind the back (Figure 5.10 a). The addition of the xiphoid process marker during stage 3 of this study also reduced the risk of data loss due to torso marker obstruction as only 3 markers were needed to construct the torso segment during data analysis. It was also observed that participants found maintaining the correct position in the medial-lateral orientations difficult due to the minimal contact area between the body and the table (Figure 5.8). During stage 3 of this study a rigid board was introduced perpendicularly to the table to provide increased stability for the participants and to ensure that a straight back was maintained perpendicularly to the ground in the medial-lateral conditions (Figure 5.10 b).



(a)



(b)

Figure 5.10: Alterations to the medial-lateral (a) and anterior (b) positions for the static extreme method.

Practicality conclusion

The static extremes method met the practicality criteria within stage 2 of this study and was taken forward for accuracy and precision assessment in stage 3. The kneeling and lying (on right and left sides) positions were altered to improve the quality of the data obtained for the accuracy and precision aspect of this study (stage 3).

Stage 3: Static extremes accuracy and precision testing

Accuracy and precision method

Stage 3 of testing for the static extremes method took place on the same day as the gold-standard buoyancy data was collected in water, with the same 14 participants (Table 4.1) using the same marker set (Figure 4.1). Two alterations were made to the static extreme method as described in the previous section in order to reduce the risk of marker obstruction and to improve the standardisation of participant posture in each condition.

Participants performed all six positions in the biomechanics laboratory. Once stationary in each position, three 1 s recordings were taken at 200 Hz using the optoelectronic camera system. Data was identified in QTM, filtered in Visual 3D using a generalised cross validatory (quintic) spline, and converted to relative data as described in section 5.4.1. The six static extremes of nipple position were identified and an estimate of the neutral nipple position was calculated as described for the practicality study.

Accuracy and precision results

Table 5.10 shows the nipple position in each of the six conditions. The maximum and minimum nipple positions along each axis (highlighted in grey in Table 5.10) were used to calculate the neutral nipple position estimates for each participant presented in Table 5.11.

Table 5.10: Mean static extreme positions of the left nipple during accuracy and precision assessment of neutral position methods.

	Breast Size	Condition	Mean static extreme left nipple position (mm)		
			Anterior-posterior	Medial-lateral	Superior-inferior
Participant 1	32B	Anterior	60.4	70.9	-152.3
		Posterior	30.4	99.0	-132.1
		Medial	41.3	74.8	-135.3
		Lateral	4.3	113.3	-119.9
		Superior	48.5	85.4	-127.3
		Inferior	35.8	88.4	-154.2
Participant 2	32B	Anterior	42.1	72.0	-173.0
		Posterior	29.6	90.6	-165.4
		Medial	48.1	50.8	-171.8
		Lateral	1.2	99.4	-151.4
		Superior	35.2	77.7	-159.9
		Inferior	31.5	78.9	-180.8
Participant 3	32B	Anterior	60.4	89.3	-146.0
		Posterior	29.2	104.6	-126.9
		Medial	53.9	68.7	-143.5
		Lateral	22.0	118.7	-128.7
		Superior	51.7	95.5	-122.1
		Inferior	42.5	98.8	-152.4
Participant 4	34B	Anterior	Left nipple obscured		
		Posterior	9.5	141.7	-159.3
		Medial	20.1	107.0	-160.0
		Lateral	1.7	150.3	-158.7
		Superior	24.4	136.2	-153.2
		Inferior	15.0	128.5	-192.4

Chapter 5: Developing alternative methods for identifying the neutral breast position

Participant 5	32C	Anterior	63.2	91.4	-160.4
		Posterior	35.5	115.4	-132.0
		Medial	45.8	78.6	-120.3
		Lateral	33.2	126.7	-124.3
		Superior	51.8	109.6	-133.4
		Inferior	41.9	104.5	-161.4
Participant 6	32C	Anterior	61.9	86.4	-162.0
		Posterior	36.5	105.0	-144.2
		Medial	57.8	66.6	-152.9
		Lateral	35.2	116.6	-148.5
		Superior	54.8	88.9	-124.6
		Inferior	46.1	95.8	-167.8
Participant 7	32D	Anterior	52.5	82.2	-147.7
		Posterior	28.8	105.4	-126.7
		Medial	33.3	92.1	-121.2
		Lateral	29.0	107.9	-127.0
		Superior	53.1	86.6	-119.2
		Inferior	29.3	99.5	-145.6
Participant 8	32D	Anterior	54.2	117.3	-126.9
		Posterior	8.2	132.9	-106.4
		Medial	62.4	86.7	-133.3
		Lateral	-0.8	133.0	-137.8
		Superior	26.1	130.5	-106.4
		Inferior	18.4	132.3	-149.8
Participant 9	32D	Anterior	63.5	90.8	-169.2
		Posterior	23.9	109.2	-134.5
		Medial	52.0	70.9	-145.4
		Lateral	14.2	108.0	-161.1
		Superior	44.6	93.0	-118.8
		Inferior	33.4	104.6	-168.6
Participant 10	34D	Anterior	77.8	79.7	-176.9
		Posterior	36.5	114.0	-146.0
		Medial	46.8	91.9	-139.6
		Lateral	27.9	125.1	-144.7
		Superior	55.2	83.6	-124.6
		Inferior	44.1	113.3	-168.6
Participant 11	32DD	Anterior	62.2	99.2	-141.0
		Posterior	39.0	104.8	-132.5
		Medial	69.7	70.0	-131.3
		Lateral	51.3	115.8	-131.0
		Superior	62.2	98.3	-128.8
		Inferior	45.4	107.0	-151.4

Chapter 5: Developing alternative methods for identifying the neutral breast position

Participant 12	30E	Anterior	95.0	85.5	-157.4
		Posterior	44.1	115.9	-129.4
		Medial	86.2	56.1	-145.4
		Lateral	23.2	125.5	-153.6
		Superior	81.0	98.5	-121.8
		Inferior	65.8	97.6	-179.8
Participant 13	34DD	Anterior	100.7	88.3	-198.7
		Posterior	71.0	110.3	-171.6
		Medial	82.0	49.0	-170.1
		Lateral	78.1	138.2	-166.8
		Superior	77.5	106.4	-136.5
		Inferior	67.7	107.2	-207.4
Participant 14	34DD	Anterior	Left rib and xiphoid process obscured		
		Posterior	38.9	132.1	-122.3
		Medial	76.2	62.5	-133.8
		Lateral	56.3	137.6	-136.5
		Superior	77.2	110.2	-96.0
		Inferior	50.1	112.4	-171.8
Mean		Anterior	66.2	87.7	-159.3
		Posterior	32.9	112.9	-137.8
		Medial	55.4	73.3	-143.1
		Lateral	26.9	122.6	-142.2
		Superior	53.1	100.0	-126.6
		Inferior	40.5	104.9	-168.0

Table 5.11: Mean neutral nipple position measured using the static extremes and gold-standard methods.

	Breast Size	Estimated neutral nipple position using static extremes (mm)			Gold-standard neutral nipple position (mm)		
		Anterior-posterior	Medial-lateral	Superior-inferior	Anterior-posterior	Medial-lateral	Superior-inferior
Participant 1	32B	45.5	94.0	-140.7	46.6	85.7	-134.5
Participant 2	32B	35.8	75.1	-170.3	44.2	73.6	-165.0
Participant 3	32B	44.8	93.7	-137.3	48.1	92.1	-130.4
Participant 4	34B	-	128.7	-172.8	24.5	127.7	-153.4
Participant 5	32C	49.3	102.6	-147.4	52.4	103.9	-135.0
Participant 6	32C	49.2	91.6	-146.2	55.4	91.6	-145.0
Participant 7	32D	40.6	100.0	-132.4	47.6	87.8	-126.4
Participant 8	32D	31.2	109.8	-128.1	51.1	116.5	-125.8
Participant 9	32D	43.7	89.4	-143.7	44.4	102.2	-144.6
Participant 10	34D	57.2	108.5	-146.6	53.3	97.2	-153.2
Participant 11	32DD	50.6	92.9	-140.1	63.8	92.0	-129.0
Participant 12	30E	69.5	90.8	-150.8	85.4	88.2	-145.2
Participant 13	34DD	85.8	93.6	-172.0	83.4	90.9	-176.1
Participant 14	34DD	-	100.1	-133.9	74.2	107.3	-128.8
Mean		50.3	97.9	-147.3	55.3	96.9	-142.3
Standard deviation		14.9	12.4	14.6	16.5	13.7	15.3

Table 5.12: Absolute difference (to the gold-standard value) and standard deviation in neutral nipple position measured using the static extremes method.

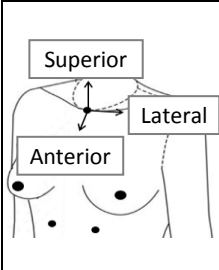
	Breast Size	Absolute difference to gold-standard nipple position (mm)			Standard deviation in nipple position (mm)		
		Anterior-posterior	Medial-lateral	Superior-inferior	Anterior-posterior	Medial-lateral	Superior-inferior
Participant 1	32B	1.2	8.3	6.2	-	0.5	0.3
Participant 2	32B	8.3	1.5	5.3	0.6	0.6	0.4
Participant 3	32B	3.3	1.6	6.9	0.1	0.4	0.1
Participant 4	34B	-	0.9	19.4	-	0.3	1.1
Participant 5	32C	3.1	1.3	12.4	0.2	0.3	0.7
Participant 6	32C	6.2	0.2	1.3	0.1	0.3	0.6
Participant 7	32D	7.0	12.2	6.0	0.1	0.1	0.2
Participant 8	32D	19.9	6.7	2.3	1.0	0.9	0.5
Participant 9	32D	0.7	12.8	0.9	0.5	0.3	0.0
Participant 10	34D	3.8	11.3	6.6	0.2	0.4	0.7
Participant 11	32DD	13.2	0.8	11.1	0.6	0.1	0.5
Participant 12	30E	15.9	2.6	5.6	0.2	0.6	0.0
Participant 13	34DD	2.5	2.7	4.1	0.4	0.4	0.4
Participant 14	34DD	-	7.2	5.0	-	1.4	0.4
Mean		7.1	5.0	6.7	0.4	0.5	0.4
Maximum		19.9	12.8	19.4	1.0	1.4	1.1

Table 5.13: Paired samples t-test results (compared to gold-standard values) and typical error of measurement (TEM) values for the static extremes method.

Static extremes	Anterior-posterior	Medial-lateral	Superior-inferior
t-value (t)	2.867	-0.548	2.797
Significance (p)	0.015*	0.593	0.015*
Effect size (r)	0.654†	0.150	0.613†
TEM (mm)	0.4	0.5	0.5

* denotes a significant difference ($p < 0.05$), † denotes a large effect size ($r > 0.5$)

Discussion

Accuracy assessment of the static extremes method demonstrated that the maximum absolute difference values (to the gold-standard neutral nipple position) exceeded the acceptable criterion (5 mm) (Table 5.12). Statistically significant differences were observed in the anterior-posterior and superior-inferior components of the estimated and neutral nipple position compared to the gold-standard measurements (Table 5.13). These findings indicate that the static extreme method did not accurately replicate the gold-standard neutral nipple position. However, precision analysis demonstrates highly precise measurements of nipple position in the static extremes study, with SD values all below 1.5 mm and TEMs below 0.5 mm in each direction. Inspection of the individual data in Table 5.11, combined with the statistically significant differences recorded in Table 5.13, suggests that the estimated neutral nipple position using the static extreme method was typically posterior and inferior to the gold-standard neutral position. A better estimate of the neutral nipple position may therefore be obtained by altering the definition of the neutral position in reference to the extreme positions of the nipple. For example, using 60% of the superior distance between the inferior and superior static extremes may have improved the accuracy of the superior-inferior component of the estimated neutral nipple position; although further optimisation of this method was outside the scope of this programme of work.

Despite attempts to improve the quality of the data obtained in this study, there were persistent problems with recording the extreme anterior position of the nipple. One participant obscured their left nipple marker and a second obscured two torso markers, preventing the construction of the torso segment during data analysis. Several attempts were made to improve the camera set-up and participant positioning during testing but the data could not be collected. It was anticipated that the inclusion of more optoelectronic cameras, or the use of a higher table during testing, may enable a more complete view of the underside of the torso to be recorded and may consequently improve marker capture in the kneeling position.

Chapter 5: Developing alternative methods for identifying the neutral breast position

An interesting observation from the data in Table 5.10 was that the body orientations used to produce the extreme static positions did not always result in the extreme left nipple co-ordinate in the intended direction. This was predominantly the case in the posterior extreme of the nipple, with many participants experiencing the minimum posterior position while lying on their left hand side and not on their back as anticipated. This was most likely due to the flattening of the medial aspect of the breast while lying on one side; similar to the flattening of the upper poles during standing described previously (Figure 4.9). The deformation of the breast as it changes position may contribute to the multi-directional changes in nipple position that occurred with each different body orientation. The extent of breast deformation was hypothesised to be individual specific and related to factors such as breast composition, body temperature and breast shape, although these factors were not quantified within this study.

Conclusion

All participants were able to complete the static extreme testing protocol although measurement of the anterior extreme of nipple position was problematic in stages 2 and 3 of this study. The static extreme method produced highly precise estimates of the neutral nipple position, with maximum SDs of 1.4 mm and TEMs of 0.5 mm, although acceptable accuracy was not achieved within this study. The static extreme method was therefore not recommended for identifying the neutral nipple position in future research. However, further developments to the testing protocol, such as additional cameras, and optimisation of the calculation procedure, may lead to improved neutral position estimates using this method.

5.4.1d. Drop landing

Introduction

The drop landing neutral position method was a novel concept developed from scientific theory. During free fall the whole body (including breasts) accelerates downwards due to gravity, as the breast is not attached rigidly to the torso there is a slight time lag between the body and breast during movement (Price *et al.*, 2009; Scurr, White, *et al.*, 2009). This lag combined with the elastic nature of the breast's supporting structures (Gefen & Dilmoney, 2007; Haake & Scurr, 2011; Yu & Zhou, 2012; Zhou, 2011) was hypothesised to result in a period of breast oscillation during the initial stage of free-fall. The displacement pattern of the nipple during a drop landing was anticipated to show damped oscillations, comparable to the pattern observed during the breast drop method (Figure 5.4). During the breast drop method the breast fell under gravity and the resulting nipple motion exhibited oscillations about the static gravity-loaded position of the nipple. The concept of the drop landing was to allow the body to drop as opposed to the breast, therefore initiating breast oscillations due to the elasticity of the breast's internal structures without any contribution from the ground reaction force. It was postulated that elimination of the ground reaction force on the breast would result in damped oscillations about the neutral nipple position as opposed to the static gravity-loaded nipple position. The neutral nipple position could therefore be estimated as the point about which nipple oscillations occur during free-fall (Figure 5.11).

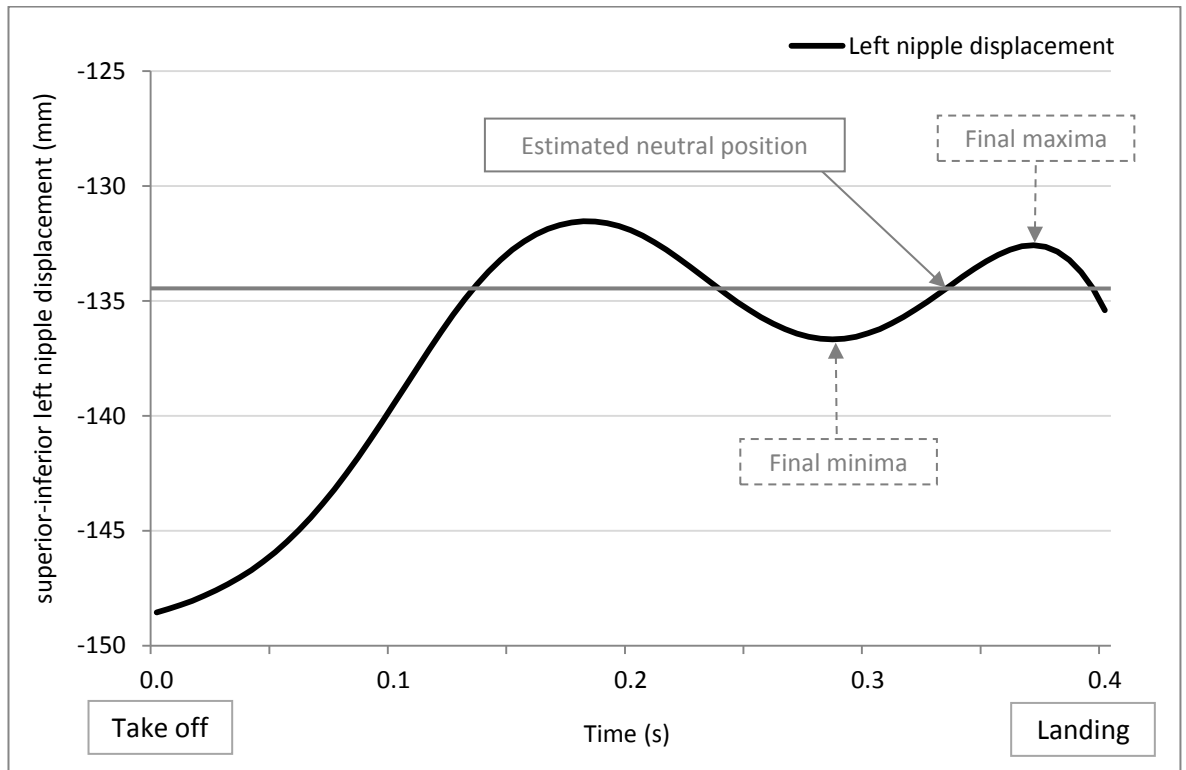


Figure 5.11: Example relative superior-inferior left nipple displacement during a drop landing.

As this was a novel method, an important methodological consideration was the drop-time required to allow multiple breast oscillations to occur during free-fall. In 2011, Haake and Scurr presented a graph of superior-inferior nipple displacement during a breast drop for a participant with breast size 32C (Figure 5.2a). The breast drop nipple displacement pattern demonstrated that the duration of the nipple oscillations was approximately 0.6 s. This therefore represented the minimum drop (free-fall) time required to produce similar oscillations during a drop landing. Using the constant acceleration equations (Equation 5.1), the corresponding drop height was calculated to be 1.8 m.

Equation 5.1:
$$s = ut + \frac{1}{2} at^2$$

where s is the drop height; u is the initial velocity of the breast; t is the drop time; and a is gravitational acceleration.

Chapter 5: Developing alternative methods for identifying the neutral breast position

Due to location and safety considerations, this height was not viable within the laboratory. Instead, two lower heights were used in the practicality testing to investigate whether the nipple would complete at least one oscillation in free-fall before landing, from which the neutral position could be estimated. The first drop height selected was 1.35 m which represented the maximum height achievable within the biomechanics laboratory (constrained by ceiling height). The second height selected was 1.10 m based on an initial pilot test during which participant technique was assessed, and it was observed that at heights above 1.10 m participants were less able to maintain a consistent drop technique over multiple trials. Some participants also became more fearful of performing the drop landing as the drop height increased, meaning that a lower height may be beneficial in terms of participant involvement if it is found to replicate the same breast oscillation pattern. Due to the limited drop height used in this study, the breast was not anticipated to settle in its neutral position during free-fall. Instead it was assumed that damped oscillations would occur about the neutral nipple position, allowing the neutral position to be estimated using the mid-point of the final breast oscillation during free-fall (Figure 5.11).

Stage 2: Drop landing practicality testing

Practicality method

Four participants gave informed consent to take part in this practicality study (breast sizes 32 to 34, A to DD). Each participant had four retro-reflective markers applied to their breast and torso as described previously (Figure 3.2). Three 19 mm diameter markers were also used to aid identification of the take-off and landing stages of each drop landing; one marker was positioned on the landing mat, and the remaining two were attached to the participants' left and right heels using hypoallergenic tape.

A gymnastics pommel horse was used to provide an adjustable platform for participants to perform the drop landing. Two gymnastics safety mats were positioned for landing and a step ladder was used to provide access to the pommel horse (Figure 5.12).

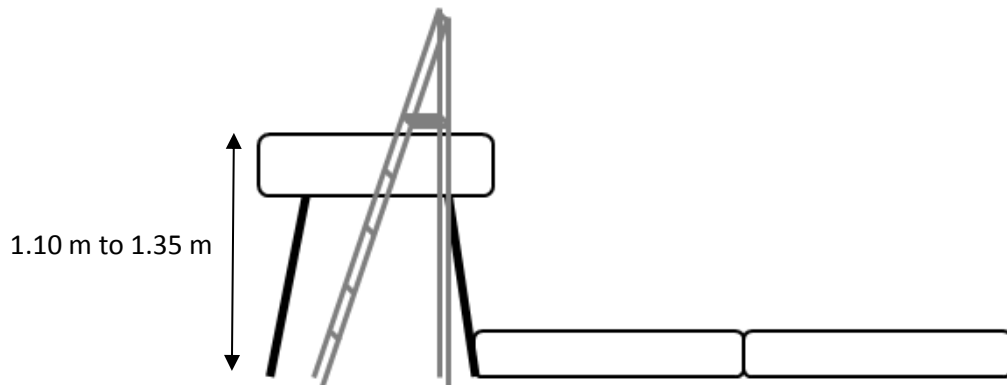


Figure 5.12: Platform used in the drop landing neutral position method.

During the drop landing participants remained as upright as possible and linked their hands behind their back to minimise the effect of underlying muscle action on the position of the nipple. Each drop landing was initiated by stepping from one foot off the end of the pommel horse. The nipple and torso markers were tracked at 200 Hz from take-off (identified by movement of the marker on the participant's supporting foot) to the point of landing (identified by the movement of the marker on the landing mat). Participants were reminded to bend their knees on landing but to try and remain upright. Three trials were performed at each height (1.10 m and 1.35 m).

The breast and torso marker trajectories were identified in QTM and analysed in Visual 3D as described in section 5.4.1. Local maxima and minima in the superior-inferior left nipple displacement data between take-off and landing were identified within Visual 3D. The mid-point between the 3D nipple positions at the final superior-inferior maxima and minima was used to estimate the neutral nipple position. The mean neutral position was then calculated for each drop height.

Practicality results

Table 5.14: Practicality results for the drop landing method.

Practicality measure	Outcome
Successful implementation in the laboratory?	Yes
Estimate of the neutral nipple position achieved?	Yes

Estimated neutral position data from this practicality study were presented in Appendix H.

Practicality discussion

This method was quick to perform in the laboratory, and all participants included in the practicality study were able to complete the testing protocol. Calculation of the neutral position was successful for most trials although there were a few cases where the breast did not oscillate as expected, predominantly at the lower drop height. Although the greater drop height should have consistently resulted in more nipple oscillations before landing, in practice participants tended to lean forward during free-fall in anticipation of a harder landing which prevented the required superior-inferior oscillation of the nipple. This loss of data at the both testing heights resulted in further preliminary testing to identify an optimum drop height for this method.

Further preliminary testing

A secondary stage of practicality testing was implemented for this method with the aim of identifying the optimum drop height for estimating the neutral nipple position before taking this method through to stage 3 of this study. Five participants (breast size 32 to 34, B to DD) took part in this secondary practicality study to investigate the effect of increasing drop height on the left nipple movement relative to the torso. Four incremental height drop landings were selected (1.05 m, 1.15 m, 1.25 m and 1.35 m) and participants performed five trials from each height. Participants remained as upright as possible and stepped from one foot off the end of the pommel horse. The breast and

torso markers were tracked at 200 Hz from take-off to landing using optoelectronic cameras, and the oscillation of the breast relative to the torso was recorded as described previously.

The example data presented in Figure 5.13 demonstrates the typical oscillatory patterns observed during this secondary study. For all participants the starting position of the nipple was inferior to the nipple position during free-fall, therefore providing some evidence to support the previously untested theory that the breast oscillates about its neutral position during free-fall. However, the nature of the oscillations varied across the different drop heights implemented in this study. At the lowest height (1.05 m), the fall time was often insufficient to allow complete oscillation of the nipple before landing (Figure 5.13 a). At 1.15 m, there were more successful trials, with a clear oscillatory pattern emerging (Figure 5.13 b). The damped oscillations were most clearly observed at the two greatest heights (1.25 m and 1.35 m), as the increased fall time allowed more nipple oscillations to occur during flight (Figure 5.13 c and d), although the oscillatory pattern from the 1.35 m drop was sometimes distorted. Visual observations indicated that participants were most cautious when dropping from the greatest height and were less able to maintain an upright posture during flight. Considering that drop heights of both 1.25 m and 1.35 m produced the anticipated oscillatory nipple displacement most frequently across trials, but that participants became more anxious and less consistent as the drop height increased, it was decided to use only the 1.25 m platform in the accuracy and precision assessment aspect of this study.

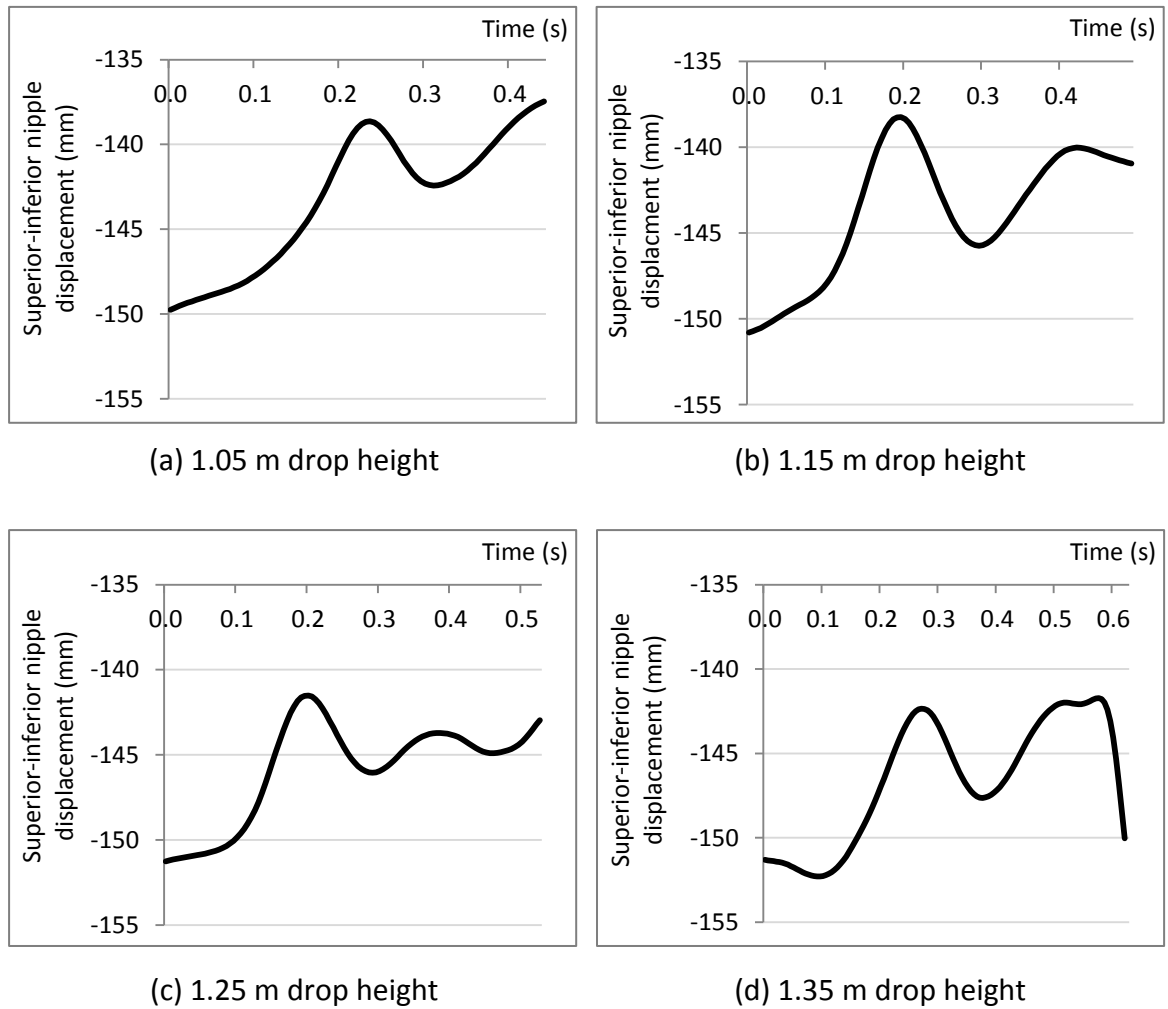


Figure 5.13: Example superior-inferior left nipple displacement for a 32C participant during a drop landing performed from four different drop heights.

Practicality conclusion

Initial practicality testing of the drop landing method demonstrated that this method could be performed successfully in the laboratory. Consideration of nipple displacement data, participant confidence, and consistency of jump technique led to the selection of a 1.25 m platform for use in stage 3 of this study.

Stage 3: Drop landing accuracy and precision testing

Accuracy and precision method

Stage 3 of testing for the drop landing method took place on the same day as the gold-standard buoyancy data was collected in soybean oil, with the same 14 participants (Table 4.1) using the same marker set (Figure 4.1). Each participant had retro-reflective markers placed on their breast and torso as described previously (Figure 4.1) with two additional 12 mm diameter markers placed on the participants' right and left heels, and three additional 12 mm diameter markers placed on the landing mat to allow identification of the take-off and landing phases of each drop landing trial.

The laboratory was set up as described for the practicality study, with the gymnastics pommel horse set to a height of 1.25 m (Figure 5.12). Each participant performed several familiarisation drop landings before recording the last 5 drop landing trials at 200 Hz using the optoelectronic camera system. Marker trajectory data were identified in QTM, filtered in Visual 3D using a generalised cross validatory (quintic) spline, and converted to relative nipple displacement data as described in section 5.4.1. The start of each drop landing trial was identified in Visual 3D using event markers created at the point where the heel marker of the leading leg passed below the level of the pommel horse. An event marker was also created at landing, identified using the first movement of any of the three markers placed on the landing mat. The superior-inferior displacement of the left nipple was analysed using Visual 3D during the flight phase of each drop landing (between the start and landing events). Analogous to the breast drop method, forces in the anterior-posterior and medial-lateral directions were assumed to be in equilibrium during free-fall enabling the neutral nipple position to be estimated as the mid-point between the 3D nipple positions identified at the final maxima and minima in superior-inferior nipple displacement. The final three drop landing trials in which at least one full nipple oscillation occurred during free-fall were used to calculate three estimates of the neutral nipple position for each participant.

Accuracy and precision results

Table 5.15: Mean neutral nipple position measured using the drop landing and gold-standard methods.

	Breast Size	Estimated neutral nipple position using static extremes (mm)			Gold-standard neutral nipple position (mm)		
		Anterior-posterior	Medial-lateral	Superior-inferior	Anterior-posterior	Medial-lateral	Superior-inferior
Participant 1	32B	39.6	90.7	-146.5	46.6	85.7	-134.5
Participant 2	32B	34.0	88.7	-165.4	44.2	73.6	-165.0
Participant 3	32B	50.6	97.3	-138.2	48.1	92.1	-130.4
Participant 4	34B	14.4	135.9	-159.4	24.5	127.7	-153.4
Participant 5	32C	49.6	101.8	-141.0	52.4	103.9	-135.0
Participant 6	32C	45.4	101.5	-140.2	55.4	91.6	-145.0
Participant 7	32D	39.9	97.8	-132.1	47.6	87.8	-126.4
Participant 8	32D	43.7	120.9	-118.9	51.1	116.5	-125.8
Participant 9	32D	35.0	109.6	-146.9	44.4	102.2	-144.6
Participant 10	34D	49.0	105.9	-162.0	53.3	97.2	-153.2
Participant 11	32DD	52.0	103.1	-132.0	63.8	92.0	-129.0
Participant 12	30E	62.6	115.1	-138.8	85.4	88.2	-145.2
Participant 13	34DD	74.9	104.1	-181.2	83.4	90.9	-176.1
Participant 14	34DD	No nipple oscillation			74.2	107.3	-128.8
Mean		45.4	105.6	-146.3	55.3	96.9	-142.3
Standard deviation		14.5	12.7	16.7	16.5	13.7	15.3

Table 5.16: Absolute difference (to the gold-standard value) and standard deviation in neutral nipple position measured using the drop landing method.

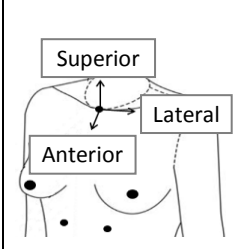
	Breast Size	Absolute difference to gold-standard nipple position (mm)			Standard deviation in nipple position (mm)		
		Anterior-posterior	Medial-lateral	Superior-inferior	Anterior-posterior	Medial-lateral	Superior-inferior
Participant 1	32B	7.1	5.0	12.0	1.5	1.2	2.0
Participant 2	32B	10.2	15.1	1.1	1.9	1.4	1.5
Participant 3	32B	2.4	5.2	7.8	1.0	1.8	1.1
Participant 4	34B	10.1	8.2	6.0	3.1	0.6	2.1
Participant 5	32C	2.8	2.2	6.0	1.6	2.0	2.1
Participant 6	32C	10.0	9.9	4.8	1.9	1.1	1.1
Participant 7	32D	7.7	10.0	5.7	0.5	0.7	1.9
Participant 8	32D	7.6	4.4	6.9	7.2	0.5	2.3
Participant 9	32D	9.4	7.4	2.2	1.1	2.9	1.2
Participant 10	34D	4.4	8.7	8.7	2.6	2.3	2.7
Participant 11	32DD	11.9	11.1	3.0	2.5	0.8	1.9
Participant 12	30E	22.8	26.9	6.4	2.0	1.7	1.2
Participant 13	34DD	8.5	13.1	5.1	1.2	3.5	3.8
Participant 14	34DD	-	-	-	-	-	-
Mean		8.8	9.8	5.8	2.2	1.6	1.9
Maximum		22.8	26.9	12.0	7.2	3.5	3.8

Table 5.17: Paired samples t-test results (compared to gold-standard values) and typical error of measurement (TEM) values for the drop landing method.

Drop landing	Anterior-posterior	Medial-lateral	Superior-inferior
t-value (t)	5.267	-5.008	1.824
Significance (p)	0.000*	0.000*	0.093
Effect size (r)	0.835†	0.822†	0.466
TEM (mm)	2.3	2.0	1.9

* denotes a significant difference ($p < 0.05$), † denotes a large effect size ($r > 0.5$)

Discussion

Although some participants were hesitant to perform the drop landing method during the third stage of this study, an estimate of the neutral nipple position was successfully attained for 13 out of the 14 participants. The unsuccessful trials for participant 14 were due to the nipple not displaying the required oscillation pattern during free-fall. Instead, this participant's nipple continued to move superiorly from take-off until landing. This unexpected behaviour may have occurred due to a combination of the participant's age, her relatively large breast size, her repeated participation in bare-breasted activity, and her previous experience of sun-burn on her breasts (Table 4.1). Each of these factors may have contributed to pre-existing damage of the participant's breast skin, reducing its elasticity and preventing the breast from oscillating during the initial stages of free-fall. With the exception of this participant, all other participants were able to complete at least three successful trials of the breast drop method.

Accuracy assessment of the breast drop method demonstrated statistically significant differences in both the anterior-posterior and medial-lateral directions (Table 5.17). Absolute differences (to the gold-standard values) were smallest in the superior-inferior direction, although maximum differences in all components of the neutral nipple position estimate exceeded the acceptable accuracy criterion (5 mm) (Table 5.16). Acceptable precision was demonstrated for the superior-inferior component of the neutral nipple position using both the SD (up to 3.8 mm) (Table 5.16) and TEM (1.9 mm) (Table 5.17) precision criteria.

The theory underlying the drop landing method only considered the superior-inferior oscillation of the breast during free-fall so it was perhaps not surprising that this component of the neutral nipple position was most accurately and precisely estimated using this method. The drop landing method demonstrated the potential to accurately and precisely estimate the superior-inferior neutral nipple position for a selection of the participants assessed within this thesis. However, it was considered that participant factors such as age, skin elasticity, fitness level, and breast size may have reduced the accuracy of this method when evaluated for the group as a whole.

Conclusion

Acceptable precision was achieved when estimating the medial-lateral and superior-inferior components of the neutral nipple position using the drop landing method, but acceptable accuracy was not achieved for all participants within this study. The drop landing method was therefore not recommended for future research aiming to identify the neutral nipple position. Factors such as participant age, skin elasticity, and drop technique may have influenced the accuracy evaluation of the drop landing method within this thesis.

5.4.1e. Zero acceleration during treadmill activity

Introduction

The zero acceleration method was a novel neutral position method based on fundamental scientific principles. Newton's second law states that the resultant force (F_R) on an object is proportional to its rate of change of momentum (p) (Equation 5.2), where momentum equals mass (m) multiplied by velocity (v). Assuming no change in mass, then zero breast acceleration (a) equates to zero resultant force on the breast.

Equation 5.2:
$$F_R = \frac{dp}{dt} = \frac{d(m.v)}{dt} = m \cdot \frac{dv}{dt} = m \cdot a$$

In the static standing position, both gravity and its reaction force act on the breast tissue. These two forces are in equilibrium and the breast remains stationary with zero acceleration. The reason that this position does not represent the neutral breast position is because gravity (acting inferiorly on the centre of mass) and the reaction force (acting superiorly on the attachment points of the breast to the torso) are misaligned, effectively creating a bending force on the breast causing it to deform (Figure 2.2).

The ground reaction force on the breast can be eliminated by removing any contact between the body and the ground, which is achieved regularly during the flight phase of activities such as running or jumping. In the no-contact state, if the acceleration of the breast is zero then all the forces acting on the breast must be in equilibrium. This concept could be used to estimate the neutral nipple position by hypothesising that each time the forces on the breast are in equilibrium (without ground contact) the nipple may return to its neutral position. One consideration regarding this theory was that the nipple acceleration would also be zero whenever the breast was moving with constant velocity, potentially resulting in many zero acceleration nipple positions that would not necessarily represent the neutral position. However, this had not yet been investigated within the literature, meaning that this study provided the first opportunity to evaluate the use of zero-acceleration nipple position to estimate the neutral nipple position. Running was

Chapter 5: Developing alternative methods for identifying the neutral breast position used initially to induce the required flight phases for this study due to its frequent use within existing breast motion research (Zhou *et al.*, 2011).

Stage 2: Zero acceleration (running) practicality testing

Practicality method

Two participants (breast sizes 32C and 34D) gave informed consent to take part in this practicality study. Each participant had four retro-reflective markers applied to their breast and torso as described previously (Figure 3.2). Two 19 mm spherical retro-reflective markers were also attached to the participants' right and left heels using hypoallergenic tape to allow the flight phase to be identified during each gait while treadmill running.

As treadmill activity had not been previously used for the purpose of identifying the neutral nipple position, an incremental-speed treadmill test was chosen to investigate which speeds would be most suited to this purpose. The incremental-speed treadmill test began at jogging pace (8 kph), and treadmill speed was increased by 1 kph every five gait cycles (counted by a second female researcher) up to a maximum speed of 14 kph. Lower treadmill speeds were not included in this study as the required flight phase would not occur during walking (Cappellini, Ivanenko, Poppele, & Lacquaniti, 2006). During the treadmill test, the breast and torso markers were tracked at 200 Hz using the optoelectronic camera system. The marker trajectories were identified in QTM and analysed in Visual 3D as described in section 5.4.1.

An important factor for consideration when calculating acceleration data for use in this method was the distinction between global and relative nipple acceleration. Throughout this thesis displacement data has been presented in relative co-ordinates using the torso as the reference frame. This allowed the nipple position to be easily identified in relation to the torso origin (defined at the proximal end of the torso segment) irrespective of the orientation or location of the torso. The use of relative nipple displacement data to calculate relative nipple acceleration would quantify the change in nipple velocity with

Chapter 5: Developing alternative methods for identifying the neutral breast position

respect to the torso. In this scenario, any zero acceleration points would effectively consider the torso to be an inertial reference frame and would neglect any force contribution from the torso when calculating resultant force on the breast. The alternative approach is to derive acceleration from the global position of the nipple (*i.e.* relative to the laboratory), resulting in the identification of zero acceleration points at which all forces, including those exerted by the torso on the breast, are in equilibrium. As this was the first study aiming to identify a neutral breast position using zero points in nipple acceleration data, both relative and global acceleration data were used. Nipple acceleration was calculated twice in Visual 3D, once using the second derivative of the relative left nipple displacement (in meters), and once using the second derivative of the global left nipple displacement (in meters). Nipple displacement and acceleration, and right and left heel displacement data were exported to Excel for further analysis.

The vertical trajectory of each heel marker was plotted in Excel and was used to identify the flight phase(s) of each gait cycle at each treadmill speed (*i.e.* neither foot was in contact with the ground) (Figure 5.14). Nipple displacement and acceleration data that did not occur during flight were excluded from further analysis. The acceleration (relative and global) data obtained during flight were plotted in Excel to identify any zero-acceleration occurrences.

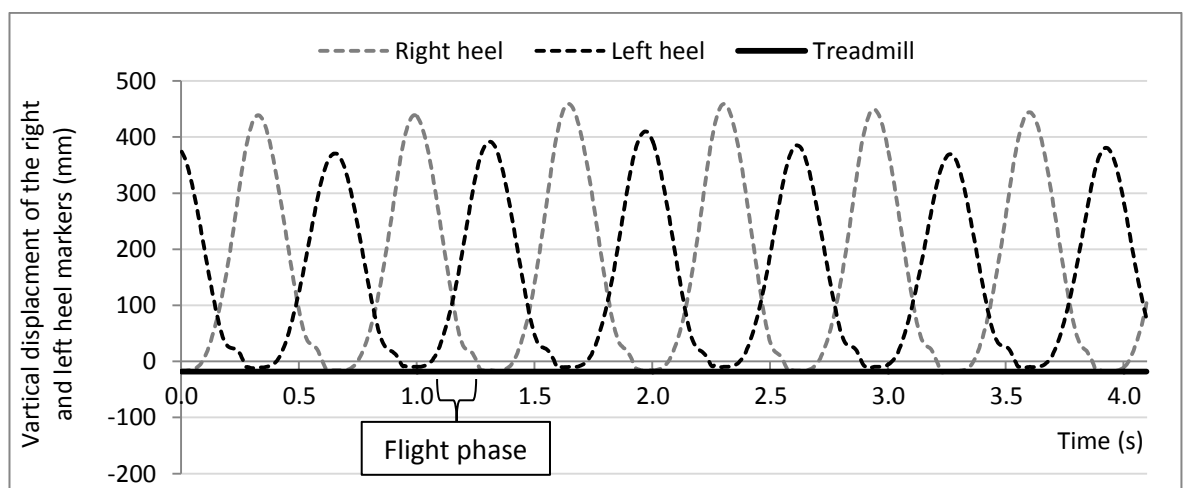


Figure 5.14: Example right and left heel vertical displacement data during treadmill running at 14 kph.

Chapter 5: Developing alternative methods for identifying the neutral breast position

To ensure no potential zero-acceleration points were missed, a maximum error margin for acceleration was calculated. This error was based on the tracking error in the optoelectronic camera system (0.25 mm). The maximum displacement error between two consecutive data points would therefore be 0.50 mm, this resulted in a maximum velocity error of $0.2 \text{ m}\cdot\text{s}^{-1}$ (with a sampling frequency of 200 Hz) between two velocity points, which in turn gave a maximum acceleration error (using two velocities) of $40 \text{ m}\cdot\text{s}^{-2}$. This is a large error margin for the acceleration data considering the original focus was to look for 'zero-points', however it was considered important to include the maximum error margin at this initial stage of practicality testing. If this method was successful then more work could be done on improving the accuracy of data collection and reducing errors in acceleration calculations. Estimates of the neutral nipple position were therefore obtained using nipple displacement during flight at time points in which nipple acceleration (relative or global) was between $-40 \text{ m}\cdot\text{s}^{-2}$ and $40 \text{ m}\cdot\text{s}^{-2}$.

Practicality results

Table 5.18: Practicality results for the zero-acceleration during running method.

Practicality measure	Outcome
Successful implementation in the laboratory?	Yes
Estimate of the neutral nipple position achieved?	No

Estimated neutral position data from this practicality study were presented in Appendix I.

Practicality discussion

Analysis of the treadmill data from this practicality study showed that there were very few time points at which the participant was not in contact with the ground (Figure 5.14). This resulted in a small set of data points from which to assess nipple acceleration. In agreement with previous studies, high levels of three dimensional nipple displacement (and therefore acceleration) were observed during treadmill running (Scurr, White, & Hedger, 2011). This further reduced the probability of measuring zero resultant acceleration at any time point, as the three directional components of nipple acceleration

Chapter 5: Developing alternative methods for identifying the neutral breast position would have to approach zero simultaneously. Despite the inclusion of both relative and global nipple acceleration data, and allowing for errors of $\pm 40 \text{ m.s}^{-2}$ in the acceleration calculation, there were no zero-acceleration points identified for the nipple using this method (Appendix I). It was proposed that the substitution of jumping as opposed to treadmill activity may increase the probability of detecting zero-acceleration occurrences due to increased flight time and decreased torso rotation. The suitability of a zero-acceleration during jumping method for predicting the neutral nipple position was investigated further in the next section.

Practicality conclusion

As no zero-acceleration points occurred during running, this method was excluded as a potential method for estimating the neutral nipple position and was not included in stage 3 of this study.

5.4.1f. Zero acceleration during jumping activity

Introduction

This zero-acceleration neutral position method was based on the same underlying theory as described in section 5.4.1e, except the kinematics of the nipple were assessed during trampette jumping as opposed to running. It was anticipated that there would be reduced torso rotation and an increased flight-time during trampette jumping compared to running, which may therefore result in a higher probability of detecting occurrences of zero nipple acceleration during flight.

Stage 2: Zero acceleration (jumping) practicality testing

Practicality method

Four participants gave informed consent to take part in this practicality study (breast sizes 32 to 34, C to DD). Each participant had four retro-reflective markers applied to their breast and torso as described previously (Figure 3.2). Two 19 mm spherical retro-reflective markers were also attached to the participants' right and left heels using hypoallergenic tape to allow the flight phase to be identified during each trampette jump.

Participants performed two 10 s trials of jumping on the trampette, once with the participant jumping continuously at a self-selected comfortable jump height, and once at the participant's maximum jumping height. While jumping, participants linked their hands behind their back and remained as upright as possible. During each jumping trial, the breast and torso markers were tracked at 200 Hz using the optoelectronic camera system. The marker trajectories were identified in QTM and analysed in Visual 3D as described in section 5.4.1. Nipple acceleration was calculated twice in Visual 3D, once using the second derivative of the relative left nipple displacement, and once using the second derivative of the global left nipple displacement. Nipple displacement and acceleration, and right and left heel displacement data were exported to Excel for further analysis.

The vertical trajectory of each heel marker was plotted in Excel and was used to identify the flight phase(s) of each jump (*i.e.* neither foot was in contact with the trampette), in a similar process as described in section 5.4.1e. Nipple displacement and acceleration data that did not occur during flight were excluded from further analysis. The acceleration (relative and global) data that was obtained during flight were plotted in Excel to identify any zero-acceleration occurrences. An error margin of $\pm 40 \text{ m.s}^{-2}$ was included to account for errors in acceleration data caused by small inaccuracies during marker tracking. Estimates of the neutral nipple position were therefore obtained using nipple displacement during flight at time points in which nipple acceleration (relative or global) was between -40 m.s^{-2} and 40 m.s^{-2} .

Practicality results

Table 5.19: Practicality results for the zero-acceleration during jumping method.

Practicality measure	Outcome
Successful implementation in the laboratory?	Yes
Estimate of the neutral nipple position achieved?	No

Estimated neutral position data from this practicality study were presented in Appendix J.

Practicality discussion

As anticipated, the jumping activity greatly reduced the medial-lateral and anterior-posterior motion of the nipple. However, on analysis of the nipple acceleration data it was observed that the nipple acceleration rarely exceed 20 m.s^{-2} during trampette jumping, meaning that almost the entire range of nipple displacement was included in the neutral position estimate. This finding exposed a considerable problem with this method since the acceleration calculation has too large an error to be used to identify zero-acceleration points of the nipple (even with a twofold improvement in accuracy). Alternative methods for measuring acceleration, such as three dimensional

Chapter 5: Developing alternative methods for identifying the neutral breast position accelerometers, may allow this method to be implemented in future although this was not investigated within this study.

Practicality conclusion

The errors associated the derivation of acceleration data from nipple displacement were too large to distinguish the zero-acceleration points of the nipple during this practicality study. This neutral position method was excluded from further testing within this thesis, although it was acknowledged that alternative methods for measuring nipple acceleration may have improved the practicality of this method in the laboratory.

5.4.1g. Gravity loaded static position

Introduction

Although not intended to replicate the neutral position of the nipple, the static gravity-loaded nipple position was also incorporated into this study as this position had previously been implemented by Scurr *et al.*, in place of the neutral position, for calculations of breast extension and breast strain (Scurr, Bridgman, *et al.*, 2009; Scurr, White, Milligan, *et al.*, 2011a). Comparison of the gravity-loaded and gold-standard neutral nipple positions therefore provides an indication of the error associated with neglecting the gravitational effect on the breast when assessing breast kinematics.

Stage 2: Gravity-loaded static position practicality testing

Measurements of the static gravity-loaded nipple position have been described and successfully implemented in previous sections of this thesis (sections 3.3 and 3.4). Consequently this method was taken straight forward to Stage 3 for accuracy and precision assessment against the gold-standard method.

Stage 3: Gravity-loaded static nipple position accuracy and precision testing

Accuracy and precision method

Stage 3 of testing for the gravity-loaded static nipple position method took place on the same days as the gold-standard buoyancy data were collected in water and soybean oil (three trials on each day), with the same 14 participants (Table 4.1) using the same marker set (Figure 4.1). Each participant had retro-reflective markers placed on their breast and torso as described previously (Figure 4.1). Participants stood stationary in the centre of the biomechanics laboratory with their back straight and their arms relaxed by their sides. The 3D position of each marker was recorded at 200 Hz for three 1 s trials on the day of the water testing and three on the day of the soybean oil testing as described in section 4.3.1. The mean nipple position from these six trials was calculated as

Chapter 5: Developing alternative methods for identifying the neutral breast position described in section 4.3.2 and was used to represent the gravity-loaded nipple position for each participant.

Accuracy and precision results

The mean gravity-loaded nipple positions were presented in Table 4.2. Accuracy and precision results are shown in Table 5.20 and Table 5.21 respectively.

Table 5.20: Absolute difference (to the gold-standard value) and standard deviation in neutral nipple position measured using the gravity-loaded static nipple position method.

	Breast Size	Absolute difference to gold-standard nipple position (mm)			Standard deviation in nipple position (mm)		
		Anterior-posterior	Medial-lateral	Superior-inferior	Anterior-posterior	Medial-lateral	Superior-inferior
Participant 1	32B	11.5	3.0	20.7	0.7	0.5	1.0
Participant 2	32B	15.5	7.0	13.4	3.3	4.1	4.0
Participant 3	32B	4.2	5.3	22.1	2.2	1.8	1.4
Participant 4	34B	11.2	2.4	32.6	2.4	1.9	7.2
Participant 5	32C	9.8	3.0	26.8	1.4	4.0	0.5
Participant 6	32C	13.2	5.2	18.7	4.3	1.3	4.6
Participant 7	32D	15.0	7.2	21.5	3.6	5.0	2.8
Participant 8	32D	25.6	13.4	27.5	7.8	3.0	4.0
Participant 9	32D	14.1	4.5	24.8	3.4	2.4	1.1
Participant 10	34D	12.5	15.7	13.9	4.4	1.0	2.5
Participant 11	32DD	17.0	11.5	22.7	1.9	3.8	0.3
Participant 12	30E	23.5	14.3	34.1	4.3	5.5	0.8
Participant 13	34DD	17.3	13.6	35.9	2.4	3.3	5.2
Participant 14	34DD	23.3	4.2	45.7	1.6	1.5	3.2
Mean		15.3	7.9	25.7	3.1	2.8	2.8
Maximum		25.6	15.7	45.7	7.8	5.5	7.2

Table 5.21: Paired samples t-test results (compared to gold-standard values) and typical error of measurement (TEM) values for the gravity-loaded static nipple position method.

Gravity-loaded	Anterior-posterior	Medial-lateral	Superior-inferior
t-value (t)	9.773	-5.100	10.819
Significance (p)	0.000*	0.000*	0.000*
Effect size (r)	0.938†	0.817†	0.949†
TEM (mm)	2.5	2.0	2.0

* denotes a significant difference ($p < 0.05$), † denotes a large effect size ($r > 0.5$)

Discussion

Accuracy assessment of this method demonstrated that the gravity-loaded nipple position was significantly different to the neutral nipple position (Table 5.21), with absolute differences of up to 25.6 mm, 15.7 mm and 45.7 mm in the anterior-posterior, medial-lateral and superior-inferior directions respectively (Table 5.20). These results suggest that neglect of the neutral nipple position may have a considerable effect on measurements of dynamic breast extension or breast strain. Larger-breasted participants in this study generally had greater differences between the gravity-loaded and neutral nipple positions, supporting the earlier suggestion (section 2.4.1) that women with larger breasts experience greater static breast strain than their smaller-breasted counterparts, although this will be investigated further in chapter 7.

Precision analysis of the gravity-loaded nipple position measurements revealed some interesting results. Although TEM values were all within acceptable limits (2.5 mm or lower) (Table 5.21), within-participant SD in nipple position (up to 7.8 mm) exceeded the acceptable precision criteria defined within this thesis (Table 5.20). This was particularly surprising as the acceptable SD criteria were developed from the data collected in this study (described in section 4.4.4). The observation that the SD within each component of nipple position exceeded the maximum SD of the resultant data suggested that inconsistencies in static nipple measurements were predominantly due to redistribution of the breast tissue in the LCS of the torso, as opposed to absolute changes in breast size. Redistribution of breast tissue in the reference frame of the torso may have been due to

Chapter 5: Developing alternative methods for identifying the neutral breast position changes in participant posture between trials (Figure 4.11), or possibly due to changes in breast shape caused by external factors (such as breast support worn prior to testing) which were not controlled during this study.

Conclusion

The static-gravity loaded nipple position could not accurately or precisely estimate the neutral nipple position attained using the gold-standard buoyancy method. The magnitude of error (up to 45.7 mm in any one direction) was large enough to effect measures of breast strain if not accounted for during testing. It was therefore recommended that all future measurements of breast strain should incorporate the neutral nipple (or breast) position as the zero-point for calculations.

5.5. Comparison of the alternative neutral position methods against the gold-standard buoyancy method

Having evaluated seven alternative neutral position methods in sections 5.4.1a to 5.4.1g, this section summarises the results from each study and provides a direct comparison of each alternative neutral position method against the gold-standard buoyancy method. Methods that did not successfully estimate the neutral nipple position in stage 3 of this study (and those excluded in stage 1 and 2) were not included in this comparison as these methods would not be recommended for future use (Figure 5.15). Comparisons are made between the measurements of estimated neutral nipple position (section 5.5.1), and between the accuracy (section 5.5.2) and precision (section 5.5.3) of these estimates.

Stage 1 (Review of methods)	Stage 2 (Practicality)	Stage 3 (Accuracy and precision)
<p>Buoyancy (gold-standard)</p> <ul style="list-style-type: none"> • Buoyancy (water) • Breast drop • Mathematical model • Static extremes • Drop landing • Extensometer • Terminal velocity • Zero acceleration • Force measuring bra • <i>Gravity-loaded position</i> 	<p>Buoyancy (gold-standard)</p> <ul style="list-style-type: none"> • Buoyancy (water) • Breast drop • Static extremes • Drop landing • Zero acceleration • <i>Gravity-loaded position</i> 	<p>Buoyancy (gold-standard)</p> <ul style="list-style-type: none"> • Buoyancy (water) • Breast drop • Static extremes • Drop landing • <i>Gravity-loaded position</i>

Figure 5.15: Summary of the included and excluded alternative neutral position methods evaluated in this programme of work.

5.5.1. Neutral nipple position estimates

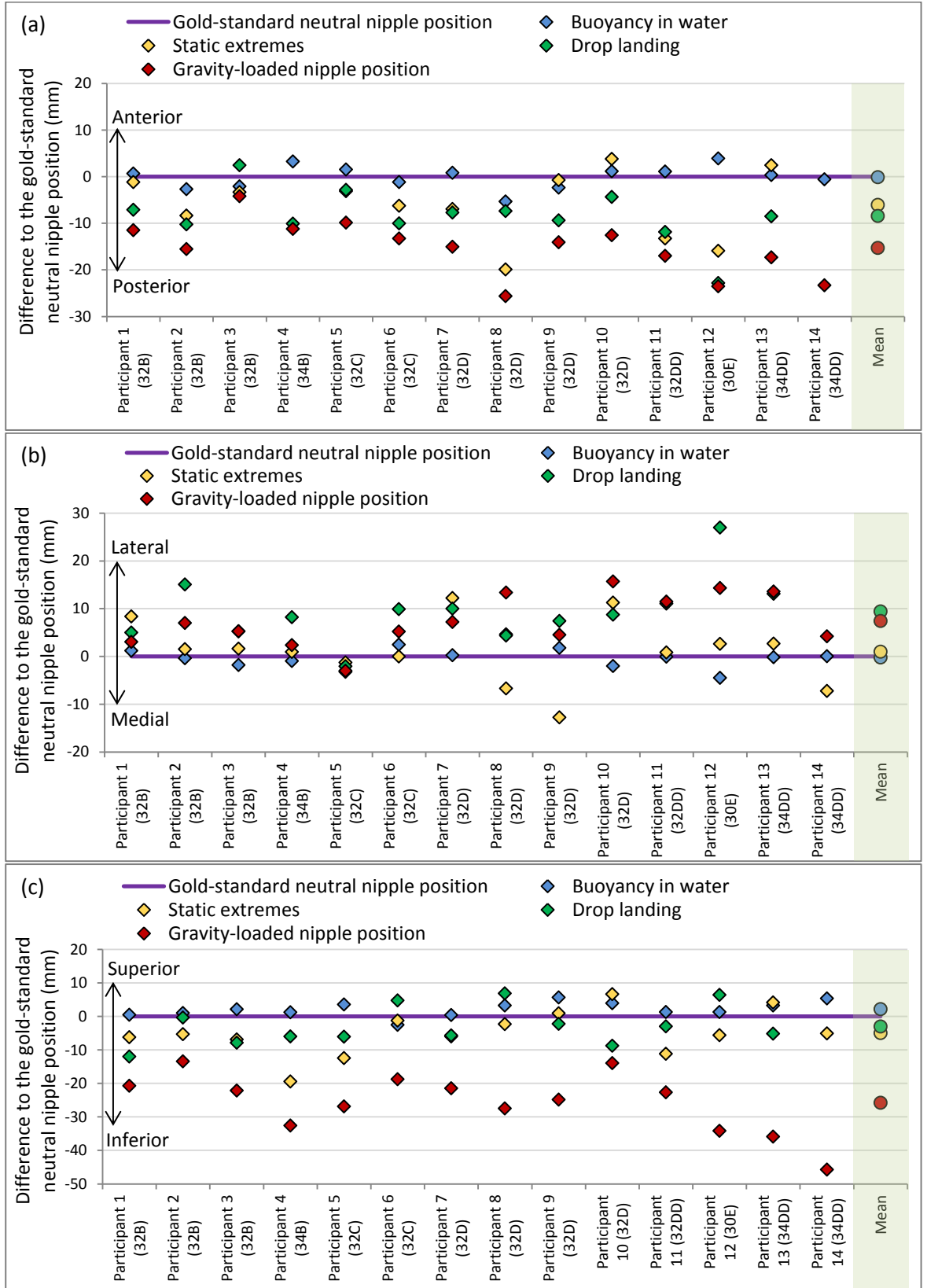


Figure 5.16: Anterior-posterior (a), medial-lateral (b) and superior-inferior (c) components of the gold-standard and estimated neutral nipple positions obtained using each of the alternative neutral position methods (n = 14).

5.5.2. Accuracy of the neutral nipple position estimates

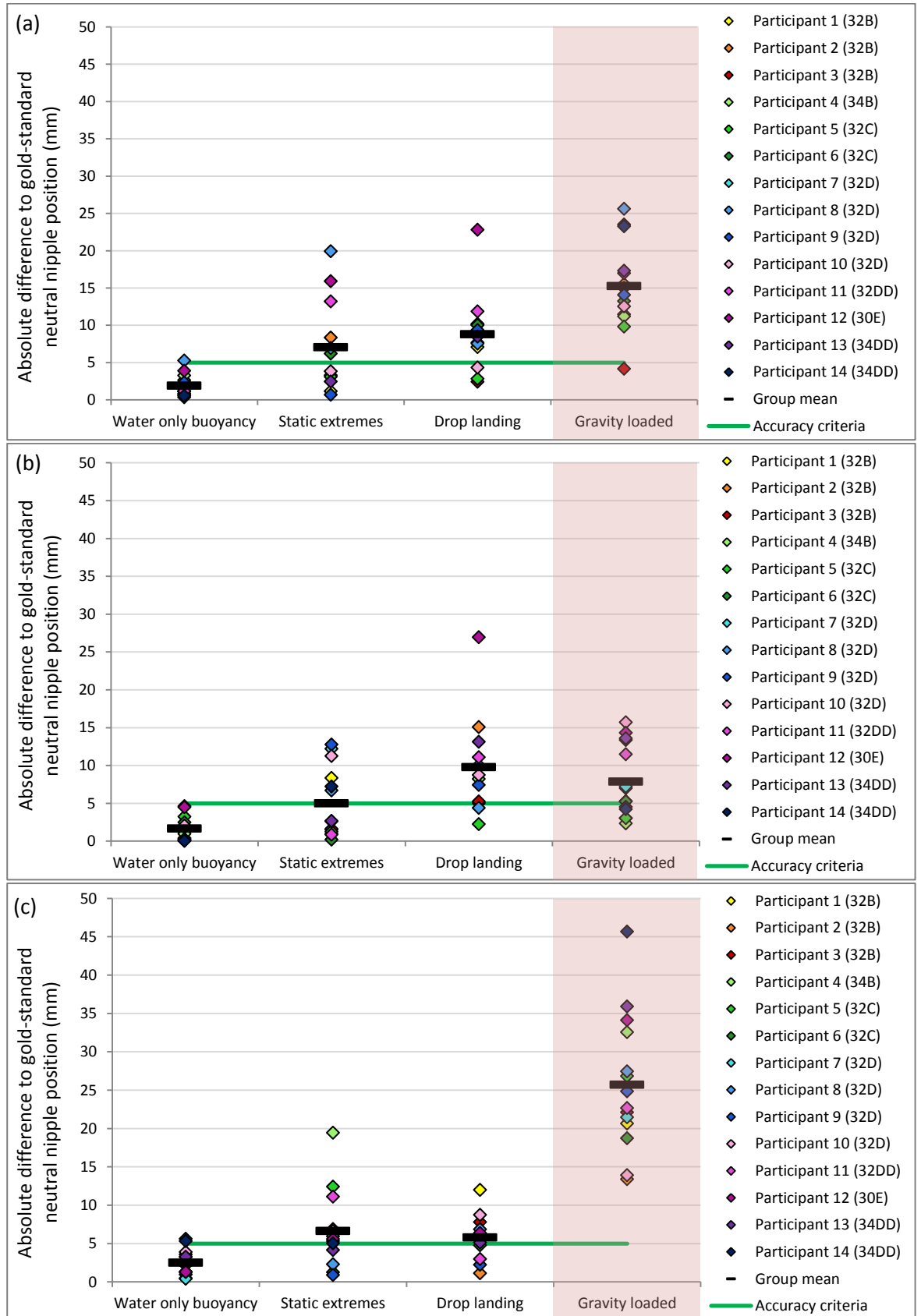


Figure 5.17: Anterior-posterior (a), medial-lateral (b) and superior-inferior (c) absolute difference in nipple position compared to the gold-standard position (n = 14).

5.5.3. Precision of the neutral nipple position estimates

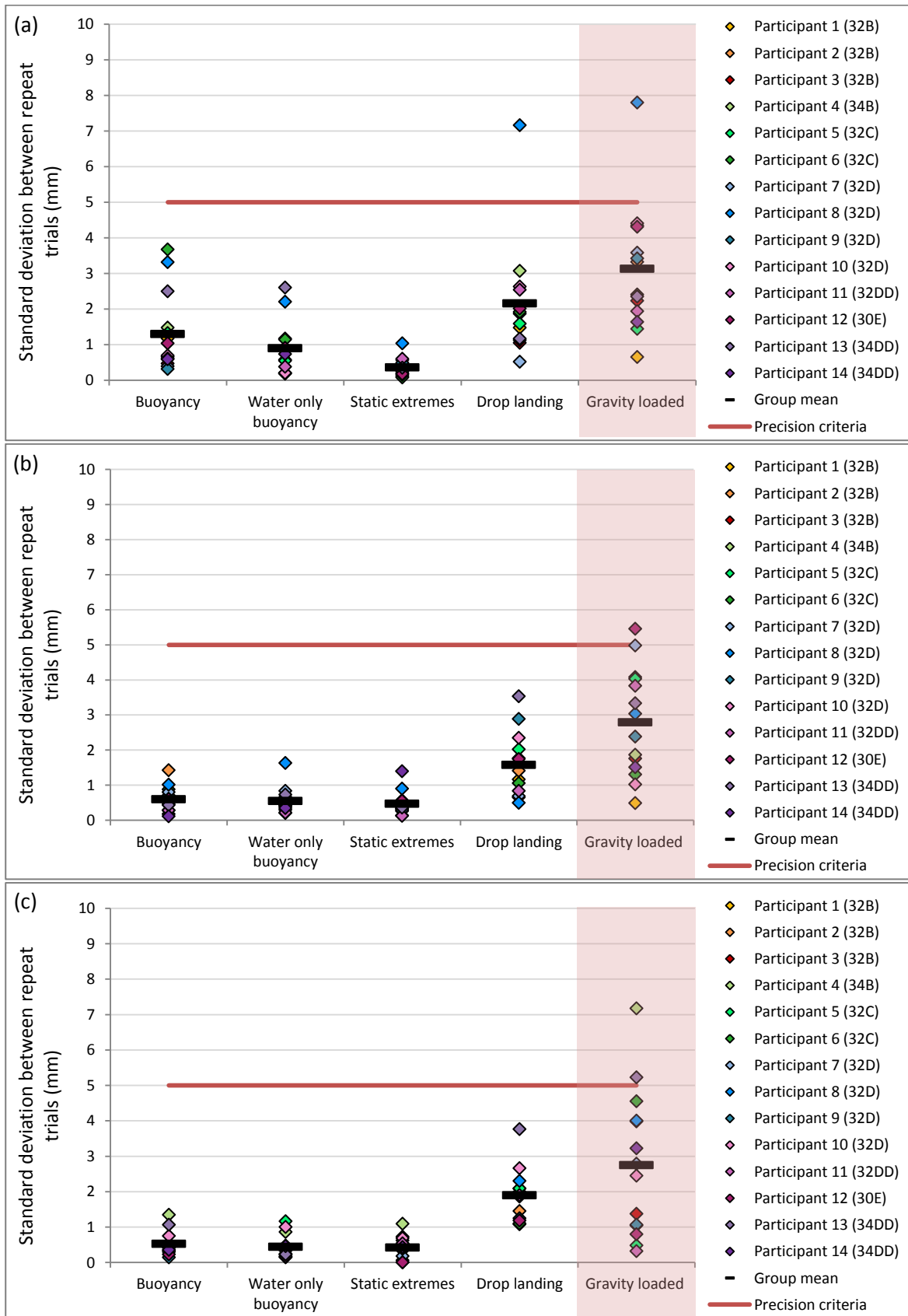


Figure 5.18: Anterior-posterior (a), medial-lateral (b) and superior-inferior (c) standard deviation in nipple position compared to the gold-standard position (n = 14).

5.6. Discussion

Comparisons of the neutral nipple position estimates obtained using each alternative method demonstrated that the shortlisted alternative methods generally provided a better estimate of the neutral position than the gravity-loaded nipple position (Figure 5.16). Accuracy and precision assessment of each method demonstrated that although all methods were able to achieve acceptable precision when estimating at least one component of the gold-standard neutral nipple position, only the buoyancy in water method achieved acceptable accuracy (in the medial-lateral direction only) when evaluated using the criterion defined within this thesis (absolute differences ≤ 5 mm). The accuracy criterion was defined using the maximum reported accuracy of anthropometric breast measurements taken in the static position (Hansson *et al.*, 2014). It was considered that this maximum level of accuracy may not be required for all applications of the neutral nipple position within future dynamic research or product development. For example, the FE breast models developed by Rajagopal (2007) and Zain-UI-Abdein (2013) had errors up to 11.4 mm (for 2 participants) and 10.77 mm (for 3 participants) respectively when predicting the deformation effect of gravity on the breast. Based on this, it was proposed that absolute differences (to the gold-standard method) below 10 mm could be used to identify neutral position methods that offered an improvement on the current published methods for predicting the breast position without the influence of gravity.

Consideration of this suggestion when evaluating the methods presented in this chapter demonstrates that only the buoyancy in water method was able to achieve the 10 mm level of accuracy, and acceptable precision, for all participants when estimating all three components of the neutral nipple position (maximum absolute differences of 5.3 mm (SD ≤ 2.6 mm), 4.6 mm (SD ≤ 1.6 mm), and 5.6 mm (SD ≤ 1.2 mm) in the anterior-posterior, medial-lateral and superior-inferior directions respectively) (Figure 5.17 and Figure 5.18). It was observed that the maximum absolute differences in the anterior-posterior and superior-inferior components of the neutral nipple position estimated using buoyancy in water were close to the original accuracy criterion of 5 mm. Stricter control over the time

interval between testing sessions, and of the participants included within this study may have reduced the error in the neutral nipple position estimates obtained using buoyancy in water to within the original 5 mm accuracy limit.

None of the other alternative neutral position methods achieved the 10 mm level of accuracy when estimating the anterior-posterior component of the neutral nipple position. The limited success of the alternative methods when predicting this component of the neutral nipple position may have been due to focusing on the inferior effect of gravity on the breast. Several of the alternative methods were developed on the assumption that gravity acted predominantly inferiorly on the breast and that it was the inferior force on the breast that should be counteracted when aiming to identify the neutral nipple position. However, results from the gold-standard method demonstrated that gravity also had a large effect posteriorly on nipple position (up to 25.6 mm) (Table 4.4). This was an unexpected result which was not anticipated prior to developing the alternative neutral position methods.

Although none of the land-based alternative neutral position methods (*i.e.* excluding buoyancy in water) achieved acceptable accuracy when estimating the medial-lateral component of the neutral nipple position, the 10 mm accuracy level was almost met in the superior-inferior direction by the drop landing (absolute differences ≤ 12.0 mm; SD ≤ 3.8 mm) and static extreme methods (absolute differences ≤ 19.4 mm; SD ≤ 1.1 mm) (Figure 5.16). One participant in the drop landing method, and three in the static extreme method caused the maximum absolute differences to exceed 10 mm when compared to the gold-standard results. Consideration of the highly precise nature of the static extreme method meant that it may be possible achieve an improved accuracy level by adapting the calculation procedures used to estimate the neutral nipple position. The drop landing method also demonstrated the potential to accurately and precisely predict the superior-inferior component of the neutral nipple position, with the exception of one participant, although the drop height implemented in this method may restrict its suitability for use with a wider participant sample.

5.7. Conclusion

The gold-standard neutral position method presented in Chapter 4 represents the most accurate estimation of the neutral nipple position as none of the alternative neutral position methods investigated within this chapter were able to replicate the neutral nipple position within the 5 mm accuracy criterion. In situations where the gold-standard method is unachievable, results of this study demonstrated that the buoyancy in water method produced the most accurate, and suitably precise, estimation of the 3D neutral nipple position (absolute differences ≤ 5.6 mm; SD ≤ 2.6 mm).

None of the other land-based neutral position methods were able to successfully estimate all components of the neutral nipple position. However, the drop landing and the static extremes methods both demonstrated the potential to precisely estimate at least one component of the neutral nipple position with an accuracy that improves upon the error associated with existing FE breast models (absolute differences ≤ 10 mm). It is recommended that these alternative methods undergo extensive validity testing before using them in lieu of the gold-standard or water only buoyancy methods.

The gold-standard neutral position attained in Chapter 4 was used throughout the remainder of this thesis when incorporating the neutral position into measurements of breast motion and breast strain.

6. Incorporating the neutral nipple position into measurements of breast motion

6.1. Introduction

This chapter addresses the third aim of the thesis, which was to assess breast motion relative to the neutral position during treadmill activity. Previous assessments of breast motion have typically reported nipple ROM along one or more axes of the torso reference frame (Mills, Lomax, *et al.*, 2014; Monari *et al.*, 2013; Risius, Milligan, *et al.*, 2014; Risius, Milligan, & Scurr, 2012; Scurr, Galbraith, Wood, *et al.*, 2007; Scurr, White, *et al.*, 2009; White *et al.*, 2012, 2008, 2010). Measurements of nipple ROM enable the extent of nipple motion to be quantified, but this measurement may not directly relate to strain, pain, or damage to the breast structure as there is no consideration for the position about which this nipple motion occurs.

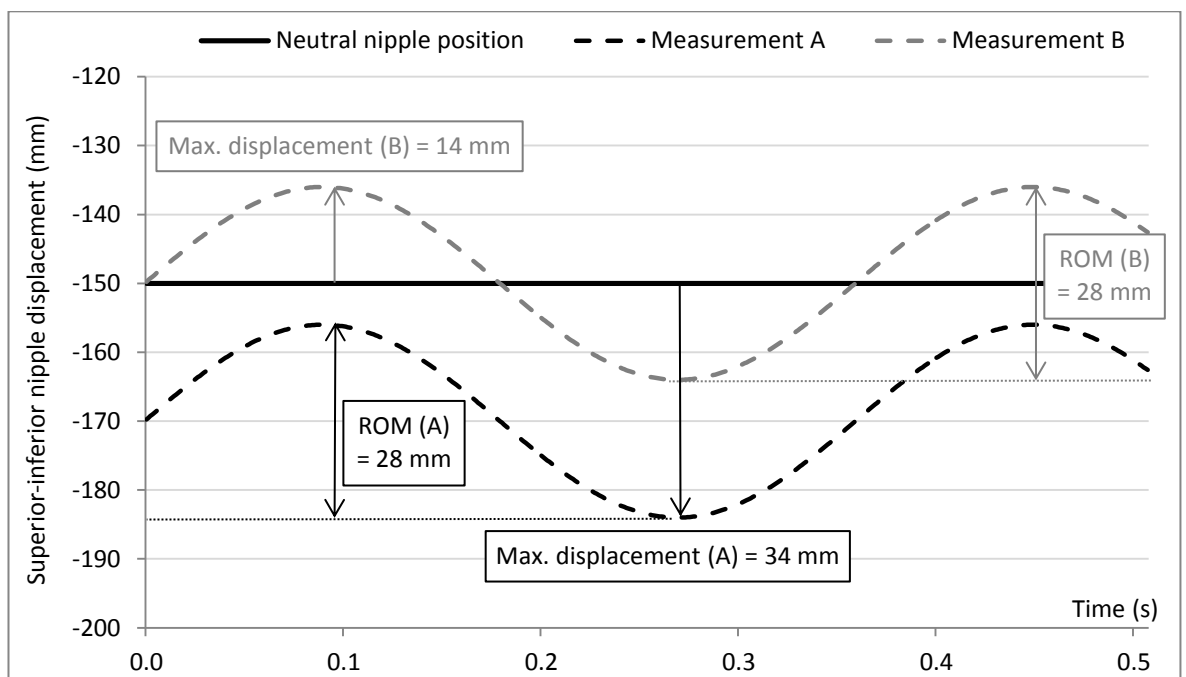


Figure 6.1: Example nipple motion data demonstrating equal nipple range of motion and differing maximum nipple displacements when measured from the neutral nipple position.

Chapter 6: Incorporating the neutral nipple position into measurements of breast motion

Figure 6.1 illustrates that two measurements of nipple motion (A and B) may exhibit the same ROM about a differing mid-point. Based on the work within this thesis, nipple motion that occurs within a limited range about the neutral nipple position may be less damaging to the breast skin, and may cause less breast pain, than nipple motion that occurs further from the neutral nipple position. It is therefore important to consider the neutral nipple position when measuring nipple motion. Incorporating the neutral position into measurements of nipple motion may be particularly beneficial for the development of improved breast support garments. For example, if the data in Figure 6.1 were obtained in two different bra conditions, existing measurement methods using ROM (Milligan *et al.*, 2014; Mills, Lomax, *et al.*, 2014; Mills, Risius, *et al.*, 2014; Risius, Milligan, *et al.*, 2014; Scurr, White, & Hedger, 2011; Zhou *et al.*, 2009) would be unable to distinguish between the appropriateness of support provided by each bra. However, by incorporating measurement of maximum nipple displacement from the neutral nipple position it could be suggested that bra B offered superior protection to the breast as nipple motion was constrained about the neutral nipple position therefore reducing the maximum strain on the breast skin. Evaluation of breast support garments based on the neutral position, as opposed to calculating the reduction in nipple ROM from the unsupported condition (Zhou *et al.*, 2009), may also eliminate the need for potentially painful and embarrassing bare-breasted activity trials (McGhee *et al.*, 2013; Zhou *et al.*, 2011).

The neutral nipple position established in Chapter 4 represents the optimum position of the nipple in terms of minimising strain on the breast skin. Incorporation of the neutral nipple position into measurements of nipple motion was anticipated to provide a more appropriate assessment of nipple motion than measurements of nipple ROM for both product assessment and for future breast motion research. Measurements of nipple displacement from the neutral position would enable nipple motion to be assessed in six directions relative to the torso; a distinction to be made between motions that increase or decrease strain on the breast; and potentially a better understanding of the relationship between nipple motion and motion-induced breast pain. Each of these potential benefits were investigated within this chapter by comparing the existing nipple ROM method to the proposed nipple displacement method for assessing breast motion

Chapter 6: Incorporating the neutral nipple position into measurements of breast motion during treadmill activity. Incremental-speed treadmill activity, incorporating several walking and running speeds, was used to initiate breast motion within this study. The treadmill speed ranged from 4 kph to 14 kph during this study, which was based on the range of treadmill speeds reported in previous breast motion studies (Scurr, White, & Hedger, 2011; Zhou *et al.*, 2011).

The relationship between breast pain and nipple motion was investigated using both nipple motion measurement techniques to evaluate which method was more appropriate for assessing motion-induced breast pain. As described in previous research (Haake *et al.*, 2012; Mason *et al.*, 1999; McGhee *et al.*, 2007; Mills, Risius, *et al.*, 2014; Scurr *et al.*, 2010), breast pain was assessed using an 11-point numerical rating scale labelled from 0 (comfortable) to 10 (painful) (Mason *et al.*, 1999).

6.2. Aims

1. Compare measurements of nipple motion using nipple ROM and nipple displacement from the neutral nipple position during incremental-speed treadmill activity.
2. Compare the relationships between breast pain and both nipple ROM and maximum nipple displacement from the neutral nipple position during incremental-speed treadmill activity.

6.3. Method

This study was conducted alongside the neutral position study (Chapter 4) using the same 14 participants (Table 4.1). Each participant had retro-reflective markers placed on their breast and torso as described previously (Figure 4.1) with two additional 12 mm diameter markers placed on the participants' right and left heels to allow identification of gait cycles during data analysis. Participants had their neutral nipple position measured using the gold-standard buoyancy method described in section 4.3, and performed an incremental-speed treadmill test. The treadmill test began at 4 kph and increased by 1

Chapter 6: Incorporating the neutral nipple position into measurements of breast motion kph every 7 gait cycles to a maximum speed of 14 kph. At each treadmill speed participants verbally rated their breast pain using an 11-point numerical rating scale (Appendix K). Breast and torso markers were recorded at 200 Hz using the optoelectronic camera system and manual event markers were added during data collection to identify the transitions between treadmill speeds. Marker trajectory data were identified in QTM, filtered in Visual 3D using a generalised cross validity (quintic) spline, and converted to relative data as described in section 5.4.1. The start of each gait cycle was identified using event markers in Visual 3D which were created automatically using the anterior-posterior velocity of the heel marker (Zeni Jr *et al.*, 2008).

Nipple ROM was calculated in Visual 3D by subtracting the minimum from the maximum relative left nipple displacement during each gait cycle. Mean nipple ROM was calculated for the last three gait cycles at each treadmill speed across all participants. Nipple displacement from the neutral position was calculated by subtracting the neutral nipple position for each participant (identified in Chapter 4 (Table 4.3)) from that participant's instantaneous relative left nipple displacement data during the treadmill test. Maximum nipple displacement from the neutral position was identified in all six anatomical directions during the last three gait cycles for each participant at each treadmill speed. The mean maximum nipple displacement in each direction was calculated for each treadmill speed.

The relationship between nipple motion (measured using both procedures) and perceived breast pain was investigated statistically. A Spearman's rho correlation was performed between perceived breast pain and nipple ROM, and between perceived breast pain and maximum nipple displacement from the neutral position, at each treadmill speed using SPSS (IBM SPSS statistics version 22). Correlation coefficients of ± 0.1 , ± 0.3 , and ± 0.5 indicated weak, moderate and strong correlations respectively (Field, 2009).

6.4. Results

Nipple displacement data for three gait cycles of running (14 kph) for one participant (Participant 6, 32C) were illustrated in Figure 6.2 and Figure 6.3. These example data

Chapter 6: Incorporating the neutral nipple position into measurements of breast motion displayed similar oscillatory patterns in each direction to those reported in previous breast motion studies (Scurr *et al.*, 2010; Scurr, White, *et al.*, 2009; Yu & Zhou, 2012). The nipple oscillated approximately once per gait cycle in the anterior-posterior (Figure 6.2 a) and medial-lateral directions (Figure 6.2 b), and a double oscillation occurred in the superior-inferior direction per gait cycle (Figure 6.2 c). Nipple range-of motion was generally greatest in the superior-inferior direction as has been previously reported for bare-breasted treadmill activity (Mills, Loveridge, *et al.*, 2014b; Scurr, White, & Hedger, 2011; Scurr, White, *et al.*, 2009). A comparison of nipple displacement during running at 14 kph to the neutral and gravity-loaded nipple positions for participant 6 demonstrated that nipple oscillations occurred about the gravity-loaded position in the anterior-posterior and medial-lateral directions. In the superior-inferior direction the nipple oscillated about a point midway between the neutral and gravity-loaded positions. The superior displacement of nipple oscillations during treadmill running has previously been reported by Campbell (2007), although the neutral nipple position was not considered in Campbell's research.

When viewed in the frontal (Figure 6.3 a) or sagittal (Figure 6.3 a) plane, the displacement of the nipple during running (14 kph) follows the characteristic 'butterfly' or 'figure-of-eight' trajectory (Scurr, 2007; Zhou *et al.*, 2012b; Zhou, 2011). Nipple trajectories have not previously been reported with reference to the neutral or gravity-loaded nipple position, and it was interesting to observe that the nipple trajectory passes through (or close to) both the neutral and gravity-loaded nipple position in the sagittal plane (Figure 6.3 b) but does not pass through either position in the frontal plane (Figure 6.3 a).

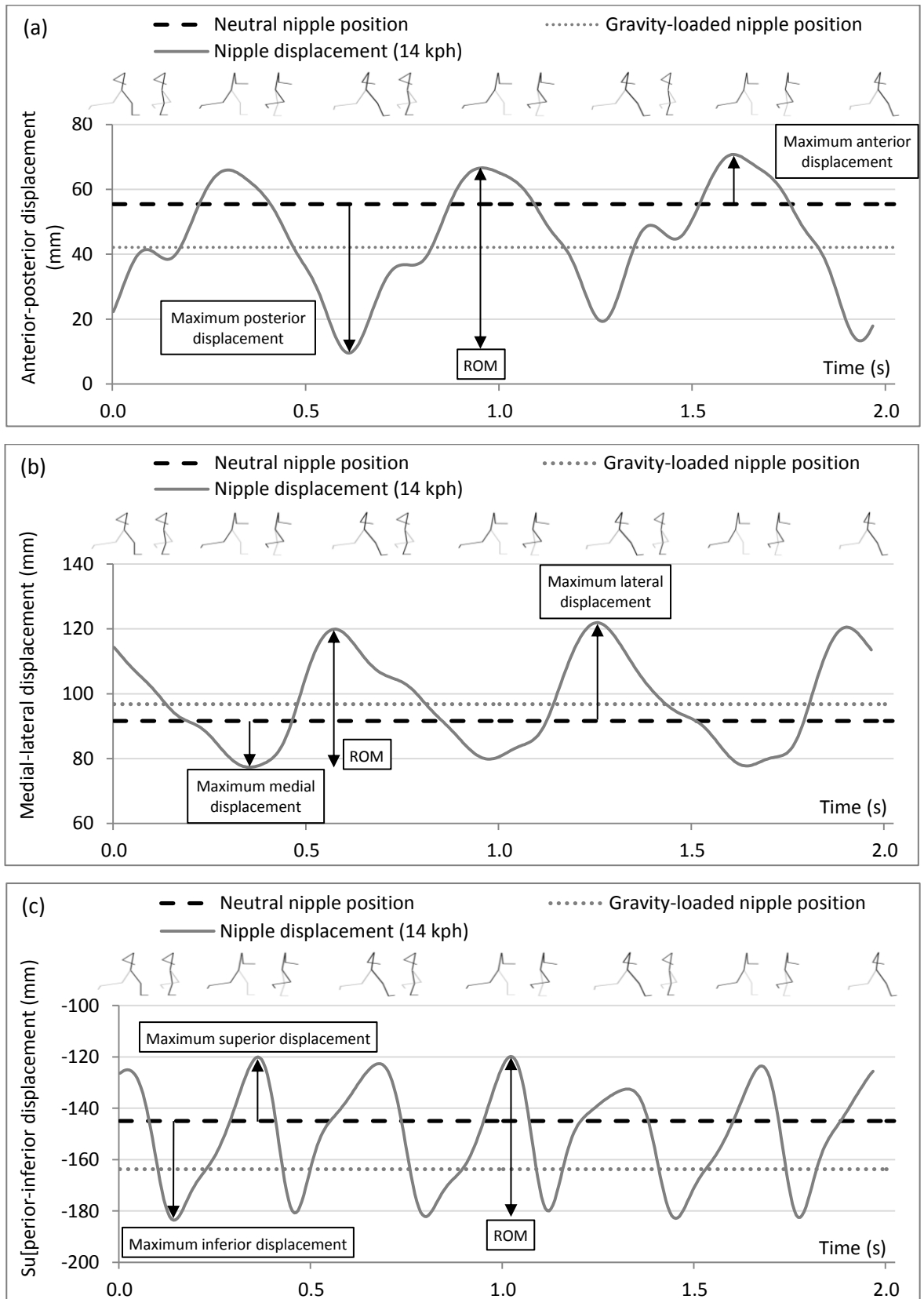


Figure 6.2: Anterior-posterior (a), medial-lateral (b), and superior-inferior (c) nipple displacement for one participant (Participant 6, 32C) during three gait cycles of treadmill running at 14 kph.

Chapter 6: Incorporating the neutral nipple position into measurements of breast motion

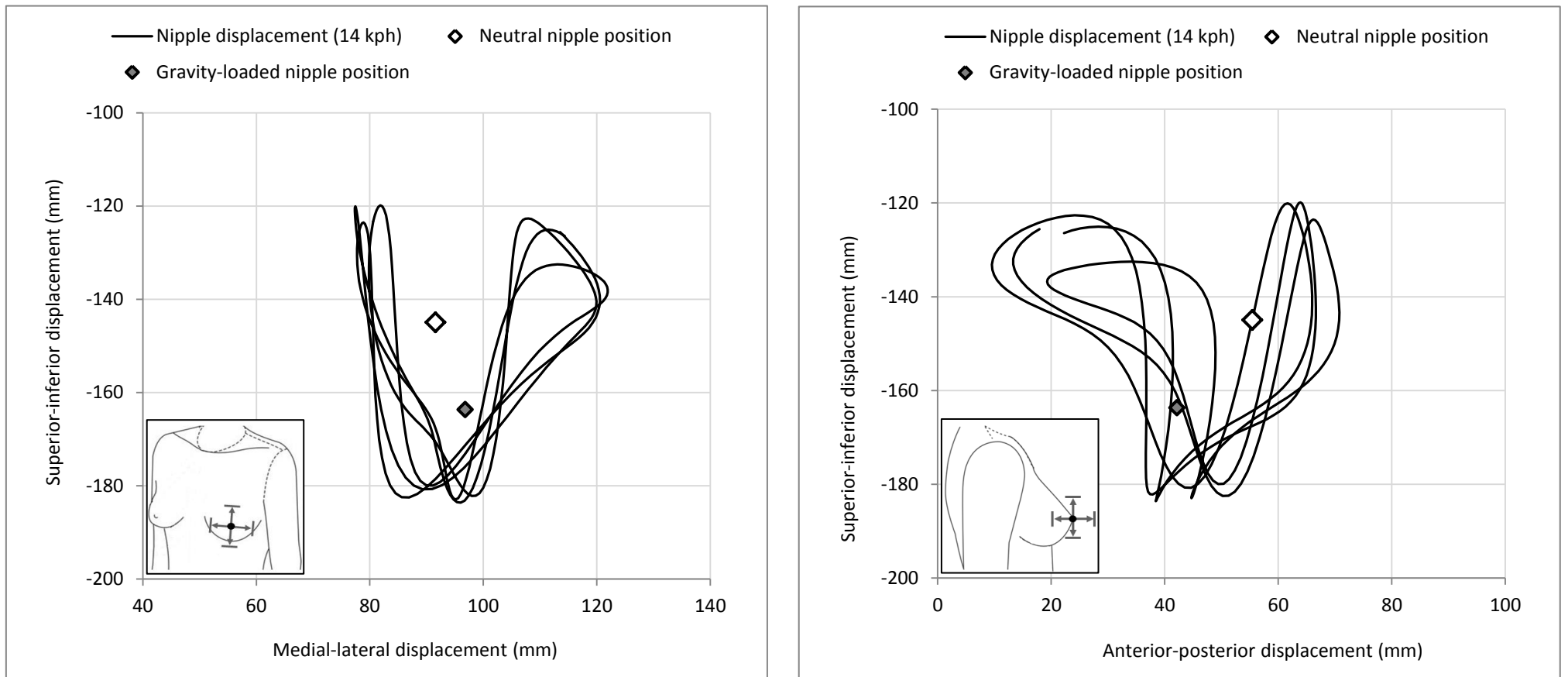


Figure 6.3: Nipple displacement in the frontal (a) and sagittal (b) plane for one participant (Participant 6, 32C) during three gait cycles of treadmill running at 14 kph.

Chapter 6: Incorporating the neutral nipple position into measurements of breast motion

Mean and mode data were calculated across the participant sample within this study to investigate the relationships between nipple range of motion, nipple displacement from the neutral position, and breast pain. Perceived breast pain data are presented for each participant and as a mode in Figure 6.4. Within-participant data demonstrate a trend for increasing breast pain with increasing treadmill speed. However, between participant pain ratings are highly varied (up to a 10 point spread at 14 kph) and mode pain scores suggest that breast pain increases with treadmill speed up to 10 kph where there is a plateau followed by a reduction in pain at the two highest treadmill speeds.

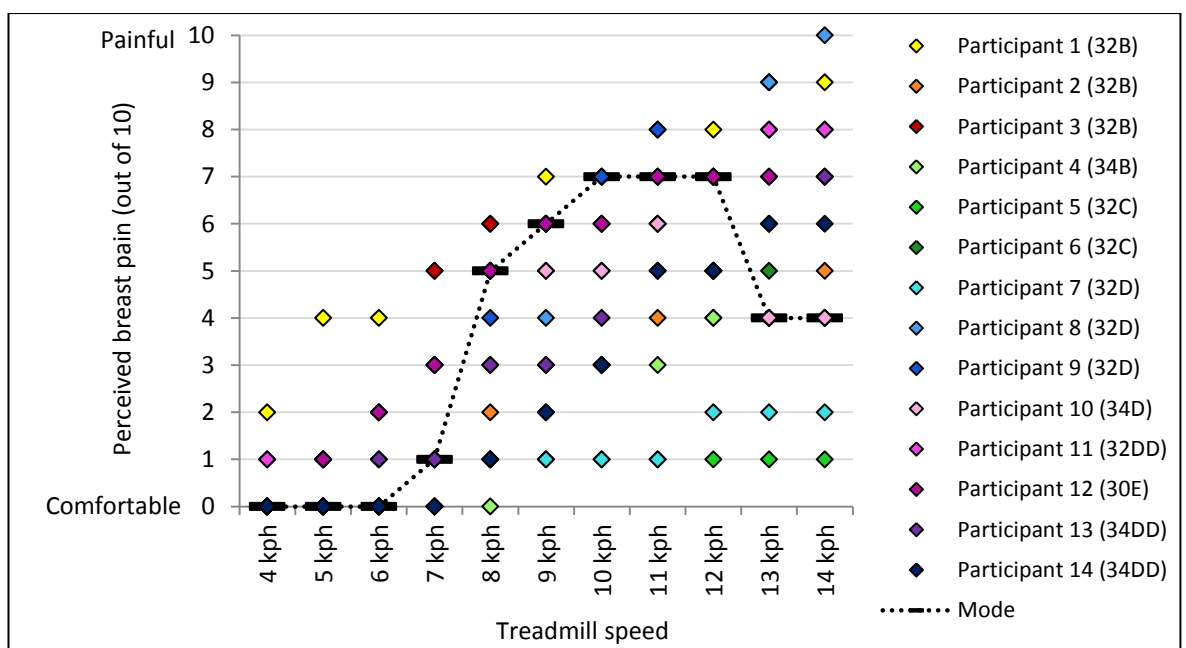


Figure 6.4: Breast pain scores at each speed of an incremental-speed treadmill test.

Measurements of nipple ROM demonstrate increasing nipple motion in all directions with increasing treadmill speed (Figure 6.5). At walking speeds (up to 7 kph) nipple motion is predominantly in the anterior-posterior and medial-lateral directions, suggesting a swinging motion of the breast. However, at speeds above 8 kph there is a large increase in superior-inferior nipple motion, indicating a transition from swinging to bouncing breast motion. A direct comparison between mean measurements of nipple ROM and maximum displacement from the neutral position while running at 14 kph is shown in Figure 6.6. The displacement data in demonstrates that nipple motion does not occur symmetrically about the neutral position during treadmill running, particularly along the

Chapter 6: Incorporating the neutral nipple position into measurements of breast motion superior-inferior axis where the nipple displaced almost three times further in the inferior than in the superior direction (Figure 6.6).

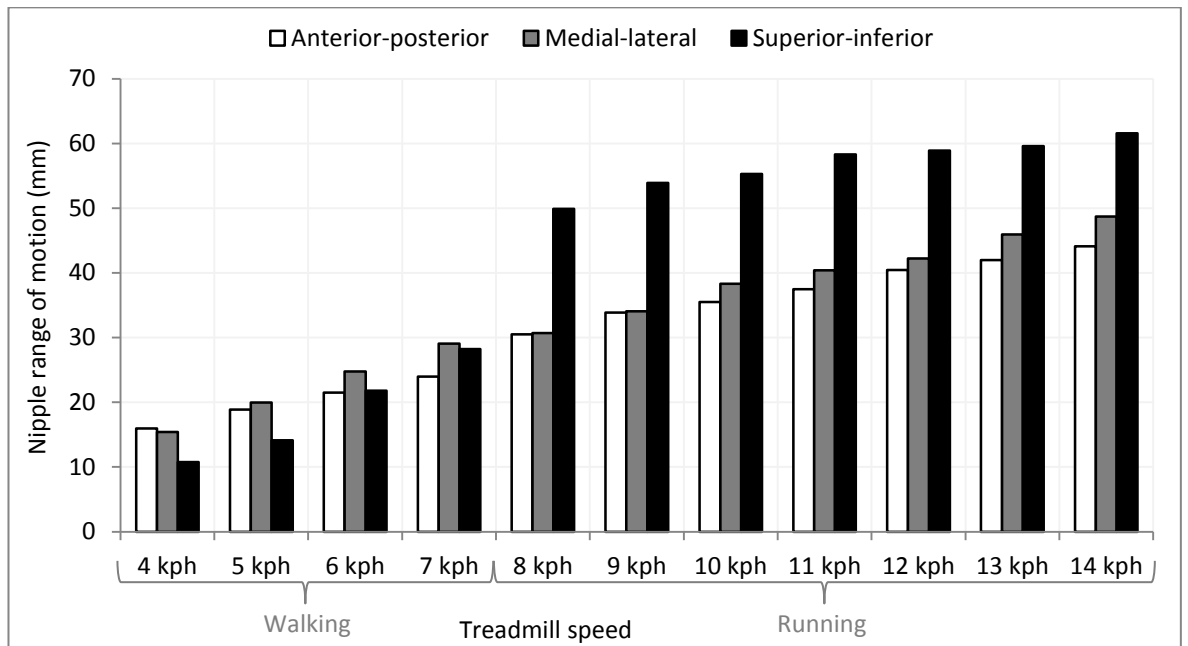


Figure 6.5: Mean left nipple range of motion at each speed of an incremental-speed treadmill test (n = 14).

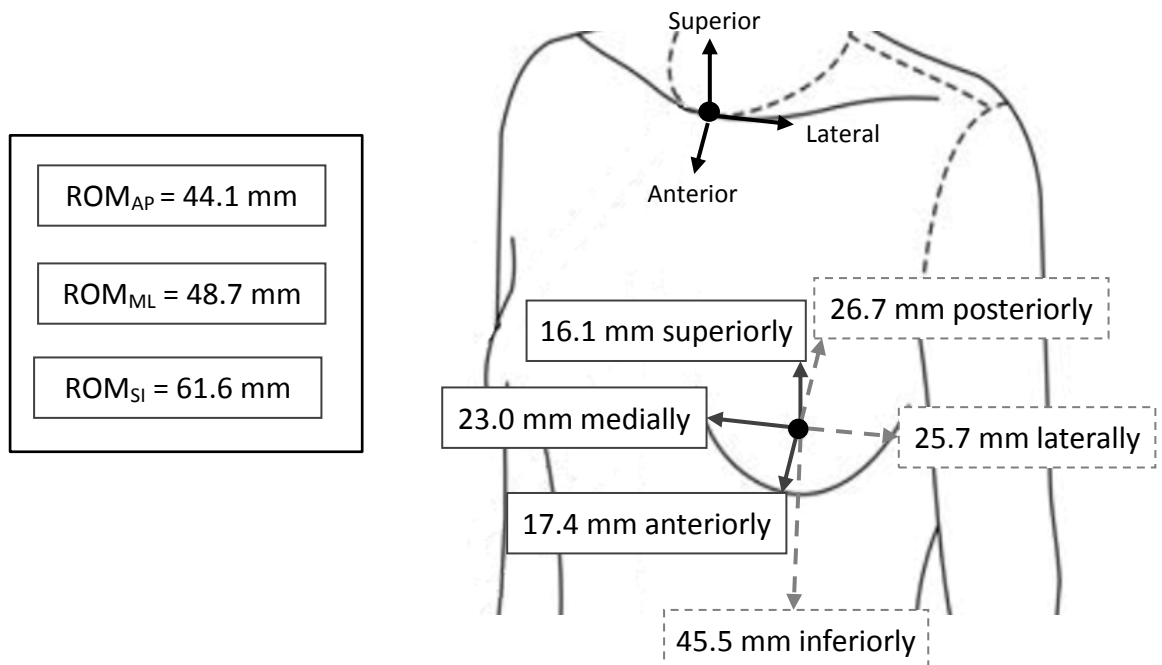


Figure 6.6: Mean ROM and peak displacements of the nipple from the neutral position during running at 14 kph (n = 14).

Chapter 6: Incorporating the neutral nipple position into measurements of breast motion

Measurements of maximum nipple displacement are illustrated at each treadmill speed in the frontal and sagittal planes of the breast in Figure 6.7 and Figure 6.8 respectively. The mean neutral and gravity-loaded nipple positions are also included in these figures to aid interpretation of the data. Maximum nipple displacement data demonstrate a similar transition in nipple motion at 8 kph to that observed in the ROM data, with a large increase in superior-inferior nipple motion occurring at this speed. Closer inspection of the maximum nipple displacement data shows that although there was an increase in nipple motion at higher treadmill speeds (above 8 kph), the position about which this motion occurred (the motion mid-point) moved closer to the neutral nipple position as treadmill speed increased. This shift of the motion mid-point resulted in slightly smaller maximum nipple displacements occurring in the superior and medial directions at 8 kph than those that occurred at lower treadmill speeds (Figure 6.7).

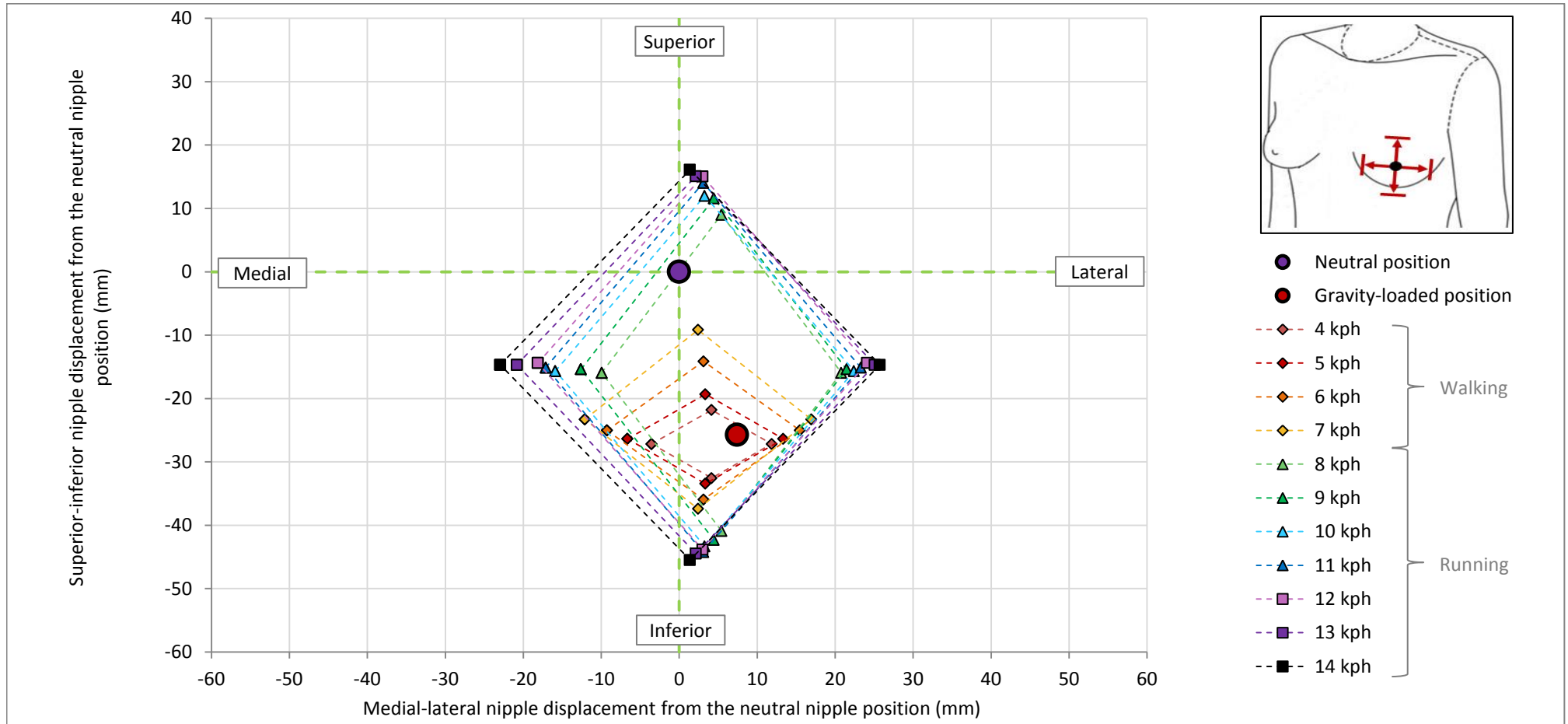


Figure 6.7: Mean maximum nipple displacement from the neutral nipple position in the frontal plane during an incremental-speed treadmill test (n = 14).

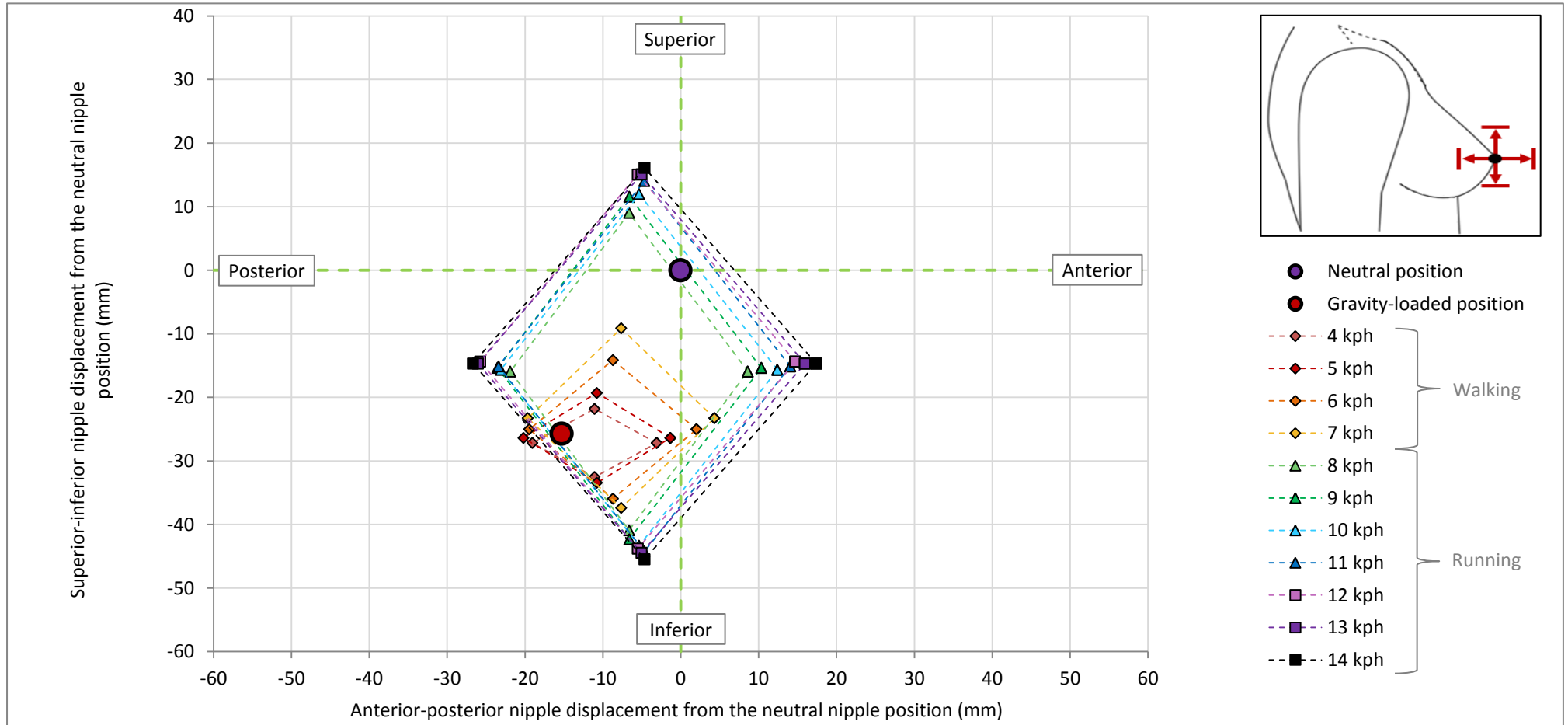


Figure 6.8: Mean maximum nipple displacement from the neutral nipple position in the sagittal plane during an incremental-speed treadmill test (n = 14).

Significant strong correlations were found between breast pain and all three components of nipple ROM, but not all directions of nipple displacement were correlated to breast pain (Table 6.1).

Table 6.1: Correlations between breast pain, nipple ROM and maximum nipple displacement from the neutral nipple position during an incremental-speed treadmill test.

		Spearman's correlation coefficient (r)	Significance (p)
Breast pain and nipple ROM	Anterior-posterior	0.588	0.000*
	Medial-lateral	0.525	0.000*
	Superior-inferior	0.660	0.000*
Breast pain and maximum nipple displacement from the neutral nipple position	Anterior	0.533	0.000*
	Posterior	0.277	0.001*
	Medial	0.346	0.000*
	Lateral	0.581	0.000*
	Superior	0.725	0.000*
	Inferior	0.219	0.006

* denotes a significant correlation ($p < 0.05$)

6.5. Discussion

This chapter aimed to investigate the effect of incorporating the neutral nipple position into measurements of nipple motion when compared to the traditional method of assessing nipple ROM. Nipple ROM results demonstrate a similar pattern to those reported in previous studies with the greatest amount of nipple motion occurring in the superior-inferior direction, particularly at speeds above 7 kph (Figure 6.5) (Scurr, White, & Hedger, 2011). Consideration of the nipple ROM data alone leads to the suggestion that breast support garments should focus on reducing breast motion in the superior-inferior direction.

More detailed bra design recommendations can be obtained using the maximum displacement data measured from the neutral nipple position. Evaluation of the maximum displacement values demonstrate that the nipple consistently displaces

Chapter 6: Incorporating the neutral nipple position into measurements of breast motion furthest from the neutral position in the inferior direction, with mean maximum displacements in this direction ranging from 32.5 mm during walking (4 kph) up to 45.5 mm during running (14 kph) (Figure 6.6 and Figure 6.7). Mean maximum nipple displacements were all below 30 mm in the medial, lateral and posterior directions, and below 20 mm in the superior and anterior directions (Figure 6.7 and Figure 6.8). Based on these displacement breast support garments aiming to protect the breast against damaging skin strains should focus on reducing the inferior displacement of the breast. Interestingly, these data show that the superior displacement of the breast decreased following the transition from walking to running (Figure 6.7), suggesting that the increased superior motion of the breast during running may not cause increased strain (or risk of damage) on the breast skin. This observation highlights the importance of measuring breast motion in six directions (from the neutral position) when making recommendations for breast support garments.

Incorporation of the neutral nipple position into measurements of nipple motion also provided the opportunity to evaluate the position of the nipple during treadmill activity. The data in Figure 6.7 and Figure 6.8 illustrate that the mid-point of nipple motion moved closer to the neutral position and further from the gravity-loaded position with increasing treadmill speed in both the frontal and sagittal plane. This finding suggests that the breast moved about an improved position, in terms of reducing skin strain, as treadmill speed increased (particularly at speeds above 7 kph). Although the mid-point of nipple motion was closer to the neutral nipple position during running than walking, the maximum nipple displacement values in all directions generally increased with increasing treadmill speed due to the increased ROM of the nipple at each speed. It was anticipated that the benefit of assessing breast positioning (using the mid-point of nipple motion) in addition to breast motion may be enhanced when comparing the performance of different breast support garments as opposed to evaluating bare-breasted nipple motion. Nipple ROM is typically reduced with the addition of a breast support garment during treadmill running (Scurr, White, & Hedger, 2011) which may mean that breast positioning becomes a more important factor when calculating maximum nipple displacements from the neutral position (*i.e.* positioning the breast closer to the neutral position inside the bra would reduce maximum displacement measurements from the neutral position).

Chapter 6: Incorporating the neutral nipple position into measurements of breast motion

Using the neutral nipple position to represent the optimum nipple position when evaluating breast support garments would enable both breast positioning and breast motion control to be quantified.

A final consequence of incorporating the neutral breast position into measurements of nipple motion is the ability to distinguish between breast motions that increase (away from the neutral position) or decrease (towards the neutral position) strain on the breast skin. Results from this chapter suggest that the breast does move towards the neutral position during treadmill running at speeds above 8 kph (Figure 6.7 and Figure 6.8), providing some evidence to support the idea of beneficial breast motion. As beneficial breast motion is a new concept within breast biomechanics it would be interesting to investigate whether certain activities or support conditions could be used to maximise the beneficial motion and minimise the negative motion of the breast during physical activity.

The second aim of this chapter was to evaluate the relationship between nipple motion (measured using ROM and maximum displacement) and breast pain. The bare-breasted pain data collected in this study demonstrate significant strong correlations to nipple ROM in all three directions, which is in line with the results from previous breast motion research (Mason *et al.*, 1999; Scurr *et al.*, 2010; White, 2013). The novel aspect of this study was the incorporation of the neutral position into measurements of nipple motion. It was anticipated that measurements of maximum nipple displacement from the neutral nipple position would correlate more strongly to breast pain than measurements of ROM because the neutral position represented the optimum breast position for each participant in terms of minimising breast skin strain. Results demonstrated that maximum superior nipple displacement was the most strongly correlated to breast pain, and that this correlation was stronger than the correlations between pain and nipple ROM. Interestingly, this finding suggests that breast support garments aiming to reduce breast pain should focus on reducing superior and lateral breast displacement, which would contradict the recommendations made based on the displacement data.

Breast pain was also more strongly correlated to maximum lateral nipple displacement than to the corresponding medial-lateral ROM. These strong correlations suggest that

Chapter 6: Incorporating the neutral nipple position into measurements of breast motion

participants experienced more breast pain when their breast displaced further from the neutral position as anticipated. However, this result was not replicated in all six anatomical directions. The relationship between breast pain and maximum nipple displacement was weaker than to the corresponding ROM measurement in the anterior, posterior, medial and inferior directions (Table 6.1). The relationships between breast pain and maximum nipple displacement were particularly weak in the inferior and posterior directions. The weak and non-significant correlation in the inferior direction was particularly interesting as this suggests that increased inferior nipple displacement from the neutral position does not cause increased breast pain despite displacement data indicating that the breast displaces furthest from the neutral position in this direction. One possible explanation for this conflicting result can be provided by considering that the inferior and posterior directions were found to be most affected by gravitational loading in Chapter 4 (Table 4.4). It has previously been reported that the pain response to a continuous stimulus can weaken and eventually disappear over time (Edes & Dallenbach, 1936). Participants in this study may therefore have experienced a reduced pain response in the inferior and posterior directions because they had become accustomed to the continual inferior and posterior action of gravity on the nipple. A second factor which may also have affected the relationships observed in this study between breast pain and nipple motion was the method used to assess pain. Methods for quantifying pain, including numerical rating scales such as the one implemented within this study, were developed for assessing within-participant pain (Ho, Spence, & Murphy, 1996). Subjective perceptions of pain can be influenced by an individual's previous experiences of pain, which makes it difficult to combine or compare self-reported pain data between participants (Kane *et al.*, 2005). High between-participant variation in perceived breast pain was evident in the data presented in Figure 6.4 and may have affected the correlations observed between pain and nipple motion within in this study.

6.6. Conclusion

Incorporation of the neutral nipple position into measurements of nipple motion revealed that nipple displacement predominantly occurs in the inferior direction during treadmill running. Additionally it was observed that the nipple motion occurred about a mid-point that was closer to the neutral nipple at higher treadmill speeds, supporting the idea of beneficial breast motion in terms of reducing breast skin strain. Breast pain correlated strongly to nipple ROM in all directions, but was most strongly correlated to superior nipple displacement from the neutral position. Evaluation of both pain and displacement data leads to the contradictory recommendations that breast support garments aiming to reduce the risk of breast skin damage should limit inferior nipple displacement, whereas garments aiming to reduce breast pain should limit superior nipple displacement during treadmill activity.

The results presented within this chapter provide some indication of the relationships between breast motion, potential breast damage, and breast pain. However, measurements of breast skin strain, combined with the previously published strain failure limits for human skin (Silver *et al.*, 2001), may provide improved estimates of the risk of breast skin damage and stronger correlations to breast pain. Breast skin strain and its relationship to breast pain were investigated in the following chapter.

7. Static and dynamic breast strain

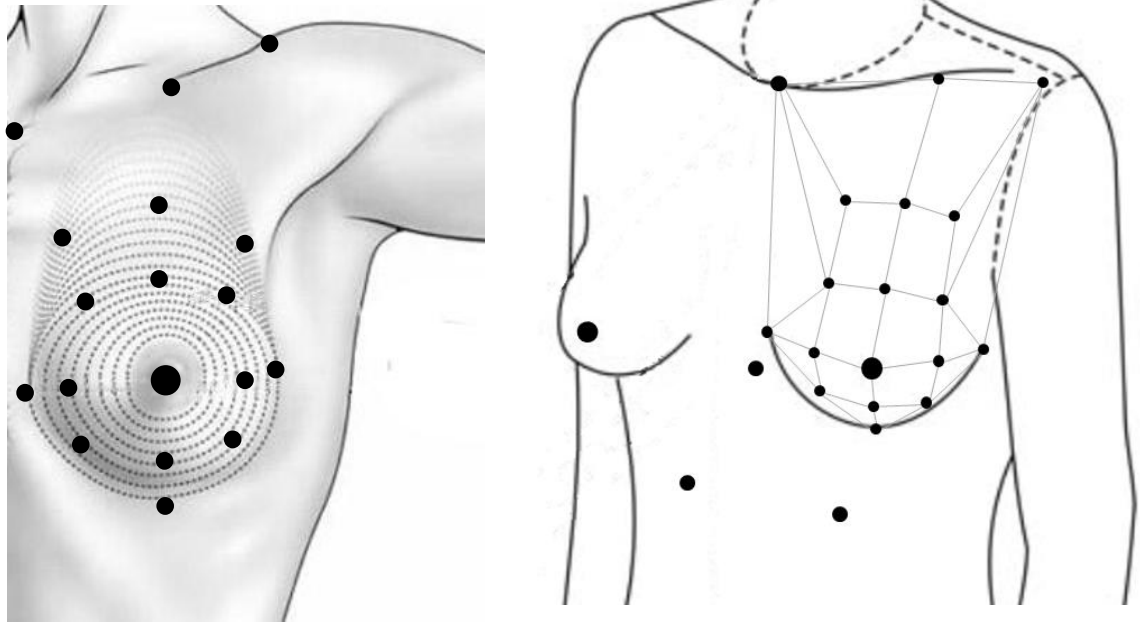
7.1. Introduction

This chapter represents the first attempt to incorporate a gold-standard measurement of the neutral breast position (described in Chapter 4) into the measurement of static and dynamic breast skin strain. It was proposed that the gold-standard neutral breast position represents a more accurate reference position for the assessment of breast strain, which would lead to more accurate strain measurements and a better understanding of the effect of breast loading on the supporting structures of the breast. As discussed in section 2.4, the risk of breast ptosis caused by skin strain could be estimated by applying the published failure limits of human skin (60% strain) to measurements of strain on the breast skin (Silver *et al.*, 2001). Furthermore, strain on the neural network within the breast skin may be a contributory factor to motion-induced breast pain (Chadbourne *et al.*, 2001). Consequently assessment of breast skin strain may provide a better predictor of breast pain than previously investigated variables such as ROM, velocity or acceleration (Zhou *et al.*, 2011).

The second novel aspect of this study was the implementation of a marker array on the breast when measuring dynamic breast strain. Although an array has been implemented in previous research assessing the effect of gravity on the breast, no strain values were calculated and only the static condition was investigated (Rajagopal, 2007). Existing dynamic breast strain studies have focused on data obtained using a suprasternal notch and nipple marker (Haake *et al.*, 2012; Haake & Scurr, 2011). The use of two markers to calculate breast strain limits the interpretation of the resulting strain data as measured values represent the percentage extension of the straight line extending from the suprasternal notch to the nipple, and not necessarily the strain occurring on any particular breast structure. Application of a marker array over the breast skin provides a better representation of the breast's curved surface. Improved breast surface approximation enables measurements of strain to better replicate the strain experienced by the breast skin, which is important for the evaluation of whether skin strain failure limits have been exceeded. Strain data obtained using an array also permits the

evaluation of skin strain in different regions of the breast. As the breast is composed of soft tissue and does not move as a rigid object against the torso, there may be regions of breast skin that are more susceptible than others to excessive levels of breast strain during particular activities. Identification of highly strained breast regions may inform the development of better breast support garments that provide increased levels of support to regions of the breast where it is most needed.

The marker array implemented within this study was described in section 4.3.1 (Figure 4.1). For the calculation of strain using Equation 2.1 (section 2.4.1), it was necessary to define the marker pairings that would be used to calculate the neutral and loaded (strained) length of each segment of skin over the breast surface. Consideration was given to the direction of the Langer lines on the female breast described in section 2.4.2. Langer lines are used to illustrate the preferred direction of the collagen and elastin fibres within the skin (Daly, 1982; Gibson *et al.*, 1969) and were depicted by Jatoi *et al.* as a series of concentric circles about the nipple (Jatoi, Kaufmann, & Petit, 2006). The marker array used within this chapter is shown overlaying the Langer lines in Figure 7.1 a. It was observed that the parallel and perpendicular directions of the Langer lines (and therefore skin tension) on the female breast could be approximated using a rectangular series of marker pairings (Figure 7.1 b). Previous research has shown that skin samples taken perpendicular to Langer lines (longitudinal breast lines) fail at lower loads than samples taken parallel to the Langer lines (latitudinal breast lines) regardless of strain rate (Ottenio *et al.*, 2014). It was therefore interesting to investigate whether there were differences between skin strains measured in the longitudinal (superior-inferior) and latitudinal (medial-lateral) directions on the breast skin. If no differences are present then this may suggest that breast skin is more likely to be damaged by loading that occurs in the superior-inferior direction as the skin fails more easily when strained in this direction, although it was acknowledged that the Langer line orientation may differ within the same breast region between individuals (Finlay, 1970; Flynn *et al.*, 2011).



(a) Breast markers and Langer lines

(b) Rectangular breast segmentation

Figure 7.1: Breast marker location on the breast with reference to the Langer lines of the breast (a) (Jatoi *et al.*, 2006); and the rectangular marker pairings used for the calculation of breast strain (b).

For clarity within this chapter, the term ‘static strain’ refers to the breast strain caused by gravity and ‘dynamic strain’ refers to the total breast strain (including gravitational strain) that occurs during dynamic activity. Incremental-speed treadmill activity was used to initiate dynamic breast strain within this study. A range of walking and running speeds were used to represent the common physical activities that women may experience in both their daily living and sporting contexts.

7.2. Aims

1. Calculate the static and dynamic strain on different regions of the breast skin.
2. Estimate the risk of breast skin damage caused by static and dynamic breast skin strain.
3. Assess the relationships between breast skin strain and breast pain during incremental-speed treadmill activity.

7.3. Method

7.3.1. Experimental procedure

The neutral position data collected for this strain study were collected at the same time, using the same participants, as the neutral position data presented in Chapter 4. Participants had the marker array illustrated in Figure 4.1 applied to their left breast and torso using henna. During testing, retro-reflective markers were applied over the henna using hypoallergenic tape (6 mm diameter markers on the breast array (excluding nipple); 12 mm diameter markers on the torso and left nipple). The total mass of the markers on the breast was 1.7×10^{-4} kg, which was assessed using a Mettler PC400 balance (Mettler Toledo, Switzerland). Participants then followed the same testing procedures described in section 4.3.1.

The static skin strain data were collected using the gravity-loaded breast position measurements taken at the same times as the buoyancy testing in both water and soybean oil as described in section 4.3.1. Dynamic skin strain data were collected at the same time as the treadmill data presented in Chapter 6, using the incremental-speed treadmill test procedures described in section 6.3. In each testing condition (neutral position, gravity-loaded position, and 11 treadmill speeds), participants verbally rated their breast pain using an 11-point numerical rating scale labelled from 0 (comfortable) to

10 (painful) (Mason *et al.*, 1999). Breast pain data were recorded using the breast pain scales shown in Appendix K.

7.3.2. Data analysis

The co-ordinate data from the water, soybean oil, static laboratory trials and dynamic treadmill trials were imported to Visual 3D. A separate torso segment model was created for each participant in each experimental condition as described in sections 3.4 and 4.3.2. Raw marker co-ordinate data was filtered in Visual 3D using a generalised cross validatory (quintic) spline and each participant's torso model was recalculated. The displacement of each breast marker was then converted into the local co-ordinate system of the torso. A total of 35 inter-marker distances were calculated in each condition using the resultant separation between the marker pairings shown in Figure 7.1 b. Gait cycles were identified in the treadmill data as described in section 6.3 and instantaneous marker separations were calculated for the final 3 gait cycles of each treadmill speed for each participant.

Due to the quantity of data obtained within this strain study it was necessary to separate each stage of the data analysis to achieve the aims outlined within this chapter. Static breast strain was investigated first, followed by dynamic breast strain, and finally the comparison between strain and pain data. The dynamic strain data was analysed in three separate stages with each stage focusing on increasingly detailed strain data within fewer dynamic conditions. Additionally, error analysis was conducted on the static strain data to assess the accuracy of the strain values presented within this thesis. These analyses are presented in the following sections:

7.3.2a Static breast skin strain

7.3.2b Peak regional breast skin strain during treadmill activity

7.3.2c Peak segmental breast skin strain during treadmill activity

7.3.2d Instantaneous segmental breast skin strain over one gait cycle at 14 kph
– A case study

7.3.2e Peak breast skin strain and breast pain

7.3.2f Error analysis of breast strain data

7.3.2a. Static breast skin strain

Method

The neutral inter-marker separation (L_0) was defined as the mid-point between the mean separation of consecutive markers in water and in soybean oil (three trials in each condition). Static skin strain was calculated using Equation 2.1; where L_0 was defined using the neutral marker separations and L was defined as the mean marker separation calculated from the six gravity loaded static trials (three from each testing session). For comparison to previous research, a first order approximation of static strain was also calculated using the resultant suprasternal notch to nipple distance in the neutral and gravity-loaded conditions as described by Haake (Haake *et al.*, 2012; Haake & Scurr, 2011). The risk of breast skin damage caused by static breast strain was estimated by comparing the static strain values for each participant to the skin strain limits reported by Silver (2001) (30% represents skin resistance and 60% represents the onset of skin failure).

Results

Analysis of individual static strain data revealed high between-participant variation in strain values across the breast skin, with differences of up to 74% in strain for the same marker pairing between individuals. Individual static strain data are illustrated in Appendix L, with Figure 7.2 providing a demonstration of the general distribution of static strain over the breast for 14 participants with breast sizes ranging from 32 to 34 under band and B to E cup size.

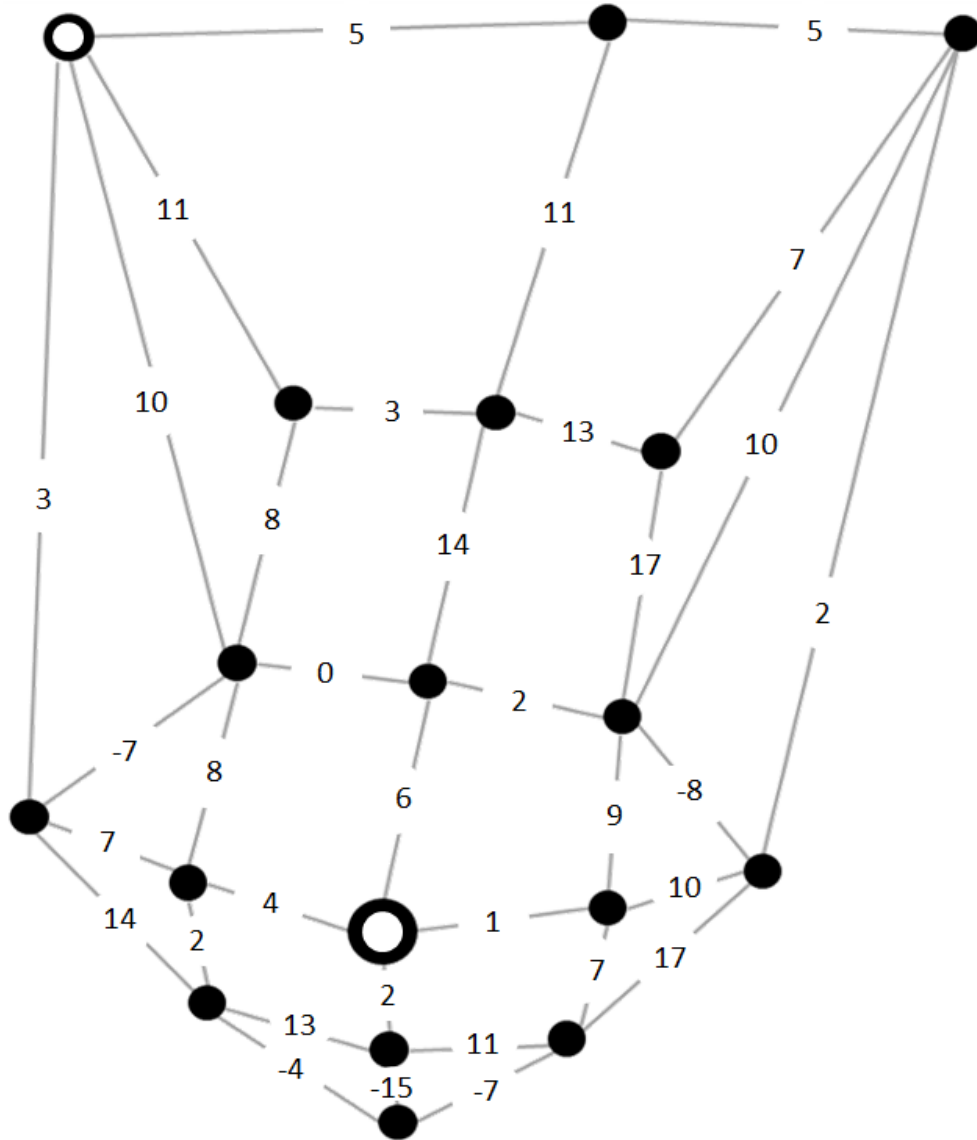


Figure 7.2: Mean percentage static skin strain across the breast for 14 participants with breast sizes 32 to 34 under band and B to E cup size. The two white markers represent the locations of the suprasternal notch and the left nipple.

Table 7.1 demonstrates the previously published method of assessing breast strain using the distance between the suprasternal notch and nipple marker (Haake & Scurr, 2011), compared to the peak breast skin strain measured for each participant using the marker array. Results demonstrate that the two strain analysis methods produce static strain values of the same order or magnitude as those presented in Haake’s previous work (Haake *et al.*, 2012; Haake & Scurr, 2011). However, the two marker method consistently underestimated the peak static strain on the breast skin (by up to 59%) compared to the strain measured using a marker array, which may have implications for the assessment of

potential skin damage. In this study, one participant experienced up to 75% static breast strain, suggesting that the effect of gravity alone may be sufficient to damage this individual's breast skin (Table 7.1).

Table 7.1: First order static breast strain calculated using the resultant distance between the suprasternal notch and nipple marker compared to peak static strain obtained using a breast array.

Participant number	Breast size	Neutral suprasternal notch to nipple length (mm)	Gravity loaded suprasternal notch to nipple length (mm)	First order breast strain using two markers (%)	Peak breast strain using the array data (%)
Participant 1	32B	166.2	182.2	10	48
Participant 2	32B	186.0	197.9	6	18
Participant 3	32B	166.7	186.2	12	26
Participant 4	34B	201.1	227.4	13	30
Participant 5	32C	178.2	195.4	10	18
Participant 6	32C	180.3	194.8	8	23
Participant 7	32D	161.1	178.9	11	27
Participant 8	32D	179.1	202.7	13	18
Participant 9	32D	182.6	202.5	11	14
Participant 10	34D	189.2	205.8	9	25
Participant 11	32DD	170.8	189.5	11	16
Participant 12	30E	190.3	215.8	13	32
Participant 13	34DD	215.0	245.5	14	58
Participant 14	34DD	183.4	213.3	16	75
Mean		182.1	202.7	11	30
Standard deviation		14.3	18.2	3	18

Discussion

Static strain data demonstrated diverse strain values across the breast skin, with differences between different breast segments of up to 110% strain in the static condition for one participant (Participant 14, Appendix L). There was also high between-participant variation in the static strain data, with differences up to 74% strain for the same breast segment across participants (Appendix L). Peak static strain values typically occurred on

the outer upper region of the breast, with strains in this region reaching a maximum of 75% for one participant in the static condition (Table 7.1).

Peak strain values in the static condition were higher than anticipated, with Participants 1, 12, and 13 experiencing strains in the skin resistance zone ($> 30\%$) and Participant 14 experiencing potentially damaging skin strain ($> 60\%$). The implication that gravity alone could be causing permanent damage to the breast skin is surprising and the lack of existing static breast strain data makes it difficult to assess the credibility of these results. On one hand the prevalence of ptosis among mature women (Rinker, Veneracion, & Walsh, 2010), and the reports of markedly elongated breasts among tribal women who do not wear breast support (Gunkel & Handler, 1969; Morgan, 1997), suggest that the breast can experience damaging skin strains. However, it was acknowledged that the straight-line approximation method used to calculate strain within this thesis may have led to an over-estimation of breast skin strain (Figure 7.3). Although the marker array used to represent the breast surface was more detailed than those presented in previous breast strain studies, the inter-marker separations were too large to negate the possibility of skin curvature between markers in the neutral position (L_0). Consequently, some inter-marker extension (ΔL) may have been caused by flattening of the skin surface (dotted line in Figure 7.3), and may have incorrectly been attributed to increased skin strain.

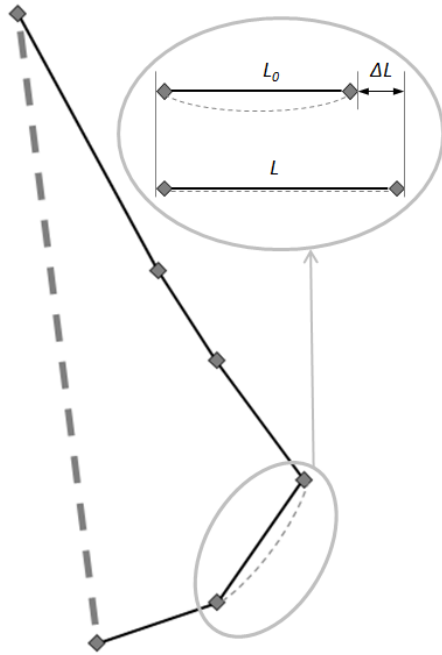


Figure 7.3: Example data demonstrating the potential for over-estimations of skin strain ($\Delta L/L_0$) arising from using the straight line approximation between breast markers.

Inspection of individual static strain arrays in Appendix L demonstrates that the smaller breasted participants tended to have less strain on the inner region of the breast mid-line (through the nipple) and more strain on the outer regions of the breast, a trend which was reversed in the larger breasted participants. This finding suggests that the larger breasts were pulled laterally to a greater extent than the smaller breasts during static standing. Increased static lateral breast movement of larger breasts from the neutral breast position may have been caused by a greater lateral gravitational force on the breast, differences in the natural shape of the breast skin, or possibly due to pre-existing breast skin damage in the large-breasted participants. An increased lateral breast position has previously been associated with breast ptosis (Brown *et al.*, 1999), and results from this study demonstrate that the strain failure limit for skin was exceeded by some participants in the static condition. Failure of the collagen fibres within the lateral regions of the breast may have resulted in a permanent extension of the skin in this region, causing the bulk of the breast to move laterally under gravity from its neutral position.

It was anticipated that the highest static strains would occur along the longitudinal lines of the breast due to increased skin elasticity in this direction (Gibson *et al.*, 1969), and because gravity was anticipated to act predominantly along the longitudinal breast direction in the static standing position. However, aside from the three largest breasted participants, the peak static strain for most participants occurred in the latitudinal direction, either at the nipple line in the lower regions of the breast. It was proposed that these high latitudinal strains were caused by an inferior shift of the breast bulk in the gravity loaded condition. Breast shape data presented in Appendix E illustrate that the participants' breast shapes became less hemispherical and more tear-drop shaped when moving from the neutral to the gravity-loaded static condition (as described previously in Figure 4.9). Latitudinal strain may have been caused by inferior movement of the breast bulk from the nipple line to the base of the breast, causing the skin near the breast-mid line to become extended to accommodate the altered breast shape.

Comparison of static strain data calculated using the marker array to data obtained using the previously published first order method using the suprasternal notch to nipple distance, demonstrated that the first order method underestimated static breast strain by up to 59% (Table 7.1). The use of only two markers to estimate breast strain does not account for the changes in breast shape and anisotropic skin response that have been shown to occur during gravitational breast loading, and is therefore not recommended for assessing breast strain in future research. Peak static strain values obtained using the marker array within this study ranged from 14% to 75% (Table 7.3). The magnitudes of these values demonstrate the importance of identifying the neutral breast position before calculating breast strain, particularly if assessing the risk of skin damage. Measuring skin strain from the gravity loaded position, as performed by Scurr in 2009, may lead to the omission of potentially damaging skin strain caused by static gravitational loading of the breast (Scurr, Bridgman, *et al.*, 2009).

7.3.2b. Peak regional breast skin strain during treadmill activity

Method

Dynamic skin strain was calculated instantaneously for three gait cycles at each speed using Equation 2.1, where L_0 was defined using the neutral marker separations and L was defined as the instantaneous marker separation over the gait cycle. For the regional strain analysis the breast surface was divided into eight regions as illustrated in Figure 7.4. These regions were based on the four mid-lines of the breast previously used in breast motion research (Zhou *et al.*, 2012b) and the four breast quadrants described in clinical breast research (Lemaine & Simmons, 2013). The peak strain value occurring at any time point within each gait cycle between any of the marker pairings within each breast region was calculated for each participant at each treadmill speed. The peak regional strains from the final 3 gait cycles were meaned to provide a mean peak breast strain for each participant at each treadmill speed within each breast region. These peak regional strain values provided an indication of which breast regions experience the greatest breast strain for each participant across eleven different treadmill speeds. The risk of breast skin damage caused dynamic breast strain was evaluated by comparing the peak dynamic skin strain values for each participant to the skin strain limits reported by Silver (2001) (30% represents skin resistance and 60% represents the onset of skin failure).

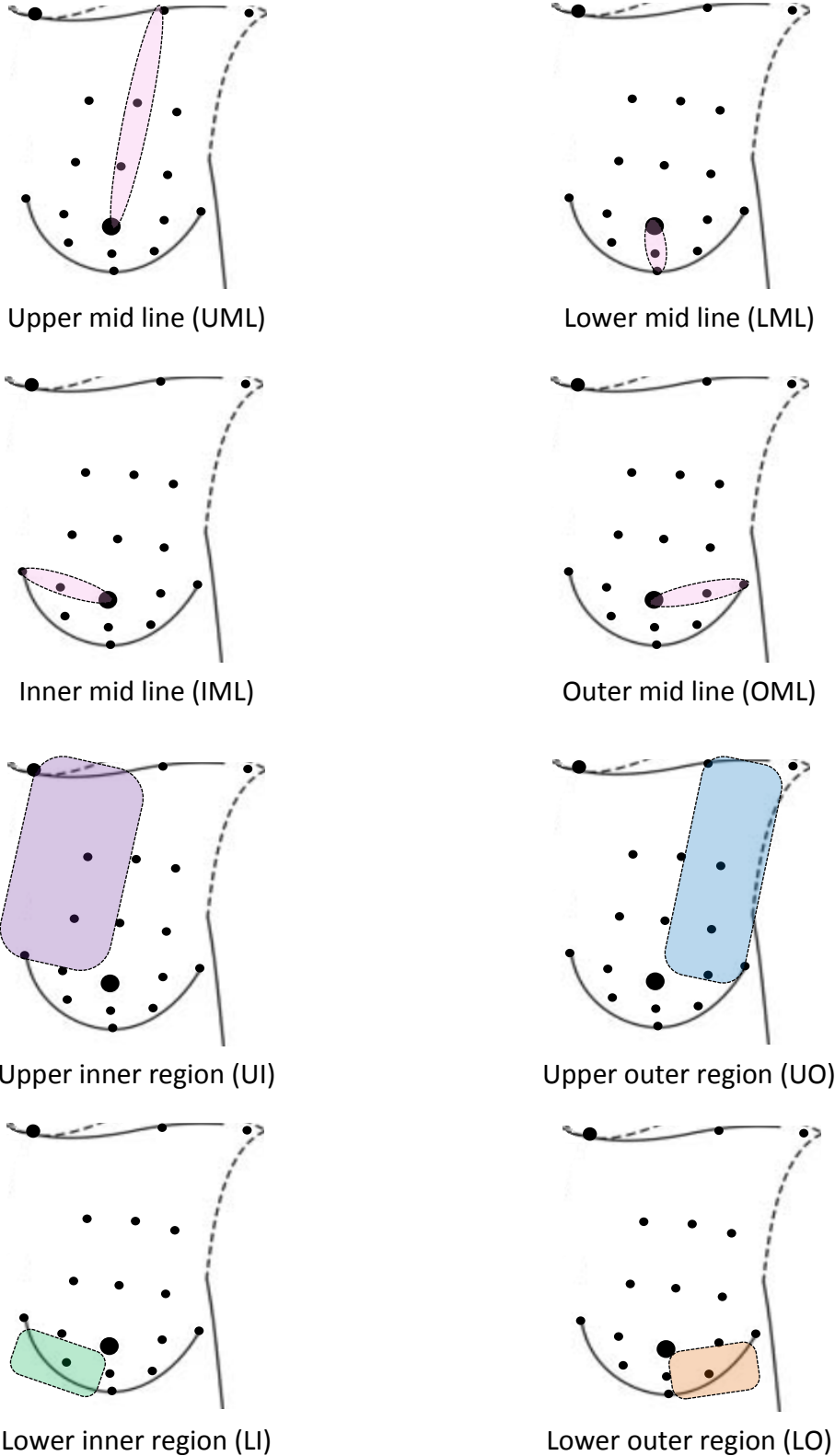


Figure 7.4: Breast regions defined for strain analysis: mid-lines (pink); upper inner (purple); upper outer (blue); lower inner (green); and lower outer (orange).

Results

Figure 7.5 to Figure 7.12 illustrate the peak breast skin strain in each breast region across the static and dynamic conditions for each participant. The neutral position (green), skin resistance (orange), and skin failure (red) strain limits are shown as dashed lines to illustrate the potential for breast skin damage in each condition.

Upper mid-line

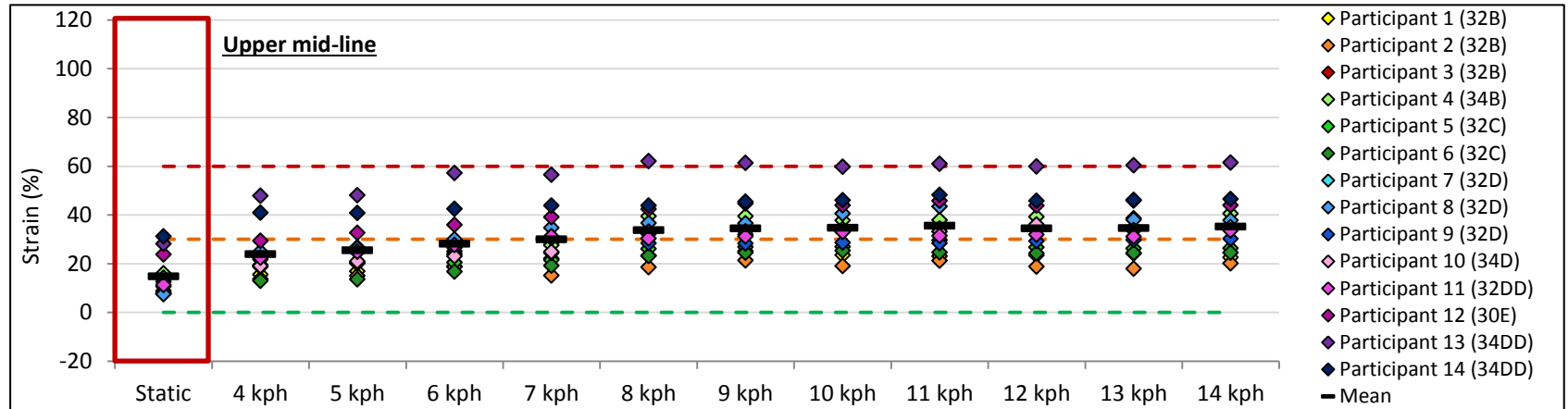
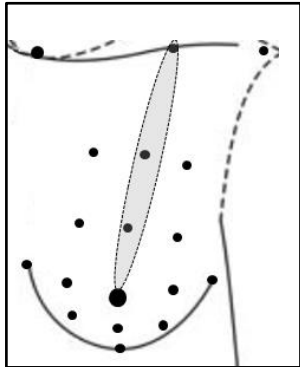


Figure 7.5: Mean peak skin strain values along the upper mid-line of the breast during static standing and incremental-speed treadmill activity.

Lower mid-line

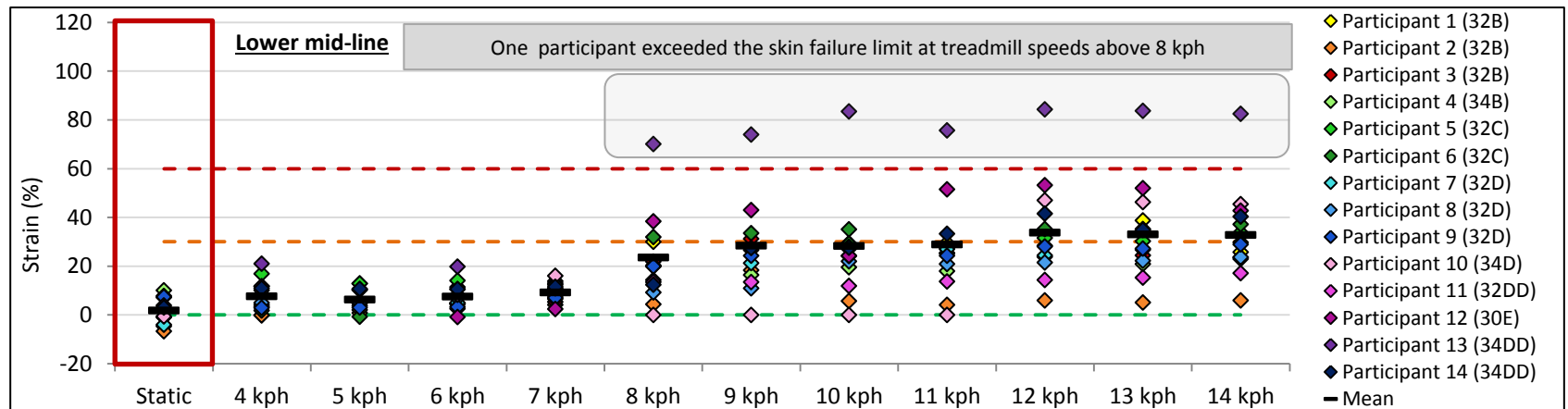
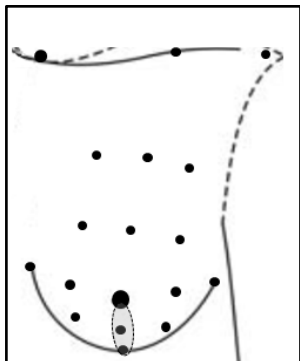


Figure 7.6: Mean peak skin strain values along the lower mid-line of the breast during static standing and incremental-speed treadmill activity.

Inner mid-line

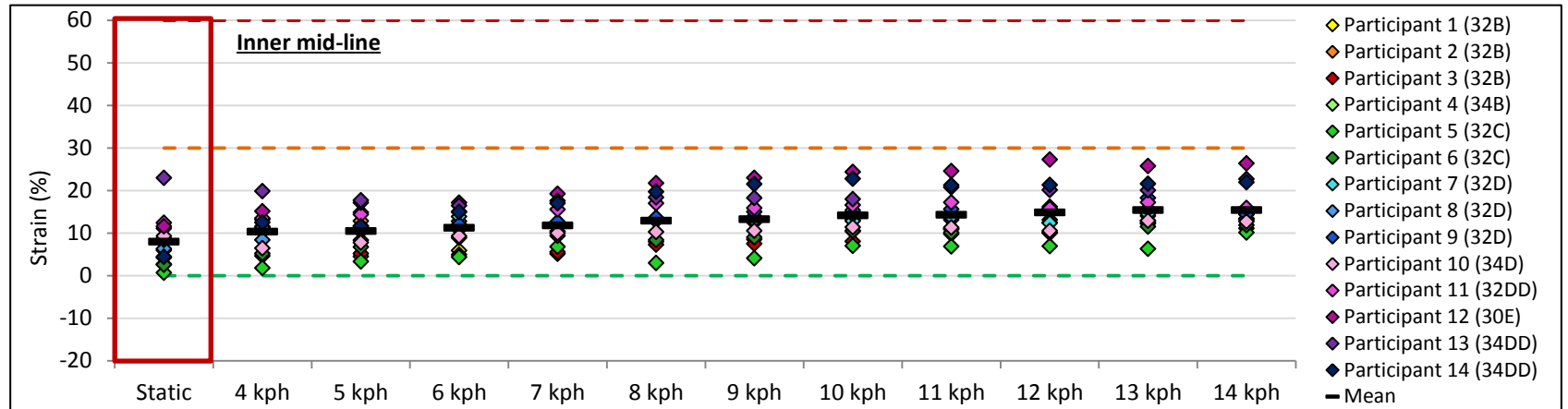
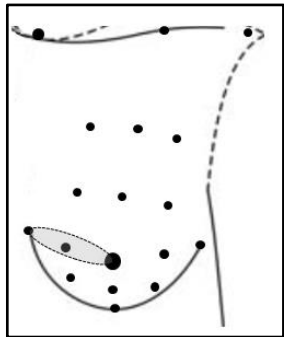


Figure 7.7: Mean peak skin strain values along the inner mid-line of the breast during static standing and incremental-speed treadmill activity.

Outer mid-line

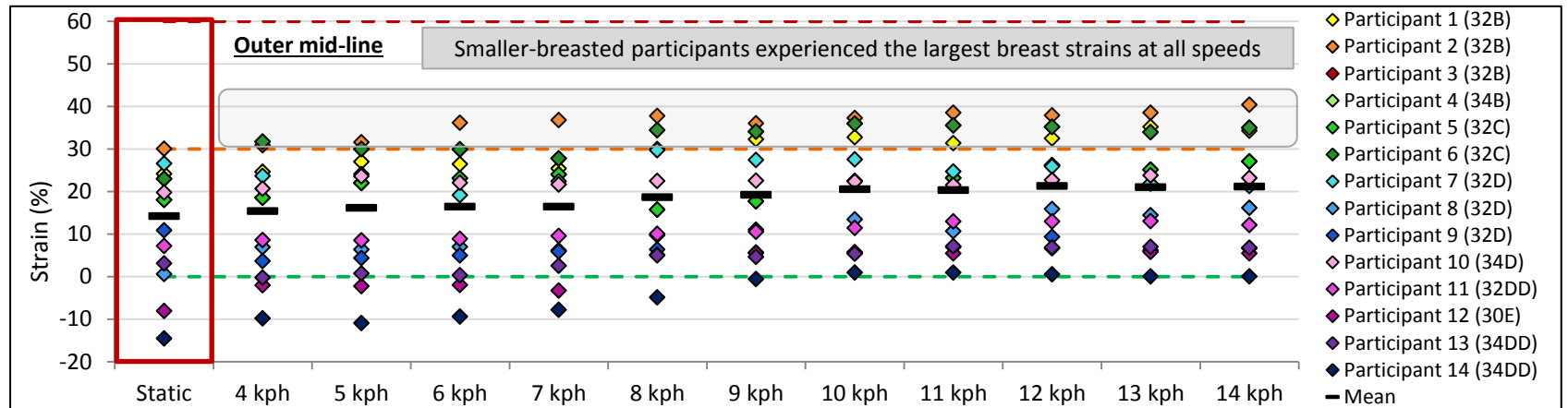
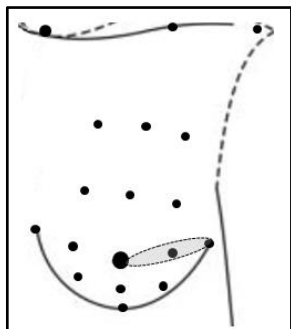


Figure 7.8: Mean peak skin strain values along the outer mid-line of the breast during static standing and incremental-speed treadmill activity.

Upper inner breast

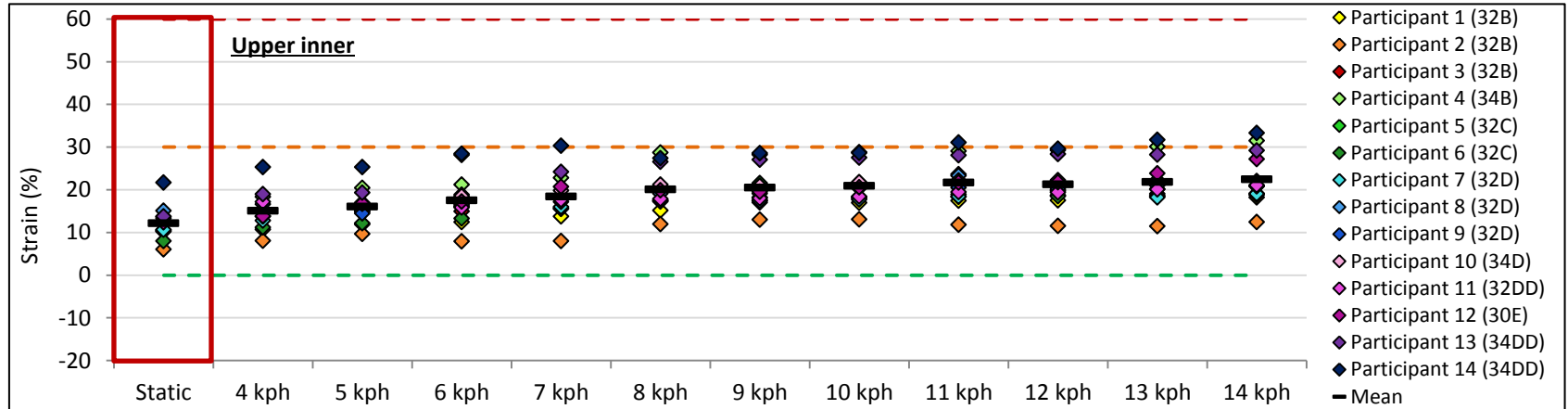
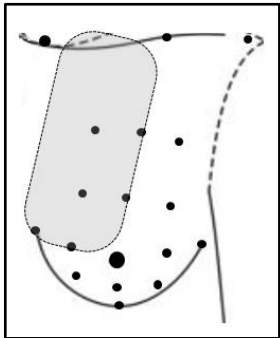


Figure 7.9: Mean peak skin strain values in the upper inner region of the breast during static standing and incremental-speed treadmill activity.

Upper outer breast

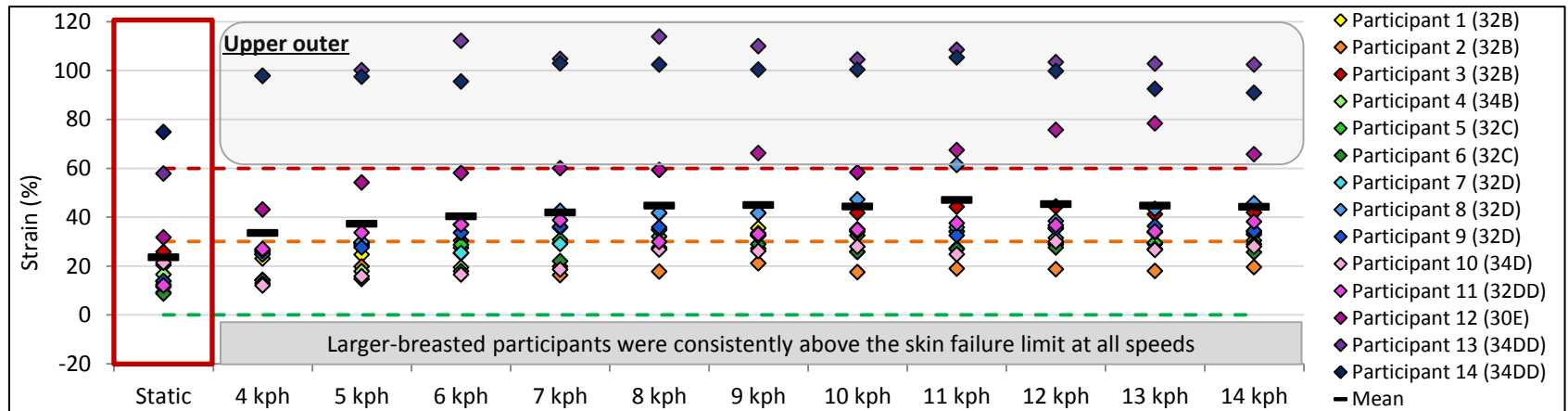
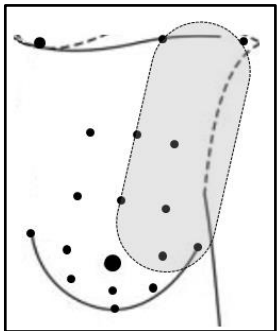


Figure 7.10: Mean peak skin strain values in the upper outer region of the breast during static standing and incremental-speed treadmill activity.

Lower inner breast

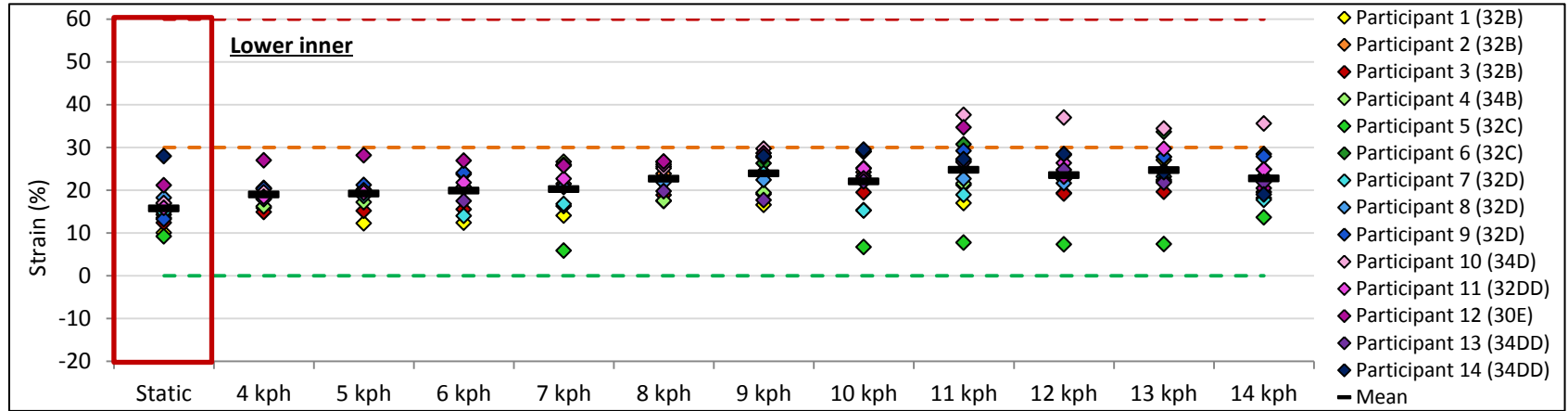
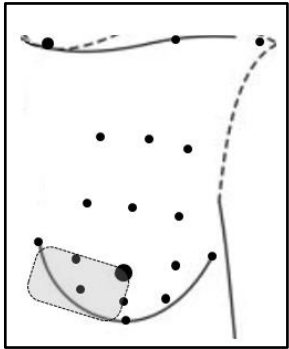


Figure 7.11: Mean peak skin strain values in the lower inner region of the breast during static standing and incremental-speed treadmill activity.

Lower outer breast

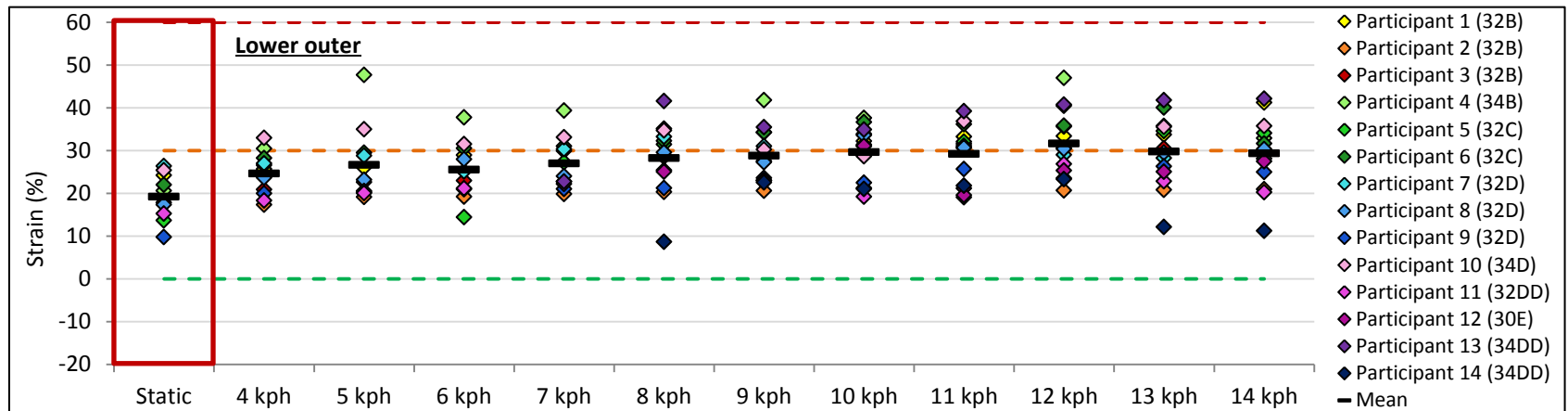
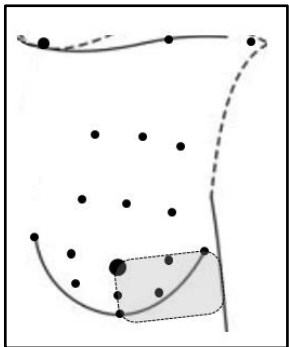


Figure 7.12: Mean peak skin strain values in the lower outer region of the breast during static standing and incremental-speed treadmill activity.

Discussion

This study represents the first attempt to quantify static and dynamic strain on the breast skin using a marker array. As observed in the static condition, dynamic breast strain was greatest in the upper outer breast region, with one participant experiencing strain up to 114% (Figure 7.10). The skin failure limit was exceeded by up to four participants in the upper-outer breast region at all treadmill speeds (Figure 7.10), and by one participant in the lower mid-line of the breast while running at speeds above 8 kph (Figure 7.6). The finding that some participants experienced potentially damaging skin strains during bare-breasted activity leads to the recommendation that women should not exercise on a treadmill without wearing breast support. This recommendation may have ethical implications for breast motion research that uses bare-breasted activity trials as the standard against which to evaluate bra performance (Zhou *et al.*, 2009)

For most breast regions there was a gradual increase in mean peak breast skin strain as treadmill speed increased, although the lower mid-line of the breast did demonstrate a clear transition from walking to running at 8 kph (Figure 7.6). It was proposed that increased superior-inferior torso displacement during running elicited a bouncing breast motion as opposed to the swinging motion that was present during walking. Breast bounce may have caused high levels of strain in the lower breast region when the breast moved superiorly relative to the torso.

7.3.2c. Peak segmental breast skin strain during treadmill activity

Method

For this analysis, the breast surface was divided into 35 segments as illustrated in Figure 7.13. The peak skin strain value occurring in each breast segment in the static condition and at any point within each gait cycle at three selected treadmill speeds (5 kph, 8 kph, and 14 kph) was calculated for each participant. The mean peak strain was calculated in the dynamic conditions by meaning the peak strain values within each breast segment over the last 3 gait cycles at each selected treadmill speed. These treadmill speeds were selected to illustrate the changes in breast skin strain that occurred between walking, slower running, and faster running (Keller *et al.*, 1996; Miller & Stamford, 1987). Calculation of peak segmental strain values enabled the identification of specific segments of the breast skin that were prone to high strain values for each participant during static standing and selected dynamic treadmill activities. The risk of breast skin damage caused by dynamic breast strain was evaluated by comparing the peak dynamic skin strain values for each participant to the skin strain limits reported by Silver (2001) (30% represents skin resistance and 60% represents the onset of skin failure).

UML (pink) = Upper mid-line	LML (pink) = Lower mid-line
IML (pink) = Inner mid-line	OML (pink) = Outer mid-line
UI (purple) = Upper-inner region	UO (blue) = Upper-outer region
LI (green) = Lower-inner region	LO (orange) = Lower-outer region
H = Horizontal (latitudinal)	V = Vertical (longitudinal)

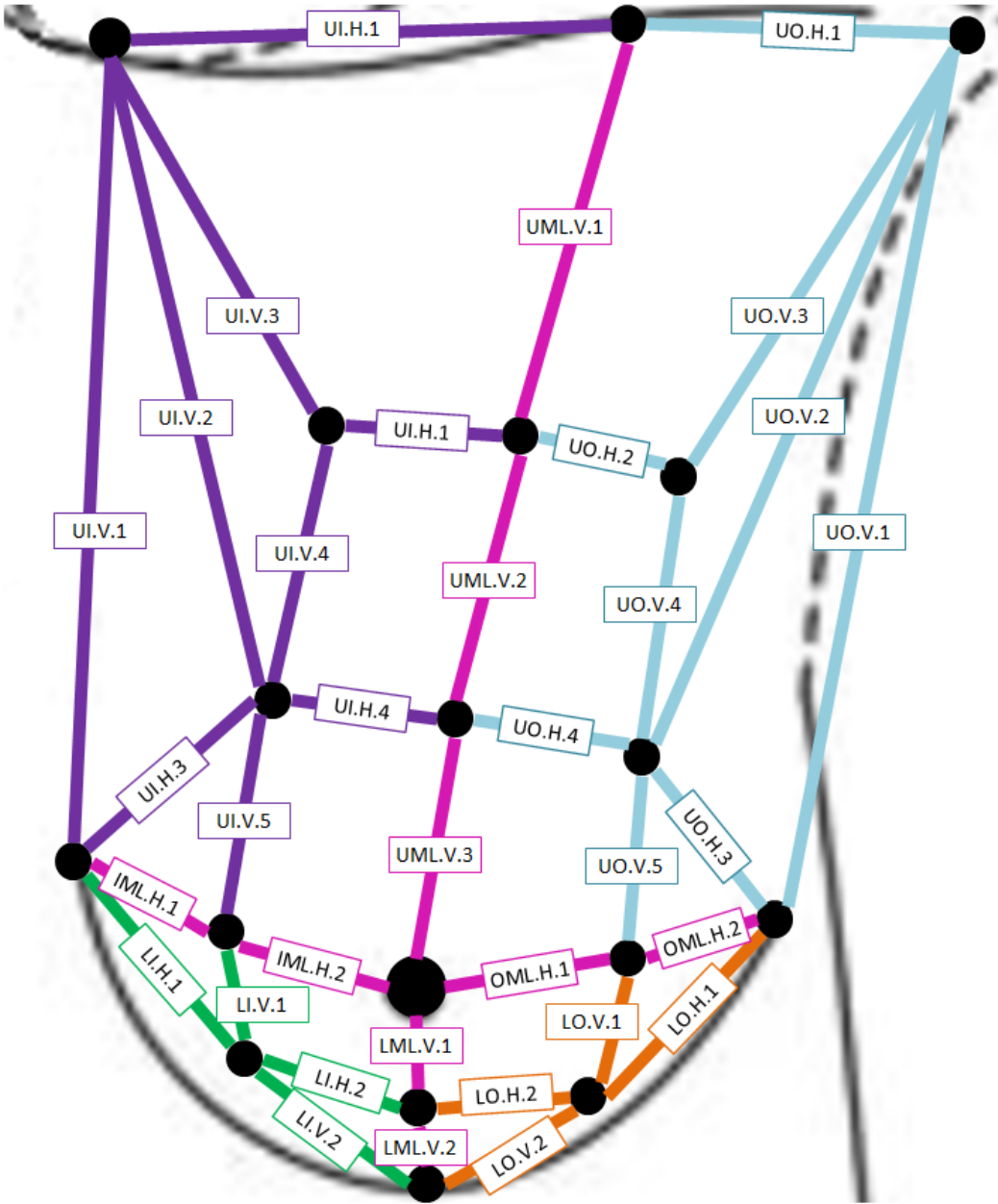


Figure 7.13: Breast skin segments defined within each breast region for strain analysis.

Results

Segmental analysis of breast skin strain demonstrated that within each breast region some parts of the breast skin were compressed (negative strain values) while others were strained (positive strain values). This was particularly evident in the static condition (Figure 7.14). The highest strain values were consistently seen in the UO.V.4 segment in the upper-outer region of the breast (Figure 7.14 to Figure 7.17). Potentially damaging strains above 60% were only observed in the OU.V.4 and LML.V.2 segments of the breast, and only for the three largest-breasted participants. Interestingly, the magnitude of breast strain in certain breast segments, such as UI.V.2, UI.V.3 and IML.H.2, was similar across all breast sizes and activity levels. However, other breast segments such as UO.H.3 and OML.H.2 demonstrated varied strain responses across participants, with the smallest-breasted participants experiencing the largest strains and the largest-breasted participants experiencing the smallest, sometimes negative, strains.

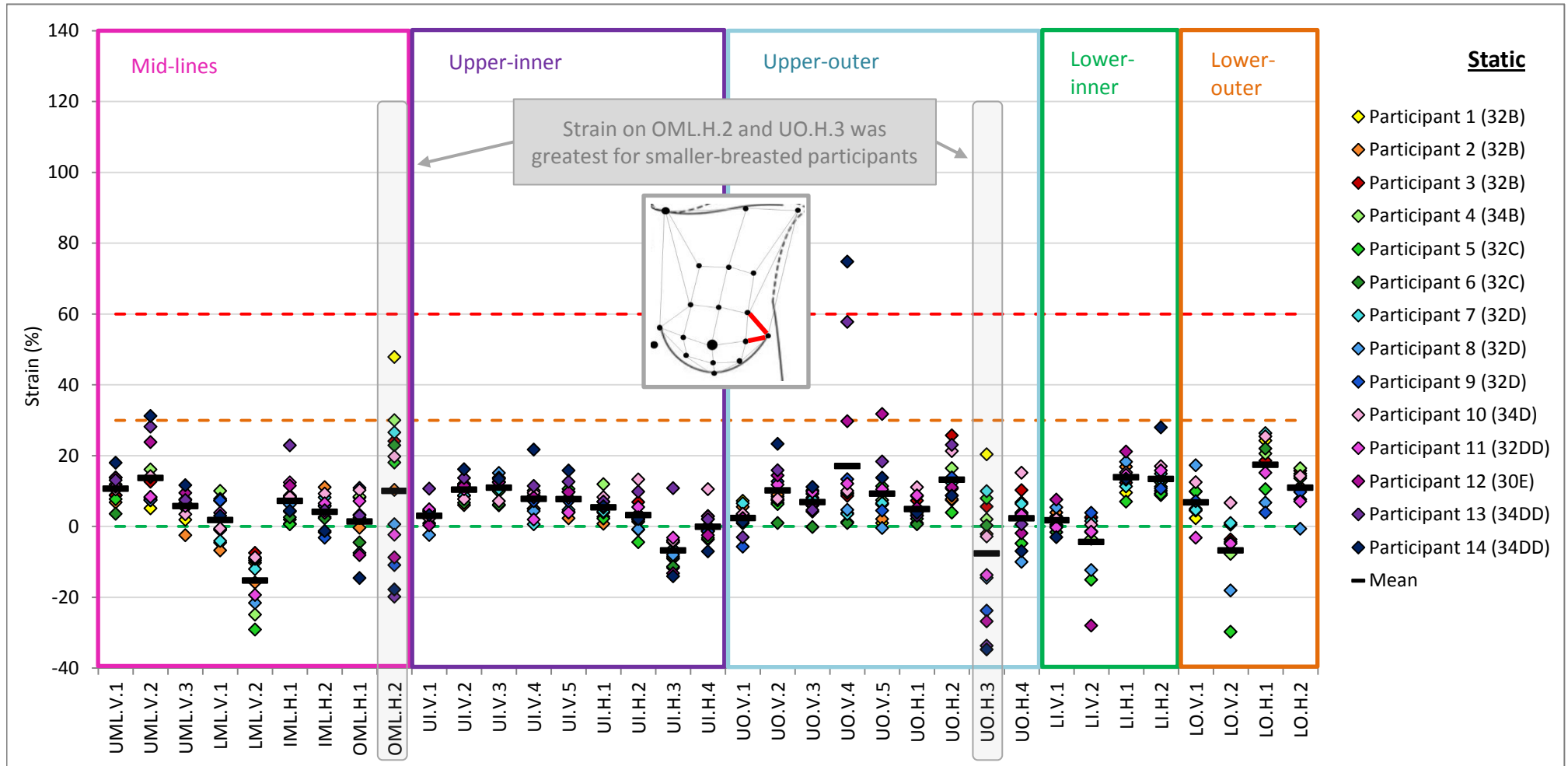


Figure 7.14: Peak skin strain in each breast segment while standing stationary in the laboratory.

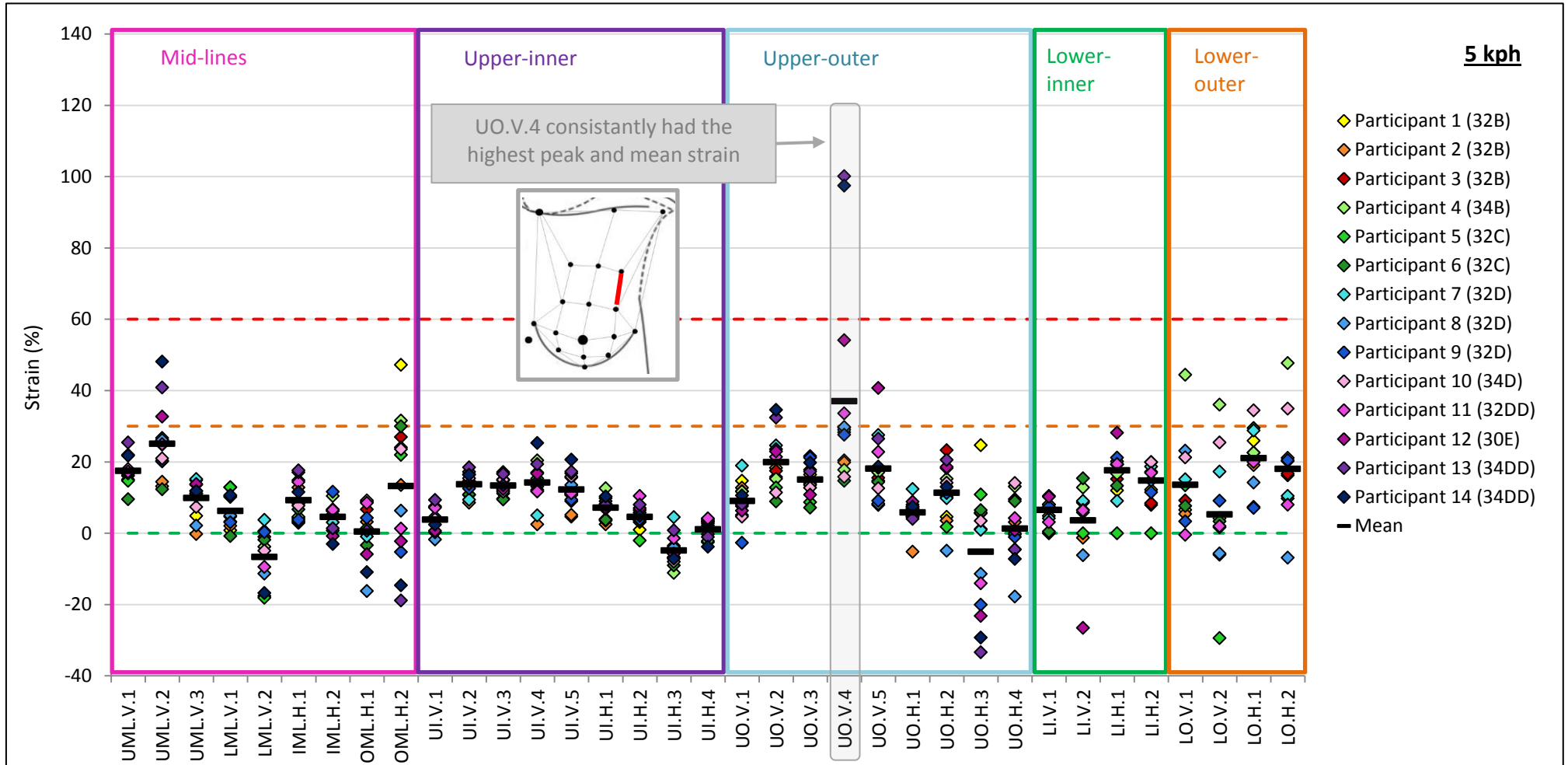


Figure 7.15: Peak skin strain in each breast segment while walking at 5 kph on the treadmill.

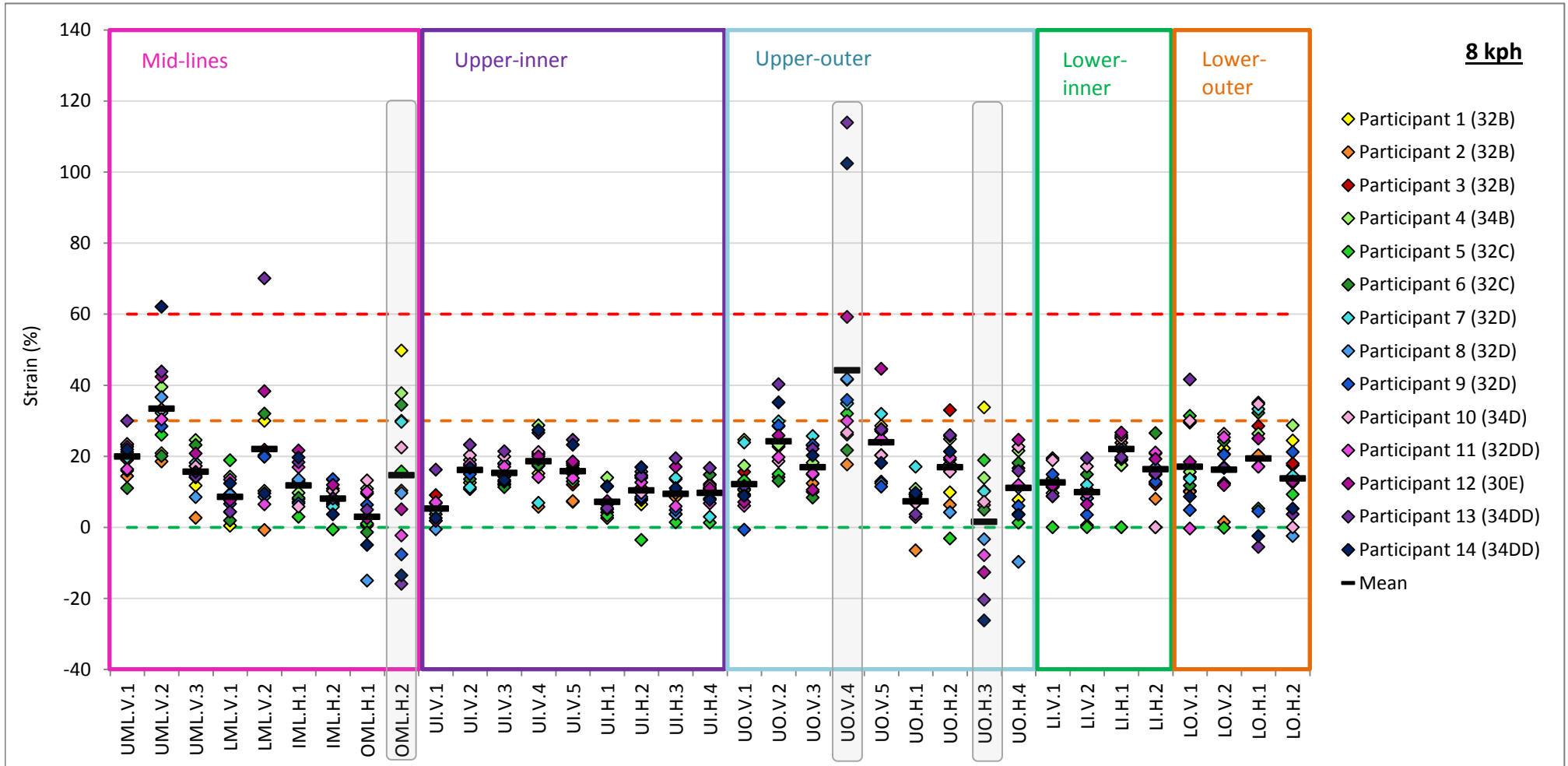


Figure 7.16: Peak skin strain in each breast segment while running at 8 kph on the treadmill.

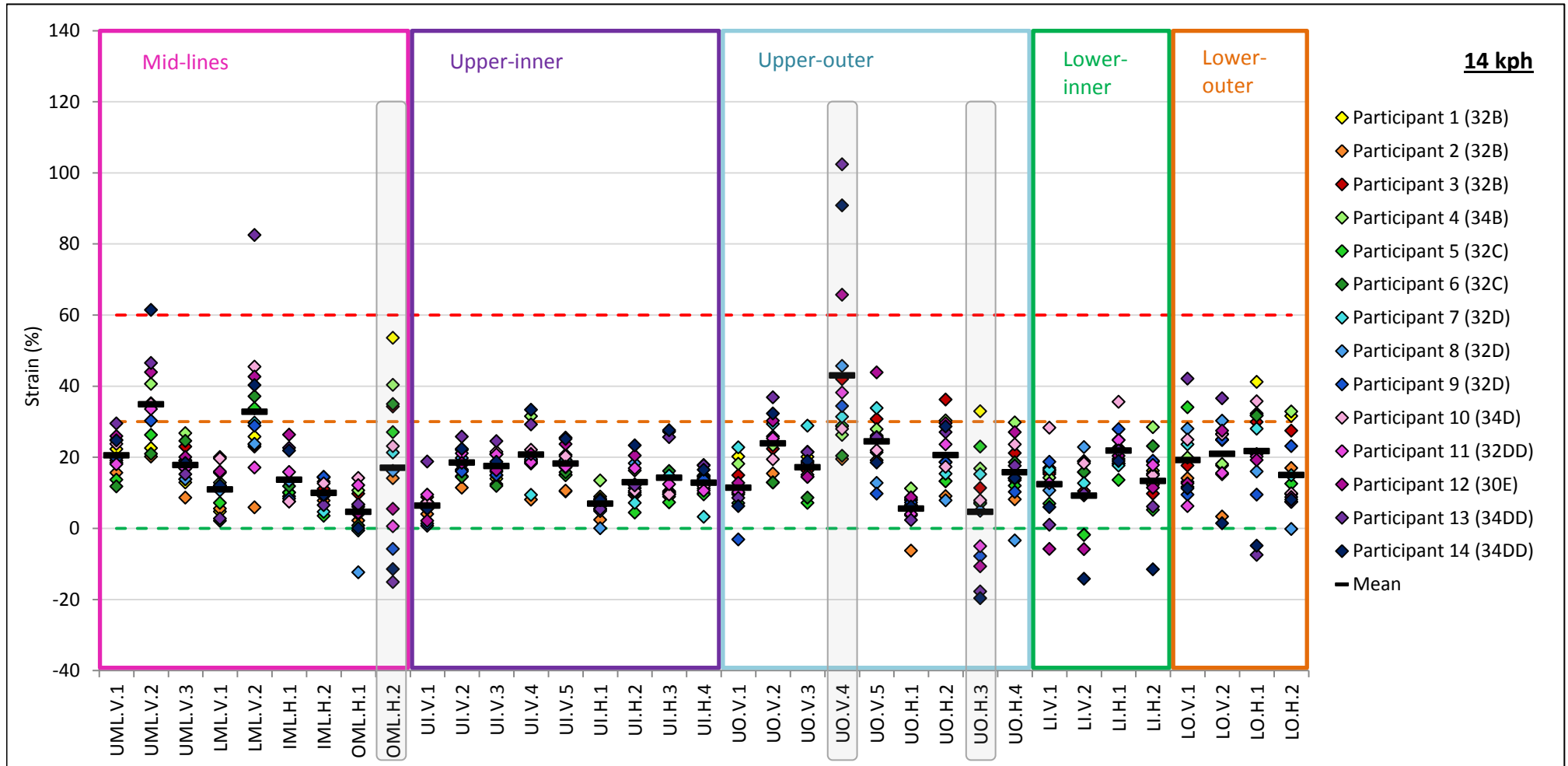


Figure 7.17: Peak skin strain in each breast segment while running at 14 kph on the treadmill.

Discussion

The results from the segmental breast skin strain analysis demonstrate that peak dynamic breast strain consistently occurred in the UO.V.4 segment of the breast. High strain values within this segment suggest that it is the longitudinal breast skin located in the middle of the upper-outer breast region that is most susceptible to damage during treadmill activity. Excessive strain leading to permanent extension of the UO.V.4 skin segment may compromise the natural support provided by the skin in this area of the breast which may subsequently contribute to the inferior and lateral movement of the breast that has been reported to occur with ptosis (Brown *et al.*, 1999). The UO.V.4 breast segment therefore represents a key focus area for the development of breast support garments as garments that can reduce strain in this breast segment may be able to better protect the breast from motion-induced breast pain or breast damage.

Although peak segmental breast strain values were typically observed in the larger-breasted participants, interestingly for segments OML.H.2 and UO.H.3 strain values became increasingly large with decreasing breast size in all conditions (Figure 7.14 to Figure 7.17). Increased breast bulk beneath the mid-line of the breast may have led to the increased strain in segments OML.H.2 and UO.H.3 for the smaller-breasted participants compared to the larger-breasted participants where the breast bulk typically sits at the base of the breast. These findings demonstrate that although large-breasted women were found to experience the largest peak skin strains during treadmill activity (up to 114%), smaller-breasted women may also be susceptible to high skin strains (up to 54%) along the outer mid-line of the breast during running.

Scurr's (2009) findings that smaller-breasted participants experienced more breast strain than their larger-breasted counterparts during running was previously attributed to neglect of the pre-existing breast strain caused by gravity. However, results of this study demonstrate that the location in which breast strain is measured may influence the relationship between breast size and breast strain. It is therefore important to evaluate strain over the entire surface of the breast to ensure that appropriate conclusions are drawn from breast strain data.

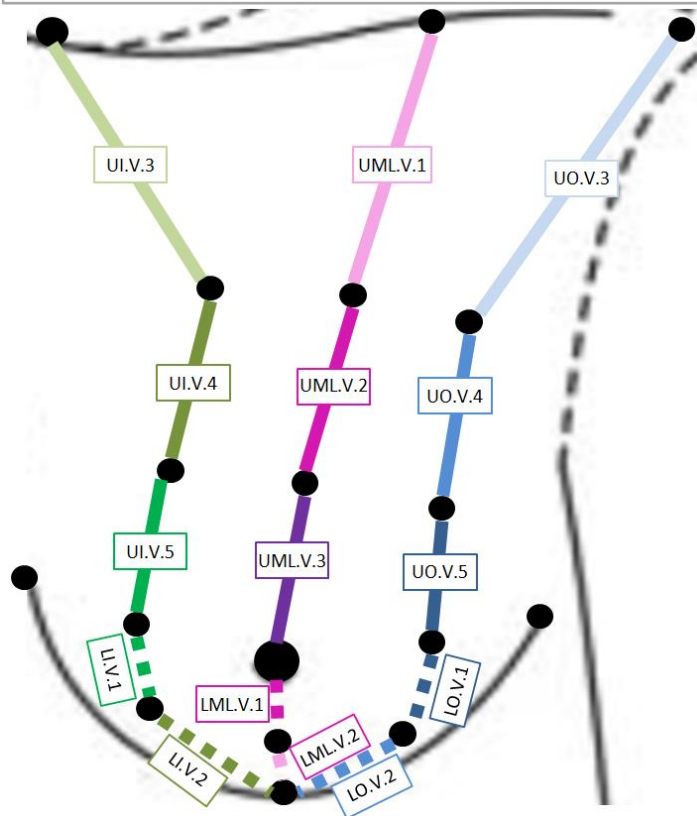
Based on previous research reporting that human torso skin would extend further in the superior-inferior direction than in the medial lateral direction before failure (Daly, 1982; Gibson *et al.*, 1969), it was anticipated that higher skin strain values would be observed along the longitudinal breast lines than along the latitudinal breast lines. Although higher strains were observed in the longitudinal direction on the upper regions of the breast, strains on the lower breast regions were similar in both directions. This suggests that loading of the upper breast during treadmill activity resulted in a predominantly longitudinal extension of the breast skin whereas loading of the lower breast led to extension of the breast skin in both directions. Considering that the skin may be more susceptible to damage when loaded in the latitudinal direction it may be beneficial to reduce this component of skin extension when aiming to reduce the negative effects of breast strain.

7.3.2d. Instantaneous segmental breast skin strain over one gait cycle at 14 kph – A case study

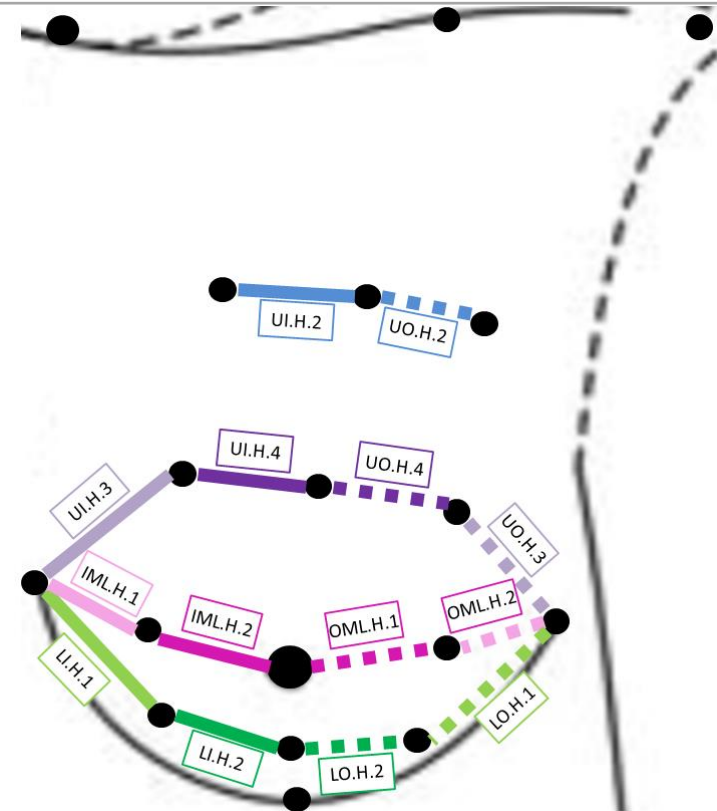
Method

Instantaneous segmental breast skin strain was investigated for one participant (size 32DD) over one gait cycle of treadmill running at 14 kph. For this case study the breast was divided into longitudinal and latitudinal breast lines representing superior-inferior and medial-lateral marker pairings respectively (Figure 7.18). Analysis of these frame-by-frame strain data enabled the interaction between different breast segments to be evaluated in detail for one participant during the running gait cycle. Within this analysis the gait cycle was divided into five stages. Left and right heel strike was identified using the anterior-posterior velocity of the left and right heel markers as described previously. The right and left stance phases and the two flight phases were identified qualitatively from the motion analysis data. A comparison between the measured skin strain values in the longitudinal and latitudinal directions provided an indication of the effect of natural skin tension (Langer lines) on the directional strain response of the breast skin.

UML = Upper mid-line	IML = Inner mid-line	UI = Upper-inner region	LI = Lower-inner region	H = Horizontal (latitudinal)
LML = Lower mid-line	OML = Outer mid-line	UO = Upper-outer region	LO = Lower-outer region	V = Vertical (longitudinal)



(a) Longitudinal (superior-inferior) breast lines



(b) Latitudinal (medial-lateral) breast lines

Figure 7.18: Longitudinal (a) and latitudinal (b) breast lines defined for case study strain analysis.

Results

Frame by frame analysis of the breast skin strain data for Participant 11 (32DD) demonstrates that the upper longitudinal lines of the left breast experience their minimum strains upon left and right heel strike, with peak longitudinal strains occurring during the stance phases of the gait (Figure 7.19). The lower sections of the breast (excluding LO.V.1) demonstrate contrary behaviour; with peak strains occurring at right and left heel strike and minimum strains occurring during stance. The strain experienced by the inner lower longitudinal line of the breast (LI.V.1) mirrors the strain experienced by the outer lower breast (LO.V.1), demonstrating a lateral shift in the breast during the gait cycle (Figure 7.19).

The latitudinal breast lines shown in Figure 7.20 suggest a symmetrical skin strain distribution across the breast; with the inner and outer aspects of each breast line behaving similarly during the gait cycle. Interestingly, the lower latitudinal breast lines behave similarly to the upper longitudinal breast lines during the gait cycle and the upper latitudinal breast lines have a similar strain pattern to the lower longitudinal lines. This behaviour suggests a complex skin 2D deformation was required to accommodate the motion of this participant's breast against their torso during running. A comparison between the latitudinal (Figure 7.20) and longitudinal (Figure 7.19) strains about each breast marker demonstrates that as strain increased in one direction it decreased in the perpendicular direction, indicating the incompressible nature of the breast skin.

Longitudinal breast lines

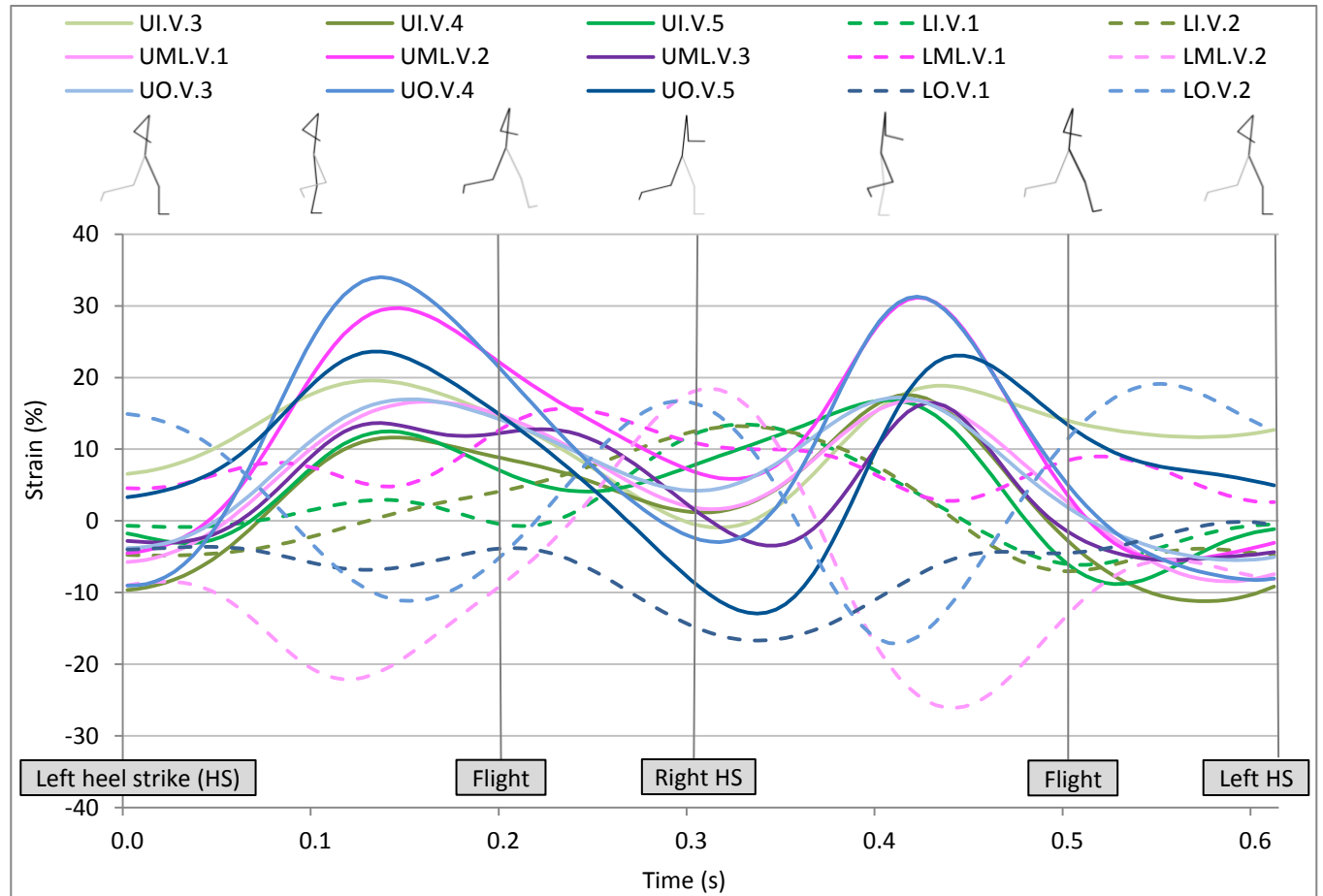
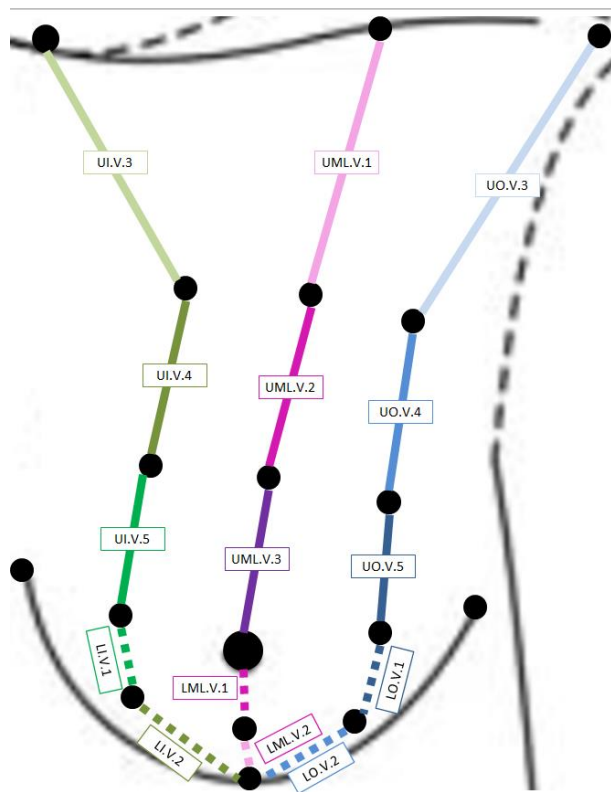


Figure 7.19: Longitudinal skin strain across the breast of Participant 11 (32DD) for one gait cycle during treadmill running at 14 kph.

Latitudinal breast lines

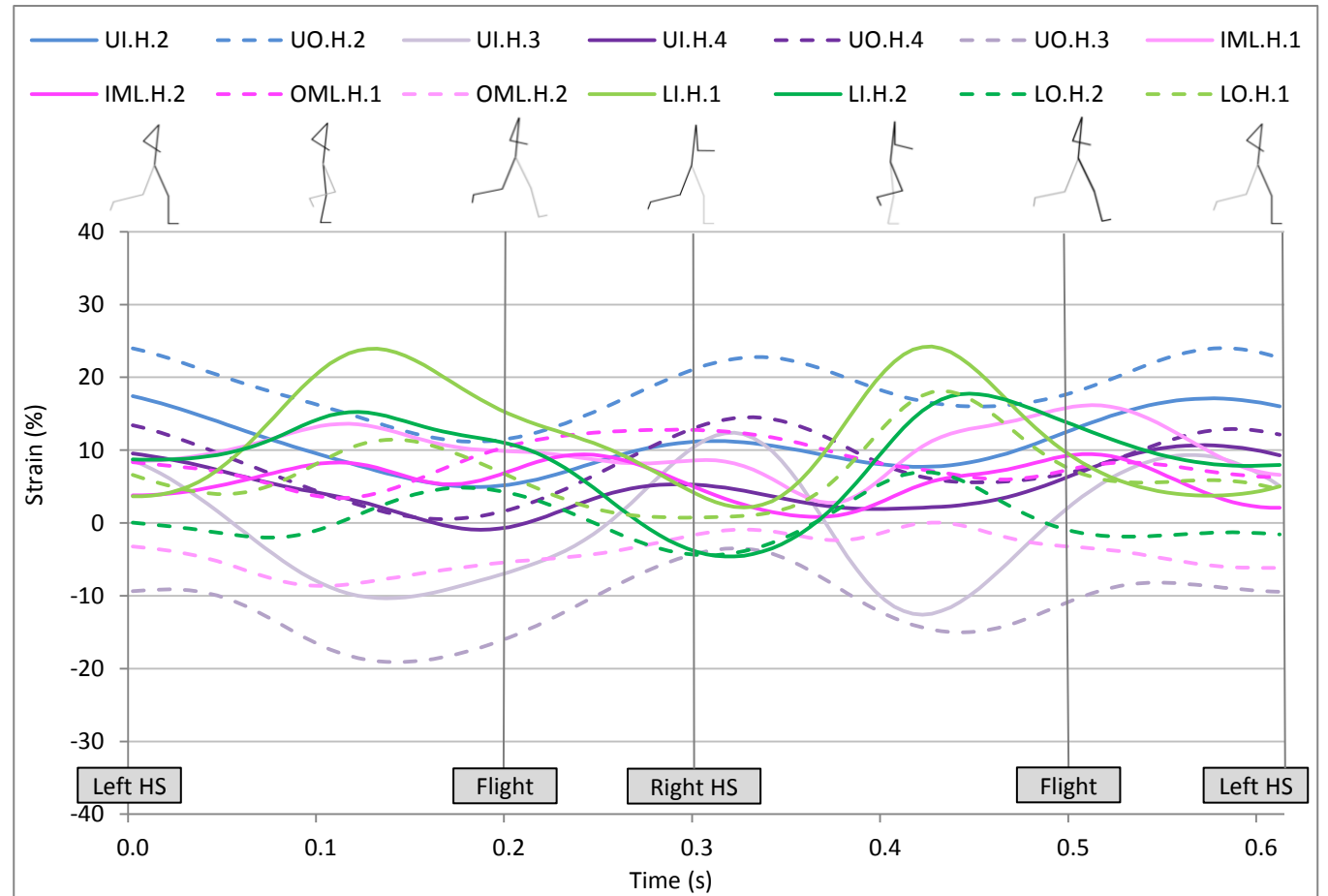
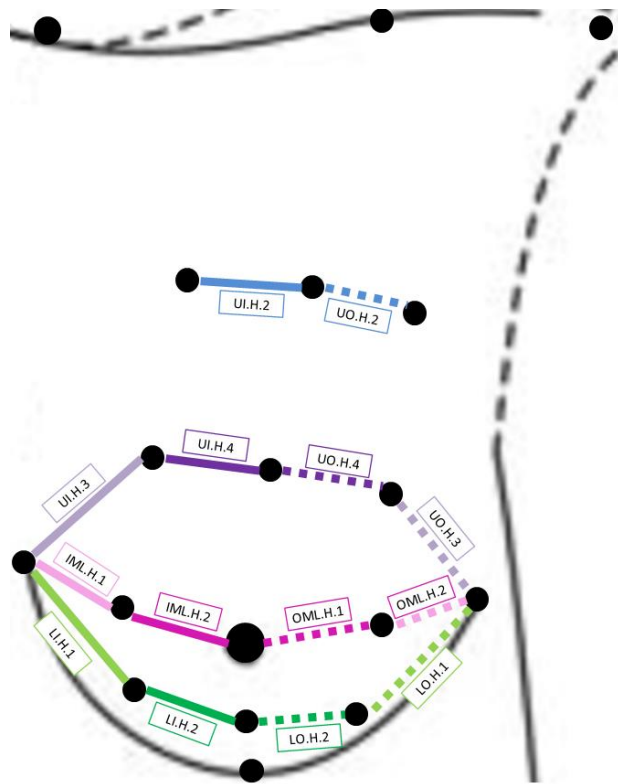


Figure 7.20: Latitudinal skin strain across the breast of Participant 11 (32DD) for one gait cycle during treadmill running at 14 kph.

Discussion

The results from this case study showed that each segment of the breast skin experienced a series of peak skin strain values during one gait cycle of running at 14 kph. The greatest dynamic skin strains occurred in the upper mid-line (UML.V.2 segment) and upper-outer region (UO.V.4 segment) of the breast, indicating that these areas may be particularly prone to damaging strains during bare-breasted treadmill activity. Peak strain locations across the breast surface are illustrated in Figure 7.21 to demonstrate the interaction of the different breast sections during running. Peak strain occurred around the edges of the breast during the stance phases of the gait cycle, whereas peak strain around the nipple occurred during flight and at heel strike. It was suggested that the transfer of strain from the (posterior) edges of the breast to the (anterior) nipple during flight was caused by the anterior propulsion of the breast bulk within the breast during the transition from stance to flight. It was also observed that although some instantaneous strain data demonstrate a double oscillation of the breast over the gait cycle (Figure 7.19 and Figure 7.20), not all breast segments experienced equal strain magnitudes during both breast oscillations, and some breast segments showed only a single strain peak during the gait cycle.

The frame-by-frame presentation of skin strain data within this case study demonstrated the interaction of the different skin segments over the breast during the gait cycle. Previous research has reported that the nipple undergoes a figure-of-eight motion during treadmill running (Scurr, White, *et al.*, 2009). A similar motion was observed in this study, with the bulk of the (left) breast tissue moving medially following left foot stance (Figure 7.21 b to c) and laterally following right foot stance (Figure 7.21 e to f). Peak longitudinal strains occurred during the stance phases of the gait as the breast bulk fell to the base of the breast (also causing latitudinal strain in the lower regions of the breast). Following the stance phase, the breast bulk proceeded to move superiorly on the torso causing the breast base to become longitudinally strained and the upper breast to experience peak latitudinal strains. The peak change in strain over the gait cycle for Participant 11 occurred in the UO.V.4 segment between left foot stance and right heel strike (Figure 7.19). During this transition a 37% change in strain occurred in 0.18 s, illustrating the

rapid strain response of the breast skin during bare-breasted running. The observed strain rate (206% per second) was higher than those typically used to obtain strain failure limits for human skin (Gallagher *et al.*, 2012). Although strain rate does not affect the strain failure limit of skin, it can influence other mechanical factors such as ultimate tensile strength (Otténio *et al.*, 2014). Strain rate may therefore be an important consideration for the future use of breast strain data within biomechanical research or for the development of FE breast models.

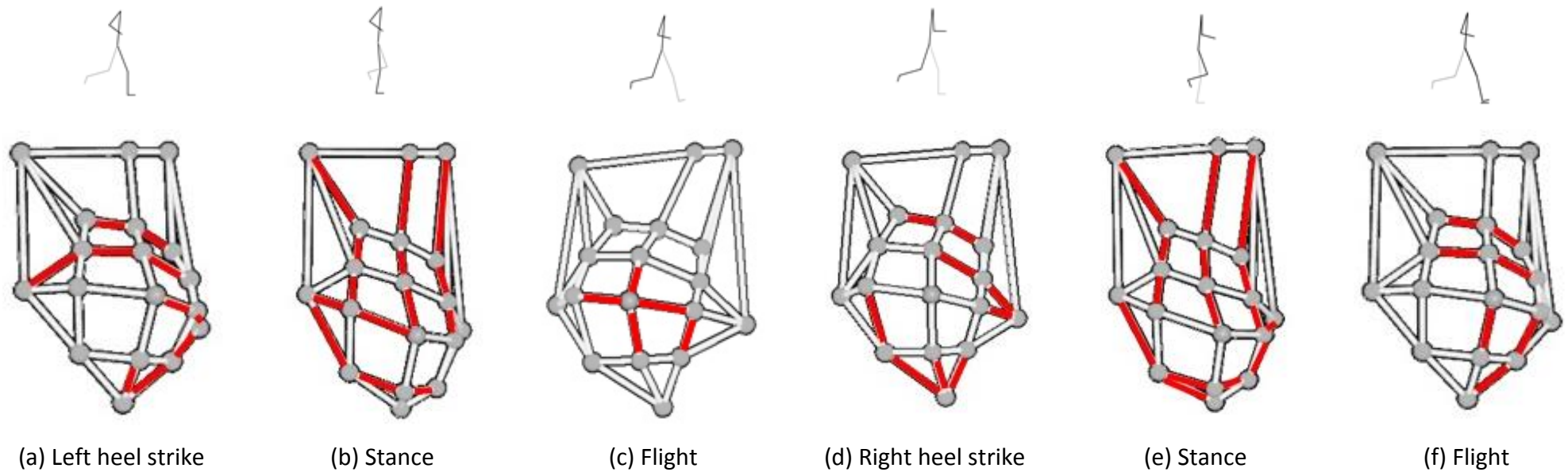


Figure 7.21: Diagrammatic representation of the points during the gait cycle (at 14 kph) for one participant (size 32DD) at which each breast skin segment experienced peak strain (red).

7.3.2e. Peak breast skin strain and breast pain

Method

The relationship between breast skin strain and perceived breast pain was investigated statistically. A Spearman's rho correlation was performed between the mean peak dynamic strain over three gait cycles (occurring anywhere over the breast surface) and the reported breast pain at each treadmill speed using SPSS (IBM SPSS statistics version 22). Correlation coefficients of ± 0.1 , ± 0.3 , and ± 0.5 indicated small, moderate and large effect sizes (Field, 2009). Mean peak strain values were used in the statistical correlation because participants rated their overall breast pain at each treadmill speed, and in the static condition, and did not distinguish between pain that occurred in different regions or segments of the breast.

Results

Table 7.2: Breast pain scores in the static standing condition and at each speed of the incremental-speed treadmill test.

Participant number	Breast size	Breast pain scores (out of 10)											
		Static	4 kph	5 kph	6 kph	7 kph	8 kph	9 kph	10 kph	11 kph	12 kph	13 kph	14 kph
Participant 1	32B	0	2	4	4	5	6	7	7	8	8	9	9
Participant 2	32B	0	0	0	0	1	2	3	3	4	4	4	5
Participant 3	32B	0	0	1	1	5	6	6	7	7	7	8	8
Participant 4	34B	0	0	0	0	0	0	2	3	3	4	4	4
Participant 5	32C	0	0	0	0	0	1	1	1	1	1	1	1
Participant 6	32C	0	0	0	0	1	5	5	6	6	5	5	4
Participant 7	32D	0	0	0	0	0	1	1	1	1	2	2	2
Participant 8	32D	1	1	1	2	3	3	4	5	6	7	9	10
Participant 9	32D	0	0	0	0	1	4	6	7	8	7	7	7
Participant 10	34D	0	0	0	0	3	5	5	5	6	5	4	4
Participant 11	32DD	0	1	1	2	3	5	6	6	7	7	8	8
Participant 12	30E	0	0	1	2	3	5	6	6	7	7	7	7
Participant 13	34DD	0	0	0	1	1	3	3	4	5	5	6	7
Participant 14	34DD	0	0	0	0	0	1	2	3	5	5	6	6
Mode		0	0	0	0	1	5	6	7	7	7	4	4

Table 7.3: Mean peak breast skin strain (occurring in any breast segment over three gait cycles) at each speed of the incremental-speed treadmill test.

Participant number	Breast size	Mean peak breast strain (in any breast segment) (%)											
		Static	4 kph	5 kph	6 kph	7 kph	8 kph	9 kph	10 kph	11 kph	12 kph	13 kph	14 kph
Participant 1	32B	48	47	47	50	45	50	50	54	53	52	55	54
Participant 2	32B	18	20	20	25	21	24	24	24	25	24	25	25
Participant 3	32B	26	25	30	30	36	42	42	42	44	44	41	42
Participant 4	34B	30	31	48	38	39	40	42	38	39	47	39	41
Participant 5	32C	18	27	28	29	31	32	33	34	34	36	35	34
Participant 6	32C	23	32	30	30	31	34	34	37	36	36	40	37
Participant 7	32D	27	27	29	27	30	35	32	34	36	34	34	35
Participant 8	32D	18	25	30	37	42	42	42	47	61	38	43	46
Participant 9	32D	14	26	28	34	36	36	32	34	33	35	36	34
Participant 10	34D	25	33	35	32	33	35	33	34	38	47	46	45
Participant 11	32DD	16	27	34	37	39	30	33	35	38	37	34	38
Participant 12	30E	32	43	54	58	60	59	66	58	67	76	78	66
Participant 13	34DD	58	98	100	112	105	114	110	105	109	103	103	102
Participant 14	34DD	75	98	97	95	103	102	100	100	105	100	92	91
Mean		30	40	44	45	47	48	48	48	51	51	50	49

Interestingly, it was observed that many participants reported no breast pain (Table 7.2) while standing statically despite experiencing high levels of static breast strain (up to 75%) (Table 7.3). It was suggested that continual gravitational loading of the breast skin may have caused the participants' pain responses to adapt such that static standing did not cause breast pain, as previously proposed in Chapter 6. Consequently, motion-induced breast pain may be more strongly correlated to the peak change in strain from the static position than to the absolute peak breast strain. To investigate this further, a second statistical correlation was performed between the perceived breast pain during the incremental-speed treadmill test and the mean peak increase in breast strain from the static condition (Table 7.5). Peak increases in breast strain were calculated using the mean maximum increase in breast strain over three gait cycles, in any region of the breast, from the static condition (Table 7.4). These peak increases did not necessarily occur in the same region of the breast as the peak values reported in Table 7.3, hence the disparities in data values.

Table 7.4: Mean maximum change in breast skin strain compared to the static condition (in any breast segment) over three gait cycles at each speed of the incremental-speed treadmill test.

Participant number	Breast size	Mean maximum within-segment change in breast strain from the static condition (%)											
		Static	4 kph	5 kph	6 kph	7 kph	8 kph	9 kph	10 kph	11 kph	12 kph	13 kph	14 kph
Participant 1	32B		16	19	23	28	40	39	40	40	43	49	36
Participant 2	32B		7	11	16	11	15	25	17	16	20	20	22
Participant 3	32B		16	21	22	27	33	39	35	36	36	33	33
Participant 4	34B		15	44	22	24	35	41	44	43	49	46	49
Participant 5	32C		17	19	25	27	49	56	58	57	61	59	63
Participant 6	32C		20	17	19	21	42	43	45	35	45	45	47
Participant 7	32D		22	26	21	26	32	33	40	39	36	39	42
Participant 8	32D		20	25	32	38	37	37	44	57	43	44	48
Participant 9	32D		15	15	20	23	29	33	33	33	37	36	38
Participant 10	34D		19	21	17	20	20	20	20	34	56	55	54
Participant 11	32DD		15	22	25	27	30	33	31	33	31	33	36
Participant 12	30E		13	24	28	30	38	43	34	52	53	52	43
Participant 13	34DD		40	42	54	47	70	74	83	76	84	84	83
Participant 14	34DD		23	23	26	28	31	30	30	34	41	37	42
Mean			18	23	25	27	36	39	40	42	45	45	45
Standard deviation			7	9	9	8	13	13	16	14	15	15	14

Table 7.5: Correlations between breast pain, peak breast skin strain and peak change in breast skin strain during an incremental-speed treadmill test.

	Spearman's correlation Coefficient (r)	Significance (p)
Breast pain and peak dynamic breast strain	0.361	0.000*
Breast pain and peak change in breast strain from the static condition during dynamic activity	0.462	0.000*

* denotes a significant correlation ($p < 0.05$)

Discussion

Bare-breasted treadmill activity has been reported to cause high levels of breast pain (Mason *et al.*, 1999). Several authors have speculated that motion-induced breast pain may be caused by excessive breast strain (Brown *et al.*, 2014; Haake & Scurr, 2011; Knight, Wheat, Driscoll, & Haake, 2014; Mason *et al.*, 1999; Scurr, Bridgman, *et al.*, 2009). Results of this study demonstrated that peak breast skin strain was significantly moderately correlated to perceived breast pain during an incremental-speed treadmill test (Table 7.5). Inspection of individual participant data presented in Table 7.2 and Table 7.3 reveals distinct patterns within both the pain and strain data. For most participants the pain data (Table 7.2) demonstrates a gradual increase with treadmill speed, with nine out of fourteen participants reporting their maximum pain at the highest treadmill speed (although this trend is not reflected in the mode data). In contrast, only one participant (Participant 2) experienced their greatest breast strain at the highest treadmill speed (Table 7.3). The majority of participants experienced peak breast strain at speeds between 11 kph and 13 kph, although Participants 11 and 13 experienced peak breast strains at 7 kph and 8 kph respectively. The disparity between the patterns observed in breast pain and peak strain data may have arisen due to several contributing factors.

The nipple displacement data previously presented in Chapter 6 demonstrated that the nipple experienced increasingly large displacements from the neutral nipple position during incremental-speed treadmill activity (Figure 6.7 and Figure 6.8). It was therefore anticipated that the breast skin would also experience increasing strain with increasing treadmill speed. However, results indicated that peak breast strain did not occur at the highest treadmill speed for 8 out of the 14 participants within this study (Table 7.3). The apparent decrease in peak strain occurring at the highest treadmill speeds may have been caused by marker occlusion occurring while the breast skin experienced its peak strain. Although the nipple marker (used in Chapter 6) could be tracked throughout the dynamic trial for all participants, the additional breast markers in the array were frequently obscured by the motion of the breast or upper body, particularly at the higher treadmill speeds. Marker occlusion may have led to an under-estimation of strain as higher peak strains may have occurred during the time points at which strain could not be calculated.

The positive relationship between breast pain and treadmill speed may suggest that the participants' reported breast pain was influenced by the perception that higher treadmill speeds would induce greater levels of breast pain. The extent of the psychological influence on breast pain could be investigated in future research by implementing randomised-speed treadmill tests during which participants are not informed of their activity speed when reporting their level of breast pain. It was also observed that several participants within this study reported no breast pain while standing despite high levels of static breast skin strain (up to 75%). Adaptations to pain responses have been reported in previous literature, where the pain response to a continuous stimulus weakens and eventually disappears over time (Edes & Dallenbach, 1936). Nerve damage has also been reported to cause altered pain perceptions (Steeds, 2009). As discussed previously, excessive skin stretching may lead to nerve damage which may have been a contributory factor to the low static pain scores within this study, particularly for the participants whose static strain was close to or exceeded the 60% failure limit for skin. It was subsequently proposed that motion-induced breast pain may be more strongly correlated to the peak change in strain from the static position than to the absolute peak breast strain. However, correlation results demonstrated that a moderate relationship was maintained despite consideration of static skin strain (Table 7.5).

Subjective perceptions of pain are difficult to measure and can be influenced by an individual's previous experiences of pain (Kane *et al.*, 2005). This study implemented a numerical rating scale for assessing pain which has previously been used within breast motion research (Mason *et al.*, 1999), but which is predominantly intended for use in a clinical setting for assessing chronic within-patient pain (Bijur, Latimer, & Gallagher, 2003). Although numerical rating scales have been shown to be reliable for measuring acute pain (Berthier, Potel, Leconte, Touze, & Baron, 1998), their application for comparing pain across individuals is questionable due to varying individual perceptions of discomfort (Kane *et al.*, 2005). Inspection of individual pain data demonstrates high between-participant variation, with the pain rating at 14 kph ranging from 1 to 10 within the participant sample (Table 7.2). Inconsistencies in pain ratings between individuals make it difficult to draw meaningful correlations between pain and breast strain for the

sample group as a whole within this study. Normalisation of participant pain data to each individual's maximum pain score (analogous to the normalisation of breast motion data based on the bare-breasted condition (Zhou *et al.*, 2009)), or use of a case study approach to the assessment of pain may have produced stronger correlations between pain and strain, although these were not investigated within this thesis.

A second consideration for the pain data collected within this study was the selection of a single number to represent overall breast pain. In retrospect, it may have been advantageous to collect separate pain ratings for different regions of the breast, or to identify the region of the breast that caused the most pain for each participant during treadmill activity. This may have enabled a focus on specific breast regions when identifying the relationships between skin strain and breast pain. Previous literature has identified that certain parts of the body are more or less susceptible to pain than others due to the specific functionality of the nerves present in that area (Steeds, 2009). Consequently the selection of peak breast skin strain values, irrespective of breast region, for use in the correlation analysis may have led to the inclusion of large skin strain values within non-painful breast regions resulting in the moderate correlation between pain and strain observed in this study.

7.3.2f. Error analysis of breast strain data

Method

Strain data reported within this thesis were calculated using Equation 2.1. This calculation involved measurements of both neutral and loaded skin lengths. As such, the errors in the strain values were derived from a combination of the measurement errors present in both the neutral and loaded conditions. Strain errors were estimated using the quotient rule (Equation 7.1), where E is the error in measurement; M is the measured value; ΔL is the skin extension; L_0 is the neutral skin length; and L is the loaded skin length (Taylor, 1982).

Equation 7.1:

$$E_{Strain} = M_{Strain} \left(\left(\frac{E_{\Delta L}}{M_{\Delta L}} \right) + \left(\frac{E_{L_0}}{M_{L_0}} \right) \right) = M_{Strain} \left(\left(\frac{E_L + E_{L_0}}{M_{\Delta L}} \right) + \left(\frac{E_{L_0}}{M_{L_0}} \right) \right)$$

Typical and maximum error values were defined for the neutral and loaded skin length measurements to enable both typical and maximum errors to be estimated for the strain data. Accuracy assessment of the gold-standard neutral position method presented in Chapter 4 (section 4.4.3) showed that the typical and maximum resultant errors in digitised co-ordinate data obtained using underwater cameras were 0.7 mm and 1.1 mm respectively (Table 4.6). Typical and maximum errors present in the loaded co-ordinate data were estimated using previously reported tracking errors associated with optoelectronic camera systems. In 2013 Milligan investigated the accuracy of an optoelectronic camera system (8 cameras) sampling at 200 Hz and found mean and maximum tracking errors of 0.4 mm and 0.5 mm respectively (Milligan, 2013). Estimates of typical (1.1 mm) and maximum (1.6 mm) errors in skin extension were then calculated as the sum of errors in the neutral and loaded skin measurements. Strain error was calculated using Equation 7.1 for all skin segments for each participant in the static condition. Typical strain error estimates involved the assumption of mean errors in all measurements of neutral and loaded skin lengths, whereas maximum strain error estimates involved the assumption of maximum errors in all measured neutral and extended skin lengths.

Results

Mean maximum and typical static strain errors for each skin segment are illustrated in Figure 7.22. When averaged across 35 skin segments and 14 participants the typical and maximum errors in the static strain data were 2% and 3% respectively, with the greatest errors generally occurring in the upper-outer and lower-outer breast regions (Figure 7.22).

Analysis of individual data (available in Appendix M) demonstrated that the peak typical and maximum strain errors (for any one skin segment in any one participant) were 7% and 10% respectively. These peak strain error values both occurred in the UO.V.4 skin segment for Participant 14, which was calculated to experience 75% static strain (Appendix M). Incorporation of the maximum potential error of $\pm 10\%$ in the measured skin strain for this skin segment does not change the conclusion that Participant 14 may have experienced potentially damaging gravity-induced skin strain (above 60%).

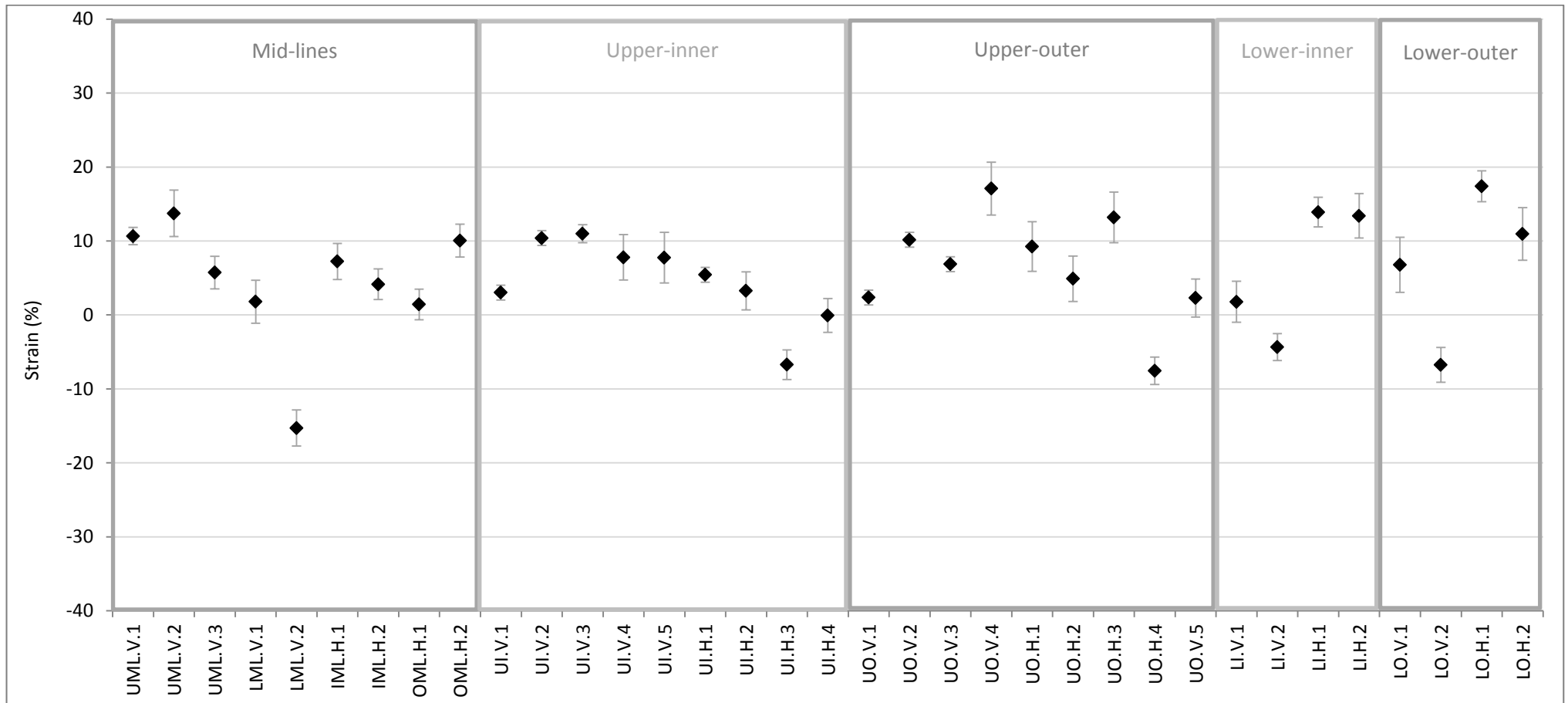


Figure 7.22: Mean static strain in each skin segment within each breast region. Error bars represent the mean typical error in each strain value (n = 14).

7.4. Discussion

This study was the first to implement a gold-standard measurement of the neutral breast position, and to use a marker array to assess static and dynamic breast skin strain. Results demonstrated that one participant experienced potentially damaging static breast strain (75%), with four participants experiencing potentially damaging breast strain during treadmill running (up to 114%). These findings suggest that women who do not wear breast support for either static or dynamic activities may risk damaging their breast skin, resulting in permanent skin extension and breast ptosis. The high strain values reported in this study may also have ethical implications for future breast biomechanics research in which bare-breasted activity is used to assess bra performance (Zhou *et al.*, 2009). It is therefore recommended that alternative methods, such as nipple displacement from the neutral position (Chapter 6), are developed for the assessment of breast support garments. Results of the static strain study also support the earlier discussion (section 2.4) that previously published reports of larger-breasted women experiencing less breast strain than smaller-breasted women during treadmill activity (Scurr, Bridgman, *et al.*, 2009) may have been due to neglect of the pre-existing strain caused by gravity.

Although the skin strain values reported within this chapter were high, limitations associated with data collection meant that the actual strain occurring on the breast skin could only be approximated. Firstly, the straight-line approximation implemented between consecutive markers on the breast skin may have led to over-estimated strain values due to incorrect incorporation rigid body motion (*i.e.* skin flattening). Secondly, the locations of the markers on the breast, particularly on the lower breast regions, meant that intermittent marker obstructions were present for all participants during the incremental-speed treadmill test. The loss of data during each participant trial meant that higher skin strains may have been present within the missing data. This problem was especially prevalent among the larger-breasted participants at all speeds, and for the lower breast region of all participants. Consideration must therefore be given to the interpretation of mean and peak strain values presented within this thesis as they may underestimate the risk of breast damage caused by static and dynamic breast loading. Missing strain data may also have contributed to the statistical correlation results being

weaker than anticipated as some participants may have experienced larger strains than could be measured during the incremental-speed treadmill test. The quality of the data collection could be improved in future by incorporating more optoelectronic cameras into the laboratory set-up when collecting data using a marker array. However, the requirement for direct line-of sight between markers and the optoelectronic cameras may present a persistent problem if testing larger-breasted, or ptotic, participants whose breast tissue rests against the torso. A similar marker obstruction problem may also occur during the assessment of breast strain inside a support garment. It was therefore recommended that alternative motion capture systems, which do not require direct line-of-sight from marker to sensor (*e.g.* six degrees of freedom electromagnetic sensors), should be investigated for collecting breast strain data in future projects.

Despite these limitations, the methods presented within this chapter offer a progression from previous breast strain assessment methods which have either implemented a marker array statically or used a first order strain approximation (using two markers) dynamically. Quantification of the extent, duration and specific regions of breast skin strain during the gait cycle may enable the risk of breast skin damage, and the associated breast pain, to be reduced by developing more appropriate breast support garments. Improved understanding of static and dynamic breast deformation may also enable the development of improved FE breast models for use within clinical research.

7.5. Conclusions

Potentially damaging breast skin strains (75%) were present in the upper outer breast region for one participant (size 34DD) while standing stationary in the laboratory and for four participants during the incremental-speed treadmill test (up to 114% skin strain). These results highlight the importance of including static skin strain (from the neutral position) when assessing dynamic strain during exercise and suggest that exercising without breast support may cause permanent damage to the breast skin leading to ptosis. The previously published two marker method for calculating breast strain was not recommended for future research due to large under-estimations (up to 59%) of static breast skin strain when compared to strain data obtained using a marker array.

Additionally, a disparity was identified between the low strain rates used previously to identify the failure limits for human skin (Gallagher *et al.*, 2012) and the high strain rate observed in the breast skin during treadmill running (206% per second).

A significant moderate relationship was found between breast skin strain and breast pain. This was weaker than anticipated and may have been caused by several factors such as differences in participant pain perception and marker obstruction during collection of the strain data. Alternative motion capture systems that do not rely on visual data could be considered for the future assessment of breast skin strain.

8. Combining breast displacement and skin strain data

8.1. Introduction

Breast position, breast motion, and breast strain data have so far been presented discretely in chapters 4 to 7 of this thesis, and the main focus of the strain analyses has been the estimation of skin damage. However, strain data can also be used to gain valuable insight into the mechanical behaviour of the breast under external loading. The novel nature of the data obtained within this thesis enabled the first investigation into the effects of gravity and dynamic activity on the breast skin. A single participant's data (Participant 11, 32DD) were considered within this chapter to enable the clear presentation of data sets at each stage of analysis.

8.2. Aim

1. Investigate gravity- and motion-induced breast displacements and the consequential static and dynamic strains on the breast skin.

8.3. Method

The methods used to collect and analyse the data presented in this chapter were previously detailed in the following sections of the thesis:

Static data

Nipple only	Sections 4.3.1 and 4.3.2
Breast array	Sections 7.3.1 and 7.3.2a

Dynamic data

Nipple only	Section 6.3
Breast array	Sections 7.3.1, 7.3.2b, 7.3.2c, and 7.3.2d

Displacement and strain data were combined initially in the static condition to investigate the effect of gravity on the nipple and breast. This was followed by the analysis of

dynamic displacement and strain data obtained during treadmill running at 14 kph, which was used to investigate the effect of motion on the nipple and breast.

8.4. Results and discussion

8.4.1. Static data

The nipple was initially used to provide a single representative point on the breast when describing the effect of gravity on breast position. The neutral and gravity-loaded nipple positions for Participant 11 were previously reported in in Chapter 4 (Table 4.2 and Table 4.3). The effect of gravity on nipple position can be seen in Figure 8.1, which includes a diagrammatic representation of the breast in the neutral position. The magnitude and direction of gravity-induced nipple displacement from the neutral nipple position are shown in Figure 8.2. These data demonstrate the small lateral effect (11.5 mm), and larger posterior (17.0 mm) and inferior (22.7 mm) effects, of gravity on nipple position (Chapter 4).

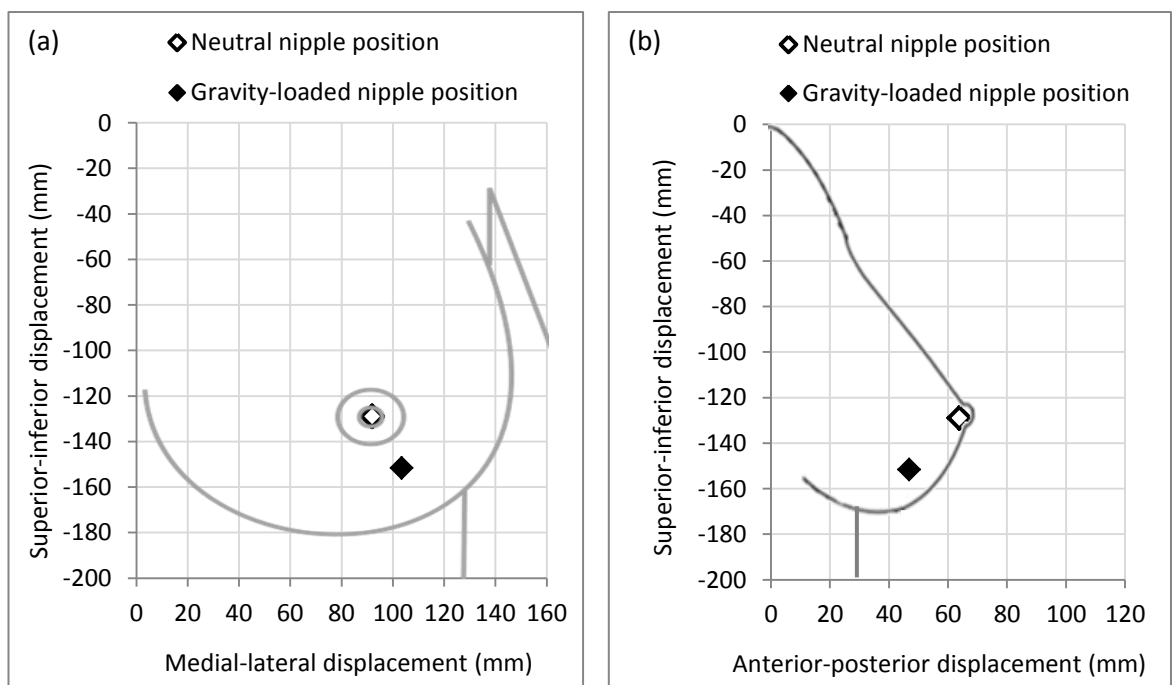


Figure 8.1: Neutral and gravity-loaded nipple position (and representative breast outline) in the frontal (a) and sagittal (b) plane (Participant 11, 32DD).

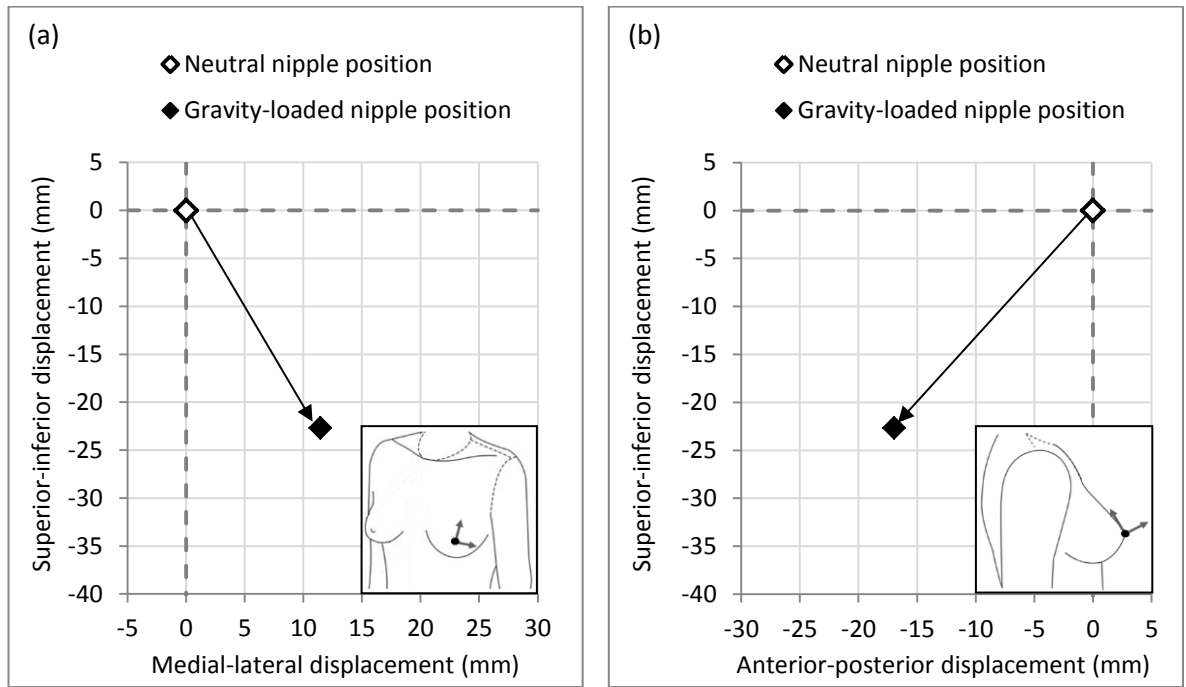


Figure 8.2: Static gravity-induced displacement of the nipple from the neutral nipple position in the frontal (a) and sagittal (b) plane (Participant 11, 32DD).

Although the data in Figure 8.1 and Figure 8.2 show the effect of gravity on nipple position only, these data provide an initial indication of how the breast as a whole may behave under gravitational loading. Marker array data obtained within this thesis (described in Chapter 7) provided opportunity to investigate the deforming and strain-inducing effects of gravity over the breast surface for the first time in breast research. The neutral and gravity-loaded positions of the longitudinal and latitudinal breast mid-lines for Participant 11 are shown in Figure 8.3 (all participants' data are shown in Appendix E). As anticipated from the nipple data, gravity caused a small lateral displacement of the longitudinal breast mid-line (Figure 8.3 a), with larger displacements occurring in the posterior and inferior directions (Figure 8.3 a and b). Comparison of the neutral and gravity-loaded data presented in the sagittal plane demonstrates the change in breast shape that occurred with gravitational loading (Figure 8.3 b). In the gravity-loaded condition the upper breast regions flatten against the torso while the lower breast regions distort to accommodate the inferior position of the interior breast bulk. These effects combine to create the typical tear-drop breast shape (Avşar *et al.*, 2010; Lee, 2011) and to explain why the nipple moves both posteriorly and inferiorly when under the influence of gravity.



Figure 8.3: Static gravity-induced displacement of the breast mid-lines from the neutral breast position in the frontal (a) and sagittal (b) plane (Participant 11, 32DD).

Measurement of the gravity-induced displacement of the breast surface provided the basis for static strain analysis. Static breast skin strains were calculated for the breast mid-lines using Equation 2.1 and are shown in Figure 8.4. The static strain values reflect the gravity-induced breast displacement observed over the breast surface. The lateral displacement of the breast causes positive strain to occur on the three medial segments, and negative strain (compression) to occur on the most lateral segment of the breast skin along the latitudinal breast mid-line (Figure 8.4 a). A similar pattern was observed along the longitudinal breast mid-line, with positive strains occurring on the superior skin segments and negative strain occurring on the most inferior skin segment (Figure 8.4 b). This longitudinal strain pattern reflects the posterior and inferior displacement of the breast caused by gravitational loading.

Static skin strains across the latitudinal and longitudinal breast mid-lines are shown graphically in Figure 8.5 a and b. These figures demonstrate that in the gravity-loaded condition the medial and superior segments of the breast skin experience tension (positive strain), while the lateral and inferior skin segments experience compression (negative strain). Interestingly, for this participant, the transition point between tension and compression of the breast skin occurs laterally and inferiorly to the nipple (Figure 8.5). As the nipple has previously been used to represent the centre of breast mass (Zhou *et al.*, 2012b) it was anticipated that the nipple may also define the transition point for static strains over the breast surface. The data in Figure 8.4 suggest that although the nipple may be positioned approximately over the centre of the breast mass in the neutral position, this is not the case in the gravity-loaded position. As the breast bulk shifts inferiorly and laterally due to gravity (Figure 8.4), so does the transition point for skin strains measured on the breast surface (Figure 8.5).

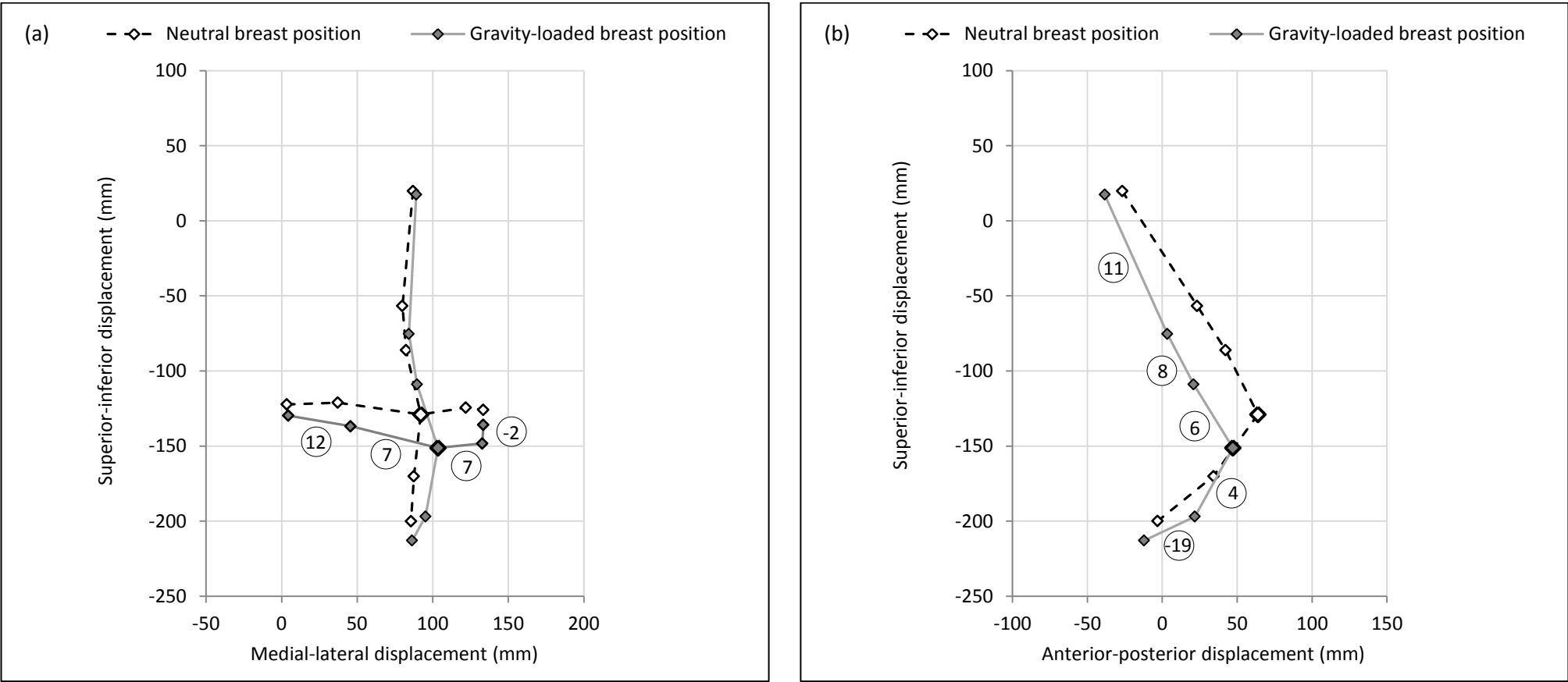


Figure 8.4: Static gravity-induced skin strain on the breast mid-lines in the frontal (a) and sagittal (b) plane (Participant 11, 32DD).

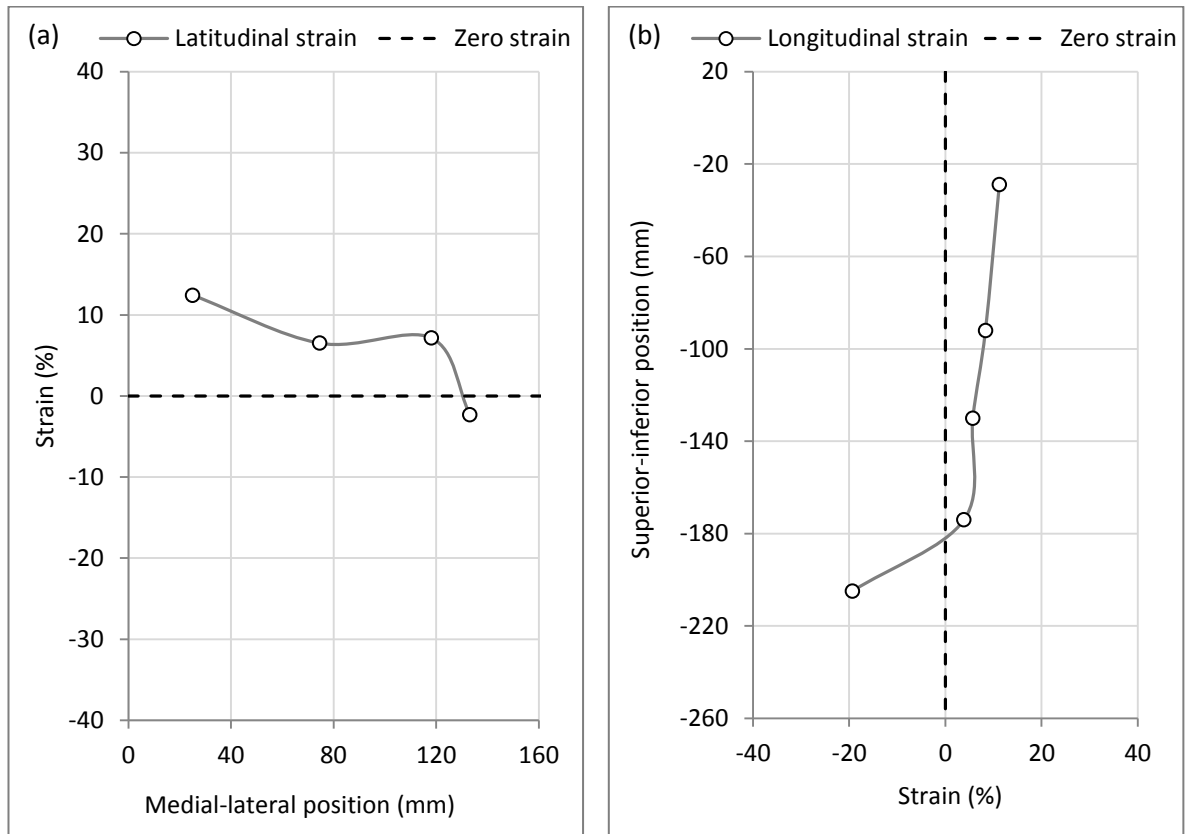


Figure 8.5: Static breast skin strain along the medial-lateral (a) and superior-inferior (b) breast mid-lines in each skin segment position (Participant 11, 32DD).

8.4.2. Dynamic data

Nipple displacement data for one gait cycle of treadmill running at 14 kph are shown in Figure 8.6. These data display a similar three-dimensional oscillatory behaviour to that described in Chapter 6 (Figure 6.2). The corresponding motion-induced skin strains for the mid-lines of the breast are shown for each frame during the gait cycle in Figure 8.7 and Figure 8.8.

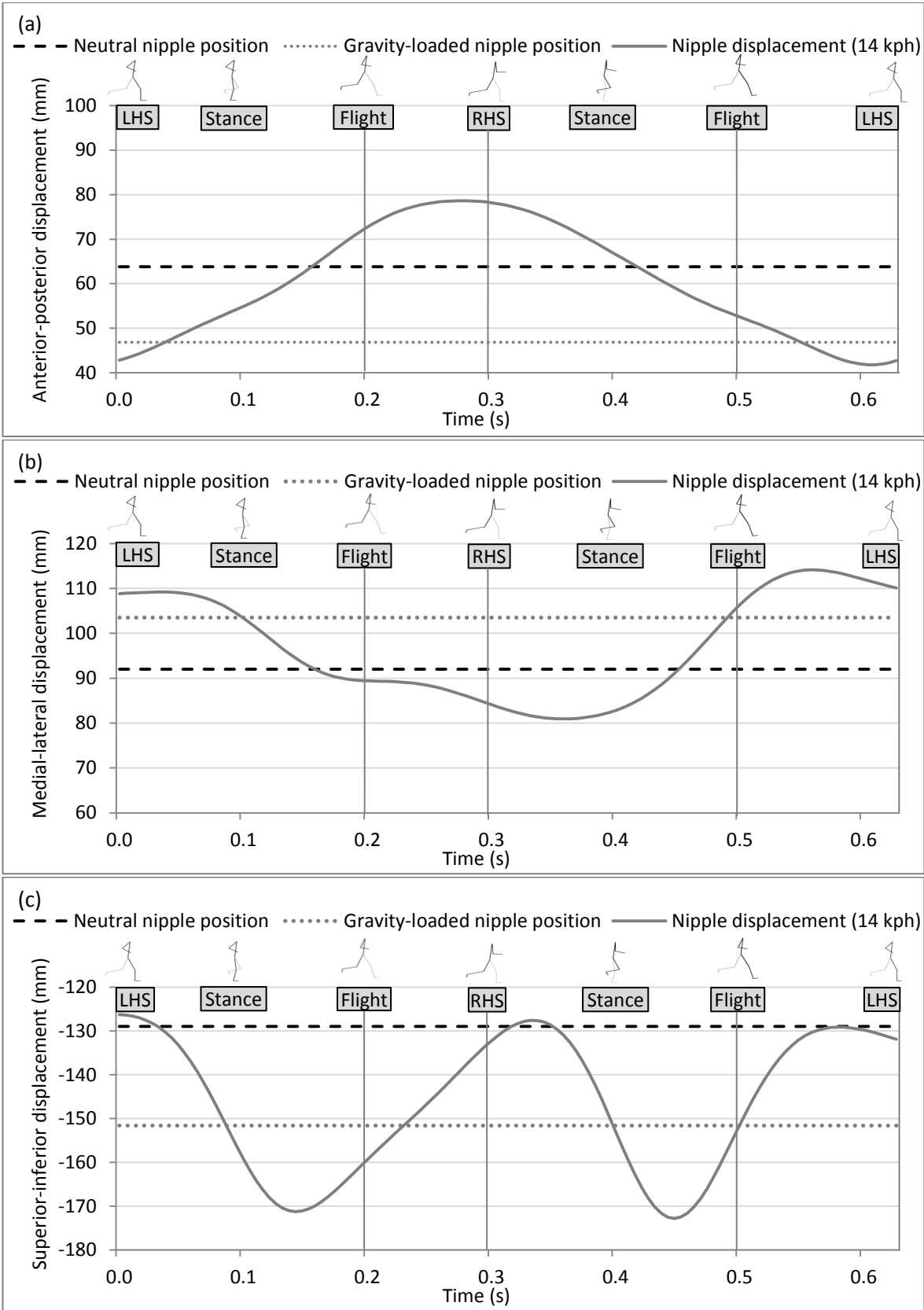


Figure 8.6: Anterior-posterior (a), medial-lateral (b), and superior-inferior (c) nipple displacement relative to the neutral nipple position during one gait cycle of treadmill running at 14 kph (Participant 11, 32DD).

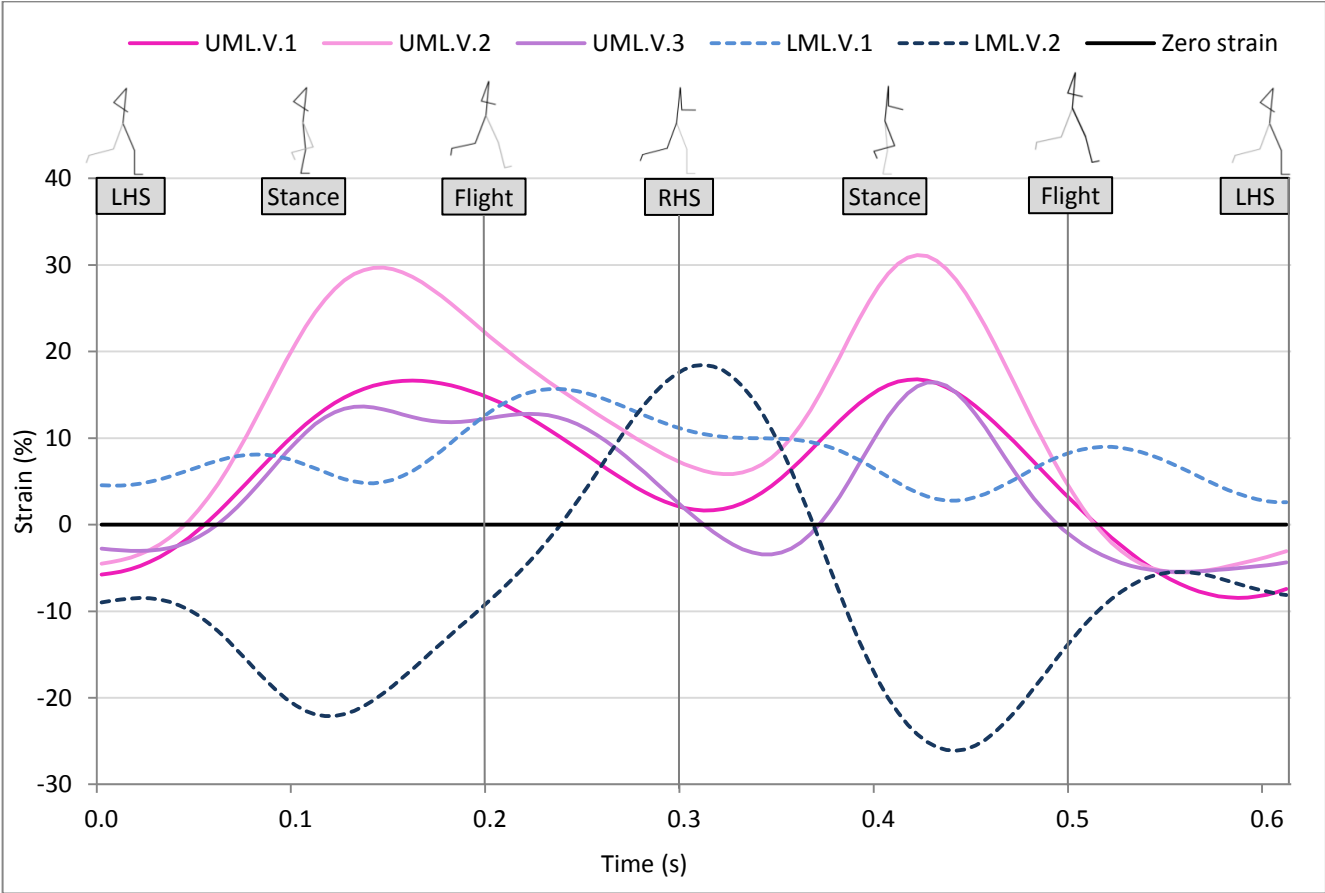
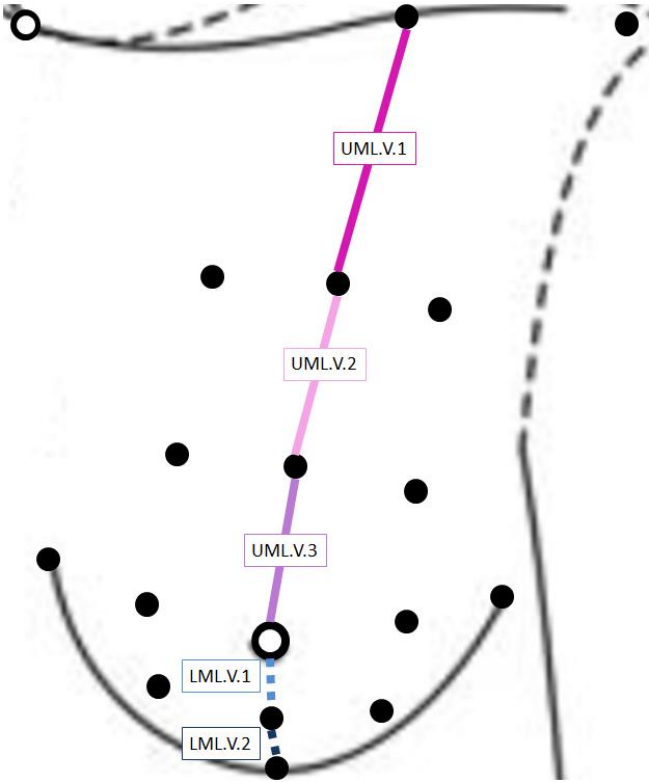


Figure 8.7: Longitudinal skin strain on the breast mid-line during one gait cycle of treadmill running at 14 kph (Participant 11, 32DD).

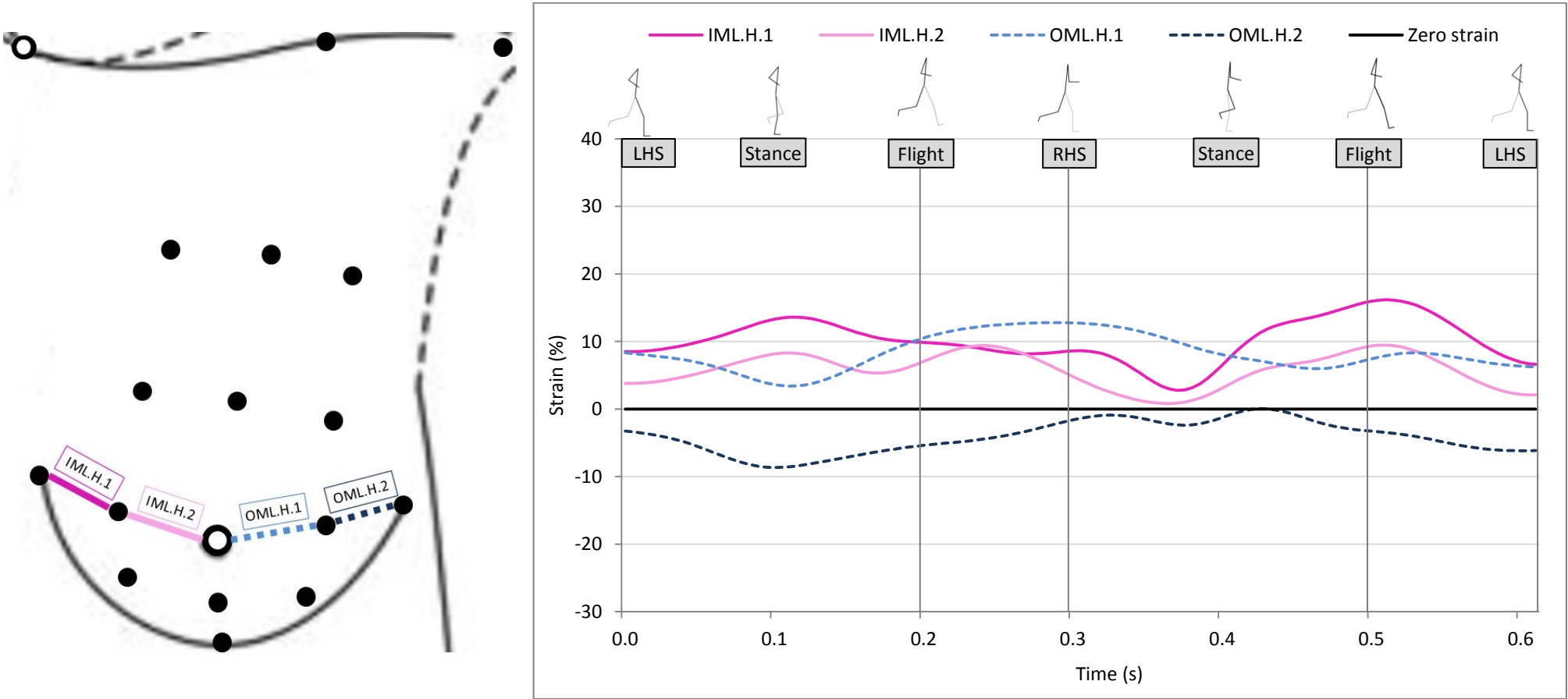


Figure 8.8: Latitudinal skin strain on the breast mid-line during one gait cycle of treadmill running at 14 kph (Participant 11, 32DD).

Perhaps the most straight-forward dynamic data to understand are longitudinal skin strains caused by superior-inferior breast motion during treadmill running. A comparison of nipple motion shown in Figure 8.6 c and strain data in Figure 8.7 demonstrates that during the stance phases of the gait (following heel strike) the nipple moved inferiorly with respect to the torso. This inferior motion caused increased strain (tension) in the upper breast skin segments and decreased strain (compression) in the lower breast skin segments. This relationship was reversed for the flight phases of the gait during which the nipple moved superiorly relative to the torso.

The relationship between anterior-posterior (Figure 8.6 a) and medial-lateral (Figure 8.6 b) nipple motion and skin strain was more subtle. In the longitudinal direction (Figure 8.7) it was observed that although most skin segments experienced similar strain patterns for both halves of the gait cycle, the most inferior skin segment (LML.V.2) had a single peak strain value which occurred following right heel strike. This may be explained by the peak anterior motion of the nipple that also occurred following right heel strike (approximately 0.35 s). Nipple motion data indicated that the breast was in a similar superior position relative to the torso following right and left heel strikes, but that the anterior displacement was greatest following right heel strike. Consequently, it makes sense that the greatest skin strain would occur when the breast was extended anteriorly rather than compressed posteriorly relative to the torso.

In the latitudinal direction the breast skin strains were generally smaller than in the longitudinal direction (Figure 8.8), and the strain pattern resembled the medial-lateral displacement pattern of the nipple (Figure 8.6 b). In the first half of the gait cycle, following left heel strike, the nipple moves medially relative to the torso. This medial motion caused increased skin strain in the lateral segments of the breast and slightly reduced skin strain in the medial segments. In the second half of the gait, following right heel strike, the nipple moved laterally causing decreased strain on the lateral skin segments and increased strain on the medial skin segments.

Dynamic strains occurring in each skin segment on the longitudinal and latitudinal breast mid-lines are shown for key time points in the gait cycle in Figure 8.9 a and Figure 8.9 b. These data demonstrate the transitions from positive to negative strains during the gait cycle for each skin segment along the breast mid-lines. Results suggest that the skin segments on the upper mid-breast (UML.V.2) and at the base of the breast (LML.V.2) are subjected to a greater range of skin strains during treadmill running than the skin segments closer to the nipple. This differing strain behaviour along the breast mid-lines may be caused by the hemispherical shape of the breast and the underlying breast anatomy. Breast tissue typically extends from the second to the sixth or seventh rib in the superior-inferior direction (Macéa & Fregnani, 2006). The breast is broadest at its contact point on the torso and is generally narrowest at the nipple (the apex of the breast) (Figure 8.10). Assuming Participant 11 had a typical breast anatomy it was suggested that the most superior longitudinal skin segment (UML.V.1) may have predominantly overlaid the soft tissue of the torso rather than the breast (Figure 8.10 b). Consequently, the skin segments overlaying the broadest cross-section of the breast may have been UML.V.2; LML.V.2; IML.H.1; and OML.H.2 (Figure 8.10 a and b). Greater dynamic loading caused by a larger underlying breast mass may explain why these skin segments experienced the largest positive and negative strains during the gait cycle (Figure 8.9).

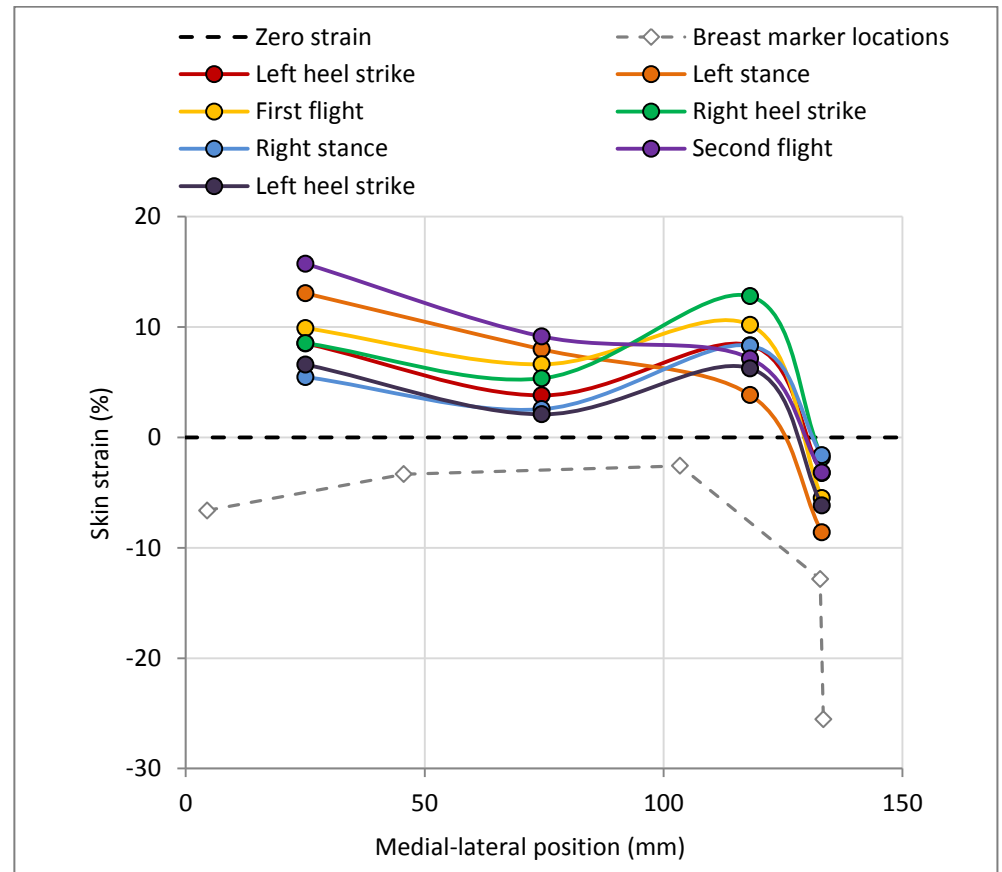
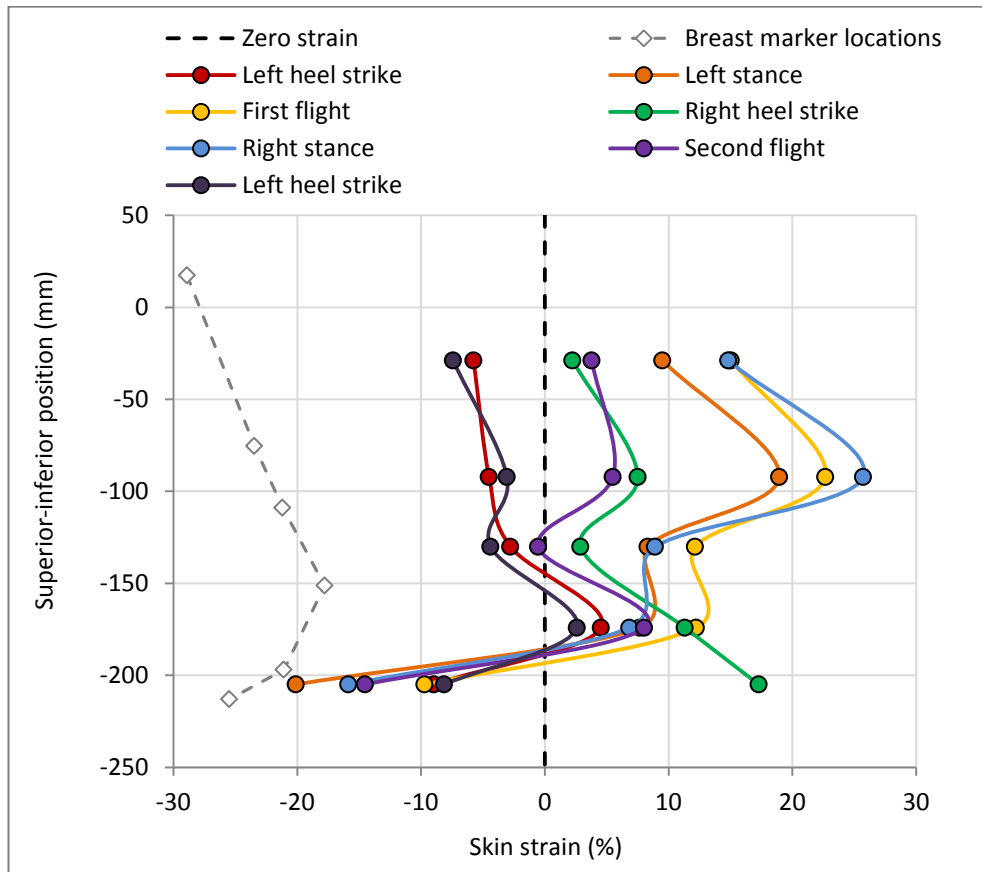


Figure 8.9: Longitudinal (a) and latitudinal (b) breast skin strain at the mid-point of each skin segment during one gait cycle of treadmill running at 14 kph (Participant 11, 32DD). The locations of the breast mid-line markers are illustrated in grey.

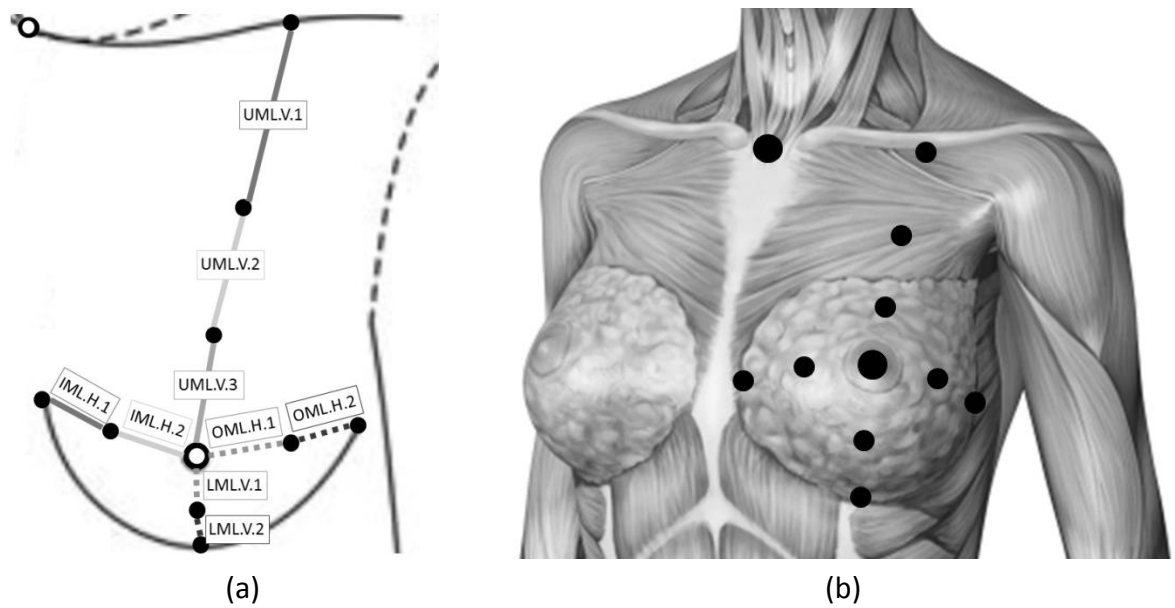


Figure 8.10: Marker locations used to define the longitudinal and latitudinal breast mid-lines with reference to the underlying breast anatomy.

Having identified how the dynamic motion of the breast causes fluctuating strains across the mid-lines of the breast skin during the gait cycle, the final stage of this chapter focuses on the identification of a representative breast position in which peak skin strain may occur. This representative position was identified using the peak resultant displacement of the nipple from the torso origin during one gait cycle of treadmill running at 14 kph (shown in Figure 8.11). The position of the nipple at this time point is shown in the frontal plane in Figure 8.12.

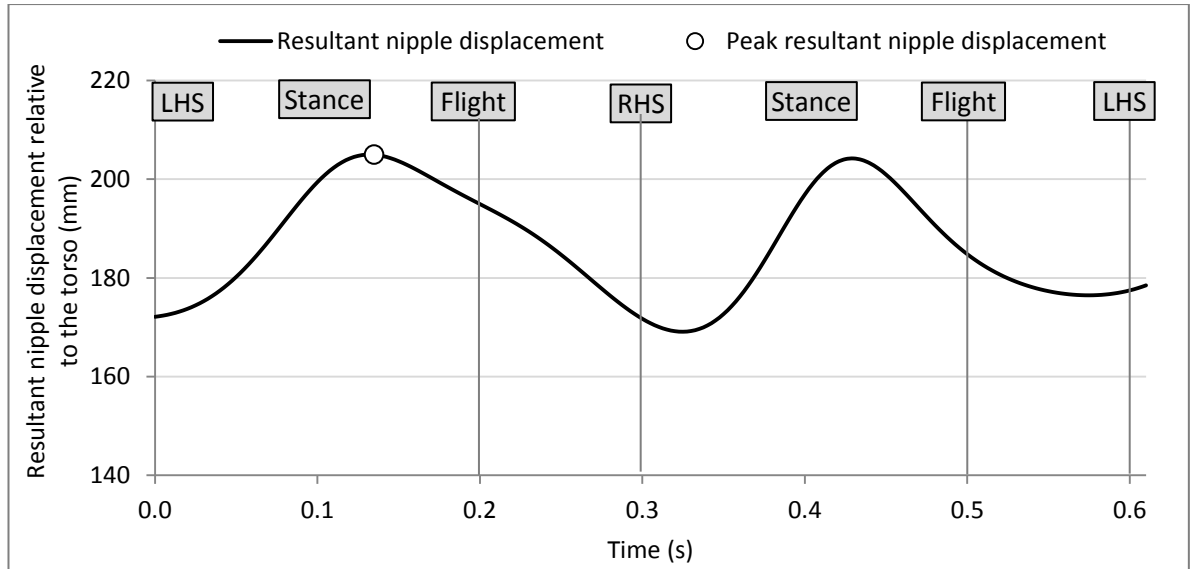


Figure 8.11: Resultant nipple displacement relative to the torso during one gait cycle of treadmill running at 14 kph (Participant 11, 32DD).

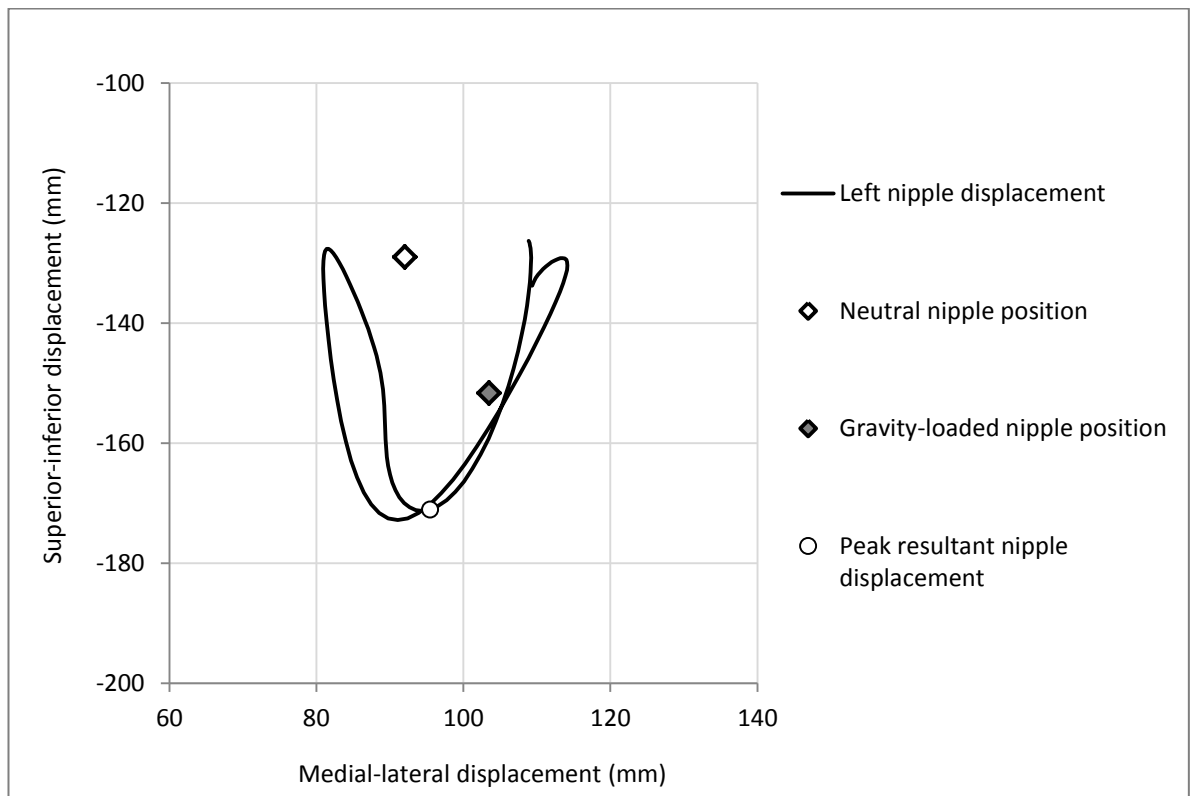


Figure 8.12: Nipple displacement in the frontal plane during one gait cycle of treadmill running at 14 kph (Participant 11, 32DD).

Maximum resultant displacement of the nipple from the torso occurred at 0.145 s, which was during the first stance phase of the gait (Figure 8.11). Instantaneous skin strain data across the breast surface at this time point are illustrated in Figure 8.13. These results demonstrate that the greatest positive skin strains (tension) at this instant occurred in the upper-outer breast region longitudinally (UO.V.4 segment at 34% strain) and in the lower-inner breast region latitudinally (LI.H.1 segment at 24% strain). Simultaneously, the greatest negative skin strains (compression) occurred in the lower (LML.V.2 segment at -22% strain) and outer (UO.H.3 segment at -19% strain) breast regions. No potentially damaging skin strains were observed at this instant during the gait cycle, although skin strains were generally greater in segments further from the nipple.

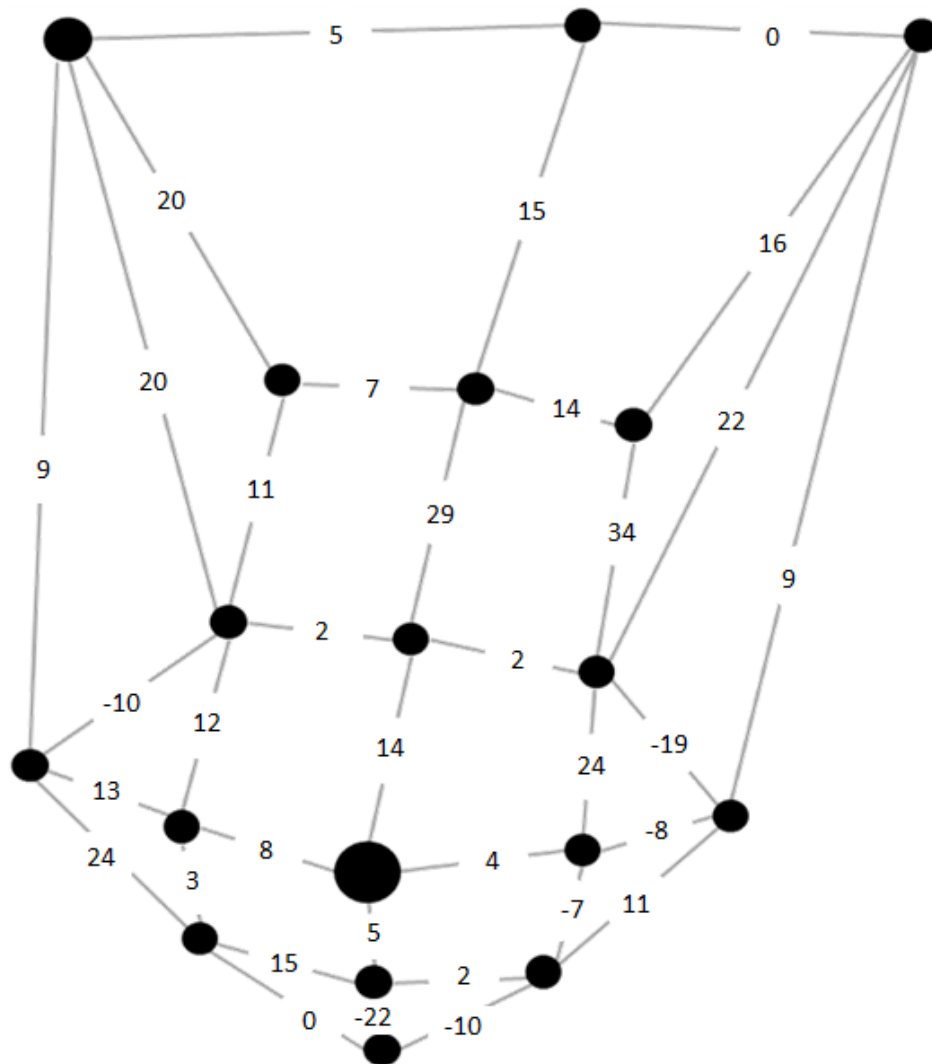


Figure 8.13: Breast skin strain at the instant of peak resultant nipple displacement from the torso during one gait cycle of treadmill running at 14 kph (Participant 11, 32DD).

8.5. Conclusion

Breast displacement and skin strain data were combined in this chapter to provide a comprehensive analysis of the effects of gravitational and dynamic loading on the breast skin. Gravitational loading caused the nipple to move posteriorly, laterally and inferiorly on the torso. These static displacements caused positive skin strains (tension) on the upper (11%) and medial (12%) breast mid-lines and negative skin strains (compression) on the lower (-19%) and lateral (-2%) breast mid-lines.

Dynamic loading of the breast during treadmill running at 14 kph produced a typical figure-of-eight nipple displacement pattern. The oscillatory behaviour of the nipple during running was reflected in the rapidly fluctuating skin strains observed across the breast surface. Peak positive (tension) and negative (compression) skin strains occurred along the upper breast mid-line during the stance (31%) and heel strike (-8%) phases of the gait cycle respectively. The lower breast mid-line displayed the opposite skin strain behaviour, with peak positive and negative strains occurring during the heel strike (18%) and stance (-26%) phases of the gait cycle respectively.

The nipple was maximally displaced from the torso during the first stance phase of the gait (at 0.145 s). At this key time point the greatest positive skin strain (tension) occurred in the upper-outer breast region (UO.V.4 segment at 34% strain) and the greatest negative skin strain (compression) occurred along the lower breast mid-line (LML.V.2 segment at -22% strain). Future implementation of the methods presented within this chapter may lead to a more holistic understanding of the breast's behaviour to external loading, which may have beneficial implications for both clinical (gravitational loading), and biomechanical (dynamic loading) research.

9. Thesis review

9.1. General discussion

This thesis aimed to identify a gold-standard method for estimating the neutral breast position and to incorporate this position into measurements of breast motion and breast strain. The key outcome of this work was the estimation of potential breast damage caused by static and dynamic skin strain, the measurement of which had previously been unachievable due to difficulties accounting for the deforming effect of gravity on the breast (Gao & Desai, 2010). In addition to damage estimation, the methods and results presented within this thesis contribute to the understanding of motion-induced breast pain, and have important implications for the general (female) public, for future breast research, and for the design of improved breast support garments.

The risk of breast skin damage was estimated by comparing the reported strain failure limit for human skin (60%) (Silver *et al.*, 2001) to the measured strain on the breast skin. This skin strain failure limit could only be appropriately applied to measurements of skin strain calculated from the neutral breast position. The study described in Chapter 7 represents the first attempt to measure the neutral position of the breast skin, and subsequently to estimate the risk of breast skin damage caused by static and dynamic strain. Results demonstrated potentially damaging breast skin strains both statically (up to 75%) and during treadmill activity (up to 114%) in the bare-breasted condition. These findings highlight the importance of supporting the breast during both daily and sporting activities. Although previous literature has strongly promoted the use of appropriate breast support, generally these recommendations are focused on reducing breast pain (Mason *et al.*, 1999), or embarrassment (Bowles *et al.*, 2008) associated with excessive breast motion during exercise. The demonstration of potential damage and increased risk of breast ptosis associated with bare-breasted activity provides a persuasive argument for women who may not otherwise experience breast pain or embarrassment during exercise. The risk of breast skin damage associated with bare-breasted activity identified within this thesis may also have ethical implications for breast biomechanics research. Future breast motion studies should consider presenting kinematic breast data

relative to the neutral breast position, rather than to the potentially damaging bare-breasted condition as has been the conventional approach (Scurr, White, & Hedger, 2011; Zhou *et al.*, 2011, 2009).

In addition to estimating breast damage, the understanding and reduction of breast pain were also important factors underpinning the work conducted within this thesis. Existing research has postulated that breast strain during dynamic activity may contribute to motion-induced breast pain (Bowles, 2012; Haake & Scurr, 2011; Mason *et al.*, 1999; Milligan, 2013; Scurr, Bridgman, *et al.*, 2009). Measurement of breast strain using a marker array within this thesis provided the first opportunity to investigate the relationship between breast skin strain and breast pain. Significant moderate correlations were found between these variables, suggesting that motion-induced breast pain may be reduced by limiting the dynamic strain experienced by the breast skin. The strength of this correlation was weaker than anticipated based on previous reports of strain-induced pain in other areas of the body (Hirsch *et al.*, 1960; Markolf *et al.*, 1989; McArdle *et al.*, 2010; Micheli & Wood, 1995; Quinn *et al.*, 2007), and may have been due to the highly varied perceptions of breast pain reported within this study.

Breast pain was also investigated in relation to the displacement of the nipple from the neutral nipple position (in the anterior, posterior, medial, lateral, superior, and inferior directions) during treadmill running. Interestingly, superior nipple displacement from the neutral position was most strongly correlated to breast pain, with weaker correlations in the other five directions. Correlations were particularly weak in the inferior and posterior directions, which were the directions shown to be most affected by gravity in Chapter 4, and by dynamic treadmill activity in Chapter 6. It was suggested that participants may have experienced a reduced pain response to inferior and posterior nipple displacements due to the continual effect of gravity these directions. This directional difference in the observed relationships between breast pain and nipple motion could not have been identified using conventional measurements of nipple ROM, and contribute to the understanding of motion-induced breast pain. Results from this study could be used to inform the development of breast support garments that reduce breast pain by limiting the superior displacement of the nipple from the neutral position during dynamic activity.

Several aspects of the work conducted within this thesis have applications within future breast research. The systematic review of quantitative breast density literature presented in Chapter 3 was conducted to inform the development of the gold-standard neutral position method. However, the mean breast mass-density estimate obtained from this work (948 kg.m^{-3}) could be beneficially implemented in both biomechanical and clinical research. Breast mass-density has been widely approximated within the literature, with estimated breast mass-density values ranging from 780 kg.m^{-3} to 2250 kg.m^{-3} (Li *et al.*, 2003; McGhee *et al.*, 2013). Identification of an improved mean breast mass-density estimate may lead to more accurate calculations of dependant biomechanical variables such as mass, force, or momentum. In a clinical setting, improved breast mass-density estimation may lead to improved FE breast models (Dufaye *et al.*, 2013; Rajagopal, 2007), and to a better understanding of the loads placed on breast implants or surgical repairs enabling more appropriate surgical techniques, or implant filler materials, to be developed (Armstrong & Jones, 2000; Gefen & Dilmoney, 2007).

Identification of the neutral position within this thesis enabled the effect of gravity on the breast to be assessed (Chapters 4 and 7). Gravity caused the nipple to move posteriorly (up to 25.6 mm), laterally (up to 15.7 mm), and inferiorly (up to 45.7 mm) relative to the torso, and induced skin strains up to 75%. The magnitudes of these results highlight the extent of gravitational deformation experienced by the breast in the static position. It is therefore important for future research to consider the effect of gravity when drawing conclusions from kinematic breast data or when estimating breast skin damage from measurements of strain. The experimentally obtained measurement of the neutral and gravity-loaded breast positions also provides valuable data for the development of FE breast models. The lack of such experimental data in previous research has meant that existing FE breast models are prone to relatively large errors, particularly on the breast surface, when predicting the behaviour of the breast under external loading (Azar *et al.*, 2002; Tanner *et al.*, 2006). Incorporation of the neutral breast position as the reference state for mapping breast structures has also been shown to improve the prediction ability of clinical breast FE models when estimating the breast deformation caused by medical imaging or surgery (Rajagopal, 2007).

Incorporation of the neutral breast position into measurements of breast motion and breast strain also has important implications for the development and assessment of breast support garments. Firstly, the neutral position could be used to represent the optimum breast position in terms of reducing strain on the breast skin. Based on the results presented in Chapter 4, a breast support garment should move the nipple anteriorly, medially and superiorly to counteract the effect of gravity on the breast. Subsequent measurements of nipple displacement from the neutral position, which relate to the mechanical loading of the breast skin, could provide a more detailed assessment of breast motion than conventional measurements of nipple ROM (Scurr, White, & Hedger, 2011). During treadmill running the majority of nipple displacement away from the neutral nipple position was found to occur in the inferior direction (Chapter 6). Breast support garments may reduce the risk of breast damage caused by skin strain by limiting the inferior displacement of the nipple during dynamic activity. Interestingly, breast pain was most strongly correlated to the superior displacement of the nipple from the neutral nipple position, suggesting that breast support garments that limit superior breast displacement may reduce the associated breast pain.

Skin strain analysis could also be incorporated into bra design and evaluation. Potentially damaging skin strains were demonstrated in both the static and dynamic conditions assessed within this thesis, particularly in the upper-outer region of the breast (Chapter 7). This information could inform the development of garments that provide increased support to the upper-outer region of the breast, which is most at risk of experiencing damaging skin strains. A bra that supports the breast in the neutral position and restricts breast motion to the elastic strain limits of the breast skin may protect the breast from damage, reduce the risk of ptosis, and minimise motion-induced breast pain. Consideration of the neutral position when evaluating breast support garments would enable both breast positioning and breast motion control to be assessed; potentially leading to the classification of garments according to how well they protect the breast against the effects of static and dynamic loading. Although several recommendations were made within this thesis regarding the development of improved breast support garments, only the bare-breasted condition was assessed within this programme of work.

Future research could apply the methods presented within this thesis to evaluate the ability of breast support garments to statically position the breast in the neutral position and to dynamically reduce strain on the breast skin.

The combination of breast displacement and strain data within Chapter 8 of this thesis (for Participant 11 (32DD)) enabled a comprehensive analysis of the effects of gravitational and dynamic loading on the breast skin, and provided a novel contribution to the development of breast research. Gravitational loading caused the nipple to move posteriorly, laterally and inferiorly on the torso. This gravity-induced displacement caused positive strains (tension) on the upper (11%) and medial (12%) breast mid-lines and negative skin strains (compression) on the lower (-19%) and lateral (-2%) breast mid-lines. Dynamic loading of the breast during treadmill running at 14 kph produced a typical figure-of-eight nipple displacement pattern. The corresponding strain data suggested that the breast bulk followed a similar displacement pattern, which caused rapid fluctuations from positive (tension) to negative (compression) skin strains across the surface of the breast during the gait cycle. The upper and lower breast mid-lines experienced the greatest strains during the stance (31%) and right heel strike (18%) phases of the gait cycle. The work presented within Chapter 8 of this thesis also demonstrated the potential to assess instantaneous breast skin strain at a key time point during the gait cycle, which was identified using nipple displacement data. If certain breast displacements (identified using a nipple marker) could be linked to important features in skin strain data then this novel approach could be used to streamline breast skin strain analysis in future research by selecting certain key time points before performing strain calculations. Detailed assessment of gravity- or motion-induced deformation of the breast surface and the resulting skin strain provides important information regarding the breast's response to external loading. This information could be used in a clinical setting to improve FE breast models, or to better understand the breast's response to static loading during surgery. The strain response of the breast skin to dynamic loading is useful for generating a holistic understanding of breast motion within biomechanical breast research, and for the development of breast support garments that offer tailored support across the breast surface to minimise dynamic skin strains.

9.2. Delimitations and limitations

Delimitations were defined as factors that were under the control of the researcher and were considered when determining the scope of this programme of work. Limitations were defined as an aspect of the research that was out of the control of the researcher that could have potentially influenced the outcome.

A delimitation of this work was the estimation of breast damage based on measurements of external breast strain (on the breast skin). Internal breast strain was not assessed within this thesis as this could not be measured dynamically with the available technology. Additionally, it was acknowledged that the internal structures of the breast may not be positioned in their neutral position when using the gold-standard neutral position method developed within this thesis as the buoyancy force can only counteract the effect of gravity at the breast surface (Gao & Desai, 2010).

The location of breast and torso markers used to calculate relative breast position also constitutes a delimitation within this programme of work. The torso marker set was selected based on the current recommendations for breast motion research (Scurr, White, & Hedger, 2011; Zhou *et al.*, 2011). However, during methodological development it was identified that high levels of soft tissue motion over the ribs caused the torso origin to shift away from the suprasternal notch when using this marker set (section 3.4). This problem was reduced within this thesis by creating a fixed rib torso segment, but a small error may have still been present when comparing nipple position between static and dynamic conditions with differing levels of soft tissue motion. Further research may be required to continue the development of improved torso marker sets for use within breast motion research.

Participant criteria implemented within this programme of work affects both the accuracy of the data obtained and the generalisability of the methods developed in this thesis. Exclusion criteria were based on previous publications that reported decreased skin elasticity with age and UV exposure (Fisher *et al.*, 1997; Smalls *et al.*, 2006). Participants

were only included if they were younger than 30 years old (Fujimura *et al.*, 2007) and had not exposed their breasts to UV radiation within the last three months (Gambichler *et al.*, 2006). These criteria were imposed in an attempt to ensure all participants' breast skin was elastic and would return to its neutral position when supported by the buoyant forces from water and soybean oil. However, no further assessment was conducted to verify the elasticity of each participant's skin before conducting the gold-standard neutral breast position study. The methods presented within this thesis for identifying the neutral breast position were based on the assumption that participant breast skin was elastic and would return almost instantaneously to its neutral position if the effect of gravity was removed. Consequently, it may not be possible to identify the neutral breast position of women who do not meet the participant inclusion criteria as they may have already experienced irreversible damage to their breast skin. The methods and results from this thesis are therefore only applicable to women who have not yet caused irreversible damage to their breast skin and could not be applied to a wider participant sample.

Although the neutral position methods developed within this thesis enabled a pioneering investigation into gravity- and motion-induced breast skin strain, there were limitations associated with these methods that may have affected the estimation of breast skin damage within this thesis. One of the main limitations was the time interval between testing sessions for some participants. Ideally all participants would have completed the water and soybean oil immersions, all the alternative neutral position tests, and the incremental-speed treadmill test within a single testing session to minimise any changes in breast size between measurements. However, due to limited facilities and participant availability, testing had to be conducted over a two week period. This time interval may have meant that some participants experienced changes in breast size, shape or position between sessions which may have affected the neutral position estimates and any subsequent measurements of nipple displacement or skin strain.

During the breast skin strain investigation, the data collected using the optoelectronic camera system was incomplete due to intermittent obstruction of the markers in the breast array for some participants. Improved skin strain measurements could be

achieved in future research following the development of alternative motion capture systems that do not require markers to be visible at all times. Several alternative systems for motion capture do currently exist (such as inertial measurement units; electromagnetic tracking; or LED and photodiode systems) (Lee *et al.*, 2012; Nasseri *et al.*, 2012). However, further work would be required to develop a system with a high sampling frequency and unobtrusive makers/sensors that could be positioned beneath a support garment with minimal effect on breast (or bra) motion. Additionally, the skin failure limits imposed within the thesis were based on representative values of previously published data, which has predominantly been obtained from cadaver or animal skin extended low strain rates (Gallagher *et al.*, 2012). More appropriate skin failure limits may be attainable by studying female breast skin at strain rates that approximate those observed during treadmill running (206% per second). Alternatively, a more accurate evaluation of the damaging effect of breast strain on the skin could be achieved by measuring the properties of each participant's breast skin to quantify the extent of skin damage caused by static or dynamic breast strain.

When developing the methods within this thesis, consideration was given to the assessment method used for measuring motion-induced breast pain. A numerical rating scale was selected based on its use within previous breast motion research (Mason *et al.*, 1999), although it was acknowledged that perceptions of pain are difficult to measure and could be influenced by an individual's previous experiences of pain (Kane *et al.*, 2005). Without a quantitative measure of pain, correlations between breast motion, breast skin strain, and breast pain across individuals may have been affected by varying individual perceptions of discomfort. Normalisation of participant pain data to each individual's maximum pain score may have produced stronger correlations between pain and strain, although these were not investigated within this thesis. Breast pain is known to negatively affect a high proportion of active females (Gehlsen & Albohm, 1980), so the development of improved breast pain assessment methods represents a worthy area of future research. An improved quantification of breast pain may enable the causes of breast pain to be better understood and improved solutions to be developed.

9.3. Conclusions

This programme of work was the first to obtain accurate (measurement errors ≤ 1.4 mm) and precise (TEMs ≤ 1.2 mm, SDs ≤ 3.7 mm) gold-standard measurements of the neutral breast position using the buoyant force from both water and soybean oil. Gold-standard neutral breast position measurements were used to evaluate the accuracy and precision of alternative neutral position methods, and to investigate the relationships between breast motion, breast damage, and breast pain. Results demonstrated that:

- The gold-standard neutral nipple position was anterior, medial, and superior to the gravity-loaded nipple position.
- Alternative neutral breast position methods did not produce accurate and precise estimates of the gold-standard neutral nipple position.
- The nipple displaced furthest from the neutral nipple position in the inferior direction during treadmill activity.
- Breast pain was most strongly correlated to superior nipple displacement from the neutral nipple position during treadmill activity.
- Gravity induced potentially damaging static breast skin strains (up to 75%).
- Potentially damaging skin strains were present at all stages (4 kph to 14 kph) of an incremental-speed treadmill test (up to 114%), particularly in the longitudinal direction in the upper-outer region of the breast.
- Skin strain data across the breast surface complied with the anticipated behaviour of the breast based on static and dynamic displacements of the nipple.

Incorporation of the neutral breast position into future breast research may lead to an improved understanding of the effect of gravity on the breast; more appropriate assessment of breast motion and breast damage; and a deeper understanding of motion-induced breast pain. Development of breast support garments that position the breast in the neutral position and restrict motion to within the reversible strain limits of the skin may protect the breast from gravity- and motion-induced skin damage and the associated breast pain.

References

- Ader, D., & Shriver, C. (1998). Update on clinical and research issues in cyclical mastalgia. *The Breast Journal*, 4(1), 25–32.
- Akin, D., & Howard, R. (1992). Neutral buoyancy simulation of space telerobotics operations. In *SPIE 1612, Cooperative Intelligent Robotics in Space II* (p. 414).
- Al-Himdani, S., Ud-Din, S., Gilmore, S., & Bayat, A. (2014). Striae distensae: A comprehensive review and evidence-based evaluation of prophylaxis and treatment. *British Journal of Dermatology*, 170, 527–547. <http://doi.org/10.1111/bjd.12681>
- Anscombe, F. (1973). Graphs in statistical analysis. *The American Statistician*, 21(1), 17–21. <http://doi.org/10.1038/nmeth.1829>
- Archambeau, J., Pezner, R., & Wasserman, T. (1995). Pathophysiology of irradiated skin and breast. *International Journal of Radiation Oncology, Biology, Physics*, 31(5), 1171–1185.
- Armstrong, A., & Jones, B. (2000). Patient satisfaction with Trilucent (TM) breast implants. *British Journal of Plastic Surgery*, 53(6), 479–483. <http://doi.org/10.1054/bjps.2000.3386>
- Atkinson, G., & Nevill, A. (1998). Statistical methods for assessing measurement error (reliability) in variables relevant to sports medicine. *Sports Medicine*, 26(4), 217–238.
- Aung, S., Ngim, R., & Lee, S. (1995). Evaluation of the laser scanner as a surface measuring tool and its accuracy compared with direct facial anthropometric measurements. *British Journal of Plastic Surgery*, 48(8), 551–558. Retrieved from <http://www.ncbi.nlm.nih.gov/pubmed/8548155>
- Avşar, D., Aygıt, A., Benlier, E., Top, H., & Taşkinalp, O. (2010). Anthropometric breast measurement: a study of 385 Turkish female students. *Aesthetic Surgery Journal*, 30(1), 44–50. <http://doi.org/10.1177/1090820X09358078>
- Azar, F., Metaxas, D., & Schnall, M. (2002). Methods for modeling and predicting mechanical deformations of the breast under external perturbations. *Medical Image Analysis*, 6(1), 1–27.
- Baines, C. (1998). Menstrual cycle variation in mammographic breast density: So who cares? *Journal of the National Cancer Institute*, 90(12), 875–876.
- Barbosa, A., Raggi, G., dos Santos Cardoso Sa, C., Costa, M., de Lima Jr, J., & Tanaka, C. (2012). Postural control in women with breast hypertrophy. *Clinics*, 67(7), 757–760. [http://doi.org/10.6061/clinics/2012\(07\)09](http://doi.org/10.6061/clinics/2012(07)09)

- Batterham, A., & George, K. (2000). Reliability in evidence-based clinical practice: a primer for allied health professionals. *Physical Therapy in Sport, 1*(2), 54–62. <http://doi.org/10.1054/ptsp.2000.0010>.
- Batterham, A., & Hopkins, W. (2006). Making meaningful inferences about magnitudes. *International Journal of Sports Physiology and Performance, 1*(1), 50–57. Retrieved from <http://www.ncbi.nlm.nih.gov/pubmed/19114737>
- Beck, T., Foerster, E., Buchröder, H., Schmidt, V., & Döring, J. (2014). The measurement accuracy of passive radon instruments. *Radiation Protection Dosimetry, 158*(1), 59–67. <http://doi.org/10.1093/rpd/nct182>
- Belavý, D., Miokovic, T., Armbrecht, G., Richardson, C., Rittweger, J., & Felsenberg, D. (2009). Differential atrophy of the lower-limb musculature during prolonged bed-rest. *European Journal of Applied Physiology, 107*(4), 489–99. <http://doi.org/10.1007/s00421-009-1136-0>
- Bennett, M. (2009). *Differences in upper body posture and postural muscle activation in females with larger breast sizes. (Unpublished masters thesis)*. Boise State University.
- Berthier, F., Potel, G., Leconte, P., Touze, M.-D., & Baron, D. (1998). Comparative study of methods of measuring acute pain intensity in an ED. *The American Journal of Emergency Medicine, 16*, 132–136. [http://doi.org/10.1016/S0735-6757\(98\)90029-8](http://doi.org/10.1016/S0735-6757(98)90029-8)
- Betzler, N. (2010). *The effect of differing shaft dynamics on the biomechanics of the golf swing. (Unpublished doctoral thesis)*. Edinburgh Napier University.
- Bijur, P., Latimer, C., & Gallagher, E. (2003). Validation of a verbally administered numerical rating scale of acute pain for use in the emergency department. *Academic Emergency Medicine, 10*(4), 390–392. <http://doi.org/10.1197/aemj.10.4.390>
- Bland, J., & Altman, D. (1986). Statistical methods for assessing agreement between two methods of clinical measurement. *Lancet, 327*(8476), 307–10. Retrieved from <http://www.ncbi.nlm.nih.gov/pubmed/2868172>
- Boschma, A. (1994). *Breast support for the active woman: relationship to 3D kinematics of running. (Unpublished masters thesis)*. Oregon State University, Corvallis.
- Bowles, K. (2012). *Sports bra design for active women. (Unpublished doctoral thesis)*. University of Wollongong.
- Bowles, K., Steele, J., & Munro, B. (2008). What are the breast support choices of Australian women during physical activity? *British Journal of Sports Medicine, 42*(8), 670–673. <http://doi.org/10.1136/bjism.2008.046219>
- Boyd, N., Lockwood, G., Byng, J., Little, L., Yaffe, M., & Tritchler, D. (1998). The relationship of anthropometric measures to radiological features of the breast in premenopausal women. *British Journal of Cancer, 78*(9), 1233–1238.

- Boyd, N., Lockwood, G., Byng, J., Tritchler, D., & Yaffe, M. (1998). Mammographic densities and breast cancer risk. *Cancer Epidemiology, Biomarkers & Prevention*, 7(12), 1133–44. Retrieved from <http://www.ncbi.nlm.nih.gov/pubmed/9865433>
- Brahmbhatt, S., Sattigeri, B., Shah, H., Kumar, A., & Parikh, D. (2013). A prospective survey study on premenstrual syndrome in young and middle aged women with an emphasis on its management. *International Journal of Research in Medical Sciences*, 1(2), 69–72. <http://doi.org/10.5455/2320-6012.ijrms20130506>
- Bridgman, C., Scurr, J., White, J., Hedger, W., & Galbraith, H. (2010). Three-dimensional kinematics of the breast during a two-step star jump. *Journal of Applied Biomechanics*, 26(4), 465–472. Retrieved from <http://www.ncbi.nlm.nih.gov/pubmed/21245506>
- Brown, N., White, J., Brasher, A., & Scurr, J. (2014). The experience of breast pain (mastalgia) in female runners of the 2012 London Marathon and its effect on exercise behaviour. *British Journal of Sports Medicine*, 48(4), 320–325. <http://doi.org/10.1136/bjsports-2013-092175>
- Brown, N., White, J., Milligan, A., Risius, D., Ayres, B., Hedger, W., & Scurr, J. (2012). The relationship between breast size and anthropometric characteristics. *American Journal of Human Biology*, 24(2), 158–64. <http://doi.org/10.1002/ajhb.22212>
- Brown, T., Ringrose, C., Hyland, R., Cole, A., & Brotherston, T. (1999). A method of assessing female breast morphometry and its clinical application. *British Journal of Plastic Surgery*, 52(5), 355–359. <http://doi.org/10.1054/bjps.1999.3110>
- Bruton, A., Conway, J., & Holgate, S. (2000). Reliability: What is it, and how is it measured? *Physiotherapy*, 86(2), 94–99.
- Burnett, E., White, J., & Scurr, J. (2014). The influence of the breast on physical activity participation in females. *Journal of Physical Activity & Health*. <http://doi.org/http://dx.doi.org/10.1123/jpah.2013-0236>
- Camomilla, V., Donati, M., Stagni, R., & Cappozzo, A. (2009). Non-invasive assessment of superficial soft tissue local displacements during movement: a feasibility study. *Journal of Biomechanics*, 42(7), 931–7. <http://doi.org/10.1016/j.jbiomech.2009.01.008>
- Campbell, T., Munro, B., Wallace, G., & Steele, J. (2007). Can fabric sensors monitor breast motion? *Journal of Biomechanics*, 40(13), 3056–3059. <http://doi.org/10.1016/j.jbiomech.2007.01.020>
- Cappellini, G., Ivanenko, Y., Poppele, R., & Lacquaniti, F. (2006). Motor patterns in human walking and running. *Journal of Neurophysiology*, 95(6), 3426–3437. <http://doi.org/10.1152/jn.00081.2006>

- Cappozzo, A., Della Croce, U., Leardini, A., & Chiari, L. (2005). Human movement analysis using stereophotogrammetry. Part 1: theoretical background. *Gait & Posture*, *21*(2), 186–96. <http://doi.org/10.1016/j.gaitpost.2004.01.010>
- Cargill. (2009). Material safety data sheet: RBD soybean oil.
- Carmichael, S. (2014). The tangled web of Langer's lines. *Clinical Anatomy*, *27*(2), 162–168. <http://doi.org/10.1002/ca.22278>
- Cavanagh, P., Licata, A., & Rice, A. (2005). Exercise and pharmacological countermeasures for bone loss during long-duration space flight. *Gravitational and Space Biology*, *18*(2), 39–58.
- Chadbourne, E., Zhang, S., Gordon, M., Ro, E., Ross, S., Schnur, P., & Schneider-Redden, P. (2001). Clinical outcomes in reduction mammoplasty: a systematic review and meta-analysis of published studies. *Mayo Clinic Proceedings*, *76*(5), 503–510.
- Chan, S., Su, M.-Y., Lei, F.-J., Wu, J.-P., Lin, M., Nalcioglu, O., ... Chen, J.-H. (2011). Menstrual cycle-related fluctuations in breast density measured by using three-dimensional MR imaging. *Radiology*, *261*(3), 744–51. <http://doi.org/10.1148/radiol.11110506>
- Chandrashekar, N., Mansouri, H., Slauterbeck, J., & Hashemi, J. (2006). Sex-based differences in the tensile properties of the human anterior cruciate ligament. *Journal of Biomechanics*, *39*(16), 2943–2950. <http://doi.org/10.1016/j.jbiomech.2005.10.031>
- Chang, A., Agredano, Y., & Kimball, A. (2004). Risk factors associated with striae gravidarum. *Journal of the American Academy of Dermatology*, *51*, 881–885. <http://doi.org/10.1016/j.jaad.2004.05.030>
- Chen, C.-M., LaBat, K., & Bye, E. (2011). Bust prominence related to bra fit problems. *International Journal of Consumer Studies*, *35*(6), 695–701. <http://doi.org/10.1111/j.1470-6431.2010.00984.x>
- Chen, J., Zhou, L., Zhang, Y., & Ferreiro, D. (2013). Human motion tracking with wireless wearable sensor network: experience and lessons. *KSII Transactions on Internet and Information Systems*, *7*(5), 998–1014.
- Chen, L., Ng, S.-P., Yu, W., Zhou, J., & Wan, K. (2013). A study of breast motion using non-linear dynamic FE analysis. *Ergonomics*, *56*(5), 868–78. <http://doi.org/10.1080/00140139.2013.777798>
- Chen, X., Wang, J., & Jiang, D. (2012). Can nipple be used as a good indicator of breast in breast motion research? *World Academy of Science, Engineering and Technology*, *71*, 1008–1011.

- Chiari, L., Della Croce, U., Leardini, A., & Cappozzo, A. (2005). Human movement analysis using stereophotogrammetry. Part 2: instrumental errors. *Gait & Posture*, *21*(2), 197–211. <http://doi.org/10.1016/j.gaitpost.2004.04.004>
- Chu, D., LeBlanc, R., D'Ambrosia, P., D'Ambrosia, R., Baratta, R., & Solomonow, M. (2003). Neuromuscular disorder in response to anterior cruciate ligament creep. *Clinical Biomechanics*, *18*, 222–230. [http://doi.org/10.1016/S0268-0033\(03\)00002-0](http://doi.org/10.1016/S0268-0033(03)00002-0)
- Chuang, G., & Gilchrest, B. (2012). Ultraviolet-fluorescent tattoo location of cutaneous biopsy site. *Dermatologic Surgery*, *38*(3), 479–483. <http://doi.org/10.1111/j.1524-4725.2011.02238.x>
- Ciatto, S., Visioli, C., Paci, E., & Zappa, M. (2004). Breast density as a determinant of interval cancer at mammographic screening. *British Journal of Cancer*, *90*(2), 393–396. <http://doi.org/10.1038/sj.bjc.6601548>
- Clark, J., Cheng, J., & Leung, K. (1996). Mechanical properties of normal skin and hypertrophic scars. *Burns*, *22*(6), 443–446.
- Coltman, K., McGhee, D., Riddiford-Harland, D., & Steele, J. (2013). Does breast size affect posture? In *24th Congress of the International Society of Biomechanics* (pp. 10–11). Brazil.
- Coutts, A., & Duffield, R. (2010). Validity and reliability of GPS devices for measuring movement demands of team sports. *Journal of Science and Medicine in Sport*, *13*, 133–135. <http://doi.org/10.1016/j.jsams.2008.09.015>
- Currell, K., & Jeukendrup, A. (2008). Validity, reliability and sensitivity of measures of sporting performance. *Sports Medicine*, *38*(4), 297–316. Retrieved from <http://www.ncbi.nlm.nih.gov/pubmed/18348590>
- D'Apuzzo, N. (2012). 3D human body scanning technologies overview, trends, applications. In *3rd International Conference and Exhibition on 3D Body Scanning Technologies* (pp. 1–49).
- Daly, C. (1982). Biomechanical properties of dermis. *The Journal of Investigative Dermatology*, *79* Suppl 1, 17s–20s. Retrieved from <http://www.ncbi.nlm.nih.gov/pubmed/7086188>
- De Groote, A., Wantier, M., Cheron, G., Estenne, M., & Paiva, M. (1997). Chest wall motion during tidal breathing. *Journal of Applied Physiology*, *83*, 1531–1537.
- Dehghani, H., Doyley, M., Pogue, B., Jiang, S., Geng, J., & Paulsen, K. (2004). Breast deformation modelling for image reconstruction in near infrared optical tomography. *Physics in Medicine and Biology*, *49*, 1131–1145. <http://doi.org/10.1088/0031-9155/49/7/004>

- Di Lernia, V., Bonci, A., Cattania, M., & Bisighini, G. (2001). Striae rubrae on the thighs of female monozygotic twins. *Pediatric Dermatology*, *18*(3), 261–264.
- Diorio, C., Pollak, M., Byrne, C., Mâsse, B., Hébert-Croteau, N., Yaffe, M., ... Brisson, J. (2005). Insulin-like growth factor-I, IGF-binding protein-3, and mammographic breast density. *Cancer Epidemiology, Biomarkers & Prevention*, *14*(5), 1065–1073. <http://doi.org/10.1158/1055-9965.EPI-04-0706>
- Duan, Z., Yuan, Z., Liao, X., Si, W., & Zhao, J. (2011). 3D tracking and positioning of surgical instruments in virtual surgery simulation. *Journal of Multimedia*, *6*(6), 502–510. <http://doi.org/10.4304/jmm.6.6.502-509>
- Dufaye, G., Cherouat, A., & Bachmann, J. (2013). Advanced modelling of the mechanical behaviour of biological tissues: application to 3D breast deformation. *Computer Methods in Biomechanics and Biomedical Engineering*, *16*(S1), 305–307. <http://doi.org/10.1080/10255842.2013.815917>
- Duric, N., Boyd, N., Littrup, P., Sak, M., Myc, L., Li, C., ... Albrecht, T. (2013). Breast density measurements with ultrasound tomography: A comparison with film and digital mammography. *Medical Physics*, *40*(1), 1–12.
- Durnin, J., & Womersley, J. (1974). Body fat assessed from total body density and its estimation from skinfold thickness: measurements on 481 men and women aged from 16 to 72 years. *British Journal of Nutrition*, *32*(01), 77–97. <http://doi.org/10.1079/BJN19740060>
- Edes, B., & Dallenbach, K. (1936). The adaptation of pain aroused by cold. *The American Journal of Psychology*, *48*(2), 307–315.
- Edgecomb, S., & Norton, K. (2006). Comparison of global positioning and computer-based tracking systems for measuring player movement distance during Australian football. *Journal of Science and Medicine in Sport*, *9*(1-2), 25–32. <http://doi.org/10.1016/j.jsams.2006.01.003>
- Edin, B. (2001). Cutaneous afferents provide information about knee joint movements in humans. *The Journal of Physiology*, *531*(1), 289–297. Retrieved from <http://www.pubmedcentral.nih.gov/articlerender.fcgi?artid=2278439&tool=pmcentrez&rendertype=abstract>
- Edin, B. (2004). Quantitative analyses of dynamic strain sensitivity in human skin mechanoreceptors. *Journal of Neurophysiology*, *92*(6), 3233–3243. <http://doi.org/10.1152/jn.00628.2004>
- Edin, B., & Johansson, N. (1995). Skin strain patterns provide kinaesthetic information to the human central nervous system. *The Journal of Physiology*, *487*(1), 243–51. Retrieved from <http://www.pubmedcentral.nih.gov/articlerender.fcgi?artid=1156613&tool=pmcentrez&rendertype=abstract>

- Edsander-Nord, Å., Wickman, M., & Jurell, G. (1996). Measurement of breast volume with thermoplastic casts. *Scandinavian Journal of Plastic and Reconstructive Surgery and Hand Surgery*, 30(2), 129–132.
- Esteban, B., Riba, J.-R., Baquero, G., Rius, A., & Puig, R. (2012). Temperature dependence of density and viscosity of vegetable oils. *Biomass and Bioenergy*, 42, 164–171. <http://doi.org/10.1016/j.biombioe.2012.03.007>
- Farinella, G., Impoco, G., Gallo, G., Spoto, S., & Catanuto, G. (2006). Unambiguous analysis of woman breast shape for plastic surgery outcome evaluation. In *Eurographics Italian Chapter Conference (Vol. 1, pp. 255–261)*.
- Field, A. (2009). *Discovering statistics using SPSS*. Sage publications.
- Findley, W., & Davis, F. (2013). *Creep and relaxation of nonlinear viscoelastic materials*. Courier Corporation. [http://doi.org/10.1016/0032-3861\(78\)90187-8](http://doi.org/10.1016/0032-3861(78)90187-8)
- Finlay, B. (1970). Dynamic mechanical testing of human skin “in vivo”. *Journal of Biomechanics*, 3, 557–68.
- Fisher, G., Wang, Z., Datta, S., Varani, J., Kang, S., & Voorhees, J. (1997). Pathophysiology of premature skin aging induced by ultraviolet light. *The New England Journal of Medicine*, 337(20), 1419–1428. <http://doi.org/10.1056/NEJM199711133372003>
- Flynn, C., Taberner, A., & Nielsen, P. (2011). Measurement of the force-displacement response of *in vivo* human skin under a rich set of deformations. *Medical Engineering & Physics*, 33(5), 610–619. <http://doi.org/10.1016/j.medengphy.2010.12.017>
- Fotouh, S. (2006). Augmentation of asymmetric breasts. *Egyptian Journal of Plastic and Reconstructive Surgery.*, 30(1), 63–67.
- Fujimura, T., Haketa, K., Hotta, M., & Kitahara, T. (2007). Loss of skin elasticity precedes to rapid increase of wrinkle levels. *Journal of Dermatological Science*, 47(3), 233–239. <http://doi.org/10.1016/j.jdermsci.2007.05.002>
- Gallagher, A., Ní Anniadh, A., Bruyere, K., Otténio, M., Xie, H., & Gilchrist, M. (2012). Dynamic tensile properties of human skin. In *2012 IRCOBI Conference Proceedings. International Research Council on the Biomechanics of Injury*.
- Gambichler, T., Matip, R., Moussa, G., Altmeyer, P., & Hoffmann, K. (2006). *In vivo* data of epidermal thickness evaluated by optical coherence tomography: effects of age, gender, skin type, and anatomic site. *Journal of Dermatological Science*, 44(3), 145–152. <http://doi.org/10.1016/j.jdermsci.2006.09.008>
- Gao, B., & Zheng, N. (2008). Investigation of soft tissue movement during level walking: translations and rotations of skin markers. *Journal of Biomechanics*, 41(15), 3189–3195. <http://doi.org/10.1016/j.jbiomech.2008.08.028>

- Gao, Z., & Desai, J. (2010). Estimating zero-strain states of very soft tissue under gravity loading using digital image correlation. *Medical Image Analysis*, *14*(2), 126–137. <http://doi.org/10.1016/j.media.2009.11.002>
- Gapstur, S., López, P., Colangelo, L., Wolfman, J., Van Horn, L., & Hendrick, R. (2003). Associations of breast cancer risk factors with breast density in Hispanic women. *Cancer Epidemiology, Biomarkers & Prevention*, *12*(10), 1074–1080.
- Gefen, A., & Dilmoney, B. (2007). Mechanics of the normal woman's breast. *Technology and Health Care*, *15*, 259–271.
- Gehlsen, G., & Albohm, M. (1980). Evaluation of sports bras. *The Physician and Sportsmedicine*, *8*(10), 89–96.
- Ghosh, K., Brandt, K., Sellers, T., Reynolds, C., Scott, C., Maloney, S., ... Vachon, C. (2008). Association of mammographic density with the pathology of subsequent breast cancer among postmenopausal women. *Cancer Epidemiology, Biomarkers & Prevention*, *17*(4), 872–879. <http://doi.org/10.1158/1055-9965.EPI-07-0559>
- Giakas, G., & Baltzopoulos, V. (1997a). A comparison of automatic filtering techniques applied to biomechanical walking data. *Journal of Biomechanics*, *30*(8), 847–850.
- Giakas, G., & Baltzopoulos, V. (1997b). Optimal digital filtering requires a different cut-off frequency strategy for the determination of the higher derivatives. *Journal of Biomechanics*, *30*(8), 851–855.
- Gibson, T., Stark, H., & Evans, J. (1969). Directional variation in extensibility of human skin *in vivo*. *Journal of Biomechanics*, *2*(2), 201–204. Retrieved from <http://www.ncbi.nlm.nih.gov/pubmed/16335105>
- Gierach, G., Loud, J., Chow, C., Prindiville, S., Eng-Wong, J., Soballe, P., ... Greene, M. (2011). Mammographic density does not differ between unaffected BRCA1/2 mutation carriers and women at low-to-average risk of breast cancer. *Breast Cancer Research and Treatment*, *123*(1), 245–255. <http://doi.org/10.1007/s10549-010-0749-7>.Mammographic
- Gilmore, S., Vaughan, B., Madzvamuse, A., & Maini, P. (2012). A mechanochemical model of striae distensae. *Mathematical Biosciences*, *240*(2), 141–147. <http://doi.org/10.1016/j.mbs.2012.06.007>
- Gissane, C. (2012). The P value, do you know what it means? *Physiotherapy Practise and Research*, *33*, 105–106. <http://doi.org/10.3233/PPR-2012-0004>
- Gissane, C. (2013). Extracting meaning from research – using confidence intervals. *Physiotherapy Practise and Research*, *34*(1), 47–49. <http://doi.org/10.3233/PPR-2012-0010>

- Gopinath, P., Wan, E., Holdcroft, A., Facer, P., Davis, J., Smith, G., ... Anand, P. (2005). Increased capsaicin receptor TRPV1 in skin nerve fibres and related vanilloid receptors TRPV3 and TRPV4 in keratinocytes in human breast pain. *BMC Women's Health*, 5(1), 2. <http://doi.org/10.1186/1472-6874-5-2>
- Graham, S., Bronskill, M., Byng, J., Yaffe, M., & Boyd, N. (1996). Quantitative correlation of breast tissue parameters using magnetic resonance and X-ray mammography. *British Journal of Cancer*, 73(2), 162–168.
- Gram, I., Bremnes, Y., Ursin, G., Maskarinec, G., Bjurstam, N., & Lund, E. (2005). Percentage density, Wolfe's and Tabár's mammographic patterns: agreement and association with risk factors for breast cancer. *Breast Cancer Research*, 7(5), R854–R861. <http://doi.org/10.1186/bcr1308>
- Greenbaum, A., Heslop, T., Morris, J., & Dunn, K. (2003). An investigation of the suitability of bra fit in women referred for reduction mammoplasty. *British Journal of Plastic Surgery*, 56(3), 230–236. [http://doi.org/10.1016/S0007-1226\(03\)00122-X](http://doi.org/10.1016/S0007-1226(03)00122-X)
- Griffin, M. (2004). Beating the bounce. *The Age*, August(1), 1. Retrieved from www.theage.com.au/articles/2004/08/27/1093518087807.html?oneclick=true.
- Griffiths, A., & Murphy, F. (2012). The use of henna as an alternative skin marker in breast disease. *Radiography*, 18(4), 279–286. <http://doi.org/10.1016/j.radi.2012.05.003>
- Gunkel, A., & Handler, J. (1969). A Swiss medical doctor's description of Barbados in 1661. *The Journal of the Barbados Museum and Historical Society*, (33), 3–13.
- Gutierrez-Farewik, E., Bartonek, A., & Saraste, H. (2006). Comparison and evaluation of two common methods to measure center of mass displacement in three dimensions during gait. *Human Movement Science*, 25(2), 238–256. <http://doi.org/10.1016/j.humov.2005.11.001>
- Haake, S., Milligan, A., & Scurr, J. (2012). Can measures of strain and acceleration be used to predict breast discomfort during running? *Journal of Sports Engineering and Technology*, 227(3), 209–216. <http://doi.org/10.1177/1754337112456799>
- Haake, S., & Scurr, J. (2010). A dynamic model of the breast during exercise. *Sports Engineering*, 12(4), 189–197. <http://doi.org/10.1007/s12283-010-0046-z>
- Haake, S., & Scurr, J. (2011). A method to estimate strain in the breast during exercise. *Sports Engineering*, 14(1), 49–56. <http://doi.org/10.1007/s12283-011-0071-6>
- Haars, G., van Noord, P., van Gils, C., Grobbee, D., & Peeters, P. (2005). Measurements of breast density: no ratio for a ratio. *Cancer Epidemiology, Biomarkers & Prevention*, 14(11 Pt 1), 2634–2640. <http://doi.org/10.1158/1055-9965.EPI-05-0824>
- Hadi, M. (2000). Sports brassiere: Is it a solution for mastalgia? *The Breast Journal*, 6(6), 407–409. Retrieved from <http://www.ncbi.nlm.nih.gov/pubmed/11348400>

- Hansson, E., Manjer, J., & Ringberg, A. (2014). Inter-observer reliability of clinical measurement of suprasternal notch-nipple distance and breast ptosis. *Indian Journal of Plastic Surgery*, *47*(1), 61. <http://doi.org/10.4103/0970-0358.129625>
- Harvey, J., & Bovbjerg, V. (2004). Quantitative assessment of mammographic breast density: relationship with breast cancer risk. *Radiology*, *230*(1), 29–41.
- Hassiotou, F., & Geddes, D. (2012). Anatomy of the human mammary gland: current status of knowledge. *Clinical Anatomy*, *000*(July). <http://doi.org/10.1002/ca.22165>
- Haut, R. (1989). The effects of orientation and location on the strength of dorsal rat skin in high and low speed tensile failure experiments. *Journal of Biomechanical Engineering*, *111*(2), 136–140.
- Heath, T. (1897). *The works of Archimedes*. Cambridge: University Press.
- Heng, D., Gao, F., Jong, R., Fishell, E., Yaffe, M., Martin, L., ... Boyd, N. (2004). Risk factors for breast cancer associated with mammographic features in singaporean chinese women. *Cancer Epidemiology, Biomarkers & Prevention*, *13*(11), 1751–1758.
- Hennessey, S., Huszti, E., Gunasekura, A., Salleh, A., Martin, L., Minkin, S., ... Boyd, N. (2014). Bilateral symmetry of breast tissue composition by magnetic resonance in young women and adults. *Cancer Causes & Control*, *25*(4), 491–7. <http://doi.org/10.1007/s10552-014-0351-0>
- Henry, F., Piérard-Franchimont, C., Pans, A., & Piérard, G. (1997). Striae distensae of pregnancy. An *in vivo* biomechanical evaluation. *International Journal of Dermatology*, *36*, 506–508.
- Henseler, H., Khambay, B., Bowman, A., Smith, J., Siebert, J., Oehler, S., ... Ray, A. (2011). Investigation into accuracy and reproducibility of a 3D breast imaging system using multiple stereo cameras. *Journal of Plastic, Reconstructive & Aesthetic Surgery*, *64*(5), 577–582. <http://doi.org/10.1016/j.bjps.2010.08.044>
- Henseler, H., Smith, J., Bowman, A., Khambay, B., Ju, X., Ayoub, A., & Ray, A. (2013). Subjective versus objective assessment of breast reconstruction. *Journal of Plastic, Reconstructive & Aesthetic Surgery*, *66*(5), 634–9. <http://doi.org/10.1016/j.bjps.2013.01.006>
- Hermanns, J.-F., & Piérard, G. (2006). High-resolution epiluminescence colorimetry of striae distensae. *Journal of the European Academy of Dermatology and Venereology*, *20*, 282–287. <http://doi.org/10.1111/j.1468-3083.2006.01426.x>
- Heymsfield, S., Wang, J., Kehayias, J., Heshka, S., Lichtman, S., & Pierson Jr, R. (1989). Chemical determination of human body density *in vivo*: relevance to hydrodensitometry. *The American Journal of Clinical Nutrition*, *50*(6), 1282–1289.

- Hindle, W. (1991). The breast and exercise. In *Caring for the exercising woman*. (pp. 83–92). New York: Elsevier Science Publishing.
- Hirsch, C., Ingelmark, B.-E., & Miller, M. (1960). The anatomical basis for low back pain: Studies on the presence of sensory nerve endings in ligamentous, capsular and intervertebral disc structures in the human lumbar spine. *Acta Orthopaedica*, 33(1-4), 1–17.
- Hirshowitz, B., Kaufman, T., & Ullman, J. (1986). Reconstruction of the tip of the nose and ala by load cycling of the nasal skin and harnessing of extra skin. *Plastic and Reconstructive Surgery*, 77(2), 316–319. Retrieved from http://journals.lww.com/plasreconsurg/Abstract/1986/02000/Reconstruction_of_the_Tip_of_the_Nose_and_Ala_by.29.aspx
- Ho, K., Spence, J., & Murphy, M. (1996). Review of pain-measurement tools. *Annals of Emergency Medicine*, 27(4), 427–432.
- Hofstra, W., Sont, J., Sterk, P., Neijens, H., Kuethe, M., & Duiverman, E. (1997). Sample size estimation in studies monitoring exercise-induced bronchoconstriction in asthmatic children. *Thorax*, 52(8), 739–741. Retrieved from <http://www.pubmedcentral.nih.gov/articlerender.fcgi?artid=1758619&tool=pmcentrez&rendertype=abstract>
- Hopkins, W. (2000a). A new view of statistics.
- Hopkins, W. (2000b). Measures of reliability in sports medicine and science. *Sports Medicine*, 30(1), 1–15. <http://doi.org/10.2165/00007256-200030010-00001>
- Hopkins, W. (2001). Clinical vs statistical significance. *Sportscience*, 5(3), 1–4.
- Hopkins, W. (2002). Probabilities of clinical or practical significance. *Sportscience*, 6(201), 589.
- Hopkins, W. (2004). Bias in Bland-Altman but not regression validity analyses. *Sportscience*, 8(4), 42–46.
- Huerta, D., Sosa, V., Vargas, M., & Ruiz-Suárez, J. (2005). Archimedes' principle in fluidized granular systems. *Physical Review E- Statistical, Nonlinear and Soft Matter Physics*, 72(3 Pt 1), 031307. <http://doi.org/10.1103/PhysRevE.72.031307>
- Hull, M., Berns, G., Varma, H., & Patterson, H. (1996). Strain in the medial collateral ligament of the human knee under single and combined loads. *Journal of Biomechanics*, 29(2), 199–206.
- Hunter, L., & Togan, C. (1985). The bra controversy: Are sports bras a necessity? *Plastic and Reconstructive Surgery*, 75(5), 781.

- Hussain, Z., Roberts, N., Whitehouse, G., García-Fiñana, M., & Percy, D. (1999). Estimation of breast volume and its variation during the menstrual cycle using MRI and stereology. *The British Journal of Radiology*, *72*(855), 236–245.
- Igarashi, T., Nishino, K., & Nayar, S. (2005). *The appearance of human skin. Technical report*. New York.
- Inui, M., Murase, K., & Tsutsumi, S. (2012). Investigation breasts' form and internal structure by wearing a brassiere from MRI images. *International Journal of Clothing Science and Technology*, *24*(2/3), 170–180.
- Issaacs, A. (2009). *Oxford dictionary of physics*. (Vol. 12). Oxford University Press. <http://doi.org/10.1063/1.3060976>
- Jacquet, E., Josse, G., Khatyr, F., & Garcin, C. (2008). A new experimental method for measuring skin's natural tension. *Skin Research and Technology*, *14*, 1–7. <http://doi.org/10.1111/j.1600-0846.2007.00259.x>
- Janiszewski, P., Saunders, T., & Ross, R. (2010). Breast volume is an independent predictor of visceral and ectopic fat in premenopausal women. *Obesity*, *18*(6), 1183–1187. <http://doi.org/10.1038/oby.2009.336>
- Jatoi, I., Kaufmann, M., & Petit, J. (2006). *Atlas of breast surgery*. Heidelberg: Springer.
- Jobson, S., Nevill, A., Palmer, G., Jeukendrup, A., Doherty, M., & Atkinson, G. (2007). *The ecological validity of laboratory cycling: Does body size explain the difference between laboratory- and field-based cycling performance?* *Journal of Sports Sciences* (Vol. 25). <http://doi.org/10.1080/02640410701619937>
- Kane, R., Bershady, B., Rockwood, T., Saleh, K., & Islam, N. (2005). Visual Analog Scale pain reporting was standardized. *Journal of Clinical Epidemiology*, *58*(6), 618–623. <http://doi.org/10.1016/j.jclinepi.2004.11.017>
- Katariya, R., Forrest, A., & Gravelle, I. (1974). Breast volumes in cancer of the breast. *British Journal of Cancer*, *29*, 270–273.
- Katch, V., Campaigne, B., Freedson, P., Sady, S., Katch, F., & Behnke, A. (1980). Contribution of breast volume and weight to body fat distribution in females. *American Journal of Physical Anthropology*, *53*(1), 93–100. <http://doi.org/10.1002/ajpa.1330530113>
- Kececi, Y., & Sir, E. (2014). Prediction of resection weight in reduction mammoplasty based on anthropometric measurements. *Breast Care*, *9*(1), 41–45. <http://doi.org/10.1159/000358753>
- Kelemen, L., Pankratz, V., Sellers, T., Brandt, K., Wang, A., Janney, C., ... Vachon, C. (2008). Age-specific trends in mammographic density: the Minnesota breast cancer family

- study. *American Journal of Epidemiology*, 167(9), 1027–1036. <http://doi.org/10.1093/aje/kwn063>
- Kell, G. (1975). Density, thermal expansivity, and compressibility of liquid water from 0° to 150°C: correlations and tables for atmospheric pressure and saturation reviewed and expressed on 1968 temperature scale. *Journal of Chemical and Engineering Data*, 20(1), 97–105.
- Keller, T., Weisberger, A., Ray, J., Hasan, S., Shiavi, R., & Spengler, D. (1996). Relationship between vertical ground reaction force and speed during walking, slow jogging, and running. *Clinical Biomechanics*, 11(5), 253–259. [http://doi.org/10.1016/0268-0033\(95\)00068-2](http://doi.org/10.1016/0268-0033(95)00068-2)
- Kelly, J., & Sale, C. (2008). Validity and reliability of body composition measurement using the TANITA BC418-MA. In *Annual Conference of the British Association of Sport and Exercise Sciences* (Vol. 26 Suppl 2, pp. S106–S107). <http://doi.org/10.1080/02640410802306202>
- Kiernan, J., & Rajakumar, R. (2013). *Barr's the human nervous system: An anatomical viewpoint*. (Wilkins. & Williams, Eds.). Lippincott.
- Kikufuji, N., & Tokura, H. (2002). Disturbance of the duration of the menstrual cycle under the influence of tight clothing. *Biological Rhythm Research*, 33(3), 279–285.
- Kim, M., Reece, G., Beahm, E., Miller, M., Atkinson, E., & Markey, M. (2007). Objective assessment of aesthetic outcomes of breast cancer treatment: measuring ptosis from clinical photographs. *Computers in Biology and Medicine*, 37(1), 49–59. <http://doi.org/10.1016/j.compbiomed.2005.10.007>
- Kim, M., Sbalchiero, J., Reece, G., Miller, M., Beahm, E., & Markey, M. (2008). Assessment of breast aesthetics. *Plastic and Reconstructive Surgery*, 121(4), 186e–194e. <http://doi.org/10.1097/01.prs.0000304593.74672.b8.Assessment>
- Klein, L., Heiple, K., Torzilli, P., Goldberg, V., & Burstein, A. (1989). Prevention of ligament and meniscus atrophy by active joint motion in a non-weight-bearing model. *Journal of Orthopaedic Research*, 7(1), 80–85.
- Knight, M., Wheat, J., Driscoll, H., & Haake, S. (2014). A novel method to find the neutral position of the breast. *Procedia Engineering*, 72, 20–25. <http://doi.org/10.1016/j.proeng.2014.06.007>
- Knudson, D. (2009). Significant and meaningful effects in sports biomechanics research. *Sports Biomechanics*, 8(1), 96–104. <http://doi.org/10.1080/14763140802629966>
- Koff, E., & Benavage, A. (1998). Breast size perception and satisfaction , body image , and psychological functioning in Caucasian and Asian American college women. *Sex Roles*, 38(7), 655–673.

- Kontaxis, A., Cutti, A., Johnson, G., & Veeger, H. (2009). A framework for the definition of standardized protocols for measuring upper-extremity kinematics. *Clinical Biomechanics*, 24(3), 246–253. <http://doi.org/10.1016/j.clinbiomech.2008.12.009>
- Kopans, D. (2008). Basic physics and doubts about relationship between mammographically determined tissue density and breast cancer risk. *Radiology*, 246(2), 348–353.
- Kornguth, P., Keefe, F., & Conaway, M. (1996). Pain during mammography: characteristics and relationship to demographic and medical variables. *Pain*, 66(2-3), 187–194. Retrieved from <http://www.ncbi.nlm.nih.gov/pubmed/8880840>
- Kowalski, K. (1989). *Applications of a three-dimensional position and attitude sensing system for neutral buoyancy space simulation. (Unpublished masters thesis)*. Massachusetts Institute of Technology.
- Krenzer, G., Starr, C., & Branson, D. (2005). Development of a sports bra prototype. *Clothing and Textiles Research Journal*, 23(2), 131–134. <http://doi.org/10.1177/0887302X0502300206>
- Kwon, Y.-H., & Casebolt, J. (2006). Effects of light refraction on the accuracy of camera calibration and reconstruction in underwater motion analysis. *Sports Biomechanics*, 5(2), 315–340. <http://doi.org/10.1080/14763140608522881>
- Lamb, K., Eston, R., & Corns, D. (1999). Reliability of ratings of perceived exertion during progressive treadmill exercise. *British Journal of Sports Medicine*, 33(5), 336–339. Retrieved from <http://www.pubmedcentral.nih.gov/articlerender.fcgi?artid=1756195&tool=pmcentrez&rendertype=abstract>
- Langer, K. (1861). *Zur anatomie und physiologie der haut*.
- Leardini, A., Chiari, L., Della Croce, U., & Cappozzo, A. (2005). Human movement analysis using stereophotogrammetry. Part 3. Soft tissue artifact assessment and compensation. *Gait & Posture*, 21(2), 212–25. <http://doi.org/10.1016/j.gaitpost.2004.05.002>
- Lee, A. (2011). *Breast image fusion using biomechanics. (Unpublished doctoral thesis)*. The University of Auckland.
- Lee, H.-E., Kim, S., Choi, C., Bang, W.-C., Kim, J., & Kim, C. (2012). High-precision 6-DOF motion tracking architecture with compact low-cost sensors for 3D manipulation. In *IEEE International Conference on Consumer Electronics* (pp. 193–194). <http://doi.org/10.1109/ICCE.2012.6161824>
- Lee, H.-Y., Hong, K., Kim, E., & Ae, E. (2004). Measurement protocol of women's nude breasts using a 3D scanning technique. *Applied Ergonomics*, 35(4), 353–359. <http://doi.org/10.1016/j.apergo.2004.03.004>

- Lee, K., Rho, Y., Jang, S., Suh, M., & Song, J. (1994). Decreased expression of collagen and fibronectin genes in striae distensae tissue. *Clinical and Experimental Dermatology*. <http://doi.org/10.1111/j.1365-2230.1994.tb01196.x>
- Lee, N., Rusinek, H., Weinreb, J., Chandra, R., Toth, H., Singer, C., & Newstead, G. (1997). Fatty and fibroglandular tissue volumes in the breasts of women 20-83 years old: comparison of X-ray mammography and computer-assisted MR imaging. *American Journal Of Roentgenology*, *168*(2), 501–506.
- Lemaine, V., & Simmons, P. (2013). The adolescent female: Breast and reproductive embryology and anatomy. *Clinical Anatomy*, *26*(1), 22–28. <http://doi.org/10.1002/ca.22167>
- Li, Y., Zhang, X., & Yeung, K. (2003). A 3D Biomechanical model for numerical simulation of dynamic mechanical interactions of bra and breast during wear. *Sen'i Gakkaishi*, *59*(1), 12–21.
- Lim, J., Hong, J., Chen, W., & Weerasooriya, T. (2011). Mechanical response of pig skin under dynamic tensile loading. *International Journal of Impact Engineering*, *38*(2-3), 130–135. <http://doi.org/10.1016/j.ijimpeng.2010.09.003>
- Lim, K., Chew, C., Chen, P., Jeyapalina, S., Ho, H., Rappel, J., & Lim, B. (2008). New extensometer to measure *in vivo* uniaxial mechanical properties of human skin. *Journal of Biomechanics*, *41*(5), 931–936. <http://doi.org/10.1016/j.jbiomech.2008.01.004>
- Losken, A., Fishman, I., Denson, D., Moyer, H., & Carlson, G. (2005). An objective evaluation of breast symmetry and shape differences using 3-dimensional images. *Annals of Plastic Surgery*, *55*(6), 571–575.
- Losken, A., Seify, H., Denson, D., Paredes, A., & Carlson, G. (2005). Validating three-dimensional imaging of the breast. *Annals of Plastic Surgery*, *54*(5), 471–476. Retrieved from <http://www.ncbi.nlm.nih.gov/pubmed/15838205>
- Lu, T.-W., & O'Connor, J. (1999). Bone position estimation from skin marker co-ordinates using global optimisation with joint constraints. *Journal of Biomechanics*, *32*(2), 129–134.
- Macéa, J., & Fregnani, J. (2006). Anatomy of the thoracic wall, axilla and breast. *International Journal of Morphology*, *24*(4), 691–704.
- MacNeil, J., & Boyd, S. (2007). Accuracy of high-resolution peripheral quantitative computed tomography for measurement of bone quality. *Medical Engineering & Physics*, *29*(10), 1096–1105. <http://doi.org/10.1016/j.medengphy.2006.11.002>
- Malini, S., O'Brian Smith, E., & Goldzieher, J. (1985). Measurement of breast volume by ultrasound during normal menstrual cycles and with oral contraceptive use. *Obstetrics & Gynecology*, *66*(4), 538–541.

- Mallucci, P., & Branford, O. (2012). Concepts in aesthetic breast dimensions: analysis of the ideal breast. *Journal of Plastic, Reconstructive & Aesthetic Surgery*, *65*(1), 8–16. <http://doi.org/10.1016/j.bjps.2011.08.006>
- Maltz, A., Bjerke, W., Belanger, M., Franzen, K., Brodsky, M., Sierpina, V., & Kreitzer, M. (2013). Evaluation and treatment of breast pain: an integrative medicine learning activity. *The Journal of Science and Healing*, *9*(4), 255–259. <http://doi.org/10.1016/j.explore.2013.04.011>
- Manning, J., Scutt, D., Whitehouse, G., & Leinster, S. (1997). Breast asymmetry and phenotypic quality in women. *Evolution and Human Behavior*, *18*(4), 223–236.
- Manning, J., Scutt, D., Whitehouse, G., Leinster, S., & Walton, J. (1996). Asymmetry and the menstrual cycle in women. *Ethology and Sociobiology*, *17*(2), 129–143. [http://doi.org/10.1016/0162-3095\(96\)00001-5](http://doi.org/10.1016/0162-3095(96)00001-5)
- Markolf, K., Schmalzried, T., & Ferkel, R. (1989). Torsional strength of the ankle *in vitro*: The supination-external rotation injury. *Clinical Orthopaedics and Related Research*, *246*, 266–272. Retrieved from <http://www.ncbi.nlm.nih.gov/pubmed/2248656>
- Maskarinec, G., Meng, L., & Ursin, G. (2001). Ethnic differences in mammographic densities. *International Journal of Epidemiology*, *30*, 959–965.
- Maskarinec, G., Nagata, C., Shimizu, H., & Kashiki, Y. (2002). Comparison of mammographic densities and their determinants in women from Japan and Hawaii. *International Journal of Cancer*, *102*(1), 29–33. <http://doi.org/10.1002/ijc.10673>
- Maskarinec, G., Pagano, I., Lurie, G., Wilkens, L., & Kolonel, L. (2005). Mammographic density and breast cancer risk: the multiethnic cohort study. *American Journal of Epidemiology*, *162*(8), 743–752. <http://doi.org/10.1093/aje/kwi270>
- Maskarinec, G., Williams, A., & Kaaks, R. (2003). A cross-sectional investigation of breast density and insulin-like growth factor I. *International Journal of Cancer*, *107*(6), 991–996. <http://doi.org/10.1002/ijc.11505>
- Mason, B., Page, K.-A., & Fallon, K. (1999). An analysis of movement and discomfort of the female breast during exercise and the effects of breast support in three cases. *Science and Medicine in Sport*, *2*(2), 134–144.
- Mayagoitia, R., Nene, A., & Veltink, P. (2002). Accelerometer and rate gyroscope measurement of kinematics: an inexpensive alternative to optical motion analysis systems. *Journal of Biomechanics*, *35*(4), 537–542. Retrieved from <http://www.ncbi.nlm.nih.gov/pubmed/11934425>
- McArdle, W., Katch, F., & Katch, V. (2010). *Exercise physiology nutrition, energy, and human performance*. (Williams & Wilkins, Eds.). Lippincott.

- McGhee, D., & Steele, J. (2006). How do respiratory state and measurement method affect bra size calculations? *British Journal of Sports Medicine*, *40*(12), 970–974. <http://doi.org/10.1136/bjism.2005.025171>
- McGhee, D., & Steele, J. (2010a). Breast elevation and compression decrease exercise-induced breast discomfort. *Medicine and Science in Sports and Exercise*, *42*(7), 1333–1338.
- McGhee, D., & Steele, J. (2010b). Optimising breast support in female patients through correct bra fit. A cross-sectional study. *Journal of Science and Medicine in Sport*, *13*, 568–572. <http://doi.org/10.1016/j.jsams.2010.03.003>
- McGhee, D., & Steele, J. (2011). Breast volume and bra size. *International Journal of Clothing Science and Technology*, *23*(5), 351–360.
- McGhee, D., Steele, J., & Power, B. (2007). Does deep water running reduce exercise-induced breast discomfort? *British Journal of Sports Medicine*, *41*(12), 879–883. <http://doi.org/10.1136/bjism.2007.036251>
- McGhee, D., Steele, J., & Zealey, W. (2010). Effects of high and low breast support on breast kinematics and kinetics during treadmill running. *Journal of Science and Medicine in Sport*, *12*, e143. <http://doi.org/10.1016/j.jsams.2009.10.298>
- McGhee, D., Steele, J., Zealey, W., & Takacs, G. (2013). Bra-breast forces generated in women with large breasts while standing and during treadmill running: Implications for sports bra design. *Applied Ergonomics*, *44*(1), 112–118. <http://doi.org/10.1016/j.apergo.2012.05.006>
- Mead, J. (1960). Control of respiratory frequency. *Journal of Applied Physiology*, *15*, 325–336. Retrieved from <http://jap.physiology.org/content/15/3/325.short>
- Micheli, L., & Wood, R. (1995). Back pain in young athletes significant differences from adults in causes and patterns. *Archives of Pediatrics and Adolescent Medicine*, *149*(1), 15–18.
- Miller, J., & Stamford, B. (1987). Intensity and energy cost of weighted walking vs. running for men and women. *Journal of Applied Physiology*, *62*(4), 1497–1501.
- Miller, K. (2001). How to test very soft biological tissues in extension? *Journal of Biomechanics*, *34*(5), 651–657.
- Milligan, A. (2013). *The effect of breast support on running biomechanics. (Unpublished doctoral thesis)*. University of Portsmouth. Retrieved from <http://eprints.port.ac.uk/14846/>
- Milligan, A., Mills, C., & Scurr, J. (2014). Within-participant variance in multiplanar breast kinematics during five kilometre treadmill running. *Journal of Applied Biomechanics*.

- Milligan, D., Drife, J., & Short, R. (1975). Changes in breast volume during normal menstrual cycle and after oral contraceptives. *British Medical Journal*, 4(5995), 494–496.
- Mills, C., Lomax, M., Ayres, B., & Scurr, J. (2014). The movement of the trunk and breast during front crawl and breaststroke swimming. *Journal of Sports Sciences*, (September), 1–10. <http://doi.org/10.1080/02640414.2014.946951>
- Mills, C., Loveridge, A., Milligan, A., Risius, D., & Scurr, J. (2014a). Can axes conventions of the trunk reference frame influence breast displacement calculation during running? *Journal of Biomechanics*, 47(2), 575–578. <http://doi.org/10.1016/j.jbiomech.2013.11.041>
- Mills, C., Loveridge, A., Milligan, A., Risius, D., & Scurr, J. (2014b). Is torso soft tissue motion really an artefact within breast biomechanics research? *Journal of Biomechanics*, 47(11), 2606–2610. <http://doi.org/10.1016/j.jbiomech.2014.05.023>
- Mills, C., Risius, D., & Scurr, J. (2014). Breast motion asymmetry during running. *Journal of Sports Sciences*. <http://doi.org/10.1080/02640414.2014.962575>
- Mills, C., Scurr, J., & Wood, L. (2011). A protocol for monitoring soft tissue motion under compression garments during drop landings. *Journal of Biomechanics*, 44(9), 1821–1823. <http://doi.org/10.1016/j.jbiomech.2011.04.019>
- Moller, A., Soler, M., & Thornhill, R. (1995). Breast asymmetry, sexual selection, and human reproductive success. *Ethology and Sociobiology*, 16(3), 207–219.
- Monari, D., Desloovere, K., Bar-On, L., Molenaers, G., & Jaspers, E. (2013). The effect of different breast support conditions on multiplanar breast kinematics and kinetics during running. *Gait & Posture*, 38, S95. <http://doi.org/10.1016/j.gaitpost.2013.07.196>
- Moore, J., & Kennedy, S. (2000). Causes of chronic pelvic pain. *Baillière's Clinical Obstetrics and Gynaecology*, 14(3), 389–402. <http://doi.org/10.1053/beog.1999.0082>
- Morgan, J. (1997). “Some Could Suckle over Their Shoulder”: Male Travelers, Female Bodies, and the Gendering of Racial Ideology, 1500-1770. *The William and Mary Quarterly*, 54(1), 167–192.
- Mori, Y., Kioka, E., & Tokura, H. (2002). Effects of pressure on the skin exerted by clothing on responses of urinary catecholamines and cortisol, heart rate and nocturnal urinary melatonin in humans. *International Journal of Biometeorology*, 47(1), 1–5.
- Morrow Jr., J., & Jackson, A. (1993). How “significant” is your reliability? *Research Quarterly for Exercise and Sport*, 64(3), 352–355. Retrieved from <http://www.ncbi.nlm.nih.gov/pubmed/8235058>

- Nagy, E., Vicente-Rodriguez, G., Manios, Y., Béghin, L., Iliescu, C., Censi, L., ... Molnar, D. (2008). Harmonization process and reliability assessment of anthropometric measurements in a multicenter study in adolescents. *International Journal of Obesity*, 32(5), S58–S65. <http://doi.org/10.1038/ijo.2008.184>
- Nakanishi, Y., Kimura, T., & Yokoo, Y. (1999). Maximal physiological responses to deep water running at thermoneutral temperature. *Journal of Physiological Anthropology*, 18(2), 31–35. Retrieved from <http://www.ncbi.nlm.nih.gov/pubmed/10388156>
- Nasseri, M., Dean, E., Nair, S., Eder, M., Knoll, A., Maier, M., & Lohmann, C. (2012). Clinical motion tracking and motion analysis during ophthalmic surgery using electromagnetic tracking system. In *5th International Conference on BioMedical Engineering and Informatics* (pp. 1058–1062). <http://doi.org/10.1109/BMEI.2012.6512987>
- Newman, D. (1993). Human locomotion and workload for simulated lunar and Martian environments. *Acta Astronautica*, 29(8), 613–620.
- Ng, E., & Sudharsan, N. (2001). An improved three-dimensional direct numerical modelling and thermal analysis of a female breast with tumour. *Journal of Engineering in Medicine*, 215, 25–37. <http://doi.org/10.1243/0954411011533508>
- Ng, E., & Sudharsan, N. (2004). Computer simulation in conjunction with medical thermography as an adjunct tool for early detection of breast cancer. *BMC Cancer*, 4, 17. <http://doi.org/10.1186/1471-2407-4-17>
- Ní Annaidh, A., Bruyère, K., Destrade, M., Gilchrist, M., & Otténio, M. (2012). Characterization of the anisotropic mechanical properties of excised human skin. *Journal of the Mechanical Behavior of Biomedical Materials*, 5(1), 139–148. <http://doi.org/10.1016/j.jmbbm.2011.08.016>
- Nie, K., Chen, J.-H., Chan, S., Chau, M.-K., Yu, H., Bahri, S., ... Su, M.-Y. (2008). Development of a quantitative method for analysis of breast density based on three-dimensional breast MRI. *Medical Physics*, 35(12), 5253–5262. <http://doi.org/10.1118/1.3002306>
- Noyes, F., & Grood, E. (1976). The strength of the anterior cruciate ligament in humans and Rhesus monkeys. *The Journal of Bone and Joint Surgery*, 58, 1074–1082.
- Otténio, M., Tran, D., Ní Annaidh, A., Gilchrist, M., & Bruyère, K. (2014). Strain rate and anisotropy effects on the tensile failure characteristics of human skin. *Journal of the Mechanical Behavior of Biomedical Materials*. <http://doi.org/10.1016/j.jmbbm.2014.10.006>
- Page, K.-A., & Steele, J. (1999). Breast motion and sports brassiere design implications for future research. *Sports Medicine*, 27(4), 205–211.

- Parmar, C., West, M., Pathak, S., Nelson, J., & Martin, L. (2011). Weight versus volume in breast surgery: an observational study. *Journal of the Royal Society of Medicine Short Reports*, 2(11), 87. <http://doi.org/10.1258/shorts.2011.011070>
- Payton, C. (2008). Motion analysis using video. In *Biomechanical evaluation of movement in sport and exercise: the British Association of Sport and Exercise Sciences guidelines* (pp. 8–30).
- Pechter, E. (2008). An improved technique for determining bra size with applicability to breast surgery. *Plastic and Reconstructive Surgery*, 121(5), 348e–350e. <http://doi.org/10.1097/PRS.0b013e31816b1161>
- Popkin, B., & Doak, C. (1998). The obesity epidemic is a worldwide phenomenon. *Nutrition Reviews*, 56(4), 106–114.
- Price, G., Sharrock, P., Marchant, T., Parkhurst, J., Burton, D., Jain, P., ... Moore, C. (2009). An analysis of breast motion using high-frequency, dense surface points captured by an optical sensor during radiotherapy treatment delivery. *Physics in Medicine and Biology*, 54(21), 6515–6533. <http://doi.org/10.1088/0031-9155/54/21/005>
- Provenzano, P., Heisey, D., Hayashi, K., Lakes, R., & Vanderby Jr., R. (2002). Subfailure damage in ligament: a structural and cellular evaluation. *Journal of Applied Physiology*, 92(1), 362–371.
- Provenzano, P., Lakes, R., Keenan, T., & Vanderby Jr., R. (2001). Nonlinear ligament viscoelasticity. *Annals of Biomedical Engineering*, 29(10), 908–914. <http://doi.org/10.1114/1.1408926>
- Pryde, E. (1980). Physical properties of soybean oil. In *Handbook of Soy Oil Processing and Utilization* (Vol. 00030, pp. 33–47).
- Qualisys Motion Capture Systems. (2008). Qualisys motion capture accessories.
- Qualisys Motion Capture Systems. (2014). Qualisys Oqus product information.
- Quinn, K., Lee, K., Ahaghotu, C., & Winkelstein, B. (2007). Structural changes in the cervical facet capsular ligament: potential contributions to pain following subfailure loading. *Stapp Car Crash Journal*, 51(October), 169–187. Retrieved from <http://www.ncbi.nlm.nih.gov/pubmed/18278597>
- Rafi, M., Tunio, M., Hashmi, A., & Ahmed, Z. (2009). Comparison of three methods for skin markings in conformal radiotherapy , temporary markers , and permanent Steritatt CIVCO® tattooing: patients' comfort and radiographers' satisfaction. *The South African Radiographer*, 47(2), 20–22.
- Rajagopal, V. (2007). *Modelling breast tissue mechanics under gravity loading*. (Unpublished doctoral thesis). The University of Auckland.

- Rajagopal, V., Lee, A., Chung, J.-H., Warren, R., Highnam, R., Nash, M., & Nielsen, P. (2008). Creating individual-specific biomechanical models of the breast for medical image analysis. *Academic Radiology*, *15*(11), 1425–1436. <http://doi.org/10.1016/j.acra.2008.07.017>
- Ramakrishnan, R., Khan, S., & Badve, S. (2002). Morphological changes in breast tissue with menstrual cycle. *Modern Pathology*, *15*(12), 1348–1356. <http://doi.org/10.1097/01.MP.0000039566.20817.46>
- Ramiao, N., Martins, P., & Fernandes, A. (2013). Biomechanical properties of breast tissue. In *2013 IEEE 3rd Portuguese Meeting in Bioengineering* (pp. 1–6). Ieee. <http://doi.org/10.1109/ENBENG.2013.6518432>
- Rathod, S., Munshi, A., & Agarwal, J. (2012). Skin markings methods and guidelines: a reality in image guidance radiotherapy era. *South Asian Journal of Cancer*, *1*(1), 27–29. <http://doi.org/10.4103/2278-330X.96502>
- Razzano, S., D'Alessio, M., & D'Alession, R. (2014). The importance of the breast aging process in the treatment of breast asymmetries. *Anaplastology*, *03*(02), 3–4. <http://doi.org/10.4172/2161-1173.1000130>
- Reilly, T., & Atkinson, G. (2009). *Contemporary sport, leisure and ergonomics*. Abingdon: Routledge.
- Richards, J. (1999). The measurement of human motion: A comparison of commercially available systems. *Human Movement Science*, *18*(5), 589–602. [http://doi.org/10.1016/S0167-9457\(99\)00023-8](http://doi.org/10.1016/S0167-9457(99)00023-8)
- Rigby, B., Hirai, N., Spikes, J., & Eyring, H. (1959). The mechanical properties of rat tail tendon. *The Journal of General Physiology*, *43*(2), 265–283.
- Rinker, B., Veneracion, M., & Walsh, C. (2010). Breast ptosis: Causes and cure. *Annals of Plastic Surgery*, *64*(5), 579–584.
- Risius, D., Milligan, A., Mills, C., & Scurr, J. (2014). Multiplanar breast kinematics during different exercise modalities. *European Journal of Sport Science*, (June), 1–7. <http://doi.org/10.1080/17461391.2014.928914>
- Risius, D., Milligan, A., & Scurr, J. (2012). Biomechanical breast support requirements for younger and older women during walking. In *Helal and Harries prize and Olympics Meeting*.
- Risius, D., Thelwell, R., Wagstaff, C., & Scurr, J. (2012). Influential factors of bra purchasing in older women. *Journal of Fashion Marketing and Management*, *16*(3), 366–380. <http://doi.org/10.1108/13612021211246099>

- Risius, D., Thelwell, R., Wagstaff, C., & Scurr, J. (2014). The influence of ageing on bra preferences and self-perception of breasts among mature women. *European Journal of Ageing, 11*, 233–240. <http://doi.org/10.1007/s10433-014-0310-3>
- Robens, E., Gast, T., & Straube, B. (1989). Applications of buoyancy. *Thermochimica Acta, 152*(1), 149–156.
- Robertson, D., Caldwell, G., Hamill, J., Kamen, G., & Whittle, S. (2004). *Research methods in biomechanics*. Human Kinetics.
- Robinson, J., & Short, R. (1977). Changes in breast sensitivity at puberty, during the menstrual cycle, and at parturition. *British Medical Journal, 1*(6070), 1188–1191. Retrieved from <http://www.pubmedcentral.nih.gov/articlerender.fcgi?artid=1606822&tool=pmcentrez&rendertype=abstract>
- Robinton, E., & Mood, E. (1966). A quantitative and qualitative appraisal of microbial pollution of water by swimmers: a preliminary report. *Journal of Hygiene, 64*, 489–499.
- Roetenberg, D., Luinge, H., & Slycke, P. (2013). Xsens MVN: Full 6DOF human motion tracking using miniature inertial sensors. *Xsens Technologies*, 1–9. Retrieved from http://www.xsens.com/images/stories/PDF/MVN_white_paper.pdf
- Rong, Z. (2006). *Breast sizing and development of a 3D seamless bra*. (Unpublished doctoral thesis). The Hong Kong Polytechnic University, Hong Kong.
- Rusinkiewicz, S., Hall-Holt, O., & Levoy, M. (2002). Real-time 3D model acquisition. *ACM Transactions on Graphics, 21*(3), 1–9. <http://doi.org/10.1145/566654.566600>
- Saftlas, A., Hoover, R., Brinton, L., Szklo, M., Olson, D., Salane, M., & Wolfe, J. (1991). Mammographic densities and risk of breast cancer. *Cancer, 67*(11), 2833–2838.
- Samani, A., Bishop, J., Yaffe, M., & Plewes, D. (2001). Biomechanical 3-D finite element modeling of the human breast using MRI data. *IEEE Transactions on Medical Imaging, 20*(4), 271–279. <http://doi.org/10.1109/42.921476>
- Sapir, R., Patlas, M., Strano, S., Hadas-halpern, I., & Cherny, N. (2003). Does Mammography Hurt? *Journal of Pain and Symptom Management., 25*(1), 53–63.
- Scheck, F. (2010). *Mechanics: from Newton's Laws to deterministic chaos*. Springer.
- Scurr, J. (2007). Bouncing breasts; a credible area of scientific research. *The Sport and Exercise Scientist*.
- Scurr, J., Bridgman, C., Hedger, W., & White, J. (2009). Multi-planar breast strain during incremental treadmill activity. *Journal of Sports Sciences, 27*(S2), S29. <http://doi.org/10.1080/02640410903195819>

- Scurr, J., Galbraith, H., Hedger, W., & White, C. (2007). A procedure for the analysis of three dimensional breast displacement during treadmill exercise. In *Annual Congress of the ECSS*.
- Scurr, J., Galbraith, H., Wood, L., & Steele, J. (2007). The biomechanics of breast bounce. In *Annual Conference of the British Association of Sport and Exercise Sciences* (Vol. 25, p. S39). <http://doi.org/10.1080/02640410701619937>
- Scurr, J., White, J., & Hedger, W. (2009). Breast displacement in three dimensions during the walking and running gait cycles. *Journal of Applied Biomechanics*, 25(4), 322–329.
- Scurr, J., White, J., & Hedger, W. (2010). The effect of breast support on the kinematics of the breast during the running gait cycle. *Journal of Sports Sciences*, 28(10), 1103–1109. <http://doi.org/10.1080/02640414.2010.497542>
- Scurr, J., White, J., & Hedger, W. (2011). Supported and unsupported breast displacement in three dimensions across treadmill activity levels. *Journal of Sports Sciences*, 29(1), 55–61. <http://doi.org/10.1080/02640414.2010.521944>
- Scurr, J., White, J., Milligan, A., Risius, D., & Hedger, W. (2011a). Breast extension during treadmill running: A case study. In *16th Annual Congress of the European College of Sport Science* (p. 468).
- Scurr, J., White, J., Milligan, A., Risius, D., & Hedger, W. (2011b). Vertical breast extension during treadmill running. In *29th Conference of the International Society of Biomechanics in Sports* (Vol. 11, p. 617).
- Scutt, D., Lancaster, G., & Manning, J. (2006). Breast asymmetry and predisposition to breast cancer. *Breast Cancer Research*, 8(2), R14. <http://doi.org/10.1186/bcr1388>
- Segal, K., Gutin, B., Presta, E., Wang, J., & Van Itallie, T. (1985). Estimation of human body composition by electrical impedance methods: a comparative study. *Journal of Applied Physiology*, 58(5), 1565–1571.
- Senie, R., Rosen, P., Lesser, M., Snyder, R., Schottenfeld, D., & Duthie, K. (1980). Breast carcinoma II: factors related to the predominance of left-sided disease. *Cancer*, 46(7), 1705–1713.
- Shepherd, J., Kerlikowske, K., Smith-Bindman, R., Genant, H., & Cummings, S. (2002). Measurement of breast density with dual X-ray absorptiometry: feasibility. *Radiology*, 223(14), 554–557.
- Shepherd, J., Malkov, S., Fan, B., Laidevant, A., Novotny, R., & Maskarinec, G. (2008). Breast density assessment in adolescent girls using dual-energy X-ray absorptiometry: a feasibility study. *Cancer Epidemiology, Biomarkers & Prevention*, 17(7), 1709–1713. <http://doi.org/10.1158/1055-9965.EPI-08-0006>

- Silver, F., Freeman, J., & DeVore, D. (2001). Viscoelastic properties of human skin and processed dermis. *Skin Research and Technology*, 7(1), 18–23.
- Smalls, L., Wickett, R., & Visscher, M. (2006). Effect of dermal thickness, tissue composition, and body site on skin biomechanical properties. *Skin Research and Technology*, 12(1), 43–49.
- Smith, C., & Havenith, G. (2012). Body mapping of sweating patterns in athletes: a sex comparison. *Medicine and Science in Sports and Exercise*, 44(12), 2350–61. <http://doi.org/10.1249/MSS.0b013e318267b0c4>
- Smutz, W., Drexler, M., Berglund, L., Growney, E., & An, K.-N. (1996). Accuracy of a video strain measurement system. *Journal of Biomechanics*, 29(6), 813–817.
- Soltanian, H., Liu, M., Cash, A., & Iglesias, R. (2012). Determinants of breast appearance and aging in identical twins. *Aesthetic Surgery Journal*, 32(7), 846–860. <http://doi.org/10.1177/1090820X12455660>
- Sonnergaard, J. (2006). On the misinterpretation of the correlation coefficient in pharmaceutical sciences. *International Journal of Pharmaceutical Sciences.*, 321(1), 12–17.
- Stagni, R., Fantozzi, S., Cappello, A., & Leardini, A. (2005). Quantification of soft tissue artefact in motion analysis by combining 3D fluoroscopy and stereophotogrammetry: a study on two subjects. *Clinical Biomechanics*, 20(3), 320–329. <http://doi.org/10.1016/j.clinbiomech.2004.11.012>
- Stark, H. (1977). Directional variations in the extensibility of human skin. *British Journal of Plastic Surgery*, 30, 105–114. [http://doi.org/10.1016/S0022-3468\(78\)80028-1](http://doi.org/10.1016/S0022-3468(78)80028-1)
- Steeds, C. (2009). The anatomy and physiology of pain. *Surgery*, 27(12), 507–511. <http://doi.org/10.1016/j.mpsur.2009.10.013>
- Steele, J. (2013). The biomechanics of better bras: Improving support and comfort during exercise. In *31st Conference of the International Society of Biomechanics in Sports*. Taipei.
- Sturm, R., Ringel, J., & Andreyeva, T. (2004). Increasing obesity rates and disability trends. *Health Affairs*, 23(2), 199–205. <http://doi.org/10.1377/hlthaff.23.2.199>
- Sutradhar, A., & Miller, M. (2012). *In vivo* measurement of breast skin elasticity and breast skin thickness. *Skin Research and Technology*, 0(11), 1–9. <http://doi.org/10.1111/j.1600-0846.2012.00627.x>
- Tanner, C., Schnabel, J., Hill, D., Hawkes, D., Leach, M., & Hose, D. (2006). Factors influencing the accuracy of biomechanical breast models. *Medical Physics*, 33(6), 1758–1769. <http://doi.org/10.1118/1.2198315>

- Tanner, C., White, M., Guarino, S., Douek, M., & Hawkes, D. (2009). Anisotropic behaviour of breast tissue for large compressions. In *IEEE International Symposium on Biomedical Imaging: From Nano to Macro* (pp. 1223–1226).
- Tatla, T., & Lafferty, K. (2002). Making your mark again in surgery. *Annals of the Royal College of Surgeons of England*, *84*(2), 129–130.
- Taylor, J. R. (1982). *An introduction to error analysis: The study of uncertainties in physical measurements*. (2nd editio). University Science Books.
- Toms, S., Lemons, J., Bartolucci, A., & Eberhardt, A. (2002). Nonlinear stress-strain behavior of periodontal ligament under orthodontic loading. *American Journal of Orthodontics and Dentofacial Orthopedics*, *122*(2), 174–179. <http://doi.org/10.1067/mod.2002.124997>
- Torres-Mejía, G., De Stavola, B., Allen, D., Pérez-Gavilán, J., Ferreira, J., Fentiman, I., & Dos Santos Silva, I. (2005). Mammographic features and subsequent risk of breast cancer: a comparison of qualitative and quantitative evaluations in the Guernsey prospective studies. *Cancer Epidemiology, Biomarkers & Prevention*, *14*(5), 1052–1059. <http://doi.org/10.1158/1055-9965.EPI-04-0717>
- Tsai, T.-Y., Lu, T.-W., Kuo, M.-Y., & Lin, C.-C. (2011). Effects of soft tissue artifacts on the calculated kinematics and kinetics of the knee during stair-ascent. *Journal of Biomechanics*, *44*(6), 1182–8. <http://doi.org/10.1016/j.jbiomech.2011.01.009>
- Turner, A., & Dujon, D. (2005). Predicting cup size after reduction mammoplasty. *British Journal of Plastic Surgery*, *58*(3), 290–298.
- Turner, J. (1979). *Buoyancy effects in fluids*. Cambridge University Press.
- U.S. Department of Health and Human Services. (2014). Fluoroscopy. Retrieved June 26, 2014, from <http://www.fda.gov/Radiation-EmittingProducts/RadiationEmittingProductsandProcedures/MedicalImaging/MedicalX-Rays/ucm115354.htm>
- Ulijaszek, S., & Kerr, D. (1999). Anthropometric measurement error and the assessment of nutritional status. *British Journal of Nutrition*, *82*(3), 165–177.
- Ursin, G., Parisky, Y., Pike, M., & Spicer, D. (2001). Mammographic Density Changes During the Menstrual Cycle. *Cancer Epidemiology, Biomarkers & Prevention*, *10*(2), 141–142.
- Vachon, C., Pankratz, V., Scott, C., Maloney, S., Ghosh, K., Brandt, K., ... Sellers, T. (2007). Longitudinal trends in mammographic percent density and breast cancer risk. *Cancer Epidemiology, Biomarkers & Prevention*, *16*(5), 921–928. <http://doi.org/10.1158/1055-9965.EPI-06-1047>

- Van Bogart, J. (2000). Motion analysis technologies. In G. F. Harris; & P. A. Smith (Eds.), *Pediatric Gait: A New Millennium in Clinical Care and Motion Analysis Technology* (pp. 166–172). Institute of Electrical and Electronics Engineers. <http://doi.org/10.1109/PG.2000.858890>
- Van Duijnhoven, F., Bezemer, I., Peeters, P., Roest, M., Uitterlinden, A., Grobbee, D., & van Gils, C. (2005). Polymorphisms in the estrogen receptor alpha gene and mammographic density. *Cancer Epidemiology, Biomarkers & Prevention*, *14*(11), 2655–2660. <http://doi.org/10.1158/1055-9965.EPI-05-0398>
- Vandeweyer, E., & Hertens, D. (2002). Quantification of glands and fat in breast tissue: an experimental determination. *Annals of Anatomy*, *184*(2), 181–184.
- Vassileva, S., & Hristakieva, E. (2007). Medical applications of tattooing. *Clinics in Dermatology*, *25*(4), 367–374. <http://doi.org/10.1016/j.clindermatol.2007.05.014>
- Veitch, D., Burford, K., Dench, P., Dean, N., & Griffin, P. (2012). Measurement of breast volume using body scan technology (computer-aided anthropometry). *Work*, *41*, 4038–4045. <http://doi.org/10.3233/WOR-2012-0068-4038>
- Vint, P., & Hinrichs, R. (1996). Endpoint error in smoothing and differentiating raw kinematic data: An evaluation of four popular methods. *Journal of Biomechanics*, *29*(12), 1637–1642. [http://doi.org/10.1016/0021-9290\(96\)00079-6](http://doi.org/10.1016/0021-9290(96)00079-6)
- Vogel, H. (1972). Influence of age, treatment with corticosteroids and strain rate on mechanical properties of rat skin. *Biochimica et Biophysica Acta (BBA)-General Subjects*, *286*(1), 79–83.
- Wallace, M., Wallace, A., Lee, J., & Dobke, M. (1996). Pain after breast surgery: a survey of 282 women. *Pain*, *66*, 195–205.
- Wang, L., Chen, D., & Lin, B. (2011). Effects of side strap and elastic hems of bra materials on clothing pressure comfort. *Journal of Fiber Bioengineering and Informatics*, *4*(2), 187–198. <http://doi.org/10.3993/jfbi06201109>
- Weinberg, S., Scott, N., Neiswanger, K., Brandon, C., & Marazita, M. (2004). Digital three-dimensional photogrammetry: evaluation of anthropometric precision and accuracy using a Genex 3D camera system. *The Cleft Palate-Craniofacial Journal.*, *41*(5), 507–518. <http://doi.org/10.1597/03-066.1>
- Weir, J. (2005). Quantifying the test-retest reliability using the intraclass correlation coefficient and the SEM. *Journal of Strength and Conditioning Research*, *19*(1), 231–240.
- Wheat, J., Choppin, S., & Goyal, A. (2014). Development and assessment of a Microsoft Kinect based system for imaging the breast in three dimensions. *Medical Engineering & Physics*. <http://doi.org/10.1016/j.medengphy.2013.12.018>

- White, J. (2013). *Breast support implications for female recreational athletes. (Unpublished doctoral thesis)*. University of Portsmouth.
- White, J., Mills, C., & Scurr, J. (2012). Multi-planar breast kinematics and breast comfort during intermittent treadmill exercise. In *BASES Biomechanics Interest Group 27th Easter Meeting* (Vol. 81, p. 40).
- White, J., & Scurr, J. (2012). Evaluation of professional bra fitting criteria for bra selection and fitting in the UK. *Ergonomics*, 55(6), 704–711. <http://doi.org/10.1080/00140139.2011.647096>
- White, J., Scurr, J., & Hedger, W. (2008). A comparison of three-dimensional breast displacement and breast comfort during overground and treadmill running. In *Annual Conference of the British Association of Sport and Exercise Sciences*. (Vol. 26, pp. S33–S34). <http://doi.org/10.1080/02640410802306202>
- White, J., Scurr, J., & Hedger, W. (2009). Kinematics of the bare-breast during a maximum vertical jump. "Abstracts", *Journal of Sports Sciences*, 27(S2), S32. <http://doi.org/10.1080/02640410903195819>
- White, J., Scurr, J., & Hedger, W. (2010). Three-dimensional breast displacement and breast comfort in small and large breasted women during jumping and agility tasks. In *15th Annual Congress of the European College of Sport Science*. (p. 138).
- White, J., Scurr, J., & Smith, N. (2009). The effect of breast support on kinetics during overground running performance. *Ergonomics*, 52(4), 492–8. <http://doi.org/10.1080/00140130802707907>
- Whittingham, L., Roberts, B., Weir, R., Caine, M., & Forrester, S. (2012). Determination of a suitable torso marker set to measure breast kinematics during running. In *BASES Biomechanics Interest Group 27th Easter Meeting* (p. 41).
- WHO Multicentre Growth Reference Study Group, I. (2006). Reliability of anthropometric measurements in the WHO Multicentre Growth Reference Study. *Acta Pædiatrica*, 450, 38–46. <http://doi.org/10.1080/08035320500494464>
- Williams, S., Schmidt, R., Disselhorst-Klug, C., & Rau, G. (2006). An upper body model for the kinematical analysis of the joint chain of the human arm. *Journal of Biomechanics*, 39(13), 2419–2429. <http://doi.org/10.1016/j.jbiomech.2005.07.023>
- Wilson, M., & Sellwood, R. (1976). Therapeutic value of a supporting brassiere in mastodynia. *British Medical Journal*, 2(July), 90. Retrieved from <http://www.pubmedcentral.nih.gov/articlerender.fcgi?artid=1687763&tool=pmcentrez&rendertype=abstract>
- Winter, G. (2006). Some factors affecting skin and wound healing. *Journal of Tissue Viability*, 16(2), 20–23. [http://doi.org/10.1016/S0965-206X\(06\)62006-8](http://doi.org/10.1016/S0965-206X(06)62006-8)

- Wojcinski, S., Cassel, M., Farrokh, A., Soliman, A., Hille, U., Schmidt, W., ... Hillemanns, P. (2012). Variations in the elasticity of breast tissue during the menstrual cycle determined by real-time sonoelastography. *Journal of Ultrasound Medicine*, *31*, 63–72.
- Wood, K., Cameron, M., & Fitzgerald, K. (2008). Breast size, bra fit and thoracic pain in young women: a correlational study. *Chiropractic & Osteopathy*, *16*(1), 1–7. <http://doi.org/10.1186/1746-1340-16-1>
- World Health Organization. (2000). *Obesity: preventing and managing the global epidemic*.
- Wright, J., & Schuknecht, H. (1972). Atrophy of the spiral ligament. *Archives of Otolaryngology—Head & Neck Surgery*, *96*(1), 16–21. Retrieved from <http://www.ncbi.nlm.nih.gov/pubmed/12021504>
- Wright, M. (2002). Graphical analysis of bra size calculation procedures. *International Journal of Clothing Science and Technology*, *14*(1), 41–45.
- Wu, G., van der Helm, F., Veeger, H., Makhsous, M., Van Roy, P., Anglin, C., ... Buchholz, B. (2005). ISB recommendation on definitions of joint coordinate systems of various joints for the reporting of human joint motion—Part II: shoulder, elbow, wrist and hand. *Journal of Biomechanics*, *38*(5), 981–992.
- Wu, Y., Thalmann, N., & Thalmann, D. (1995). A dynamic wrinkle model in facial animation and skin aging. *The Journal of Visualization and Computer Animation*, *6*(4), 195–205.
- Wurstbauer, K., Sedlmayer, F., & Kogelnik, H. (2001). Skin markings in external radiotherapy by temporary tattooing with henna: improvement of accuracy and increased patient comfort. *International Journal of Radiation Oncology, Biology, Physics*, *50*(1), 179–181.
- Yaghjian, L., Colditz, G., Collins, L., Schnitt, S., Rosner, B., Vachon, C., & Tamimi, R. (2011). Mammographic breast density and subsequent risk of breast cancer in postmenopausal women according to tumor characteristics. *Journal of the National Cancer Institute*, *103*(15), 1179–1189. <http://doi.org/10.1093/jnci/djr225>
- Ying, B., Wang, Y., Liu, F., & Zhang, X. (2011). Study on the definition of moulded bra cup features and parametric modeling. *Journal of Fiber Bioengineering and Informatics*, *4*(4), 389–402. <http://doi.org/10.3993/jfbi12201109>
- Yu, B., Gabriel, D., Noble, L., & An, K.-N. (1999). Estimate of the optimum cutoff frequency for the Butterworth low-pass digital filter. *Journal of Applied Biomechanics*, *15*, 318–329.

- Yu, W., & Zhou, J. (2012). Three-dimensional movements of pert and ptotic breasts. *Journal of Fiber Bioengineering and Informatics*, 5(2), 139–150. <http://doi.org/10.3993/jfbi06201203>
- Zain-Ul-Abdein, M., Morestin, F., Bouten, L., & Cornolo, J. (2013). Numerical simulation of breast deformation under static conditions. *Computer Methods in Biomechanics and Biomedical Engineering*, 16(S1), 50–51. <http://doi.org/10.1080/10255842.2013.815857>
- Zeni Jr, J., Richards, J., & Higginson, J. (2008). Two simple methods for determining gait events during treadmill and overground walking using kinematic data. *Gait Posture*, 27(4), 710–714.
- Zhang, Z. (2001). *Camera calibration. Department of Communication Technology.*
- Zheng, R., Yu, W., & Fan, J. (2007). Development of a new chinese bra sizing system based on breast anthropometric measurements. *International Journal of Industrial Ergonomics*, 37(8), 697–705. <http://doi.org/10.1016/j.ergon.2007.05.008>
- Zhou, J. (2011). *New methods of evaluating breast motion in braless and sports bra conditions. (Unpublished doctoral thesis).* The Hong Kong Polytechnic University, Hong Kong.
- Zhou, J., Yu, W., & Ng, S.-P. (2011). Methods of studying breast motion in sports bras: a review. *Textile Research Journal*, 81(12), 1234–1248. <http://doi.org/10.1177/0040517511399959>
- Zhou, J., Yu, W., & Ng, S.-P. (2012a). Identifying effective design features of commercial sports bras. *Textile Research Journal*, 83(14), 1500–1513. <http://doi.org/10.1177/0040517512464289>
- Zhou, J., Yu, W., & Ng, S.-P. (2012b). Studies of three-dimensional trajectories of breast movement for better bra design. *Textile Research Journal*, 82(3), 242–254. <http://doi.org/10.1177/0040517511435004>
- Zhou, J., Yu, W., Ng, S.-P., & Hale, J. (2009). Evaluation of shock absorbing performance of sports bras. *Journal of Fiber Bioengineering and Informatics*, 2(2), 108–113. <http://doi.org/10.3993/jfbi09200906>
- Zhu, R., & Zhou, Z. (2004). A real-time articulated human motion tracking using tri-axis inertial/magnetic sensors package. *IEEE Transactions on Neural Systems and Rehabilitation Engineering*, 12(2), 295–302. <http://doi.org/10.1109/TNSRE.2004.827825>

Appendices

Appendix A

Mean left nipple position relative to the torso during three 2 s static trials with normal breathing, held exhalation, and held inhalation.


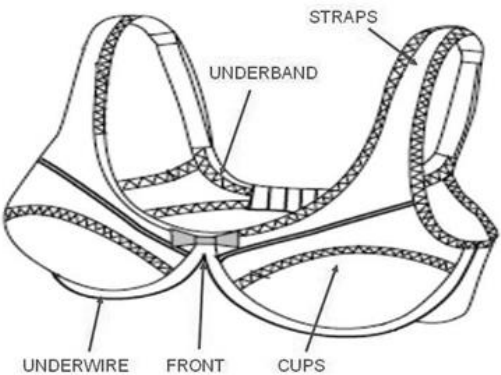
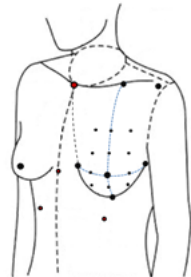
Participant	Breast size	Mean static left nipple position relative to the torso (mm)								
		2 s normal breathing			2 s held exhale			2 s held inhale		
		Anterior-posterior	Medial-lateral	Superior-inferior	Anterior-posterior	Medial-lateral	Superior-inferior	Anterior-posterior	Medial-lateral	Superior-inferior
Participant I	32A	34.8	88.6	-163.6	34.8	87.1	-168.4	45.9	92.5	-157.5
Participant II	32B	40.4	102.7	-153.3	41.2	99.3	-155.5	53.3	101.6	-148.4
Participant III	32B	35.4	91.7	-161.5	34.0	92.3	-161.0	46.5	95.9	-150.8
Participant IV	32C	44.1	102.1	-164.1	41.6	102.5	-165.3	47.7	106.6	-159.5
Participant V	32D	40.2	94.1	-151.6	39.6	94.8	-150.1	41.0	94.7	-152.1
Participant VI	32D	35.9	106.5	-164.2	34.6	105.2	-165.8	50.0	109.9	-149.9
Participant VII	34D	48.0	117.7	-187.2	52.7	115.7	-187.8	54.5	121.6	-178.1
Participant VIII	34D	53.2	106.4	-179.7	56.3	103.7	-184.9	64.3	104.3	-174.4
Participant IX	34DD	55.1	109.8	-181.7	56.1	107.2	-183.8	66.2	108.3	-173.2
Participant X	34E	65.1	110.1	-191.3	65.9	109.0	-192.9	68.6	110.2	-190.6
Participant XI	32F	62.2	102.6	-205.0	69.4	92.9	-210.1	71.7	101.3	-200.3
Participant XII	30GG	61.9	111.9	-218.0	62.5	110.1	-221.2	71.4	115.8	-210.2
Mean		48.0	103.7	-176.8	49.1	101.6	-178.9	56.7	105.2	-170.4
TEM		0.7	0.4	0.7	0.7	1.1	1.0	1.6	1.2	1.1

Appendix B

Mean left nipple position relative to the torso during three repeat trials of 2.00 s, 1.00 s, 0.50 s and 0.25 s normal breathing.

Participant	Breast size	Mean static left nipple position relative to the torso (mm)														
		10.00 s normal breathing			2.00 s normal breathing			1.00 s normal breathing			0.50 s normal breathing			0.25 s normal breathing		
		Anterior-posterior	Medial-lateral	Superior-inferior	Anterior-posterior	Medial-lateral	Superior-inferior	Anterior-posterior	Medial-lateral	Superior-inferior	Anterior-posterior	Medial-lateral	Superior-inferior	Anterior-posterior	Medial-lateral	Superior-inferior
Participant I	32A	35.2	87.7	-161.9	34.8	88.6	-163.6	34.7	88.6	-163.6	34.7	88.7	-163.6	34.7	88.7	-163.5
Participant II	32B	40.5	102.5	-153.1	40.4	102.7	-153.3	40.5	102.7	-153.3	40.5	102.7	-153.2	40.6	102.6	-153.2
Participant III	32B	33.3	92.7	-159.1	35.4	91.7	-161.5	35.3	91.7	-161.5	35.2	91.7	-161.5	35.1	91.7	-161.5
Participant IV	32C	43.7	102.9	-161.6	44.1	102.1	-164.1	44.0	102.2	-164.1	43.9	102.2	-164.0	43.9	102.3	-163.9
Participant V	32D	40.7	93.9	-150.6	40.2	94.1	-151.6	40.3	94.1	-151.6	40.3	94.1	-151.4	40.3	94.1	-151.4
Participant VI	32D	34.4	108.4	-160.0	35.9	106.5	-164.2	36.0	106.5	-164.2	36.1	106.5	-164.2	36.2	106.5	-164.1
Participant VII	34D	50.9	116.4	-183.5	48.0	117.7	-187.2	48.3	117.5	-187.2	48.6	117.4	-187.0	48.7	117.3	-186.9
Participant VIII	34D	53.9	104.9	-180.3	53.2	106.4	-179.7	53.5	106.3	-179.7	53.9	106.1	-179.7	54.2	106.1	-179.5
Participant IX	34DD	52.5	114.4	-176.5	55.1	109.8	-181.7	55.2	109.7	-181.7	55.2	109.7	-181.7	55.3	109.8	-181.7
Participant X	34E	63.8	111.7	-187.7	65.1	110.1	-191.3	65.1	110.0	-191.3	65.2	109.9	-191.3	65.3	109.8	-191.3
Participant XI	32F	62.6	103.0	-203.7	62.2	102.6	-205.0	62.3	102.4	-205.0	62.4	102.2	-204.9	62.5	102.2	-204.9
Participant XII	30GG	62.2	111.5	-216.4	61.9	111.9	-218.0	61.9	111.9	-218.0	61.9	112.0	-217.9	61.9	112.0	-217.9
Mean		47.8	104.2	-174.5	48.0	103.7	-176.8	48.1	103.6	-176.7	48.2	103.6	-176.6	48.2	103.6	-176.6
TEM		0.7	0.4	1.2	0.7	0.4	0.7	0.8	0.4	0.7	0.7	0.5	0.7	0.7	0.6	0.8

Appendix C

<p>RGBH</p> <p>  </p> <p>SESSION 0</p> <p>Date: Time:</p> <p> <input type="checkbox"/> Skin test – application of a surgical dressing to the torso <input type="checkbox"/> Bra fit – assessed bra size: </p> 	<p>SESSION 1</p> <p>Date: Time:</p> <p> <input type="checkbox"/> Health history questionnaire <input type="checkbox"/> Breast health questionnaire <input type="checkbox"/> Marker application using surgical marker <input type="checkbox"/> Marker application using henna </p>  <p>What to bring:</p> <ul style="list-style-type: none"> o A non-underwired, crop-top, or loose-fitting bra (minimises irritation) o A top that covers the marker positions – marks will be very visible for the first 48 hours. <p>Advice following the session:</p> <ul style="list-style-type: none"> o Avoid activities that may make you hot and sweaty while the surgical tape is still on your torso o Try to keep the tape on for 48 hours following application o Remove the tape immediately if you notice your skin becoming red or itchy o Please check your marks daily to ensure they are not faded and re-apply using the surgical marker if required (you will receive a daily email reminder)
---------------------------------------------------------------------------------------------------------------------------------------------------------------------------------------------------------------------------------------------------------------------------------------------------------------------------------------------------------------------------------------------------------------------------------	-------------------------------------------------------------------------------------------------------------------------------------------------------------------------------------------------------------------------------------------------------------------------------------------------------------------------------------------------------------------------------------------------------------------------------------------------------------------------------------------------------------------------------------------------------------------------------------------------------------------------------------------------------------------------------------------------------------------------------------------------------------------------------------------------------------------------------------------------------------------------------------------------------------------------------------------------------------------------------------------------------------------------------------------------------------------------------------------------------------------------------------------------------------------------------------------------------------------------------------

SESSION 2

Date: Time:

- Application of reflective markers
- Static extreme experiment
- Breast drop
- Trampette jumping
- Treadmill walking, jogging and running
- Water tank experiment



What to bring:

- o Trainers and shorts/leggings for running
- o A hair bobble
- o A drink
- o A jacket or loose top for modesty between experiments
- o A swimsuit or bikini bottoms (can be provided if required)

Advice for the session:

- o Please ensure the surgical tape has been removed **before** attending this session
- o Towels, swimsuits and bath robes will be available for this session but you can bring your own if you prefer

SESSION 3

Date: 11/04/13 Time:

- Application of reflective markers
- Drop landing from a pommel horse
- Shower with antimicrobial gel
- Application of black markers
- Oil tank experiment



What to bring:

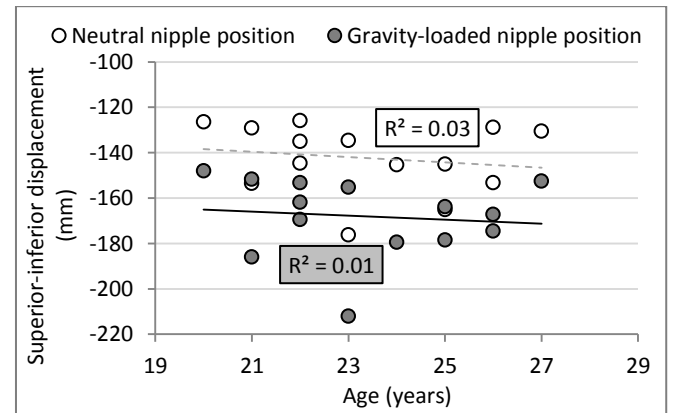
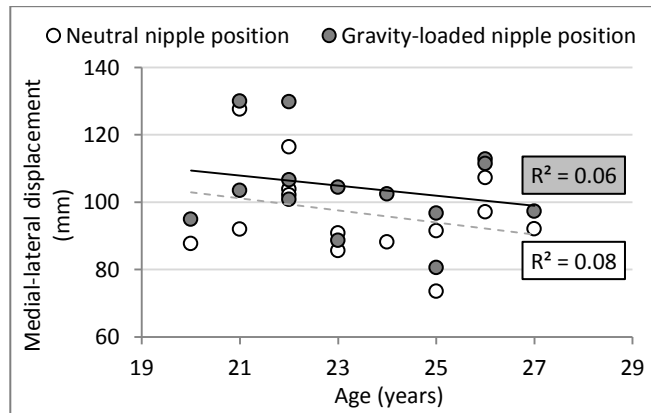
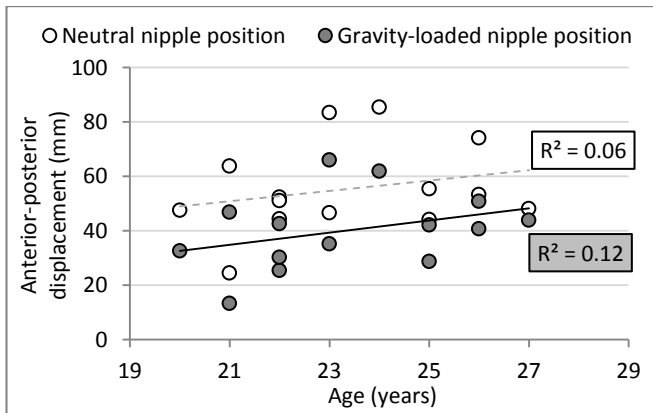
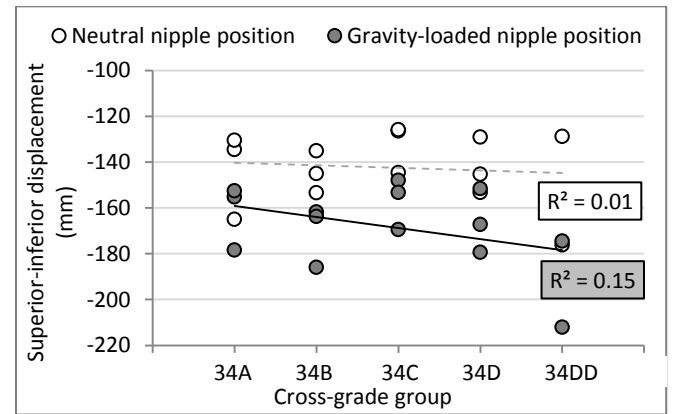
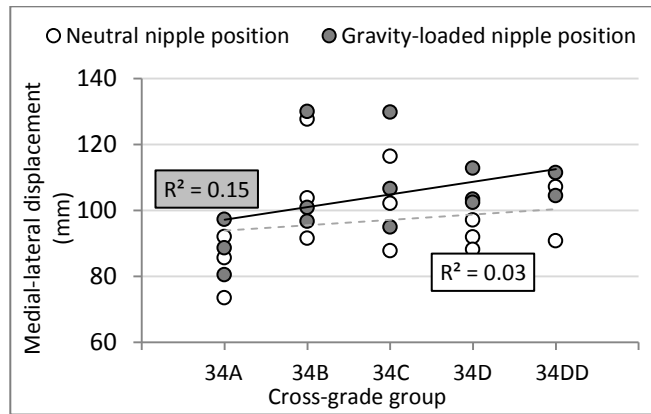
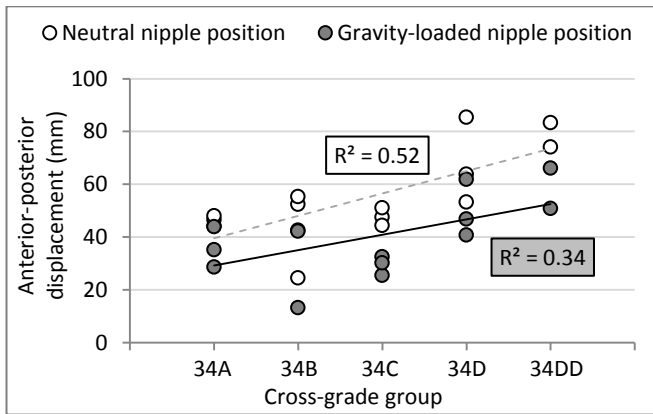
- o Trainers and shorts/leggings for jumping
- o A hair bobble

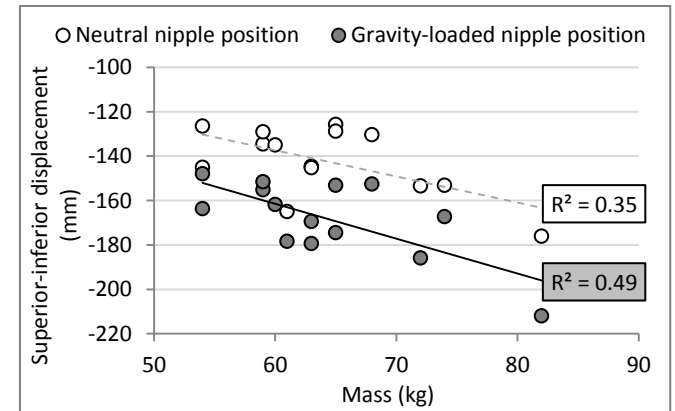
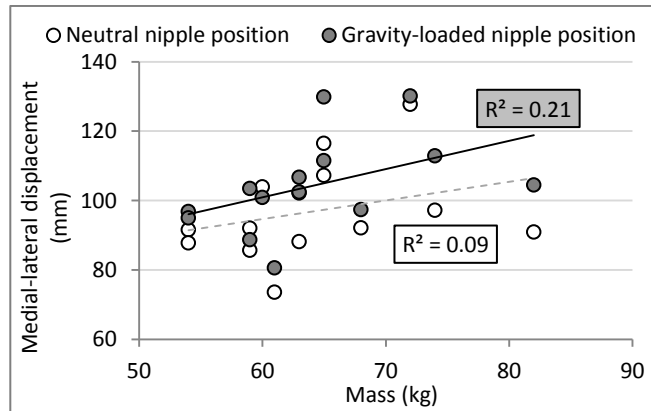
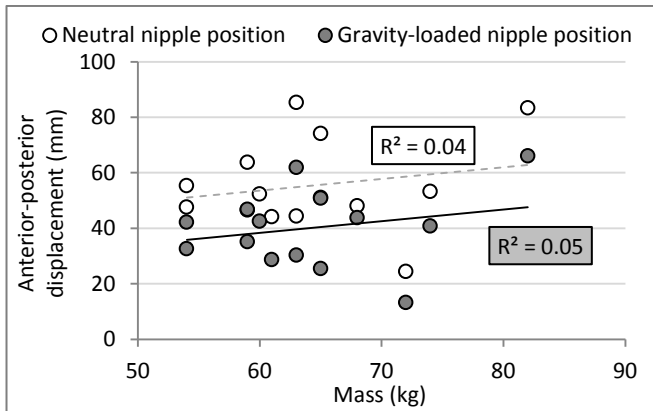
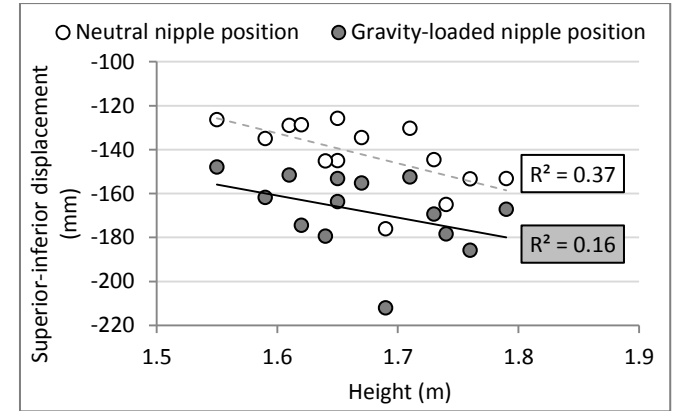
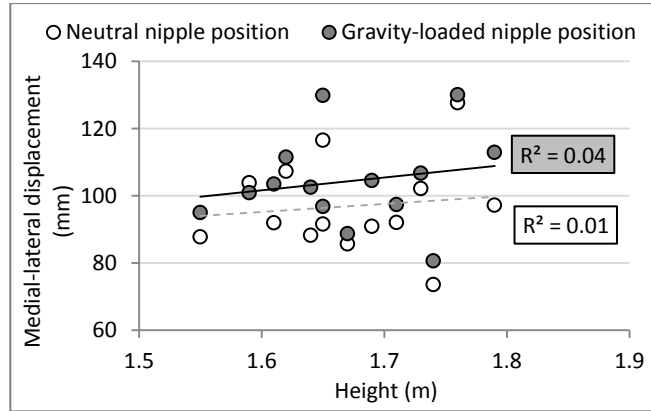
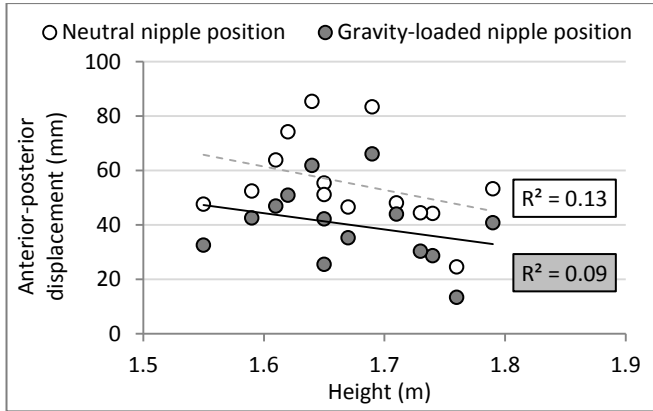
Advice for the session:

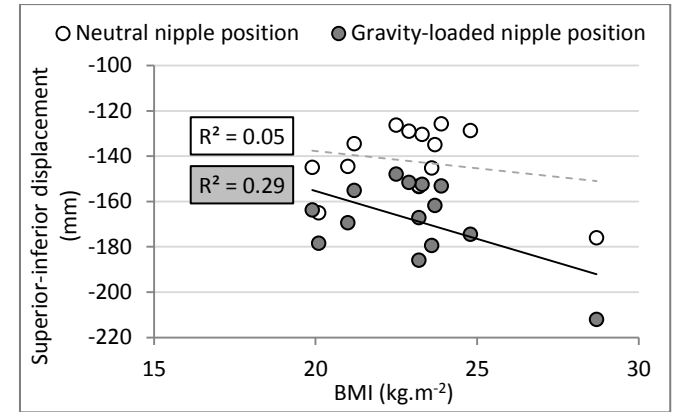
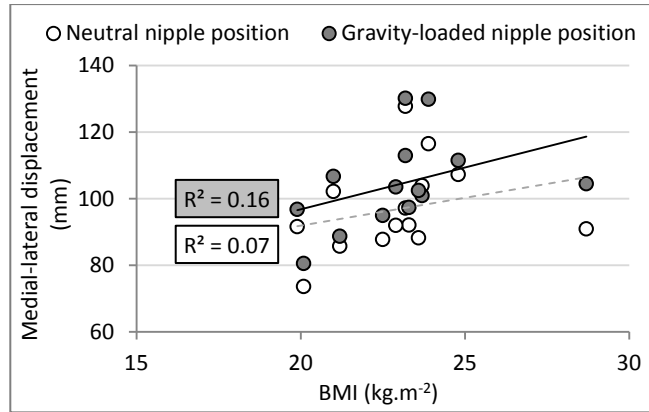
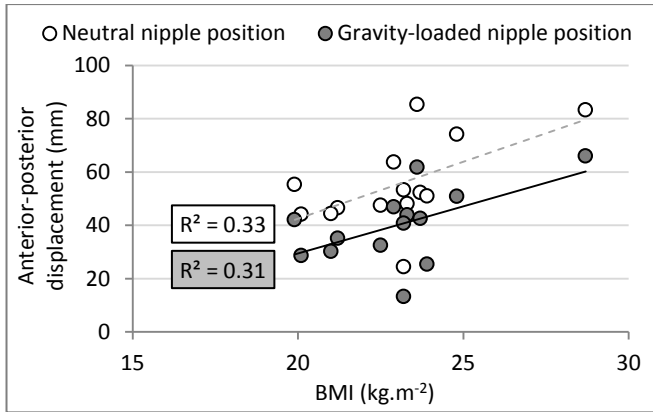
- o Towels, swimsuits and bath robes will be provided for this session but you can bring your own if you prefer (they will get oily)
- o Although there will be shower facilities for use after this experiment, your skin may still be a little oily so consider the clothes you wear to this session.

Appendix D

Correlations between participants' physical characteristics and their neutral (unloaded) and gravity-loaded nipple positions (relative to the torso origin).

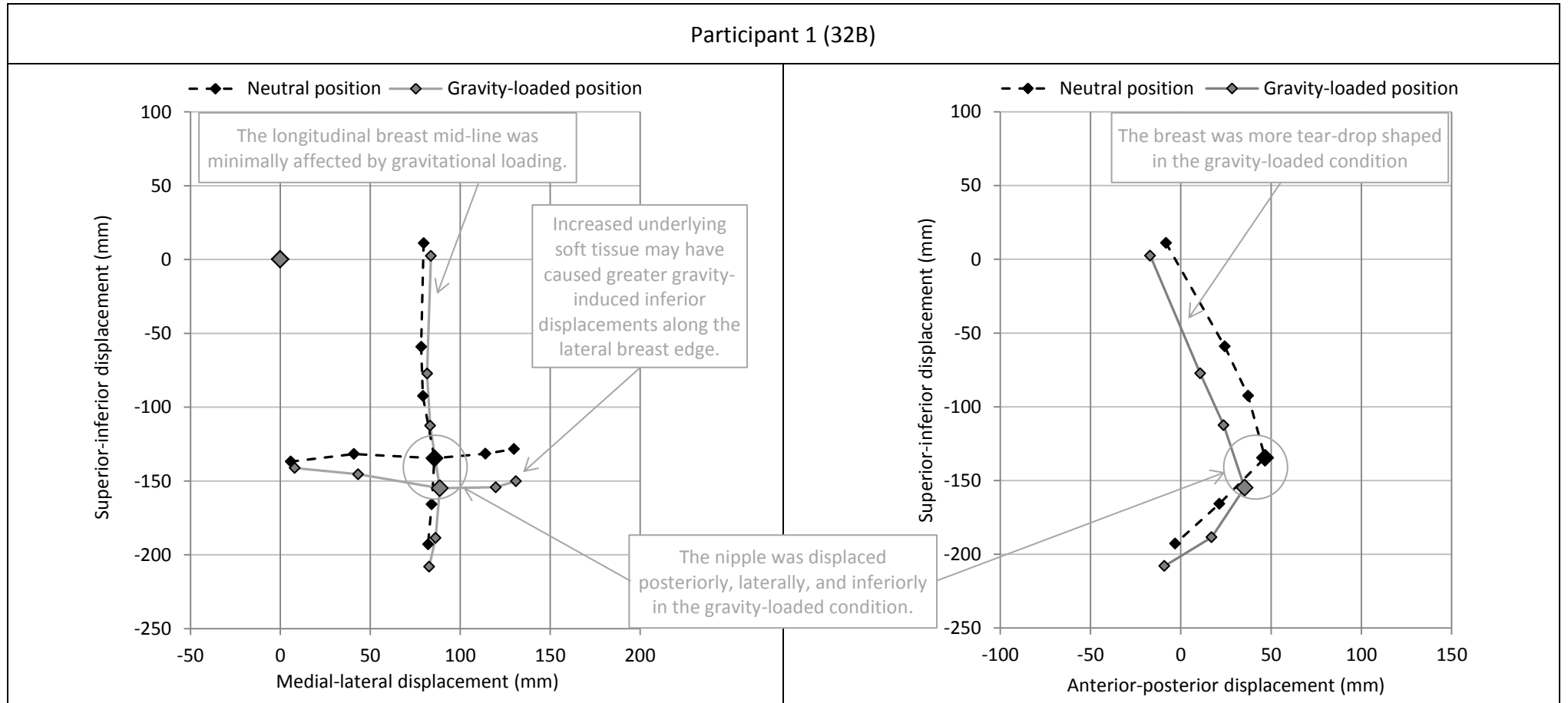




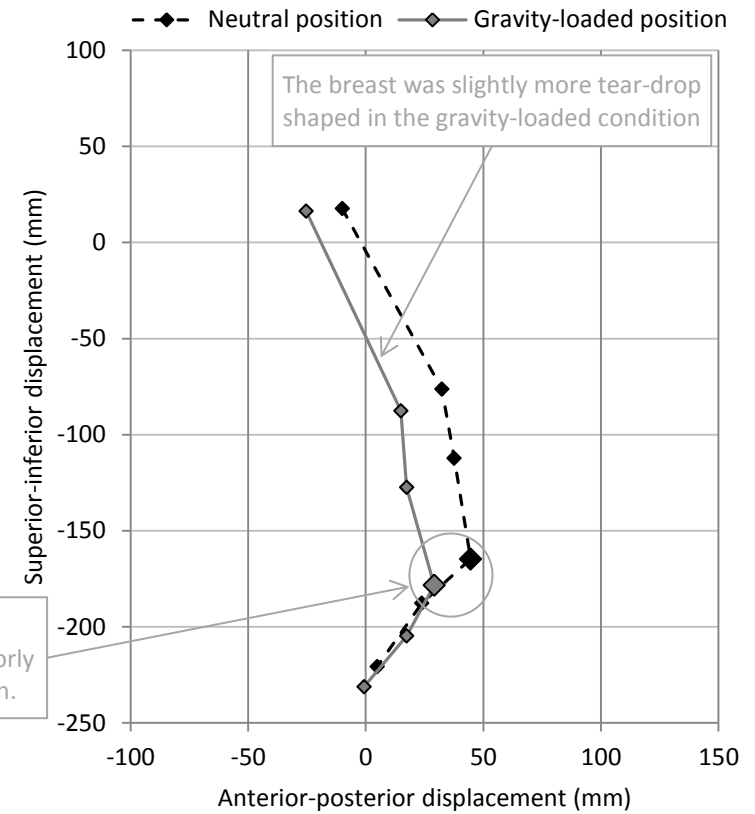
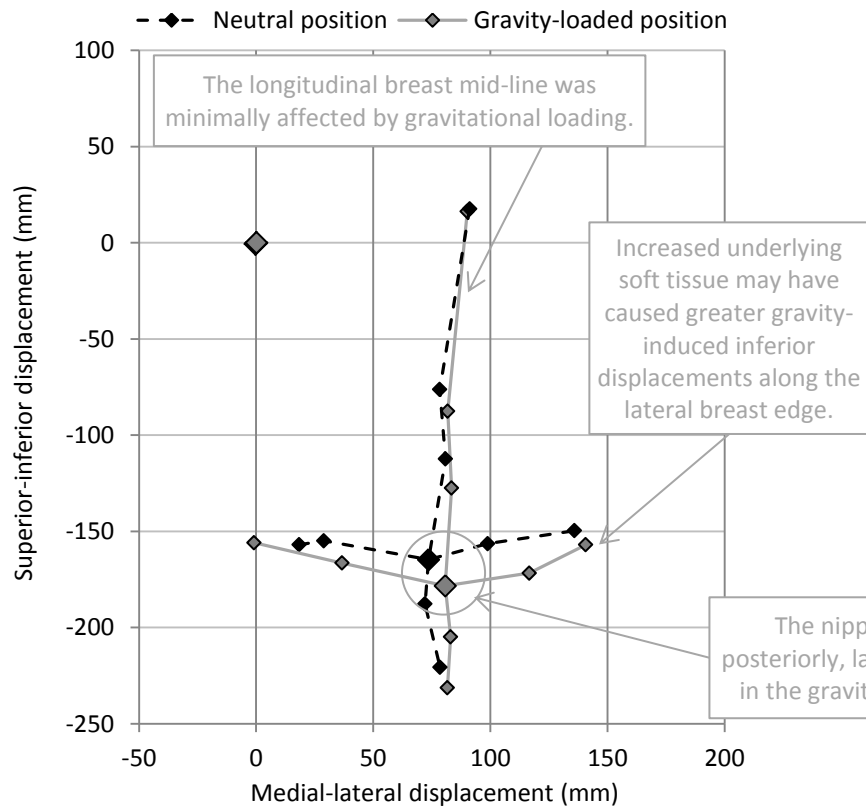


Appendix E

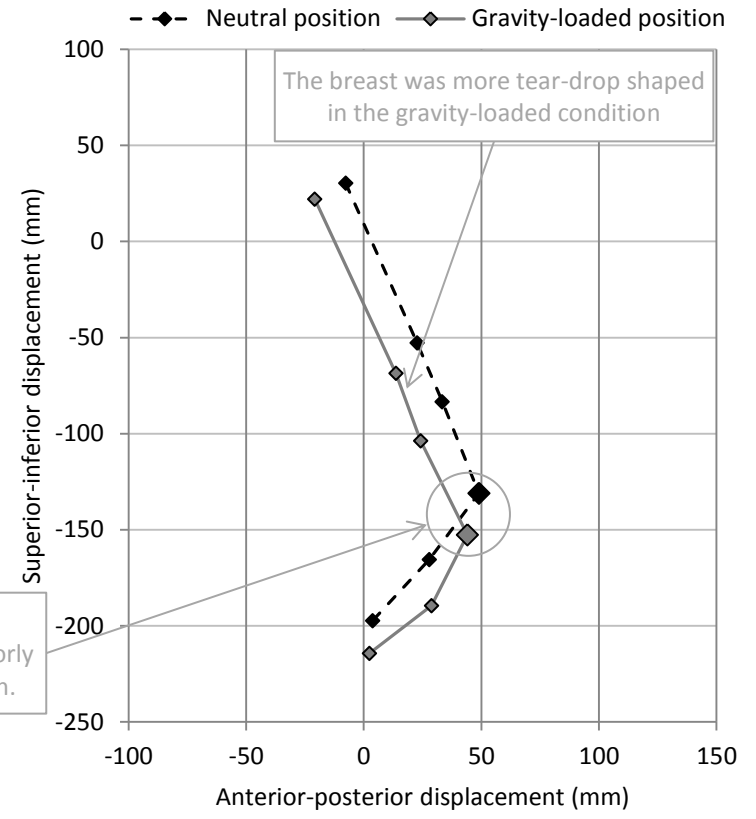
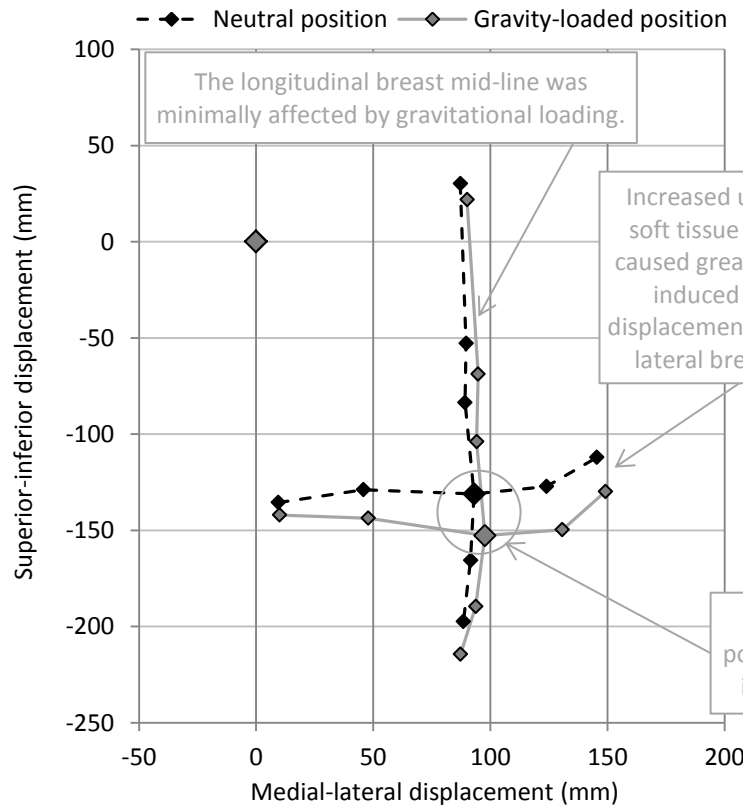
Frontal and sagittal views of each participant's breast mid-line markers in the neutral and gravity-loaded conditions.



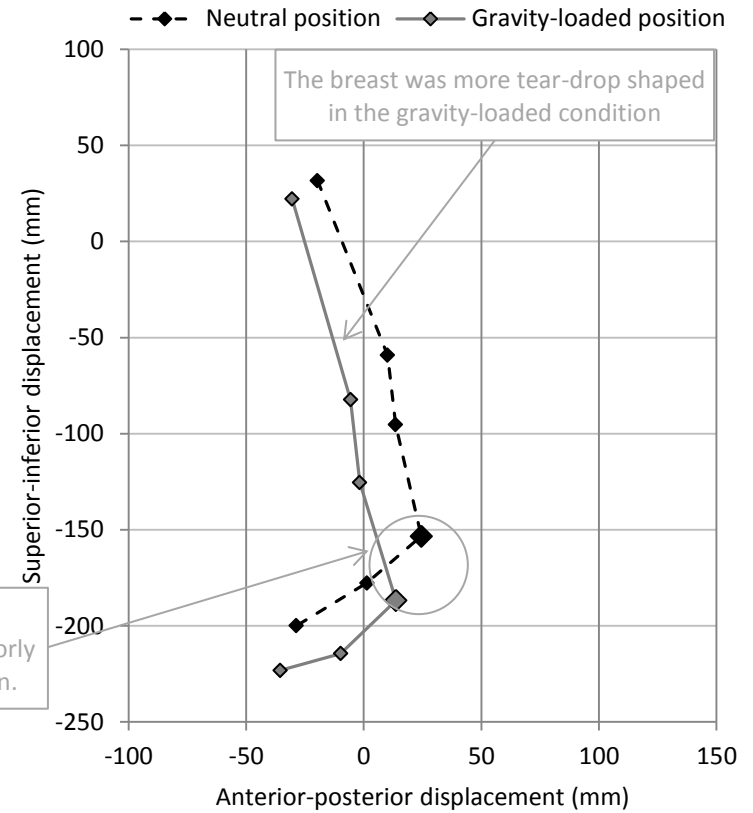
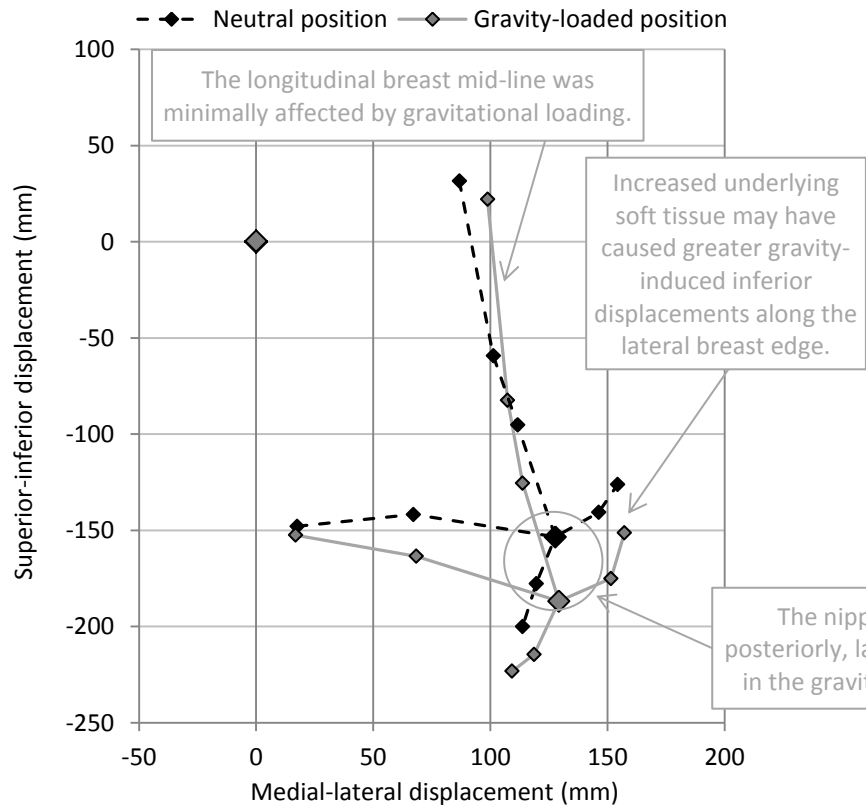
Participant 2 (32B)



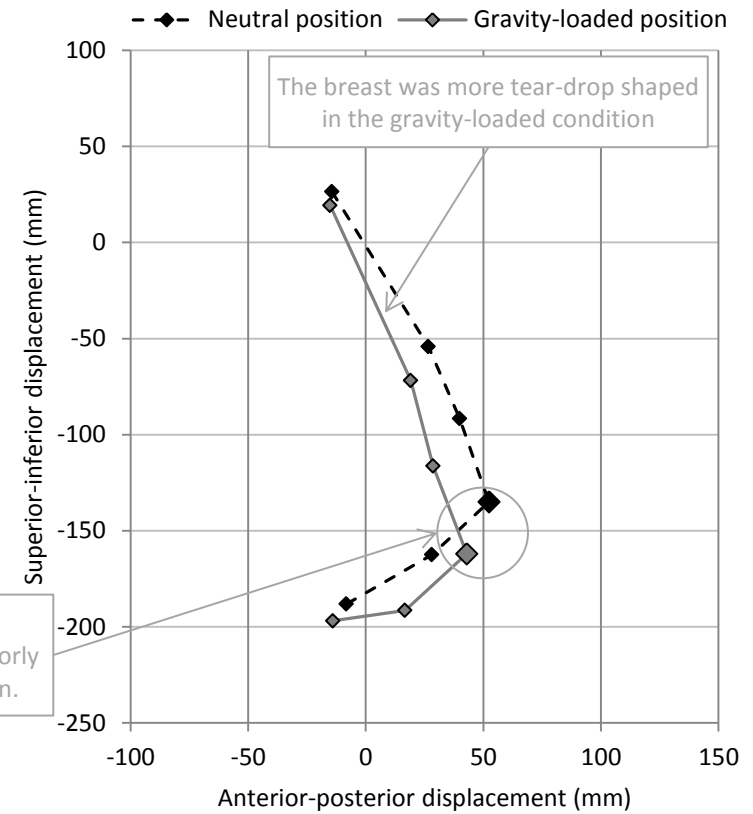
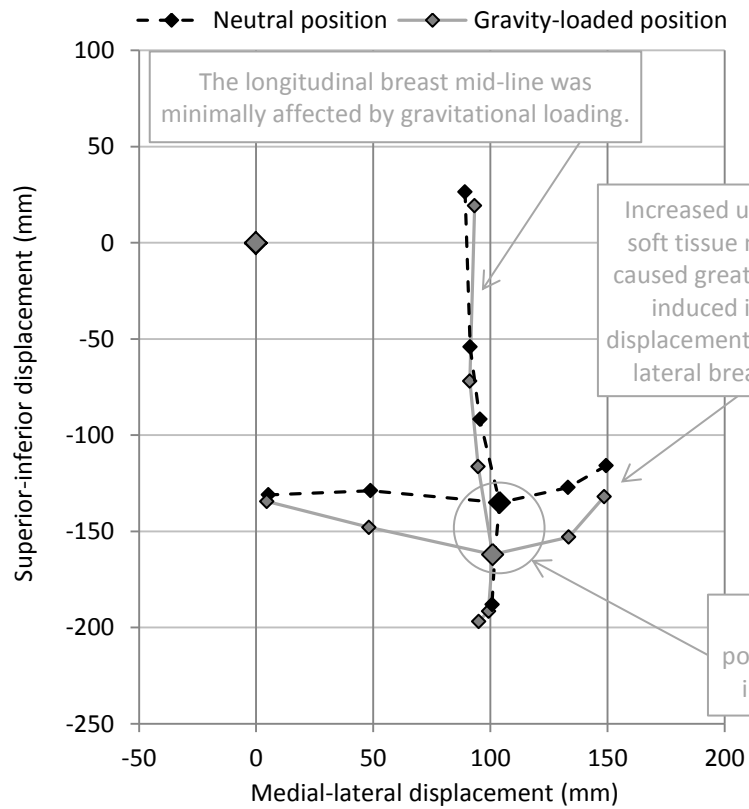
Participant 3 (32B)



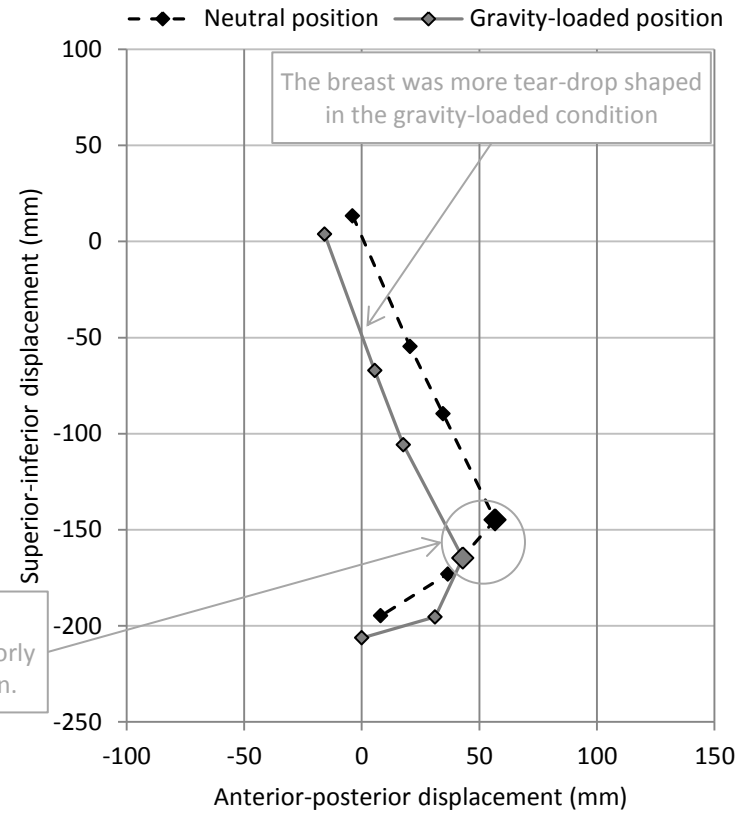
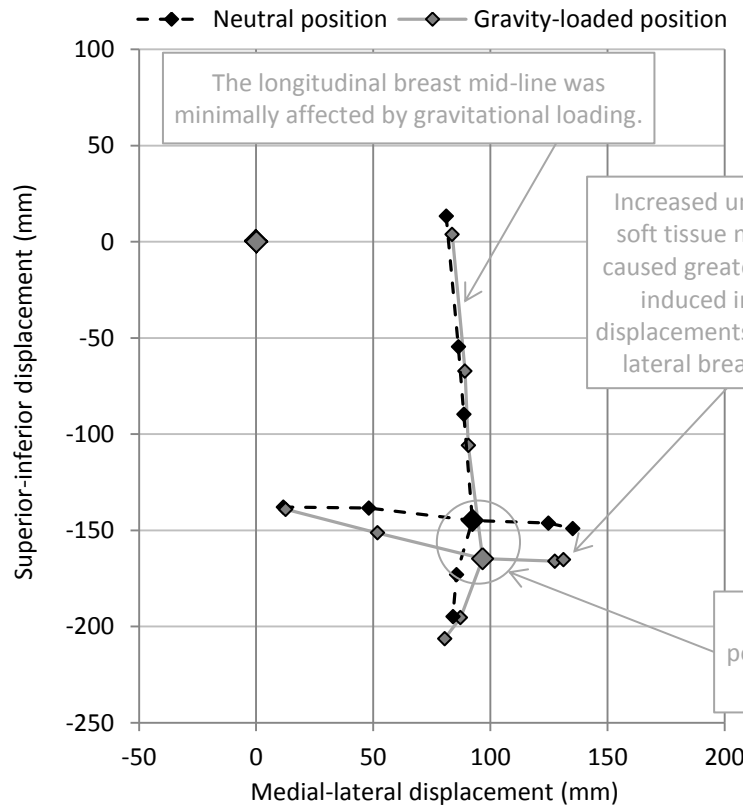
Participant 4 (34B)



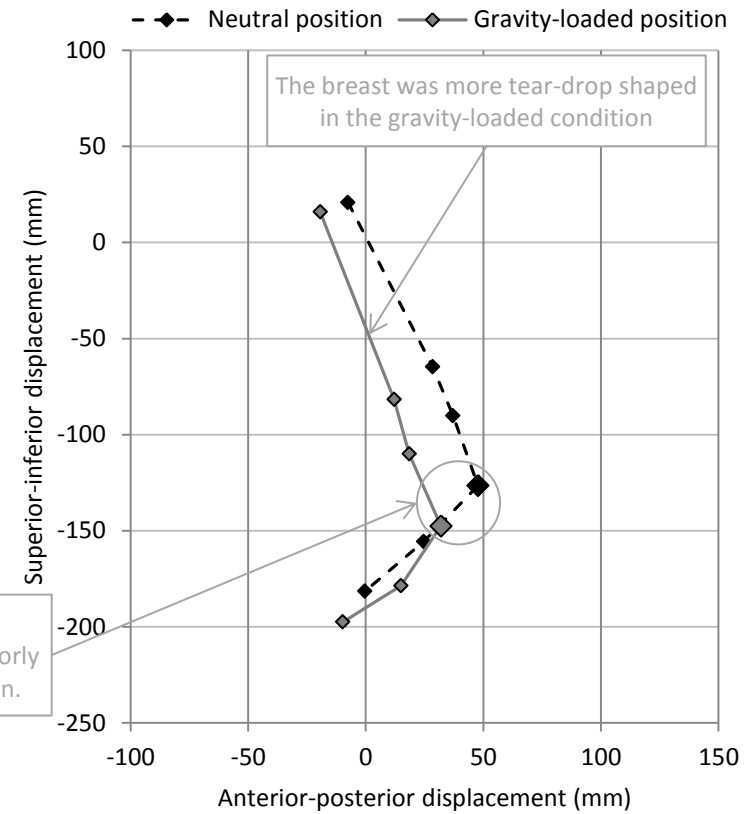
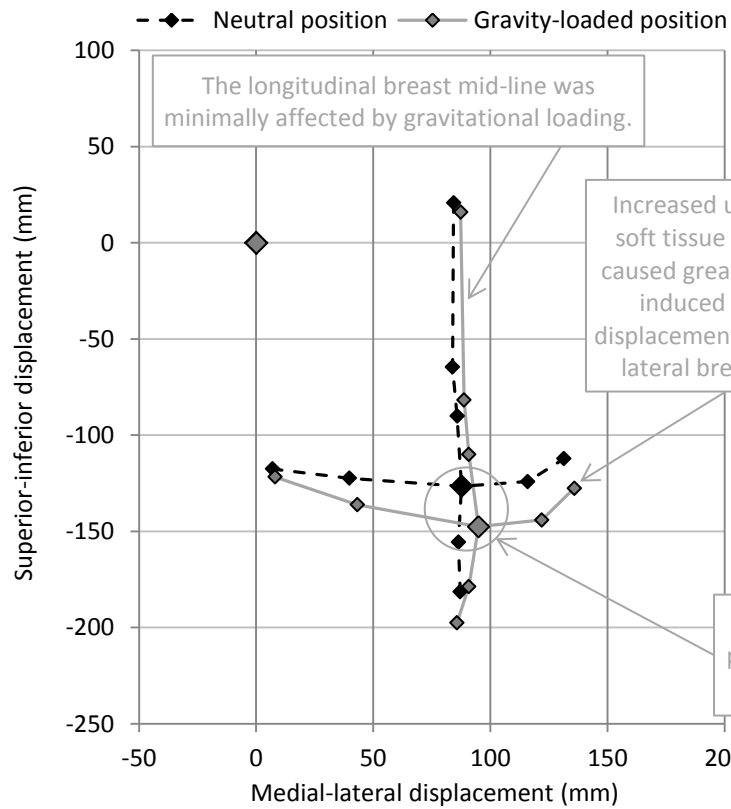
Participant 5 (32C)



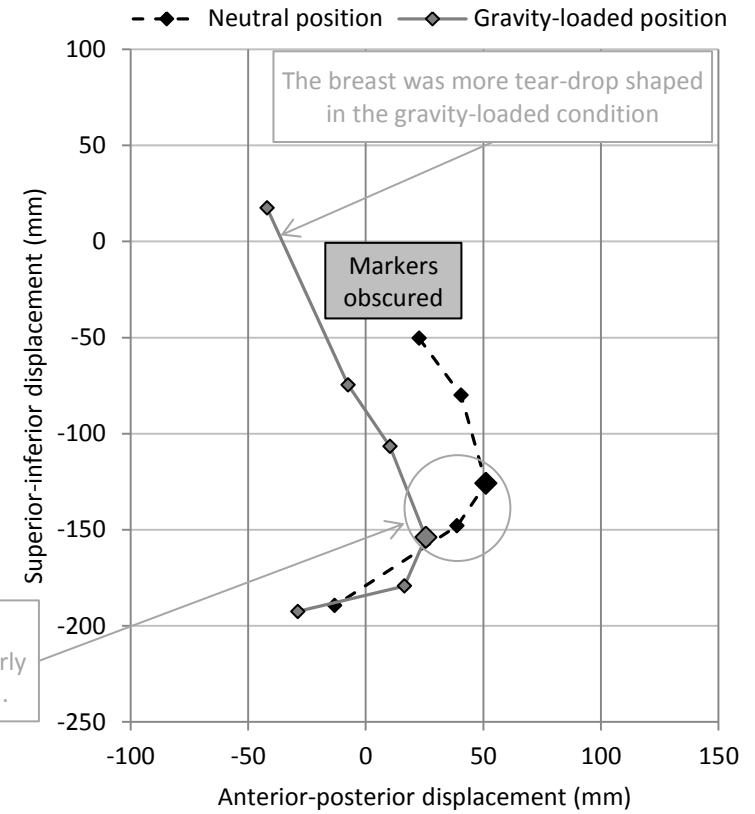
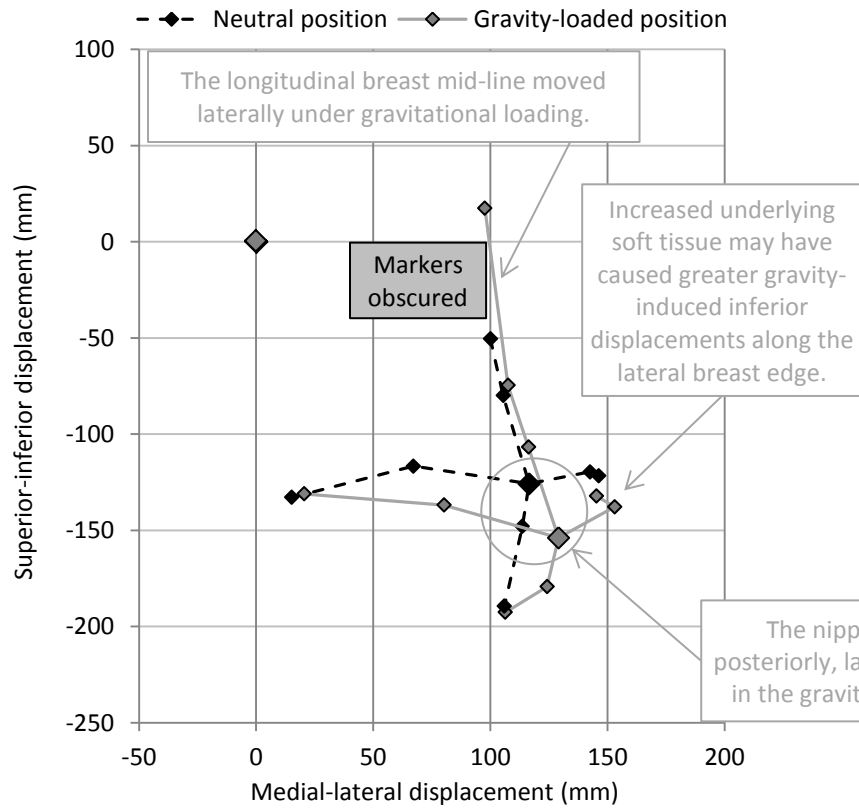
Participant 6 (32C)



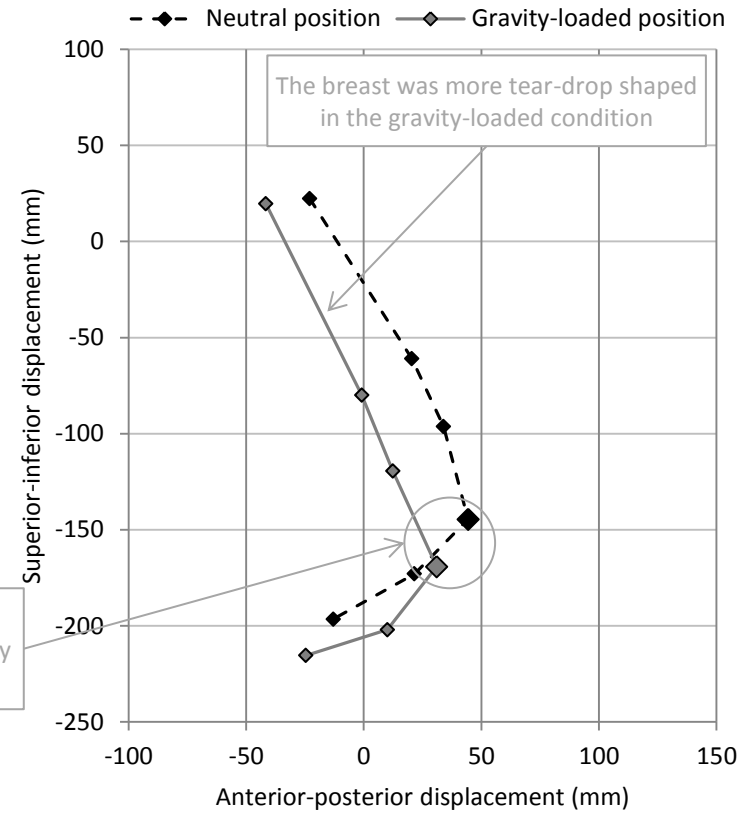
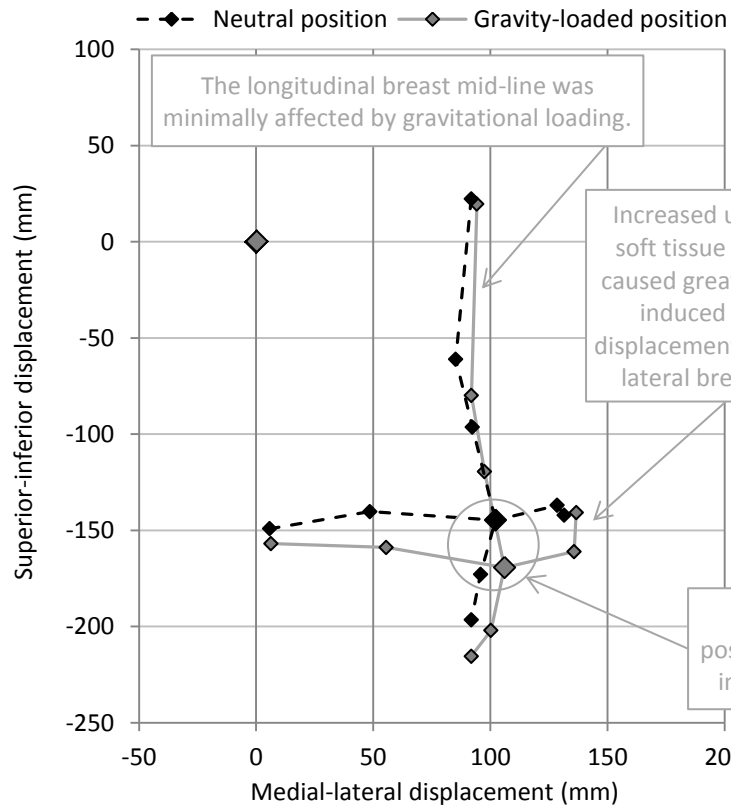
Participant 7 (32D)



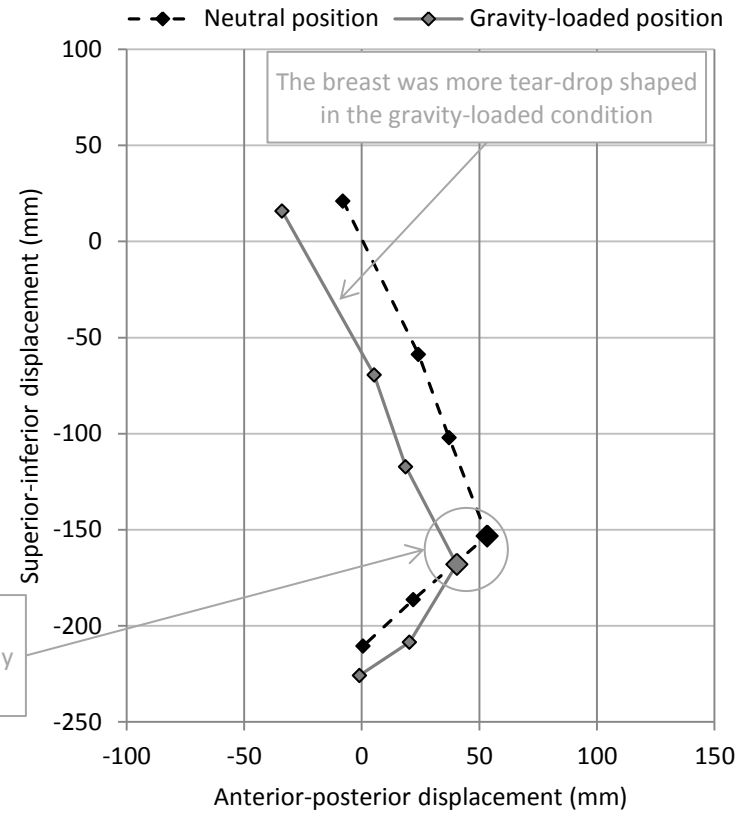
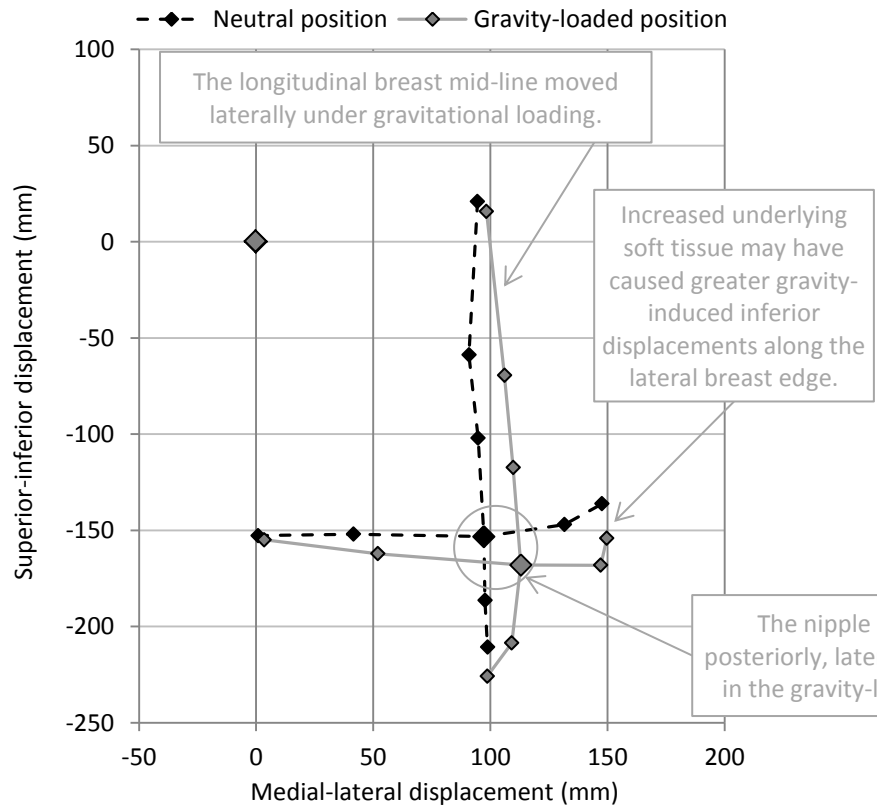
Participant 8 (32D)



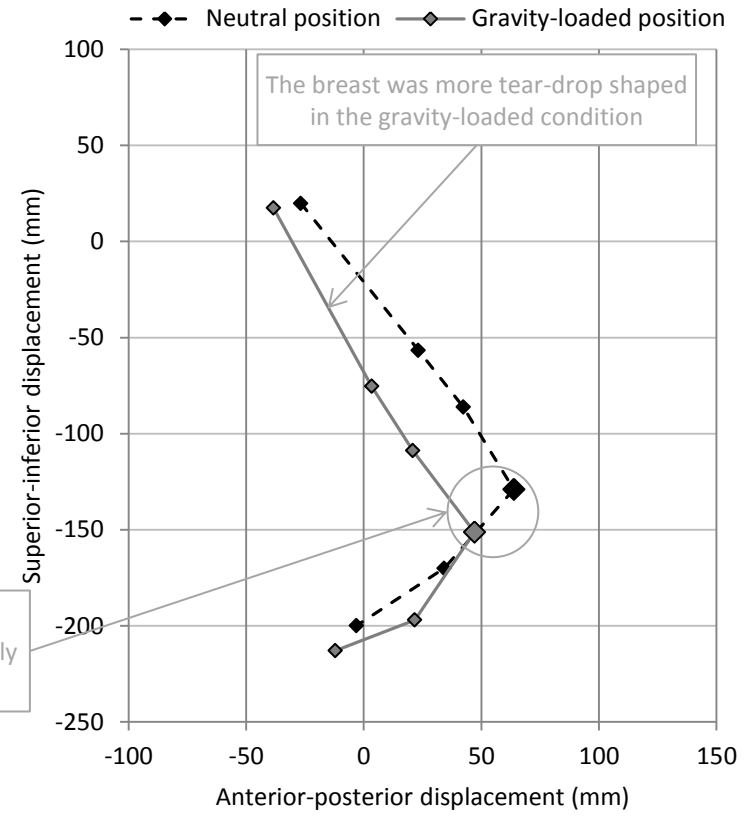
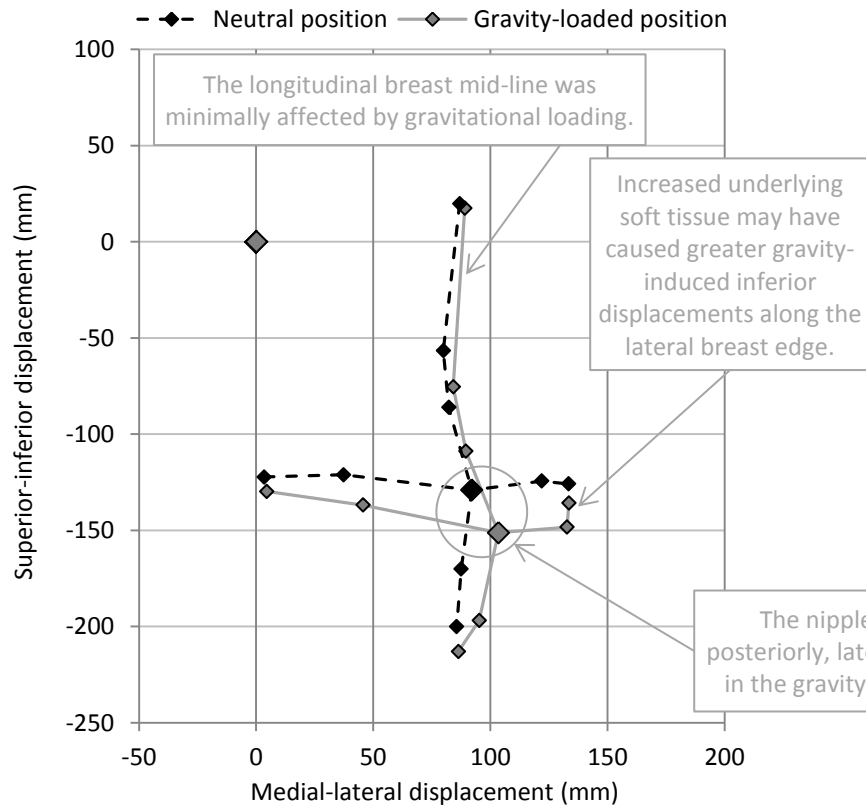
Participant 9 (32D)



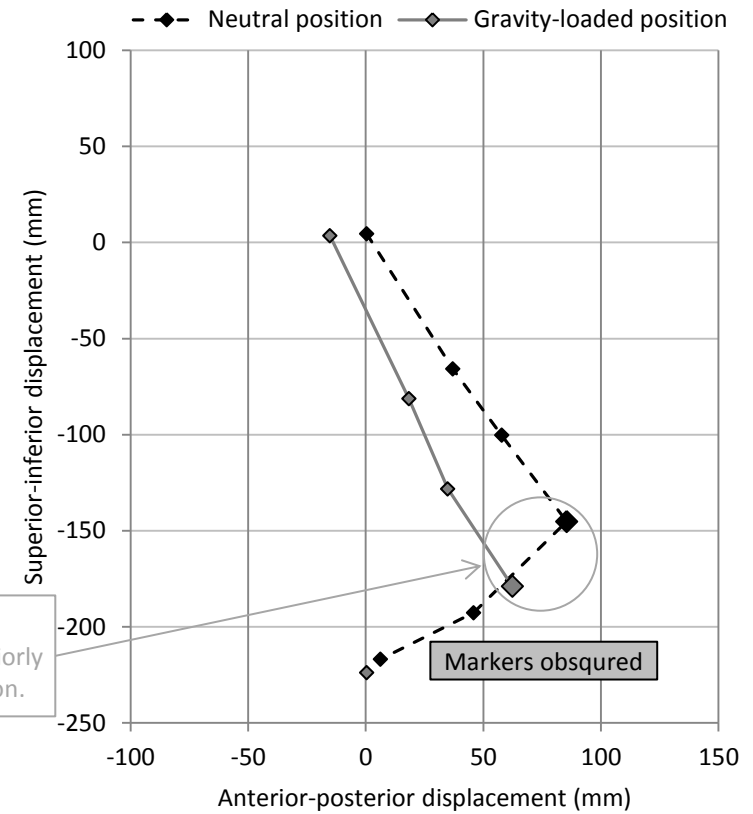
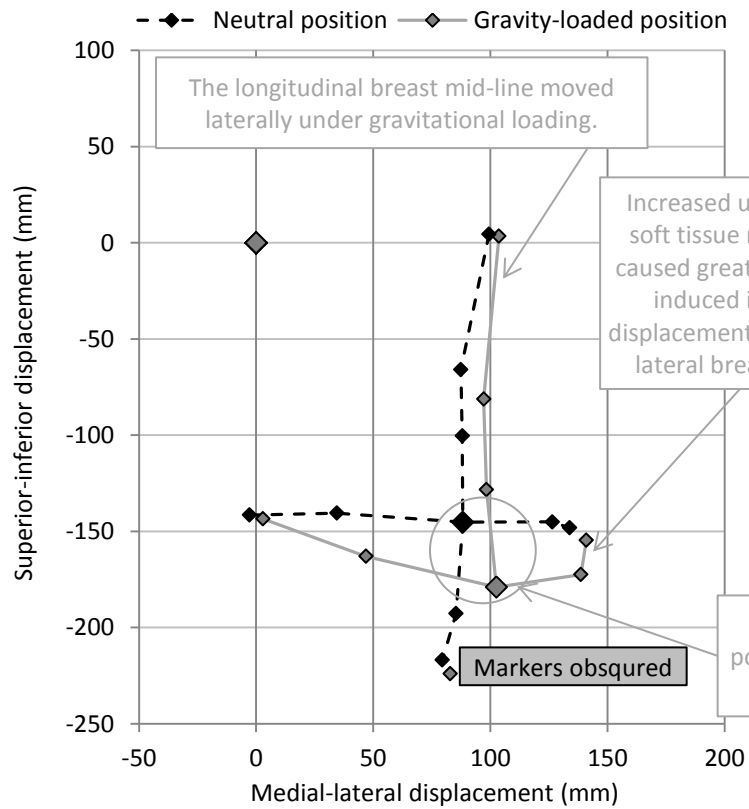
Participant 10 (34D)



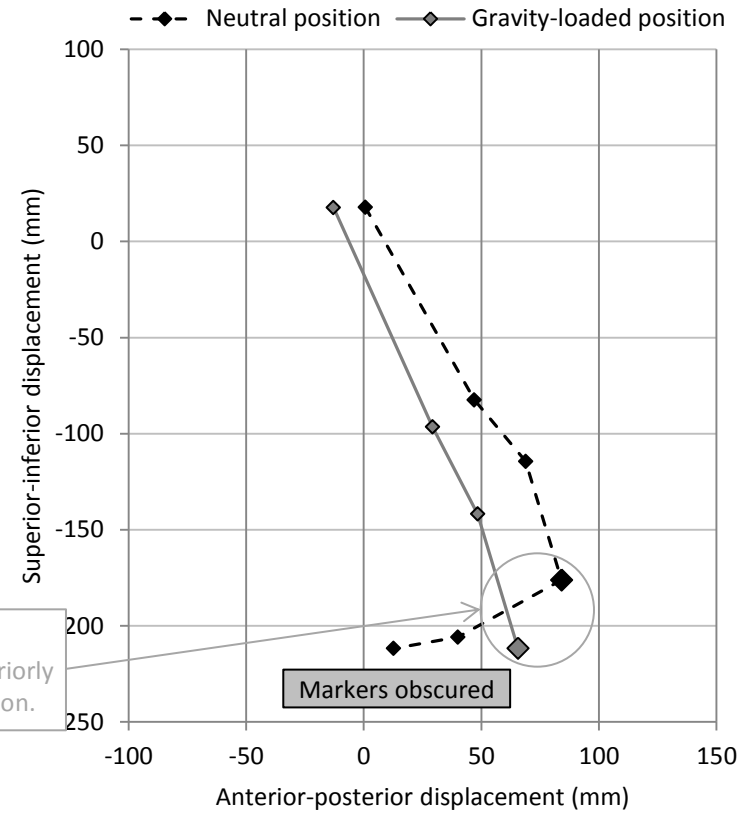
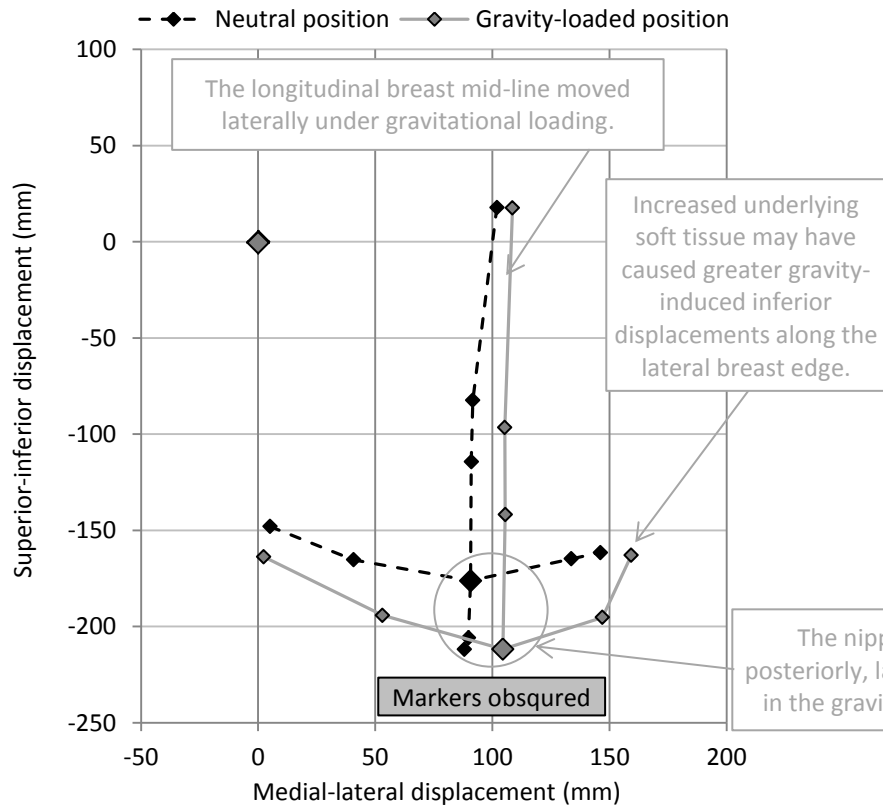
Participant 11 (32DD)



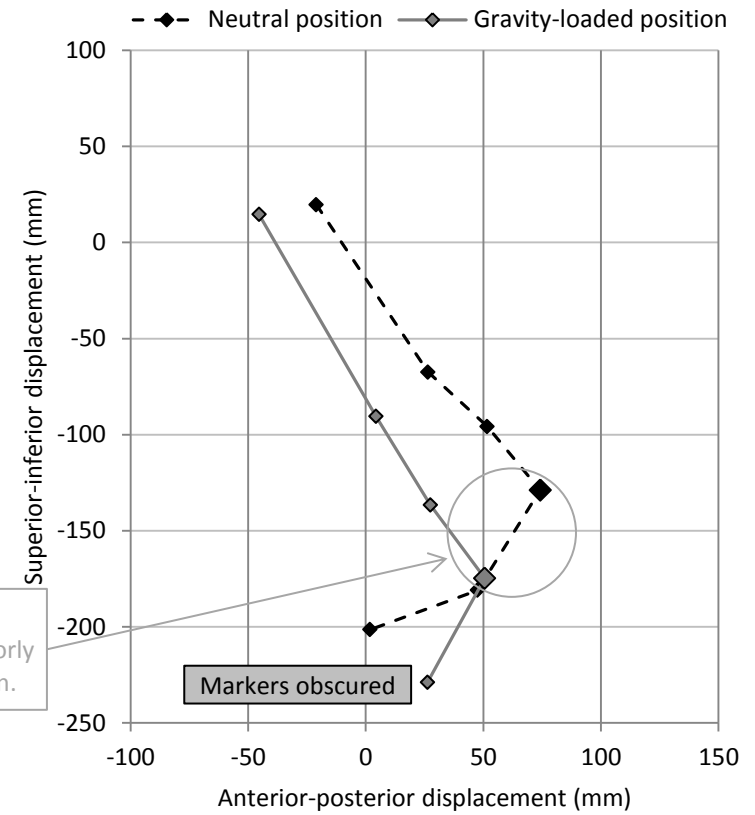
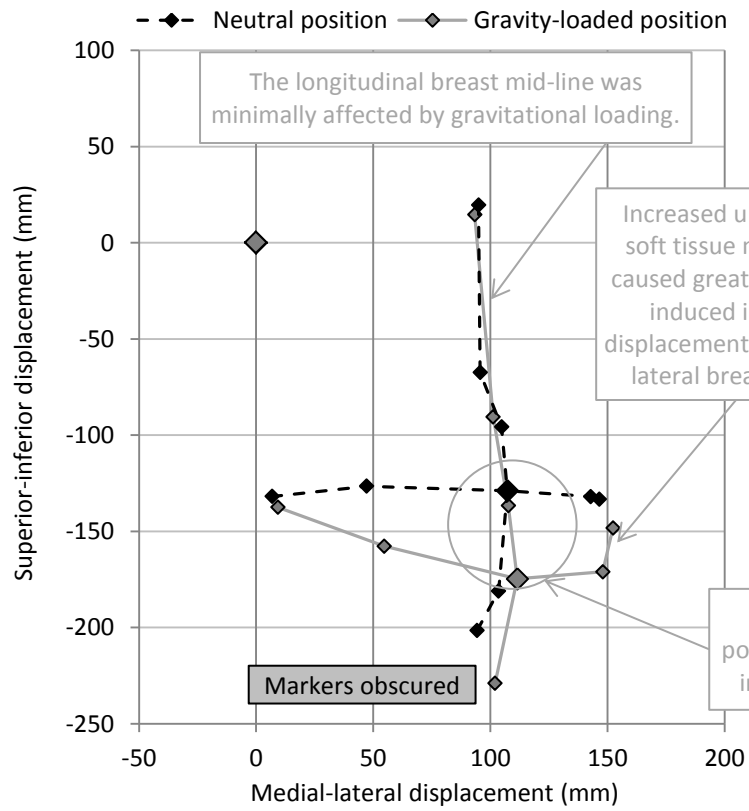
Participant 12 (30E)



Participant 13 (34DD)



Participant 14 (34DD)



Appendix F

Estimated neutral nipple position during the practicality testing of the breast drop method.

Participant	Breast size	Breast drop method	Neutral nipple position estimated using breast drop (mm)		
			Anterior-posterior	Medial-lateral	Superior-inferior
Participant B	32C	Hand oscillation 1	62.1	97.3	-141.6
		Hand oscillation 2	60.9	102.6	-161.4
		Theraband	49.9	109.1	-123.6
Participant C	32C	Hand oscillation 1	51.6	107.8	-130.4
		Hand oscillation 2	46.7	109.9	-138.7
Participant D	34C	Hand oscillation 1	54.0	95.4	-135.2
		Hand oscillation 2	50.9	117.4	-151.8
Participant E	34D	Hand oscillation 1	58.2	95.4	-128.9
		Theraband	43.9	108.9	-83.1
Participant F	34DD	Hand oscillation 1	49.6	124.4	-130.4
		Theraband	38.3	133.4	-120.0

Appendix G

Estimated neutral nipple position during the practicality testing of the static extreme method.

Participant	Breast size	Neutral nipple position estimated using static extremes (mm)		
		Anterior-posterior	Medial-lateral	Superior-inferior
Participant B	32C	63.1	89.6	-148.0
Participant C	32C	53.0	110.8	-113.1
Participant D	34C	No data	100.4	-138.7
Participant E	34D	58.4	102.5	-102.3
Participant F	34DD	69.9	111.8	-133.9
Participant G	30 HH	93.9	105.1	-185.0

Appendix H

Estimated neutral nipple position during the practicality testing of the drop landing method.

Participant Number	Breast size	Drop height (m)	Neutral nipple position estimated using drop landing (mm)		
			Anterior-posterior	Medial-lateral	Superior-inferior
Participant A	32A	1.35	59.1	95.0	-141.6
Participant B	32C	1.10	67.2	100.4	-147.5
		1.35	61.6	106.6	-154.0
Participant E	34D	1.10	56.5	100.6	-134.3
		1.35	59.1	101.0	-131.2
Participant F	34DD	1.10	54.6	137.8	-137.2
		1.35	61.7	124.1	-132.4

Appendix I

Estimated neutral nipple position during the practicality testing of the zero acceleration during running method.

Participant Number	Breast size	Treadmill speed (kph)	Neutral nipple position estimated using zero acceleration during running (mm)		
			Anterior-posterior	Medial-lateral	Superior-inferior
Participant B	32C	8	No zero-acceleration occurrences		
		9	No zero-acceleration occurrences		
		10	No zero-acceleration occurrences		
		11	No zero-acceleration occurrences		
		12	No zero-acceleration occurrences		
		13	No zero-acceleration occurrences		
		14	No zero-acceleration occurrences		
Participant E	34D	8	No zero-acceleration occurrences		
		9	No zero-acceleration occurrences		
		10	No zero-acceleration occurrences		

Appendix J

Estimated neutral nipple position during the practicality testing of the zero acceleration during jumping method.

Participant Number	Breast size	Jumping height (acceleration type)	Number of zero acceleration points	Neutral nipple position estimated using zero acceleration during jumping (mm)		
				Anterior-posterior	Medial-lateral	Superior-inferior
Participant B	32C	Comfortable (relative)	1495	58.2	107.5	-146.9
		Comfortable (global)	1397	57.8	107.6	-147.9
		Maximum (relative)	1488	58.4	107.4	-153.5
		Maximum (global)	1404	58.1	107.5	-154.2
Participant C	32C	Comfortable (relative)	1532	43.8	118.3	-112.9
		Comfortable (global)	1400	43.5	118.7	-114.4
		Maximum (relative)	1426	40.8	117.9	-116.3
		Maximum (global)	1300	40.3	117.9	-117.6
Participant E	34D	Comfortable (relative)	1157	55.9	106.1	-108.8
		Comfortable (global)	1083	55.8	106.3	-110.0
		Maximum (relative)	1076	59.1	102.7	-118.2
		Maximum (global)	1058	59.2	102.8	-118.2
Participant F	34DD	Comfortable (relative)	96	45.0	107.2	-120.0
		Comfortable (global)	238	37.6	85.8	-101.4
		Maximum (relative)	686	58.4	135.8	-144.5
		Maximum (global)	1228	52.7	122.2	-129.4

Appendix K
BREAST COMFORT QUESTIONNAIRE

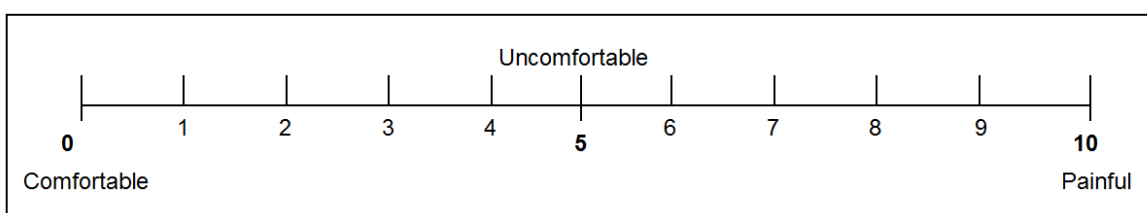


Participant Number: _____ Date: _____

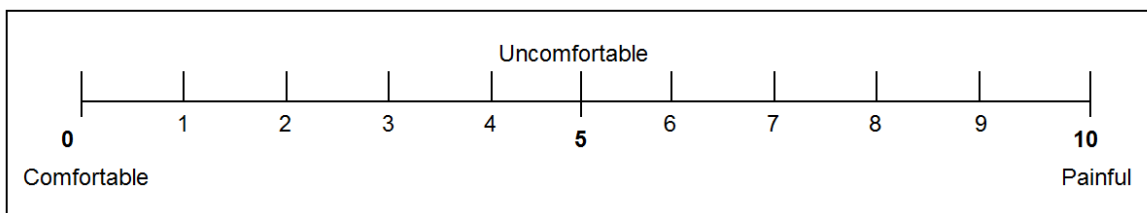
Please rate how comfortable your **breasts** felt during the following trials.

Treadmill Running

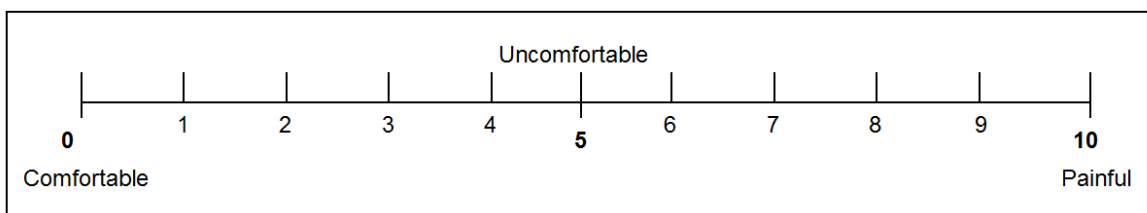
Walking (4 kph to 7 kph)



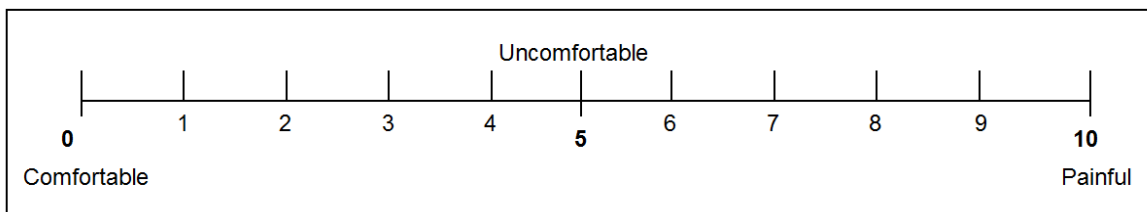
Jogging (8 kph to 11 kph)



Running (12 kph to 14 kph)

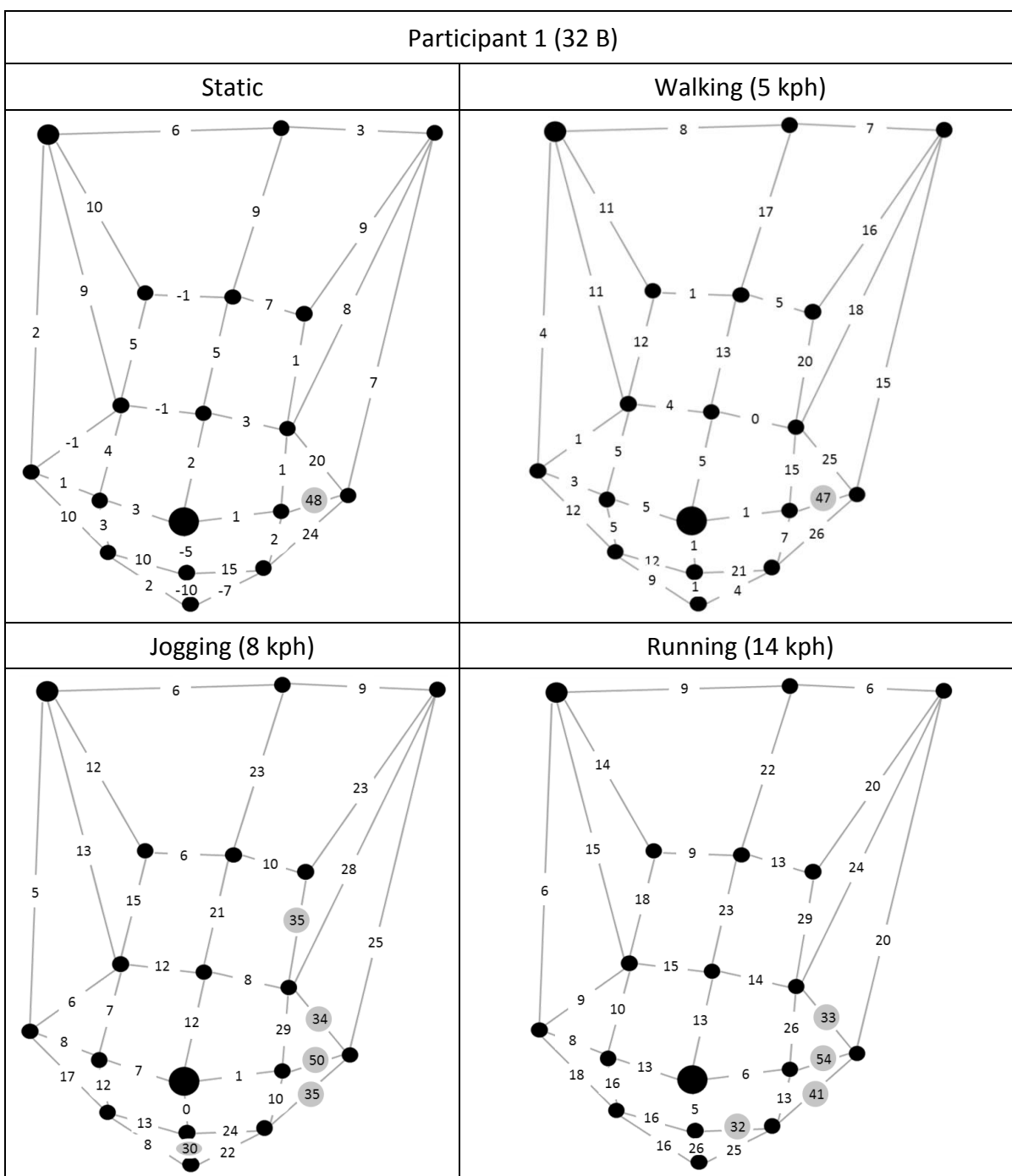


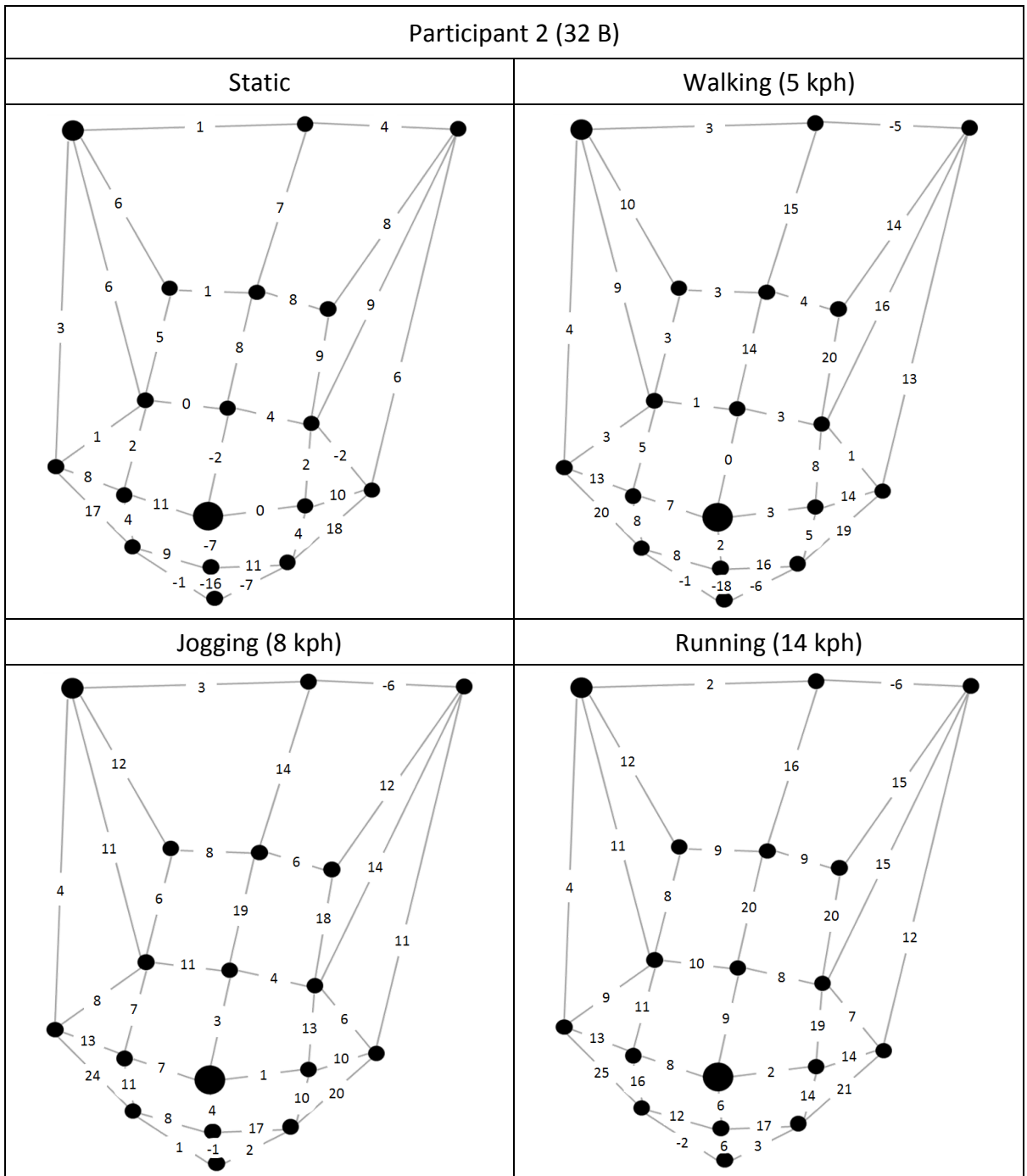
Static standing

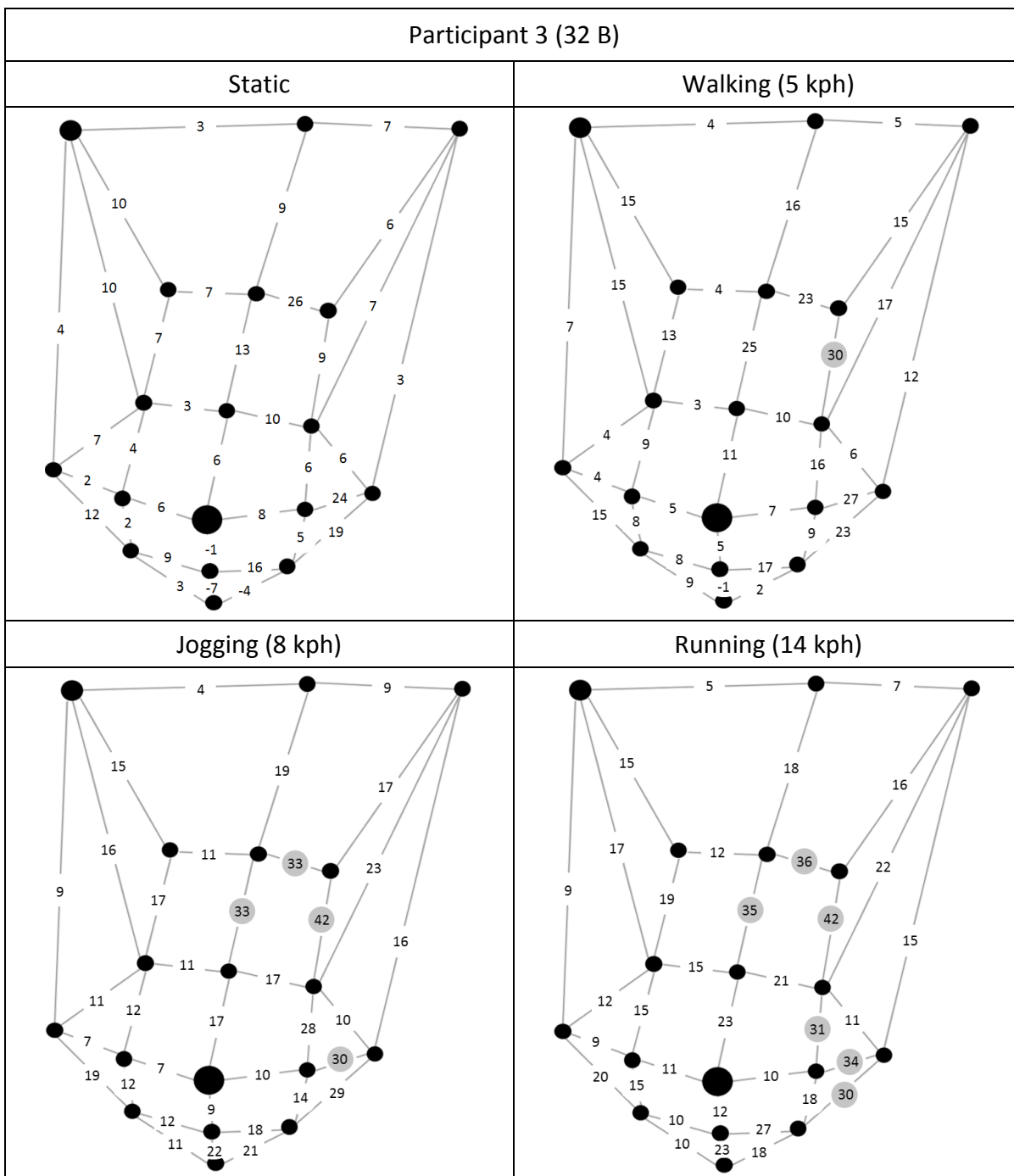


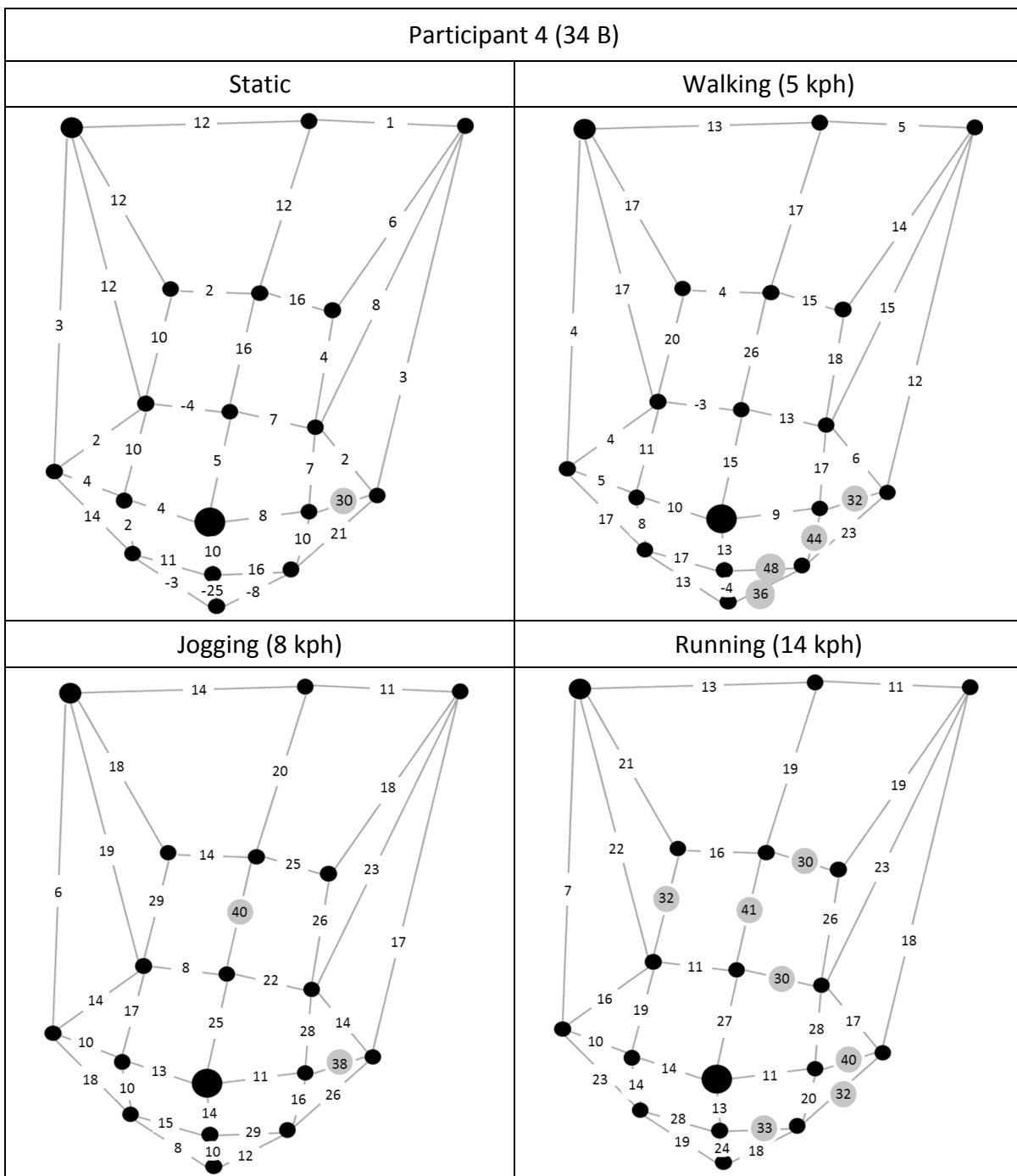
Appendix L

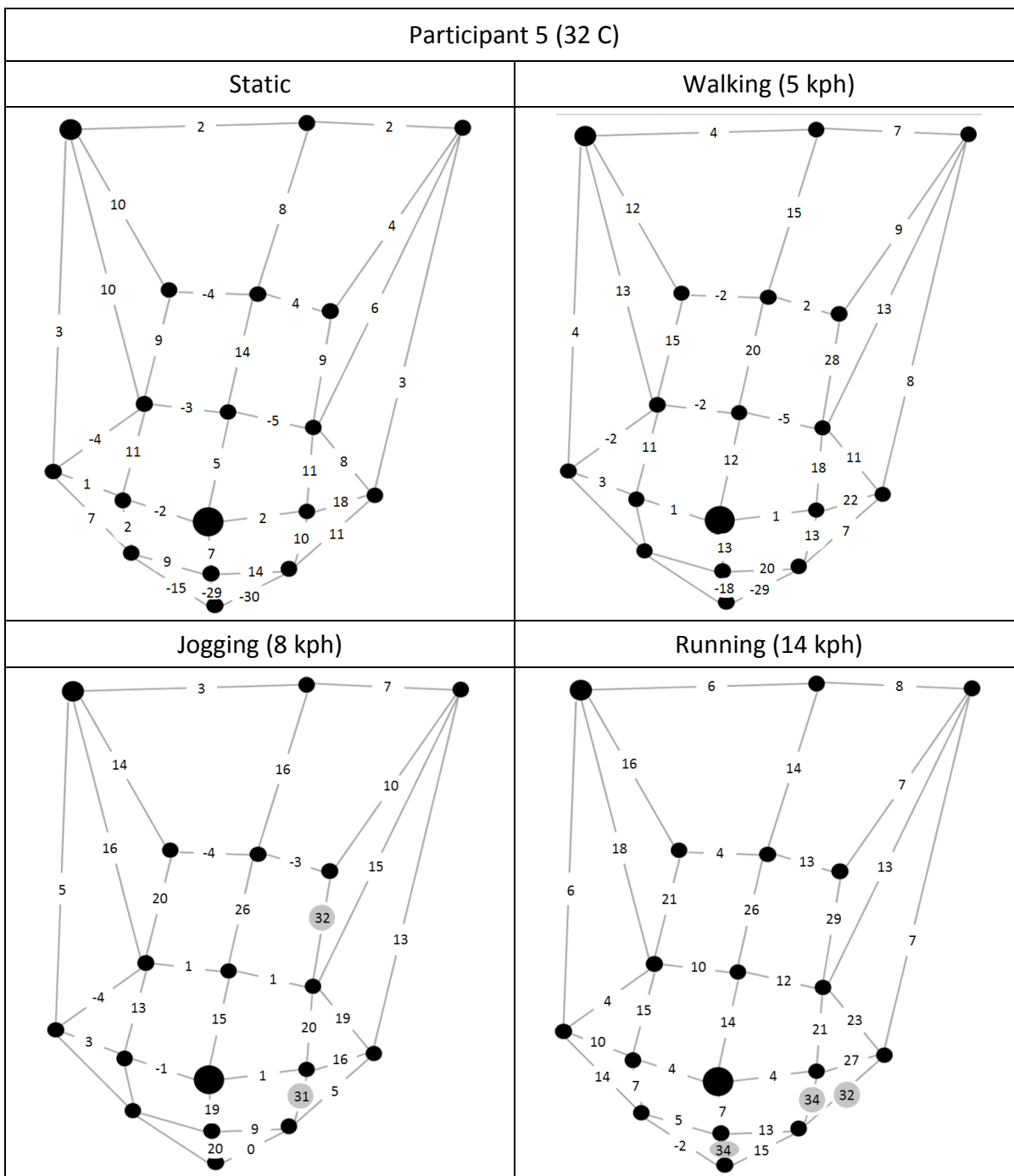
Mean peak strain (over three gait cycles) across the breast skin during static and dynamic conditions. Grey highlighting signifies that strain values are within the skin resistance zone (between 30% and 60% strain), and black signifies strain values within the skin failure zone (strain $\geq 60\%$). Missing data values occurred due to marker obstruction during data collection.

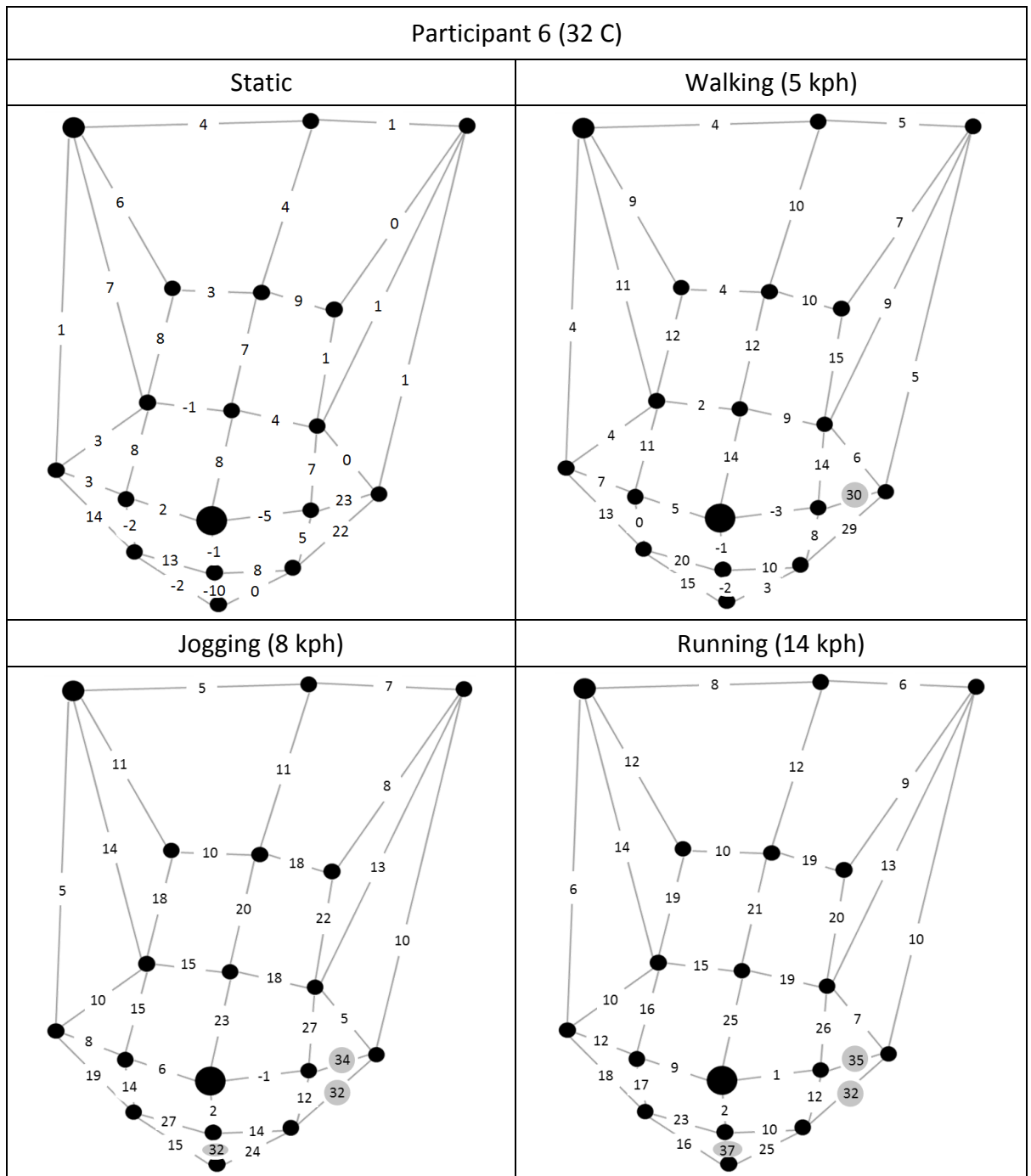


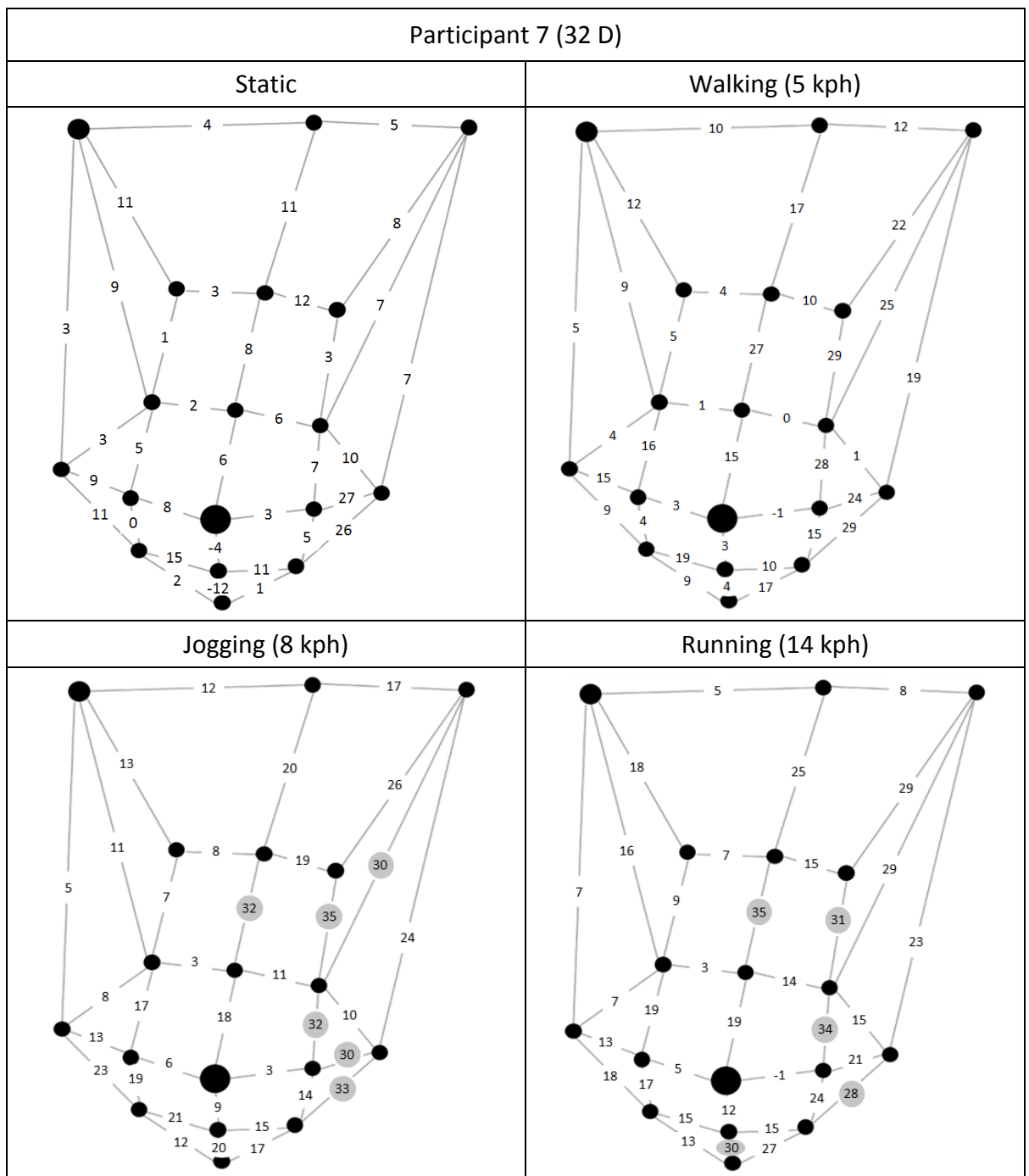


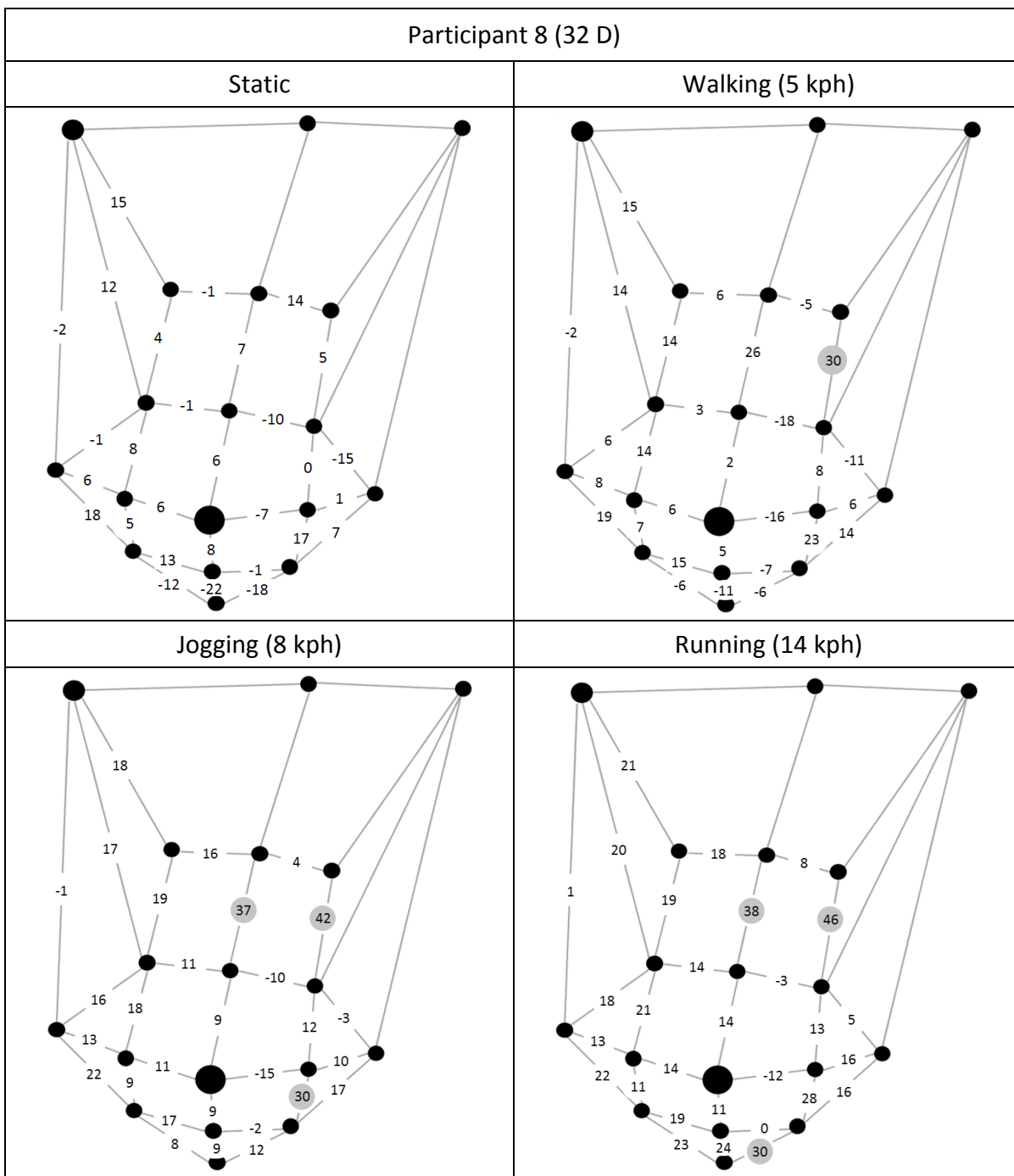


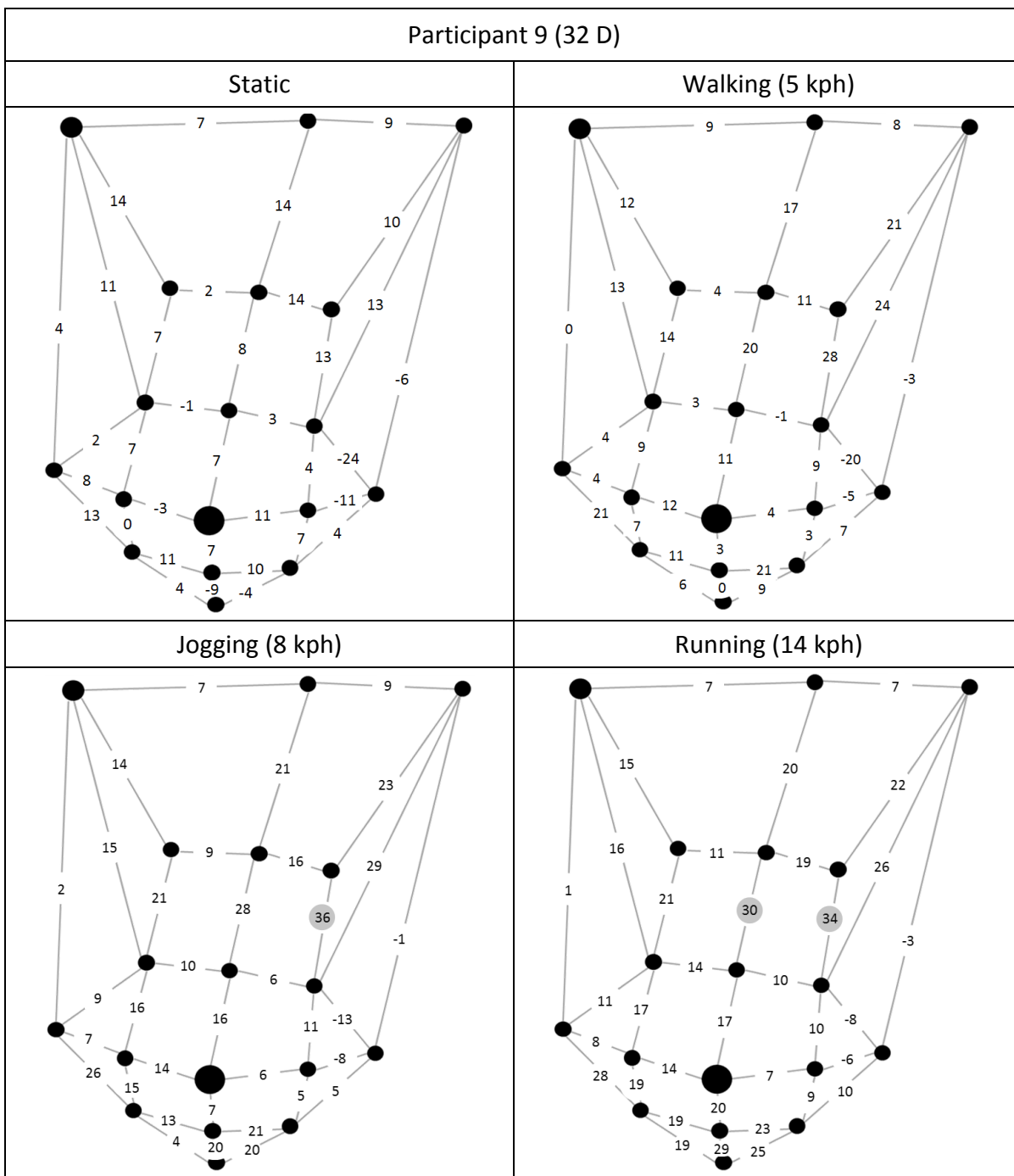


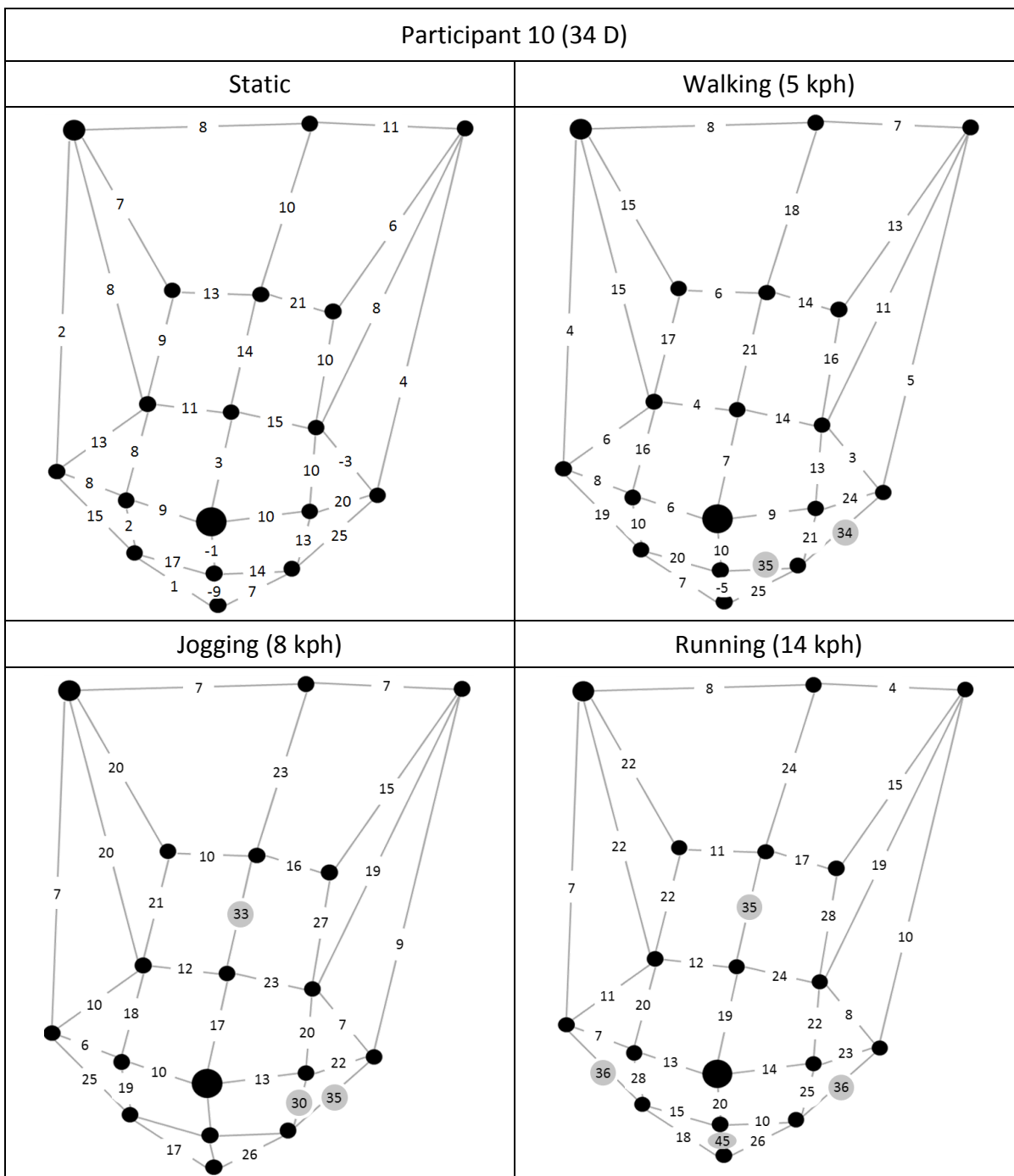


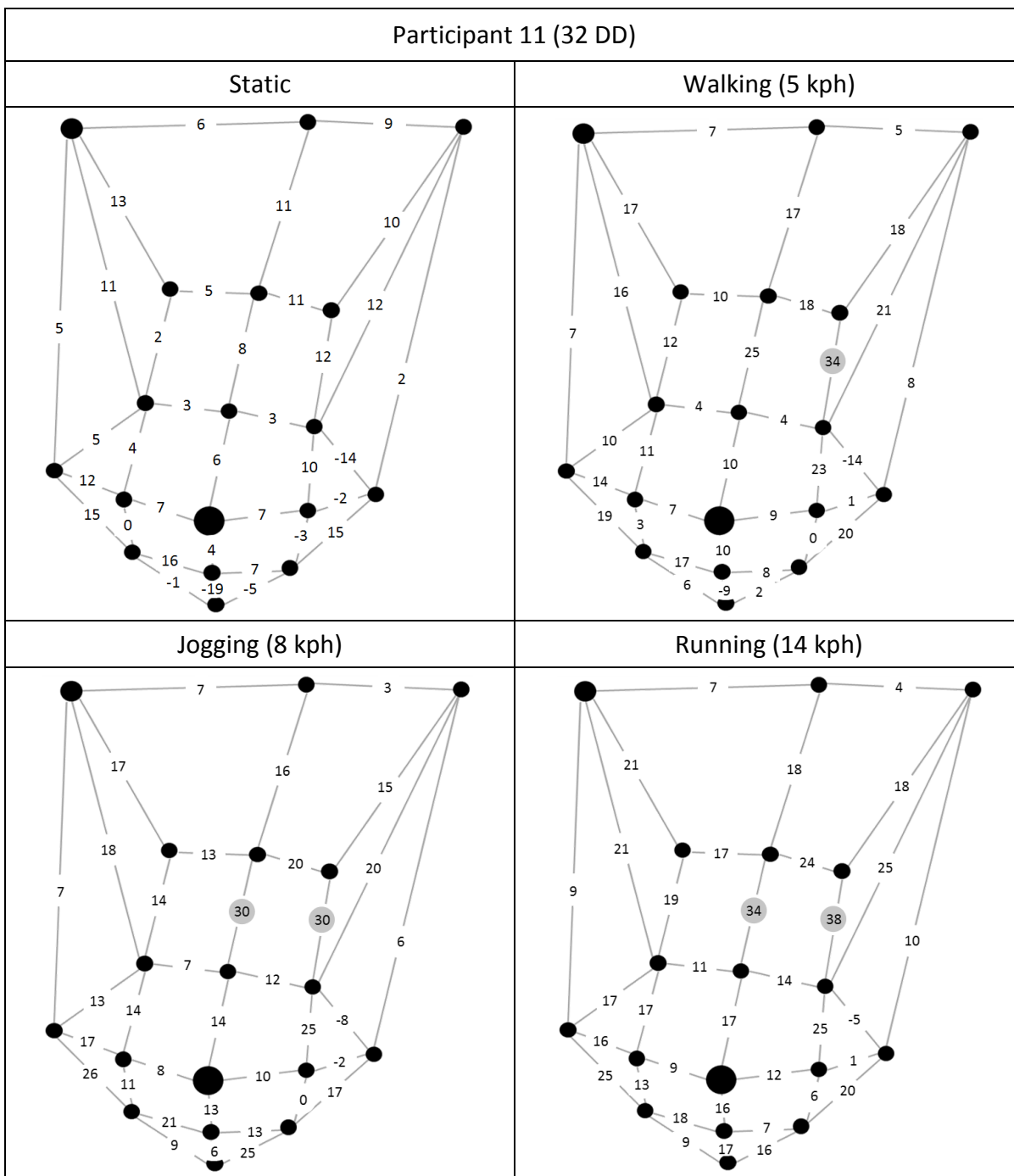


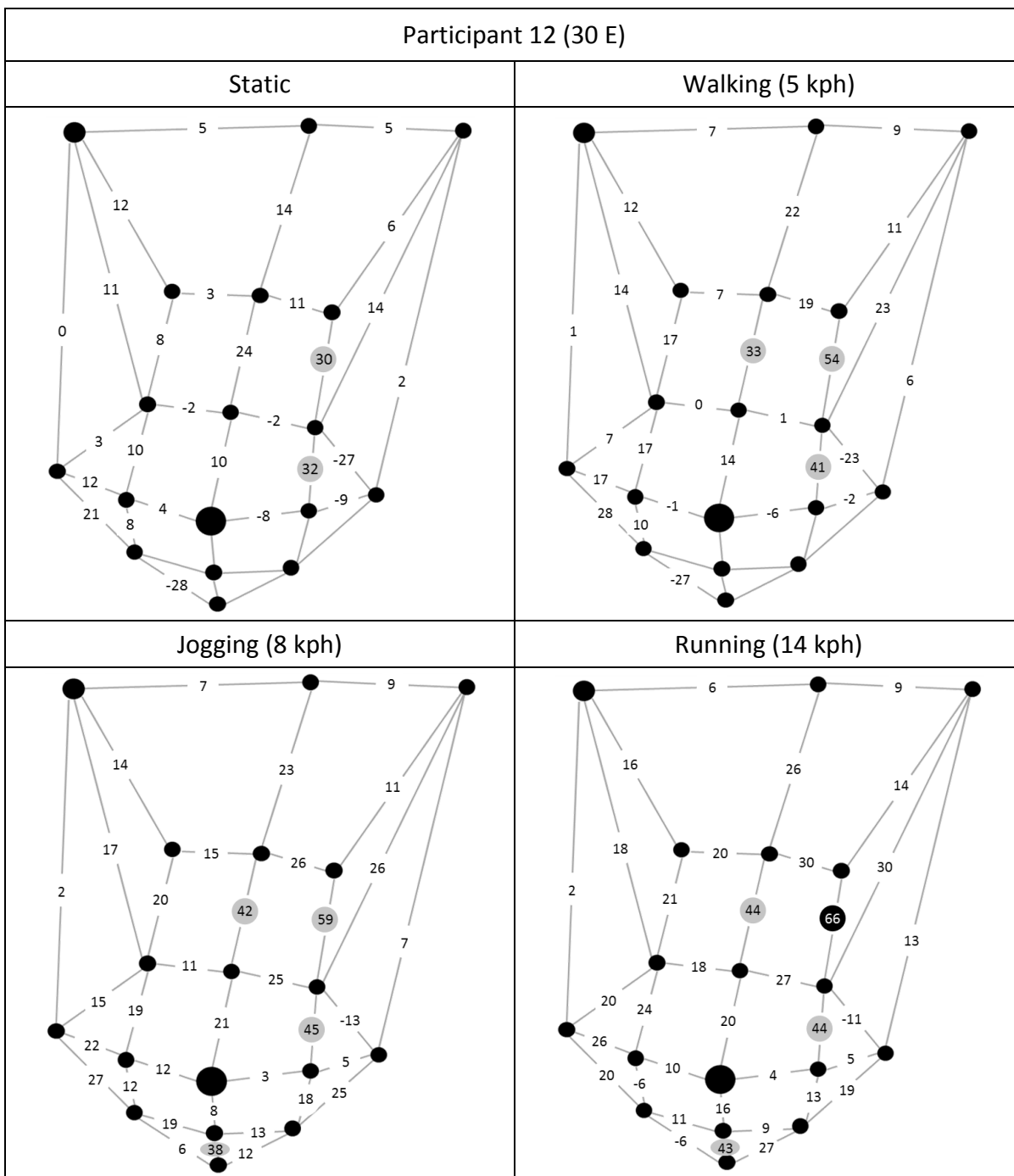


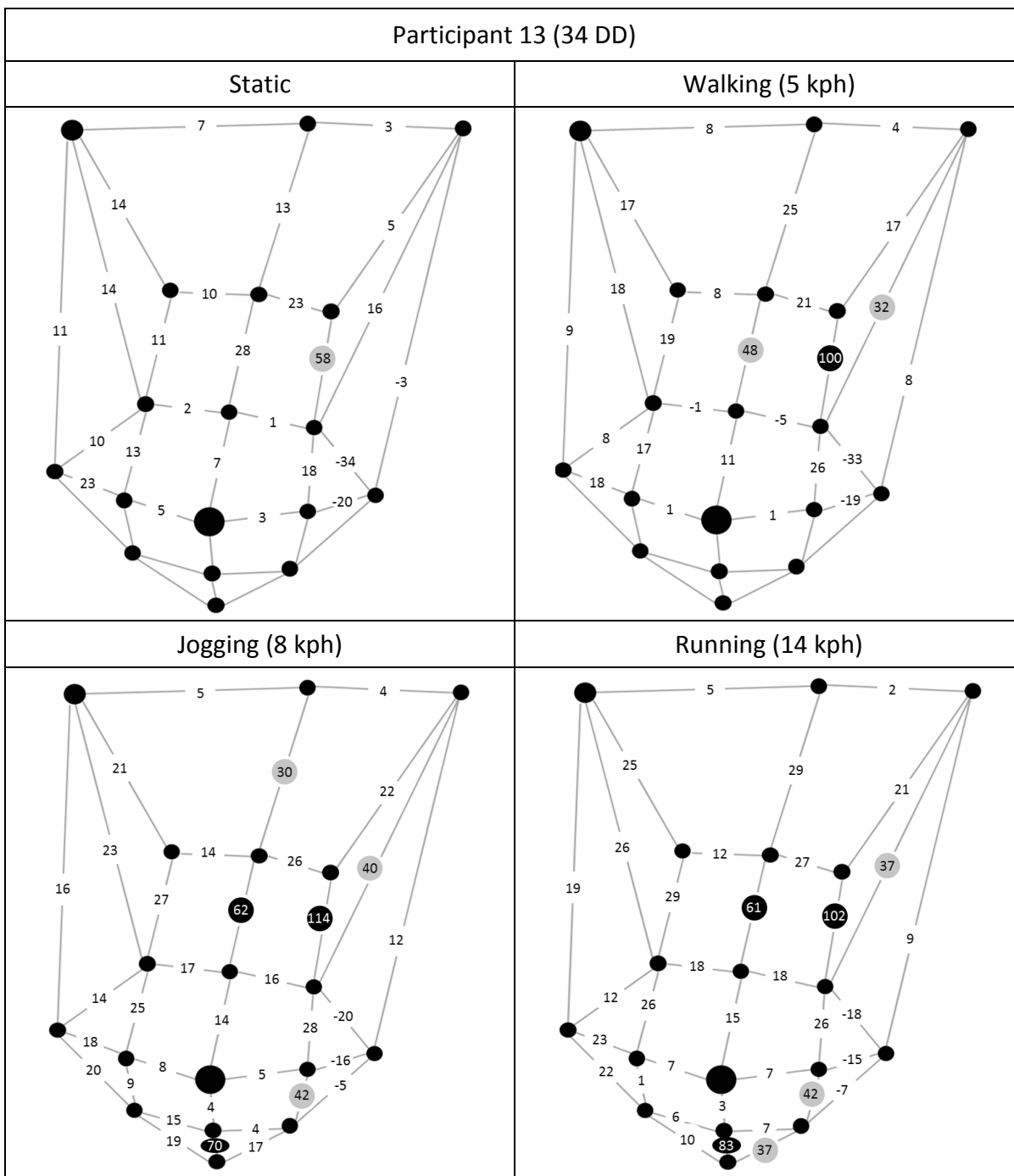


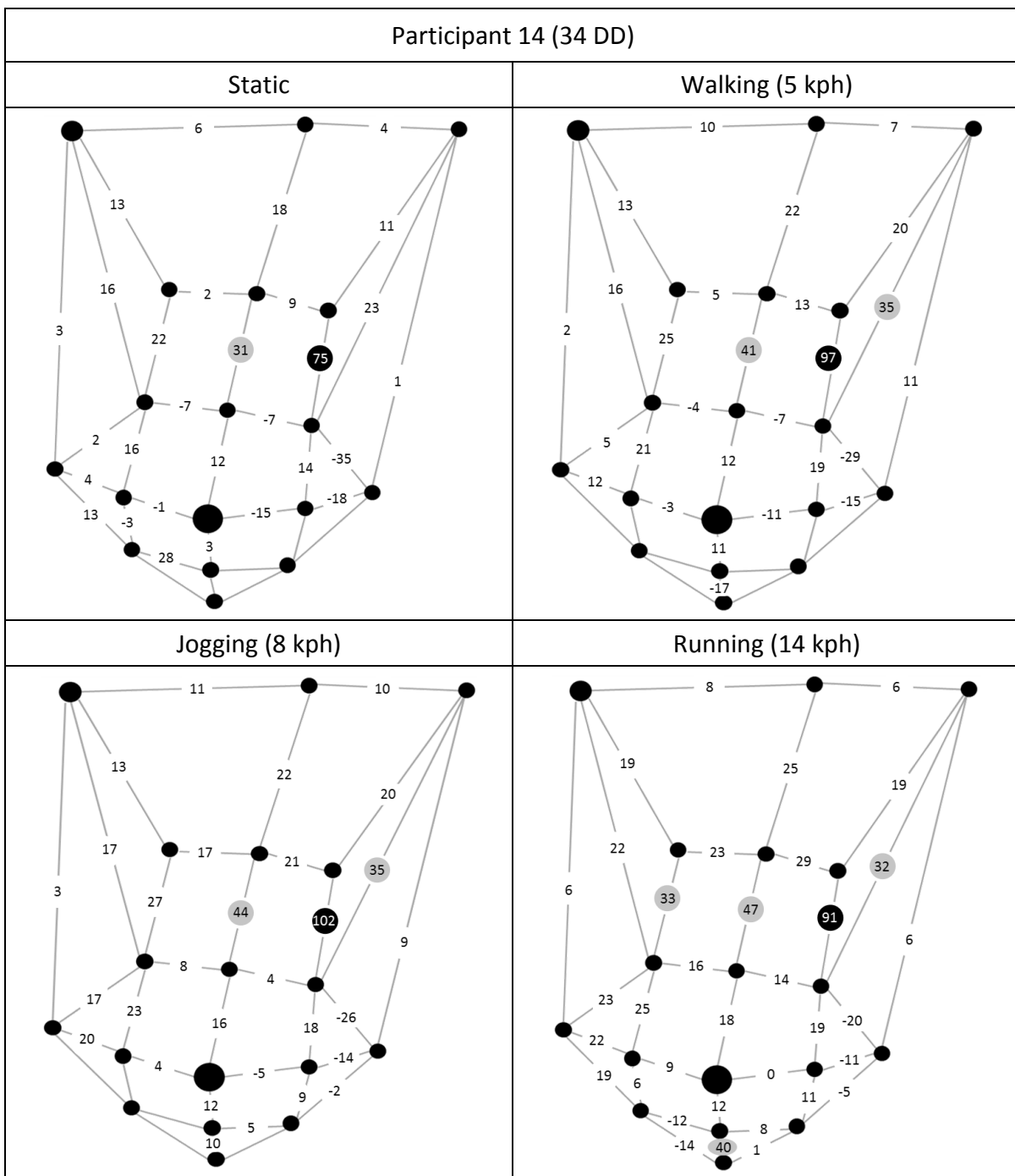












Appendix M

Static strain values for each skin segment for each participant and the maximum and typical errors in each strain value.

Static strain values (%)	Participant 1 (32B)	Participant 2 (32B)	Participant 3 (32B)	Participant 4 (34B)	Participant 5 (32C)	Participant 6 (32C)	Participant 7 (32D)	Participant 8 (32D)	Participant 9 (32D)	Participant 10 (34D)	Participant 11 (32DD)	Participant 12 (30E)	Participant 13 (34DD)	Participant 14 (34DD)	Mean
UML.V.1	9	7	9	12	8	4	11		14	10	11	14	13	18	11
UML.V.2	5	8	13	16	14	7	8	7	8	14	8	24	28	31	14
UML.V.3	2	-2	6	5	5	8	6	6	7	3	6	10	7	12	6
LML.V.1	-5	-7	-1	10	7	-1	-4	8	7	-1	4			3	2
LML.V.2	-10	-16	-7	-25	-29	-10	-12	-22	-9	-9	-19				-15
IML.H.1	1	8	2	4	1	3	9	6	8	8	12	12	23	4	7
IML.H.2	3	11	6	4	-2	2	8	6	-3	9	7	4	5	-1	4
OML.H.1	1	0	8	8	2	-5	3	-7	11	10	7	-8	3	-15	1
OML.H.2	48	10	24	30	18	23	27	1	-11	20	-2	-9	-20	-18	10
UI.V.1	2	3	4	3	3	1	3	-2	4	2	5	0	11	3	3
UI.V.2	9	6	10	12	10	7	9	12	11	8	11	11	14	16	10
UI.V.3	10	6	10	12	10	6	11	15	14	7	13	12	14	13	11
UI.V.4	5	5	7	10	9	8	1	4	7	9	2	8	11	22	8
UI.V.5	4	2	4	10	11	8	5	8	7	8	4	10	13	16	8
UI.H.1	6	1	3	12	2	4	4		7	8	6	5	7	6	5
UI.H.2	-1	1	7	2	-4	3	3	-1	2	13	5	3	10	2	3
UI.H.3	-9	-4	-7	-9	-12	-11	-6	-8	-4	-4	-3	-13	11	-14	-7
UI.H.4	-1	0	3	-4	-3	-1	2	-1	-1	11	3	-2	2	-7	0

Appendices

UO.V.1	7	6	3	3	3	1	7		-6	4	2	2	-3	1	2
UO.V.2	8	9	7	8	6	1	7		13	8	12	14	16	23	10
UO.V.3	9	8	6	6	4	0	8		10	6	10	6	5	11	7
UO.V.4	1	9	9	4	9	1	3	5	13	10	12	30	58	75	17
UO.V.5	1	2	6	7	11	7	7	0	4	10	10	32	18	14	9
UO.H.1	3	4	7	1	2	1	5		9	11	9	5	3	4	5
UO.H.2	7	8	26	16	4	9	12	14	14	21	11	11	23	9	13
UO.H.3	20	-2	6	2	8	0	10	-15	-24	-3	-14	-27	-34	-35	-8
UO.H.4	3	4	10	7	-5	4	6	-10	3	15	3	-2	1	-7	2
LI.V.1	3	4	2	2	2	-2	0	5	0	2	0	8		-3	2
LI.V.2	2	-1	3	-3	-15	-2	2	-12	4	1	-1	-28			-4
LI.H.1	10	17	12	14	7	14	11	18	13	15	15	21		13	14
LI.H.2	10	9	9	11	9	13	15	13	11	17	16			28	13
LO.V.1	2	4	5	10	10	5	5	17	7	13	-3				7
LO.V.2	-7	-7	-4	-8	-30	0	1	-18	-4	7	-5				-7
LO.H.1	24	18	19	21	11	22	26	7	4	25	15				17
LO.H.2	15	11	16	16	14	8	11	-1	10	14	7				11

Appendices

Static strain error (%)	Participant 1 (32B)		Participant 2 (32B)		Participant 3 (32B)		Participant 4 (34B)		Participant 5 (32C)		Participant 6 (32C)		Participant 7 (32D)		Participant 8 (32D)		Participant 9 (32D)		Participant 10 (34D)		Participant 11 (32DD)		Participant 12 (30E)		Participant 13 (34DD)		Participant 14 (34DD)		Mean	
	Maximum	Typical	Maximum	Typical	Maximum	Typical	Maximum	Typical	Maximum	Typical	Maximum	Typical	Maximum	Typical	Maximum	Typical	Maximum	Typical	Maximum	Typical	Maximum	Typical	Maximum	Typical	Maximum	Typical	Maximum	Typical		
UML.V.1	2	2	2	1	2	1	2	1	2	1	2	2	2	1			2	1	2	1	2	1	2	1	2	1	2	1	1	2
UML.V.2	5	3	5	3	5	4	5	3	4	3	4	3	6	4	5	3	4	3	4	3	5	3	5	3	5	3	5	3	3	5
UML.V.3	4	3	3	2	3	2	3	2	4	2	3	2	4	3	3	2	3	2	3	2	3	2	3	2	3	2	4	3	2	3
LML.V.1	4	3	5	3	4	3	5	3	5	3	5	3	4	3	7	5	5	3	3	2	3	2					3	2	3	4
LML.V.2	4	3	4	3	4	3	3	2	3	2	4	3	4	3	2	1	4	2	5	3	3	2							2	4
IML.H.1	4	3	4	3	4	3	3	2	3	2	4	3	4	3	3	2	3	2	3	2	4	3	4	2	3	2	3	2	2	4
IML.H.2	4	2	4	3	3	2	3	2	3	2	4	2	3	2	3	2	3	2	3	2	3	2	3	2	3	2	3	2	2	3
OML.H.1	4	3	3	2	4	3	3	2	3	2	3	2	4	2	3	2	3	2	3	2	3	2	2	2	3	2	2	1	2	3
OML.H.2	6	4	3	2	4	3	5	3	4	2	5	3	5	3	3	2	2	1	4	3	2	2	2	1	1	1	2	1	2	3
UI.V.1	1	1	1	1	1	1	1	1	1	1	1	1	1	1	1	1	1	1	1	1	1	1	1	1	1	1	1	1	1	1
UI.V.2	1	1	1	1	2	1	1	1	1	1	1	1	2	1	1	1	1	1	1	1	2	1	1	1	1	1	1	1	1	1
UI.V.3	2	1	2	1	2	2	2	1	2	1	2	2	2	1	2	1	2	1	2	1	2	2	2	1	2	1	2	1	1	2
UI.V.4	4	3	5	3	4	3	5	4	5	3	4	3	5	4	4	3	4	3	4	3	4	3	4	2	4	3	5	3	3	4
UI.V.5	5	4	5	3	4	3	5	3	5	4	4	3	5	4	6	4	4	3	4	3	5	3	4	3	4	3	7	5	3	5
UI.H.1	2	1	2	1	2	1	2	1	2	1	2	1	2	1			2	1	2	1	2	1	2	1	2	1	2	1	1	2
UI.H.2	4	3	4	3	4	3	3	2	3	2	4	3	4	3	4	3	4	3	3	2	5	3	4	2	3	2	3	2	3	4
UI.H.3	3	2	3	2	3	2	2	2	3	2	3	2	3	2	2	2	2	2	2	3	2	3	2	3	2	3	2	3	2	3
UI.H.4	4	3	3	2	4	3	3	2	3	2	4	3	4	2	4	2	4	2	3	2	4	3	3	2	3	2	2	2	2	3

Appendix N



Faculty of Science
University of Portsmouth
St Michael's Building
White Swan Road
PORTSMOUTH
PO1 2DT

Amy Loveridge
Department of Sport and Exercise Science
Spinnaker Building
University of Portsmouth
Portsmouth
PO1 2ER

30th January 2013

FAVOURABLE OPINION

Protocol Title: A comparison of experimental methods to assess the neutral position of the breast (SFEC Appl 2012-014; SFEC Opinion 2013-001)

Date Reviewed: 7th Jan 2013 to 30th Jan 2013

Dear Amy,

Thank you for resubmitting your protocol for ethical review and for the clarifications provided.

Your responses have been reviewed and I am pleased to inform you that your application has been given a favourable opinion by the Science Faculty Ethics Committee. Please notify us in the future of any substantial amendments that may be required and send us a final study report.

Good luck with the study.

A handwritten signature in black ink, appearing to read 'Clare Eglin'.

Clare Eglin
DSES, Science Faculty Ethics Committee

CC -
Dr Chris Markham – Chair of SFEC
Dr Jim House – Vice Chair of SFEC
Holly Shawyer – Faculty Administrator


Appendix O

FORM UPR16**Research Ethics Review Checklist**

Please complete and return the form to Research Section, Quality Management Division, Academic Registry, University House, with your thesis, prior to examination

Postgraduate Research Student (PGRS) Information		Student ID:	649848
Candidate Name:	Amy Zena Loveridge		
Department:	DSES	First Supervisor:	Professor Joanna Scurr
Start Date: (or progression date for Prof Doc students)	1 st February 2012		
Study Mode and Route:	Part-time <input checked="" type="checkbox"/>	MPhil <input type="checkbox"/>	Integrated Doctorate (NewRoute) <input type="checkbox"/>
	Full-time <input type="checkbox"/>	MD <input type="checkbox"/>	Prof Doc (PD) <input type="checkbox"/>
		PhD <input type="checkbox"/>	
Title of Thesis:	Incorporating the neutral breast position into measurements of breast motion and breast strain		
Thesis Word Count: (excluding ancillary data)	79,891		
<p>If you are unsure about any of the following, please contact the local representative on your Faculty Ethics Committee for advice. Please note that it is your responsibility to follow the University's Ethics Policy and any relevant University, academic or professional guidelines in the conduct of your study</p> <p>Although the Ethics Committee may have given your study a favourable opinion, the final responsibility for the ethical conduct of this work lies with the researcher(s).</p>			
<p>UKRIO Finished Research Checklist: (If you would like to know more about the checklist, please see your Faculty or Departmental Ethics Committee rep or see the online version of the full checklist at: http://www.ukrio.org/what-we-do/code-of-practice-for-research/)</p>			
a) Have all of your research and findings been reported accurately, honestly and within a reasonable time frame?	YES/NO [±]		
b) Have all contributions to knowledge been acknowledged?	YES/NO [±]		
c) Have you complied with all agreements relating to intellectual property, publication and authorship?	YES/NO [±]		
d) Has your research data been retained in a secure and accessible form and will it remain so for the required duration?	YES/NO [±]		
e) Does your research comply with all legal, ethical, and contractual requirements?	YES/NO [±]		

*Delete as appropriate

Candidate Statement:	
I have considered the ethical dimensions of the above named research project, and have successfully obtained the necessary ethical approval(s)	
Ethical review number(s) from Faculty Ethics Committee (or from NRES/SCREC):	2013-001
Signed: <i>(Student)</i> 	Date: 20/04/15
If you have <i>not</i> submitted your work for ethical review, and/or you have answered 'No' to one or more of questions a) to e), please explain why this is so:	
Signed: <i>(Student)</i>	Date: